CISBAT 2015

FUTURE BUILDINGS & DISTRICTS SUSTAINABILITY FROM NANO TO URBAN SCALE

International Scientific Conference
9-11 September 2015, EPFL, Lausanne, Switzerland

PROCEEDINGS VOL. II

CISBAT

Schweizerische Eidgenossenschaft
Confédération suisse
Confederazione Svizzera
Confederaziun svizra

Swiss Federal Office of Energy SFOE

IBPSA-CH

Cambridge University

Massachusetts Institute of Technology

CISBAT 2015

International Scientific Conference
9-11 September 2015, EPFL, Lausanne, Switzerland

FUTURE BUILDINGS & DISTRICTS –
SUSTAINABILITY FROM NANO TO URBAN SCALE

ISBN Electronic version: 978-2-9701052-2-0
ISBN Print-version: Vol.I 978-2-9701052-0-6 Vol.II 978-2-9701052-1-3

Conference Host / Editor
Solar Energy and Building Physics Laboratory (LESO-PB)
Ecole Polytechnique Fédérale de Lausanne (EPFL)
Station 18, CH - 1015 Lausanne / Switzerland, leso@epfl.ch , http://leso.epfl.ch
Conference Chair: Prof. J.-L. Scartezzini
Conference Manager: Barbara Smith

Scientific partners
Cambridge University, United Kingdom
Massachusetts Institute of Technology, USA
Swiss Chapter of International Building Performance Simulation Association, Switzerland

Under the patronage of
Swiss Federal Office of Energy (SFOE)
Ecole Polytechnique Fédérale de Lausanne (EPFL)

Schweizerische Eidgenossenschaft
Confédération suisse
Confederazione Svizzera
Confederaziun svizra

Swiss Federal Office of Energy SFOE

Cambridge University

Massachusetts Institute of Technology

IBPSA-CH

sccer | future energy efficient buildings & districts

PREFACE

"Future Buildings and Districts – From Nano to Urban Scale" was the topic of the international scientific conference CISBAT 2015, which took place in the Swiss lakeside city of Lausanne from 9 to 11 September 2015.

Designed as a platform for interdisciplinary dialog and presentations of innovative research and development in the field of sustainability in the built environment, the conference covered a wide range of subjects from solar nanotechnologies to the simulation of buildings and urban districts.

CISBAT 2015 was the 13th edition of CISBAT, whose vocation is to present new perspectives offered by renewable energies in the built environment as well as the latest results of research and development in sustainable building technology, in a setting that encourages networking at the international level. The conference assembled building scientists, engineers, urban planners and building designers from all over the world in an effort to promote clean technologies for sustainable buildings and cities. Close to 170 scientific papers were presented during three intense days of conference.

CISBAT 2015 was organized in scientific partnership with the Massachusetts Institute of Technology (MIT) and Cambridge University. Furthermore, the organizing committee was proud to be able to count on an international team of renowned scientists to ensure the quality of presented papers. The conference also teamed up for the third time with the Swiss Chapter of the International Building Performance Simulation Association (IBPSA-CH) to strengthen the subject of “Building Simulation”, one of the conference's leading topics.

Finally we were proud to host an outreach event of the Swiss Competence Centre for Energy Research “Future Energy Efficient Buildings and Districts” (SCCER FEEB&D) as well as a Workshop on Grid-Supportive Buildings organised by Fraunhofer IBP and E.ON Energy Research Center, RWTH Aachen.

Organised under the auspices of the Swiss federal Office of Energy (SFOE) and the Federal Commission for Technology and Innovation (CTI), CISBAT 2015 connected researchers and projects and gave an exciting insight into current research and development in the field of sustainable buildings and cities. It is our greatest wish that the conference will have led to a better understanding of the issues at stake and to fruitful, creative collaboration between its participants.

Prof. Dr J.-L. Scartezzini

Chairman of CISBAT 2015
Head of Solar Energy and Building Physics Laboratory (LESO-PB), Swiss Federal Institute of Technology Lausanne (EPFL)

Note

A few figures might not be easy to interpret in this black and white version of the proceedings. For better legibility please refer to the colour figures in the electronic version of the proceedings.

CONTENTS VOL. I

Author index see back of book – Contents Vol.II see page v

Nanostructured Materials for Renewable Energies

Sustainable Building Envelopes

Daylighting and Electric Lighting

Indoor Environment Quality

Model Predictive Control

Urban Ecology and Metabolism

CONTENTS VOL. II

Integration of Renewable Energy in the Built Environment

Building Simulation (IBPSA Special Session)

Urban Simulation

Information Technologies and Software

Integration of Renewable Energy in the Built Environment

REPLICABLE RETROFITTING FOR CITYFIED LINERO DEMONSTRATOR IN LUND, SWEDEN

Jeanette Green[1], Thomas Eriksson[2,] Markus Paulsson[3], Victoria Silverberg[4]

1. *IVL Swedish Environmental Research Institute, Box 210 60, 100 31 Stockholm, Sweden*
2. *Kraftringen, Box 25, 221 00 Lund, Sweden*
3. *Miljöstrategiska enheten, Lunds Kommun, Lund Sweden*
4. *Lunds Kommuns Fastighets AB, Box 1675, 221 01, Lund, Sweden*

ABSTRACT

The overall objective of EU funded CITyFiED (repliCable and InnovaTive Future Efficient Districts and cities) project is to develop a replicable, systemic and integrated strategy to adapt European cities and urban ecosystems into the smart city of the future, focusing on reducing the energy demand and GHG emissions and increasing the use of renewable energy sources by developing and implementing innovative technologies and methodologies for building renovation, smart grid and district heating networks and their interfaces with ICTs and Mobility. One of the most important goals of this project is the development of a deep retrofitting of the buildings and innovative district heating solutions in three large scale demonstrations at Laguna-Valladolid (Spain), Soma (Turkey) and Lund (Sweden) in order to achieve powerful models suitable for replication across Europe.

This paper presents the wide intervention that will be carried out in the Linero district (Lund), which aims to reduce drastically the energy consumption and CO^2 emissions by means of passive and active measures on building and district scale. Energy conservation measures on building level will be based mainly on the retrofitting of the façade, changing of windows and heat recovery from ventilation. The interventions on district scale involve the implementation of advanced control and distribution systems, such as a smart grid for electricity and smart distribution of district heating. Finally, the tenants' energy use and the environmental impact are analyzed by means of real time visualization of energy consumption. The overall impact will be further enhanced by the integration of renewable energy from multiple production units to the large scale district heating network that heats the buildings in Linero. This includes solar energy, wind energy, biomass, geothermal heat as well as residual heat from industries for example the new research facilities in Lund, European Spallation Source (ESS) and Max IV-laboratory)

The paper also presents a model that has been developed in the CITyFiED project in order to evaluate the replication potential of the CITyFiED measures that will be deployed in 11 European cities. The model consists of three parts, energy simulation, semi-strucutred interviews for the identification of non-technological barriers and suggestion of new business models. The purpose of the model is to provide innovative, affordable solutions that are effective to address the current technical, financial, social and organizational challenges that exist in respective city.

Key words: retrofitting, district heating, smart grid, renewables, visualisation, replication

INTRODUCTION

The overall objective of EU funded CITyFiED (repliCable and InnovaTive Future Efficient Districts and cities) project is to develop a replicable, systemic and integrated strategy to adapt European cities and urban ecosystems into the smart city of the future, focusing on reducing the energy demand and GHG emissions and increasing the use of renewable energy sources by developing and implementing innovative technologies and methodologies for building renovation, smart grid and district heating networks and their interfaces with ICTs and Mobility. One of the most important goals of this project is the development of a deep retrofitting of the buildings and innovative district heating solutions in three large scale demonstrations at Laguna-Valladolid (Spain), Soma (Turkey) and Lund (Sweden) in order to achieve powerful models suitable for replication across Europe.

LINERO, A SWEDISH HOUSING DISTRICT IN NEED OF RETROFITTING

Lund is a medium-sized university city (115.000 inhabitants) with a research-intensive industry. The town dates back a thousand years, but the number of inhabitants has grown largely during the last century and a great stock of buildings from the 1960s and 1970s now needs retrofitting. Almost 90% of the heat demand is supplied by the district heating network which has a large share of renewables.

The district of Linero is found in the eastern part of Lund. Over the next few years the district is going to undergo major changes. Lunds kommunala fastighetsbolag, LKF, is currently constructing six new tower blocks with 24 flats in each. At the same time the square in the centre of Linero is being refurbished, with new shops and offices, a supermarket and two new tower blocks with 94 flats. The final phase of the district refurbishment of Linero is the renovation of the Eddan and Havamal properties. The area consists of 28 three storey building with an area 71 258 m^2 $A_{temp.}$. Today there are approximately 2,000 tenants in the area, with 681 flats owned and managed by LKF. The road Vikingavägen divides this residential area into two by a road, Havamal in the north and Eddan in the south. Of the 28 buildings in the area only 16, with an area of 40 400m^2 A_{temp}, are included in the CITyFiED project. This includes the urban block Eddan and two buildings in the urban block Havamal [1].

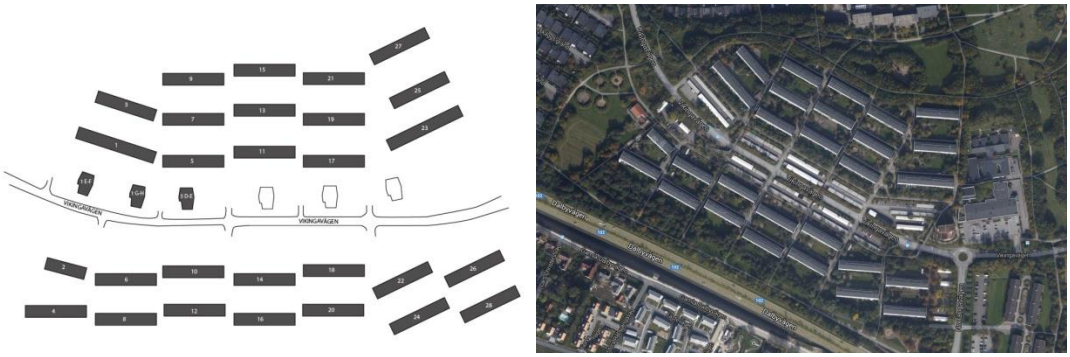

Figure 1. The road Vikingavägen divides Linero into two; Havamal and Eddan.

All buildings in the area are almost identical in appearance and design. They are all three-story buildings with a basement with a consistent orientation within the residential area. The buildings and the whole residential area is characterized by concrete façades combined with metal components.

In the Linero districts a connection from the main district heating grid is feeding two substations which in their turn are feeding the 28 buildings through a culvert network. This district heating pipe is owned by Kraftringen AB and its media is at a high temperature and pressure, approximately 95°C and 16 bar (Primary line). In each substation there is one heat exchanger for heating water and one heat exchanger for hot tap water. The district heating substation contains main pumps for heating water and hot tap water circulation. The pipe systems within the buildings are owned by LKF. The culvert network has pipes for supply and return heating water, hot tap water, hot tap water circulation and cold tap water. Inside the buildings the culvert pipes are suspended in the basement ceilings. Between the buildings they are buried underground. Auxiliary pumps for heating water and hot tap water circulation are installed at some locations due to the long pipe runs. The culvert network is from the 1970's when the area was built and is a relatively poorly insulated pipe system. The total length of the culvert network is approximately 800 m. The long culverts lead to external energy losses.

Energy simulation of heat losses in the district [1] shows that the culvert network corresponds to 13% of the total heat loss of the district. The simulations also indicates that major losses are ventilation and the building envelope; Figure 2. Airtightness tests have however indicated that the building envelope is however largely of such a high standard as to be comparable with the standards for new buildings. Consequently, the renovations will be targeted at the elements in the building envelope that can be given an improved U-value. Early investigation has also reviled that the ventilation flow in the buildings does not work as it should and does not comply with Swedish building regulations or LKF's ventilation policy.

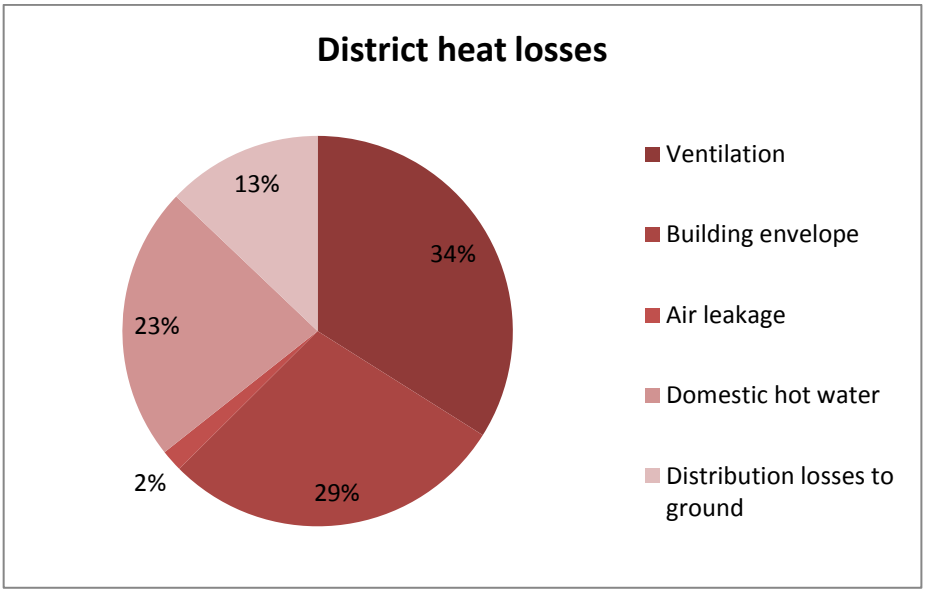

Figure 2. Distribution of heat losses in the district

GOING FOR LOWER CO2-EMISSIONS, INCREASED SHARE OF RENEWABLES AND SMART GRID INTERVENTIONS

The final retrofitting strategy [1] included in CITyFiED is in line with the Swedish Building Regulation incentives to reduce bought energy consumption exceeding the goal of 31% for energy efficiency measures (Table 1) and reaching a share of 87% for renewable energy sources for the district included in the CITyFiED project. It also meets the demand for ventilation according to Swedish regulation. It is in line with the affordability demands for the

tenants and presents an overall decreased environmental impact in regard to CO_2 and Primary energy (Table 1).

		Energy consumption [kWh/(m² year)]	Primary energy consumption [kWh/(m² year)]	Greenhouse gas emissions [g/(m² year)]
Current situation	District heating	127	80	10,457
	Electricity[1]	31	65	4,960
After renovation	District heating	68	38	4,566
	Electricity	38	77	5,942
Total reduction		**52**	**31**	**4,909**
Savings		**38%**	**21%**	**32%**

Table 1 Results from the district energy simulation

The retrofitting strategy includes following measures:

- Replacement of the one existing district heating substations to 6 new custom and prefabricated efficient modulars.
- Replacing windows on the south side floor 1 and 2
- Replacing balcony doors on the south side floor 1 and 2
- Additional wall insulation on the southern long side of floor 1 and 2
- Additional roof insulation
- Reduction of the interior temperature
- Replacement of radiator thermostat
- Glazing of balconies
- Change stairwell lighting to LED and install presence control
- Change the lightning in the cellar to LED and install presence control
- Change the lighting at the entrance and gable ends to LED
- New culvert solution
- Upgrading of the ventilation system
- Exhaust air heat pump
- Individual metering and billing
- Replace bathtubs with shower

The overall impact will be further enhanced by the integration of renewable energy from multiple production units to the large scale district heating network that heats the buildings in Linero. This includes solar energy, wind energy; biomass, geothermal heat as well as residual heat from industries for example the new research facilities in Lund, European Spallation Source (ESS) and Max IV-laboratory increasing the share of renewables from 74, 8% to 94.1% of the district heating.

The smart grid interventions in the district include new electricity generation from photovoltaics and new electricity use by an EV charger. At least 70 kWp roof mounted photovoltaics will be installed in the project, divided on at least two of the buildings. The installation of photovoltaics will be connected to the electricity system of the building and the electricity production will primarily feed the building and reduce the need of bought electricity. In cases when the production exceeds the consumption of the building the excess electricity is fed to the grid and sold to the chosen electricity trading company. The display

[1] Includes the total electricity in the district, lighting and domestic electricity

showing the solar production data will be combined with the visualisation tools for showing the energy use in the buildings and in the district. Combining display of energy use and local energy production is intended to increase the awareness of the energy flow in the district for the people living in the area.

An EV charger will be installed in the demo area in order to give the tenants easy access to quick and well-functioning charging infrastructure that fits their needs, both now and in the future. The charger will be configured in order to host one car for car-sharing and one other private car at the same time. In order to facilitate well-functioning car-sharing-functionality, the charger will be configured to enable full charging within one hour. The EV charger will be connected to the 400 V grid and the location will be easily accessed by the tenants.

Visualization will be implemented on three level; district, building and home level. Home level will focus on household electricity use, since that is the parameter that the tenant has the ability and the incitement to influence on the Swedish demo site. A solution giving the tenant real-time visualization of the household electricity consumption will be implemented. In the application for energy visualisation of the apartment, possibilities for controlling loads are integrated. The solution will be made available to the tenant through mobile devices such as tablets and smart phones. Building level will include electricity, heating, and local solar PV production. The solution for visualization on building will instead be made available to the tenant through stationary screens in the buildings. On district level aggregated use of energy will be visualized in order to evaluate the energy use of the demo site as a whole. The energy use of the buildings in the demo site area will be intercomparable. On district level aggregated use of energy will be visualized in order to evaluate the energy use of the demo site as a whole. District level visualization will be made available to the tenants on the most suitable common areas synced with the renovation process.

Other interventions concerns monitoring of energy flow, power quality and fault analysis in the demo site. The purpose of the enhanced monitoring is to increase the energy awareness of the people living in the area in order to reduce the electricity consumption and for the distribution system operator to get a better control of the electricity quality in the grid in order to enable a high penetration of further local electrical generation in the area. Noise on the power lines, originated from for example electronic devices connected to the power grid, can sometimes interfere the communication. With an increase in photovoltaics and other local electricity production sources connected to the grid by power electronic converters these problems are assumed to increase. In order to handle this communication problem the new generation power line communication, G3-PLC, will be tested in CITyFiED.

REPLICATING THE RESULTS IN EUROPE

In order to investigate the potential for replication of the CITyFiED results demonstrated in the three demo sites of CITyFIED in other cities a framework for a feasibility model for building technology and retrofitting has been developed in the CITyFIED project [2]. The feasibility model is based on known concepts for modelling energy demand in buildings together with and energy system modelling approaches. As a complement to the quantitative model, a methodology for semi structured interviews has also been developed. The methodology will be used to find out what non-technological aspects such as financial, organizational, cultural, juridical and social can either boost the replication potential or hinder it. In addition to this Business model should be defined according with city council criteria and taking into account stakeholders at district level.

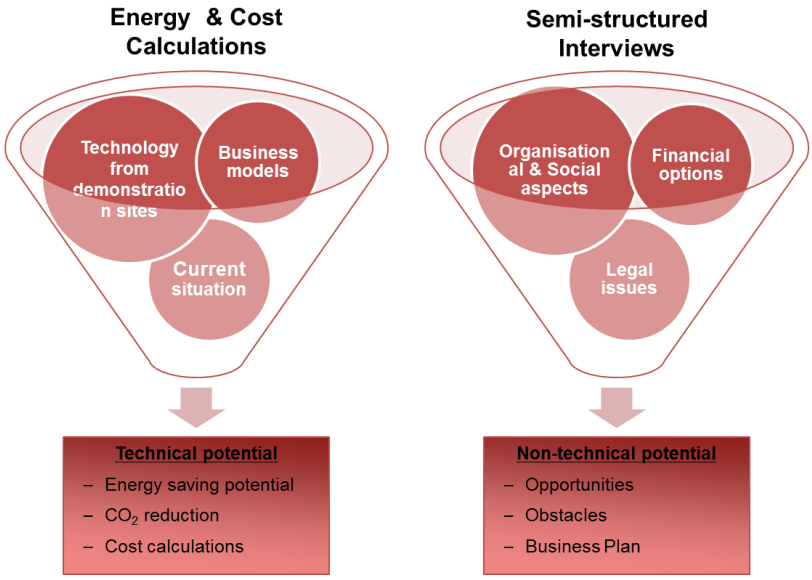

Figure 3. Replication model of CITyFIED

As a first step of deploying this process a refining process of several cities was performed including a selection of appropriate city districts for detailed analysis according to e.g. energy systems, building typology, climate, how well the city is represented by the area where it is located in the district, financial options, social aspects, etc. As a result of this a CITyFiED city cluster was established including 11 districts in 11 European cities. The next step in the CITyFiED project is to deploy the replication model in order to demonstrate the replication potential of the CITyFiED measures implemented in the three demo sites.

CONCLUSIONS

Despite many existing initiatives on buildings retrofitting, the systemic renovation strategies at district or city level are still not generalized enough in Europe or in Sweden. It is clear that some general barriers are holding the massive deployment of this kind of interventions back. Even if the technology is available there is a need for more affordable solutions and new business models. The Demo site in Lund, along with the demo sites in Soma and Valladolid, will evaluate several interventions for smart city retrofitting, this along with a strong effort to spread the benefits of the integrated refurbishment in other European cities will provide and promote innovative and affordable solutions that are effective to address the current technical, financial, social and organizational challenges in many European cities.

REFERENSER

1. Green, J. Faraguna, C (IVL). Eriksson, T. Skarrie, H (Kraftringen), Silverberg, V. (LKF): CITyFiED D 4.6 Implementation plan for the Swedish Demonstrator. 2015
2. Green, J. Adolfsson, I. Faraguna, C. Karlsson, A. Lätt ,A. Sandö, P. Jarnehammar, A (IVL), Birkedal, L (LUND), Vasallo, A. Martin, A (CARTIF): CITyFiED D1.4 Model for evaluation of replication potential. Intermediate version. 2015

BALANCING OPERATIONAL AND EMBODIED EMISSIONS FOR THE ENERGY CONCEPT OF AN EXPERIMENTAL RESEARCH AND LIVING UNIT

G. Lydon; A. Willmann; J. Hofer; Z. Nagy; A. Schlüter.

Chair of Architecture and Building Systems, Institute of Technology in Architecture, ETH Zurich, John von Neumann Weg 9, 8093, Switzerland.

ABSTRACT

In a European context, energy standards in the built environment have made a valuable contribution to the sustainability of the industry over the past twenty years. The current cycle focuses predominantly on the thermal properties of the building envelope. As space heating and cooling with domestic water heating currently accounts for 60% of global energy consumption in buildings, this aspect will remain a key mechanism for building energy improvements. When considering 2050 energy targets, significant energy efficiency improvements will be required for new and renovated buildings in the next 5 – 10 years.

This research investigates the constraints placed on modern architecture by the influence of building energy regulation in the context of the HiLo module at NEST. Current building regulations are encouraging a convergence towards heavily insulated enclosures with minimised glazing, with the key design parameter being geometrical compactness. This assumes that the operational energy costs outweigh the costs of the embodied energy in the building materials and the construction process. As the building energy codes become increasingly severe for building designers, it is essential that innovation is central to architecture and regulatory assessment procedures become more sophisticated.

The goal of the HiLo module is to investigate if sustainable design related the total building lifecycle (BLC), rather than solely determined by an operational energy saving approach, will enhance architecturally and structurally challenging projects. This paper highlights the importance of the adaption of an early stage integrated design approach. In addition, it will demonstrate that considering the BLC will lead to more advanced sustainability focused outcomes for the built environment, without placing overbearing restrictions on architecture.

Keywords: Embodied Energy, Buildings, Integrated Design, Building Lifecycle.

1. INTRODUCTION

NEST (Next Evolution in Sustainable Building Technologies) is a district scale project by Empa and Eawag in partnership with the ETH Domain, to demonstrate innovation in the built environment [1]. NEST provides a basic infrastructure and access to an advanced ground source geothermal system, in the form of the backbone which, can accept up to fifteen modular buildings. This creates a unique setting for academic groups and innovative companies to implement research under real-world conditions. NEST serves as an interactive demonstration and research facility for the design of sustainable buildings and districts.

As one of the first NEST modules, HiLo utilises innovative design elements, specifications, materials, construction schemes and control systems which are informed by the principles of sustainable development [2]. The key objective of HiLo is to demonstrate that an integrated design process, which considers the lowering of both embodied and operational energy allows for sustainable design solutions without severe architectural compromises. Further, HiLo exhibits innovation in the domains of building energy efficiency and structural design while fostering a unique architectural expression.

Figure 1: Rendering of the exterior of the HiLo module.

HiLo is planned as an energy-plus module in operation phase and will be equipped with sensors providing a stream of thermal, lighting, energy consumption and external environment data. HiLo is currently at an advanced design phase, and is due to commence construction in early 2016.

The total building lifecycle energy consists of operational and embodied energy. Embodied energy considers the contribution during the construction, demolition and disposal phases (direct), which includes the production of materials (indirect). The operational energy is related to the use of the building, including heating, cooling, lighting and equipment [3].

Embodied energy has traditionally been neglected from the energy analysis of buildings. However, as recent improvements in the energy performance of buildings have been focused on operational energy (i.e. insulation, heat recovery ventilation), the proportion of embodied energy relative to operational energy has become more significant.

This paper introduces and discusses the energy concept of HiLo, in particular, the influence of the design of the thin concrete shell roof, as it offers the clearest example of balancing the operational performance with the embodied energy.

2. BACKGROUND

HiLo is headed jointly by the Chair of Architecture and Building Systems (A/S) and the BLOCK Research Group (BRG) at the Institute of Technology in Architecture at ETH Zurich. The academic leaders are supported by Supermanoeuvre Architects of Sydney, Australia and ZJA Zwarts & Jansma Architects of Amsterdam, Netherlands. This core team has developed the concept and building permit design phases for the project by respecting the dual brief of delivering a building, which confirms to current Swiss construction regulations and a project which will provide five years of operational phase research.

HiLo exhibits four core innovations:

- Integrated, thin shell roof [3,4]
- Funicular floor system [5]
- Adaptive solar facade [6]
- Occupant centred control [7].

The HiLo innovations are led by domain experts with involvement from associated disciplines. As buildings have a relatively long lifecycle, an integrated approach is seen a promising method of moving the construction industry towards 2050 energy targets [8].

Integrated design provides a platform to examine interdisciplinary early stage energy concepts and allows the full potential of energy savings to be realised over the building lifecycle (BLC). A simple example of the integrated approach is the adaption of a single CAD software system by the structural, energy and architecture core team members. The CAD platform is linked directly to the advanced analysis software used by each domain. This provided a method for the easy exchange of concepts and results, despite the complexity of the geometry. This integrated approach is used to develop outcomes, which are relevant in the context of the built environment and not limited to a laboratory setting.

3. INTEGRATED, THIN SHELL ROOF

The thin shell roof has been numerically optimised to deliver a highly efficient structural element [4]. This efficiency is translated into an architecturally elegant form through the use of the touchdown points (the connection locations from the roof to the main structure, see Figures 1 and 4). The improvement in structural performance reduces the overall volume of concrete by up to two-thirds compared to a typical concrete roof section (Figure 3). The shell roof is cast by a reusable and lightweight cable-net and fabric formwork system, which is expected to have less environmental impact compared to a standard method.

In order to visually highlight the structural efficiency of the shell roof, a key part of the design brief is to provide a highly glazed facade (Figure 1). The integrated approach considering all aspects in an early stage, allowed for the provision of the large glazed facade, while complying with the Swiss regulations.

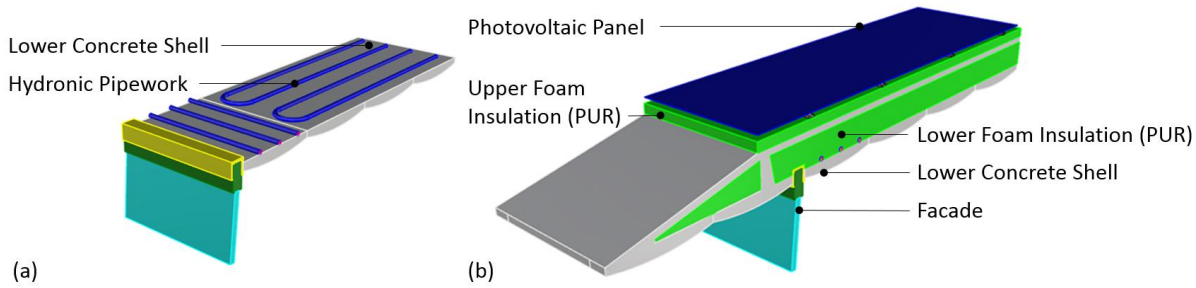

Figure 2: Integrated, thin composite shell roof, (a) Cutaway View (b) Isometric View.

The roof shell integrates multiple functions besides the structure. First, it is a thermally active element due to the integrated hydronic pipework (Figure 2a). This provides heating and cooling through the thin concrete radiant panel at ceiling level. Second, photovoltaic panels are integrated with the concrete shell (Figure 2b), on surfaces with complex geometry to utilise non-typical building envelopes as a resource for local renewable energy harvesting during the BLC.

Due to the shape and the materials, the roof offers further benefits, e.g. thermal mass. Thermal mass refers to the use of the internal materials of the building to absorb internal or solar heat gains, this process dampens internal air temperature fluctuations. As the exposed internal concrete shell constitutes a significant thermal mass resource, which is ideally distributed at ceiling level over the entire main space, it is engaged with a mixed ventilation strategy in the management of solar gains during the summer period. The natural component of the ventilation system is aided by the roof shape, which was optimised for a range of parameters during the current design phase. For example, the combination of a head height parameter and

a glazing reduction parameter, resulted in a roof shape, which funnels air by buoyancy or cross ventilation to five boundary points at which facade openings are applied.

In terms of energy compliance, the negative features, such as the highly glazed facade are captured by the standards. However, the main beneficial features of the roof are not fully accounted for in the standards, when compared to a typical method of roof construction (see Figures 3a and 3b). These benefits include a reduction of the carbon emissions in the roof shell (see Figure 3c) and the application of the PV panels onto building elements with complex geometry. This is a limitation of the current regulations, which does not clearly encourage innovation and may need to be remedied if buildings are to be correctly assessed for energy performance over the BLC.

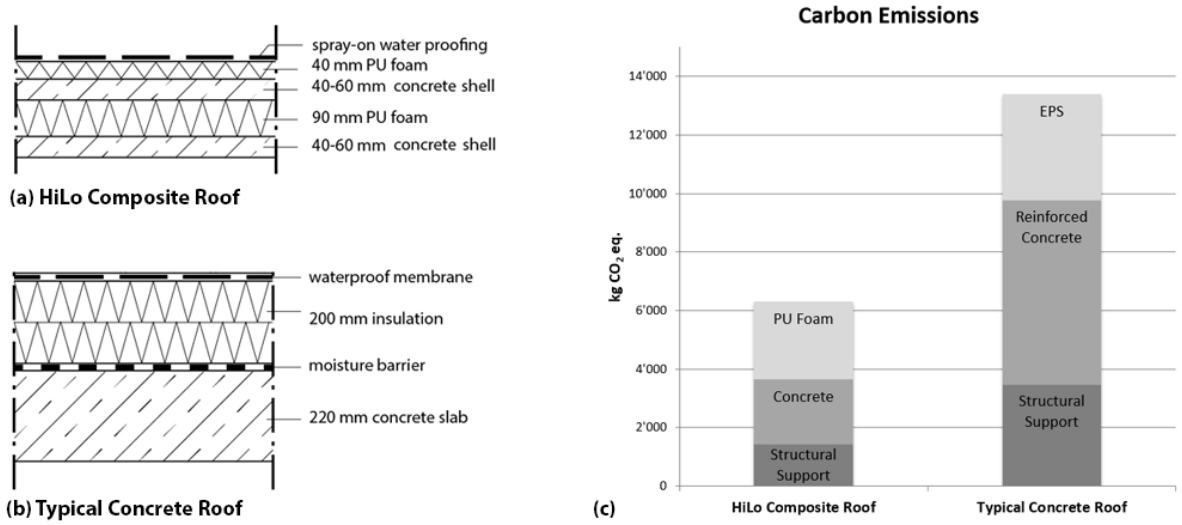

Figure 3: Carbon Emissions of the structural components of the HiLo Composite Roof and a Typical Concrete Roof.

The design of the integrated roof element has undergone many design iterations, driven by structural, thermal and aesthetic constraints. In terms of thermal performance, the key transition was the change from a single shell to the current composite shell. The energy related design constraints, which influenced this decision, are discussed in the next section.

4. ENERGY DESIGN OF THE SHELL ROOF

One of the main design strategies of the HiLo module is the extraction of the maximum potential from the building elements while considering the embodied energy contribution to the building lifecycle. The embodied energy analysis advises the design process, but this factor does not govern the final decisions. A balanced approach is employed by not just examining the material performance by volume, but also assessing the contribution of the material to a range of tasks. As a demonstration, this section discusses the integrated design process on the example of the roof shell.

As the roof shell is important in terms of the project research and forms a key component of the innovation strategy, it is preferred that the lower surface of the shell is not directly insulated (as shown in Figure 4). Therefore, at the roof/facade interface, the lower edge surface of the shell is exposed internally and externally. The concrete shell is an active heating element and the total external heat transfer coefficient can be up to 25 W/m^2 K. It was likely that relatively high thermal losses would occur at this location, as the roof was a single shell and was insulated with a roll applied aerogel insulation at an early design stage.

Figure 4: Rendering of the Interior of the HiLo Module.

A numerical study of the single shell roof showed that the edge losses were in excess of the amount recommend in SIA 380/1. Due to the concrete element thickness and the related structural issues, traditional methods such as thermal breaks or concrete mixes with insulation pearls (expended polystyrene) could not be readily employed to insulate the concrete shell. This is especially true in regions with large overhangs.

In order to resolve the thermal loss issue at the roof/facade interface, the structural engineers (BRG) proposed a composite roof shell, which provided thermally separate internal and external shells. As the design evolved, it was noted, based on numerical analysis of the shell, that temperature differences of the external and internal concrete shell volumes would cause stress at the composite interface layers. In order to counteract these forces, it would be typical to add steel shear connections between the shells. This approach would further complicate the construction of the formwork system and the process of placing the concrete. From the energy perspective, the improvements in the thermal performance of the roof/facade interface would be significantly reduced by the shear connection thermal losses.

The solution involved replacing the roll based aerogel insulation material with a spray-on polyurethane rigid foam (PUR), which can transfer stresses between the upper and the lower shells. As PUR is comparable to aerogel insulation in terms of embodied energy [9], the main concern related to the additional embodied energy related to an on-site spray-on application and at disposal phase. In addition, strong safety precautions must be employed during application due to respiratory hazards.

A CFD study of the single shell and the composite shell showed that the latter was superior in terms of thermal edge losses. In addition to the embodied energy contribution, the structural performance, simplification of the construction and the reduction the thermal losses (of the shell edge and the exclusion of the shear connection) during the operation phase were used to reach the final decision. These main three benefits outweighed the increase in embodied energy associated the composite shell with PUR insulation. Also, the preliminary embodied energy calculations show that the current composite shell roof design is superior to a typical

concrete roof section in terms of carbon emissions [11]. Figure 3 shows a comparison of the structural and insulation elements of the HiLo composite roof and a typical concrete roof.

5. CONCLUSION

The concept and building permit design phases of HiLo have shown that as building design becomes more sophisticated, the inclusion of an early stage integrated design approach is vital to maximising the energy efficiency potential over the BLC.

In addition, the already advanced Swiss building energy assessment regulations need to evolve to deal with new methods of construction and building materials. While it is difficult to capture every permutation of a building design in the form of a building regulation, further improvements to the standards will help to achieve the ambitious 2050 energy targets. In particular, regulations which encourage designers to optimise the required volumes of building materials while improving element durability, form and performance are needed.

As HiLo develops during the next phases, high resolution numerical analysis will be carried out to quantify results at a research level. The research phase investigation will focus on the simulation of internal comfort parameters. These results will be calibrated over the initial operation phase of the building using an array of sensors. This analysis will be used to assess the quality of the standard design methods used at the concept and building permit phases.

6. ACKNOWLEDGEMENTS

The authors would like to acknowledge the contribution of Diederik Veenendaal of the BLOCK Research Group, Agnes Weilandt of Bollinger and Grohmann GmbH, the NEST team at Empa, the Kanton of Zurich, the Swiss Federal Office of Energy (BFE) and the various consultants involved in the project. Funding from Climate-KIC through the building accelerator (BTA) program is gratefully acknowledged.

7. REFERENCES

1. Empa: NEST project website, http://nest.empa.ch/, 2015.
2. ETH Zurich: HiLo project website, http://hilo.arch.ethz.ch/, 2015.
3. Pargana, N. et al.: Comparative environmental life cycle assessment of thermal insulation materials of buildings. Energy and Buildings, 82, pp.466–481, 2014.
4. Veenendaal, D. & Block, P.: Design process for prototype concrete shells using a hybrid cable-net and fabric formwork. Engineering Structures, 75(2014), pp.39–50, 2014.
5. López, D. et al.: Prototype of an ultra-thin, concrete vaulted floor system. Proceedings of the IASS-SLTE 2014 Symposium, 2014.
6. Rossi, D. et al.: Adaptive Distributed Robotics for Environmental Performance, Occupant Comfort and Architectural Expression. IJAC, 10(03), pp.341–360, 2011.
7. Nagy, Z. et al.: Occupant Centered Lighting Control for Comfort and Energy Efficient Building Operation. Energy and Buildings, 94, pp.100–108, 2015.
8. Sorrell, S.: Making the link: climate policy and the reform of the UK construction industry. Energy Policy, 31(9), pp.865–878, 2003.
9. Cuce, E. et al.: Toward aerogel based thermal superinsulation in buildings: A comprehensive review. Renewable & Sustainable Energy Reviews, 34, pp.273–299, 2014.
10. Swiss Society of Engineers and Architects (SIA): Swiss Standard SIA 2040: Effizienzpfad Energie (Path to Energy Efficiency), SIA, Zurich, 2011.

ELECTRIC VEHICLE BATTERIES IN ENERGY STORAGE SYSTEMS: AN ECONOMIC ANALISYS FOR SWISS RESIDENTIALS

C. Menn; A. Geissler

Institut Energie am Bau, St. Jakob-Strasse 84, 4132 Muttenz, Switzerland

ABSTRACT

Battery energy storage (BES) systems for residential buildings can contribute to power grid stability. The demand for decentralized storage capacity in Switzerland is expected to rise due to political decisions that facilitate renewable energies with power fluctuations such as photovoltaics (PV). Using lithium based BES to meet this demand could have a significant environmental impact as a result of energy intensive production-processes. Furthermore, currently available conventional BES (C-BES) systems are not economically viable. Within this context, a second use of electric vehicle batteries for 2^{nd}-life-BES (2^{nd}-BES) can be an environmentally sound alternative that facilitates grid integration of residential PV-systems.

A model describing the economic viability of 2^{nd}-BES based on the Net Present Value (NPV) method is presented. On the basis of one example building each, results are given for single-family-houses (SFH) and multi-family-houses (MFH), focusing particularly on the market situation found in Switzerland.

Results show a cost advantage for 2^{nd}-BES in MFH compared to C-BES systems if a Cycle Life (CL) of 800 and more is available. In SFH, a 2^{nd}-BES shows only a slightly better economic performance than a C-BES system if a CL of 4800 and more can be guaranteed. Notwithstanding the relatively low Levelized Cost of Electricity (LCOE), the NPV for both 2^{nd}-BES and C-BES in both SFH and MFH is negative. Reasons for this are high initial system costs and an electricity tariff scheme with low incentives for consumers to store electricity.

In this paper, only the current tariff structure in Switzerland is considered. However, alternative tariff schemes, e.g. real time pricing for residential consumers, have become reality in some countries. The impact of such tariff schemes on the economic performance of 2^{nd}-BES is left to future research.

Keywords: Battery 2^{nd}-use, residential energy storage, PV, cycle life, net present value

1. INTRODUCTION

Recent cost calculations on nuclear power plants [1,2] and governmental commitment to mitigate climate change are in favour of renewable energies. Among renewable energies building integrated photovoltaics (PV) are expected to play a major role in the process of energy source transition due to a high technical potential [3] and public acceptance [4,5]. However, the grid integration of PV generated electricity and its impact on power quality is one relevant technical barrier to PV deployment [6]. In the electrical grid, power supply and demand has to match at any given time. A high fraction of often volatile PV generated electricity can lead to a disruption of this balance and jeopardize grid stability [7].

Battery energy storage (BES) is one effective measure to overcome problems of frequency fluctuation [8]. For BES in dwellings, lithium based batteries are most suitable due to high efficiencies and long Cycle Life (CL, defined as the number of charge/discharge cycles available prior to the end of useful life) [9]. Current studies show that conventional lithium based BES (C-BES) are not viable economically in the near future [10,11]. Besides weak economic performance, C-BES cause significant environmental impact due to energy intensive production-processes [12,13]. Within this context, a reuse of electric vehicle batteries, after their automotive life, in residential 2^{nd}-life-BES (2^{nd}-BES) can be an environmentally sound alternative. However, not much attention has been given to the economic viability of 2^{nd}-BES.

In this paper a model to describe the economic viability of 2^{nd}-BES and the combined PV-2^{nd}-BES system based on the Net Present Value (NPV) method is proposed. The model is based on the prosu -mers' perspective, considering Swiss market conditions in 2015. An optimal size for both the PV installation and the 2^{nd}-BES for economic viability is derived. Furthermore, the minimum necessary CL of 2^{nd}-BES is quantified. Finally, the key factors for profitability of 2^{nd}-BES are identified.

2. SYSTEM DESCRIPTION

The economic viability of 2nd-BES is calculated for Single-Family-Houses (SFH) and Multi-Family-Houses (MFH) based on one example building each. The building technology and heat demand correspond to a typical energy efficient building in Switzerland. For both building types, the Swiss average household of 3 people is assumed [14]. The example MFH consists of 7 housing units (Swiss average: 5.4 [14]). Both the SFH and MFH have a mechanical ventilation system with heat recovery. The heat generation systems for the SFH and MFH are an air source heat pumps (ASHP) and ground source heat pumps (GSHP), respectively. The buildings are located in the city of Olten.

Both C-BES and 2nd-BES are embedded in an alternating current (AC)-coupling system. The BES is charged if generated PV power exceeds the demand and storage capacity is available. If the BES is fully charged, excess electricity is fed into the power grid. The BES is discharged if the demand exceeds PV output and capacity is available. BES charge/discharge from/into the grid is not possible. This system typology is quite typical for residential buildings [11,15–17]. Both BES topologies are identical but differ in technological and economic input parameters. The PV-system is south-oriented with a 30° tilt angle and consists of polycrystalline cells. Power output is calculated by the simulation software Polysun® [18].

3. INPUT PARAMETERS

3.1. Technological parameters

The PV system size can be from one to 30 kW_p. This range covers a majority of PV installations in Switzerland [19]. BES usable capacities can be from one to 40 kWh.

C-BES typically has the maximum depth-of-discharge (DOD max.) set to 80 % of the nominal capacity [20–22]. Charge/discharge efficiency is 90 % [20–22]. Furthermore, a 0.1 % self-discharge per hour is included in the calculation [23]. CL of C-BES is assumed to be sufficient to avoid battery replacement during the 25 years' time frame investigated [24]. Neither casing or cables nor AC/DC inverter are replaced during that period.

2nd-BES are considered to have a 60 % DOD max. due to battery degradation during automotive life. A 0.3 % self-discharge per day is considered [23]. It is assumed that at the end of each year 1 % of the installed nominal capacity needs to be replaced due to battery degradation. For 2nd-BES, battery life in terms of CL available is varied (200-6400). Charge/discharge efficiency and useful life of casing and inverter correspond to the C-BES.

The electricity load for the heat pump and auxiliary energy is calculated with Polysun® [18] and is 3'250 kWh/a for the SFH and 11'540 kWh/a for the MFH, respectively. The electricity load for ventilation is 360 kWh/a for the SFH resp. 3'030 for the MFH [25]. The electricity load for domestic equipment is 3'330 for the SFH resp. 20'300 kWh/a for the MFH [26].

3.2. Economic parameters

C-BES system costs consist of 1'040 CHF per kWh nominal capacity and 10'240 CHF base costs for casing, cables and AC/DC inverter (initial costs). A 2nd-BES induces initial costs similar to a C-BES. However, costs per kWh nominal capacity of 140 CHF [27] are significantly below those for a C-BES system. A yearly decrease of 3 % is considered for 2nd-BES nominal capacity costs. Battery replacement is assumed to cost 100 CHF per occurrence. PV-system costs are 1'870 CHF/kW_p [16]. In addition, expenses for installation, cabling and maintenance are included with 9.5 % of the total PV-system costs [16].

The current Swiss subsidy-scheme for PV-systems [28] is taken into account by the model. This consists of a base contribution of 1'400 CHF issued for every PV system. Additionally, 500 CHF grants are issued per kW_p.

Two different tariffs for electricity drawn from the grid are considered here, a ‘High Tariff’ (HT) and a ‘Low Tariff’ (LT). The HT is valid between 6 a.m. and 9 p.m. during workdays and from 6 a.m. to 12 p.m. on Saturdays. The HT in the first year after installation is 0.23 CHF/kWh and the LT is 0.16 CHF/kWh [29]. After that the tariff development follows the scenario as described below. Feed-in remuneration is assumed to be 0.08 CHF/kWh [29,30].

Two different scenarios in regard to tariff development during the time frame investigated are considered. The scenarios are based on the price trend, estimated within the Swiss Energy Strategy 2050 [31,32]. The scenario "Business As Usual" (BAU) assumes a continuation of current energy policies and results in an electricity price increase of 0.52 % p.a. In the "New Energy Policies" (NEP) scenario, policies towards 1-1.5 tons of carbon emissions p.c. are assumed which imply an electricity price increase of 0.9 % p.a.

An inflation-rate of 0.84 % [33] and a nominal discount-rate of 3 % are considered [34].

4. TECHNO-ECONOMIC MODEL

In Table 1 the most important parameters of the techno-economic model are specified.

Table 1: nomenclature Techno-Economic Model.

Parameter	Description	Value
t	Index for yearly balance $t = 1, \dots, T; T = 8760$	hours
j	Indices for time frame investigated $j = 1, \dots, J; J = 25$	years
E_{Bc}	Nominal capacity of BES	kWh
E_{Bav}	Usable capacity of BES	kWh
$\Delta E_{B,t}$	Nominal BES discharge during the hour t	kWh
η_B	Discharge efficiency	-
$TR_{EG,j}$	Total feed-in payback for year j (PV to grid)	CHF
$TC_{El,j}$	Total electricity costs in year j	CHF
$TC_{PV,j}$	Total costs for PV-system in year j	CHF
$TC_{B,j}$	Total costs for BES in year j	CHF
$E_{PV,j}$	Net electricity amount generated by PV in year j	kWh
r_{real}	Real discount rate	-
SOC_t	State of charge at the end of hour t	-
ρ_{mdod}	Maximum depth of discharge	-
$CL_{use,j}$	Elapsed Cycle Life of BES in year j	-
$\theta_{CL,t}$	Binary variable for Cycle Life in hour t, values [0,1]	-

The NPV of PV-BES represents the sum of discounted cash flows within the time frame investigated minus total initial investments acc. to eqn. (1). A real discount rate is considered in the calculation based on Karathanassis [35].

$$NPV_{PVB,J} = \sum_{j=1}^{J} \frac{TR_{EG,j} + \left(TC_{El,j} \middle| E_{PV,j} = 0\right) - TC_{El,j} - TC_{PV,j} - TC_{B,j}}{(1 + r_{real})^j} - TC_{PV,0} - TC_{B,0} \text{ [CHF]} \quad (1)$$

The internal rate of return (IRR) signifies the discount rate r_{nomIRR} for which the NPV acc. to eqn. (1) equals zero after 25 years. A nominal discount rate is considered for the IRR calculation. The payback period (PBP) is defined by the year in which the sum of cash flows in eqn. (1) exceeds initial investment, given that $r_{real} = 0$.

Levelized costs of electricity (LCOE) represent the sum of discounted BES costs per kWh net discharged electricity over the time frame investigated as defined by eqn. (2.

$$LCOE_{B,J} = \frac{TC_{B,0} + \sum_{j=1}^{J} \frac{TC_{B,j}}{(1 + r_{real})^j}}{\sum_{t=1}^{8760} \left(\Delta E_{B,t} \middle| \Delta E_{B,t} < 0\right) \cdot \eta_B \cdot \mathrm{J} \cdot (-1)} \quad \text{[CHF/kWh]} \quad (2)$$

Usable BES capacity is the actual amount of energy that can be extracted acc. to eqn. (3).

$$E_{Bav} = E_{Bc} \cdot \rho_{mdod} \quad (3)$$

One CL is counted for hour t if SOC reaches 1-DOD-max. acc. to eqn. (4).

$$\theta_{CL,t} = \begin{cases} 1 & \mathrm{SOC}_{t-1} \neq 1 - \rho_{mdod},\ \mathrm{SOC}_t = 1 - \rho_{mdod} \\ 0 & \text{otherwise} \end{cases} \quad (4)$$

$CL_{use,j}$ for year j is calculated as acc. to eqn. (5).

$$CL_{use,j} = \sum_{t=1}^{T} \theta_{CL,t} \quad (5)$$

5. RESULTS

5.1. System size, Quality requirements and Profitability

Optimal system size differs between building types and CL available (Figure 1). A 2nd-BES usable capacity of 1-2 kWh for SFH and 3-7 kWh for MFH are found to be best if 4800 CL or more are available. Optimal PV-size is found to be 3 kW_p for SFH and 11-15 kW_p for MFH.

2nd-BES is in most cases economically advantageous as compared to C-BES for both building types investigated (Figure 1). In SFH, LCOE of 2nd-BES are generally below C-BES if usable capacity exceeds 1 kWh. However, cost advantages remain relatively small notwithstanding increasing CL available. In MFH, 2nd-BES systems are more favourable than C-BES if a CL of 800 is exceeded. This cost advantage increases with an increase of available CL.

Profitability differs between building types and system components. For SFH, a 3 kW_p PV reduces the yearly energy bill by 452 CHF (-33 %) and a NPV of 3'200 CHF results over 25 years (NEP-scenario, PBP: 9 years, IRR: 12 %). By including a 2 kWh 2nd-BES, more energy from the power grid is substituted and an additional 86 CHF p.a. can be economized. However, the resulting higher self-consumption rate (57 % to 71 %) decreases revenues from excess generated electricity by 40 CHF thus BES contribution is 46 CHF p.a. These revenues do not cover 2nd-BES (CL 6400) system costs over the time frame investigated (2nd-BES NPV: -11'600 CHF) and consequently, a NPV of -8'400 CHF results for the PV-2nd-BES. As shown in Figure 1, no profitable PV-2nd-BES system combination can be found for SFH.

In contrast to SFH, a PV-2nd-BES for MFH is profitable if CL exceeds 1600 cycles in the scenario BAU and already at 200 cycles in the NEP scenario (Figure 1). E.g. a 15 kW_p PV reduces the energy bill by 2'405 CHF p.a. (-34 %) and results in a NPV of 13'300 CHF after 25 years (NEP-scenario, PBP: 11 years, IRR: 9 %). By adding a 7 kWh 2nd-BES (6400 CL), additional gains of 164 CHF p.a. occur. This revenue does not cover total 2nd-BES costs over the time frame investigated (NPV: -11'100 CHF). Nonetheless, in combination with the PV system a NPV of 2'200 CHF results after 25 years (NEP-scenario, PBP: 16 years, IRR: 4 %).

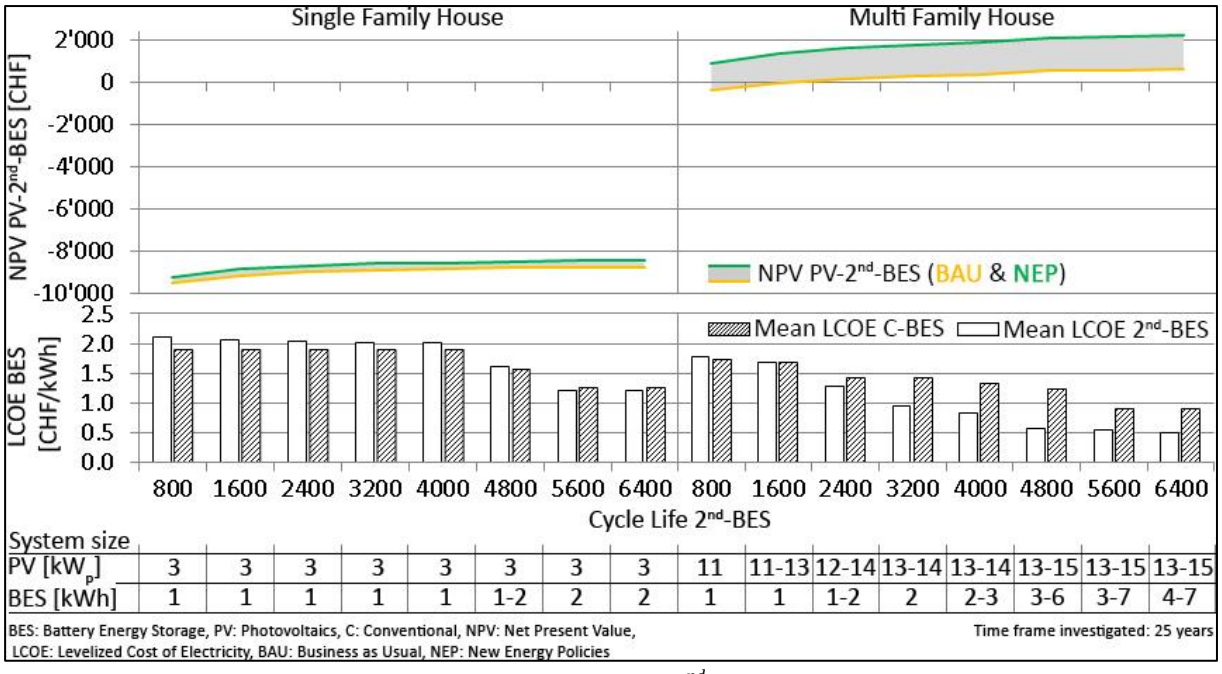

Figure 1: NPV and mean LCOE for SFH- and MFH-PV-2nd-BES with optimal system size.

5.2. Sensitivity analysis

Based on a ±33 % value variation of a number of parameters a sensitivity analysis of the NPV of 2nd-BES is conducted. Results show that the parameters "initial system cost" and "HT price" can be seen to have the largest impact (Figure 2). A 33 % decrease of initial 2nd-BES-system costs unsurprisingly improves the NPV by a large margin (31 %). The 33 % increase of HT electricity price increases the NPV by 13 %. This strong dependency of BES economic performance and electricity market prices can also be found in previous research on PV-BES systems [10,11]. Furthermore, a relatively strong decrease in NPV is found (-10 %) if DOD max. is lowered further to 40 %. For system optimization interdependencies of parameters need to be considered, e.g. a DOD max. reduction can increase expected CL of 2nd-BES.

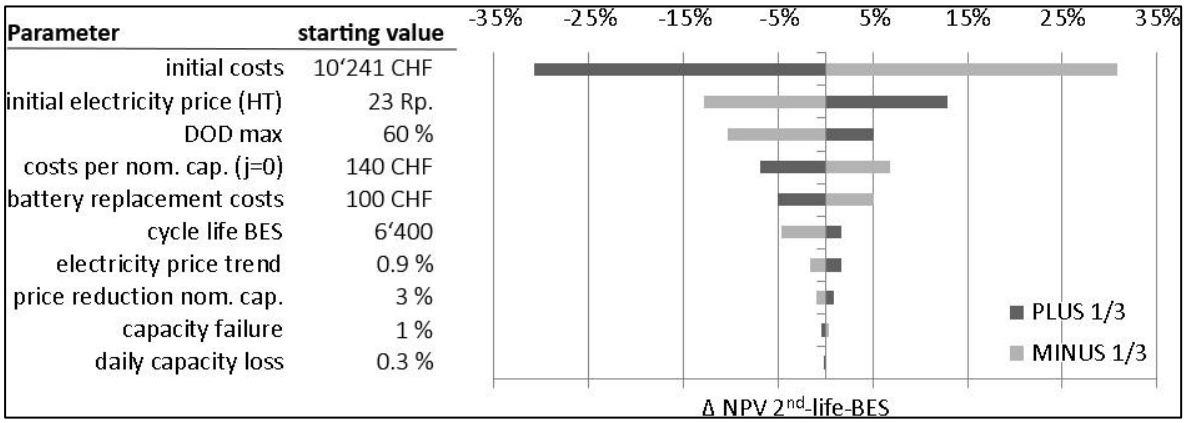

Figure 2: Sensitivity analysis for MFH, scenario NEP, 15 kW_p PV- 7 kWh 2nd-BES (6400 CL).

6. CONCLUSIONS

PV systems in combination with 2nd-BES (PV-2nd-BES) can be dimensioned for MFH such that they are economically viable. For SFH, no economically viable PV-2nd-BES system can be found under current market boundary conditions. This is mainly due to the optimal system size of PV-2nd-BES, which is larger for MFH than for SFH.

Under current market boundary conditions, no profitable 2nd-BES system dimensions for either SFH or MFH can be found. Nonetheless, mean LCOE in MFH 2nd-BES systems is favourable as compared to C-BES mean LCOE, provided that more than 800 cycles are available per battery in the 2nd-BES system. SFH 2nd-BES are more favourable than C-BES systems if CL > 4800 can be guaranteed. However, mean LCOE of 2nd-life BES fall only slightly below C-BES systems and remain on a high level. Main drivers for more economically viable 2nd-BES are a reduction of initial system costs and an adapted structure of electricity prices.

Results shown here will contribute to the product development of 2nd-BES. Producers can use the design values "min. CL", "max. initial system costs" and "DOD max. configuration" as target values or threshold values. Furthermore, the findings in regard to optimal system size can contribute in project assessment to maximize profits.

The results are based on a very simple, current Swiss electricity tariff scheme for residential consumers. The results show the importance of introducing alternative pricing-models. The model developed can be used in future research to assess the economic viability of BES in combination with more sophisticated tariff schemes. Current Swiss tariffs do not take the positive impact of local storage capacity on power grid stability and the reduction of the necessity to reinforce the power grid into consideration.

ACKNOWLEGEMENTS

This paper is based on research done in the scope of the project "Gebrauchte Batterien als Stromspeicher" (UTF 473.03.14) funded by the Federal Office for the Environment (BAFU).

REFERENCES

1. Boccard N. The cost of nuclear electricity: France after Fukushima. Energy Policy. 2014;66(0):450–61.
2. Harris G, Heptonstall P, Gross R, Handley D. Cost estimates for nuclear power in the {UK}. Energy Policy. 2013;62(0):431–42.
3. Hoogwijk M, Graus W. Global potential of renewable energy sources: a literature assessment. Backgr Rep Prep Order REN21 Ecofys PECSNL072975. 2008;

4. DECC. Public Attitudes Tracker - Wave 11 [Internet]. London: Department of Energy and Climate Change; 2014. Available from: https://www.gov.uk/government/uploads/system/uploads/attachment_data/file/369848/Summary_of_Wave_11_findings_of_DECC_Public_Attitudes_Tracker.pdf
5. University of Hawai'i. Public Attitudes about Renewable Energy in Hawai'i [Internet]. 2014 [cited 2015 Mar 20]. Available from: http://uhfamily.hawaii.edu/publications/brochures/9314e_14101012_COF_RenewableEnergy_Report-FINAL.pdf
6. Azadian F, Radzi MAM. A general approach toward building integrated photovoltaic systems and its implementation barriers: A review. Renew Sustain Energy Rev. 2013;22(0):527–38.
7. Eltawil MA, Zhao Z. Grid-connected photovoltaic power systems: Technical and potential problems—A review. Renew Sustain Energy Rev. 2010;14(1):112–29.
8. Ehara T. Overcoming PV grid issues in urban areas. Int Energy Agency Photovolt Power Syst Program Rep IEA-PVPS T10-06-2009 [Internet]. 2009 [cited 2015.3.20]; Available from: http://www.iea-pvps-task10.org/IMG/pdf/rep10_06.pdf
9. Wang X, Adelmann P, Reindl T. Use of LiFePO4 Batteries in Stand-Alone Solar System. PV Asia Pac Conf 2011. 2012;25(0):135–40.
10. Mulder G, Six D, Claessens B, Broes T, Omar N, van Mierlo J. The dimensioning of PV-battery systems depending on the incentive and selling price conditions. Appl Energy. 2013;111(0):1126–35.
11. Rudolf V, Papastergiou KD. Financial analysis of utility scale photovoltaic plants with battery energy storage. Energy Policy. 2013;63(0):139–46.
12. McManus MC. Environmental consequences of the use of batteries in low carbon systems: The impact of battery production. Appl Energy. 2012;93(0):288–95.
13. Kim D, Menn C, Geissler A, Hengevoss D. Quantifizierung des Umweltnutzens von gebrauchten Batterien aus der Elektromobilität als gebäudeintegrierte 2nd-Life Stromspeichersysteme. Submitt Bauphys. 2015;
14. BFS. Bau- und Wohnungswesen - Die wichtigsten Zahlen [Internet]. Neuchâtel; 2013 [cited 2015 Mar 23]. Available from: http://www.bfs.admin.ch/bfs/portal/de/index/themen/09/01/key.html
15. Castillo-Cagigal M, Caamaño-Martín E, Matallanas E, Masa-Bote D, Gutiérrez A, Monasterio-Huelin F, et al. PV self-consumption optimization with storage and Active DSM for the residential sector. Sol Energy. 2011;85(9):2338–48.
16. Hoppmann J, Volland J, Schmidt TS, Hoffmann VH. The economic viability of battery storage for residential solar photovoltaic systems – A review and a simulation model. Renew Sustain Energy Rev. 2014;39(0):1101–18.
17. Schmiegel AU, Kleine A. Optimized Operation Strategies for PV Storages Systems Yield Limitations, Optimized Battery Configuration and the Benefit of a Perfect Forecast. 8th Int Renew Energy Storage Conf Exhib IRES 2013. 2014;46(0):104–13.
18. vela solaris. Polysun [Internet]. vela solaris; 2015 [cited 2015 Apr 21]. Available from: http://www.velasolaris.com/
19. Swissolar. Markterhebung Sonnenenergie 2013.Teilstatistik der Schweizerischen Statistik der erneuerbaren Energien [Internet]. BFE; 2014 [cited 2015 Mar 24]. Available from: http://www.bfe.admin.ch/php/modules/publikationen/stream.php?extlang=de&name=de_84850551.pdf&endung=Markterhebung%20Sonnenenergie%202013
20. C.A.R.M.E.N. C.A.R.M.E.N. - Marktübersicht für Batteriespeichersysteme [Internet]. Straubing; 2014. Available from: http://www.carmen-ev.de/sonne-wind-co/stromspeicher/batterien/813-marktuebersicht-fuer-batteriespeichersysteme
21. Märtel C. Hersteller von Lithium Akkus (AC) für Photovoltaik Anlagen [Internet]. 2014. Available from: http://www.photovoltaik-web.de/batteriesysteme-akkusysteme-pv/hersteller-speicherloesungen/ac-lithium.html
22. Forst M. Marktüberblick: Diese Speichersysteme gibt es derzeit - Solarstrom- [Internet]. 2013. Available from: http://www.focus.de/immobilien/energiesparen/solarenergie/tid-31894/strom-im-eigenen-keller-speichern-marktueberblick-diese-speichersysteme-gibt-es-derzeit-_aid_1017799.html
23. Chen H, Cong TN, Yang W, Tan C, Li Y, Ding Y. Progress in electrical energy storage system: A critical review. Prog Nat Sci. 2009;19(3):291–312.
24. Battke B, Schmidt TS, Grosspietsch D, Hoffmann VH. A review and probabilistic model of lifecycle costs of stationary batteries in multiple applications. Renew Sustain Energy Rev. 2013;25(0):240–50.
25. MINERGIE. MINERGIE-A Datenbank. Muttenz: MINERGIE Agentur Bau; 2014.
26. Nipkow J. Der typische Haushalt-Stromverbrauch: Neue Haushalt-Kategorien und typische Stromverbrauchswerte [Internet]. Zürich; 2013. Available from: http://www.energieeffizienz.ch/dam/files/Der_typische_Haushalt-SV-SAFE-Dez-2013.pdf
27. Biketec. Preis für gebrauchte Flyer Batterien. (inkl. Transport) [Internet]. Huttwil; 2014. Available from: http://www.flyer-bikes.com/startseite/
28. Swissgrid. Swissgrid - Vergütung [Internet]. 2015 [cited 2015 Mar 13]. Available from: http://www.swissgrid.ch/swissgrid/de/home/experts/topics/renewable_energies/remuneration_re/eiv/compensation.html
29. ElCom. Tarif-Rohdaten der schweizerischen Verteilnetzbetreiber [Internet]. 2014. Available from: http://www.elcom.admin.ch/themen/00002/00097/index.html?lang=de&download=NHzLpZeg7t,lnp6I0NTU042l2Z6ln1acy4Zn4Z2qZpnO2Yuq2Z6gpJCDdX97e2ym162epYbg2c_JjKbNoKSn6A–
30. Neukomm R, editor. Einspeisen mit Orientierung am Bezugstarif [Internet]. Bern: Schweizerische Vereinigung für Sonnenenergie SSES; 2013. Available from: http://www.sses.ch/fileadmin/x_bibli/8_downFiles/2_aktuelles/energie/Einspeisen_Poster_PV-Konferenz_Basel_2013_03.pdf
31. IEA. World energy outlook 2010 [Internet]. Paris: International Energy Agency (IEA); 2010. Available from: http://www.worldenergyoutlook.org/media/weo2010.pdf
32. prognos. Die Energieperspektiven für die Schweiz bis 2050: Energienachfrage und Elektrizitätsangebot in der Schweiz 2000 - 2050 [Internet]. Basel: Bundesamt für Energie; 2012. Available from: http://www.bfe.admin.ch/themen/00526/00527/index.html?dossier_id=05024&lang=de
33. BFS. Schweizerische Preisindizes 1914-2014 [Internet]. 2014a. Available from: http://www.bfs.admin.ch/bfs/portal/de/index/themen/05/01/100.html
34. sia. Wirtschaftlichkeitsrechnung für Investitionen im Hochbau. Zürich: Schweiz. Ingenier- und Architektenverein; 2004.
35. Karathanassis G. The net present value method under conditions of anticipated inflation. University of Aston in Birmingham, Management Centre; 1980.

EUROPEAN MAPPING OF SEASONAL PERFORMANCES OF AIR-SOURCE AND GEOTHERMAL HEAT PUMPS FOR RESIDENTIAL APPLICATIONS

Romain Nouvel[1]; Mariela Cotrado[1]; Dirk Pietruschka[1]

1: HFT Stuttgart – zafh.net, Germany

ABSTRACT

The Coefficient of Performance (COP) of heat pumps, provided by manufacturers, quantifies the heat pump efficiency in nominal conditions (laboratory tests). Therefore, it is generally far from its actual on-site performance.

In order to evaluate realistic heat pump potential in a specific climatic region for a specific use, the Seasonal Performance Factor (SPF) has been mapped for air-source and ground-source heat pump configurations in whole Europe, with a 200 km spatial resolution.

This paper presents the results of this work, as well as the different assumptions, models and calibration used to process it. Further development are finally proposed, laying in particular on the web-based GIS technologies.

Keywords: Coefficient of Performance, Seasonal Performance Factor, Heat pump potential

INTRODUCTION

The Coefficient of Performance (COP) of heat pumps provided by manufacturers quantifies the heat pump efficiency in nominal conditions, i.e. during laboratory tests, with standard and constant boundary conditions. However, heat pump performance depends in particular strongly on the on-site heat source and heat load temperatures, according to the Theorem of Carnot.

In order to evaluate realistically the heat pump potential in a specific climatic region for a specific use, the Seasonal Performance Factor (SPF) should be considered. It represents the final energy efficiency of the whole system over the whole heating/cooling season, calculated as the overall useful energy output to the overall driving final energy input. Standardized in the norm EN 15316-4 [1], it takes into consideration the variable heating and/or cooling demands, the variable heat source and sink temperatures, and includes the auxiliary energy demand like defrost cycle, circulation pumps/fans of the primary loop, storage, back-up heaters.

For HVAC planners, installers as well as building owners, this performance factor is essential to compare heat pumps with conventional heating systems, with regards to environmental criteria (e.g. primary energy saving and reduced CO2 emissions) and economic factors (e.g. yearly energy costs, pay-back period). However, the calculation of SPF applied to a given building in a given location is not trivial, involving different datasets and dynamic models which require specific competences and time.

In the perspective of identifying the renewable energy potentials in whole Europe, we've automatized the modelling and calculation process of the Seasonal Performance Factor, providing the decision takers with several European SPF mappings for air-source and ground-source heat pumps. This paper presents only the case of well-insulated refurbished/modern

residential buildings. Further mappings related to other building usage (e.g. office) and insulation levels have been realized in the framework of the European Project FP7 Inspire [2].

METHODOLOGY

In order to realize a mapping of SPF over the whole Europe, a specific methodology has been developed, integrating the weather data of 300 European weather stations, a model of ground temperature, a model of heat demand profile representative for modern residential buildings, and a calibrated model for the heat pump.

Weather data source

The weather datasets used in this climatic analysis come from the database of Meteonorm 7. They contain hourly values of ambient air temperature, humidity, pressure, solar radiations, cloudiness and other meteorological parameters for a 1-year period, derived from hourly measurements recorded over the period 2000-2009.

To create meteorological mappings of Europe, more than 300 weather stations in the whole Europe, Maghreb, Middle-east and Russia have been considered, for a final spatial resolution of 200-300 km.

Figure 1: 334 considered weather station for the study (Meteonorm7 Data).

Limited phenomena which cause localised temperature peaks have been avoided. Thus, only weather stations at an altitude below 1000 metres have been considered.

Ground temperature modelling

The ground temperature variation in a specific place at a specific depth is an important criterion for the choice of a ground-source heat pump.

Under the topsoil layer (first 30 centimetres), the ground temperature isn't influenced anymore by the daily outside temperature variations, but by the monthly mean ambient air temperature evolution.

An important parameter impacting strongly the ground temperature is the thermal diffusivity of the soil, depending mainly on the soil structure. The soil structure is a very local parameter, with soil compositions variable in all Europe. There is not a general tendency per climate region, since the geological characteristics are much localised. As a simplification in this study, the thermal diffusivity of the soil has been taken constant for all geographical locations fixed at 0.05 m²/day which corresponds to the European average.

The ground temperature has been modelled according to the equation of Kasuda, as function of the time of the year and the depth below the surface.

Building heat demand modelling

For this European mapping, space heating demands representative of well-insulated refurbished/modern residential buildings have been considered, considering that building insulation standard adapts to local climates, so that the annual space heating demand reach 40 kWh/m².yr. The hourly distribution of this space heating demand is assumed to be proportional to the Heating Degree Days base 12.

Considering the domestic hot water demand, also covered with the heat pump, a typical annual demand of 20 kWh/m².yr, distributed uniformly over the whole day (and year) has been assumed.

The hypotheses concerning the supply hot water temperatures correspond to the mean values from a large scale measurement study [2].

Hypotheses:

- Supply hot water temperature for space heating: 36°C
- Supply hot water temperature for DHW: 52°C
- Heating demand = 40 kWh/m².a (distributed over the year, proportionally to the Heating Degree Days base 12)
- DHW demand = 20 kWh/m².a (distributed uniformly over the year)

Heat pump modelling

For this European scale modelling study, a simplified model of heat pump based on the Carnot efficiency is used:

$$COP = \eta_C * \frac{T_{hw}}{T_{hw} - T_{source}} \quad (1)$$

Where

- T_{hw} : supply hot water temperature for space heating or DHW [in Kelvin]
- T_{source} : temperature of the heat source, in our case ambient air or ground [in Kelvin]
- η_C : Carnot performance factor, defining as the quotient of the real over the ideal from the Carnot reversible cycle.

The value of the Carnot performance factor depends on the efficiency of the heat pump installation. Generally, it varies from 0.3 for small scale heat pumps designed for domestic use, to 0.65 for the most efficient heat pumps.

In our simplified model, auxiliary energy consumption needed for the circulation pumps/fans of the primary loop (evaporator side), heating rods and defrost cycles (necessary to melt the ice formed on the outdoor unit's heat exchanger when the ambient temperature gets below 0°C) are counted in the considered Carnot performance factor

Model calibration

The Carnot performance factor has been calibrated for both air-source and ground source heat pumps, based the results of a recent 3-years measurement campaign in 77 German residential buildings equipped with air-source and ground-source heat pumps [3].

According to the technical report, the mean SPF measured on the air-source heat pumps of this study reached 2.88, for an average heating demand of 72 kWh/m².a, an average DHW demand of 16 kWh/m².a, a supplied hot water temperature of 36°C for space heating and 52°C for DHW. The heat pumps have an average $COP_{A2/W35}$= 3.48, for a Carnot performance factor of 0.36.

For the ground-source pumps with horizontal collectors, the mean measured SPF reached 3.75, for approximately the same heat demands and supply hot water. The heat pumps present $COP_{B0/W35}$ = 4.66, for a Carnot performance factor of 0.36 identical to the air-source heat pumps.

EUROPEAN MAPPING OF AIR-SOURCE AND GROUND-SOURCE HEAT PUMP PERFORMANCES

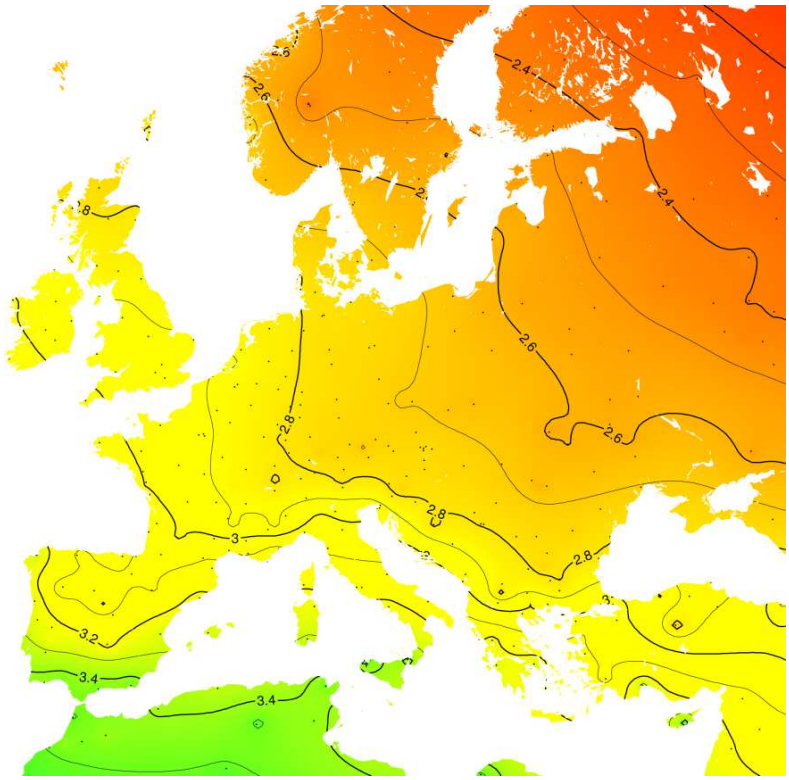

Figure 2: Seasonal Coefficient of Performance of Air source heat pumps in Europe, residential buildings.

Figure 2 represents the European Mapping of SPF of air-source heat pump, generated by using the methodology previously described.

The SPF of air-source heat pump varies between 2.4 and 3.4 in European modern residential buildings. With an average Primary Energy Factor for electricity of 2.5 in Europe, the primary energy-conversion factor of a heat pump is in the northern half of Europe is barely more than 1 (equivalent to an high efficiency condensing gas boiler).

Figure 3 represents the Seasonal Performance Factor of ground-source heat pumps with horizontal collectors (buried 2 meters deep into the soil) in Europe.

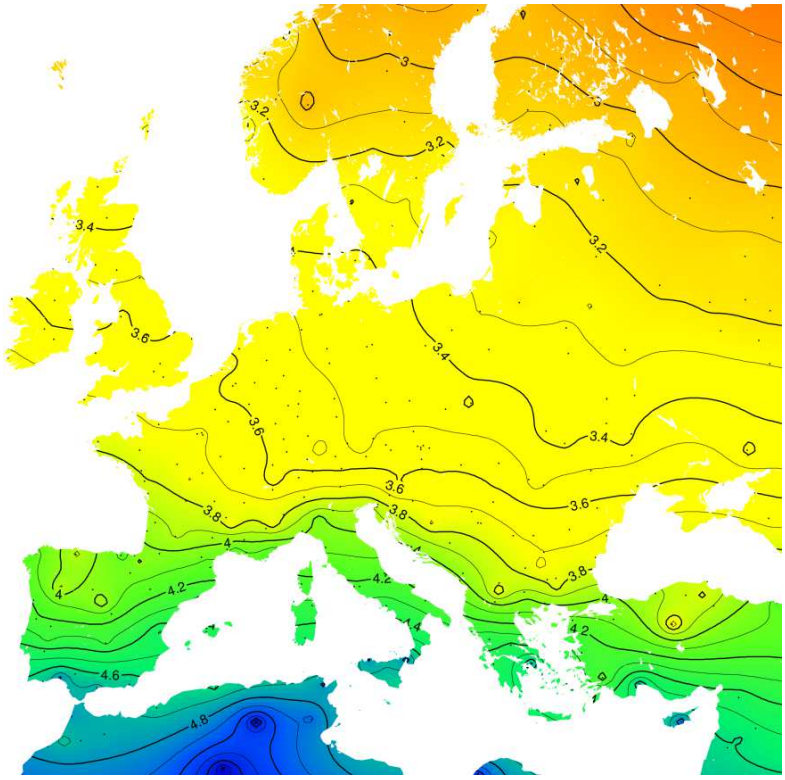

Figure 3: Seasonal Coefficient of Performance of Ground-source heat pumps in Europe, residential buildings.

In Europe, the Seasonal Performance Factor of ground-source heat pump can vary between 3 and 4.6 in refurbished residential buildings, between 0.5 and 1 higher than the ones of air-source heat pump.

In the European Project FP7 Inspire, the same study has been realised for office buildings. Because they don't require domestic hot water, whose temperature is higher than for space heating, the calculated SPF are higher than for residential buildings, up to +0.5 in some European regions.

CONCLUSION AND PERSPECTIVES

These European mappings provide an important decision making support for HVAC planners, installers as well as citizens, wondering about the benefit of installing a heat pump in a specific region of Europe.

By considering this locally simulated SPF instead of the single nominal COP as it is widely done, planning failures with dramatic consequences on both economic and environmental

levels will be avoided. For instance, in particular regions of Europa, heat pumps may have a worse environmental impact that conventional gas boilers. This first version of European SPF mapping focuses on the different models and their data requirements. For ground source heat pumps the required size of the geothermal system can vary significantly according to the found ground configuration and humidity. The influence of these differences are not considered in the calculations.

However, a very natural evolution of the presented analysis would be a conversion of these static mappings in a Geographical Information System (GIS). Additionally to the navigability benefits, GIS technologies would enable to take into account other geo-localized parameters such as the very local soil properties or precipitation, for a more precise estimation of the ground-source heat pump potential. The European Project ThermoMap, which aimed at mapping the very shallow (up to 10m) Geothermal Potential, has already developed a GIS layer of the soil thermal conductivity, it could be very easily integrated for the purpose addressed here.

By using web-based GIS, all the assumptions of this paper related to the building (insulation level, domestic hot water demand) and the heat pumps system (Carnot efficiency) could be specified interactively in a web platform, in order to improve the customization of the calculation and obtain more precise results.

For the regions of Europe with a cooling demand, a much needed further development is the modelling of reversible heat pumps producing also cooling in summer. In this case, the whole yearly impact of the heat pump system would be considered. However, the cooling loads are much more complex to model at large scale for the mid European climates, depending highly on the building design, internal load situation and passive strategies. Reflecting this issue, no Cooling Degree Day method has been standardized until now in Europe, contrary to countries like U.S.A.

ACKNOWLEDGMENT

The research leading to these results has received funding from the European Union's Seventh Programme for research, technological development and demonstration under grant agreement No 314461. The European Union is not liable for any use that may be made of the information contained in this document which is merely representing the authors view.

REFERENCES

1. Norm EN 15316-4-2 (2008): Heating systems in buildings – Method for calculation of system energy requirements and system efficiencies – Part 4-2: Space heating generatino systems, heat pump systems
2. European project iNSPiRE - Development of Systemic Packages for Deep Energy Renovation of Residential and Tertiary Buildings including Envelope and Systems. Project web-site: http://www.inspirefp7.eu/ (May 2015)
3. M. Miara: Messtechnische Untersuchung von Wärmepumpenamlagen zur Analyse und Bewertung der Effizienz im realen Betrieb. Final technical report of the project „Wärmepumpen Effizienz“ subsidised by the Bundesministerium für Wirtschaft und technologie. 2011.

AKTIVA – DESIGN AND INTEGRATION OF BUILDING OUTER SURFACES FOR MULTI-FUNCTIONAL SPACE HEATING AND COOLING APPLICATIONS

Wemhöner Carsten[1]; Kluser Reto[1]; Schweizer Raphael[1]; Afjei Thomas[2]; Müller Andreas[2]

1: IET Institute of Energy Technologies, HSR University of Applied Sciences Rapperswil, Oberseestrasse 10, 8640 Rapperswil, Switzerland

2: Institute of Energy in Building, University of Applied Sciences Northwestern Switzerland, St. Jakobs-Strasse 84, 4132 Muttenz, Switzerland

ABSTRACT

In modern highly-insulated buildings the summer operation is getting more important and comfort cooling of buildings becomes increasingly an issue, in particular for office buildings. Free cooling during night-time by convection and radiation of an activated outer surface such as an absorber or collector has rarely been considered in practical operation for Swiss climate conditions, yet, but has shown interesting potentials in recent studies. An even more beneficial operation, though, would be to use the same outer surface also for space heating in winter operation, for instance as a heat source for a heat pump, as well as in summer operation for DHW heating. Thus, the objective of the project is the optimisation of properties of outer building surfaces for both heating and cooling operation, e.g. regarding the selectivity of the outer surface. Furthermore, adapted options for the system integration into a hydronic system are investigated by simulations. The results of the simulations are compared to lab measurements.

As first step the properties of an unglazed collector with different degrees of selective coating and different inclination angles have been lab-tested. In parallel, a collector model based on the data sheet parameters has been implemented in Matlab-Simulink and compared to the lab test data with good agreement. Subsequently, the unglazed collector has been integrated into a system simulation model consisting of a heat pump or chiller, respectively, a source storage connected to the collector for the winter heat pump operation as well as a direct connection of the collector to the differently oriented building zones for summer cooling. The building zones are equipped with thermally-activated building systems (TABS), which are often applied in office buildings and offer favourable conditions for low temperature heating and high temperature free-cooling operation.

Simulation results show a high degree of coverage for the Zurich average year weather data according to SIA 2028 for both operation modes. For single office use based on SIA 2024 loads, degree of coverage of winter source energy is about 75% corresponding to an SPF of the heat pump around 4. In summer cooling mode, about 90% of the cooling energy can be covered by free cooling. Results vary depending on the selectivity and inclination, so based on the requirements parameters can be optimised for heating or cooling. An integration of the source storage in cooling mode increases the degree of coverage up to 10%, in particular in adverse conditions like high selectivity of the collector or warm summer climate like Lugano warm year. As result of the project recommendation on the design, integration and control of outer surfaces for multi-functional operation in different applications will be concluded and verified by lab measurements of enhanced prototypes.

Keywords: Renewable heating, free cooling, unglazed solar collector, multi-functional façade, heat pump

INTRODUCTION

New buildings in Switzerland have U-values around 0.2 W/(m^2K) and are therefore well insulated. The internal loads, however, tend to increase. As a result, comfort cooling in office buildings becomes increasingly an issue, but should not lead to excessing electricity use for cooling in summer. Different free-cooling techniques have established as cooling options mainly in office buildings, though. By direct use of environmental heat sinks like the ground or outside air they offer an energy-efficient way to increase the cooling performance, since the sole energy expense is the circulation of the fluid. However, each passive cooling technology has its specific limitations. Space cooling by radiation or night-time convection of an activated outer building surfaces has yet rarely be considered or validated in practical operations for Swiss climate conditions, despite promising potentials [1]. A further synergy exists when the same system is used for space heating operation in winter or domestic hot water production (DHW) in summer, as well.

Thus, the objective of the project AKTIVA is the optimisation of properties of the outer building elements, which could be designed as absorbers or collectors, for multi-functional application, e.g. regarding the selectivity and inclination angle. As result, renewable heating and cooling fraction as well as design and applications ranges of the system are evaluated.

METHODS

Within the project AKTIVA system simulations based on lab-measurement of the component characteristics are accomplished. On the one hand, lab-measurements of the characteristics of the outer surface are performed at the University of Applied Sciences Northwestern Switzerland in Muttenz. On the other hand, the HSR University of Applied Sciences Rapperswil is modelling and simulating the system with an integrated multi-functional absorber using the simulation environment Matlab-Simulink with the CARNOT Toolbox [2]. The industrial project partner Energie Solaire SA in Sierre, which produces unglazed absorbers for different applications, supports the project with the absorbers and know-how.

Lab-Measurements

Three unglazed collectors of the industrial partner Energie Solaire SA with different selective coatings ($\varepsilon = 0.15$, $\varepsilon = 0.3$, $\varepsilon = 0.9$) were measured regarding their heating and cooling capacity. The collectors are connected to a hydraulic system which emulates respectively simulates different operating conditions. In a first step, the cooling potential during the night was investigated, which depends on the ambient temperature (convection) as well as the sky temperature (radiation). Furthermore, the impact of different inclination angles was examined regarding the cooling and heating capacity, since a small inclination is better for cooling whereas higher inclination angles typical for façade integration has advantages in heating.

Collector Modelling

In order to evaluate the outer surface performance over the year-round operation a model of the unglazed collector has been implemented based on the model-approach of Stegmann et. al [3], which depends on the results of the European collector test standard EN 12975 [4]. The model includes the effects of direct and diffuse solar radiation, heat emission as well as condensation due to sky- and ambient temperatures. Subsequently, the simulated data of the collector model were validated with measurement data of the unglazed lab-collector.

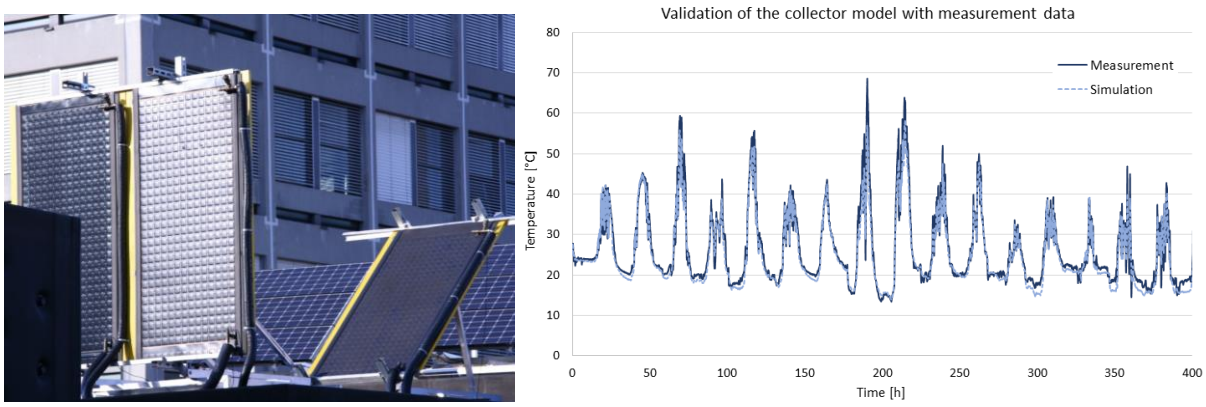

Figure 2: Experimental setup of the unglazed absorbers with different selectivity and inclination (left) and comparison of measured and simulated data of the outlet-temperature of the non-selective collector of ε = 0.9 (right).

Figure 2 shows good agreement of measured and simulated data. Only small deviations in the range of up to 3 K occur in particular situations.

System Simulations

After validation the collector model was integrated into an adapted hydraulic system to evaluate the components and system key figures. Therefore, the model was coupled with a heat pump, source storage and a heating and a cooling load. By this integration, the operation modes heating with collector source, direct heating from the collector, simultaneous heating and cooling with the heat pump, active cooling with the heat pump and recooling with the collector as well as free-cooling with the collector can be covered. Figure 3 shows the system integration.

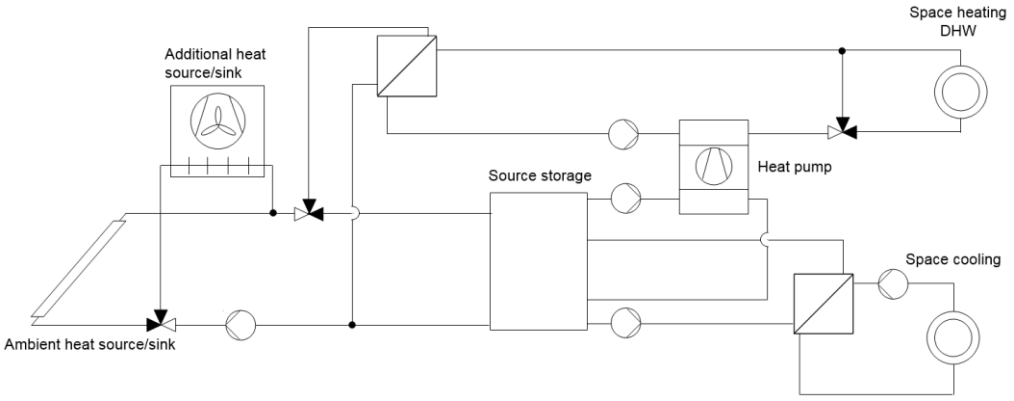

Figure 3: Hydraulic system integration to simulate and evaluate the cooling and heating potential of multi-functional component use

The emission system in the room zones are TABS of 30 cm concrete with core activation resulting in maximum supply temperature of 29 °C in the heating mode. During winter period, the collector is connected to the storage and serves as a heat source for the heat pump. In summer period, however, the collector can be directly connected to the TABS, or as variant can be connected parallel to the source storage, and cooling is covered from the storage. The heat pump can be used as a backup chiller. Winter heating operation covers the period of October-March, while summer cooling takes place in the period of April – September.

RESULTS

Simulation results for multi-functional use of collector and source storage

Figure 5 summarises performance results as uniform metric "degree of coverage" of the collector for both space heating and cooling mode. The components in the hydronic integration are chosen in that way that each component can be used for both space heating and space cooling mode. However, the requirements for the components are partly opposite for the two operation modes, implying optimisation potentials of component parameters and design depending on the prevalent loads.

The heating and cooling loads are assumed for two single office zones with façades in north and south direction and a glazing fraction of 60%. Weather conditions are Zurich Meteoschweiz average year and Lugano warm year according to SIA Merkblatt 2028 [5]. Data for the internal loads are taken of SIA Merkblatt 2024 [6]. The collector design corresponds to 0.33 $m^2_{coll.}/m^2_{ERA}$. A brine-storage with 10 l/m^2_{ERA} is integrated as source storage. Resulting room temperatures correspond to the temperature requirement according to the SIA 180 [7].

Four cases have been simulated in order to evaluate the heating and cooling potential for the extreme characteristics of the collector operation, considering the inclination and emission coefficient. The inclination varies between 5° and 90°, which corresponds to collectors on a flat roof or façade-integrated collectors. The emission coefficient varies between 0.1 and 0.9 for a selective collector and non-selective collector, respectively. Figure 5 left shows the degree of coverage for the collector either as a free-cooling system or as source for the heat pump in all four cases. All cases are considered without storage use in cooling mode and with the collector as only heat source in heating mode.

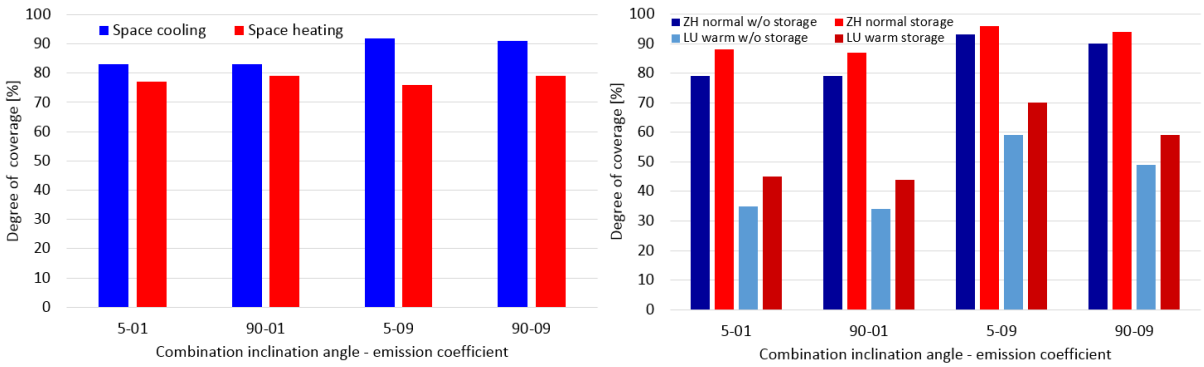

Figure 5: Degree of coverage for a multi-functional collector use by inclination and emission coefficient (left) and free-cooling fraction with multi-functional use of source storage (right)

The degree of coverage during space heating mode can be recalculated as the seasonal performance factor (SPF) of the heat pump. A fraction of source energy of 75% (i.e. 25% compressor energy) corresponds to an SPF of 4. The relatively high SPF-values are a result of the favourably low supply temperature for TABS. During cooling mode, the degree of coverage represents the fraction of free-cooling on the totally used cooling energy. The missing fraction has to be supplied by an active back-up of the heat pump in chiller mode. Due to small temperature difference in the operation of the unglazed collectors as heat pump source, the emission coefficient has a lower influence to the degree of coverage and differences between the selective and non-selective collectors are small. However, the effect on the cooling performance is higher even though the ambient temperatures during the night are relatively low in Zurich with a temperature below 15° C in 85% of all night hours.

Thus, the inclination has a relatively small influence to the cooling power in this case, since the convective heat rejection still reaches high shares.

Multi-functional use of the source storage both in heating and cooling mode is evaluated in Figure 5 right. It can be seen that the increase of the degree of coverage by free-cooling depends on the situation. For limited surface characteristic, i.e. low emission coefficient, or adverse ambient conditions, i.e. hot summer climate of Lugano warm year, the storage use in cooling operation can increase the degree of coverage by about 10%. However, with favourable conditions in Zurich average summer climate and good surface properties of an emission coefficient of 0.9 and 5° inclination, differences decrease to about 3%.

Design aspects

Parameter variations have been accomplished to evaluate the dependency of SPF in winter heating and degree of coverage in summer cooling mode, respectively. Figure 6 left shows the impact of the collector design on the SPF for two extremes of inclination/emission of 5°/0.9 (cooling optimised) and 90°/0.1 (heating optimised). For increasing collector area the performance increases digressively. Both designs reach good SPF values above 4, even with low collector areas of 0.1 $m^2_{coll.}/m^2_{ERA}$. By the selective coating and good inclination, though, the SPF can be increased by about 0.5, up to absolute values above 5. In cooling mode, characteristic is vice versa. For cooling optimised designs the free-cooling fraction can be increased by 0.15 and more up to values above 90% for the same inclination angle of 5°. This is even the case in moderate night-time temperature in the Swiss middle land of Zurich normal summer with about 85% of night-time temperatures below 15 °C allowing higher convective shares. In the hotter climates of southern Switzerland, differences are even more pronounced due to limited convective losses.

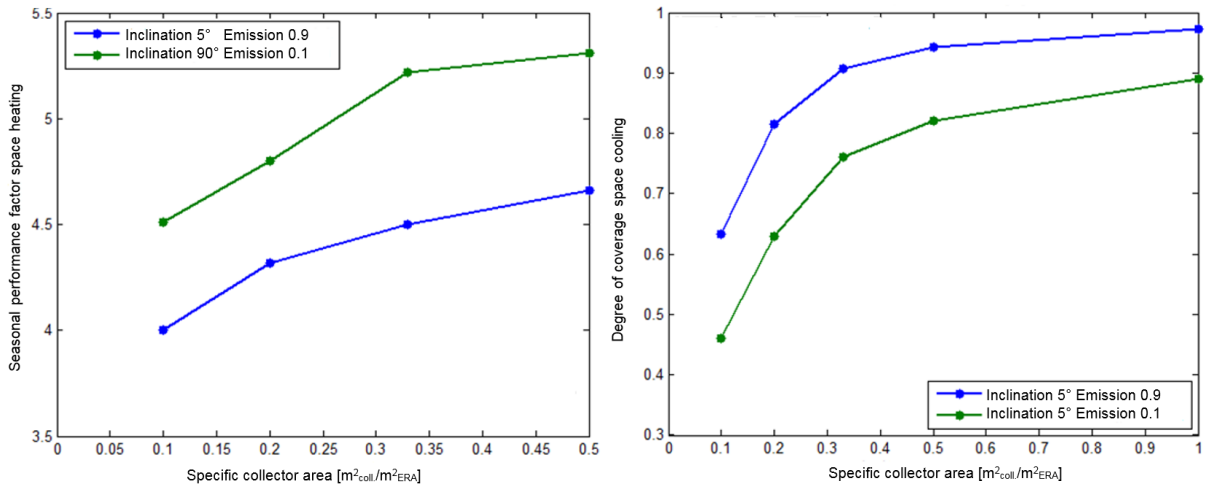

Figure 6: Seasonal performance factor and degree of coverage of multi-functional collector for different combinations of inclination and emission in Zurich Meteoschweiz average year.

CONCLUSION

A multi-functional system configuration based on the core components heat pump and solar collector has been lab-tested, modelled and simulated for different characteristic of the collector surface. The system integration is done in a way that all system components are suited for multi-functional use for space heating and cooling. In both operation modes, high degree of coverage is confirmed by the simulation. However, depending on the prevalent load situation an optimisation of the characteristic can be accomplished.

A further use of the source storage as cold storage for the cooling mode can increase the degree of coverage of passive cooling operation by further 10% in particular in more restrictive boundary conditions of higher night-time temperatures or limited properties of the surface regarding cooling operation.

Also the design has an impact, since larger collector areas increase both, source conditions for the heating operation and free-cooling shares.

In unfavourable weather conditions, though, the operation limits of the components, e.g. the lower temperature limit of the heat pump, may require an additional source or back-up systems. On the other hand, in favourable conditions, a direct solar space heating operation and DHW heating in transitional periods is probable, but has not been investigated, yet.

Further investigations and potentials are seen in control optimisations and design depending on different load conditions, since the yield of environmental energy in both space heating and cooling is strongly linked to the temperature levels of the surface. Thus, if operational temperatures can be enhanced by the control of the system, an enhanced degree of coverage is expected. Further simulation will be carried out to evaluate these impacts.

ACKNOWLEDGEMENTS

The project AKTIVA is a national contribution to the Annex 40 in the IEA Heat pump programme (HPP) on heat pump systems for nearly Zero Energy buildings. Information on the IEA HPP Annex 40 can be found on http://www.annex40.net. The funding and advice of the Swiss Federal Office of Energy for the project AKTIVA and the IEA HPP Annex 40 is highly acknowledged. Gratitude is expressed to the industrial project partner Energie solaire SA for the support, know-how and prototype collectors in the project.

REFERENCES

1. Wemhöner, C., Genkinger A., Afjei T.: Kühlen über thermisch aktivierte Aussenflächen. Feasibility study, University of Applied Sciences Northwestern Switzerland, 2011
2. Solar-Institute: CARNOT-Blockset 5.3, Germany, 2012
3. Stegmann, M., Bertram, E., Rockendorf, G., Jassen, S.: Modell eines unverglasten photovoltaisch-thermischen Kollektors basierend auf genormten Prüfverfahren, 22. Solarthermisches Symposium, Kloster Banz, 2012
4. EN 12975-2: Thermal solar systems and components – Solar collectors – part 2: test methods, CEN, Brussel, 2006
5. Swiss Society of Engineers and Architects: SIA Merkblatt 2024 – Standardnutzungs-bedingungen für die Energie- und Gebäudetechnik, Zurich, 2006
6. Swiss Society of Engineers and Architects: SIA Merkblatt 2028 - Wetterdaten für die Energie- und Gebäudetechnik, Zurich, 2006
7. Swiss Society of Engineers and Architects: SIA 180 – Wärmeschutz, Feuchteschutz und Raumklima in Gebäuden, Zurich, 2014

A MACHINE LEARNING METHODOLOGY FOR ESTIMATING ROOF-TOP PHOTOVOLTAIC SOLAR ENERGY POTENTIAL IN SWITZERLAND

D. Assouline[1], N. Mohajeri[1]; J.-L. Scartezzini[1]

[1]*Solar Energy and Building Physics Laboratory (LESO-PB), Ecole Polytechnique Fédérale de Lausanne (EPFL), 1015 Lausanne, Switzerland*

ABSTRACT

Solar photovoltaic (PV) deployment on existing building roof-tops has proven to be one of the most viable large scale resources of sustainable energy for urban areas. While there have been many studies on roof-top integrated PV systems at building and neighborhood scale, estimating the PV energy potential through the available roof surface area in large scale, however, remains a challenge. This study proposes a methodology to estimate the roof-top solar PV potential for existing buildings at the commune level (the smallest administrative division) in Switzerland. In addition, while several studies suggest physical models to assess the photovoltaic solar energy potential, the current study proposes a computational data-based learning approach, using the following four steps: (1) monthly estimation of the main solar irradiance components (global horizontal, direct normal, diffuse horizontal) for the entire Switzerland, that is, the total amount of solar energy available from the Sun (2) processing of training and testing population and building data at a commune level, (3) estimation of the available roof-top surface (A_R), average roof tilted angle (β), and average shading coefficient (S) for buildings in the urban areas, for each commune, (4) combination of the available roof-top surface area for each commune with the solar potential along with other parameters so as to estimate the actual solar PV potential. The first step is achieved through a Support Vector Regression (SVR), using solar irradiance satellite data with an average RMSE of 1.68 W/m^2. In the second step, GIS have been used to aggregate the data at a commune level. In the third step, a supervised learning algorithm using SVR has been used so as to estimate A_R, β and S in existing buildings, which can be extremely difficult data to obtain at a large scale. We use (i) population and building density data, (ii) land use data, and (iii) building typologies as input features. Aggregated values for A_R, β and S for 46 communes in Geneva canton are used as a training output (labeled data) for the learning process. Finally, in the fourth step, by combining solar irradiance and building parameters predictions, we estimate the solar PV potential at the national scale.

Keywords: Rooftop Photovoltaics, Machine Learning, large scale solar potential, GIS, Support Vector Regression

INTRODUCTION

To lead to a better use and a more efficient management of renewable energies in urban environments, where the energy demand is often concentrated, the assessment of local energy potential is required. While many renewable resources are considered, one of them stands out for its almost unlimited power and everlasting presence: the sun. Consequently, solar PV panels on existing building roof-tops have proven to be an efficient and viable large scale resource of sustainable energy for urban areas. To estimate the roof-top solar potential, an assessment of the available solar energy coming to these urban areas as well as the surface area available on buildings (facades and roofs) for solar power plants is required. These assessments have been addressed at multiples scales, with various methods and using different parameters (e.g. building and population density, shade effect, number and orientation of buildings). However, very few

studies explore the large scale solar PV potential. For example, study have been done in Spain at municipality level [1] and in Canada-Ontario at regional level [2].
This paper presents, for the first time, a machine learning methodology to estimate the rooftop PV potential of urban areas at large scale. A valuable characteristic of the method is its scalability, since it could be applicable from communal or regional to continental scales, depending on the level of aggregation of the available data. The methodology applies to Switzerland and estimates the rooftop PV potential of each commune, as the smallest Swiss administrative entity. It captures only urban areas defined by the CORINE Land Cover database (including residential, industrial and commercial buildings) enhanced for Switzerland [3]. This help us to capture accurately building density within the urban areas as one of the input variables. The data have been processed using a Geographical Information System (GIS); further processing including machine learning procedures have been performed in Python. All GIS data have been projected and processed in CH1903-LV03, the Swiss GIS coordinate system.

METHODOLOGY

There are several approaches to estimate the solar potential on rooftops. One method has been developed based on a hierarchical approach, as presented in [1]. It is composed of three main potential steps: (i) the physical potential is the solar power available, that is, the solar irradiance coming to the zones of interest; (ii) the geographical potential is the portion of the physical potential captured over the restricted area, more specifically here the available area for PV installation on roofs; and (iii) the technical potential is the actual electricity generated by the PV panel (considering its efficiency, varying between 10% and 40%) based on the geographical potential. Considering the legal issues and socio-economics aspects can be added as another step, that is, the societal potential.
To achieve the potential steps, we adopted a data-based learning approach, known as Machine Learning (ML). In ML, a certain amount of data is given to the machine so that it learns how this type of data is structured, and build directly models from data instead of calibrating prebuilt models with the data. This help us to predict similar unknown data. Supervised learning (SL), a machine learning task, is used to derive a model from labeled training data. Here we are interested in finding a function f that relates an input to an output vector, $\mathbf{x}$ and $\mathbf{y}$, so that $\mathbf{y} = f(\mathbf{x})$, given a training data of observed - known - points (x_i, y_i).
One of the most popular SL algorithms is the Support Vector Machine algorithm [4]. It is often superior to classic interpolation since it can handle higher dimension data, often offers a lower computation time and a lower RMSE (Root Mean Square Error). Support Vector Regression, the SVM regression algorithm, has been used in this study. When using SVR, 75% of the known data is used as the training set , and 25% as the testing set (to test models built in the training set), for which the test RMSE is computed. K-fold cross validation is performed on the training set to tune the hyperparameters. The next following parts will present the application of the first two potential steps to our case, the technical and societal steps being not addressed here.

APPLICATION TO SWITZERLAND DATA

Physical potential (solar irradiance maps)

Solar monthly maps have been derived for the solar global horizontal (GHI), and horizontal diffuse and normal direct irradiances (respectively DHI and DNI), in order to account for the tilted angle of the roofs in our calculation. Hourly values of DNI computed on a virtual moving plane following the sun trajectory perpendicularly have been used. In addition, hourly GHI and DHI values from the HC3 (HelioClim-3) database have been used. These values have been extracted from 100 different sites in Switzerland available in the SoDa web service [5]. The data span from February 2004 to May 2015. Monthly values were extracted from the hourly series

by averaging the irradiances over 24 hours for each day of the month - taking the null values of the night into account. This helps us to finally obtain an average value of the solar irradiance received (in W/m^2) per month.
In order to test the efficiency of various algorithms, a yearly GHI map was computed, using SVR and several classical spatial interpolation techniques. These include Inverse Distance Weighting (IDW), Radial Basis Functions (RBF), General Regression Neural Networks 2D (GRNN) and Simple Kriging (SK). One of the SVR derived map is showed in Figure 1. Table 1 presents the RMSE for each technique, showing the best results with SVR.

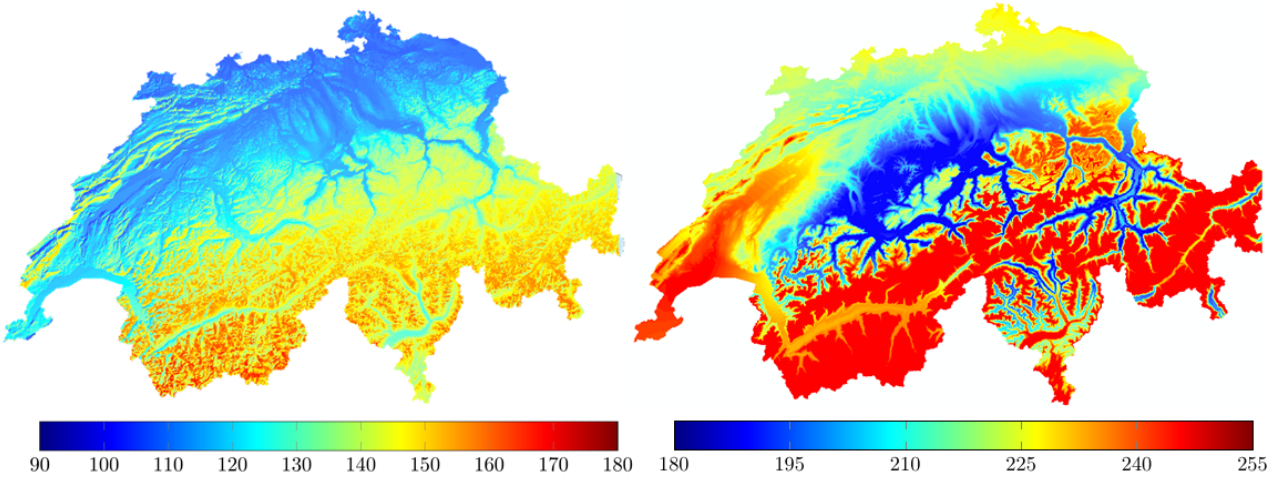

Figure 1: Left: Solar annual GHI map of Switzerland, in W/m^2, obtained with SVR, using spatial coordinates and terrain parameters derived from DEM's. Right: Solar DNI map for July, in W/m^2, using spatial coordinates and weather parameters.

	IDW	**RBF**	**GRNN2D**	**SK**	**SVR2D**	**SVR3D**	**SVRTerrain**
Test RMSE (W/m^2)	2.65	2.10	2.42	1.85	1.37	1.65	1.72

Table 1: RMSE summary of interpolation techniques for deriving a swiss GHI solar irradiance map.

Since the SVR algorithm is superior to the other 2D interpolating methods, it has been chosen for monthly mappings of DNI, DHI and GHI. An example of DNI map is showed in Figure 1. Latitude, longitude, altitude and weather parameters are chosen as input features. Temperature, precipitation, sunshine duration, and cloud cover data were gathered to account for the weather behavior, tremendously impacting on solar prediction. The raster basis for the prediction maps was a Digital Elevation Model (DEM) that covers all Switzerland (RIMINI DEM available in the Swisstopo website, available at http://www.swisstopo.admin.ch) and re-sampled to a resolution of 200m $\times$ 200m. The global tilted irradiance (GTI) on a non horizontal surface (i.e. a tilted roof) is given by the classical following equations:

$$GTI = R_d D_h + B_n \cos(\theta) + \rho R_r G_h \tag{1}$$

$$\cos(\theta) = \sin(\theta_z)\sin(\beta)\sin(\gamma_s - \gamma) + \cos(\theta_z)\sin(\beta) \tag{2}$$

Where D_h, B_n and G_h are respectively DHI, DNI, and GHI, θ is the angle of incidence of the sun rays on the tilted plane, R_d and R_r are diffuse and reflected factors (given by physical isotropic or anisotropic models), ρ is the foreground's albedo (taken here as 0.2), and θ_z , γ_s, β, and γ are respectively the sun zenith angle, sun azimuth angle, tilt angle of the surface, and the azimuth angle of the surface. Thus, all these parameters require to be aggregated at the communal level. The azimuth of a tilted surface is defined as the angle between the North and the horizontal projection of normal vector to the plane. To obtain an azimuth value for the average building

in each commune, we made the following assumptions: (i) the footprint is rectangular and symmetric, (ii) the roof consists in two tilted surfaces with the same slope, and the A_R is equally shared between the two sides of the roof, and (iii) the roofs are likely to follow the direction of the longest walls, meaning that the azimuths of one of the two roof tilted surface are given by the smallest walls direction which is perpendicular to them. The rooftop azimuths are aggregated in each commune considering the main direction - most frequent azimuth from a histogram with 20 degree bin width. We computed monthly raster maps for the suns altitude and azimuth with SVR, based on hourly data for various points in Switzerland, considering again the suggested days per month in [6], at 1:00 PM. Raster maps offer much more resolution than the aggregated maps that only offer one value per commune, thus we decided to clip these sun position raster values within the CORINE urban areas, and average the clipped cells within these areas. Slope estimation, needed to obtain the GTI, will be addressed in the next part.

Available communal roof area, average slope and shading estimation

Precise data on various parameters of buildings are very rarely available. Some of these parameters directly influence the solar potential and are necessary for a geographical potential study: for example, the available area for PV installation on rooftops (A_R), the average slope of the building rooftops (the slanting angle of the roof from a horizontal plane), and the shading effect caused by surrounding buildings. While most studies arbitrarily choose correction coefficients to account for the first and the third parameter, we evaluated these coefficients based on the building characteristics and properties of the urban areas. We use machine learning methods to estimate an aggregated value of these unknown buildings parameters in every Swiss commune by extrapolating them from the Geneva canton, where accurate data is available through SITG open access website (http://ge.ch/sitg/). This database contains available roof surface for PV panels and the average slope for each building in the canton. The shading factor is extracted for each commune in Geneva from a DOM (Digital Orthophoto Map), a DEM that takes buildings and vegetation into account. This computes the hillshade raster map from the DOM with the Spatial Analyst toolbox in ArcMap. As hillshade depends on the sun altitude and azimuth, we repeated the DOM extraction for each month, by taking into account a monthly sun position, corresponding to typical days per month [6], and calculating the hillshade for this position.

The portions of the hillshade corresponding to the building rooftops were then clipped in order to extract an aggregated shading value within each commune in Geneva. The input features for the SVR algorithm are as follows: (i) building density (D_b), (ii) population density (D_p), (iii) average building footprint area (A_f), (iv) total building footprint area, and (v) various building typologies ratios (e.g. period of construction, number of stories, main energy resource used etc.). D_b and D_p as well as the building areas were extracted from a 2D footprint building data which covers all Switzerland, VEC25 from the Swisstopo website. The building typologies data were taken from the swiss Federal Office of Statistics (OFS). All these features have been aggregated within the urban areas defined by CORINE Land Cover in different communes in order to obtain one value for each Swiss commune. The average roof slope and A_R have been extracted from the SITG database. These values are also aggregated within the urban area along with the shading factor from the DOM in order to present one value for each commune in Geneva. A correction coefficient c_R has then been computed from A_R ($c_R = A_R/A_f$) for each commune in Geneva. Average roof slope, shading coefficient and c_R are the outputs in the ML algorithm in order to predict the same variables for every Swiss commune. SVR have been used for all three variables separately. The RMSE obtained for each of them are presented in Table 2, along with RMSE obtained for GHI, DNI, and DHI predictions. It resulted in one A_R map (calculated as $c_R A_f$ in each commune), one slope map, and 12 monthly shading maps. The slope aggregated values are used to finalize the computation of GTI in each CORINE area.

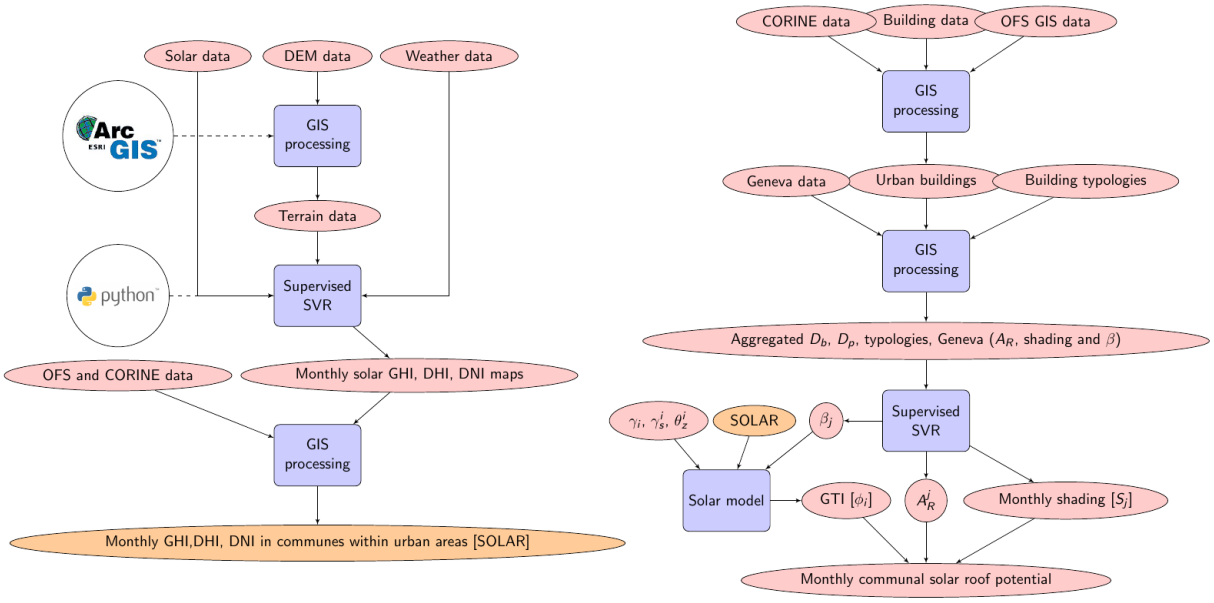

Figure 2: Methodology scheme. Left and right diagrams respectively describe physical and geographical potential steps. A_R^j and β_j are the available rooftop area for PV installation and the roofs average tilt angle in each commune, θ_z^i , γ_s^i, and γ_i are respectively the sun altitude and azimuth angles, and the main azimuth of the roofs in each CORINE area.

	GHI (W/m^2)	**DNI (W/m^2)**	**DHI (W/m^2)**	C_R (0 $\leq$**ratio**$\leq$ 1)	β (°)	**Shade**(0 $\leq$**coeff**$\leq$ 255)
Test RMSE	1.29	2.97	0.76	0.0164	0.54	2.14

Table 2: RMSE summary of various parameters predicted with SVR. In case of monthly derived parameters, the given value is the average of the monthly RMSE's.

Geographical potential (multi-layer approach)

The geographical potential has been obtained from the combination of aggregated GTI values with the previously presented predicted commune aggregated maps. A scheme of the complete methodology is showed in Figure 2.
We computed the solar potentials of the CORINE urban areas of a commune, and summed them to obtain the total commune potential. The values that are are already aggregated by the prediction (for example A_R) are taken the same for each urban area within the commune. For each month, the total available solar power on rooftops P_j for each commune j is computed as follows:

$$P_j = \sum_{i=1}^{N} b_i S_j \left(\frac{A_R^j}{2} \varphi_i \left(\gamma_i\right) + \frac{A_R^j}{2} \varphi_i \left(\gamma_i + 180\right) \right) \tag{3}$$

Where the sum is computed over the CORINE urban areas i, b_i is the number of buildings in area i, S_j is the shading factor predicted in j, A_f^j is the average available rooftop area in j, φ_i is the GTI clipped in area i, given by equation (1), as a function of γ_i, the predicted roof azimuth of CORINE urban areas i. We consider both γ_i and $(\gamma_i + 180)$ to account for both sides of the roof. It should also be noted that we used the Klucher model [7] to compute R_d and the classical isotropic sky model to compute R_r in equation (1). This is computed for every considered commune, for each month, resulting in twelve final potential maps. An example of the resulted maps is showed in Figure 3 for June, along with the obtained map for c_R. The general PV potential can be clearly seen from each commune, yet, it is highly dependent on the number of buildings. As a result, values have also been divided by CORINE and total footprint areas, and inhabitants of the commune, to obtain normalized maps.

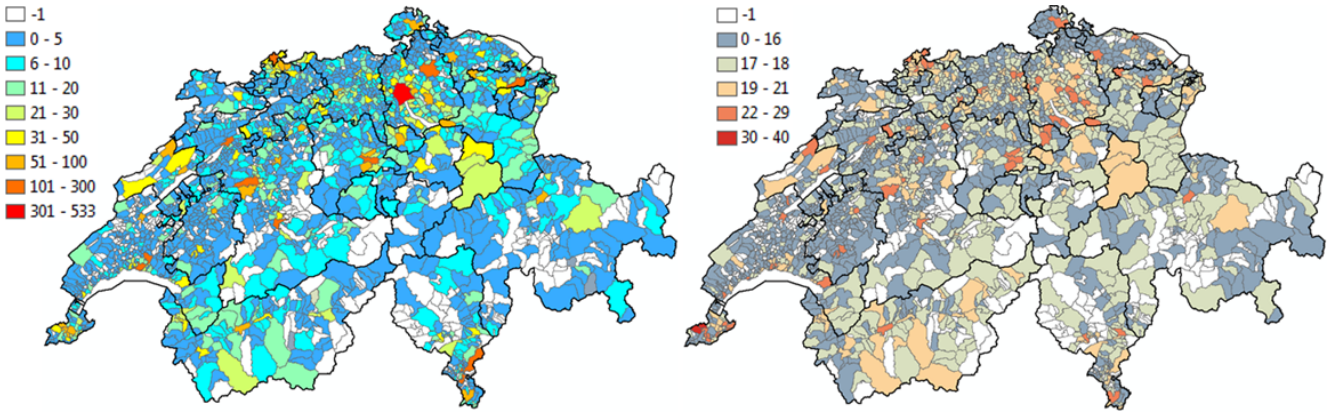

Figure 3: Left: Solar PV Potential map for June, in MW. Right: c_R map (portion of footprint area available on rooftop), in percentages (-1 is for unconsidered communes).

CONCLUSION

A Machine Learning methodology coupled with ArcGIS has been used to estimate rooftop solar PV potentials for 1895 communes in Switzerland. The ML methodology is very useful for considering a significant range of parameters when estimating solar irradiances and additional characteristics with reasonable errors. To the best of our knowledge, such a scale for estimating solar PV potentials has not been considered before for Switzerland. Given the level of aggregation (commune) and the the amount of data available, several assumptions and approximations had to be made. There are several limitations regarding the data and the methods of estimation which needs to be addressed in the future. Some of these limitation are as follows: (i) the inconstistency between different data sources for communes, buildings and population, resulting in several communes not considered, (ii) the lack of precise data for other cantons in Switzerland apart from Geneva, which causes the question of generalization to all other communes in Switzerland; (iii) here only the urban areas defined by CORINE Land Cover are considered, meaning that buildings in the rural areas might be missing in this study. While the aggregation results at commune level are very useful and have implications for planning and policy making, estimating the rooftop solar potentials at the neighborhood level is also necessary. In the future we plan to extend these results to the pixel level so as to make them more accurate.

ACKNOWLEDGEMENTS

This work is part of the SCCER Future Energy Efficient Buildings and Districts (FEEB&D) supported by the Commission for Technology and Innovation (CTI).

REFERENCES

1. Izquierdo, S., Rodrigues, M., and Fueyo, N.: A method for estimating the geographical distribution of the available roof surface area for large-scale photovoltaic energy-potential evaluations. *Solar Energy*, 82(10):929–939, Oct. 2008.
2. Wiginton, L., Nguyen, H., and Pearce, J.: Quantifying rooftop solar photovoltaic potential for regional renewable energy policy. *Computers, Environment and Urban Systems*, 34(4):345–357, 2010.
3. Steinmeier, C.: Corine land cover 2000/2006. 2013.
4. Cortes, C. and Vapnik, V.: Support-vector networks. *Machine Learning*, 20(3):273–297, 1995.
5. Ratto, P. T., Reise, C., Remund, C., Wald, L., Albuisson, M., Best, C., Delamare, C., Gaboardi, E., Hammer, A., Heinemann, D., Kift, R., Lefvre, M., Leroy, S., Martinoli, M., Mnard, L., Goot, E. V. D., Vanroy, F., and Webb, A. Soda: a web service on solar radiation.
6. Klein, S.: Calculation of monthly average insolation on tilted surfaces. *Solar energy*, 19(4):325–329, 1977.
7. Klucher, T. M.: Evaluation of models to predict insolation on tilted surfaces. *Solar energy*, 23(2):111–114, 1979.

SOLAR ENERGY FOR ZERO ENERGY BUILDINGS – A COMPARISON BETWEEN SOLAR THERMAL, PV AND PHOTOVOLTAIC-THERMAL (PV/T) SYSTEMS

C. Good; I. Andresen; A.G. Hestnes

Norwegian University of Science and Technology (NTNU), Department of Architectural Design, History and Technology, Alfred Getz vei 3, NO-7491 Trondheim, Norway

ABSTRACT

In a net zero energy building, the energy needed to operate the building is met by renewable energy generated on site. Buildings require energy both in the form of heat and electricity, and hybrid photovoltaic-thermal (PV/T) modules are therefore an interesting technology for building applications. This paper describes a comparative simulation study of solar thermal, photovoltaic (PV) and PV/T systems on a Norwegian residential building model, with the objective to reach net zero energy balance. The results show that PV/T systems can reach a higher energy output than separate solar thermal and PV installations, but the building with only state-of-the-art PV modules and no thermal collectors gets closest to meeting the nZEB requirements.

Keywords: net zero energy building, PV/T, PV, solar thermal, import/export balance

INTRODUCTION

Buildings account for around a third of the global energy use. Making buildings more energy efficient is therefore an important tool in the effort to reduce global greenhouse gas emissions. In a net zero energy building (nZEB), the amount of energy required to operate the building is generated by renewable energy sources on or near the building [1]. During a specified period of time, typically a year, the building reaches a net zero energy balance.

Utilization of solar energy is one of the main strategies used for on-site renewable energy generation. Buildings require energy both in the form of heat and electricity during operation, which can be provided by solar thermal collectors and photovoltaic (PV) modules. In projects with ambitious energy targets or limited available area for installations, solar thermal collectors and PV modules may be competing for the available space on the buildings' roof and facades.

PV/T modules

In a hybrid photovoltaic-thermal (PV/T) module, electricity and heat are generated simultaneously. This can lead to a high total efficiency per module area and possibly a reduced use of space compared to separate systems. PV/T technology has so far not had a commercial breakthrough comparable to that of PV or solar thermal, but the interest in the technology is increasing, especially in connection to low or zero energy buildings [2].

PV modules convert only around 10-20 % of the radiation to electricity, while the rest is reflected or dissipated as heat in the module. The basic idea behind PV/T technology is to utilize more of the incoming solar radiation by also harvesting the waste heat from PV modules. Since PV cell efficiency typically decreases with increased cell temperature, removing the waste heat can also lead to an increased electricity output.

A number of PV/T technologies are available. For flat plate PV/T modules, a basic distinction can be made between covered and uncovered modules. Simply put, an uncovered PV/T module is a PV module with cooling. It produces an equal or larger amount of electricity than a regular PV module, and in addition some low-temperature heat. A covered PV/T module is similar to a solar thermal collector with added PV cells. Since the extra cover prevents heat loss from convection, this type of module has a higher heat output than an uncovered one. A recent market study from Germany found 41 producers of PV/T modules, out of which 30 were marketing uncovered modules [3].

This paper describes a comparative simulation study of solar thermal, PV and PV/T systems, applied to the case of a Norwegian low energy residential building. The goal is to achieve a zero energy balance. The energy yield of the different systems are analysed and compared, and the building energy balance is calculated.

The building model

The building model used in the simulations is based on a concept building model developed at the Research Centre on Zero Emission Buildings (the ZEB Centre, www.zeb.no) in Trondheim, Norway. The model represents a state of the art Norwegian building, and is designed to meet the requirements of the Norwegian passive house standard [4]. The material use, embodied energy and emissions, HVAC, technical details and energy performance of the concept building model is well documented and is presented in [5].

The ZEB concept building model is a two-storey residential building with 160 m^2 heated floor area, located in Oslo in Southern Norway (59.53° N, 10.41° E). It has a simple rectangular design with a flat roof, and a footprint of 8 x 10 m (the longer sides facing north and south). Meteonorm [6] data is used in the simulation. The annual solar irradiation on an optimally inclined surface (45° south-facing) in Oslo is around 1150 kWh/m^2, and the average ambient temperature 6.3°C. The largest fraction of the solar radiation is available in the summer, when the heating demand is low, but during spring and autumn significant irradiance levels and heating demand occurs at the same time.

The energy need of the building is shown in Table 1, as determined in [5]. During the winter months, the space heating dominates, while no space heating is needed during t May to August. The DHW energy need is relatively constant during the year, as are the electricity needs. The energy needed for domestic hot water (DHW) and electricity are specified in accordance with standard values from the Norwegian standard NS 3031 [7], as are the internal heat gains from people and equipment.

Table 1: The energy need of the building as determined in [5]

Energy need	kWh/year	kWh/m2 year
Space heating	3349	20.9
Domestic hot water	3811	23.8
Electricity	4074	25.5
Total	11234	70.2

The storage tank is the centre of the buildings heating system. The solar thermal system (or thermal part of the PV/T system) is connected to the lower part of the tank with an internal heat exchanger. An air-to-water heat pump provides the auxiliary energy by feeding the upper or middle part of the tank directly, based on the required temperature. The building has a low temperature hydronic heating system with floor heating and radiators, with feed/return temperatures are 25/35°C and 30/40°C respectively. The required volume for DHW is heated

in a tank-in-tank system. The delivery temperature is 45°C at the tap, with a 55°C set point temperature in the tank. Legionella growth is prevented by heating the tank to 70°C weekly.

METHOD

Comparative study

Three versions of the building (A, B and C) are simulated to study the performance of different solar energy systems for zero energy buildings. The simulations are based on a model of the building and HVAC system which is further described in [5]. Building A has a system with a combination of solar thermal collectors and PV modules, and represents the original design of the building model. Building B has a system of PV/T and PV modules, and building C has only PV modules installed. The hydronic heating system is the same in all versions of the building, except for the dimensions of the tank and piping.

The boundary condition used in this study is the area of the roof (80 m^2) and the design objective of the installation is to reach a net zero energy balance over on year. Installing solar energy systems on flat roofs, especially in northern regions, requires that row-to-row shading is considered. It was calculated that only two rows of modules could be installed on the roof at a close to optimal tilt angle of 45°. Performance data and dimensions from modules available on the market have been used in the study. It is assumed to be are no restrictions (in time or power) on the electricity exchange with the grid. In the case of thermal energy, the generated energy from the solar collectors is only useful if it can be used directly or stored; in the latter case given that the storage is not fully loaded. The usefulness of the solar thermal output also depends on the temperature of the energy carrier.

Table 2: The characteristics of the solar modules used in the simulations.

Module	Technology	Gross area [m2]	Electric efficiency at STC* [%]	Optical efficiency η0 [%]
ST	Flat plate	2.0	-	80.0
PV	Poly-Si	1.65	15.8	-
PV/Ta	Mono-Si, uncovered, uninsulated	1.64	17.4	61.4
PV/Tb	Poly-Si, covered, insulated	2.26	12.0	71.5

**Standard test conditions: 1000 W/m^2, spectrum AM 1.5, 25°C cell temperature*

The solar thermal collectors and PV modules used in the simulation are selected to represent the average of products that are available on the market in terms of performance. The market for PV/T modules is still relatively small, and the quality of a PV module depends both on the thermal and electric performance it is difficult to find a module that represents the market average. In an attempt to account for these differences, two different PV/T modules were used in the simulations: a PV/T module with good electric performance (PV/Ta), and a covered PV/T module with good thermal performance (PV/Tb). An overview of the module characteristics is given in Table 2.

Zero energy balance

There are several ways of calculating the energy balance of a nZEB, depending among other things on the system boundary and weighting factors for different energy sources that are used. A proposal for a consistent definition was presented by Sartori et al [8].The annual import/export balance is used in the present case. That is, the balance is calculated between energy delivered, or imported, to the building ($E_{delivered}$) and the energy exported from the building ($E_{exported}$). The energy balance is then calculated according to equation (1).

$$E_{net} = |E_{exported}| - |E_{delivered}| \quad (1)$$

The balance in this case is calculated with total annaul values. A net zero energy balance is reached if E_{net} (kWh) is zero or positive. Since the auxiliary energy to the heating system of the building is provided by a heat pump the only form of delivered energy is electricity. No weighting factor is therefore necessary in this case.

The solar fraction (SF), i.e. the fraction of the thermal energy demand of the building that can be covered by the solar thermal and PV/T systems can be calculated according equation (2), where Q_{sol} (kWh) is the thermal energy from the solar energy system, Q_{dem} (kWh) is the thermal energy needed for space heating and DHW.

$$SF = \frac{Q_{sol}}{Q_{dem}} \quad (2)$$

RESULTS

The simulations are performed in the program Polysun from Vela Solaris, which is a dynamic simulation tool for solar energy solutions[9]. The main parameters used in the simulations for buildings A, B and C are shown in Table 3. In addition to the modules described above, two systems with state-of-the-art solar thermal collectors and PV modules were added (A* and C*). The differences in total installed areas are due to the use of real module dimensions are been used.

Table 3: The main parameters of the simulated system variants.

System	Description	Installed area ST/PVT/PV [m^2]	Rated electric power [kWp]	Tank volume [l]
A	ST and PV	10/0/21	3.4	1200
B1	Only PV/Ta	0/30/0	5.1	1800
B2	PV/Tc and PV	0/21/11	4.6	600
C	Only PV	0/11/18	4.7	0
A*	State-of-the-art (ST and PV)	0/8/23	4.7	1200
C*	State-of-the-art (only PV)	0/0/30	6.0	0

The annual thermal and electricity output in of the systems are shown in Figure 1, measured in kilowatt hours. The systems with highest thermal energy output (A, B3 and A*) are also the system with the highest total output with this way of calculating. The solar fraction (SF) of the thermal energy demand is shown in Table 4, together with the import/export energy balance calculations. None of the system reaches net zero energy balance ($E_{net} > 0$). The system that is closest to reaching a balance is system C*, with only state-of-the-art PV modules and no thermal collectors. This system meets 87% of the delivered electricity with exported solar electricity.

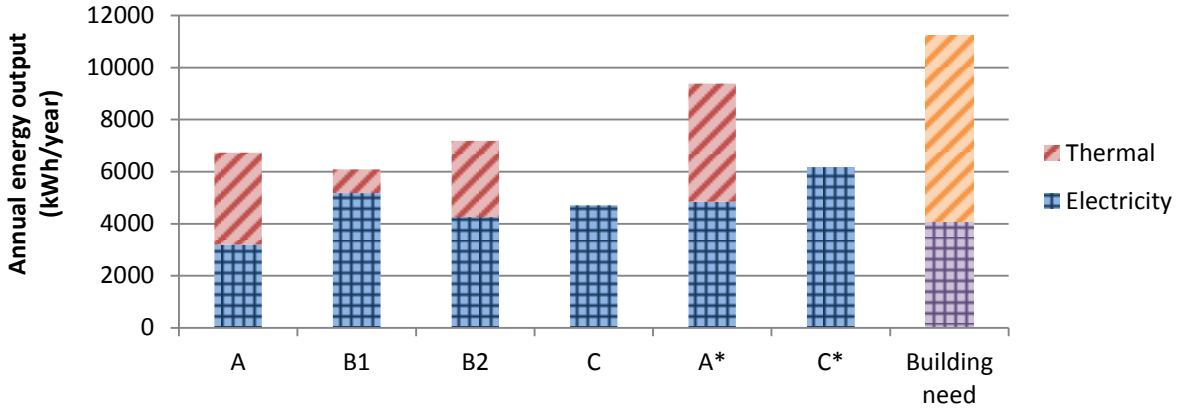

Figure 1: The annual thermal and electricity output of the different systems. The rightmost column shows the thermal and electric energy need of the building.

The state-of-the-art system with solar thermal and PV (A*) has the highest solar fraction, and is the second closest to reach a balance with 82% of the delivered energy met by on-site electricity. Of the studied systems with PV/T, the uncovered PV/T system in B1 is the closest to a balance, with 71% of the delivered electricity met by solar generated electricity. Due to the use of a heat pump for auxiliary energy, the systems with high electricity output are favoured in this calculation.

Table 4: The thermal solar fraction and annual energy balance calculations of the systems. A negative value of E_{net} means that the building has not reached a zero energy balance.

System	SF [%]	E_{net} [kWh]	$E_{exported}$/ $E_{delivered}$ [%]
A	42	-3 044	51
B1	10	-2 112	71
B2	37	-2 022	68
C	0	-2 414	66
A*	53	-1 047	82
C*	0	-945	87

DISCUSSION

The idea that hybrid PV/T modules would be able to perform better than a side by side installation of PV modules and solar thermal collectors is supported by the results of this study. However, the system with state-of-the art PV modules only comes closest to reaching a net zero energy balance. The number of different modules studied here is small, as is the number of available PV/T modules on the market. No far-reaching conclusions on PV/T technology can therefore be drawn from these results.

The system with uncovered and uninsulated PV/T modules (B1) has a higher electric yield than the one with average quality PV modules (C). However, it should be noted that the efficiency of the PV modules used here is slightly lower than that of the PV/Ta modules. The thermal output of system B1 is small and of low temperature, which means that an auxiliary heat source is necessary also during summer. Built examples from suggest that uncovered PV/T modules perform well in systems with ground source heat pumps, where the low temperature output can be used to recharge the ground storage, or as direct input to the heat pump when the temperature level is sufficient.

System B2, with a combination of PV and covered PV/T performs slightly better than system A with average solar thermal and PV, suggesting that covered PV/T modules could be

suitable for smaller residential systems, like the one studied here. However, as Adam et al. [3] found in their market survey, the number of market-available covered PV/T modules is very small. The validity of the performance data for PV/Tb module is therefore quite uncertain. A limiting factor for this technology is the high demands on module materials, which has to endure significant changes in temperature without degradation or damage.

In this study the import/export balance was calculated on a yearly basis, which means that self-consumption is not taken into account. Further work will be to include electricity use profiles in the calculation to evaluate the load match. Since an air-to-water heat pump was used as auxiliary energy source, the import/export balance included only electricity. Further work will be to consider other heat sources, such as bio energy, which requires use of weighing factors in the energy balance calculations. In addition, further work will focus on the greenhouse gas emission balance of the systems, which includes the embodied emissions of the different solar energy technologies. Alternative module layouts, e.g. a larger number of modules but at a at lower tilt angle, will also be considered in further studies.

CONCLUSION

A comparative simulation of solar energy systems on a Norwegian building model has been performed, with the objective to reach a net zero energy balance over one year. The building model is a Norwegian passive house, located in Oslo. The study looked at different combinations of solar thermal collectors, PV modules and hybrid PV/T modules in different, installed at 45° on the flat roof of the building. The annual import/export energy balance was used to calculate the zero energy balance. Since the auxiliary energy was provided by an air-to water heat pump, only electricity was considered in this balance. In this study, none of the solar energy systems managed to meet the energy demand, and a net zero energy balance was not reached in any of the versions of the building. The system that was closest to reach a balance included only state-of-the-art PV modules and no thermal collectors. Of the PV/T systems, the uncovered, uninsulated system came closest to the zero energy balance in this example, although the total energy output measured in kWh was highest from the covered PV/T system.

REFERENCES

1. Marszal, A.J., et al., *Zero Energy Building – A review of definitions and calculation methodologies.* Energy and Buildings, 2011. **43**(4): p. 971-979.
2. Chow, T.T., G.N. Tiwari, and C. Menezo, *Hybrid solar: A review on photovoltaic and thermal power integration.* International Journal of Photoenergy, 2012. **2012**.
3. Adam, M., H.P. Wirth, and R. Radosavljevic, *PVT-Marketsubersikt*. 2014.
4. Standard Norge, *NS 3700 - Criteria for passive houses and low energy houses - Residential buildings*. 2013, Standard Norge: Lysaker.
5. Houlihan Wiberg, A., et al., *A net zero emission concept analysis of a single-family house.* Energy and Buildings, 2014. **74**: p. 101-110.
6. Meteotest, *Meteonorm Database*. 2009.
7. Standard Norge, *NS 3031:2011 - Calculation of energy performance of buildings - Method and data*. 2011, Standard Norge: Lysaker.
8. Sartori, I., A. Napolitano, and K. Voss, *Net zero energy buildings: A consistent definition framework.* Energy and Buildings, 2012. **48**: p. 220-232.
9. Vela Solaris AG, *Polysun Simulation Software*. 2012, Institut für Solartechnik SPF: Rapperswil.

A HYBRID FACADE THAT COMBINES AN ALGAL BIOREACTOR WITH PHOTOVOLTAICS

T. Granata, M. Krehel, S. Wittkopf and M. Egli
Lucerne University of Applied Sciences and Arts (HSLU), Technikumstr 21 CH-6048 Horw

ABSTRACT

For an algal facade that is operated as a flat plate bioreactor, the biomass in the facade is capable of producing energy as oil, or through methane digestion of the cells, while absorbing radiation that would heat the building. However, an algal facade could also produce electricity if coupled to a photovoltaic (PV) module.

Experiments were conducted with a PV module situated behind a flat plate, algal bioreactor to determine the relative power output for such a hybrid facade compared to a PV module without the algal layer. Two container materials were tested (polypropylene and acrylic), for two algal species (a green algae and a coccolithophore), at 4 biomass concentrations. The containers were two rectangular boxes with a volume of 0.4 liters and 1 liter, corresponding to path lengths (i.e. thicknesses) of 0.9 cm and 2.8 cm, respectively. Experimental results were presented as attenuation coefficients versus algal biomass, photovoltaic power output versus scalar irradiance, and modeled power output based on biomass concentration and container thicknesses.

The acrylic container transmitted more light than the polypropylene and had statistically lower attenuation coefficients. Water in both container types had a minor contribution to attenuation while algal concentrations gave high attenuation. The highest attenuation occurred for the green algae and was a result of increased pigments. The highest coccolithophore concentration, in combination with the shorter path length, produced 95% of the maximum PV power output. Generally, power output increased with decreasing algal concentration since more light was transmitted to the PV module.

The amount of light transmitted through the container to the PV module was modeled based on light attenuation by algal biomass and container thickness. Using the model for full sunlight, we determined that with high algal concentrations and realistic facade thicknesses, high power output can be achieved from PV modules in parallel with algal growth. The next step is to build a prototype facade to assess the effect of full sunlight under these design criteria, as well as the effect of heat dissipation by the facade.

Keywords: hybrid algal facade, integrated photovoltaics, light attenuation

INTRODUCTION

Since visible light can pass through transparent facades, it is feasible to use them as algal bioreactors to create living buildings that can produce energy from biomass. Spectral light transmission through transparent facades is strongly dependent on the angle of light and the color of the facade material, with clear glass transmitting >80% of the visible spectra (400-700 nm) at angles $\leq 20^{o}$ [1]. Additionally, the thickness of the facade will attenuate light. In 2013, the first commercial algal facade, covering the surface a building, was unveiled in Hamburg, Germany [2]. Recently other designs for algal facades have been proposed [3, 4].

Commercial algal bioreactors come in various sizes (1 to 10^{6} L) and shapes (e.g. cylinders, flat plates, coils, trapezoidal channels) and are used to produce oil (i.e. lipids) for biofuels, and other compounds for pharmaceuticals and food supplements [5]. Smaller algal

bioreactors, between 200 L and 1000 L, with high illuminated surface to volume ratios, are the most productive and can achieve high oil yields [6]. One of the most efficient bioreactors for algal facades is a flat plate reactor, which has a large, rectangular surface area and thicknesses from 0.1 to 10 cm [7, 8]. A flat plate bioreactor maximizes the illuminated surface area and minimizes the light path length, such that even with high light attenuation by algae, sufficient light is transmitted through the bioreactor to promote high algal growth rates.

In this paper we present data that demonstrate that light passing through an algal bioreactor is utilized by a photovoltaic module to generate electricity. We use these data in a model to examine parameters for a full scale, hybrid algal facade capable of producing biofuel from algal oil, electricity from a PV module, and which may have implications for heat dissipation from the building envelope.

METHODS

The experiment consisted of placing transparent containers (i.e. bench scale facades) with medium and algae, on top of a 20 cm x 20 cm mono-crystalline, single-cell PV module (rated at 4 W for STP and 1000 W m^{-2} radiance) on a level bench and measuring both spectral and scalar light transmission through the containers, as well as the power generated from the PV module. Two container materials were tested (polypropylene and acrylic), for two algal species (a green algae and a coccolithophore) each at 4 biomass concentrations. The control was a container without algae, only the salts and algal nutrients (i.e. medium). The containers were two rectangular boxes with a volume of 0.4 L (polypropylene) and 1 L (acrylic), corresponding to path lengths (i.e. thicknesses) of 0.9 cm and 2.8 cm, respectively. The containers were laid flat on the PV module such that they extended beyond the edges of the PV module, ensuring that only light passing through the container impinged on the PV module and thereby avoiding edge effects. Measurements were done from high to low algal concentrations by successively diluting each sample with sterile media to attain the desired concentration.

Containers were oriented perpendicular to a light source, which simulated solar radiation using an array four of small halogen flood lamps (2000 W, 3000 K) surrounding one large lamp (1000 W, 6000 K) all hung from the ceiling. Spectral light was measured every 10 nm for visible wavelengths (400-700 nm) using a spectrometer. Scalar measurements of photosynthetically active radiation for plants, PAR, were taken with a quantum meter set to detect light from an electronic source. The total scalar irradiance on the container surface was 490 μE m^{-2} s^{-1} and varied only 4% during the experiment.

Attenuation of light in the containers was calculated from the Beer-Lambert Law as,

$$k = -\frac{ln\frac{I_z}{I_0}}{z} \quad (1)$$

where I_z was the light measured leaving the container, I_0 was the light measured impinging on top of container, and z was the container thickness. Total attenuation was given by the sum of individual attenuation coefficients based on water, container material, and algal type and biomass concentration,

$$k = k_{water} + k_{container} + k_{algae} \quad (2)$$

Graphics and ANOVA statistics were done using Kaleidagraph (v4.5) software.

RESULTS

The acrylic control container transmitted more light than the polypropylene control for thickness of 0.9 cm (95% vs. 84%) and 2.8 cm (90% vs. 73%) and had statistically lower attenuation coefficients (df=7, F=19.6, P=0.007, Table 1). There were no statistical differences in attenuation coefficients based on container thickness for either the polypropylene (P=0.101) or the acrylic (P=0.43) controls, indicating that the path length through water (medium) in the containers had a minor contribution to attenuation.

Table 1. Attenuation coefficients for algal biomass and controls (no algae).

	% Biomass Concentration	Biomass (10^6 Cells L^{-1})	K (polypropylene) (cm^{-1})	K(acrylic) (cm^{-1})
Control container*				
z=0.9 cm		0.0	0.150	0.067
z=2.8 cm		0.0	0.102	0.042
Algae container				
Coccolithophore	100	5.00	0.185	0.091
	50	2.50	0.127	0.047
	18	0.90	0.095	0.023
	7	0.36	0.082	0.012
Green	100	2.00	0.225	0.084
	40	0.80	0.185	0.081
	16	0.32	0.120	0.047
	6	0.13	0.082	0.011

* Containers with medium were used as controls.

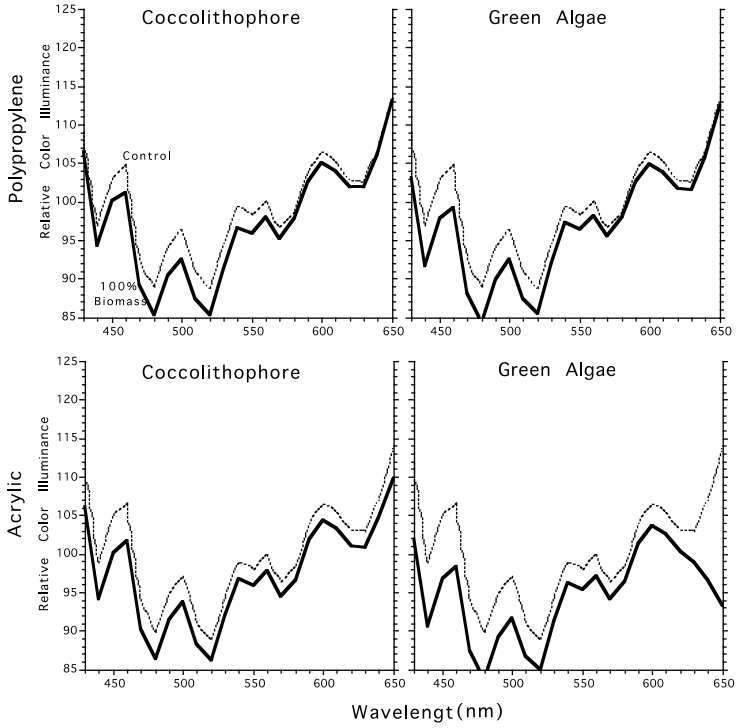

Figure 1. Spectral light transmission for cococlithophore (left) and green algae (right) in the polypropylene (top) and acrylic (bottom) container for the control with water (dashed line) and the 100% biomass concentration (solid line).

The polypropylene control had lower light transmission in the blue wavelengths (400-450 nm) than the acrylic control container, however, both controls had higher transmission than

algae at all wavelengths (Figure 1). Both algal types had strong attenuation in the blue spectral band (430-480 nm), although the green algae also attenuated in the other bands (i.e. green, yellow, and red).

The highest algal biomass concentrations produced the highest attenuation coefficients and as algal concentrations decreased, light attenuation also decreased (Table 1, Figure 2). The polypropylene container consistently had higher attenuation than the acrylic one, for all but the most dilute coccolithophore and green algae biomass concentrations (Figure 2). Green algae attenuated more light than the coccolithophore at all biomass concentrations (Figure 2).

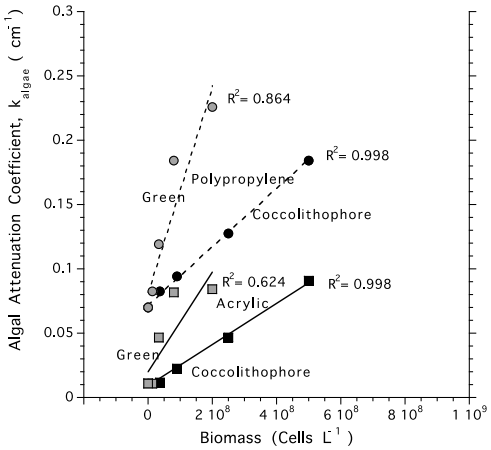

Figure 2. Attenuation coefficients versus algal biomass for coccolithophore (black) and the green algae (grey) and polypropylene (circles, dashed lines) and acrylic (squares, solid lines) containers, *where regression lines indicate the best fit.*

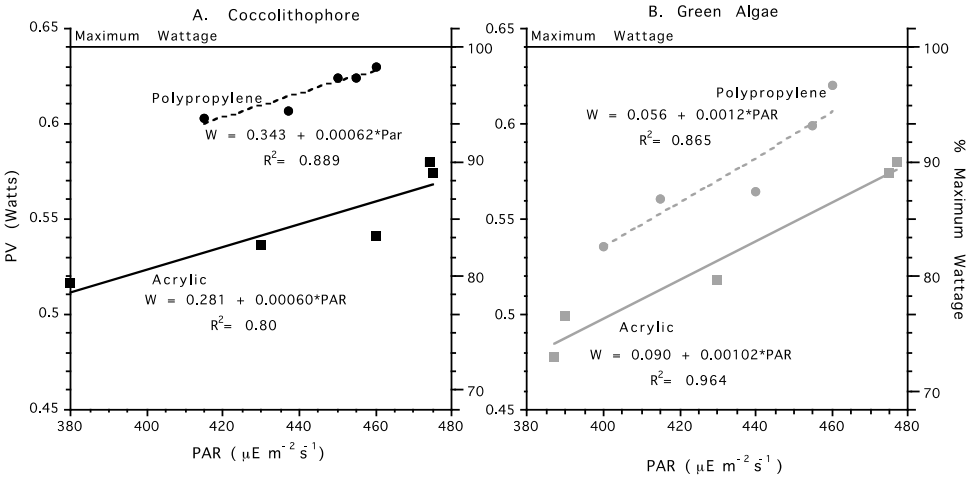

Figure 3. Photovoltaic power output as Watts (left y-axis) and percent maximum wattage (right y-axis) versus scalar irradiance (PAR) for: A. coccolithophore (black) and B. green algae (grey) in polypropylene (circles, dashed lines) and acrylic (squares, solid lines) containers. Regression lines and equations indicate the best fit. The solid horizontal line is the maximum wattage produced by the PV module with no containers.

Reducing the algal concentration resulted in reduced attenuation of light with concomitantly higher power outputs for the PV module for both container types (Figure 3). The 0.9 cm container transmitted more light and therefore produced more power than the 2.8 cm container for both the coccolithophore (Figure 3A) and green algae (Figure 3B). However, the coccolithophore had a higher power output than the green algae for the same container thickness.

The highest coccolithophore concentration, in combination with the shorter path length (0.9 cm), produced 95% of the full PV power output, while the highest green algae concentration at the shorter path length produced 84% of the maximum power. Even with the thicker container (2.8 cm), the highest algal concentrations produced 80% and 73% of the maximum power for the coccolithophore and green algae, respectively.

DISCUSSION

As discussed by Caram et al. [1], different facade materials attenuate light differently. In our work, the polypropylene container transmitted less light than the acrylic container. When algae biomass was added to the container, light transmission decreased further and attenuation increased for all but the most dilute algal biomass concentrations. The high attenuation by algae can be attributed to light absorption by photosynthetic pigments. The fact that the green algae had more pigments and was larger (7 μm) than the 3 μm coccolithophore, explains why it also had higher attenuation coefficients at similar biomass concentrations. Additionally, the spectral signatures of visible light attenuation coincided with known absorption spectra of the green algae and coccolithophore. However, algal attenuation is a result of both absorption of light by pigments and scattering of light off the cell surface [9]. Since only bulk attenuation was measured, we were not able to separate these two variables.

Even though the 2.8 cm acrylic container had lower attenuation, it let less light through than the 0.9 cm polypropylene container because it was thicker. The result of this thicker container was a longer light path, and so higher numbers of algal cells intercepting and absorbing light over the path length. Therefore, the power output from the PV module was a function of the container thickness, the algal concentration, and to some extent the container material.

A model of light attenuation in an algal facade can be parameterized as:

$$I_z(\lambda) = I_0(\lambda)e^{-k(\lambda)z} \quad (3)$$

where $I_0(\lambda)$ is the spectral irradiance at wavelengths, λ, impinging on the facade surface, $I_z(\lambda$ is the spectral irradiance passing through the facade of thickness z (i.e. front to back) and $k(\lambda$ is the spectral attenuation coefficient that accounts for the reduction of irradiance as the light passes through an algal. The scalar (PAR) form of equation 3 would be the same except irradiance would be integrated over the visible spectrum as,

$$I_{PAR} = \int_{400\,nm}^{700\,nm} I(\lambda)\, d\lambda \quad (4)$$

Using attenuation coefficients from Table 1, modeled PAR irradiances were calculated from equations 3 and 4 and used in the regression equation for power as a function of PAR for coccolithophore biomass, *PAR*(*B*), $Watts = 0.343 + 6.2x10^{-4}\ PAR(B)$ (Figure 3A), in order to determine the power generated from a prototype facade with a PV module.

The model shows that at a biomass concentration as high as 10^{11} cells L^{-1}, 78% of the maximum PV power is generated for a 0.1 cm thick facade (Figure 4). For thicknesses < 0.25 cm, enough light is transmitted to generate > 50% of the maximum PV power. The advantage of maintaining high algal concentrations is that higher yields of algal oil can be produced per unit volume of facade. Therefore, it should be possible to optimize oil production by the algae and power production by the PV panel, as well as heat dissipation by the facade. This model, however, assumes that the regression equation and *k* values are the same for a full-scale facade as for the laboratory containers. This assumption, however, must be validated for a full scale (1 m^2) facade exposed to solar irradiance and under

controlled conditions. Still, these results indicate the necessity of further research to determine if a hybrid algal facade can be deployed on buildings to provide electricity and heating oil.

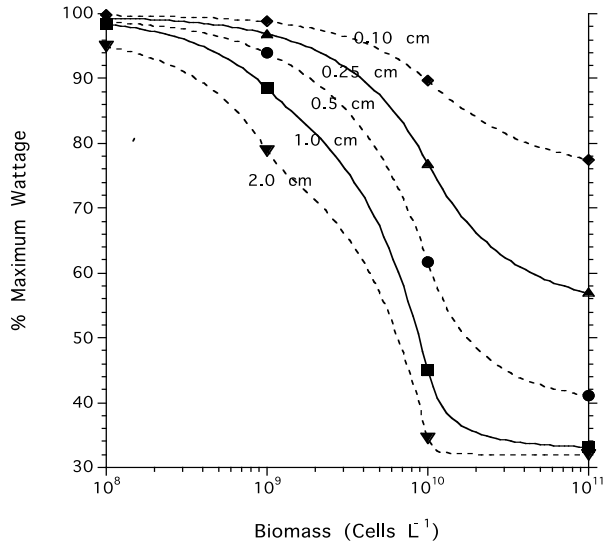

Figure 4. Modeled PV power output versus coccolithophore biomass concentration for facade thicknesses from 0.1 cm to 2.0 cm.

REFERENCES

1. Caram, R.M., J. Pizzutii, L.C. Labaki, and E.P. Sichieri: Evaluation of solar radiation transmission through transparent facades. http://www.academia.edu/3068158/Evaluation_of_Solar_Radiation_Transmission_Through_Transparent_Facades, 2014.
2. IBA Hamburg: Smart materials house, BIQ. In: International Building Exhibition Hamburg, 2013, White Paper, 2013.
3. Ratii, C.: The urban canopy. http://www.carloratti.com/project/algaetecture/, 2014.
4. Kim, K-Y.: Beyond green: growing algae facade. In: Architecture Research Center Consortium 2013-The Visibility of Research Sustainability: Visualization Sustainability and Performance, 500-505. www.arcc-journal.org/index.php/repository/article/view/211/160, 2014.
5. Borowitzka, M.A.: Commercial production of microalgae: ponds, tanks, tubes, and fermenters. Journal of Biotechnology, 70: 313–321, 1999.
6. Granata, T.: Dependency of microalgal production on biomass and the relationship to yield and bioreactor scale-up for biofuels. Energy Science & Engineering, in review, 2015.
7. Tredici, M.R., P. Carlozzi, C.G.Zittelli, and R. Materassi: A vertical alveolar panel (VAP) for outdoor mass cultivation of microalgae and cyanobacteria. Bioresource Technology, 38: 153-159, 1991.
8. Richmond, A. and Z. Cheng-Wu: Optimization of a flat plate glass reactor for mass production of *Nannochloropsis* sp. Journal of Biotechnology, 85(3): 259-269, 2001.
9. Mobley, C.D.: Optical properties of water. Chapter 12. In: Handbook of Optics, Ed. M. Bass, McGraw-Hill Inc., 1994.

OPTIMIZATION OF CONCURRENCY OF PV-GENERATION AND ENERGY DEMAND BY A HEAT PUMP – COMPARISON OF A MONITORED BUILDING AND SIMULATION DATA

Monika Hall[1]; Achim Geissler[1]

[1] *University of Applied Sciences and Arts of Northwestern Switzerland, Institute Energy in Building, St. Jakob-Strasse 84, CH - 4132 Muttenz, Switzerland*

ABSTRACT

Monitoring data of a small, well-insulated residential building shows that the electricity consumption of the heat pump amounts to approx. 30% of the total electricity consumption of the building. Shifting duty cycles of the heat pump into the daytime would therefore be a possible means to greatly increase the concurrency of electricity production and consumption and reduce the grid interaction without an expensive technical effort. Experimentally, the duty cycle of the heat pump is limited to daytime from 10 am through 7 pm. The monitored data shows this is sufficient to heat the building and the domestic hot water.

Interesting questions that arise are e.g. if such run-time limitations can also be used with a heavy (concrete) and a lightweight (wood) construction and if further reduction of the run-time is possible. Reducing run-time even more would further increase self-consumption and reduce grid interaction. The impact of the thermal mass of the construction and the limiting of the run-time are investigated by transient thermal building simulation. The simulation model with constructions "as built" is calibrated based on measurement values from temperature sensors in the living rooms and the measured heating demand of all three apartments. Simulation results are evaluated based on thermal comfort criteria in the living rooms of each apartment.

The results obtained show that for the construction types "as built" and "heavyweight" no differences in resulting thermal comfort are to be expected. Construction types "as built" and "heavy weight" show good robustness in regard to the limitation of the run-time of the heat pump. The construction type "lightweight" cannot be used with limited run-times of the heat pump without a significant drop in thermal comfort as defined by the metrics used. The paper gives detailed results for the mentioned construction types and 4 different run-time scenarios.

Keywords: Building simulation, self-consumption, heat pump, energy flexibility, thermal mass

INTRODUCTION

Due to the necessary increase of renewables the amount of volatile electricity based on solar and wind power being fed into the grid must be expected to increase, also. This will lead to big challenges in regard to the stability and capacity of the grid. In order to mitigate this effect, the direct consumption or storage of electricity based on renewables at the site of production seems prudent. In order to be able to increase the self-consumption of buildings, these must have certain flexibility in regard to their energy demand. Such flexibility must consider thermal comfort.

Measurement data gained from a small, well-insulated multi-family dwelling shows that the self-consumption of electricity generated on site by photovoltaic panels (PV) was approx. 28 % between September 2011 and April 2012 during daytime hours from 10 am to four pm each day [1]. During the remaining hours of the day, approx. 27 % of the overall electricity consumption could be attributed to the heat pump. This shows that the heat pump is the largest single consumer of electricity and therefore most promising in regard to shifting loads

into daytime hours and thus increasing self-consumption. Consequently, the run-time of the heat pump was constrained to 10 am through seven pm starting February 2013. This resulted in a shift of approx. one MWh from nighttime to daytime hours. The overall self-consumption was thus increased from 21 % (winter 2011/2012) to 34 % (winter 2013/2014). Also, the efficiency of the heat pump was increased. This is due to a reduction in the number of on-off cycles. The heating efficiency increased from 3.8 to 4.9 and the DHW efficiency increased from 3.6 to 3.9 [2]. No decrease in thermal comfort was found, even though the restriction meant that the heat pump was off 15 consecutive hours per day. The temperature decrease in the building was found to be about 1 K [1].

In the work described below, the potential of heavy weight and lightweight buildings in regard to run-time constraints is evaluated. The work is based on transient thermal building simulation. Simulation model details can be found in [3].

METHODOLOGY

General

The building performance simulation model is set up based on design values and wherever possible actual values taken from the known building usage (ESP-r [4]). The measurement data available consists of various electricity consumption values in a time-step resolution of 15 minutes. The simulation model is calibrated and validated with measurement values from the period February 10th 2013 through March 11th 2013. The ambient air temperature in this period is 1.8 ± 4.7 °C with minimum and maximum values of -12 °C and 17 °C, respectively. For validation purposes, the values measured with the temperature sensor “living room” (Figure 1) and the measured useful heat consumption are used.

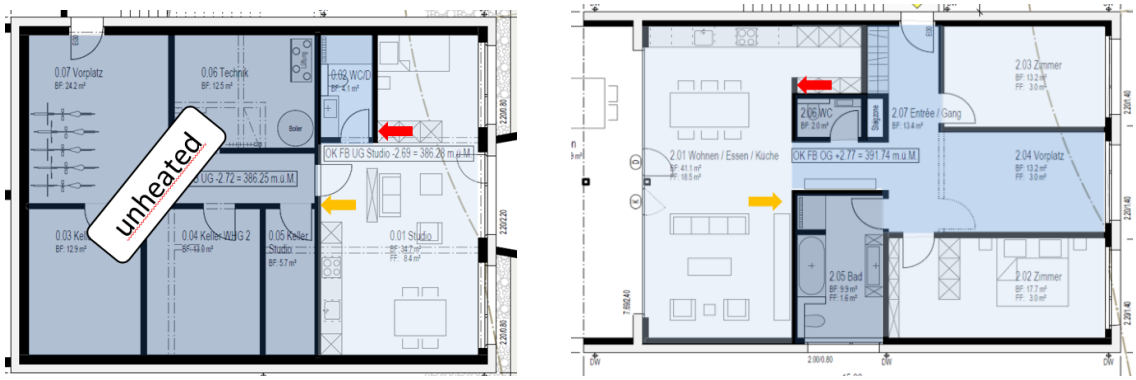

Figure 1: Layout of thermal zones for ground floor (left hand side) and first/second floor (right hand side). Positions of the temperature sensor (red) and the heating thermostat (orange) in the living rooms are given (© Setz Architektur).

Building Details

The building considered in this paper is a well-insulated small multi-unit dwelling in the Canton of Aargau, Switzerland. The two-story building has a cellar and an overall heated floor area of 320 m^2. The ground and first floors are each one flat with a heated floor area of 135 m^2. The cellar is partially above grade to the east and features a small studio with a heated floor area of 50 m^2. Detailed information in regard to the building can be found in [1, 2]. Heating and DHW is covered by a ground source heat pump (GSHP) with a nominal power of 8.9 kW. The building also features a mechanical ventilation system with heat recovery. A PV system with 20 kW peak is mounted on the roof facing south with a 10° angle to the horizontal and has a design electricity production of 18 MWh per year (Figure 2).

Figure 2: View of the multi-family dwelling studied (© Setz Architektur, FHNW IEBau).

Transient building performance simulation

The building performance simulation model is set up with 15 thermal zones, one for each room of the building (Figure 1). The non-heated area in the cellar is modelled as one thermal zone, though. Regardless of the availability of quite detailed measurement data, various necessary inputs for the building performance simulation are unknown and must therefore be based on assumptions. Specifically, the the following main assumptions are made [3]:

- The solar protection device (external venetian blind) is up at all times during the heating period.
- There is no thermally relevant air exchange between thermal zones (internal doors are closed).
- The occupation schedule in each unit is based on the current (at the time of this study) tenant situation.
- The split of electricity consumption between lighting and small power is set room-wise.
- The thermal mass of furniture and other non-constructive fittings is taken into account based on an approximate amount of clutter.
- The ventilation rate is set to a fixed, constant value room-wise. This ventilation rate includes the mechanical ventilation (w/ 80 % heat recovery) and a fraction taking occasional opening of windows into account.
- The temperature sensor "living room" is let into the wall and thus is assumed to measure a mix of air- and wall temperatures. It is assumed that this split is 33 % air temperature and 67 % wall temperature [5].

In the **actual building** ("as built"), floor and ceiling slabs, cellar walls and the roof are made of reinforced concrete. The external walls are made of aerated concrete and the internal walls are made of sand-lime brick or plasterboard. For the **heavyweight model**, external and internal walls are changed to reinforced concrete, as well. Standard wall thickness values for cast-in-place concrete are used (i.e. external walls 250 mm, internal walls 200 mm). For the **lightweight model**, above grade external walls, the ceiling/floor between first and second levels and the roof are changed to wood frame constructions. For both variants, the U-values for external walls and the roof are equal to the values of the actual building. Detailed information on the constructions used can be found in [3].

The overall heat capacity is found to be 17 kWh/K for the actual building, 21 kWh/K for the heavyweight construction and 11 kWh/K for the lightweight construction (values derived with the transient method according to [6]). The heat capacity of the furniture is calculated to be 1.8 kWh/K (derived with the simplified method according to [6] with a time period of 24 h including heat transfer coefficients).

The only changes in the models considered in the results given below are the changes to the building elements mentioned above and the run-time of the heat pump. In all other respects, the models are identical to the calibrated model of the actual building.

GSHP run-time constraints

Initially, the heat pump run-time is restrained to 10 am through 1 pm and 2 pm through 7 pm for heating purposes. In accordance with the measurement results, DHW is produced in the intermediate interval of 12 am through 1 pm. This basic setting corresponds to the setting in the actual building where eight hours were available for heating purposes in the time period considered. Subsequently, the run-time is further reduced in three steps to five hours (10 am through 1 pm and 2 pm through 4 pm).

RESULTS

Evaluation of the simulation results and comparison between run-times is based on the calculated operative temperatures of the living rooms in the three units. Also, thermal comfort criteria according to SN EN ISO 7730 [7] and SIA 180 [8] are evaluated. The following specific criteria based on hourly mean values are considered:

- SN EN ISO 7730:2006 [7]: The operative temperature must be in an interval according to the desired comfort class A (22 ± 1 °C), B (22 ± 2 °C) or C (22 ± 3 °C).
- SIA 180:2014 [8]: The operative temperature must be between 20.5 and 24.5 °C during occupied hours if the 48-hour running average of the ambient temperature is less than or equal to 12 °C, which is the case, here.

Model validation

The simulation model with constructions “as built” is calibrated based on measurement values giving useful heat supplied and values from the temperature sensors in the living rooms of all three apartments. Table 1 shows that the agreement between measured and calculated values is very good. Thus, the simulation model is considered validated.

Table 1: Measured/calculated useful heat demand and average measured/calculated temperatures at the temperature sensors "living" (actual construction, heat pump run-time: 10:00-13:00/14:00-19:00 hours).

	Heat [kWh]		Average temperature at sensor „living“ [°C]	
Floor	Measured	Calculated	Measured	Calculated
Ground	311	306 (-2%)	21.9 ± 0.4	21.9 ± 0.4
First	580	560 (-3%)	21.6 ± 0.3	21.7 ± 0.4
Second	728	710 (-2%)	22.8 ± 0.4	22.9 ± 0.4
Total	1'619	1'576 (-3)		

Operative temperatures

Figure 3 shows the cumulated frequency of calculated hourly values for operative temperatures in the zone “living room” of each floor for the three different construction types and four different run-time constraints considered. The comfort class achieved according to [7] corresponds to the level of the highest or lowest operative temperature found. Table 2 summarizes the resulting comfort classes. It can be seen that the construction “as built” and the heavyweight construction show identical results in regard to comfort class. Only in the second floor can the lightweight construction achieve a “C” for the longest run-time of the GSHP considered.

Table 2: *Comfort compliance for the living rooms according to SIA 180:2014 and SN EN ISO 7730:2006 (gf: ground floor, ff: first floor, sf: second floor).*

Heat pump run-time schedule	"as built"			"heavyweight"			"lightweight"		
	gf	ff	sf	gf	ff	sf	gf	ff	sf
10 am -13/14-19 pm	C	C	B SIA 180	C	C	B SIA 180	-	-	C
10 am -13/14-18 pm	C	C	B	C	C	B	-	-	-
10 am -13/14-17 pm	C	C	C	C	C	C	-	-	-
10 am -13/14-16 pm	-	-	-	-	-	-	-	-	-

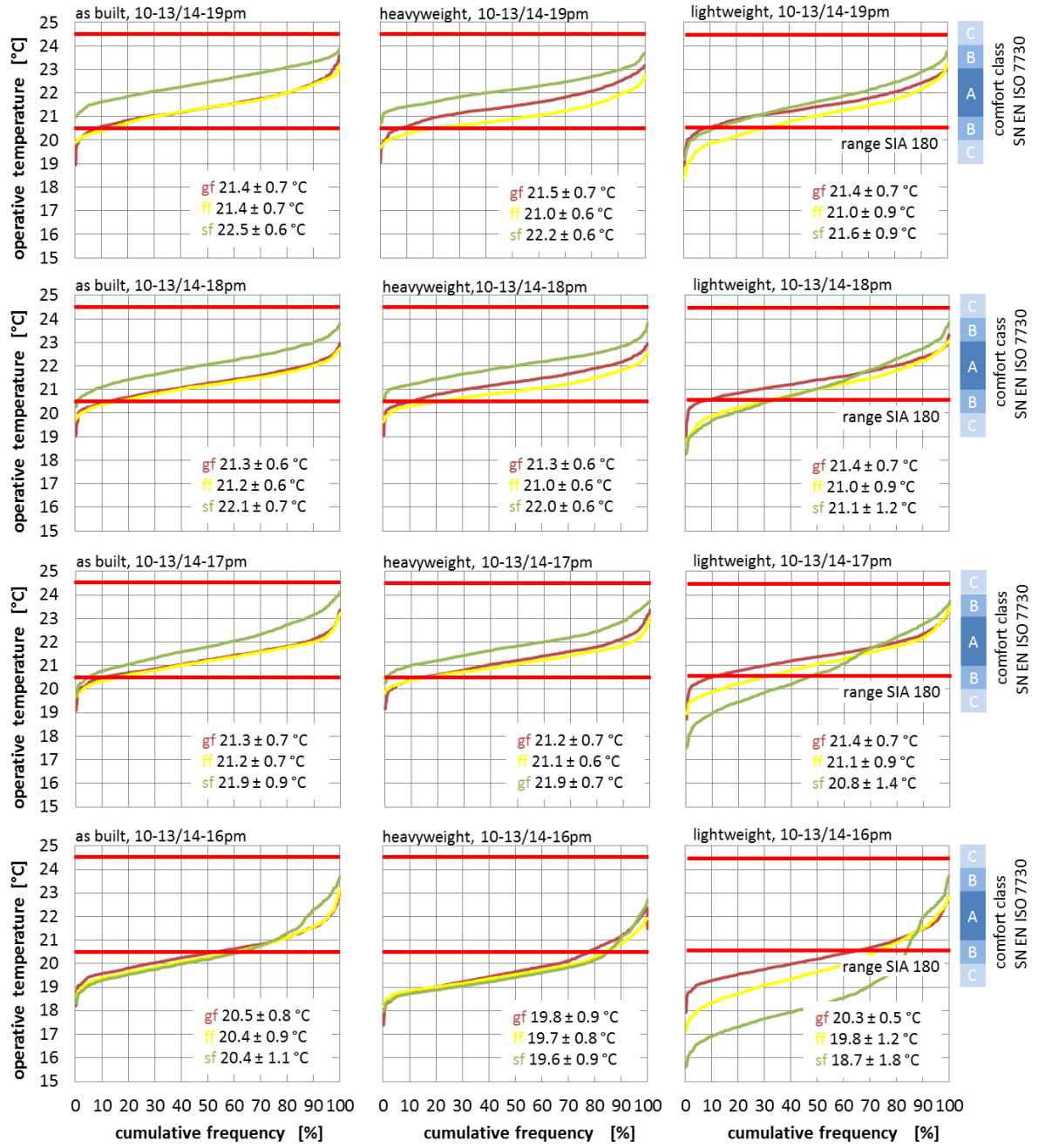

Figure 3: Cumulative frequency, mean value und standard deviation of simulated operative temperatures for the living rooms in the ground, first and second floor apartments (gf: ground floor, ff: first floor, sf: second floor).

DISCUSSION

The tenants of the measured building are highly satisfied with thermal comfort in their flats. It must be assumed that in real life the operative temperature – which was not measured – shows a similar range of values as found in the simulation. This could be interpreted such that operative temperatures falling below the threshold values according to standards for short periods of time do not lead to immediate problems in regard to thermal comfort. The tenants obviously easily accept a thermal comfort at level "C" in the highly insulated building considered here. This implies that the tenants seem to accept a shortfall in thermal comfort compared to requirements given by SIA 180:2014 [8]. In order to use the thermal mass of a building to increase energy flexibility it seems necessary to allow for such short-term shortfalls of thermal comfort.

CONCLUSION

The results show that regardless of a very high level of thermal insulation a sufficient amount of thermal storage capacity is necessary in order to be able to limit run-times of the heat pump to daylight hours without unduly compromising thermal comfort. The restriction of run-time for the heat pump (or any other heat source) to daytime hours unavoidably leads to a drop in operative temperature levels despite the high insulation standard. Ideally, thermal comfort requirements set by standards can be met by a building in which a high degree of energy flexibility is sought. The current requirements in regard to thermal comfort defined in SIA 180:2014 [8] do not allow for the degree of flexibility in building operation studied in this paper. It will likely prove desirable to adapt the requirements in said standard in order to be able to meet Swiss political goals in regard to the future power supply.

ACKNOWLEDGMENTS

The results presented in this paper are based on research funded by the Swiss Federal Office of Energy SFOE under contract number BFE SI/500645 // SI/500645-01.

REFERENCES

[1] M. Hall, F. Dorusch, and A. Geissler, "Optimierung des Eigenverbrauchs, der Eigendeckungsrate und der Netzbelastung von einem Mehrfamiliengebäude mit Elektromobilität," Bauphysik, vol. 36, no. 3, pp. 117–129, Jun. 2014

[2] F. Dorusch, M. Hall, and R. Dott, "Mehrfamilienhaus mit Elektromobilität in Rupperswil," FHNW, Institut Energie am Bau, Schlussbericht, BFE SI/500645 // SI/500645-01, www.fhnw.ch/habg/iebau, 2014

[3] M. Hall and A. Geissler, "Netzbelastung durch Nullenergiegebäude," FHNW, Institut Energie am Bau, Schlussbericht, BFE 810000723, SI/500217-02, www.fhnw.ch/habg/iebau, 2014

[4] ESRU, ESP-r (open source): A Building and Plant Energy Simulation Environment. University of Strathclyde, Glasgow; http://www.esru.strath.ac.uk. Programm Version 2013.

[5] Persönliche Mitteilung von Herrn Jürg Bichsel, Institutsleiter Institut Energie am Bau FHNW, Muttenz, vormals Firma Sauter, Basel 19.09.2013

[6] SN EN ISO 13786: Wärmetechnisches Verhalten von Bauteilen - Dynamisch-thermische Kenngrössen - Berechnungsverfahren. 2007

[7] SN EN ISO 7730: Ergonomie der thermischen Umgebung - Analytische Bestimmung und Interpretation der thermischen Behaglichkeit durch Berechnung des PMV- und des PPD-Indexes und Kriterien der lokalen thermischen Behaglichkeit. 2006

[8] SIA 180: Wärmeschutz, Feuchteschutz und Raumklima in Gebäuden. 2014

GRID IMPACT OF A NET-ZERO ENERGY BUILDING WITH BIPV USING DIFFERENT ENERGY MANAGEMENT STRATEGIES

K. Klein[1]; D. Kalz[1]; S. Herkel[1]

1: Fraunhofer-Institute for Solar Energy Systems. Heidenhofstr. 2, 79110 Freiburg, Germany

ABSTRACT

A net-zero energy office building with Building-integrated photovoltaics (BiPV), a heat pump with cooling functionality and TABS as a heat distribution system is simulated in dynamic thermohydraulic simulations in Dymola. The focus of the evaluation is the electricity exchange with the grid. The temporal mismatch between local electricity production and electricity consumption is evaluated using established indicators such as the autonomy and self-consumption. Moreover, it is analyzed during which times electricity is consumed from the grid, and how high the fraction of Wind and PV in the energy mix is during the time of consumption. The latter is quantitatively expressed using the Grid Support Coefficients GSC_{abs} and GSC_{rel} proposed by the authors.

HVAC operation accounts for roughly 43% of the total electricity consumption of the considered building. With a conventional HVAC control concept based on heating and cooling curves, an annual autonomy rate of 42% and a self-consumption rate of 43% are achieved. In an alternative control scheme, the trajectory of heat and cold delivery to the zones is altered such that the self-consumption of the locally produced electricity is maximized. The remaining electricity demand for HVAC operation, which has to be covered from the public grid, is shifted to times of a high availability of Wind and PV power in the energy system. With this energy management scheme, the autonomy and the self-consumption rate are increased to 50% and 53%, respectively. The fraction of Renewables in the electricity consumed from the public grid is increased by 15% (relative). Thermal comfort in the offices is only moderately affected by the shifting of the heating and cooling loads.

Keywords: Net-zero energy buildings, BiPV, grid-supportive, heat pumps, simulation

INTRODUCTION AND GOALS

As part of the Energy transition, the German federal government plans to cover at least 80% of its electricity consumption with renewables by the year 2050 [1]. The largest part of the renewable electricity will be generated by Wind and PV plants [1]. Due to the volatile nature of Wind and PV power, it is expected that the availability of electricity in the German energy system will fluctuate significantly. Consequently, not only the quantity, but also the time of energy consumption or production will become a relevant requirement to "grid-supportive" electricity consumers and producers. Buildings using heat pumps, compression chillers or CHP units can serve as such by adapting the operation of local heating and cooling energy production according to the availability of electricity in the grid and store the energy in thermal form.

The present study investigates how the net power exchange of a net-zero energy office building equipped with BiPV, a ground-coupled heat pump and Thermo Active Building Systems (TABS) coincides with the availability of electricity in the power grid. In office buildings, the local production also partly coincides with local electricity demand during occupancy as well as cooling loads in summer. It is analyzed to what extend the operation strategy of the heat pump or chiller can influence the overall grid exchange of a net-zero

energy office building. In this case, TABS is utilized to activate the building mass as a thermal energy storage. The influence of this thermal activation of the building structure on indoor comfort is evaluated.

REQUIREMENTS TO GRID-SUPPORTIVE BUILDINGS

The grid interaction of a net zero energy building is typically assessed in terms of the autonomy (also called load cover factor), which is the percentage of the electric load covered by local production, and the self-consumption rate (also called supply cover factor), which represents the fraction of the locally produced electricity which is consumed on-site. [2] In this article, the cover factor is defined as the ratio between the locally produced and the consumed electricity, regardless of the temporal mismatch between production and consumption.

In addition, the absolute and relative Grid Support Coefficients GSC_{abs} and GSC_{rel} are proposed in order to assess whether electricity from the public grid is consumed at times with a high or a low availability of renewables in the energy system. GSC_{abs}(WPC) is the fraction of Wind and PV energy in the consumed electricity, relative to the average fraction of renewables during the evaluation period. [3] A value greater than one indicates that electricity is consumed at an above-average availability of wind and PV in the grid. GSC_{rel} relates the value of GSC_{abs} to the worst and best achievable values on a scale of -100 to 100 in order to increase the comparability of the results. In this study, the fraction of Renewables in the German electricity mix for 2023 is used for the assessment, which was calculated from historical data and scaled with the projected future Wind and PV power from [4]. However, GSC can be applied to any meaningful, time-resolved reference quantity such as the Residual load, price signals or a time-resolved primary energy factor of the electricity mix. [3]

SIMULATION MODEL

Considered Building and office zones

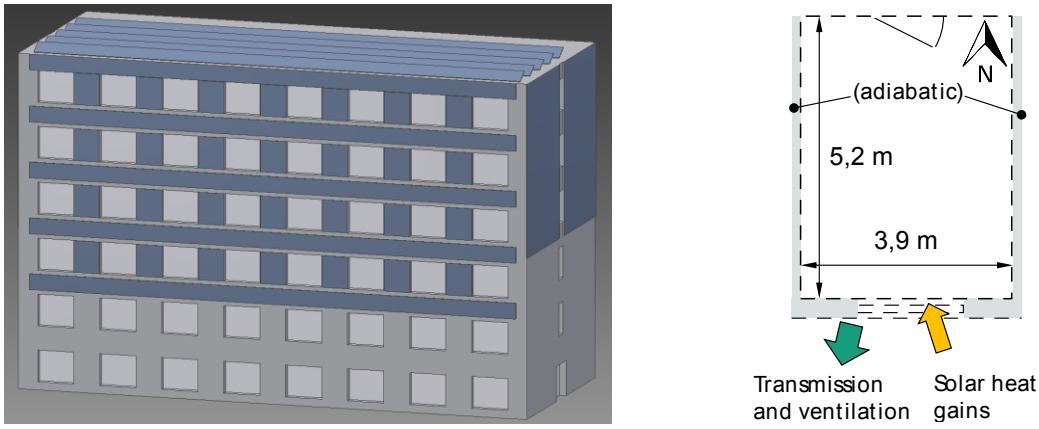

Figure 1: Building including BiPV panels in blue and geometry of south-facing office

The building considered in this study represents a generic “typical” European office building located in Mannheim/Germany. It is six storeys high and divisible into eight rows of geometrically identical three-zone-cells. Seven of these rows of cells consist of one north-facing two-person office, one south-facing two-person office, as well as a connecting corridor. The building has a floor area of 2433.6 m^2, a specific heat consumption of 33.4 kWh/m^2a and a specific cooling energy consumption of 26.7 kWh/m^2a.

Thermal properties	Value	Unit	Offices properties	Value	Unit
U-value of exterior walls	0.24	W/m^2K	Zone width	3.9	m
U-value of roof	0.2	W/m^2K	Zone depth	5.2	m
U-value of windows	1.0	W/m^2K	Zone height	3	m
g-value of windows	0.58	-	Window area (glazing)	4.68	m^2

Table 1: Geometry and properties of two-person office zone in compliance with EnEV 2014.

Usage and heat gains

It is assumed that the offices are partially occupied during workdays between 7 a.m. and 6 p.m. The assumed occupancy factor is 0.36 during the first and last two working hours as well as during noon (12 p.m.-1 p.m.) and 0.7 during the other working hours. During occupancy, the ventilation rate is 30 m^3 per person and hour. During absence, the ventilation rate is the natural air infiltration rate (air leakage) of 0.3 h^{-1}. No heat recovery is assumed.

The heat gains from people and appliances are 70 W/person and 100 W/person, respectively. It is assumed that a continuous lighting controller keeps the illuminance on the working surfaces at or above 300 lux. All assumptions concerning the usage and heat gains comply with the standard DIN-V EN ISO 18599:2011-12.

Heat and Cold supply and hydraulic system

A variable-speed, brine-water ground-coupled heat pump with cooling functionality is used as a heat and cold generator. Its specifications are taken from the data sheet for the first compressor stage of the Dimplex SI 75 TER+. Its rated heating and cooling capacities are linearly scaled to 150% in order to match the load requirement of the building. The thermal energy is delivered to the zones using Thermally Activated Building Systems (TABS), which are centrally located inside the 30 cm concrete floor slabs. The north-facing and the south-facing zones have separate hydraulic circuits.

Building-Integrated Photovoltaics

The BiPV system is designed such that the annual local energy production approximately covers the annual electricity consumption. The PV modules used are Schott Perform Poly 245, which consist of 72 polycristalline cells with an efficiency of 15% at standard test conditions. A total of 422 modules are installed: 151 on the southern façade, 88 each on the eastern and western façade and 95 on the roof. The roof-mounted modules are inclined 30°, whereas the façade-mounted modules are vertical. An inverter efficiency of 98% as well as 15% overall losses due to shading, reflection and dirt are assumed.

Simulation setup

The software environment Dymola 2014 is used for the thermohydraulic simulations. The zone model used is a 5R1C model in compliance with the modeling standards of DIN EN ISO 13790. Most other models (e.g. TABS, Pumps, valves), are taken from the Modelica Buildings library. The simulation comprises one year in 1-hour resolution.

ENERGY MANAGEMENT STRATEGIES

Reference controller: Optimized heating and cooling curves

In the reference variant, the supply water temperatures to the zones is determined by heating and cooling curves, which are linear functions of the moving 24 hour mean of the ambient temperature. The offset and slope of the heating and cooling curves as well as the temperature

limits for heating and cooling operation are optimized using GenOpt such that the operative room temperatures below 20 °C and above 26 °C during occupancy and the thermal energy consumption for one year are minimized. The pumps in the TABS circuits are operated continuously with a mass flow rate of 15 kg/(m^2h).

Alternative energy management scheme

The goals of the presented energy management scheme are a) to maximize self-consumption of the locally produced electricity and b) to consume as much of the remaining electricity consumption as possible during times with a high share of Wind and PV power in the grid.

First, the daily thermal energy demand for the zones is determined using the simulation results from the reference case, which is equivalent to an ideal load prediction. The thermal energy is then allocated to the hours with the highest surplus local PV energy after substraction of non-shiftable loads (lighting, miscellaneous loads for appliances, and heat pump operation for the conventionally-conditioned zones). In case there is no or insufficient surplus local PV energy available during one particular day, the remaining thermal demand is allocated to the hours of the day with the highest share of Wind and PV power in the grid. The load shifting is constrained by the maximum capacity of the heat pump and the maximum transmittable thermal power to the zones. In order to increase the latter, the heating curve is increased by 3 K and the cooling curve is lowered by 3 K compared to the optimized heating and cooling curves in the reference controller.

RESULTS

Annual and monthly electric energy balance of building

The simulated building consumes 71.2 MWh_{el} of electricity per year. HVAC operation, which comprises the heat pump compressor energy for heating and cooling as well as pump electricity, accounts for 43% of the consumption. Miscellaneous loads for appliances and lighting, which can be classified as non-shiftable loads, account for 37% and 20%, respectively. The annual electricity production by BiPV is equivalent to 96.5 % of the electricity consumption.

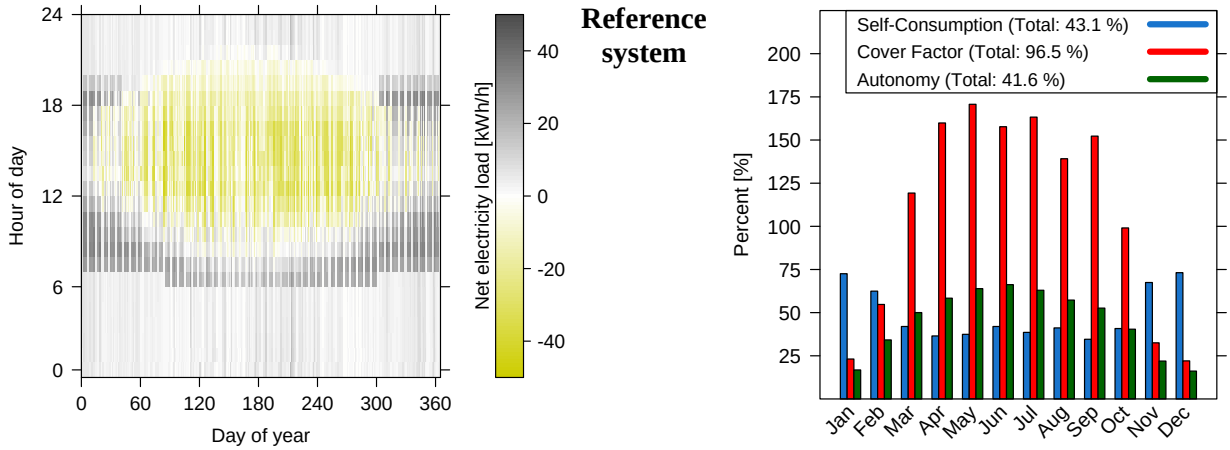

Figure 3: Results for the reference case. Left: Carpet diagram of the net electric load. Right: monthly self-consumption, cover factor and autonomy.

In the reference case with a conventional controller, the self-consumption in the base variant is only 43% and the autonomy is 41.6% due to the temporal mismatch between electricity

production and consumption. Even in the summer months, when the cover factor reaches values close to 175%, the autonomy never exceeds 75%.

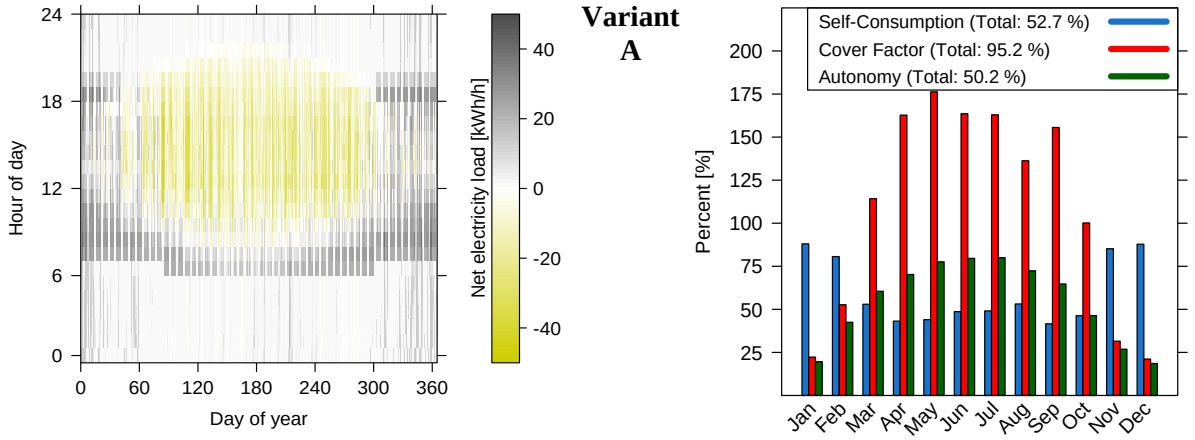

Figure 4: Results of the alternative load management scheme. Left: Carpet diagram of the net electric load. Right: monthly self-consumption, cover factor and autonomy

Using the altered energy management scheme ("Variant A"), the self-consumption and autonomy can be increased by roughly 9% (absolute). As shown in figure 4, grid consumption during the night is almost completely avoided since heat pump operation is shifted to the day. The total electricity consumption increases slightly since the seasonal performance factor of the heat pump drops from 6.52 to 6.09 due to the shifted heating and cooling curves.

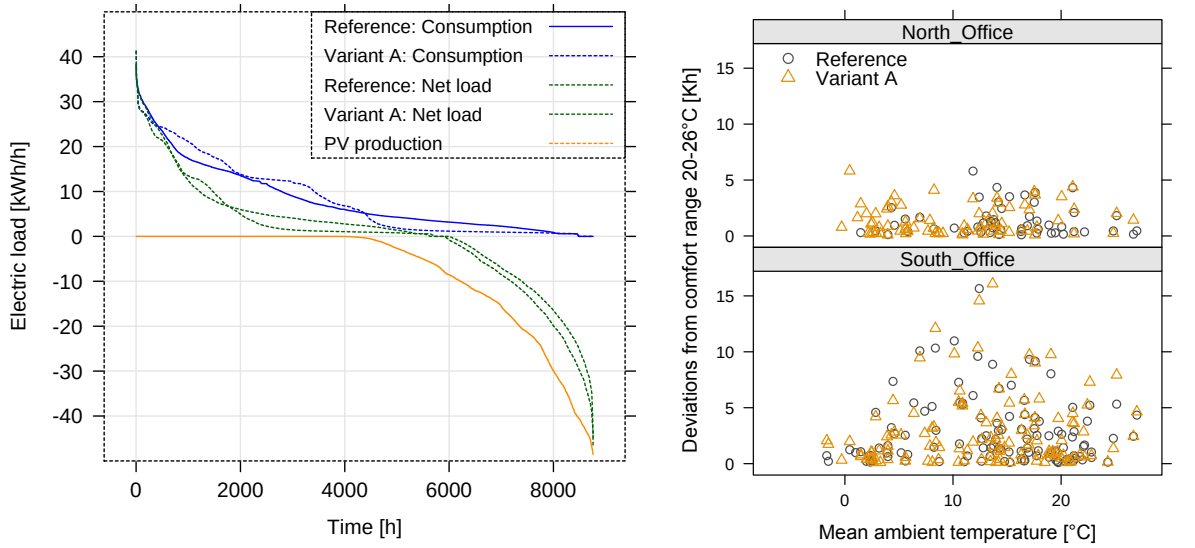

Figure 5: Left: Ordered load duration curve of consumption, net load and PV production for both variants. Right: Daily comfort violation over the mean ambient temperature

The altered energy management scheme leads to a much flatter load duration curve of the net grid exchange (figure 5, left). During 3753 hours, the building has nearly no power exchange with the grid (net load < 2 kW_{el}), which is nearly 2.5 times longer than in the reference variant. At the same time, the peak load hours (net load > 28 kW_{el}) are reduced by roughly the same factor. Thermal comfort is only moderately affected by the load shifting. In the north-facing office, deviations from the comfort range are below 5 Kelvin-hours, whereas in the south-facing office, comfort violations are several times higher throughout the year for both controllers, which is a result of higher solar heat gains.

	Comfort violations *North offices/ South offices*	**Grid consumption above 28 kW_{el}**	**GSC_{abs}/ GSC_{rel} (for fraction of Wind and PV in 2023)**		
			Grid consumption	*Feed-in*	*Heat pump compressor*
Reference	73 / 316 Kh	211 hours	0.84 / -50.6	1.55 / 70.9	1.02 / -0.5
Variant A	104 / 336 Kh	91 hours	0.97 / -25.6	1.53 / 71.6	1.41 / +74.7

Table 1: Comfort deviation and grid support for reference and alternative scheme.

With the alternative energy management scheme, the heat pump compressor's electricity consumption achieves a GSC_{abs}(WPV) value of 1.41, which means that operates at times during which the share of Renewables in the electricity mix is 41% higher than average. A GSC_{rel} value of 74.7 indicates that this value is relatively close to the optimum (100). Even though the grid consumption is reduced in quantity, its Grid Support Coefficients are only slightly improved. This is due to the non-shiftable loads, which occur mostly in the morning and evening, when the availability of Wind and PV power is low, as well as the high coincidence of local PV availability and Wind and PV availability in the grid.

CONCLUSION

In the considered net-zero energy office building, roughly 43% of the electricity consumption is used for HVAC operation, nearly in equal parts for heating and cooling. By shifting this load according to the presented energy management scheme and storing the thermal energy in the building mass, self-consumption and autonomy are increased by about 9% each. However, the time structures of grid consumption and feed-in, which are reflected by the Grid Support Coefficients (GSC_{abs} and GSC_{rel}), can only partly be influenced by due to the limited shiftable load and finite power of the heat pump. The prevalence of excess PV production in summer and low autonomy in winter highlights the limitations of load shifting using heat pumps.

The effect of the load shifting on comfort in the office zones is limited. This shows that TABS allow to store significant amounts of heat and provide a high degree of flexibility for the operation of the heat and cold generators. In order to fully seize the potential of net-zero energy buildings as grid-supportive electricity consumers, storages and producers under consideration of cost and comfort constraints, a combination of various measures has to be taken. These measures include the use of technical storages, "fuel-switch" between multi-energy heat and cold generators, and predictive control strategies for zone conditioning. Such concepts will be studied more thoroughly and presented by the authors in future work.

ACKNOWLEDGEMENT

The work presented in this article is part of the project "Netzreaktive Gebäude" funded by the German Ministry of Economic Affairs and Energy under the code 03ET1111A.

REFERENCES

1. German Federal Ministry of Economics and Technology: Energy Concept for an Environmentally Sound, Reliable and Affordable Energy Supply, 2010: Berlin.
2. Salom, J. et al.: Analysis of load match and grid interaction indicators in net zero energy buildings with simulated and monitored data. Applied Energy, 2014. 136: p. 119-131.
3. Klein, K. et al.: Netzdienlicher Betrieb von Gebäuden. Bauphysik, 2014. 36(2): p. 49-58.
4. German Transmission system operators : Grid Development Plan 2013, second draft, part 1. 2013; Available from: http://www.netzentwicklungsplan.de/en/.

VISUAL IMPACT THRESHOLDS OF PHOTOVOLTAICS ON RETROFITTED BUILDING FACADES IN DIFFERENT BUILDING ZONES USING THE SALIENCY MAP METHOD

R. Xu, S. Wittkopf

CC EASE, Lucerne University of Applied Sciences and Arts, 6048 Horw, Switzerland

ABSTRACT

The saliency map is a tool to describe the visual attention of human eye within a certain visual field. It is based on neurobiological and psychological principles. On a scale from 0-1, the lower the calculated value of a particular spot on the map is, the lower the probability of the human eyes to notice this spot. The authors have used this tool to quantitatively measure the visual change on heritage architectures before and after the Photovoltaic (PV) installation [1]. In this paper, the authors used a similar methodology to investigate the domains of allowed visual change caused by PV installation in different building zones. One existing building was used as an example and the PV color was used as the changing parameter. First, we found out how different visual changes and their quantification look like. A photo of the building in the original situation was taken, and named as the image "as is". This image was then run through about 5000 simulation iterations, each time the building façade on the image was equipped with PV with a different glazing color. After that, we investigated the visual changes that were caused by different PV color compared to the "as is" situation, and quantified them with the help of the saliency map. In the end, which amount of visual change is suitable for which type of building zone was discussed. Domains of allowed visual change were proposed. The benefit of the results could limit the negative visual impact caused by building integrated PV installation on urban buildings, retain the aesthetic balance in urban spaces, and could be integrated as thresholds in laws or regulations to guide the appropriate trend of building integrated PV installation in urban environments.

Keywords: visual assessment, solar architecture, façade retrofit, visual impact threshold

INTRODUCTION

Until today, people are still learning to deal with the combined qualities of PV that are quite unconventional: energy production and building material in one. Architects and engineers are still trying to find the balance between these two qualities. Experienced architects [2] compiled a report summarizing the experience of involving PV in architecture design. One chapter was dedicated especially to the decorative/architectural aspect of building integrated PV (BIPV), pointing out that especially in renovation projects, a careful coping with the existing façade is crucial.

Even though the new RPG clause 18a [3] and RPV clause 32a [4] were revised, only the importance of roof-integrated PV was paid attention to, façade-integrated PV was not mentioned at all. It was also stated that the installation of roof-integrated PV have higher probability of being installed in new buildings due to lower aesthetic requirements [5]. Nevertheless, façade integrated PV will gain more attention, as their daily electricity production profile fits a building electricity consumption profile better than the peak-oriented

PV power plants on roofs, and as a matter of fact, facades are not covered by snow during the winter season.

Others mentioned the importance of national policies [6]. According to this paper, different policies and regulations can lead to different results in BIPV adoption. For example in France, 59% of all PV systems are considered BIPV, in Italy 30%, Switzerland 30%, Austria 4% and Germany 1%.

Suggestions were made to assess the integration quality of BIPV [7]. The two main decisive parameters were the sensitivity of the zone where the building/building complex was located, and the visibility of the BIPV system itself. The latter one was again decided by the appearance of the PV (obviousness of size, material, color, texture, form and joints), whose obviousness was decided manually with +, +/- and – symbols. Thresholds for different quality levels of BIPV were given. This methodology allowed for quality categorizing and fast decision, but in terms of using descriptions with qualitative nature, there is still room for improvement.

PROBLEM STATEMENT

Due to lack of experience in using PV as an architectural element, at present mostly roof-integrated PV are mentioned in national laws and regulations, even though façade-integrated PV and roof-integrated PV both belong to the BIPV category. Also in current standards concerning BIPV, the laws and regulations only make vague separation between requirements in different kinds of building zones, even though different building zones clearly have different architectural standards, e.g. industrial zones would have a much lower architectural requirements compared to residential zones.

In order to prevent inappropriate BIPV designs, laws and regulations use mostly qualified and semantic descriptions to express how the expected BIPV installation should look like. This gives the responsible local authorities certain freedom in their approval process for BIPV projects. While the authors basically agree this is a successful way to prevent inappropriate BIPV designs, we must admit that façade-integrated PV has huge potentials in meeting the requirements of Energy Strategy 2050, therefore very possible to become more popular. Thus it is necessary to include the architectural requirements of not only the roof-integrated PV, but also of façade-integrated PV into regulations or laws, so that it can generally guide PV engineers, architects and other stakeholders with the “do-s” and “don’ts” when designing a BIPV project. The authors would therefore to make a proposal of another solution concerning the above-mentioned aspects.

SALIENCY MAP

The saliency map is a neurobiological and psychological tool to predict human visual attention. For every point in a certain human visual field, the probability of human paying attention to this particular spot can be calculated. These probabilities (on a sale from 0-1) can be presented on a saliency map. The Judd Saliency benchmark has evaluated the Harel & Koch [8] method as one of the most accurate algorithms available today. Their algorithm considers certain features (such as colour contrast, hue and object edge) and weights it according to position within the view for the processing of one final saliency map. Compared to other saliency algorithms, their algorithm has the advantage that the spots in the centre of the visual scene are prioritized, and also the area that are far away from the object edges are also being paid appropriate attention to. Figure 1 is an example of the saliency map application. One can see that the flower is the most salient spot in the image, meaning it has the highest possibility of being noticed by the human eye within this image. The farer away

the object is from the centre of the image (e.g. the leaf down-left), the more it tends to be suppressed.

Figure 1. An example of the saliency map application. It is possible to use a photo as an import into the saliency map tool. The photo is considered to be a snapshot of the human visual scene. Even though the proportion of the Harel & Koch map's default setting is 900 x 1200 pixel, but in reality the proportion does not matter due to saccade movement in the human eyes.

METHODOLOGY AND APPLICATION EXAMPLE

In order to find out the visual changes and their corresponding quantified descriptions, representative heritage views was chosen for the investigation. Visual changes in this paper always referred to the difference of the view perception of the scene in figure 2 ("as is" situation) before and after the PV installation. Figure 2 shows the Kapellbrücke in Lucerne Old City as an application example because it could best demonstrate how a scenic view is very sensitive to an extrinsic PV installation that did not belong here originally. The sensitivity was also amplified by the fact that the PV was installed on a precious heritage building.

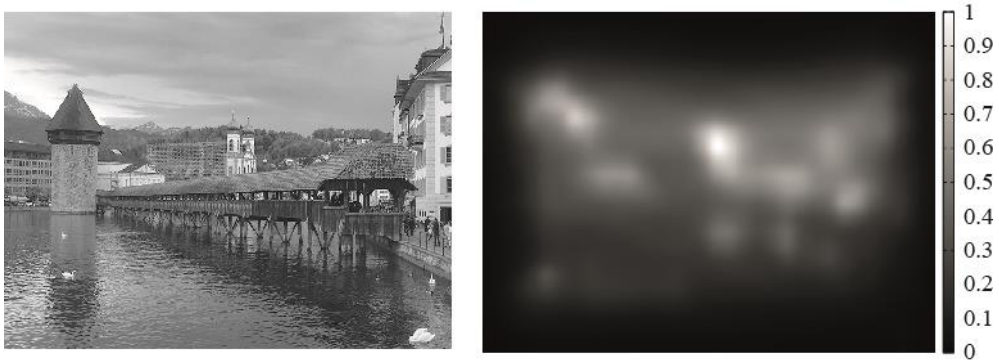

Figure 2. The image "as is" (left) and its saliency map "as is" (right).

As seen in figure 2, the Kapellbrücke consists of a water tower and a wooden bridge. However, the heritage site is not defined by the Kapellbrücke alone, but the surrounding architectures (e.g. the church in the background) also play important parts in defining the aesthetic balance of this view. The image left in figure 2 was named image "as is" and imported into the Harel & Koch algorithm. A saliency map was then generated from it (see figure 2, right). One can see that in original situation "as is", human attention is drawn to the water tower and the white church in the background first, which are the dominant attention-drawers. This was due to their colour contrast with the environment, central location and the unusual edge directions in the visual scene. Then the attention goes to the other white building with a triangle roof in the background and the roof of the bridge. The surrounding objects

such as the white architecture on the right, and the swan in the down-right corner are not salient in the map, even though they are in very heavy colour contrast with their environment. That is because they are very far away from the centre of the visual scene and are suppressed in the normalization processes.

This paper studies the visual changes caused by differently coloured PV modules in this view, as purely hypothetical installations. A square PV module was painted into the image region showing the tower, indicated as the white square in figure 3. Other parameters than the colour such as location and details (joints, mounting, cables etc.) were omitted.

Figure 3. The white square represents the locations where Photovoltaics of different colors were added.

Through an automatic image processing script, the white area was filled with different colours, which were represented by different RGB values (each 0-255). With increments of 15 for each colour channel, the output was 4913 "new" images (each with a different glazing colour) in total. Then the images "new" were imported into the Harel & Koch algorithm, resulting in 4913 saliency maps "new".

In order to find out how different PV colour affected the overall visual perception of the scene, each saliency map "new" was compared with the map "as is". The results were named Delta Saliency maps (see formula (1)).

$$\Delta Saliency\ map = |Saliency_{As\ is} - Saliency_{New}| \quad (1)$$

On Delta Saliency Maps, we have the locations marked where the saliency values of saliency maps "new" were different compared to saliency maps "as is" by an absolute value of more than 0.1 (differences under 0.1 were considered as noise). The sum of the pixels with different values were counted together, and then divided by the total pixel number of the map (in this case 900x1200). This was calculated by formula (2) and presented in figure 4.

$$Percentage_{\Delta Saliency\ map>0.1} = pixel\ number_{\Delta Saliency\ map>0.1} / (900 \times 1200) \quad (2)$$

DISCUSSION

With the different PV colour as the changing parameter, the results could provide us an insight how different visual changes and their corresponding quantifications look like.

Throughout figure 4, we can see that the white church in the background and the water tower still belonged to the most dominant objects in the image. This was especially the case with a visual change of within 30% in the scene. If the PV colour was grey-brownish that is similar to the original colour of the water tower, as seen from the images on the first row, then the overall perception of the visual scene stayed basically the same.

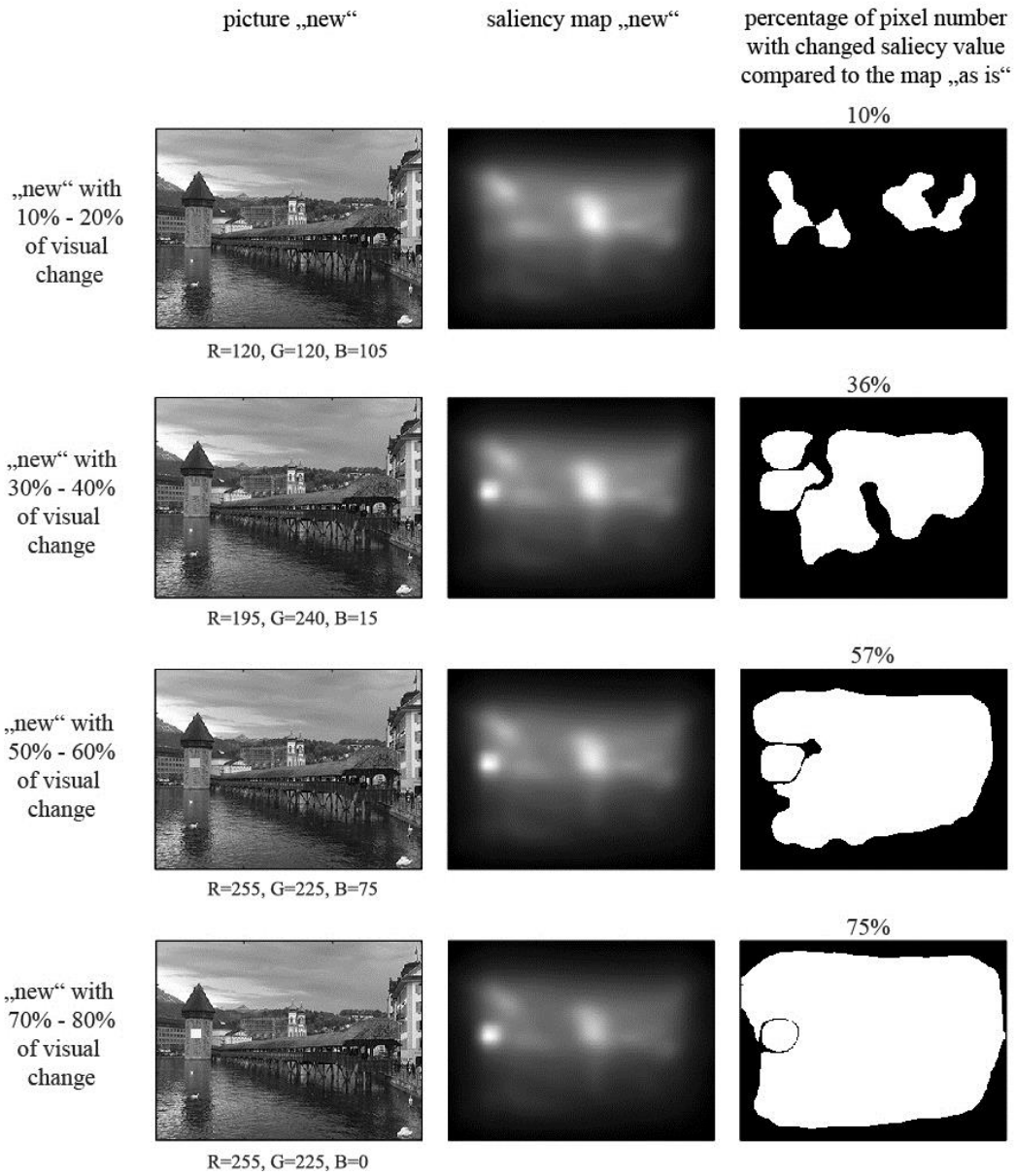

Figure 4. The saliency map and visual attention comparison for different PV module colors.

When the hue of the PV colour exceeded the one of the water tower, and the visual change went above 40%, the presence of the PV and its negative visual impact became inacceptable. It was also obvious that the more obvious the PV colour got, the larger the attention shift in the visual scene became. This is because human attention can only focus on one single object each time. Paying attention to multiple objects at the same time is not possible. So if the PV was installed on the water tower and its colour made it get attention probability of 1, then other objects will be “kicked out” of the original attention priority ranking. This is why when the visual change stayed below 40%, the colour of PV is still acceptable – the attention priority ranking in the original scene was mostly not destroyed. When the visual change went above 40%, the former attention priority ranking in the visual scene was shifted too much that the visual change became apparent to the human eye.

With the results above, the authors propose a mapping of visual changes to different building zones as summarized in table 1, for discussion.

Visual change %	Applicable zones	Preservation level	Reason
< 20%	Sensitive heritage zones.	High	The preservation value of area is high. PV and the change are almost unnoticeable to the human eye. The former visual attention ranking is mostly preserved
20% - 40%	Residential and business zones. Insensitive landscape zones.	Medium	The preservation value of the area is medium. PV is noticeable from afar. The moderate part of the former visual attention ranking is changed.
>40%	Industrial zones, renewable energy demonstration zone	Low to very low	The preservation value is low, visual changes are welcome. PV is very noticeable from far away.

Table 1

CONCLUSION

This paper investigated and quantified the possible visual changes caused by installing PV on an existing building façade using the saliency map method. Visual changes thresholds were proposed for different building zones. In order to simplify the experimentation, only one parameter was changed – the PV colour. Location and details (edge, construction joint etc.) of the PV were omitted. We found out that when the visual change stayed below 20%, the change was barely noticeable by the human eye. This range may therefore be a suitable as a threshold for sensitive zones with heritage protection. Within the range of 20%-40%, the visual change was noticeable by the human eye, but may not cause disturbance, because the major parts of visual attention ranking in the visual scene stayed the same. The visual change above 50% drew major attention to the newly installed PV panel. This range is therefore only suitable for demonstration zones where PV needs to be presented prominently.

ACKNOWLEDGEMENTS

This research was supported by the Swiss National Science Foundation as part of the project "ACTIVE INTERFACES – Holistic strategy to simplify standards, assessments and certifications for building integrated photovoltaics", project no. 153849. It also benefits from the doctoral degree support scheme of Lucerne University of Applied Sciences and Arts in collaboration with Swiss Federal Institute of Technology, Lausanne.

REFERENCES

1. R. Xu, S.Wittkopf, *Visual assessment of BIPV retrofit design proposals for selected historical buildings using the saliency map method.* Journal of Facade Design and Engineering, 2015 (In Press).
2. D. Ehrbar, A. Held, M. Hohl, E. Roesler, U. Sturm, P. Schwehr, *Methodik zur Umsetzung von solaren Strategien in der Architektur*. 2012, Hochschule Luzern.
3. *Bundesgesetz über die Raumplannung (Schweiz)*. 2014.
4. *Raumplannungsverordnung (Schweiz)*. 2015.
5. T. Müller, E. Nelson, R. Zulian, M. Ryser, *Gesamtbeurteilung von fassadenintegrierten Solarstrom-Anlagen*. 2013, Fachhochschule Nordwestschweiz: CAS Erneuerbare Energien 2013.
6. P. Heinstein, C. Ballif, L.-E. Perret-Aebi, *Building Integrated Photovoltaics (BIPV): Review, Potentials, Barriers and Myths.* Green, 2013. **3**(2).
7. M.-C. Munari Probst and C. Röcker. *Urban acceptability of building integrated solar systems: Leso QSV approach*. in *Ises*. 2011. Kassel, Germany.
8. J. Harel, C.Koch, P. Perona. *Graph-Based Visual Saliency*. in *Proceedings of Neural Information Processing Systems (NIPS)*. 2006.

MULTI-OBJECTIVE OPTIMIZATION OF THE DESIGN AND OPERATION OF AN ENERGY HUB FOR THE EMPA CAMPUS

M. Hohmann[1,2,3], C. Waibel[1,2], R. Evins[1,2], J. Carmeliet[2,4]

1: Laboratory for Urban Energy Systems, Swiss Federal Laboratories for Materials Science and Technology, EMPA, Duebendorf, Switzerland

2: Chair of Building Physics, Swiss Federal Institute of Technology, ETHZ, Zurich, Switzerland

3: Automatic Control Laboratory, Swiss Federal Institute of Technology, ETHZ, Zurich, Switzerland

4: Laboratory for Multiscale Studies in Building Physics, Swiss Federal Laboratories for Materials Science and Technology, EMPA, Duebendorf, Switzerland

ABSTRACT

This paper presents a comparison of two multi-objective optimization processes used to simultaneously select and size the components of an energy hub and to determine their optimal operation according to net present value and carbon emissions. The first is a single-level optimization process that uses a mixed-linear integer programming (MILP) model based on the energy hub concept in which time-varying demands and supply availabilities must be matched using conversion and storage options. The second is a bi-level optimization process composed of a multi-objective genetic algorithm (GA) as the upper level to optimize selection and sizing of components. A linear programme is nested within the GA as the lower level to optimize the operation of each proposed system.

The study uses measured data from the Empa research campus in Dübendorf, Switzerland for the heating, cooling and electricity demands that must be met. Appropriate values for solar availability, energy prices and equipment costs were used. The optimization process is conducted for a whole year, allowing the consideration of seasonal storage. The energy hub includes electricity, gas, solar power, and medium temperature and high temperature thermal networks. The technologies considered include boilers, chillers, photovoltaic panels, combined heat and power plants, heat pumps and storage.

Results presented give trade-off fronts of the competing objectives (carbon emissions and discounted costs) that reveal a set of optimal design solutions, including their optimized hourly operational schedules. The effectiveness of the two approaches is compared, including the convergence of the optimization, necessary computing time and the identification of solution characteristics. It is shown that the single-level optimization finds a better Pareto front in much shorter time than the bi-level approach for this problem instance.

Keywords: Multi-objective, Bi-Level, Optimisation, Energy Hub, Measured data

INTRODUCTION

Research facilities often consume large amounts of energy for heating, cooling and operation. Budget constraints and environmental considerations make it necessary to minimise costs and emissions of the energy consumption. As shown in [1], optimization techniques are increasingly used to design and operate multi-carrier energy systems. The optimization methods are used in combination with modelling frameworks such as the energy hub concept of [2]. District systems that also include cooling and operate on different temperature levels

can reduce energy consumption and emissions of buildings [3]. The design of a new energy system is a multi-objective problem as costs and environmental impacts must be considered together.

A single-level optimization process was compared to a bi-level optimization process in order to address the multi-objective problem based on monthly samples in [4]. In [5], a bi-level optimization process in combination with the energy hub model operating on an hourly basis was proposed. The contribution of this paper is the comparison of a single-level optimization process to a bi-level optimization process for a large energy system including short- and long-term storage based on hourly measurement data for a whole year, including time-varying electricity prices.

METHOD

The energy system of the research facility is modelled using the energy hub approach. The model consists of energy streams for electricity, gas, solar power, medium temperature and high temperature thermal networks, and represents their interdependencies via conversion and storage technologies. The model expresses these energy system constraints as a mixed-integer linear programming (MILP) model implemented in Matlab using Yalmip [6] and solved using IBM CPlex.

The optimization process is conducted for a whole year, allowing the consideration of seasonal storage. The temporal resolution is hourly. The objective is to minimize the net present value of the capital and operational costs. A single-level multi-objective optimization process, composed of a mixed-integer linear program, is compared to a bi-level multi-objective optimization process. The single-level optimization process is extended with the ε-constrained technique in order to obtain a multi-objective Pareto front.

Problem formulation

The energy hub concept [2] allows the modelling of multi-carrier energy systems in terms of power flows. In this paper, a slightly modified representation is used. A carrier node k connects different storage devices, expressed as $q_{t,k}^{store}$ (storing) and $q_{t,k}^{dis}$ (discharging), conversion devices, expressed as $p_{t,k}^{in}$ and $p_{t,k}^{out}$, supply grids $g_{t,k}$ and loads $l_{t,k}$. The power flows of a carrier node must be balanced at every time step t as in equation (1). Conversion devices are represented by a linear input-output relationship determined by the efficiency matrix A, as shown by equation (2). The state-of-charge of storage devices are represented by a dynamic discrete linear equation (3) and characterized by the charging and discharging matrices A_+ and A_- and the loss coefficient a. The operational decision variables are constrained by the design variables (i.e. equipment capacities) (4).

$$p_{t,k}^{out} - p_{t,k}^{in} - q_{t,k}^{store} + q_{t,k}^{dis} - l_{t,k} + g_{t,k} = 0 \ \forall t,k \tag{1}$$

$$p_t^{out} = A\, p_t^{in} \tag{2}$$

$$e_{t+1} = a\, e_t + A_+ q_t^{store} - A_- q_t^{dis} \ \forall t \tag{3}$$

$$0 \le p_t^{out} \le p_{\max},\ 0 \le q_t \le q_{\max}, 0 \le e_t \le e_{\max} \tag{4}$$

The operational decision variables at every timestep are the inputs and outputs of storage and conversion devices and the grid supply. The design variables are the output capacities of the conversion devices, the input and output capacities of the storage devices, the storage

capacities and the binary variables that state if devices are present in the energy hub. Equations (1) to (4) express the constraint set of the optimization problem.

The single-stage optimization process incorporates both the design decision variables and the operational decision variables in the MILP model. In order to conduct a multi-objective optimization, the carbon dioxide emissions are constrained by a maximum amount ε that is consecutively reduced to give a spread of solutions.

In the bi-level optimization process, the design variables are determined by the genetic algorithm NSGA-II [7] and the operation variables by a MILP model. Because the MILP does not contain capacities it solves much faster. The objective functions of the genetic algorithm are the net present value of the total costs and the carbon emissions. The linear program in the inner loop optimizes the operational costs. The GA runs for 50 generations, with a population size of 50.

Case Study

The case study is based on the Empa/Eawag research facility in Dübendorf, near Zürich, Switzerland. The energy demand data used for this study originates from hourly measurements for 2012 of electricity, cooling and heating demand. The annual total demand is found in Table 2. The demand for the medium temperature heating power has been estimated based on the profile from the high temperature grid.

Figure 1 illustrates all possible technology options of the energy hub. The high temperature (HT) grid is at 65°C. The medium temperature (MT) grid is at 38°C. The different temperature gaps of the heat pumps lead to different coefficients of performance (see Table 1). A varying percentage of biogas can be added to the gas consumption of the CHP and the boiler. The cooling towers ensure that excess power in the medium temperature grid is exhausted.

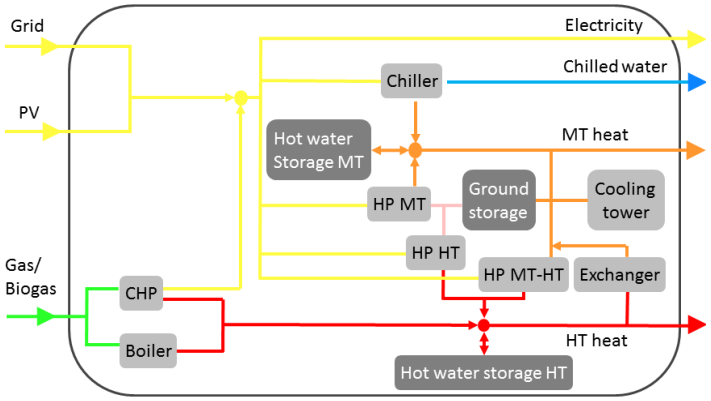

Figure 1: Energy hub of the Empa research facility

The efficiency coefficients, the unit costs and fixed costs of the equipment are listed in Table 1. The costs of the geothermal storage depend only on the input/output capacity and not on the storage capacity. The hot water tank costs depend on both the input/output capacity and the storage capacity. The costs and efficiency values are based on industry estimates. Operational costs of 0.046 CHF/kWh and carbon emissions of 0.099 tCO_2/MWh are added to the objective function for the photovoltaic panels.

The electricity prices are varying on a daily, weekly and seasonal basis. All pricing data is taken from the local distribution company. Carbon emissions are based on the European UCTE electricity mix. The time frame of the total net present costs is 20 years. The discount rate is 2.5%. Energy costs are assumed to increase by 2.5% per year.

Equipment	Efficiency/COP	Unit costs [CHF/kW]	Fixed costs [CHF]
CHP	ε_{el} : 0.3, ε_{th} : 0.4	500	500000
PV	0.18	300 [CHF/m^2]	100000
Boiler	0.7	200	50000
Chiller	ε_{cool} : 4.9, ε_{th} : 5.8	400	100000
HP MT-HT	5	550	120000
HP Ground-HT	3	550	120000
HP Ground-MT	4.5	550	120000
Heat exchanger	0.9	200	-
Pump MT-Ground	45	10	5000
Cooling tower	-	240	-
Ground storage	0.003%/hour	2000	-
MT storage	0.5%/hour	10 [CHF/kW], 4 [CHF/kWh]	10000
HT storage	0.5%/hour	10 [CHF/kW], 2 [CHF/kWh]	10000

Table 1: Parameters of the devices in the energy hub

Carrier	Price [CHF/MWh]	Carbon emissions [tCO$_2$/MWh]	Load [MWh/yr]
Electricity	0.0951-0.1361	0.594	10204
Natural gas	0.0632	0.237	-
Biogas	0.1452	0.125	-
MT heat	-	-	1369
HT heat	-	-	5627
Cooling	-	-	3899

Table 2: Parameters of the carriers, including loads to be met.

RESULTS AND DISCUSSION

The single-level optimization requires two optimization runs (one minimising emissions, the other costs) to determine the minimum and maximum emissions to use as bounds for the ε-constraints. The single-level outperforms the bi-level optimization for this type of problem, as seen in Figure 2. The computation time for the single-level problem with 16 ε points was 2.15 hours, whereas the bi-level algorithm took 28 hours for 50 generations. From the evolution of the hypervolume shown in Figure 3, it appears that the bi-level algorithm has not yet fully converged. The solutions obtained by the bi-level method after 5 generations are also shown, as this corresponds to the same runtime as the single-level case. It is clear that the optimisation has not progressed at all by this point.

Figure 4 presents the design variables of the single-level optimization solutions. The dominant mitigation measure to reduce the carbon emissions is the use of biogas in combination with the CHP. The UCTE electricity mix includes a lot of power generated by coal plants, giving very high carbon emissions for electricity. The installation of storage and heat pumps results in only a limited reduction of emissions because the heat pumps increase the electricity demand to some degree. Hence, only the use of biogas and electricity production through the CHP can reduce the emissions further. Lots of heat is wasted for very low levels emissions due to the overproduction of heat by the CHP. This mode of operation is not permitted in many countries. High capacities of the heat exchanger and the cooling tower are good indicators that excess heat from the CHP is wasted. These points on the Pareto fronts should not be considered for the implementation of the energy system. The high electricity base load and the high electricity prices favour the use of photovoltaics panels, which are

installed at the maximum capacity for all solutions (even the cheapest, since the capital cost is easily paid back through lower electricity bills within the timeframe considered).

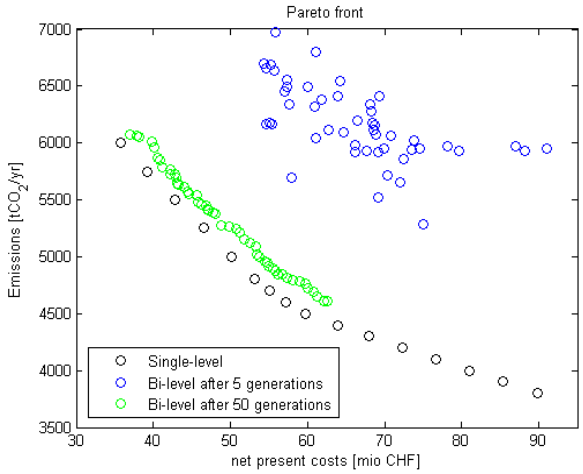

Figure 2: Pareto front for the single and bi-level optimizations

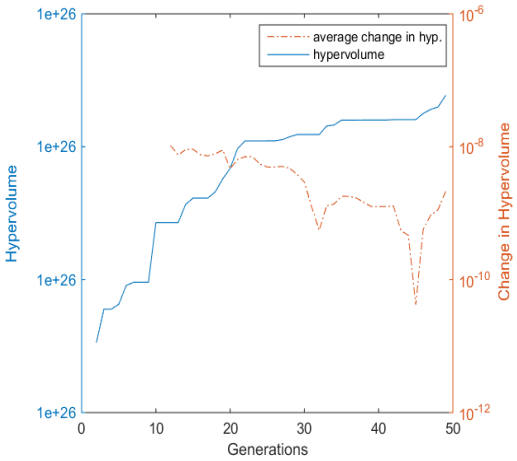

Figure 3: Hypervolume of the Pareto front and the change in hypervolume for the bi-level optimisation

CHP	PV [m²]	Boiler	Chiller	Cooling tower	HP MT-HT	Exchanger	HP Ground-HT	HP Ground-MT	Pump MT-Ground	Ground Storage	Heat Storage HT	Heat Storage MT	Heat Storage HT [kWh]	Heat Storage MT [kWh]	Biogas [%]	Costs [mioCHF]	Emissions [tCO2/yr]
1624	15000	909	172	2046	0	1235	392	239	543	632	1217	184	28534	3815	100	90	3800
1621	15000	920	172	1673	0	1033	388	238	549	625	1173	177	28215	3841	100	85	3900
1621	15000	919	172	1554	0	963	389	238	554	626	1173	177	28130	3815	100	81	4000
1621	15000	919	172	1553	0	962	389	238	554	626	1173	177	28132	3802	100	77	4100
1622	15000	915	172	1484	0	915	390	239	564	629	1175	179	28028	3740	100	72	4200
1619	15000	930	172	1162	0	517	386	232	618	618	1102	294	27132	3642	100	68	4300
1618	15000	931	172	1146	0	301	385	232	617	617	1102	311	27120	3601	100	64	4400
1604	15000	916	172	1099	0	53	392	264	612	612	1050	363	14091	4193	100	60	4500
1540	15000	1208	172	1038	195	345	420	0	420	420	519	421	2524	4703	100	57	4600
1482	15000	1339	172	1062	424	0	0	328	328	328	655	259	3206	3289	100	55	4700
1482	15000	1367	172	1088	501	0	0	343	343	343	0	628	0	3020	100	53	4800
1454	15000	1173	172	938	378	110	236	227	462	462	407	334	1438	2248	88	50	5000
1454	15000	1173	172	938	378	110	236	227	462	462	407	334	1438	2248	65	46	5250
1454	15000	1173	172	938	378	110	236	227	462	462	407	334	1438	2248	43	43	5500
1445	15000	1339	172	1079	465	0	0	331	331	331	413	303	1486	1756	20	39	5750
1450	15000	2175	172	1658	408	320	0	242	242	242	0	0	0	0	0	36	6000

Figure 4: Design variables (Input/output capacities of conversion and storage devices, storage capacities and biogas use) of selected Pareto solutions.

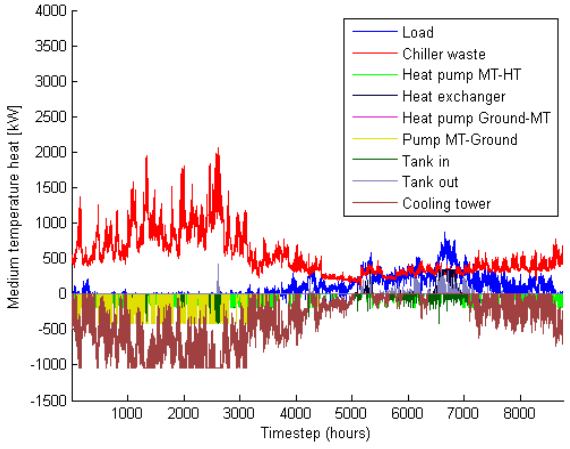

Figure 5:Operation of the medium temperature grid

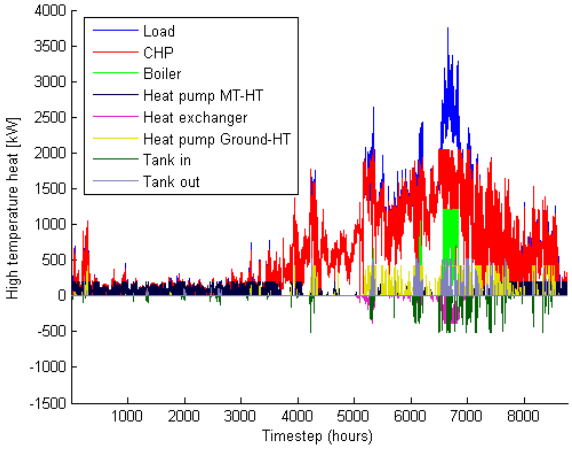

Figure 6: Operation of the high temperature grid

Figures 5 and 6 illustrate a year of operation of the medium temperature grid and the high temperature grid for the single-level solution with emissions of 4600 tCO_2/yr. The low level

of high temperature heat needed in summer is supplied by a heat pump using the waste heat from the chiller as a source. The boiler and a small heat pump using the ground as a source are switched on to meet peak demands. The necessity of reducing the emissions of the UCTE electricity mix does not allow the replacement of CHP by large heat pumps. Hence, a lot of waste heat of the chiller is exhausted via the cooling towers.

CONCLUSION

The single-level optimization finds a better Pareto front in much shorter time than the bi-level approach for this problem instance. Further investigation is needed to establish whether this is true for many types of problem (e.g. if the runtime of the MILP with sizing is higher), or if improvements to the bi-level process can overcome this (e.g. seeding with good solutions).

The case study illustrates the importance of a multi-carrier perspective on the reduction of carbon emissions. The high carbon emissions of the European electricity mix lead to high biogas consumption and costly operational solutions. PV is installed at the maximum permitted level of 15,000m^2 in all cases due to high energy prices.

Further research that considers scenarios with different electricity generation mixes is required. A more accurate modelling of the geothermal and short-term storages using temperature nodes is suggested, along with constraints on dumping excess heat from CHP if applicable.

ACKNOWLEDGEMENTS

Prof. J. Lygeros and Prof. R. Smith are thanked for their valuable help and support. This research has been financially supported by CTI within the SCCER FEEB&D (CTI.2014.0119).

REFERENCES

1. Mancarella, P. : MES (multi-energy systems): An overview of concepts and evaluation models. Energy, 65, pp 1-17, 2014.
2. Geidl, M., Koeppel, G., Favre-Perrod, P., Klockl, B., Andersson, G., & Frohlich, K. : Energy hubs for the future. IEEE Power and Energy Magazine, *5*(1), pp 24-30, 2007.
3. Lund, H., Werner, S., Wiltshire, R., Svendsen, S., Thorsen, J. E., Hvelplund, F., & Mathiesen, B. V. : 4th Generation District Heating (4GDH): Integrating smart thermal grids into future sustainable energy systems. Energy, 68, pp 1-11, 2014.
4. Fazlollahi, S., Mandel, P., Becker, G., & Maréchal, F. : Methods for multi-objective investment and operating optimization of complex energy systems. Energy, 45(1), pp 12-22, 2012.
5. Evins, R.: A Bi-Level Design and Operational Optimisation Process Applied to an Energy Centre. Journal of Building Performance Simulation, 2015.
6. YALMIP: A Toolbox for Modeling and Optimization in MATLAB. J. Löfberg. In Proceedings of the CACSD Conference, Taipei, Taiwan, 2004.
7. Deb, K., A. Pratap, S. Agarwal, and T. Meyarivan. 2002. “A Fast and Elitist Multiobjective Genetic Algorithm: NSGAII.” IEEE Transactions on Evolutionary Computation 6: 182–197.

CONCEPT DEVELOPMENT OF AN INDUSTRIAL WASTE HEAT BASED MICRO DH NETWORK

Charlotte Marguerite[1], Ralf-Roman Schmidt[1], Nicolas Pardo Garcia[1],

1: AIT Austrian Institute of Technology, Giefinggasse 2, 1210 Vienna, Austria

ABSTRACT

District heating (DH) systems are an effective and efficient way to address the challenges of urban areas in terms of energy efficiency, use of renewables and CO_2 emissions reductions [1]. The design and operation strategy of such systems is not always trivial and several questions appear, especially when integrating a significant share of fluctuating, small scale and distributed low temperature heat sources: How to optimize a network design, how to operate a network in an energy and cost efficient way? How to integrate different technologies? How to satisfy customers 'needs when they have different profiles?

This paper briefly presents the CITYOPT project, which aims at creating a web application with guidelines to support efficient planning and detailed design and operation of energy systems in urban districts. A demonstration case for testing the CITYOPT application is then presented: A concept/feasibility analyses for a micro DH network in Vienna, based on industrial waste heat at different temperature levels rejected from a nearby industrial facility. The study includes the consideration of one standard office building, two energy efficient office buildings, existing renewable energy supply (solar thermal heat and heat pumps) and thermal storages (long and short term), to balance the heat production and demand. In the future, different configurations of the district network will be modelled and tested through APROS, a multifunctional dynamic simulation tool and linked to the CITYOPT application, in order to determine the optimal design solution.

Keywords: micro-DH network, industrial waste heat; energy systems, smart cities

INTRODUCTION

The green transition of the District Heating and Cooling sector can be achieved through large-scale replication of best practice by 2020: better valorization of local resources, such as renewable (including secondary biomass and waste) and surplus energy [2]. Systems must evolve to provide more flexible solutions for instance low temperature networks and the integration of innovative thermal storage. These solutions must fit customers' profiles and be applicable to different scales from small neighborhood solutions to city wide networks. The efficient utilization of local waste heat (excess heat from industrial processes, waste incineration and power stations) together with other renewable energy (geothermal energy, large-scale solar thermal energy or large-scale heat pumps) in district heating networks becomes essential in future sustainable cities [3-5]. The integration of various sources is difficult to handle, since standard tools and operation strategies don't consider low-temperature and fluctuating sources with a significant share. These issues are addressed in the CITYOPT project and in particular in the Vienna demonstration case.

The CITYOPT project is a collaborative European project [2] whose main objective is to create applications that bring together information and guidelines for designing scenarios of energy systems and help prioritizing alternative energy solution scenarios based on social, economic and environmental criteria. The "CITYOPT Tool" will provide support for decision

makers through a platform which can be used to combine diverse input information in order to perform simulations (interactions with any simulation software will be possible) and optimizations based on the input information and mathematical models. This information can be used to build indicators which allow the performance analysis of an energy system under different conditions. In particular, the CITYOPT tool will be tested with APROS simulation software (a simulation energy software allows to model complex urban energy system in a flexible way [6]) on the Vienna case study which consists of an industrial fed micro-DH network including existing and new buildings together with short and long term storages and renewable energy supply.

This paper is structured as follows. First the method used within the project to identify the challenges of the case study is explained. Then the Vienna case study of is described. The network concept development and the challenges are presented afterwards.

METHOD

Initially, the Vienna case was selected to be studied within the CITYOPT Tool because it embodies the main challenges of future DH systems as mentioned above (various industrial waste heat, renewable and fossil heat sources, low-energy consumers and standard consumers, storages).

Several steps were necessary to develop the DH network options that will be evaluated. First of all, the supply heat sources characteristics were either manufacturer information (solar panels, heat pumps, gas boilers) together with literature or monitoring data (temperatures and fluctuations of the industrial waste heat source). The energy demand characteristics were obtained from TRNSYS simulations of the buildings, where monitoring data of the energy consumption were used to calibrate the simulation. The second step was the identification of the specific challenges from the case study, through preliminary design studies and workshops with different stakeholders and thematic experts:

- Technical challenges: hydraulic and multi-temperature level constraints, integration of various sources and consumers with low-energy demand
- Social challenges: behaviors and comfort requirements from the end-users
- Economic challenges: current and possible future business models

CASE STUDY AND CHALLENGES

The Vienna study case is based on three office buildings, TECHbase (Tb), ENERGYbase (Eb) and FUTUREbase (Fb), located in the 21st district of Vienna. Fb is under planning but not built yet. They lie in close proximity to Rail Tec Arsenal GmbH (RTA), a facility using one of European largest climatic wind tunnels. During these tests a huge amount of waste heat is rejected from the chillers to the air [7].

This case study of Vienna is a particular case of interest for the investigation in the CITYOPT Tool, since it can bring a lot of knowledge and concepts for future developments of smart and micro district heating networks (DHN). Indeed, it gathers many current and future challenges regarding DHN, such as how to integrate in a hydraulically connected system: renewable sources, industrial waste heat (fluctuating heat source, with different temperature levels), thermal storages (short term and long term) in order to satisfy the heat demand of low energy buildings and standard buildings, with respect to environmental, energetic and economic objectives. This case study is not trivial since the optimum dimensioning and design of the system components (topology of the distribution network according to multi-temperature levels and pressure levels, hydraulics of the network and control strategy) require particular

attention and the use specific tools. The different temperature levels that have to be included in the network are illustrated in Figure 1.

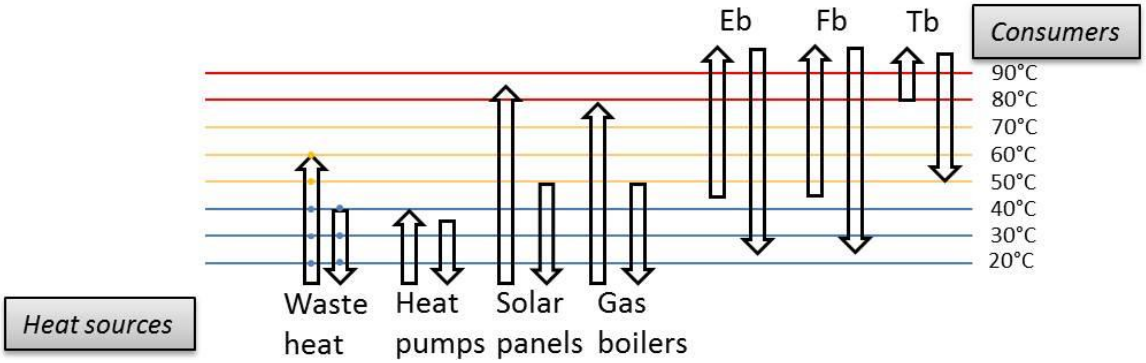

Figure 1: Supply and return temperatures of the heat sources and the consumers

Apart from the network design, the control strategy has also to be well defined in order to allow an optimum operation of the network, addressing issues such as, which situation is more profitable to store heat for long or short term, the number of prosumers who can feed the grid at the same time or how much heat can be store, considering the renewable and waste heat available. Additionally, the complexity of this system brings the need for the development of new business models which consider local price regulations, customers' needs, the prosumers integration, network operators and industrial profitability.

Moreover, this micro-DH can be used as an example that could be scaled up or adjusted to many cases of networks that have to be refurbished or extended. These are some questions that arise with this specific study case that can help for similar case studies [3-5, 8-10].

The current situation the different components is illustrated in Figure 2. A gas boiler provides heat to Tb. Fb will have a solar thermal array and potentially an additional ground source heat pump (not shown on Figure 1 for drawing reasons). Two ground source heat pumps and solar thermal panels provide heat to Eb. Fb and Eb are designed for a maximal use of the internal gains from occupants and equipment in order to almost eliminate heating demand. The average daily heat demand profile for Eb and Tb are shown on Figure 3 [11]. The test case is to connect all the components by a micro-DHN. Several scenarios are designed for the study case and will be simulated through APROS. More detailed information about this study case in [11].

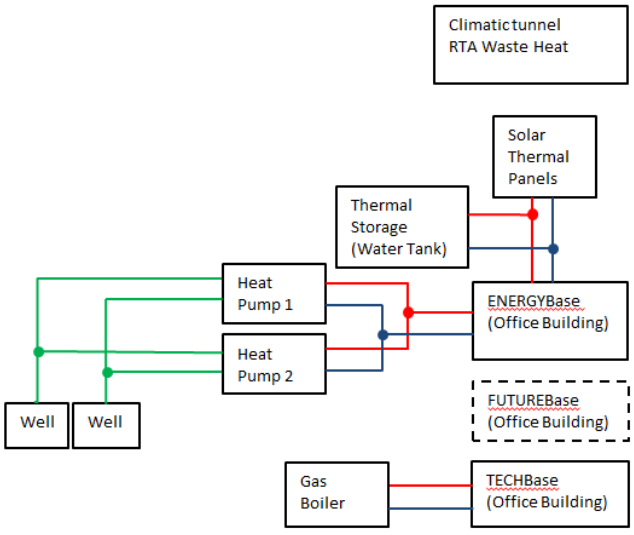

Figure 2: Base scenario –3 independent buildings and an industry are located in the same area.

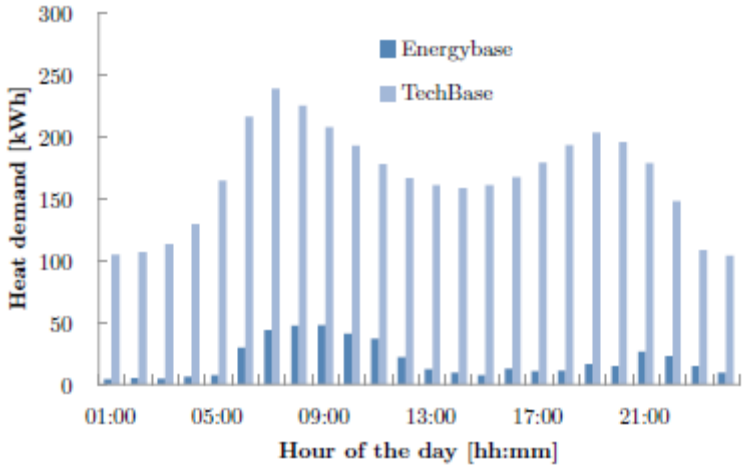

Figure 3:Average daily heat demand profile for 2010, (mathematical models [12]).

Moreover two possible storage solutions are envisaged, a water tank as mid-term storage and boreholes heat exchangers as seasonal storage, to allow the storage of excess energy from the solar thermal panels and from the RTA chiller. Depending on the experiments performed in the RTA´s climatic tunnel the temperature levels and total heat loads of the waste heat able to be supplied to thermal energy network will vary significantly, as illustrated in Figure 4. In addition to this, the periods of the facility when no experiments are taking place have to be considered. Therefore mid-term thermal storage is expected to be an important feature of the balancing system, making it a key component of the thermal energy network performance in the Vienna study case. Using the mid-term storage, the surplus heat could be stored for a few days to enable the network to balance heat generation with demand.

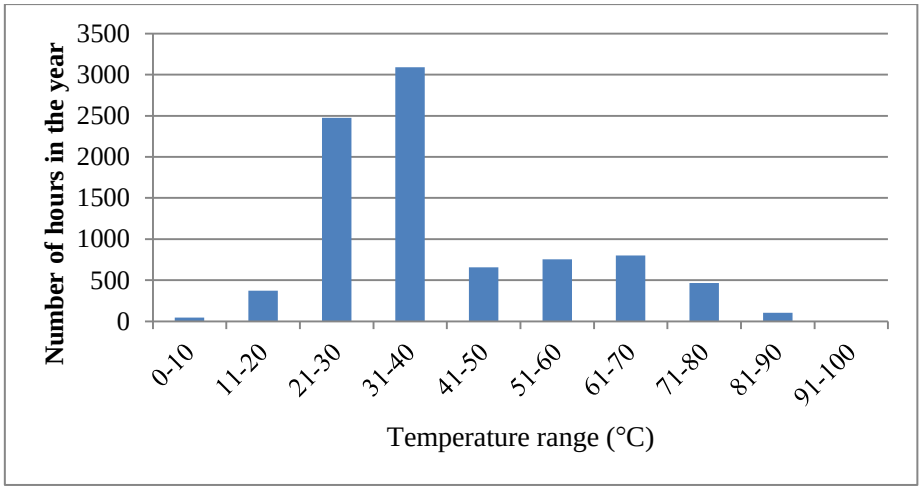

Figure 4: Frequency of temperatures that can be supplied by the industrial waste heat source. (based on a study of the heat rejection system of RTA [12]).

To produce usable information, the CITYOPT tool will perform optimizations on different scenarios which have different options in terms of the design of the water tank, ground heat exchanger, the topology of the district heating networks together with operation of the system according to the variation on the defined constraints. The best design of the district heating network will be determined according to specific criteria (optimization variables) to maximize the rejected heat to the ground, to maximize the energy efficiency of the chillers of the RTA´s climatic tunnel, to minimize the CO2 emissions of the overall system according with the

technical and economic constraints, to minimize the import of energy (gas and electricity) to the system or to minimize the energy bill of the office buildings. The optimization process should be run under several type of constraints such as: the maximum size of the water tank, the maximum area were the boreholes of the heat exchanger can be allocated, the maximum temperature of the ground which can be reached by the rejected heat, the minimum and maximum temperature levels of the warm water needed to cover the heat demand of the office buildings, economical constraints based on the investment and operational cost of the system, fluctuations on the production of the waste heat from RTA´s climatic tunnel due to its use, influence of the weather conditions in the heat production from the solar thermal panels.

DISCUSSION/ OUTLOOK

The Vienna case of micro DH-network is a challenging study case, insofar as it is a small scale network, it consists of several components, with specific characteristics, that can be connected in different ways. The four network configurations which will be designed in more detail and the Base scenario that will be later simulated in the CITYOPT tool are presented in Table 1. Various thermal, dimensioning and hydraulic issues arise for each possible design scenario, such as:

- the pipes configuration/ network topology which is more efficient (less expensive, more controllable): choosing between bi-directional use of pipes and the use of several pipes in parallel.
- how to connect the buildings to supply the grid and to take energy from the grid (a direct connection or heat exchangers),
- the number of network pumps that should be used, especially considering bi-directional flow from and to the buildings/storages (some buildings can receive and supply energy to the network)
- the possible need for (micro-)booster heat pumps to deal with the different temperature levels of supply and demand,
- the optimal size for the storages in order to optimize the balance between heat generation and demand, maximize the utilization of waste energy, to minimize the losses, costs …

Simulations and optimizations through the CITYOPT tool will address these issues and determine the optimal network design according to the key performance indicators defined (e.g. total costs, CO2 emissions, share of renewables, waste heat supplied, primary energy consumed, storages contribution …).

	Base Sc.	**Sc. 1**	**Sc. 2**	**Sc. 3**	**Sc. 4**
Micro-net	No	Yes	Yes	Yes	Yes
Water tank	No	Yes	No	No	Yes
Ground storage	No	No	Yes	No	Yes
Waste heat source	No	No	Yes	No	Yes

Table 1: Different network configurations which will be simulated.

CONCLUSION

To address the challenges of future DH systems, a small scale case study in Vienna has been selected as role model. This case study is including existing and new buildings, waste heat from an industrial climatic chamber, renewables (heat pumps, solar panels), fossil heat source (gas boiler), and storages. The design and operation of such systems, with a high share of

alternative heat sources and different customer characteristics, is complex and its optimization faces many challenges. A suitable decision environment (CITYOPT tool) will be applied in the future to the specific case study to handle the aspects mentioned above.

At the time of the writing, the CITYOPT project is still in its running phase. So far it has been decided to evaluate four configurations of networks and the Base scenario. Each of these configurations will be optimized (system design parameter, temperatures, size and power of pumps, size of storages, control strategy) and various indicators will be calculated out of the simulation results, in order to determine the best design scenario that will allow satisfying consumers' needs at the least costs and environmental impacts. The results given by the CITYOPT tool will allow decision makers and planners to design networks based on the analysis of a large panel of possibilities.

REFERENCES

1. United Nations Environment Program. http://www.unep.org/energy/districtenergyincities
2. CITYOPT project website http://www.cityopt.eu/
3. Lund, H., Moller, B., Mathiesen B.V., Dyrelund, A.: The role of district heating in future renewable energy systems, 35, pp 1381–1390, Energy, 2010.
4. Lund, H., Werner, S., Wiltshire, R., Svendsen, S., Thorsen, J.E., Hvelplund, F., Mathisen,, B.V.: 4th Generation District Heating (4GDH) Integrating smart thermal grids into future sustainable energy systems, 68, pp 1-11, Energy, 2014.
5. Schmidt, R.R., Pol, O., Page, J.: "Smart Cities: Challenges and Opportunities for Thermal Networks. Proc. of the 13th International Symposium on District Heating and Cooling, S. 29 – 37, Copenhagen, Denmark, September 2012.
6. APROS – Dynamic Process Simulation Pricess. Avialable at: www.apros.vtt.fi
7. Website of Rail Tec Arsenal GmbH http://www.rta.eu/en/
8. Werner, S.: District heating and cooling. Studentlitteratur 2013.
9. Munster, M., Morthorst, P.E., Larsen, H.V., Bregnbaek, L., Werling, J., Lindboe, H.H., Ravn, H.: The role of district heating in the future Danish energy system, 48, pp 47-55, Energy, 2012.
10. DHC+ Technology Platform: District heating and cooling – Strategic research agenda, http://www.dhcplus.eu/wp-content/uploads/2012/05/120529_DHC+SRA_final.pdf
11. Pardo, N., Nadler, F., Marguerite, C., Kelly, B.: CITYOPT – Holistic Simulation and Optimisation of Energy in Smart Cities – Vienna Study Case. 2nd ICERE conference, Vienna, 2015.
12. Girardin, A.: Thermal storage aiming at increasing the share of used heat rejected from a cooling process. EPFL and AIT, Lausanne, 2012.

THE PROPOSAL FOR A SPATIAL PLANNING SUPPORT SYSTEM TO ESTIMATE THE URBAN ENERGY DEMAND AND POTENTIAL RENEWABLE ENERGY SCENARIOS

E. Morello[1]; M. Bignardi[1]; M. A. Rudini[1]

1: Laboratorio di Simulazione Urbana 'Fausto Curti', Department of Architecture and Urban Studies, Politecnico di Milano, Milan, Italy

ABSTRACT

A simplified methodology for the estimation of energy demand (heating, electricity, hot water) and the production of renewable energy of households at the city level based on the available data and information is presented. The aim of this work is to develop a spatial planning support system, i.e. an estimation tool based on the use of geographic information systems (GIS) in order to support public administration and stakeholders towards a sustainable energy and urban planning at the local scale. For instance, assessing urban energy quantities and potential energy productions can drive urban policies and planning decision-making. The tool was applied to the case-study area of the city of Milan, Italy. Outcomes show that in terms of energy savings, the retrofitting of households reveal huge margins for improvement, whereas in terms of energy production through RES, geothermal and solar energy represent the only valid options, because other sources require the availability of open spaces, thus far beyond the saturated urbanized land of the town. Finally, the calculation procedure is easy to run and represents a versatile and adaptable energy prediction tool to be used to link energy and urban planning in a more effective way.

Keywords: energy consumption estimation model, urban heatmaps, energy-conscious urban planning, spatial planning support system, GIS.

INTRODUCTION: THE GENERAL CONTEXT AND THE OBJECTIVE OF THIS STUDY

Cities as the major actors towards energy consumption reduction. International and national programs are pushing for a drastic reduction of energy consumption, improvement of efficiency and clean energy production from renewable sources. Reports from the International Energy Agency estimate that in 2030 cities will consume about 75% of the total energy production and buildings will make use of about 40% of the global primary energy [1]. However, most of the energy related policies are addressed at the scale of the building or at the global scale (see for instance the policies on the reduction of greenhouse gases emissions). In fact, urban planning and energy planning still remain two separate dimensions. We argue that a focus on the spatial dimension of energy, which is missing in the current practice, would improve the general understanding of the phenomena. Hence, the final aim of this work is to provide municipalities with a flexible and simplified tool for the estimation of urban energies in order to allow policy- and decision makers to get a first understanding of the implied quantities, sizes and locations of the energy phenomena.

THE RESEARCH CONTEXT

In order to setup our methodology we refer to the available literature on the approaches to mapping and a series of applications on case studies. Heatmaps and urban energy maps in particular, represent the main outcome of estimation or prediction models of energy consumption and performance at the city scale.

Bottom-up and top-down models

The construction of urban energy- and heat maps can be based on different approaches depending on the scopes. Swan and Ugursal [2] present a classification of urban heatmap models based on two approaches, namely top-down and bottom-up approaches (Figure 1). Bottom-up approaches start from the analysis of energy consumption for single final uses, and from those the sampling and aggregation methods of data at the larger scale are consequently defined. The extrapolation methods of data are of two types, namely the statistical or the engineering type. The first type is based on the use of the historical information which undergoes a series of statistical procedures; the second one relies on the use of technological information, like the type and efficiency of energy appliances, which are investigated and then aggregated through three methods: the population distribution method, the archetype method and the sample method [2]. On the contrary, top-down approaches rely on aggregated data, based on historical records such as econometric variables (GDP, occupation rates, etc.) and technological variables (climate data, rate of construction/replacement of the building stock, average number of appliances per household, number of employees per household, etc.). In these models, the built fabric is considered as an energy absorber and dissipater, with no need to take into account the final uses in detail.

In general, top-down approaches are applied at the large scale (regional and national), whereas bottom-up procedures are often used at the urban or district level. Nevertheless, the overlapping of procedures within the same model is possible, and often, different methods (for example the statistical and engineering one) are integrated.

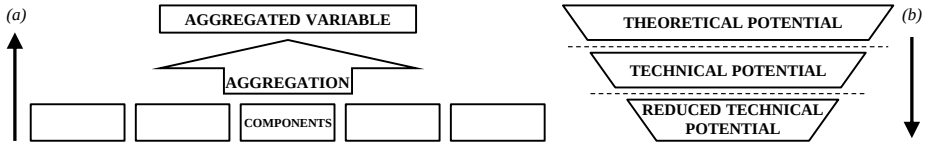

Figure 1: (a) Bottom- up and (b) top- down approaches applied in the construction of urban energy models. An elaboration from [2].

Case studies on urban energy consumption maps and renewable energy maps

The first exploration refers to the heatmaps, i.e. maps that estimate urban energy consumptions. All the analysed methods are bottom-up procedures and most of them are limited to the computation of heating consumption for the household sector alone. Only some methods include other land use than households [3, 4], and only few provide scenarios with energy reduction [5, 6, 7].

Concerning the energy production maps through RES, numerous references adopt top-down approaches [8, 9]. Some works aim at investigating the potential production of one source alone: Bergamasco and Asinari [10] provide a quick methodology for the estimation of electricity production through photovoltaic technologies at the city scale. Fiorese and Guariso [11] work on the optimization of the localization of biomass plants at the regional scale. Other studies take into account multiple energy sources to promote energy diversification [12, 13].

METHODOLOGY: THE CONSTRUCTION OF THE MODEL

We implemented a model for the estimation of the energy demand, the energy performance and the potential of renewable energy applicable to a city or larger territory. Thanks to the implementation of the methodology with GIS software, it is possible to geo-refer every estimated information.

The model is divided into three distinct parts (Figure2): (i) the current energy consumption of residential buildings of the case study (estimation of current consumptions) are defined; (ii) improved consumption scenarios based on the implementation of a number of measures to reduce the energy demand (estimations of future consumptions) are assessed;(iii), the energy demand that can be satisfied from local RES is estimated (estimation of RES potential).

Hence, this work does not only assess the current energy consumption, but designs future scenarios, evaluating possibilities and benefits in two steps: first, through an overall reduction in consumption due to the increase of efficiency, and second, through the coverage of part of the demand by local RES, thus reducing the use of conventional and imported sources.

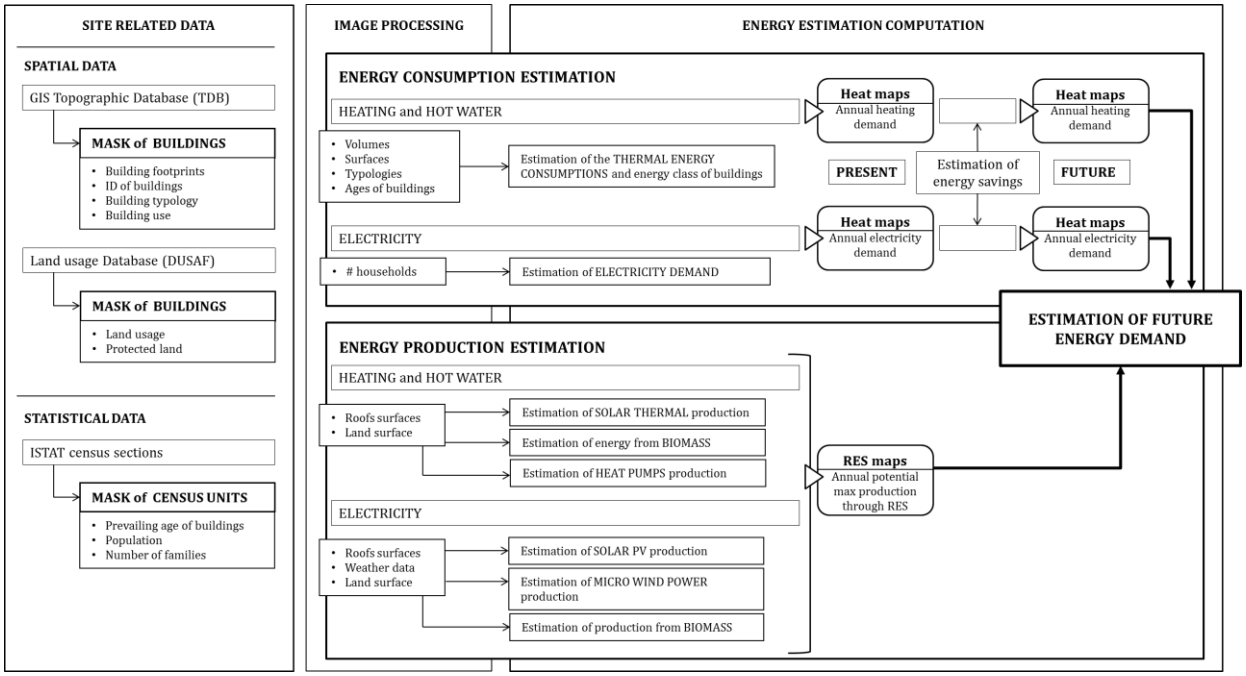

Figure 2: Conceptual scheme of the structure of the model

THE APPLICATION

We applied the model to the municipality of Milan. Past studies [4] and CEER (Catasto Energetico Edifici Regionale), i.e. the official energy cadastre that collects certificates [14] represented our main references to validate the outcomes of this work. Data available for the city of Milan and used as the main entry information are: (i) the topographic database (TDB) and statistical data from the national census referred to the local units. The first step was the construction of the database of residential buildings. A series of operations on the TBD crossing the census data have been carried out in order to eliminate noise and derive the total number of residential units. Moreover, by crossing these two databases with GIS software, we could define the age classes, the S/V ratios and the number of floors for each building, and from this the building typology.

The estimation of thermal energy demand and improved scenarios

For assessing the consumption of thermal energy for space heating and hot water production we refer to TABULA [15, i.e. a database with 28 archetypes of buildings, obtained by crossing four building typologies and seven age classes to define the thermal primary energy for each one. We aggregated the archetypes according to an engineering bottom-up approach. As a limitation, we have to state that retrofitting measures and the presence of RES on the current building stock cannot be addressed. Hence, we start from a more restrictive baseline.

Current thermal energy demand is overall very high (Table 1a). In fact, for heating 92% of the buildings belong to the worst energy class (G class), while this percentage becomes 95% for hot water. The main reason is the obsolescence of buildings; even if Milan is characterized by one of the most efficient building typology (72% of buildings are apartment blocks), about 90% of Milan stock was built before 1971, and only 4% after 1981.

Two retrofitting scenarios (a standard and an advanced one) were proposed on the basis of current best available technologies and are based on TABULA [15]. As it clearly emerges from Table 1b, there is a great difference between current and future estimated demand. For instance, the maximum potential energy saving for heating is estimated to reach 83% for a standard retrofitting, and 89% for the advanced retrofitting; for the hot water consumptions, the savings are lower, but still relevant. Hence, we can finally argue that the existing stock could be a huge source of energy savings. It is true that these predictions appear to be very optimistic, but we looked forward to long-term scenarios and considered the expected technology advancement to happen in the next 20 years.

(a) Current estimated thermal energy consumption for heating and hot water

	Heating consumptions	**Hot Water consumptions**
Average consumption (kWh/m^2/year)	258	48
Global consumption (GWh/year)	12.763	2.374

(b) Future estimated thermal energy consumption for heating and hot water

	Current consumptions	**Standard retrofitting**	**Advanced retrofitting**
Average heating consumption	258	43	26
Energy saving (%)		83,3%	89,9%
Average HW consumption	48	26	14
Energy saving (%)		45,8%	70,8%

Table 1: (a) current estimated thermal energy consumption for heating and hot water; (b) future estimated thermal energy consumption for heating and hot water

The estimation of electric energy demand and scenarios

For the current electricity consumptions we refer to MICENE dataset [16]; even if quite old, it is representative for the case study, containing most of the measures from Milan households. Considering the average annual electricity demand per household of 3.250 kWh and the number of household for every census section, the calculation for the city was easy to derive (Table 2a). In order to assess the improvement scenarios, we referred to Intelligent Energy Europe projects [17]. These quantify the maximum potential of electricity savings per household in percentages of around 40% of current electricity consumption (Table 2b).

Legend	**(a) Current demand**	**(b) Future demand**
Average yearly demand per section	345.313 kWh/year/section	207.188 kWh/year/section
Global annual municipal demand	2.058 GWh/year	1.234 GWh/year

Table 2: Estimated electricity demand for Milan aggregated on the census sections

Energy improvement scenarios through renewable energy sources

This last part of the work aims to estimate the share of the global energy demand that can be satisfied by RES, in order to reduce the import of conventional fossil fuels. It is important to stress that RES have to be found locally within the municipality borders, thus maximizing the benefit of this fuel switching and, at the same time, minimizing the 'energy transferring' (e.g. biomass transport, electricity infrastructure, pipe grids). Before introducing the results, it is important to state that the above introduced thermal energy demand scenarios already

consider various types of RES for the production of thermal energy (i.e. geothermal heat pumps and solar thermal), particularly in the advanced retrofitting scenario; hence, in this section we decided to consider those RE plants that provide electricity only. The technical potential of the following RES were considered in the model through feasibility analysis: very-small and small-wind turbines, cogeneration of biomass, biomass anaerobic digestion and solar PV systems.

Numerous RES do not represent an option. Wind turbine systems were discarded because of the low natural ventilation and the aesthetic and environmental intrusiveness make this technology not convenient. Biomass cogeneration plants is unsustainable, because Milan in 2009 has less than 30 ha of woody crops, while a cogeneration plant of 1 MW needs at least 150 ha. Anaerobic digestion plants from animal manure are not an option due to the lack of heads (Milan has just 40 swine, while a 100 kW plant needs at least 3.000); moreover, all the cattle of the municipality (424) could feed a 180 kW plant, able to satisfy 1,2% of the future electric demand (1,5 GWh/year), but this is not convenient due to the dispersion of the farms on the territory. About anaerobic digestion of crops, we have estimated that if all the arable land was converted into energy crop, we could build 21 biogas plants of 300 kW each, which could produce 50,4 GWh/year (4,1% of future electricity demand), but this is an and unsustainable scenario, if we consider a more convenient food production.

Finally, we checked the potentiality of PV systems on building roofs, and we can state that the energy output is more efficient. We estimated the available roof surface for PV panels [11]; for electricity production we drew up six different scenarios, depending on the possibility or not to install PV panels in the city centre and to install only Monocrystalline Silicon panels, only Polycrystalline Silicon panels or to install the same share of panels as currently applied in Italy (Table 3). PV systems could potentially cover from nearly a half (best scenario) to about 1/3 (worst scenario) of the future electricity demand.

Scenarios		Total production (GWh/year)	Quote on future demand (%)
PV in city center	**Mono Si scenario**	**583,1**	**47,2**
	Poli Si scenario	501,6	40,6
	IT mix scenario	522,3	42,3
NO PV city center	Mono Si scenario	483,9	39,2
	Poli Si scenario	**387,1**	**31,4**
	IT mix scenario	431,7	35,0

Table 3: *PV electricity production in Milan and table with estimated numerical data*

CONSIDERATIONS AND CONCLUSIONS

General considerations emerging from the application of the tool are as follows: (i) taking into account the spatial dimension of territories allows to give a better understanding of the potential provision of energy scenarios and the implementation of RES; (ii) the calculation procedure is easy to run even with poor entry data, mostly derived from geometrical information derived from the 3D urban model; (iii) it can be easily replicated, thus representing a versatile and adaptable energy prediction tool to be used to link energy and urban planning in a more effective way.

Specific considerations on the application in Milan are: (i) the city goes far beyond the current political boundaries that today correspond to an almost 100% urbanized land with few open spaces: hence, the metropolitan area would be the proper dimension for energy planning; (ii) the different urban tissues and locations offer alternative opportunities and corresponding energy scenarios; (iii) only a first broad estimation of RE production can give a clear understanding about the potential efficient strategies to promote and the sources to discard.

REFERENCES

1. IEA: Promoting energy efficiency investments. Case studies in the residential sector. Paris: OECD/IEA and AFD, 2008.
2. Swan, L., & Ugursal, V.: Modeling of end-use energy consumption in the residential sector: a review of modeling techniques. Renewable and Sustainable Energy Reviews, 13, pp 1819-1835, 2009.
3. Modi, V.: Spatial distribution of urban building energy consumption by end use. Energy and Buidings, 45, pp 141-151, 2012.
4. Caputo, P., Costa, G., & Ferrari, S.: A supporting method for defining energy strategies in the building sector at urban scale. Energy Policy, 55, pp 261-270, 2013.
5. Jones, P., Lannon, S., & Williams, J.: Modeling building energy use at urban scale. 7th International IBPSA Conference. Rio de Janeiro, 2001.
6. Yamaguchi, Y., Shimoda, Y., & Mizuno, M.: Proposal of a modeling approach considering urban form for evaluation of city level energy management. Energy and Buildings, 39, pp 580-592, 2007.
7. Reiter, S., & Marique, A.: Toward low energy citie - A case study of the urban area of Liège, Belgium. Journal of Industrial Ecology, 16, pp 829-838, 2012.
8. Biberacher, M., & Gadocha, S.: GIS based model to optimize the utilization of renewable energy carriers and related energy flows. 18th World IMACS congress and MODSIM09, pp 1915-1921, Anderssen RS, Braddock RD, Newham LTH editors, 2009.
9. Angelis-Dimakis, A.: Methods and tools to evaluate the availability of renewable energy sources. Renewable and Sustainable Energy Reviews, 15, pp 1182-1200, 2011.
10. Bergamasco, L., & Asinari, P.: Scalable methodology for the photovoltaic solar energy potential assessment based on available roof surface area: application to Piedmont Region (Italy). Solar Energy, 85, pp 1041-1055, 2011.
11. Fiorese, G., & Guariso, G.: A GIS-based approach to evaluate biomass potential form energy crops at regional scale. Enviromental Modelling & Software, 25, pp 702-711, 2010.
12. Vettorato, D.: Spatial comparison of renewable energy supply and energy demand fo low-carbon settlements. Cities, 28, pp 557-586, 2011.
13. Mourmouris, J., & Potolias, C.: A multi-criteria methodology for energy planning and developing renewable energy source at a regional level: A case study in Thassos, Greece. Energy Policy, 52, pp 522-530, 2013.
14. CENED, Catasto Energetico Edifici Regionali (CEER), Regione Lombardia, www.cened.it (retireved on April 2015)
15. Corrado, V., Ballarini, I., Corgnati, S., & Talà, N.: TABULA, Building Typology Brochure – Italy. Fascicolo sulla tipologia edilizia italiana. Politecnico di Torino, 2011.
16. Dipartimento di Energetica, Politecnico di Milano: MICENE, MIsure dei Consumi di ENergia Elettrica in 110 abitazioni italiane, 2004.
17. REMODECE: REsidential MOnitoring to Decrease Energy use and Carbon emissions in Europe, 2008.

ENERGY HUB MODELING FOR THE DESIGN OF SOLAR THERMAL ENERGY SYSTEMS WITH SHORT-TERM AND LONG-TERM STORAGE

A. Omu[1,2], S. Hsieh[1,2], K. Orehounig[1,2], J. Carmeliet[1,3]

1: Chair of Building Physics, Swiss Federal Institute of Technology, ETH Zürich, Stefano-Franscini-Platz 5, 8093 Zürich, Switzerland
2: Laboratory for Urban Energy Systems, EMPA, Swiss Federal Laboratories for Materials Science and Technology, Überlandstrasse 129, 8600 Dübendorf, Switzerland
3: Laboratory for Multiscale Studies in Building Physics, EMPA, Swiss Federal Laboratories for Materials Science and Technology, Überlandstrasse 129, 8600 Dübendorf, Switzerland

ABSTRACT

A mixed integer linear programming (MILP) energy hub model is developed to design a solar thermal district-heating network for a cluster of residential buildings in Rheinfelden, Switzerland. The model is employed to determine the area of roof-mounted solar thermal collectors that are required to meet the space heating and domestic hot water loads of the 11 buildings in the neighborhood. The installation and operation of electric heaters is permitted in order to supply back up heat during periods when the solar energy is not sufficient to meet thermal loads. The results of the energy hub model show that thermal energy storage (TES) is required in order to achieve solar fractions (i.e. the percentage of total energy demand that is met by solar energy) that are over 10%. Furthermore, the volume of required TES increases exponentially with the solar fraction. Due to the seasonality of space heating demand, the installation of short-term storage tanks alone is not sufficient for achieving solar fractions that are above 60%, and long-term TES units are also required. However, even when both short-term and long-term TES units are installed, 100% solar fraction is still not possible due to the loss of heat in the TES units over time. Finally, for the size and characteristics of the neighborhood analysed in this study, the decentralised storage configuration with both short-term and long-term storage units results in a cheaper energy system with a higher solar fraction, when compared with the centralised storage configurations.

Keywords: solar thermal, thermal energy storage, energy hub, optimisation, MILP

INTRODUCTION

Space heating accounts for around 70% of the final energy consumption in Swiss households. Therefore, as Switzerland looks towards its 2050 CO_2 emission targets which require an 80% reduction in per capita annual CO_2 emissions, there is a pressing need to increase the utilisation of energy efficient and renewable heating sources in the residential sector. Solar thermal collectors are an ideal candidate technology due to the abundance and sustainability of solar energy. However, in order to maximize the utilisation of solar energy, thermal energy storage (TES) is required as heating demand is typically not coincident with the availability of solar radiation. There are numerous decisions that must be made when designing these solar thermal + TES systems for residential quarters. These include determining the optimal solar thermal collector area, the required number and volume of TES units, and deciding whether the storage should be decentralised, with a TES unit located at each building, or centralised, with only a single TES unit that supplies all buildings through a district heating network. To facilitate this decision making, an energy hub model is developed in this paper to design a solar thermal district-heating network for a cluster of residential buildings. The energy hub concept, developed by [1] is a macro-level framework that is used to model the flow, conversion, and storage of multiple energy carriers within an energy system, in order to

facilitate system design and unit scheduling. Energy hub models are typically developed using mixed integer linear programming (MILP) formulations composed of linear equations that describe the conversion of input energy streams (e.g. electricity, solar radiation) to output energy streams (e.g. electricity loads, space heating loads).

The model developed in this paper is used to determine the area of roof-mounted solar thermal collectors and the volume of short-term and long term thermal energy storage units that are required in order to meet the hourly space heating and domestic hot water loads of the buildings in the neighborhood over the course of a single year. In order to ensure that the simplified energy hub formulation is able to represent the typical performance of these systems, the energy hub model is first validated against dynamic simulation models developed in EnergyPlus of the solar thermal + TES systems that are optimised for each building. It is then employed to analyse the influence of the storage configurations by comparing the annual economic cost and renewable energy utilisation of the following system configurations, 1) no storage, 2) decentralised short-term storage only and no long-term storage, 3) decentralised short-term and decentralised long-term storage, and 4) decentralised short-term and centralised long-term storage.

METHODS

An 11 building neighborhood in Rheinfelden, Switzerland was used as a case study to analyse the influence that numerous factors have on the design of solar thermal + TES systems. Three building types, single-family house (SFH), attached single-family house (aSFH), and apartments, are present in the neighborhood. EnergyPlus was employed to simulate the heating demand by utilizing the building geometries and surfaces construction materials, in combination with local weather and internal gains to determine the additional energy required to maintain an indoor air temperature set point of 20°C. It was assumed that building renovation measures were implemented in compliance with SIA 380/1 [2], while mean air temperature was set to comply with Swiss standard indoor air temperature [3]. Internal gains from occupancy, electricity appliance usage, and lighting are accounted for with respect to activity schedules taken from Swiss standards [3]. Figure 1 depicts the layout of the neighborhood, while Table 1 summarises the pertinent information about each of the buildings in the neighborhood.

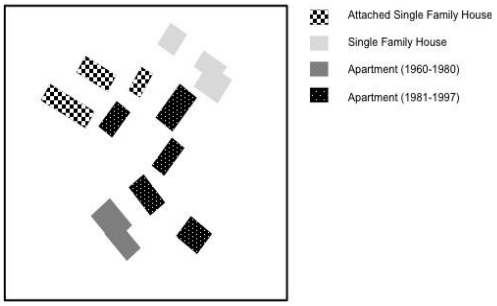

Figure 1: Layout of the 11 buildings in the quarter

Table 1: Summary of Building Information for Rheinfelden Neighborhood

		B1	B2	B3	B4	B5	B6	B7	B8	B9	B10	B11	Total
Building Type		aSFH	SFH	SFH	Apartments						aSFH	aSFH	
Heated Area	m^2	286	842	407	1745	735	945	713	945	880	1100	902	*9500*
SH Demand	MWh/yr	8.1	23.1	7.7	25.7	8.9	13.2	10.3	13.5	16.2	21.6	11.9	*160.2*
DHW Demand	MWh/yr	2.6	7.5	3.6	17.6	7.4	9.5	7.2	9.5	8.9	9.8	8.1	*91.6*
Available Roof Area	m^2	115	211	102	218	92	189	143	252	176	183	150	*1831*

Figures 2(a-c) depict the energy hub structures for the four scenarios that were modeled. In the first scenario, No Storage (Figure 2a), there is no TES unit; therefore the solar thermal collector can only generate thermal energy when there is a demand for either space heating or domestic hot water. An electric heater, run on electricity that is purchased from the grid, is utilised during periods when there is not enough solar energy to meet demand. In the second

scenario, Decentralised One Tank (Figure 2b), there is one short-term storage tank supplying heat for both space heating and domestic hot water, the electric heater is again present to supply the energy loads that cannot be met by the solar collector. The third and fourth scenarios, Decentralised and Centralised Two Tank, have the same energy hub structure (Figure 2c) in which both short-term and long-term storage tanks are charged by the heat transferred from the solar collectors, through a buffer tank. The heat stored in short-term tank is used to supply domestic hot water, while the heat stored in long-term tank is used to supply space heating. The first three scenarios are all decentralised scenarios, in which there is an energy hub at each of the 11 buildings with no energy distribution between buildings, while the fourth scenario is the centralised case, with a single energy hub at building 4 and distribution of energy to all buildings through a district-heating network.

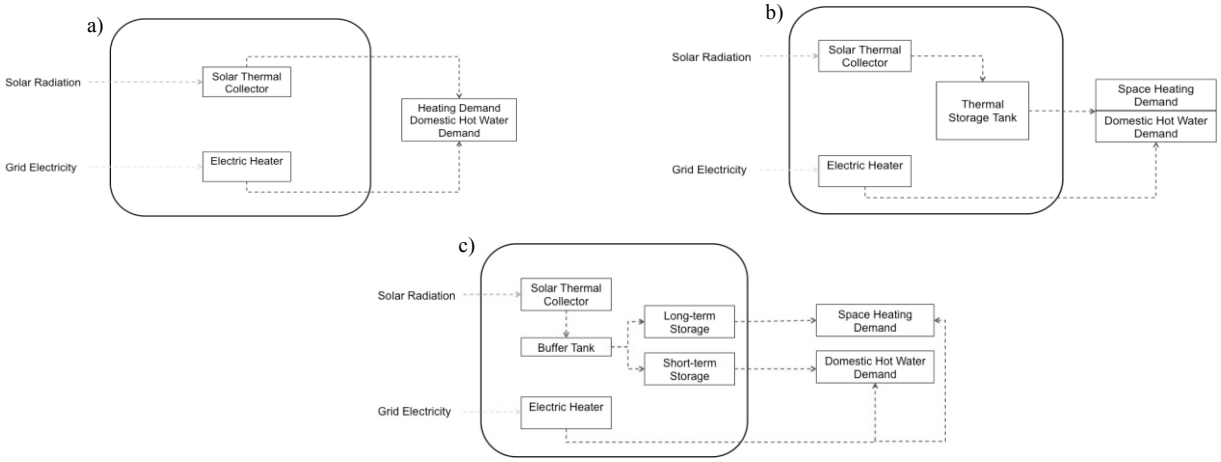

Figure 2: Energy hub structures for the four model scenarios, a) No Storage, b) Decentralised One Tank, c) Decentralised Two Tank and Centralised Two Tank.

The energy hub model contains both integer and continuous decision variables that are indexed over 5 sets, *b*, *b*', *h*, *i*, and *k*. *b* denotes the buildings in the quarter that generate energy, *b'* denotes the buildings that consume energy, *h* denotes the 8760 hourly time intervals that make up the 1 year analysis period, *i* denotes the technologies that can be included in the energy system (i.e. solar thermal collectors (ST) and electric heaters (EH)), and *k* denotes the types of storage (i.e. short-term (Short) or long-term (Long)). The model contains two integer decision variables, the number of units of technology *i* purchased at building *b* ($U_{i,b}$) and the active/inactive status of the district heating network connection between buildings *b* and *b'* ($L_{b,b'}$). The continuous variables in the model are the amount of heat generated by technology *i* at building *b* during hour *h* ($G_{i,h,b}$), the quantity of heat distributed from building *b* to building *b'* during hour *h* ($D_{h,b,b'}$), the electricity that each building *b*' purchases during each hour *h* ($EP_{h,b'}$), the amount of energy stored in storage *k* at building *b* during hour *h* ($Q^{stored}_{h,b,k}$), the amount of energy charged into storage *k* at building *b* during hour *h* ($Q^{ch}_{h,b,k}$), the amount of energy discharged from storage *k* at building *b* during hour *h* ($Q^{dish}_{h,b,k}$), and the quantity of heat lost from storage *k* at building *b* during hour *h* ($Q^{storeloss}_{h,b,k}$). The objective function (Eqn. 1) is to minimise annual economic cost of the energy system, which is the sum of the electricity and fuel costs (C_{elec} and C_{fuel}), operational and maintenance costs (C_{om}), amortised technological capital and installation costs ($C_{capital}$), amortised network cost ($C_{network}$), and the amortised storage cost (C_{store}).

$$\textbf{min}\ C_{fuel} + C_{elec} + C_{om} + C_{capital} + C_{network} + C_{store} \quad (1)$$

The objective function is minimised subject to the following constraints. Firstly, the generation of thermal energy by each technology *i* is bounded by the maximum capacity of

the technology ($MaxCap_i$) multiplied by the number of units of the technology that have been purchased at each building (Eqn. 2).

$$G_{i,b,h} \leq MaxCap_i \cdot U_{i,b} \qquad \forall i,h,b \ (2)$$

Additionally, the space heating demand ($Heating_{b',h}$) at each building *b'* during every hour *h* must be equal to the amount of energy distributed to the building from all buildings *b* during hour *h* (Eqn. 3). The amount of energy distributed from each building *b* to all buildings *b'* is equal to the amount of energy discharged from the TES units at building *b* plus any additional energy generated by the auxiliary electric heaters (Eqn. 4). Distribution heat losses are not explicitly modeled in this energy hub formulation. Instead a fixed heat loss value of ($Q^{distloss} = 4.3\%/\text{km}$) [4] is employed to take into account the losses that occur within the district heating network pipes.

$$Heating_{b',h} = \sum_b D_{h,b,b'} \qquad \forall h,b' (3)$$

$$\sum_{b'} \left(D_{h,b,b'} / \left(1 - Distance_{b,b'} \cdot Q^{distloss}\right)\right) = Q^{disch}_{h,b,k} + \sum_i G_{i,b,h} \qquad \forall h,b,k,i = EH \ (4)$$

Similarly, the domestic how water demand ($DHW_{b',h}$) at each building *b'* must be equal to the energy discharged from the storage *k* plus any energy generated by the electric heater (Eqn. 5). For the one tank scenario both space heating and domestic hot water loads can be met by the energy discharged from the single tank, and there is only one type of auxiliary electric heater installed. However, for the two tank scenarios, the short-term storage tank can only be used to supply domestic hot water loads, and the long-term storage tank can only be used to supply space-heating loads. Furthermore, a differentiation is made between the auxiliary electric heaters that are used to supply the space heating loads, and those that are used to supply the domestic hot water loads.

$$DHW_{b',h} = Q^{disch}_{h,b,k} + \sum_i G_{i,h,b} \qquad \forall h,b', i = EH \ (5)$$

Finally, the energy that is used to charge the storage tanks at each building *b* in every hour *h* is equal to the amount of energy generated by the solar thermal collectors at building *b* in hour *h* (Eqn. 6). The upper bound on this solar energy generation is calculated by multiplying the number of solar thermal collector units that are installed at each building ($U_{i,b}$) by the area of each collector ($Area_i$), the efficiency of each collector (η_i), and the amount of incident solar radiation ($Solar_h$) (Eqn. 7).

$$G_{i,b,h} = \sum_k Q^{ch}_{h,b,k} \qquad \forall h,b,i = ST \quad (6)$$

$$G_{i,b,h} \leq U_{i,b} \cdot Area_i \cdot \eta_i \cdot Solar_h \qquad \forall h,b,i = ST \quad (7)$$

Although the optimisation is a cost minimisation, the emissions are controlled using the ϵ constraint method in which a constraint is used to set an upper bound on the allowable system emissions based on the maximum CO_2 emissions that the system can produce ($MaxCO2_{b'}$) (Eqn. 8). The value of ϵ can then be reduced from 1 to 0 in order to find least cost solutions that lead to increasingly smaller CO_2 emissions.

$$\sum_h GridCO2EmissionFactor \cdot EP_{h,b'} \leq \epsilon \cdot MaxCO2_{b'} \qquad \forall b' \ (8)$$

The thermal energy storage model employed is adapted from [5] in which the amount of energy stored in each hour *h* is a function of the amount of energy stored in the previous hour ($Q^{stored}_{h,b,k}$), plus any energy charged into the storage ($Q^{ch}_{h,b,k}$), minus any energy discharged from the tank ($Q^{dish}_{h,b,k}$), minus storage losses ($Q^{storeloss}_{h,b,k}$) (Eq. 9). Both the charging and discharging efficiencies (η^{ch}_k and η^{disch}_k) are assumed to be 90%.

$$Q_{h,b,k}^{stored} = Q_{h-1,b,k}^{stored} + \eta_k^{ch} \cdot Q_{h,b,k}^{ch} - \frac{Q_{h,b,k}^{dish}}{\eta_k^{disch}} - Q_{h,b,k}^{storeloss} \qquad \forall h,b,k \quad (9)$$

Storage losses are calculated using the two parameter heat loss expression developed by [5] in which the hourly heat losses are a function of the amount of energy stored in the previous hour as well as static losses from the unusable energy in the tank (Eqn. 10).

$$Q_{h,b,k}^{storeloss} = Q_{h-1,b,k}^{stored} \cdot \theta_k^{store} + Q_{b,k}^{capacity} \cdot \left(\frac{T_k^{min} - T_k^{amb}}{T_k^{max} - T_k^{min}}\right) \cdot \theta_k^{static} \qquad \forall h,b,k \quad (10)$$

The MILP model is solved using the AIMMS Software program, which is an optimisation software program that uses the CPLEX solver. CPLEX employs a branch and bound algorithm to solve the MILP.

RESULTS AND DISCUSSION

In order to first validate the energy hub model, the solar thermal collector area was fixed at the maximum available roof area for each building and the resulting short-term and long-term storage volume sizes were determined. These design specification were then used to create dynamic simulation models for each building in EnergyPlus [6]. The system performance of the energy hub models and the corresponding EnergyPlus models were then compared in order to determine if the simplifications that are made in the linear energy hub model have a significant impact on the performance of the energy system. Solar fraction (SF) was chosen as the metric of comparison. Solar fraction, defined as the percentage of the total annual energy demand that is satisfied by solar energy, is calculated as SF = 1 – (Generation$_{ElecticHeater}$/Total Energy Demand). Figure 3 shows the solar fraction comparison of the energy hub and EnergyPlus models for the individual buildings in the three decentralised scenarios. The comparison shows that although the energy hub model is not always able to achieve solar fractions that are equal to the results of the more detailed EnergyPlus model, it typically leads to results that are within 10% of the EnergyPlus output. Additionally models show a similar trend of increasing solar fractions when going from no storage to only a short-term storage tank to both short-term and long-term storage tanks for most of the buildings.

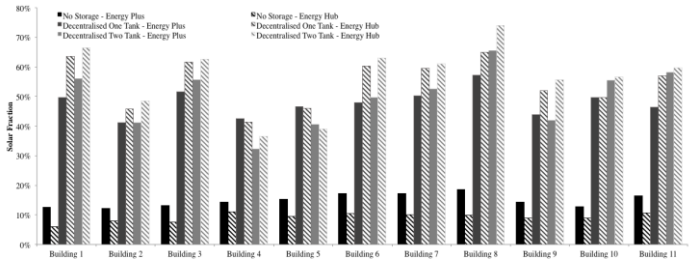

Figure 3: Comparison of solar fraction results for energy hub and EnergyPlus models for the three decentralised scenarios

In Figure 4a the aggregated optimal solar thermal collector area and required short-term and long-term storage volumes for the whole Rheinfelden neighborhood are plotted with the resulting solar fraction for the different energy hub scenarios at multiple ϵ constraint values. An increase in the solar thermal collector area and short-term and long-storage volumes leads to an increase in the solar fraction. Figure 4b shows a graph of the aggregated solar fraction and resulting total annual cost of the optimal energy systems for the entire neighborhood in all four scenarios at multiple ϵ constraint values. In the No Storage scenarios, the solar fraction does not increase beyond 10%, however, the addition of a short-term storage tank can result in solar fractions of up to 60%. When long-term storage is also available, the solar fraction can reach 90%. Increasing storage volume results in the longer storage of solar energy, which facilitates the increased utilisation of solar and thus higher solar fractions. For this quarter, the results in Figure 4b also indicate that centralisation of storage does not result in the energy

system with the highest solar fraction. This is likely due to high heat losses, both in the large centralised long-term storage tank, but also due to additional heat losses in the district heating network pipes.

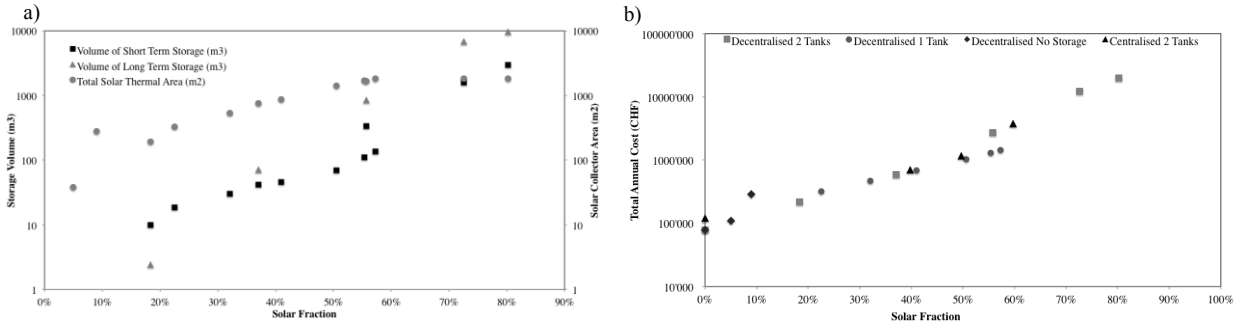

Figure 3: a) Solar thermal collector area, short-term storage volume, and long-term storage volume corresponding to the different solar fractions, b) Solar fraction and resulting annual cost of different scenarios

CONCLUSION

In this study, an energy hub model was developed in order to design the solar thermal energy system for a neighborhood in Rheinfelden, Switzerland. While dynamic simulation models are useful for accurately modeling the temperature dependent system performances, linear energy hub models were found to be an adequate simplification that facilitates optimal sizing of the system components. The temporal mismatch between thermal energy demands and solar energy availability necessitates the adoption of both short and long-term thermal energy storage units. However, even when storage is installed, 100% solar fraction is not attainable due to the characteristics of the thermal loads and the thermal losses in the TES units and district-heating network. Furthermore, as solar thermal collector area and solar fraction increase, the required storage volume increases to potentially impractical levels. Therefore it may be worth investigating other types of storage system, such as sorption storage. While these systems may have lower charging efficiencies, they also have higher storage densities and no time dependent heat losses which might make it possible to achieve solar fractions that are close 100%.

ACKNOWLEDGEMENT

This research has been financially supported by CTI within the SCCER FEEB&D (CTI.2014.0119).

REFERENCES

1. Geidl, M., Koeppel, G., Favre-Perrod, P., Klockl, B., Andersson, G., Frohlich, K., 2007. Energy hubs for the future. IEEE Power Energy Mag. 5, 24–30.
2. SIA. 2009. Thermische Energie im Hochbau. Zurich: SIA Zurich.
3. SIA. 2006. Standard-Nutzungsbedingungen für die Energie- und Gebäudetechnik. Zurich.
4. Morvaj, B., Evins, R., Carmeliet, J. 2014. Optimal selection and operation of distributed energy resources for an urban district, in: Engineering Optimization 2014. CRC Press, pp. 709–714.
5. Steen, D., Stadler, M., Cardoso, G., Groissböck, M, DeForest, N., Marnay, C. 2015. Modeling of thermal storage systems in MILP distributed energy resource models. Applied Energy. 782-792.
6. Hsieh, S., Weber, R. Dorer, V., Orehounig, K. 2015. Integration of Thermal Energy Storage at Building and Neighbourhood Scale. International Building Performance Simulation Association Conference. Hyderabad, India.

NEIGHBORHOOD ENERGY MANAGEMENT SYSTEM

GZ Gerhard Zucker[1]; FJ Florian Judex[1]; BI Branislav Iglar[1]; MB Max Blöchle[1]; FP Filip Petrushevski[1]; JH Jürgen Hubert[2]

1: AIT Austrian Institute of Technology, Energy Department,

Giefinggasse 2, 1210 Vienna, Austria

2: DERlab, Fraunhofer IWES, Königstor 59, 34119 Kassel, Germany

ABSTRACT

Increasing building energy efficiency is an important topic when attempting to achieve national and European climate goals. Energy efficiency through energy management during operation is a key issue with high leverage potential, especially neighborhood management - control systems that are capable to optimize local generation and consumption while assuring the comfort and performance of several buildings is promising. Using the recent advancements in information and communication technology it is possible to build effective neighborhood energy management systems as well as information and decision support systems with user interfaces for different stakeholders that can take the advantage of variable tariffs and diversity of supply. Beside technological aspects, the stakeholders require motivation as well as better understanding of energy and how it should be consumed.

This paper explores the approach of the EEPOS project, how to establish neighborhood energy management and examines the advantages and challenges of such a system. Although the main focus is the technology being used, we also address stakeholder integration that support the technology and allow for better market penetration. A virtual demonstrator setup explores the technical preconditions and boundaries and supports the integration of the EEPOS IT platform.

Keywords: neighborhood energy management, OGEMA, load shifting, load balancing, demand side management

INTRODUCTION

Increasing building energy efficiency is an important topic when attempting to achieve national and European climate goals [1]. Instead of only addressing individual buildings, energy efficiency can be improved through energy management during operation on the neighborhood level. Recent advancements in information and communication technology (ICT) allow the development of information and decision support systems that can optimize local generation and consumption in energy positive neighborhoods.

This paper explores the approach of the EEPOS project [2]. After a review of the related work, the IT platform is presented, including its applications. To evaluate the potential for optimization, the operation data are analyised and a virtual demonstrator is described. Finaly, the paper is concluded and a plan for future work is presented.

RELATED WORK

There has been a progress regarding ICT-supported business models for neighborhood operators during the last years, but still a big potential for improvements exists [3]. New business models for district level energy services related to smart grids and distributed energy production are under development. Hence, there are plenty of business opportunities at the neighborhood level [4]. Prosumers (producer and consumer) are really newcomers who can in

addition of consuming also generate energy and supply their extra energy it into the grid [5]. At the moment, there are no real markets for prosumers due to lack of motivation, incentives and information [6].

Most systems for energy management and building energy efficiency are designed to work with a limited set of communication technologies. Smart grid approaches for the integration of larger public sites aim at a direct control of large loads and generation capabilities. The advantage of this is clearly defined interfaces, but the disadvantage is limitations regarding intelligent control strategies.

On the building level solutions for analyzing and management of energy exist, especially for electricity, heating and water consumption. All basic routines of monitoring, analysis with reports related to buildings can be done over the internet. Functionality may include numerous reports e.g. alarm reports, monthly and yearly energy consumption, water consumptions etc. This offers a good ground, but development towards more easy access and user friendliness as well as support on the neighborhood levels is required.

In the near future buildings, building blocks and residential areas are going to be supplied by several energy sources. In many areas prosumers have begun to produce electricity and this tendency will continue but the energy gained is frequently lost due to lack of storage or demand at a given moment in time. Currently there are only very few such neighborhoods, but as the number of zero or positive energy buildings is increasing, so is the number of such neighborhoods.

Information models for energy and energy related building systems and components are currently being developed on several levels. On the one hand projects like SEMANCO [7] are creating standards for information models in the context of large levels (between neighborhood and city scale), while on the other hand e.g. the HESMOS [8] project tries the same on a building automation level.

For informing and involving end users and other relevant stakeholders an information and decision support system is required in order to take advantage of variable tariffs and diversity of supply in order to provide profound end-user motivation [9] (“personal drivers”) and understanding of energy consumption [10].

IT PLATFORM ARCHITECTURE

The goal is to design and implement an energy management system capable to optimize the local energy generation and consumption considering all energy systems (mainly heating, but also HVAC, lighting and others) in buildings and in the neighborhood. This would ideally advance the transition towards energy positive neighborhoods. The system shall also be capable to analyze consumption and use this information (as a decision support system) to integrate use of energy storages such as water tanks and intrinsic thermal storage in building structures. Neighborhood energy information and weather forecasts also contribute to the knowledge base necessary to perform energy matching with the low voltage electricity distribution grid. The architecture of the system is shown in Figure 1 (left).

The core of the NEMS is the OGEMA Framework (Open Gateway Energy Management) [11], an open-source software system developed as universal framework for energy management. To standardize energy management, OGEMA has a large range of data models which describe elements used in energy management. These can represent devices that need to be controlled (such as washing machines, cooling or heating systems), sensory information (such as temperature, brightness, local electricity consumption etc.), and external data which is needed for management (such as weather forecasts, variable electricity prices). The full

range of data models can be found at [12]. Devices represented by a particular data model can be connected to OGEMA via one of several communication driver standards (such as ZigBee, KNX, or EEBus) or via custom, model-specific hardware drivers. Application based on the OGEMA framework (OGEMA apps) are making use of both the standard data models and (where applicable) the communication drivers, and represent all aspects of energy management and monitoring. Depending on the particular access rights of the app, they can access any sensor and device connected to the running OGEMA installation and make use of persistently stored data (so-called "resources"), as well as share app-generated data with other running apps. The currently running apps as well as the status of the currently used resources can be reviewed via the administrative web interface (Figure 1, right).

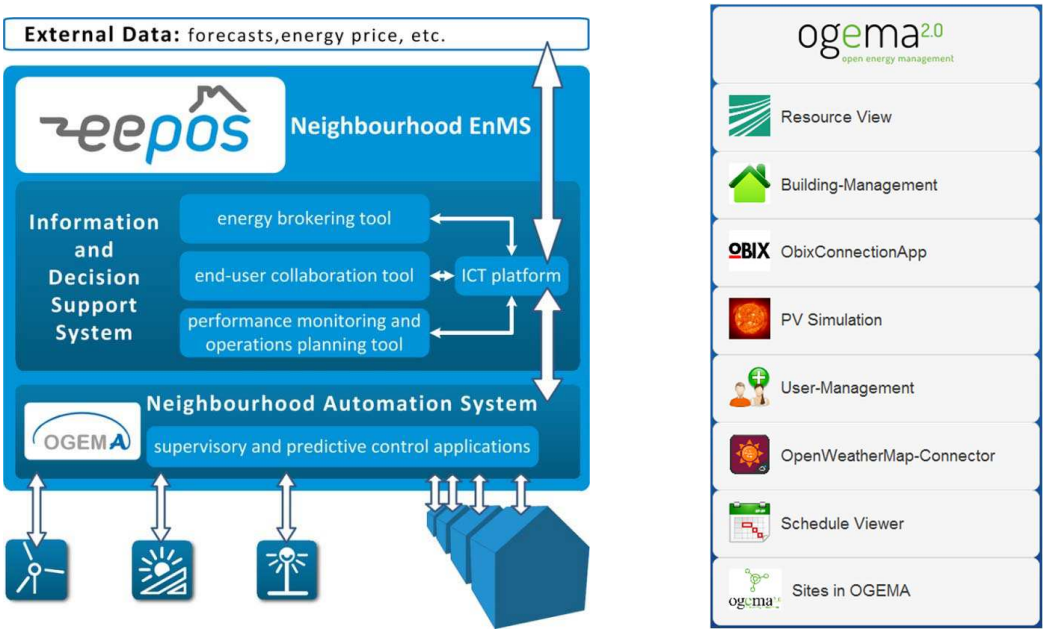

Figure 1: IT architecture of the platform (left) and OGEMA user interface (right).

APPLICATIONS

In EEPOS, OGEMA is used as the base for a Neighborhood Automation System (NAS), which monitors electricity consumption and production at the neighborhood level and attempts to shift consumption to more favorable times. The following apps are primarily used:

- **Load Prediction**: Predicts the load within a neighborhood based on past behavior.
- **PV Forecast**: Generates a forecast schedule of the PV (photovoltaic) electricity production of a particular plant, based on its location, technical specifications, geometric alignment, time of the day, and weather forecast.
- **Adaption Requester**: Based on information from the Load Prediction and PV Forecast apps as well as electricity price information, the Adaption Requester can identify time periods when electricity production exceeds demand and vice versa. To maximize the efficiency and stability of the local grid and minimize losses, this app attempts to shift the consumption of the individual households by producing a schedule of adaption requests – numeric values ranging from -2 (strongly shift electricity consumption away from this time) to +2 (strongly shift electricity consumption to this time). This information can then be sent to the individual households where the adaption requests can either be used to automatically control electricity-consuming devices or are used by the inhabitants to manually alter their consumption behavior.

Additional apps, such as **Simulated PV Plant** or **OpenWeatherMap-Connector** can be used to simulate a "virtual" PV plant or to provide additional data such as weather forecast from publicly available services [13].

THERMAL DEMAND AND SUPPLY

As a first result, the system has been used to collect baseline data for electric energy and heat consumption from a demo-site. These are used to assess the impact of the energy management measures. The main components of interest in the demo site in Langenfeld (North-Rhine-Westphalia, Germany) are a small district heating grid supplying hot water for about 70 multifamily dwellings, as well as the local heating plant providing the thermal energy. The plant is equipped with a biomass boiler (840 KW), a natural gas powered CHP (100KW thermal, 50KW electric), a natural gas boiler (1300 KW) and as a backup a boiler using marine fuel oil (also 1300KW), as well as a 24.000l hot water storage used as a buffer.

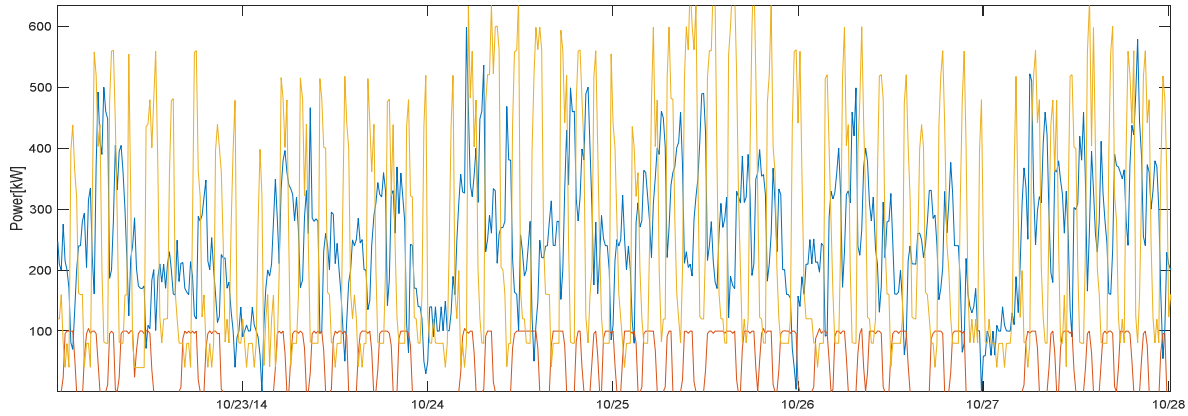

Figure 2: Thermal energy provided by the plant with biomass (yellow), gas boiler (blue) and gas powered CHP (red)

As shown in Figure 2, the CHP, the most efficient of the plants, is not operating continuously. At the same time, the gas boiler is running at power which could be actually covered by the CHP. Furthermore, when the power is combined, the CHP is running at its optimal point, with nearly the full 50KW of electrical power which, due to the fact that it is heat driven, drops to 30 KW or below in some situations. As this is clearly a problem on the demand side, proper demand side management, e.g. by ending the night set back earlier so that the energy used for this increased heating demand coincides with the domestic hot water peak in the morning, could lead to a longer operation of the CHP in the morning while decreasing the amount of thermal energy provided by the gas boiler. As the first peak in the electric grid coincides with the morning peak in thermal energy, the power produce could thus be used locally, therefore putting no strain on the grid.

The analysis showed potential for some of the dwellings that will be the focus of the demonstrator. In order to ensure scalability of the approach it was proven that the tenants are representative for average energy consumption both in quantitative and qualitative behavior.

DEMONSTRATOR

Based on the specifications of the dwellings in Langenfeld, a virtual demonstrator is created that allows to experiment with the available demand response potentials. This demonstrator uses dynamic thermal simulation tools that are used for providing qualitative information on the thermal performance of energy systems and buildings. However, the tools are not

designed to cooperate with an external controller as it is established in the Demand-Response app of EEPOS. Because the buildings at the demo site do not have significant thermal-electric coupling, it would not allow for dedicated electric load management without significant effort in instrumentation. Therefore, a building has been added virtually to the dwelling that allows executing electric demand response management. All buildings are represented in a simulation environment and backed up by real-world monitoring data.

The goals of the virtual demonstrator are to prove the methodology and show replicability of the solution. For that purpose, thermal simulation for 30 buildings in Langenfeld is performed. Thermal 3D models are created using TRNSYS or EnergyPlus. Additionally, models of CHP (combined heat and power) unit with CoP (Coefficient of Performance) 100 kW thermal, 50kW electric, gas heating unit (1300 kW) and biomass heating unit (840 kW) are created.

The simulation can deliver the following:

1. Heat demand for the next 24 hours for each building (in 10 min resolution)
2. CO2 profile for the next 24 hours (based on operation of CHP, biomass and gas)
3. Electricity production profile for the next 24 hours (based on CHP production)

The simulation does not regard duty cycles of e.g. gas heating unit and the impact on efficiency as well as losses in local distribution grid.

For the load management control, the goal is to change temperature setpoints in the apartments. For this it is necessary to provide the heat consumption for the next 24h for each apartment as well as difference in thermal consumption in 10 min resolution as reply to the adaptation requests. The heat unit control strategy is designed to minimize CO2 emissions during its operation (Table 1).

Condition	**Action**		
	CHP	**Biomass**	**Gas**
demand > 0 kW	ON	OFF	OFF
demand > 100 kW	ON	ON	OFF
demand > 940 kW	ON	ON	ON
demand <= 0 kW	OFF	OFF	OFF

Table 1: Heat unit control strategy.

The OGEMA Load Shifting App uses an algorithm with the following steps:

1. Collect all thermal load profiles of all buildings
2. Use the static “heat unit control strategy” to calculate the overall CO2 consumption
3. Issue adaptation requests to all buildings
4. Collect replies of buildings: difference in thermal consumption in 10 min resolution
5. Optimize for minimum CO2 using the “heat unit control strategy”
6. Inform building to execute the adaptation request (commit change)

A VirtualBEMS (virtual building energy management system) component waits for OGEMA adaptation requests and triggers the thermal simulation to create a response to OGEMA. This configures the simulation tool, runs the simulation and collects the simulation results. The

OGEMA Simulated Weather app is used in the VirtualBEMS simulation to get the weather forecast for the next 24 hours.

CONCLUSION AND OUTLOOK

We have presented the approach of the EEPOS IT Platform that is used for establishing neighborhood energy management by interacting with energy consumers and producers and providing services for better management of energy. The different apps are available on the OGEMA platform, while the virtual demonstrator uses existing simulation tools and links them to the communication interfaces used by the apps. The virtual demonstrator uses a real world dwelling as a foundation and the analysis of the operation data shows clear potential to optimize neighborhood energy management, which can be exploited using the EEPOS IT Platform. The next steps are the commercial exploitation of various available functions in order to advance energy efficiency on neighborhood level.

ACKNOWLEDGEMENT

The work presented here has been carried out in the frame of the EEPOS project which is co-funded by the European Commission within the Seventh Framework Programme (FP7/2007-2013) under grant agreement number 600050.

REFERENCES

1. European Commission, “The 2020 climate and energy package,” 26 March 2015. [Online]. Available: http://ec.europa.eu/clima/policies/package/index_en.htm. [Accessed 30 April 2014].
2. "EEPOS Project website," [Online]. Available: http://eepos-project.eu/. [Accessed 30 April 2015].
3. “SEMANCO Project website,” [Online]. Available: http://www.semanco-project.eu/. [Accessed 30 April 2015].
4. “HESMOS Project website,” [Online]. Available: http://hesmos.eu/. [Accessed 30 April 2015].
5. Mario Richter: Utilities’ business models for renewable energy: A review, Renewable and Sustainable Energy Reviews, Volume 16, Issue 5, June 2012, Pages 2483-2493
6. Vincenzo Giordano, Gianluca Fulli: A business case for Smart Grid technologies: A systemic perspective, Energy Policy, Volume 40, January 2012, Pages 252–259
7. Larry E. Ruff, Demand Response: Reality versus “Resource”, The Electricity Journal, Volume 15, Issue 10, December 2002, Pages 10–23
8. Can Smart Grid Technology Fix the Disconnect Between Wholesale and Retail Pricing, The Electricity Journal, Volume 24, Issue 1, January–February 2011, Pages 7-13 Ashley Brown, Raya Salter
9. Stephen Healy, Iain MacGill , From Smart Grid to Smart Energy Use, Smart Grid, 2012, ISBN: 978-0-12-386452-9 Pages 29-59
10. David P. Chassin: What Can the Smart Grid Do for You? And What Can You Do for the Smart Grid?,The Electricity Journal, Volume 23, Issue 5, June 2010, Pages 57-63
11. “OGEMA website,” [Online]. Available: http://www.ogema.org/ [Accessed 30 April 2015].
12. “OGEMA source portal,” [Online]. Available: https://www.ogema-source.net/. [Accessed 30 April 2015].
13. “OpenWeatherMap website,” [Online]. Available: http://openweathermap.org/. [Accessed 30 April 2015].

THE IMPACT OF CLIMATE CHANGE AND BUILDING RENOVATION ON HEATING RELATED CO_2 EMISSIONS ON A NEIGHBOURHOOD LEVEL

Andrić, I.[1,3]; Silva, C.[1]; Pina, A.[1]; Ferrão, P.[1]; Fournier, J.[2]; Lacarrière, B.[3]; Le Corre, O.[3];

1: Instituto Superior Técnico, Avenida Rovisco Pais 1, 1049-001 Lisbon, Portugal;

2: Veolia Recherche Et Innovation, 10 rue Jacques Daguerre, Rueil-Malmaison 92500 France;

3: École des Mines de Nantes, La Chantrerie , rue Alfred Kastler 4, 44300 Nantes, France;

ABSTRACT

Building sector is currently one of the major sources of CO_2 emissions. Considering that the largest proportion of energy in buildings in Europe is used for heating services, significant potential for emissions decrease could be exploited through heat demand reductions.

The scope of this paper is to evaluate the impacts of changed climate and building renovation on heating related CO_2 emissions on a neighborhood level. A combination of existing tools (EnergyPLAN, ArcGIS, CCWorldWeatherGen) and a tool previously developed by the authors (resistance-capacitance analogy based heat demand model [1]) were used. Three weather scenarios for the future were considered (low, medium, high temperature increase), as well as four renovation paths (no renovation, shallow, intermediate, deep renovation path). Three heating system options were taken into the account: individual electric heaters in each dwelling, natural gas distribution network with individual boilers in each dwelling and district heating network with centralized heat production in natural gas fueled boiler. Generic neighborhood configuration for Portugal was created based on the district of Alvalade that is located in Lisbon. This particular district was chosen due to the fact that it possesses desirable urban morphology and it was built during several construction periods over the last century.

The results showed that the changed climate, by itself, could decrease annual CO_2 emissions from 8% up to 34% in 2050 compared to 2010 (depending on the weather scenario and heating system considered) due to the changed weather parameters. Furthermore, building envelope renovation could enable additional 80-260ktCO_2 savings in cumulative emissions for the regarded period (2010-2050).

Keywords: climate change, emissions, heating, urban environment

INTRODUCTION

In 2009, the European Council committed the member states of the European Union to reduce the carbon-dioxide emissions to a minimum of 80% (compared to the levels from 1990) by 2050. Due to the fact that the heat demand in Europe is the main energy end-use source of emissions [2], decarbonisation of this sector could improve the achievability of the goals set.

However, the CO_2 emissions from the building heating sector could decrease due to the reduced heat demand caused by the changed climate. Increased outdoor temperatures and changed levels of solar radiation could decrease the amount of heat required to reach the comfort temperature inside the buildings. Furthermore, improvements in the building envelope thermal performance due to the new energy efficiency policies could reduce the heat transfer between the building and the environment, further decreasing the heat demand.

Additionally, the penetration of renewable energy technologies (biomass boilers, solar thermal panels, geothermal heat pumps) for heating in urban environment had an increasing trend in the previous decade with efficiency improvements and decline in prices for such technologies. However, in high-density areas, limited amount of space available for placing the geothermal heat pump installation (heat exchangers and piping) and shading of the solar panels from the surrounding buildings could compromise the use of these systems. Considering the global population increase and dense urban environment expansion rates, the possible solution could be the production of heat outside the municipalities coupled with heat distribution through the networks.

District heating networks are commonly proposed in the literature as an environmentally friendly solution for providing heating services for the built environment due to their benefits, such as centralized heat production located outside the municipalities, utilization of renewable heat sources (biomass, solar, geothermal etc.) and comfort for the consumers. The subject has been widely researched in several scientific reports [2-5]. The conclusions were that the district heating should be considered as an essential cost effective technology for the EU energy system decarbonisation.

Another solution could be the natural gas distribution networks with high efficiency individual condensing boilers within each dwelling. Global demand for natural gas is projected to rise by 65 percent from 2010 to 2040, making it the largest volume growth of any energy source [6]. Additionally, due to the rise in new technologies for extracting natural gas from unconventional sources, it is considered that natural gas could have a major role in energy transition [7,8]. Additionally, natural gas networks could be used for distribution of other gaseous fuels such as hydrogen [9].

Furthermore, we have considered electric heaters in each dwelling for this study, due to the fact that significant proportion of heat demand in southern countries like Portugal is covered by these systems. Additionally, the change in emissions due to the heat demand reduction is not so obvious due to the energy mix used for electricity production, making it an interesting research topic.

The main goal of this paper is to assess the possible heating-related CO_2 emission reductions on a neighborhood level, caused by the impacts of climate change and building renovation and taking into account several options for providing heating services to the urban environment.

METHOD

The methodology used in this paper is illustrated on Figure 1. Heat demand on a neighborhood scale was calculated by using the resistance-capacitance model (RC model) based on the thermo-electrical analogy that was developed for a previous study [1]. Heat demand is calculated on an hourly basis for each building within the studied area. The model was improved since the last case study, and its current version it capable to take into the account occupancy profiles, internal heat gains from the occupants and heat losses due to the air renewal (all on an hourly basis). Additionally, shading between the buildings was calculated depending on the season of the year considered (shading was estimated in ArcGIS). For the heat demand calculations, the model requires two main inputs: weather data and building data for the chosen case study location. Weather data consists of data for the reference year and weather scenarios for the future. Reference weather data can be obtained from the Energy Plus weather database [10] for multiple locations around the world. For the creation of the future weather scenarios (low, medium and high temperature increase) we have used the Climate Change World Weather File Generator tool [11] that uses reference

weather data and outputs from the HadCM3 global circulation model as an input to forecast the weather conditions for the future.

Building data was obtained from calculations in ArcGIS (building geometry, shading between the buildings), the municipality database (construction period, typology, no. of inhabitants) and the Building Performance Institute Europe (thermal properties of the building elements – walls, roofs, floors, windows) database [12]. For the building renovation scenarios, we have assumed improvements in the thermal properties of the building elements, introducing four levels of renovations (low, medium, high and net zero energy buildings level) and four renovation depths that consider the number of buildings renovated with each level of renovation for each year (no renovation, shallow, intermediate, deep) as suggested by BPIE report [13]. Additional information about weather and renovation scenarios was provided in [14].

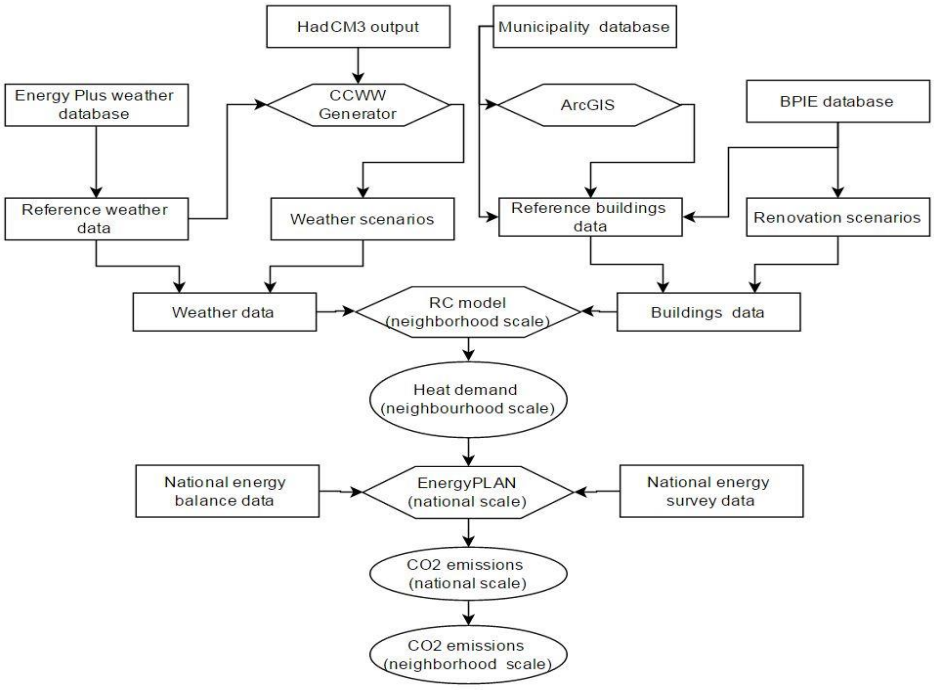

Figure 1 Methodology outline

CO_2 emissions are calculated in the EnergyPLAN software. EnergyPLAN is a deterministic model for evaluating the operation of an energy system. It has been applied for the evaluation of energy systems and strategies for increasing the penetration of renewable energy sources on a national scale for different countries, such as Norway [15], Denmark [5], China [16], USA [17] and Serbia [18]. The model is capable of taking into the account several sectors within the energy system, including the electricity sector, heating and cooling sector, and industry and traffic sectors. Primarily, the model for the whole country (Portugal) was created and verified based on the data from the national energy balance [19]. Since the energy balance does not contain data about the energy consumed for heating and cooling in Portugal, a national survey [20] was used as a source. This caused a misbalance in the results (compared to the energy balance) of only 1.2%, which we found acceptable. After the reference case calculations and model calibration, the estimated heat demands for each scenario of the studied neighborhood were introduced in the model and the emissions were calculated. The level of emissions on a neighborhood scale for each scenario was obtained through the comparison with reference case results. Fuel emission factors were obtained from the SenterNovem [21] report. Low heating values of the fuels were considered constant.

For this paper, a generic neighborhood for Portugal was created based on the Alvalade district in Lisbon. We have used this district due to the fact that it has as desirable morphology (ratio of private, public and service areas) and that it is consisted of 665 buildings constructed during various periods in the last century. In this study, we have neglected the cooling demand in the district, due to the fact that only a small number of buildings within this district have cooling systems. This is also true on the national level, since the energy survey for Portugal indicates that the amount of energy for cooling on a national level was significantly smaller than the amount of energy used for heating (13,107Mtoe compared to 533,892Mtoe in 2010, respectively [20]), despite the warm climate.

For heating systems, we have considered three scenarios: individual electric heaters, two-pipe district heating network with central boiler fueled by natural gas (network losses $\zeta_{dhn} = 0.2$, boiler efficiency $\eta_{ngn} = 0.8$) and natural gas distribution network with individual gas boilers in each dwelling (network losses $\zeta_{ngn} = 0.15$, boiler efficiency $\eta_{ngn} = 0.9$).

RESULTS AND DISCUSSION

The impact of climate change on annual heating related CO_2 emissions is represented on Figure 1 for all considered heating system scenarios (EH – electric heaters, NGDHN – district heating network with natural gas boiler, INGN – natural gas distribution network with individual gas boilers). It can be noted that the neighborhood with electric heaters has the highest emissions for all weather scenarios (36% higher than NGDHN and 43% higher than INGN). Due to the changed weather conditions, annual CO_2 emissions could decrease from 8-33% in 2050 (compared to 2010 and depending on the weather scenario) for natural gas fueled systems and 9-34% for the electric heaters scenario.

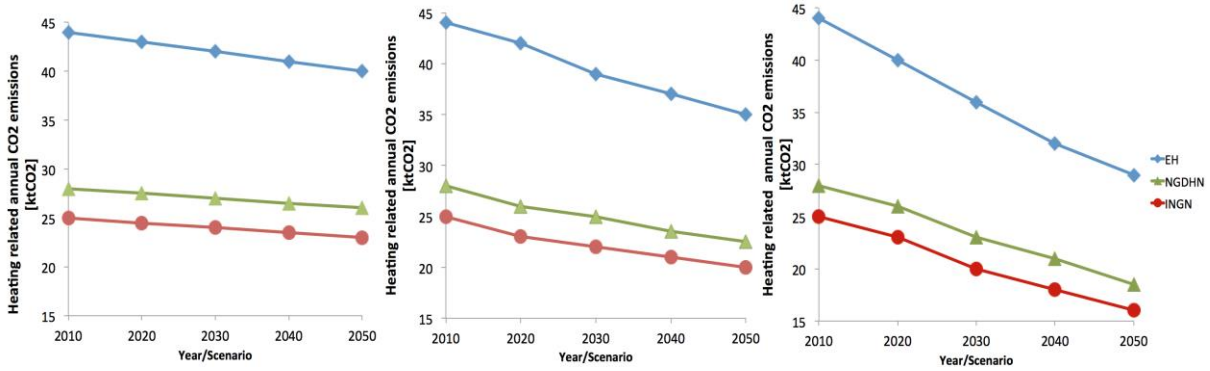

Figure 2 The impact of climate change on heating related annual CO_2 emissions on a neighborhood level (low (a), medium (b) and high temperature scenario (c))

Combined effects of climate change and building renovation (NR - no renovation, SR – shallow renovation path, MR- medium renovation path and DR – deep renovation path) on cumulative CO_2 emissions for the period 2010-2050 are illustrated on Figure 2. Building renovation could enable additional 107-260ktCO_2 emission savings for low temperature scenario, 94-245ktCO_2 for medium temperature scenario and 80-214ktCO_2 for high temperature scenario (depending on the heating system observed).

In this case study, the natural gas distribution network had the lowest emissions for all weather and renovation scenarios considered, due to the efficiency of the small individual condensing natural gas boilers and lower losses in the system (compared to traditional two-pipe district heating network). On the other hand, new low-temperature district heating networks designs have lower losses and can integrate the heat production from renewable sources such as solar thermal panels and biomass. However, there are only few such systems operating today (mostly in Nordic countries).

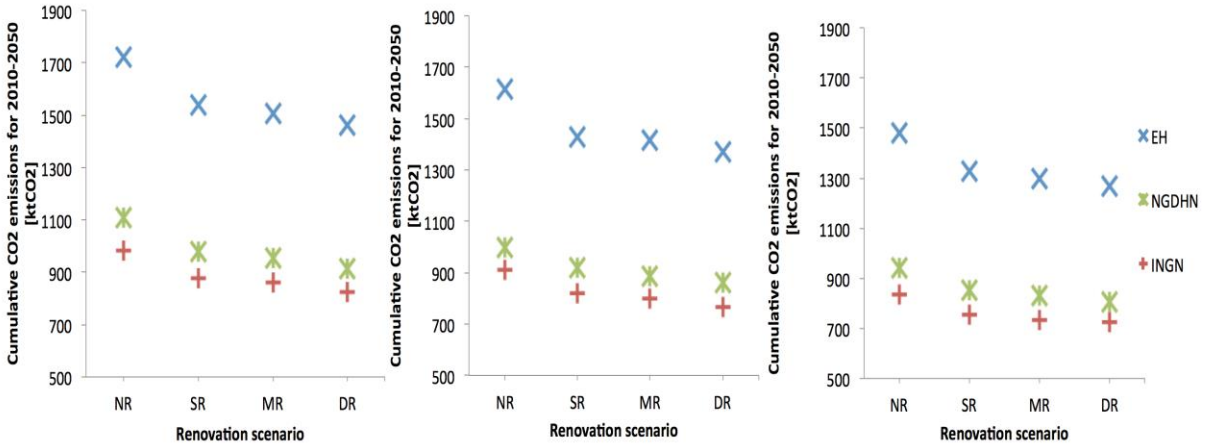

Figure 3 The impact of climate change and building renovation on heating related cumulative CO_2 emissions on a neighborhood level (low (a), medium b) and high(c)) for the period 2030-2050

CONCLUSIONS

The main goal of this paper was to evaluate the potential decrease in heating related CO_2 emissions on a neighborhood scale due to the impacts of climate change and building renovation. Additionally, different options for providing the heating services for urban environment were considered. A generic neighborhood for Portugal was created based on the Alvalade district located in Lisbon.

The results showed that just due to the changed weather variables, annual CO_2 emissions could decrease from 8% up to 34% in 2050 (compared to 2010, depending on the weather scenario and heating system considered). Additionally, building envelope renovation could enable additional 80-260ktCO_2 savings in cumulative emissions for the regarded period (2010-2050).

Furthermore, natural gas distribution network with individual boiler in each dwelling caused the lowest emissions for all weather and renovation scenarios studied (compared to electric heaters and two-pipe district heating network considered). However, new low-temperature designs for district heating networks are currently emerging, enabling the utilization of renewable sources such as solar thermal panels. Additionally, we note that for fully evaluating the emissions from the building sector, cooling demand should also be taken into the account, since the increased outdoor temperature could result in increased cooling demand, which we will address in our next case study.

REFERENCES

1. Andrić, I., Darakdjian, Q., Ferrão, P., Fournier, J., Le Corre, O., Lacarrière, B. The impact of global warming on district heating demand : the case of St Félix, DHC14 Symposium, Stockholm, 2014;
2. Connolly, D., Mathiesen, B. V., Østergaard, P. A. “Heat Roadmap Europe 2050”, Euroheat & Power p. 99, 2012;
3. Dolman, M., Abu-Ebid, M., Stambaugh, J. “Decarbonising heat in buildings 2030 - 2050. Summary report for The Committee on Climate Change.,” no. April 2012, pp. 2030–2050, 2012;
4. Scottish Goverment, “Towards Decarbonising Heat : Maximising the Opportunities for Scotland Draft Heat Generation,” 2014;

5. Lund, H., Möller, B., Mathiesen, B. V., Dyrelund, A. “The role of district heating in future renewable energy systems,” Energy, vol. 35, no. 3, pp. 1381–1390, Mar. 2010;
6. ExxonMobil Outlook for Energy: A View to 2040.Online publication, 2014. http://cdn.exxonmobil.com/~/media/Reports/Outlook%20For%20Energy/2015/2015-Outlook-for-Energy_print-resolution.pdf [last accessed: April, 2014];
7. Rafiqul Islam, M. Chapter 2 - World Gas Reserve and the Role of Unconventional Gas, In Unconventional Gas Reservoirs, edited by M. Rafiqul Islam, Gulf Professional Publishing, Boston, 2015, Pages 9-69;
8. Verdeil, E., Arik, E., Bolzon, H., Markoum, J. Governing the transition to natural gas in Mediteranean Metropolis: The case of Cairo, Istanbul and Sfax (Tunisia), Energy Policy, Volume 78, March 2015, Pages 235-245;
9. Haeseldonckx, D., D’haeseleer, W. The use of the natural-gas pipeline infrastructure for hydrogen transport in a changing market structure, International Journal of Hydrogen Energy, Volume 32, Issues 10–11, July–August 2007, Pages 1381-1386;
10. U.S. Department of Energy, Building Technologies Office, Energy Plus weather database: http://apps1.eere.energy.gov/buildings/energyplus/ [last accessed: April, 2015];
11. University of Southtempton, Climate Change World Weather Generator: http://www.energy.soton.ac.uk/ccworldweathergen/ [last accessed: April, 2014];
12. Building Performance Institute Europe, Country Factsheets - Portugal: http://www.buildingsdata.eu/country-factsheets [last accessed: April, 2014];
13. Building performance Institute Europe (BPIE), 2012. Europe’s buildings under the microscope http://www.bpie.eu/eu_buildings_under_microscope.html - .VGIoLYe6Xdk [last accessed: April 2015];
14. Andrić, I., Gomes, N., Pina, A., Ferrão, P., Fournier, J., Lacarière, B., Le Corre, O. “Modeling the combined effects of direct and indirect impacts of climate change on district heat demand in the future : the case study of Alvalade”, internal report;
15. Hagos, D. A., Gebremedhin, A., Zethraeus, B. “Towards a flexible energy system - A case study for Inland Norway,” Appl. Energy, vol. 130, pp. 41–50, 2014;
16. Xiong, W., Wang, Y., Vad, B., Lund, H., Zhang, X. “Heat roadmap China : New heat strategy to reduce energy consumption towards 2030,” Energy, 2015;
17. Zhai, P., Larsen, P., Millstein, D., Menon, S., Masanet, E. “The potential for avoided emissions from photovoltaic electricity in the United States,” Energy, vol. 47, no. 1, pp. 443–450, 2012;
18. Bjelić, I. B., Rajaković, N., Ćosić, B., Duić, N. “Increasing wind power penetration into the existing Serbian energy system,” Energy, vol. 57, pp. 30–37, 2013.;
19. DGEG (Direção General de Energia e Geologia), Balanço Energético Nacional, 2010. http://www.dgeg.pt [on Portuguese; last accessed: April 2015];
20. Instituto Nacional de Estatistica, Inquérito ao Consumo de Energia no Sector Doméstico, 2010 [on Portuguese];
21. SenterNovem, The Netherlands: list of fuels and standard CO_2 emission factors, 2005 http://www.rvo.nl/sites/default/files/2013/10/Vreuls_2005_NL_Energiedragerlijst_-Update.pdf [last accessed: April 2015];

SOLAR POWER GENERATION AND SOLAR COOLING TRIGENERATION: A NEW APPROACH OF CONCEPTUAL DESIGN FOR COUNTRIES OF MENA REGION

Y. Boukhris[1]; N. Al-Azri[2]; Y. Allani[3]

1: Industrial Engineering Departement, National school of engineers of Tunis, Tunis El Manar University, Tunisia.
2: Department of Mechanical and Industrial Engineering, College of Engineering, Sultan Qaboos University, Oman.
3: Allani Sunlife Holding SA, Suisse.

ABSTRACT

The rapid increase in population, industrial and agricultural developments in countries of the Middle East and North Africa (MENA) has resulted in proportional increase in demand for electric power. This demand increases sharply during the summer months due to the use of electricity-powered Air Conditioning (AC) systems. The usual response to this problem is to build new, time-consuming and costly power generation plants. Trigeneration or combined heat, power and cooling represents a great opportunity for the Sunbelt countries, especially in the MENAregion. The potential application covers not only the construction industry and the service sector, but also the industry, agribusiness and agriculture sectors. Specifically, we show the possibility to design a basic concept that meets all the requirements and which optimally adapts to all cultural, regulatory and economic considerations according to the studied country and the site of realization in question. We propose in this study the use of the solar thermal for heating, power generation and building cooling. The new developed solar-based technology is capable of producing power via Organic Rankine Cycle (ORC) and absorption or adsorption cooling as a byproduct/cogeneration operated by the rejected heat from the ORC. We consider also the possibility of using ice storage technology which is much cheaper than steam storage. This way, autonomous power generation and cooling (AC) can be installed in locations remote from the electricity grid, resulting in huge savings in both power transmission lines and added power capacity. We present practical results and we describe our conceptual approaches and modeling. The developed parametric model is applied to various design cases, generated from the baseline concept, and then validated by comparison with experimental approaches. We note that our model is also used to predict the future facilities operations. Thereafter, we present our current projects and test stands in two countries in the MENA region.

Keywords: Smart building, predictive model, HVAC, solar-gas trigeneration.

INTRODUCTION

The maturity of solar thermal technology used for producing hot water can be used for satisfying the rapidly increasing demand for cooling through thermal and thermodynamic pathways [2, 3]. However, innovative systems especially those including multi-generation will face a number of challenges including having affordable maintenance, rational use of natural gas as an auxiliary source, coping with the summer high demand for air conditioning, availability of storage facility and a seasonal adjustment of the hot-cold outputs.

Due to their high demand for energy per capita, most countries in the MENA region need a transitional development in the energy generation sector. Such initiatives have already been planned as in Tunisia where 30% contribution from renewable sources is targeted by 2030. Even in oil producing countries such initiatives are taken place as the case with Oman where the government is currently allocating handsome funds for the development of alternative energy producing technologies through research and development. In such efforts, the most challenging tasks will be the development of renewable energy systems that are efficient,

reliable, economically feasible and, especially important, compatibility with the climatic characteristics of the location of use.

In this context, we have developed two models of cooling systems: a classic (Type 1) and another innovative (Type 2). The performance of each system has been parametrically evaluated with the aim to identify the limitation of use at nominal conditions. Hence, upon on the availability of solar radiation, it will be possible to propose the most suitable type of installation conforming to the above-mentioned criteria. The performance of the various units is based on widely tested and proven models.

DEVELOPED CONFIGURATIONS

Regional Comparison

The design layout and outputs are to a great extent location-specific. A lucrative technology in one region might be deemed impractical in another place where it may lack compatibility with the renewable resources, availability of subsidized conventional utilities and/or the type of the most utility in demand. Table 1 shows a comparison between Tunisia and Oman which are located far apart within the MENA region.

Criteria	Tunisia	Oman
Solar radiation in urban areas	Medium 1600-1900 kWh /m^2 /year	High 1900-2300 kWh /m^2 /year
Summer daytime peak	Very critical	Critical
Heating utility and hot water	In demand	Low demand
Cooling utility	High demand in summer	In demand most of the year
Investment opportunities in innovative renewable energy technologies	Low to medium	Medium to high
State plans for alternative energy	Established	Evolving
Maturity of the thermal solar energy sector	Commonly used conventional systems	Very low
Importance of electricity production	High	High in remote areas
Electricity rates at peak	high	Medium
Electricity rate in network isolated sites	Very high	Medium

Table 1: Comparison between two countries in MENA region.

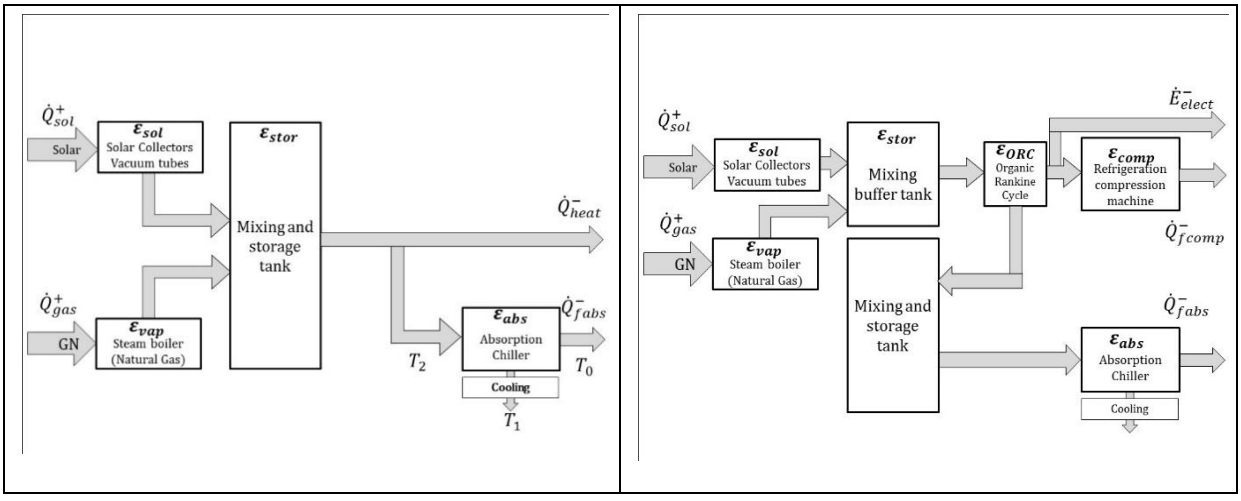

Figure 1: Schematic diagram of the installations Type 1 (Left; Tunisia) and Type 2 (Right; Oman).

PROPOSED CONFIGURATIONS

Modeling the Overall Efficiency for the Proposed Configuration Type 1

In this configuration, the heat gained from the dual input of solar and natural gas are applied directly to an absorption chiller via a storage tank where the injected steam (from a gas boiler) serves as an extra heating source for the water heated by the solar field. In addition to cooling, Type 1 allow direct use of hot water (figure 1).

The solar contribution, (τ_{sol}) is the ratio of the solar gain at the solar collectors to the total heat input of solar gain and the primary heat from natural gas:

$$\tau_{sol} = \frac{\dot{Q}_{sol}^{+}}{\dot{Q}_{sol}^{+}+\dot{Q}_{gaz}^{+}} \quad (1)$$

The ratio of the net heat produced to the sum of the heat and absorption cooling produced is given by:

$$\tau_{heat} = \frac{\dot{Q}_{heat}^{-}}{\dot{Q}_{heat}^{-}+\dot{Q}_{abs}^{+}} \quad (2)$$

The overall efficiency of the given configuration Type 1 is based on two assumptions [6]:
Assumption 1: The system is considered to produce two equally important outputs, cooling and heating:

$$\varepsilon_{g-abs} = \frac{\dot{Q}_{fabs}^{-}+\dot{Q}_{heat}^{-}}{\dot{Q}_{sol}^{+}+\dot{Q}_{gaz}^{+}} = \varepsilon_{stor}.\left(\varepsilon_{sol}.\tau_{sol} + \varepsilon_{vap}.(1-\tau_{sol})\right).\left(\tau_{heat} + \varepsilon_{abs}.(1-\tau_{heat})\right) \quad (3)$$

Assumption 2: The system produces both cooling and heating with cooling is considered the main product of interest:

$$\varepsilon'_{g-abs} = \frac{\dot{Q}_{fabs}^{-}}{\dot{Q}_{sol}^{+}+\dot{Q}_{gaz}^{+}} = \varepsilon_{stor}.\left(\varepsilon_{sol}.\tau_{sol} + \varepsilon_{vap}.(1-\tau_{sol})\right).\varepsilon_{abs}.(1-\tau_{heat}) \quad (4)$$

The change in internal energy is assumed to be zero. The system is therefore evolving in quasi-stationary operating conditions.

Modeling the Overall Efficiency for Configuration Type 2

In this configuration, the solar energy collected and steam are fed to an ORC via a buffer tank, reducing thermodynamic losses due to mixing compared to configuration Type 1. Cooling is produced by two means: from a compression machine working on the power produced by the ORC and from an absorption machine [6]. Exergy lost by the ORC is either stored or applied to the absorption machine (figure 1).

In this configuration, the solar contribution, (τ_{sol}) is the ratio of the solar gain at the solar collectors to the total heat input of solar gain and the auxiliray fuel and is given by:

$$\tau_{sol} = \frac{\dot{Q}_{sol}^{+}}{\dot{Q}_{sol}^{+}+\dot{Q}_{gaz}^{+}} \quad (5)$$

The ratio of the net electrical power produced to the sum of the net electrical power produced and that consumed by the refregiration-compression system is given by:

$$\tau_{elect} = \frac{\dot{E}_{elect}^{-}}{\dot{E}_{elect}^{+}+\dot{E}_{e.comp}^{+}} \quad (6)$$

The overall efficiency of the given configuration Type 2 is based on two assumptions [6]:

Assumption 1: The system produces two products of equal interest: cooling and electrical power.

$$\varepsilon_{g-trigen} = \frac{\dot{Q}_{fabs}^{-}+\dot{Q}_{fcomp}^{-}+\dot{E}_{elect}^{-}}{\dot{Q}_{sol}^{+}+\dot{Q}_{gaz}^{+}} =$$

$$\varepsilon_{stor}.\left(\varepsilon_{sol}.\tau_{sol} + \varepsilon_{vap}.(1-\tau_{sol})\right).\left(\varepsilon_{abs} + \varepsilon_{ORC}.(\tau_{elect} + \varepsilon_{comp}.(1-\tau_{elect}) - \varepsilon_{abs})\right) \quad (7)$$

Assumption 2: The system produces both cooling and electrical power with only cooling is considered to be the output of interest:

$$\varepsilon'_{g-trigen} = \frac{\dot{Q}^{-}_{fabs} + \dot{Q}^{-}_{fcomp}}{\dot{Q}^{+}_{sol} + \dot{Q}^{+}_{gaz}} =$$

$$= \varepsilon_{stor} \cdot \left(\varepsilon_{sol} \cdot \tau_{sol} + \varepsilon_{vap} \cdot (1 - \tau_{sol})\right) \cdot \left(\varepsilon_{abs} + \varepsilon_{ORC} \cdot (\varepsilon_{comp} \cdot (1 - \tau_{elect}) - \varepsilon_{abs})\right) \quad (8)$$

The feasibility and the optimization of such configuration must be validated at the design phase using process integration methods such as pinch technology [2, 3, 5, 6 ,7].

Modeling the Efficiency of the Absorption System

The absorption refrigerator exchanges heat with three sources given by three levels of temperatures denoted by T_{m0}, T_{m1} and T_{m2}, which are those of the evaporator, the cooling tower and the generator.

In order to address the limitations of usual models, we propose the following empirical model that has been widely validated using both dimensional and dimensionless analysis and it is inspired by the basic expressions of the COP.

$$\varepsilon_{abs} = c_0 \cdot \left(\frac{T_{m0}}{T_{m2}}\right)^{c1} \cdot \left(\frac{T_{m2} - T_{m1}}{T_{m1} - T_{m0}}\right)^{c2} \quad (9)$$

The new empirical model that we have developed has been validated through an experimental study in 2015. The experiments were conducted on the absorption chiller (dual solar-gas) with an output of 175 kW used to cool the industrial premises in an agro-industry in Tunisia.

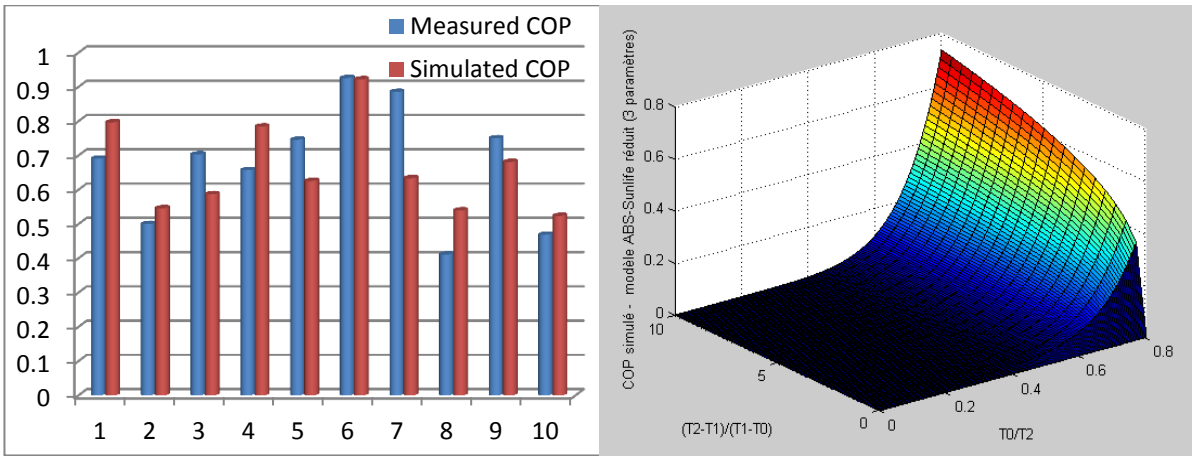

Figure 2: Simulated and measured COP based on the identified parameters.

Modeling the ORC Efficiency

The structure of the cycle has a single volumetric turbine stage using an organic fluid with the high temperature kept constant while the lower temperature is variable.

The condensation of the organic fluid does not take place at ambient temperature but at a temperature higher than that required by the absorption machine [1, 3, 4, 5] and it is also subject to the average ΔT_{pinch}.

The efficiency can be expressed by the following model where parameters d_o and d_1 are determined experimentally.

$$\varepsilon_{ORC} = d_0 \cdot (T_{ORC} - T_{m2})^{d1} \cdot (T_{ORC})^{-1} \quad (10)$$

The Efficiency Model of The Solar Field

After a thorough analysis of the most appropriate solar collectors and the selected temperature ranges, we selected the following model:

$$\varepsilon_{sol} = F'.(\tau\alpha) - \frac{F'.U_{L0}}{E_n}.(T_{m-sol} - T_a) - \frac{F'.U_{L1}}{E_n}.(T_{m-sol} - T_a)^2 \quad (11)$$

This model has been extensively validated in numerous studies involving several experimental works [1, 8].

Figure 3 shows the simulation for both configurations with Type 2 showing higher performance at all generator temperatures.

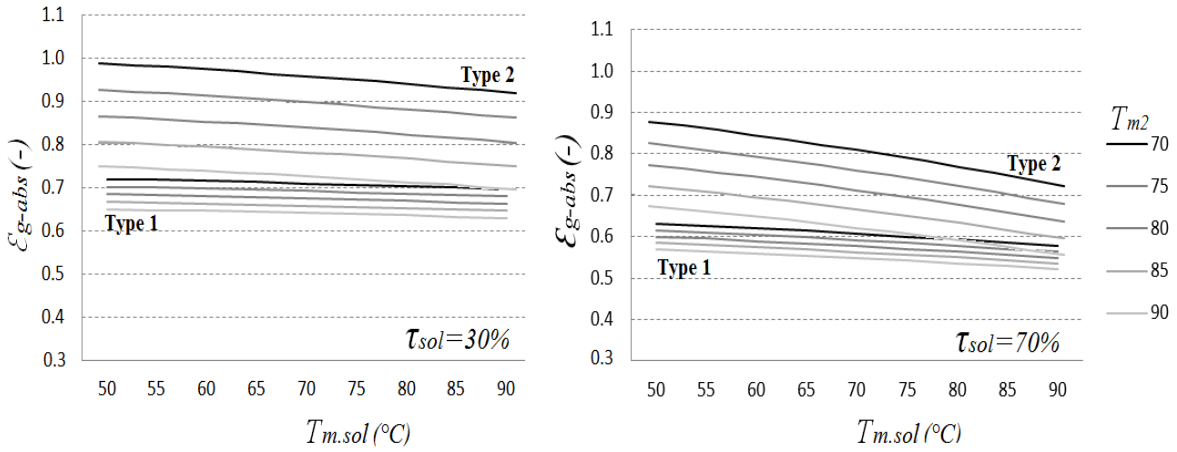

Figure 3: Simulation of Type 1 and Type 2 configurations.

COMPARATIVE STUDY

Type 1 (Tunisia): The system performance (heat and cooling) are very sensitive to the variation in temperature at the solar collectors and the generator of the absorption chiller which is due to the fluctuations in solar radiation. For solar contribution of 30% and 70%, the overall efficiency was 65% and 55%, respectively. Note that cold production is based solely on absorption chillers with the risk of crystallization due to temperature irregularities. The retrofitting in this 2 is possible.

Oman Type 2: The trigeneration performance is sensitive to the choice of the type of solar collectors but they are, in all cases, much higher than those of Type 1. This type is not adequate if the natural gas network will not cover isolated areas. For solar contribution of 30% and 70%, the overall efficiency is 81% and 65% respectively. T_{m-sol}= 140 °C (type 2) and 90°C (Type 1) ; T_{m2} = 80 °C (Type 1 and 2); E_n = 900 W/m^2, T_a = 25 °C

CONCLUSION

We have shown that it is possible to improve the performance of the conventional cooling systems through a combination of solar energy and natural gas that provide significant advantages over the existing systems. The trigeneration systems is mainly based on a cascade transfer of heat so as to give priority to a mechanical work via ORC rather than direct feed of heat to the absorption machine and it significantly improves the energy efficiency of solar cooling system. These systems can ensure maximum availability of energy (heat, cold, electricity) as well as adaptability to local conditions. We also investigated the temperature ranges of operation of the solar collectors and those of various machines (ORC, absorption) that ensure eligible annual level of performance depending on the characteristics of two typical areas considered in MENA.

SYMBOLS

Symbol	Designation	Unit	Symbol	Designation	Unit
$\dot{Q}^{+}_{sol}$	Heat from solar collectors	kW	τ_{sol}	Nominal solar contribution	(-)
$\dot{Q}^{+}_{gaz}$	Primary heat from natural gas fuel	kW	τ_{heat}	Heating utility contribution	(-)
$\dot{Q}^{+}_{heat}$		kW	τ_{elect}	Ratio of net electricity produced	(-)
$\dot{Q}^{+}_{abs}$	Thermal power provided to the absorption machine	kW	ε_{stor}	Storage tank effciency	(-)
$\dot{Q}^{-}_{fabs}$	The cooling load of the absorption machine	kW	ε_{sol}	efficiency of solar collectors	(-)
$\dot{Q}^{-}_{fcomp}$	The cooling load of the refrigeration compression machine	kW	ε_{vap}	efficiency of vapor recovery at heat engine	(-)
$\dot{E}^{-}_{e.comp}$		kW	ε_{ORC}	Effciency of ORC	(-)
$\dot{E}^{-}_{elect}$	Net electrical power produced	kW	ε_{abs}	absorption machine COP	(-)
E_n	Solar radiation	W/m^2	ε_{comp}	Refrigeration compression machine COP	(-)
T_a	Ambient temperature	°C	ε_{g-abs}	Absorober solar cooling overall effciency (Assummption 1)	(-)
T_{m-sol}	Average temperature (solar collectors)	°C	ε'_{g-abs}	Absorober solar cooling overall effciency (Assummption 2)	(-)
T_{m0}	Temperature (evaporator)	°C	$\varepsilon_{g-trigen}$	Trigeneration system overall effciency (Assummption 1)	(-)
T_{m1}	Temperature (cooling tower)	°C	$\varepsilon'_{g-trigen}$	Trigeneration system overall effciency (Assummption 2)	(-)
T_{m2}	Temperature (generator)	°C	$F'.(\tau\alpha)$	Loss factor	(-)
T_{ORC}	High temperature of the ORC	°C	U_{L0}, U_{L1}	Conductivity of solar collectors	W/m^2/°C
T_{e0}, T_{s0}	Inlet, outlet temp. of the evaporator	°C	c_0, c_1, c_2	Absorption machine coffcients	(-)
T_{e2}, T_{s2}	Inlet, outlet temp. of the generator	°C	d_0, d_1	ORC Coeffcients	(-)
$\dot{m}_0$, $\dot{m}_2$	Mass flow, evaporator & generator	Kg/s	C_{p0}, C_{p2}	Specific heats	J/kg/°C

REFERENCES

1. Henchoz, S., Buchter, F., Favrat, D., Morandin, M., Mercangoez, M.: Thermoeconomic analysais of a solar enhanced Energy storage concept based on thermodynamicscycles. Energy. Vol. 45 (1), PP 358-36, 2012.
2. Alllani, Y., Favrat, D., Von Spakovsky, M.: *CO_2*, mitigationtrough The Use Of Hybride Solar-Combined Cycles.Energy Conversion and Management. Vol. 38, PP S661-S667, 1997.
3. Kane, M., Favrat, D., Larrin, D., Allani, Y.: Small hybrid solar power system.Energy. Vol. 28 (14), PP 1247-1443, 2003.
4. Kane, M., Favrat, D., Allani, Y., Larrin, D.: Thermoeconomic Analysis of Advanced Solar-Fossil Combined Power Plants. Int. Journal of Applied Thermodynamics, Vol. 3 (4), PP 191-198, 2000.
5. Kane, M., Zanelli, T., Favrat, D., Allani Y., Glauser, E.: Conception d'une mini-centrale electro-thermo-solaire hybride adaptée aux pays en voie de développement. Proc. of The Inetrnational Conference on Solar Energy and Buildings (CISBAT'99), PP 103-108, Lussane, 1999.
6. Al-Azri, N., Al-Rawahi, N., Allani, Y.: Solar Power Generation and Solar Cooling Cogeneration. Project Report,The RESEARCH COUNCIL (TRC) Sultanate of Oman, 2012.
7. Al-Azri, N. , Al-Thubaiti, M. and El-Halwagi, M.: An algorithmic approach to the optimization of process cogeneration.Clean Technologies and Environmental Polices, Vol. 11(3), PP.329-338, 2009.
8. Allani, Y.: Caractérisation des convertisseurs héliothermiques par couplage entre modèles physiques et de représentations. Thèse de doctorat, Ecole Polytechnique Fédérale de Lausanne, 1993.

DEVELOPMENT OF A HIGH PERFORMANCE FACADE ELEMENT

S. Eicher[1]; J. Bony[1]; A. Duret[1]; M. Bunea[1]; S. Citherlet[1]

1: HEIG-VD, LESBAT, Av. des Sports 20, CH-1401 Yverdon-les-Bains

ABSTRACT

This paper presents an overview of the R&D activities for the *Bâti-Tech* project that concerns integration of solar thermal collectors into an existing, commercialised multifunctional facade element. The study involves both monitoring and test bench measurements along with dynamic simulations of the facade element integrated in a building. The existing facade concept includes thermal and acoustic insulation and PV production. The overall objective of the project is to modify the current facade element and integrate a solar thermal collecting function for building heating purposes. This project, funded by the Canton of Vaud, was launched at the end of 2013 within the framework of its "*100 millions pour les énergies renouvelables et l'efficacité énergétique*" programme. Research has indicated that the PV performance of the investigated facade is greatly affected by shading of the near surrounding. Measured stagnation temperatures of the PV panel of the facade element have also shown a limited potential for using heat from these modules for heating applications unless combined with a heat pump. Simulations have further suggested that the use of flat plate systems as a collecting device integrated in the building envelope could be interesting for space heating and domestic hot water preparation. The study is now focusing on the modification and integration of a solar thermal collector into the existing facade concept.

Keywords: multifunctional facades, building integration, active solar components

INTRODUCTION

In Switzerland, space and domestic water heating are estimated to account for more than 40% of the total energy consumption in buildings [1]. They, therefore, represent an important opportunity to enhance buildings energy and environmental performance. Improved building envelopes and equipment along with exploiting renewable energies are key to minimising heat consumption and achieve higher energy efficiency and low greenhouse gases emission.

Today, the use of renewable energy in the building sector is dominated by solar installations for space and water heating and photovoltaic systems, mainly on the roof. In order to comply with current energy efficiency policies and legislation, for example [2], facades must also be considered as multifunctional energy conversion elements. The idea of changing the building envelope primary role so that it additionally becomes an active solar element is a good opportunity to optimise building energy efficiency. Thus, this project deals with the development of a multifunctional high energy performance facade element for new and refurbished buildings. This paper summarises the project different steps, describes the facade element concept and presents the main findings in the optimisation process of the facade system under investigation.

PROJECT DESCRIPTION

The overall objective of the project is to improve the functions of an existing, commercialised facade element. The facade element to optimise is a prefabricated layer module, fully integrating thermal and acoustic insulation along with photovoltaic panels for electricity generation. The investigated system is commercialised in Switzerland under the name of *Face*

InTec© and in association with Alpic InTec AG [3] a number of buildings have already been implemented with this technology [4]. Figure 1 shows a schematic representation of the *Face InTec*© system.

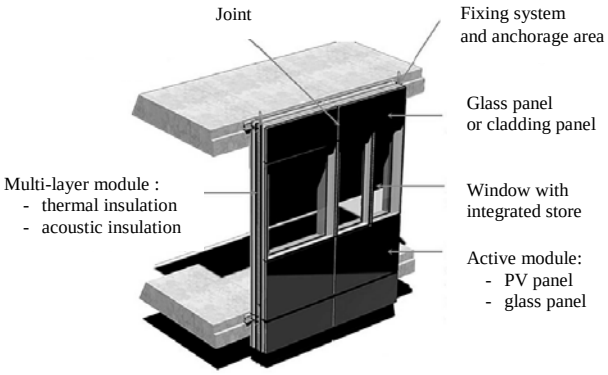

Figure 1: Schematic representation of the Face InTec© *facade element*

This project is concerned with the extension of facade element functions to include heat generation while keeping its aesthetics and modularity.

This will be achieved through a programme of work with the following sub-objectives:

- To monitor the energy performance of a pilot building installation and estimate heat recovery from the PV panel
- To study the system on a test bench, set up to characterise the facade element
- To develop a numerical model to simulate the behaviour of the facade element and predict the potential for heat recovery from different types of solar collectors. In addition, to simulate the annual performance of a building made of these elements over a wide range of conditions

Monitoring campaign

A monitoring campaign on a pilot building installation is underway allowing the evaluation of the electricity production of the *Face Intec*© elements. This helps verifying how well the PV installation is performing by comparing the actual PV production with expected targets. These latter were computed with the simulation software PVsyst [5].

The building is a two storey office situated in Lausanne with an envelope totally implemented with *Face Intec*© elements, see Figure 2.

Figure 2: Northwest and southwest facades of the pilot building

Some of these incorporate PV panels, apart from the northeast facade for which no PV panels were integrated. The building longitudinal axis runs from northeast to the southwest. The PV

installation is made of 402 micromorph modules[1] for a nominal rating of 46.2 kWp. The output is then fed to ten inverters[2]. Electricity production and module temperatures are recorded continuously since 2011 at 5 minutes intervals using a solar data logger with PC control.

Figure 3 shows a comparison between the annual PV output power per inverter (and orientation) and the corresponding simulated values for outdoor conditions based on the closest meteorological station to the building (Pully, CH).

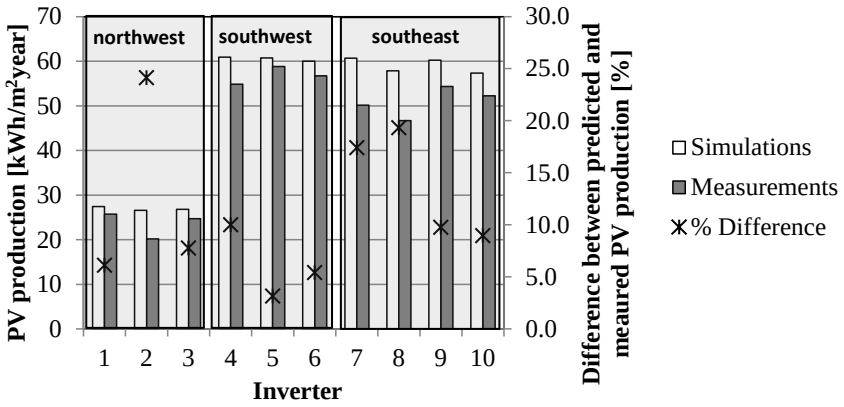

Figure 3: Comparison of predicted and measured PV production of the pilot building facade

As expected, the northwest facade presents lower electricity production in comparison with the other two facades mainly because of less exposure to the sun. Southwest and southeast facades present a similar PV production with values slightly higher for the southwest side probably due to slightly better insolation conditions.

It can also be seen that predictions are systematically higher than measurements with differences up to 24%. These are probably due to energy losses associated with module and inverter efficiency, shades, cabling, mismatch and soiling. However, a detailed analysis of the PV panels associated with these large differences have shown that due to their location, shading effects by the near surrounding and consequent mismatch losses are quite important. These effects have not been included in the simulation and result in great discrepancies, particularly for inverters 2, 7 and 8. This analysis considered direct shading using information based on both on-site observation and shadow projection on a sun-path diagram.

In order to estimate the potential for heat recovery of the *Face Intec*© facade, one PV module in the southwest facade has been fitted with two Pt1000 sensor to continuously monitor the rear-side temperature. The results revealed stagnation temperatures ranging from -8°C to 74°C on an annual basis. However, in winter the potential for applications such as space heating and domestic hot water (DHW) preparation (20°C and higher) is only about 15%. For temperature levels below 20°C, the use of a heat pump for heating purposes becomes necessary.

Test bench

A test bench comprising two independent support structures for studying the active module of *Face Intec*© is operational and equipped with different sort of sensors for monitoring purposes, see Figure 4. It allows to measure module temperatures, weather data and electricity

[1] Pramac Luce MCPH P7 115Wc
[2] Powador 6002, KACO new energy

production of the PV module. Situated in Yverdon-les-Bains, this facility offers the possibility to make comparisons between different modules under the same climate conditions. Modules undergoing testing are a PV micromorph panel, a simple glass panel and a solar thermal collector. This test bench is used not only to characterise the behaviour of the different modules but also to allow direct comparisons of performance between module types.

Figure 4: Test bench of the Face Intec© active module

Validation of results obtained on the test bench with measurements on the pilot installation was performed under near clear sky conditions. Figure 5 compares the temperature values obtained on an autumn day.

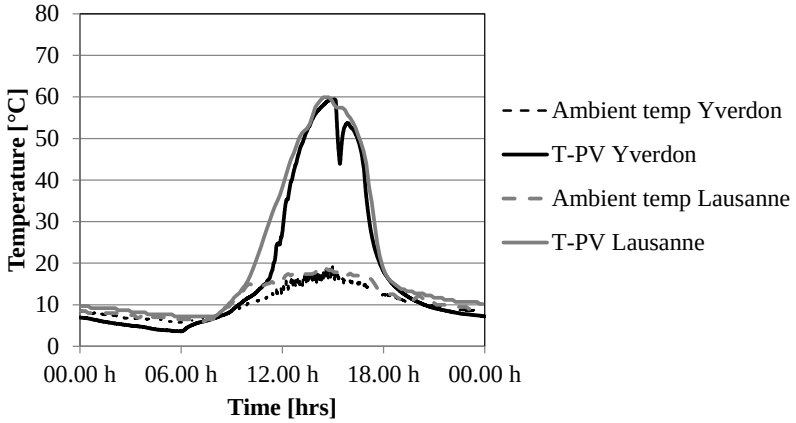

Figure 5: Comparison of test bench and pilot building PV module temperature

The daily temperature profiles of the PV module for the two locations follow the same trends with discrepancies more pronounced in the morning as some clouds partly covered Yverdon-les-Bains, reducing momentarily the solar irradiance. Another decrease of solar irradiance occurred in the afternoon at Yverdon-les-Bains due to a near surrounding object partly overcasting the tested module. The testing campaign of the different modules is ongoing and the results recorded using a Labview [6] acquisition system. This facility will allow the experimental characterisation of the performance and efficiency of the integrated heat recovery system under different climate and configuration conditions. These tests will benefit the development and design of a future solar thermal integrated *Face Intec©* element.

Simulation of the system

A dynamic model has been developed to characterise the performance of the facade active module on its own and when integrated in the building envelope. For these simulations the software TRNSYS 17 [7] was employed. The numerical model considers:

- Reference building: pilot office building at Lausanne with a heating area of 3650 m^2.

- Building space heat demand estimated with a single node model: thermal losses through the envelope and by ventilation as well as heat gains through windows and from people and equipment are accounted for.
- Building DHW demand: according to standard SIA 380/1 [8].
- Three different types of solar thermal collectors: flat plate; selective unglazed; non-selective unglazed.
- Two different Swiss climates: typical midland climate (Lausanne) and typical mountain climate (St-Cergue).

In order to assess the potential of generating heat from building integrated solar thermal devices, an analysis of the monthly average of global available solar irradiation on a south oriented surface for two slopes was performed. The resultant profiles are plotted in Figure 6 for the two surface inclinations of 30° (optimum tilt angle) and 90° (vertical facade) for the climate of Lausanne. Similar trends were observed for the mountain climate.

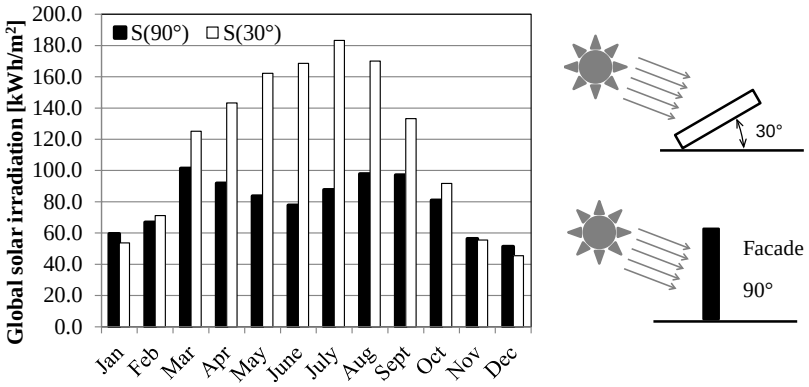

Figure 6: Average monthly distribution of the global solar irradiation on a south oriented surface for two slopes (Lausanne)

In the case of the vertical facade, it can be seen that the available solar irradiation is rather constant throughout the year, limiting summer overproduction when heating requirements are lowest (DWH only). Also, due to the high slope, solar irradiation is more important during spring and autumn. In addition, because during winter the sun is low in the sky, winter months receive an amount of irradiation comparable to that of the optimal case when energy needs are at the highest. The results indicate that vertical facades could provide a good alternative to more conventional solar thermal systems as they are able to better match the solar energy offer to the building heating demand.

Based on these profiles, the potential amount of heat that can be delivered from a solar thermal collector to the building heating system has been determined. Three different types of solar collectors able to be integrated in a façade without compromising the aesthetics were considered, see above. Variation of the inlet temperature to the collector was simulated for values between 15°C to 80°C in order to assess the effect on the heat recovery during winter months. Because results exhibit similar trends, only predictions for December are presented here. Figure 7 shows the predicted amount of heat recovered in December for the location of Lausanne for three types of solar thermal collectors placed on a south oriented vertical facade

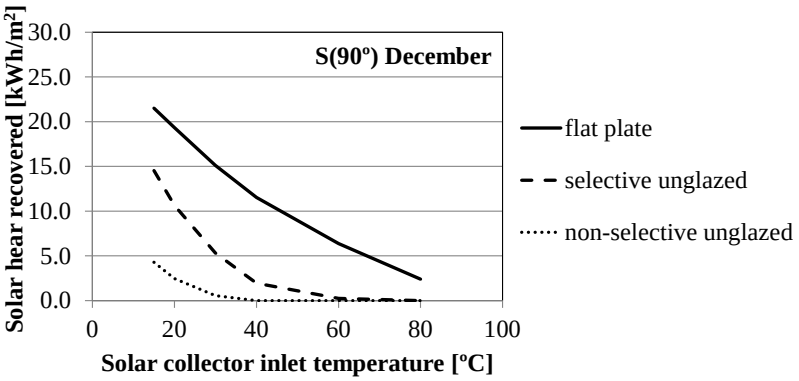

Figure 7: Predicted amount of solar heat recovered for three types of solar thermal collectors mounted on southern vertical facade

It can be seen that heat recovered by the non-selective unglazed collector is quite small when compared with that from the other two collectors. The selective unglazed collector could be an interesting option for heating purposes if combined with a heat pump to reach higher temperature levels. Finally, the flat plate presents the best solution with a predicted heat recovery at low to moderate temperature levels. Unlike unglazed collectors, their ability to collect solar energy is less dependent on the outside temperature. In all cases heat recovered decreases with increasing collector inlet temperature. The small amounts of heat recovered by the non-selective unglazed collectors suggest further that if combine with a PV module, resulting in the so-called photovoltaic thermal hybrid solar collector (PV/T), would not be appropriate for heating applications.

CONCLUSION

This paper presents the ongoing R&D activities for the *Bâti-Tech* project that deals with the integration of solar thermal collectors into an existing, commercialised multifunctional facade element. The investigation involves monitoring, test bench measurements and dynamic simulations of the facade element integrated in a building envelope. Monitoring of a pilot building facade has shown that PV performance is greatly affected by shading of the near surrounding. In addition, the potential for heat recovery from the rear-side of a PV panel is found to be small for heating applications unless combined with a heat pump. Conversely, simulations have shown promising results regarding the use of flat plate collectors integrated in the facade to better capture the available solar energy for heating applications. Based on these results, research is now focusing on the physical modification of the current facade element to include a solar thermal collecting device.

REFERENCES

1. Le bon chauffage au bon endroit. www.energie-environnement.ch/brochure-chauffage [Access April 2015].
2. Directive 2010/31/EU of the European Parliament and of the Council of 19 May 2010 on the energy performance of buildings.
3. Alpic InTec. www.alpic-intec.ch.
4. www.faceintec.com [Access April 2015].
5. PVsyst – Photovoltaic software. www.pvsyst.com.
6. LabVIEW System Design Software. www.ni.com/labview.
7. TRNSYS – Transient System Simulation Tool. www.trnsys.com.
8. Norme SIA 380/1. L'énergie thermique dans le bâtiment. SIA. Edition 2009.

PERFORMANCE OF THE ABSORPTION PROCESS IN A SEASONAL SORPTION HEAT STORAGE PROTOTYPE

B. Fumey[1]; S. Stoller[1]; R. Fricker[1]; R. Weber[1]; P. Gantenbein[2]; X. Daguenet-Frick[2]; V. Dorer[1]

1: Empa Material Science and Technology, Überlandstrasse 129, 8600 Dübendorf, Switzerland

2: HSR-SPF, Oberseestrasse 10, 8640 Rapperswil, Switzerland

ABSTRACT

Seasonal heat storage has great potential to enable renewable heating and seasonal load shifting. Nevertheless, it remains an on going challenge today. The benefits of sorption heat storage are fonud in the potentially lossless storage, when not including charging and discharging processes, and the prospective of greater volumetric energy densities compared to water. In sorption heat storage not sensible heat is stored, but the potential to regain heat. In the framework of the EU funded project COMTES a closed sorption heat storage demonstrator based on sodium hydroxide as sorbent and water as sorbate was developed and built.

The built demonstrator operates on a hybrid basis. Heat is stored in sensible hot water tanks for diurnal storage and in the sorption heat storage system for seasonal storage. This grants the possibility to utilise the benefits of both systems, namely low charging and discharging losses in sensible storage and low heat losses during storage time in sorption storage. The complete system is built into a 7 m long shipping container. A solar collector field with an active area of 18 m^2 mounted on the container serves to cover the total heat demand.

The central component of the sorption system is the interconnected absorber and desorber (AD) and evaporator and condenser (EC) unit. Both units are built as tube bundle falling film heat and mass exchangers similar to a solar thermal chiller. In initial operation with water, 6 kW of water vapour equivalent could be transported from desorber to condenser with a temperature difference between desorber and condenser of approximately 30 K. Nevertheless, absorption tests with sodium hydroxide at a concentration of 50 wt% showed much lower power output below 1 kW. It was found that even though absorption occurred, the process of water vapour absorption is slower than expected. The sodium hydroxide flows over the tube bundle with little water gained, thus releasing little heat. Results from this work and further testing of the speed of absorption have shown that novel heat and mass exchangers are required for sorption heat storage applications.

Keywords: Seasonal heat storage, sorption heat storage, absorption, heat and mass exchanger.

INTRODUCTION

In the framework of the EU funded project COMTES a closed sorption heat storage demonstrator based on sodium hydroxide (NaOH) as sorbent and water as sorbate, has been developed [1,4]. The system operates on a hybrid basis [2]. Heat is stored in sensible hot water tanks for diurnal storage and in the sorption system for seasonal storage. It is expected that the benefits of both systems can be utilised, namely low charging and discharging losses in diurnal storage and low heat losses during storage time in seasonal storage.

The complete system has been built into and onto a 7 m long shipping container [6]. Figure 1 shows the demonstrator system from the outside on the left and from the inside on the right.

Figure 1: Left: Picture of the complete system from the outside. Solar collectors with an active area of 18 m^2 are mounted on top and on the side of the shipping container. Right: Picture of the complete system from the inside. On the left is the heat and mass exchanger assembly, with the sorbent and sorbate tanks in the back, and on the right are solar pump station, fresh hot water station and floor heating pump, in the back the sensible hot water tanks are placed.

In a preliminary work, plate type heat and mass exchangers were constructed. These consisted of double floored plate shaped containments, whereby sorbent was introduced onto the plate, and a heat transport fluid passed through the plates double floored construction. In the present demonstrator, in order to reach a more continuous process, it was decided to introduce the falling film tube bundle concept, which is common in solar thermal chillers. To this accord two heat and mass exchanges were designed and constructed for the absorption and desorption as well as evaporation and condensation process respectively. Both consist of a horizontal alignment of tubes containing the heat transfer fluid and wetted by sorbent (AD unit) or sorbate (EC unit) from a horizontal liquid falling film [3]. Figure 2 shows the heat and mass exchanger design as built in the demonstrator.

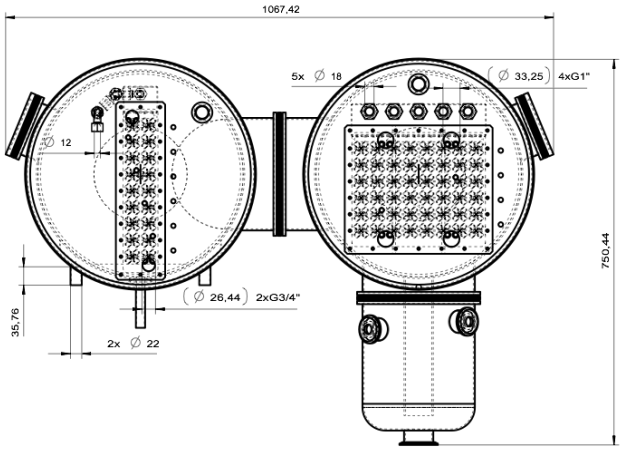

Figure 2: CAD drawing of the heat and mass exchanger, measurements in mm. On the left is the AD unit and on the right the EC unit.

RESULTS

Several absorption tests have been done with the heat and mass exchanger illustrated in Figure 2. Results of two tests are visualised in Figure 3. These illustrations show steady state average values. The blue circles indicate the tube bundle arrays for both the AD and EC units. The heat transport medium flows upward from one tube to the other, as shown by the blue arrows through the circles. The orange arrow shows the flow of the sorbent in the AD unit, this is in counter flow to the heat transport fluid. In the EC unit the sorbate flow is indicated in dark blue. Temperatures are measured inside as well as outside of the tubes at varying levels, as indicated. Volume flows of the sorbent and the heat transport fluids in both AD and EC units are indicated as well as the power input and output.

In operation it was discovered that non condensing gases have a substantial effect on the absorption process. In the figure on the left, operating at a pressure of 1.88 mbar abs. above the water vapour pressure (18.69 mbar abs.) at the given evaporator temperature stable vapour transport equivalent to 1 kW of thermal energy could be reached. On the other hand on the right, at similar settings, the measured pressure was 10.3 mbar above the water vapour pressure (17.4 mbar abs.). In this test no vapour transport was possible.

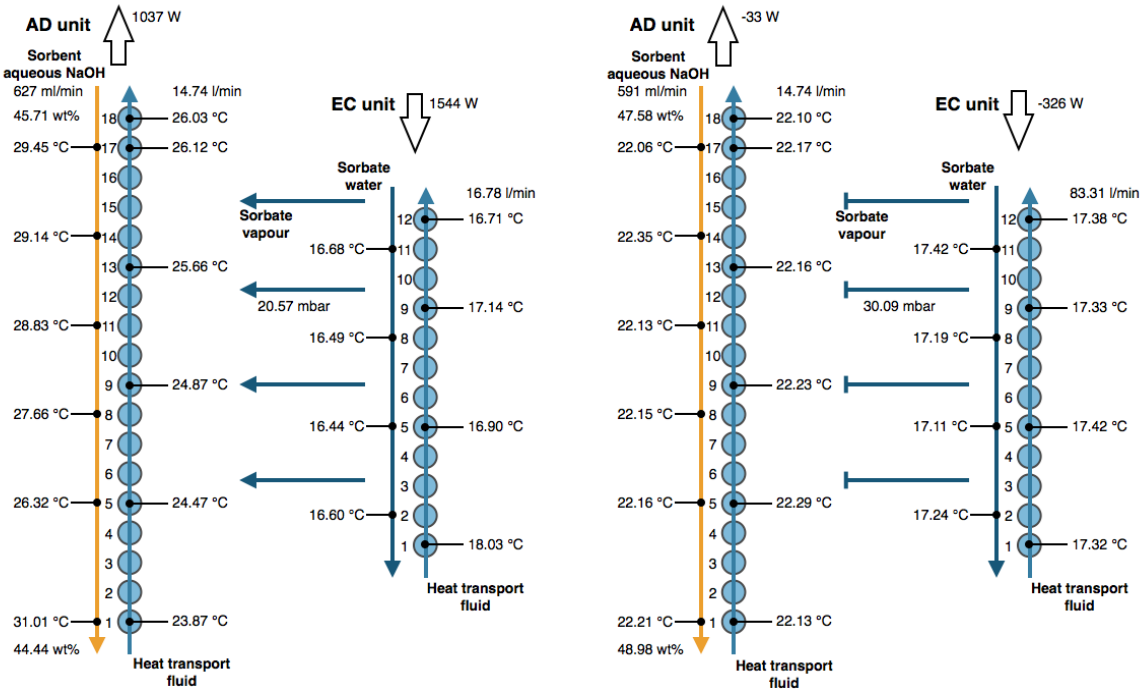

Figure 3: Illustration of the absorber / desorber (AD) and evaporator / condenser (EC) heat and mass exchanger test results. On the left is the result with nearly all non condensing gases removed, on the right a result with approximately 10 mbar pressure resulting from non condensing gases.

Even through an achieved continuous power output of approximately 1 kW, the actual temperature gain was only 2.16 °C, from 23.87 °C to 26.03 °C. Theoretically an output temperature of approximately 56 °C should be possible [5], when neglecting temperature losses. The sorbent concentration reaches only a slight reduction, which explains the low temperature gain and power output.

DISCUSSION

It appears that the conventional heat and mass exchangers as designed in this system and often used in absorption chillers [3] are not fitting the heat storage application. This can be explained as follows: Even though the process of absorption and desorption in the heat storage application is comparable to the solar chilling process, the actual operation differs strongly. Solar chilling follows a continuous full cycle process, sorbent is charged by removing sorbate followed immediately by discharging through absorbing sorbate. Sorbate is condensed and evaporated in a continuous process whereby heat is released or gained from the ambient respectively. In gaining heat from the ambient, chilling is achieved. In this process the quantity of sorbate transported between desorption and absorption is not of primary importance. In the heat storage approach on the other hand a continuous but not full cycle process is at work. This is due to the nature of its role as storage. In its operation, especially in the absorption process, it is of significant importance that a low concentration of sorbent, in other words high sorbate absorption is reached. This has direct impact on the storage energy density. Due to the dependence of the output temperature on the sorbent concentration, absorption must occur in one step and recirculation is not possible. Consequently the exposure time of the sorbent to the sorbate vapour must be sufficient to reach high sorbate uptake. In the described setup about 2 seconds are given.

A further issue is found in the formation of sorbent droplets. Figure 4 shows the AD tube bundle with the manifold evenly supplying small droplets on the first tube. Nevertheless they quickly group to form larger droplets, thus reducing the wetted area of the tube bundle and increasing the fall through time, whereby reducing both contact area and contact time of sorbent to sorbate.

Figure 4: Picture of the tube bundle in the AD unit, showing the flow of sorbent (aqueous NaOH) over the tubes. Fine droplets group, reducing the wetted surface on the tubes.

CONCLUSION

It is found that a novel heat and mass exchanger design for the absorption process in sorption heat storage is required. A possibility could be a heat and mass exchanger consisting of two separate zones. An initial area of only mass absorption, allowing preheating of the sorbent, followed by an area of mass absorption and heat release for heat transport. In the design it is critical that the sorbent is allowed adequate time for sorbate absorption, this could require a sorbent suspension in sorbate vapor time of more then one hour.

ACKNOWLEDGEMENTS

Financial support by the European Union in the seventh framework program (FP7 / 2007-2013) under the grant agreement No295568 is gratefully acknowledged. Further we gratefully acknowledge financial support by our research institutions EMPA Swiss Federal Laboratories for Materials Science and Technology and HSR-SPF University of Applied Sciences Rapperswil Switzerland.

REFERENCES

1. Benjamin Fumey, Robert Weber, Paul Gantenbein, Xavier Daguenet-Frick, Tommy Williamson, Viktor Dorer, EXPERIENCE ON THE DEVELOPMENT OF A THERMO-CHEMICAL STORAGE SYSTEM BASED ON AQUEOUS SODIUM HYDROXIDE“ Energy Procedia 57 (2014) 2426 – 2435.
2. Benjamin Fumey, Robert Weber, Paul Gantenbein, Xavier Daguenet-Frick, Tommy Williamson, Viktor Dorer, „Development of a closed sorption heat storage prototype“ Energy Procedia 46 (2014) 134 – 141
3. Xavier Daguenet-Frick, Paul Gantenbein, Elimar Frank, Benjamin Fumey, Robert Weber, Tommy Williamson, „Reaction zone development for an aqueous sodium hydroxide seasonal thermal energy storage“, Energy Procedia 57 (2014) 2426 – 2435.
4. Benjamin Fumey, Robert Weber, Paul Gantenbein, Xavier Daguenet-Frick, Tommy Williamson, Viktor Dorer, „Closed sorption heat storage based on aqueous sodium hydroxide“, Energy Procedia 48 (2014) 337 – 346.
5. Benjamin Fumey, Robert Weber, Paul Gantenbein, Xavier Daguenet-Frick, Ian Hughes, Viktor Dorer, „Limitations imposed on energy density of sorption materials in seasonal thermal storage systems“, SHC2014 China.
6. Benjamin Fumey, Robert Weber, Paul Gantenbein, Xavier Daguenet-Frick, Sascha Stoller, Reto Fricker, V. Dorer, “Operation results of a closed sorption heat storage prototype“, IRES2015 Germany

HIGHLY EFFICIENT, COST-EFFECTIVE SOLAR-GEOTHERMAL HEAT SUPPLY CONCEPT FOR MULTI-FAMILY HOUSES AND SMALL RESIDENTIAL AREAS

N. Gohl[1]; A. Loose[1]; D. Bauer[1]; H. Drueck[1]

1: Research and Testing Centre for Thermal Solar Systems (TZS), Institute of Thermodynamics and Thermal Engineering (ITW), University of Stuttgart, Pfaffenwaldring 6, 70550 Stuttgart, Germany

ABSTRACT

In order to meet the targets of the European Renewables Directive (2009/28/EC) [1], it is essential to increase both, the share of renewable energy sources used for heating applications as well as the efficiency of today's conventional heat supply systems. As a step forward to face this challenge, an innovative, sustainable heat supply concept is being developed at the Research and Testing Centre for Thermal Solar Systems (TZS) of the Institute of Thermodynamics and Thermal Engineering (ITW) of the University of Stuttgart. **This concept, which is based on solar thermal and geothermal heat generation and advanced heat storage technologies, will be realized for the first time as a heat supply system for new apartment buildings. The key feature of the system is the fact, that on an annual basis only 1 kWh of electricity will be required to generate 10 kWh of heat.**

The concept mentioned above is in principle designed in a similar way as the energy concept of so-called "solar houses" or "solar active houses" with high solar fractions > 50 %, where heat is usually generated by solar thermal collectors and stored in large-volume hot water stores. Regarding the high efficient, cost-effective solar-geothermal heat supply concept introduced in this paper, about 50 % of the annual heat demand for domestic hot water and space heating can be provided by solar energy. Another 40 % of the annual heat demand is provided by shallow geothermal energy, and only an additional 10 % of the annual heat demand is required in the form of electrical energy to operate a compression heat pump. The high efficiency of the concept is derived from an efficient combination of the used technologies in conjunction with a specially adapted control strategy and the use of innovative key products. For example, the geothermal source system is based on highly efficient, slim, helical ground heat exchangers with high specific heat transfer capacities, which are immersed only up to 10 meters in the ground. In contrast to conventional borehole heat exchangers, the installation of these innovative heat exchangers is relatively low priced and, due to the small drilling depth, no hydrogeological problems are expected.

This contribution is focused on the presentation of the above described, newly developed system concept as well as first results of the design and simulation studies for a pilot heat supply system that is planned to be realized in a complex of three multi-family houses within a total living area of approx. 3 530 m² in the German city Crailsheim, which is located 80 km north-east of Stuttgart.

The development of the concept is part of the research project '1to10 – Development, testing and demonstration of a sustainable, standardized solar-geothermal heat supply concept'. In the conceptual design phase of the project, theoretical work for the realization of such systems is performed. Another key part of the design phase is for example the issue of a stakeholder analysis and, based on this analysis the development of a constellation of stakeholders.

Keywords: solar thermal, geothermal, heat supply concept, multi-family houses

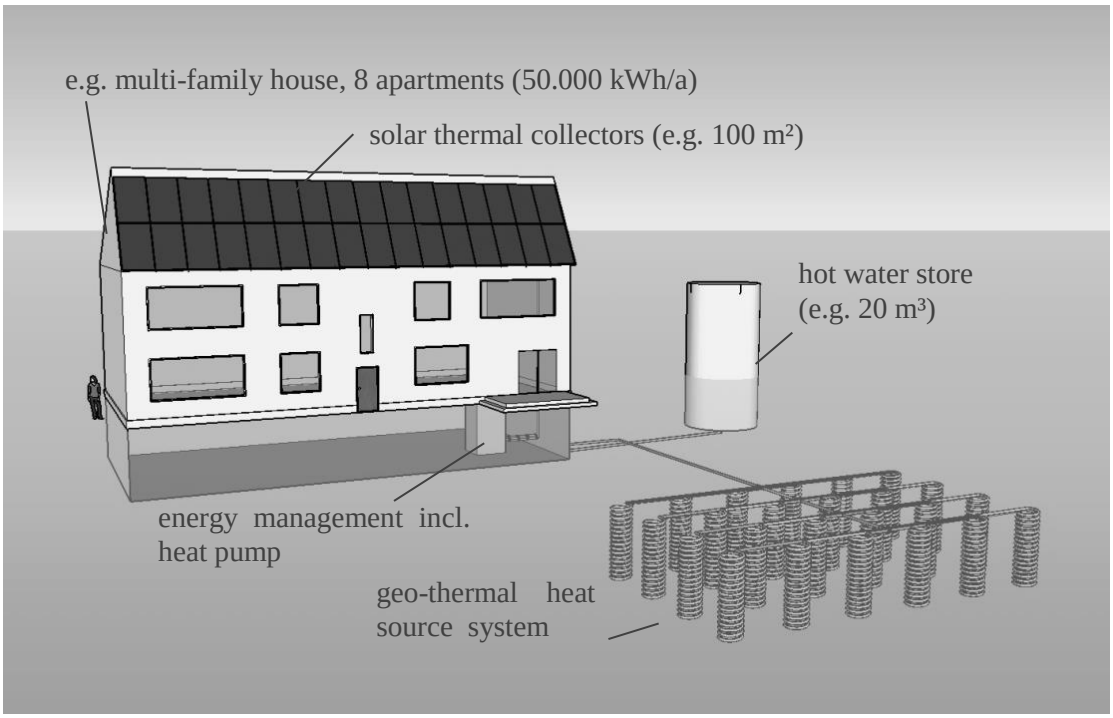

Figure 1: General 1to10 system concept

INTRODUCTION

Solar thermal as well as geothermal energy play a crucial role in the extension of the use of renewable thermal energy in Europe. The aim until 2050 is a contribution of 50 % of solar thermal energy to cover the European heating and cooling demand [2]. An essential step to reach this goal is to access the market of multi-family houses. In Germany, the share of residential units that are located in multi-family houses is 60 % of all existing residential units and this market segment is vastly untapped for solar thermal systems until now.

Essential aspects of the 1to10 heat supply concept on the basis of solar thermal and geo-thermal heat generation as well as heat storage are:

- Exceptionally high system efficiency – only 1 kWh of electricity required to generate 10 kWh of heat
- Only electrical connection required – no natural gas connection or storage for oil or wood pellets
- Large thermal capacities on both sides of the heat pumps allow relatively flexible operation times in off-peak periods which result in the stabilization of the electricity grid
- The combination of solar thermal energy and shallow geothermal energy reduces the size and therefore the investment costs of the geothermal system compared to a solely ground-coupled heat pump system.
- Consistently high energy efficiency ratios of the heat pumps and therefore low operation costs

DESCRIPTION OF THE PILOT SYSTEM

The 1to10 system (hydraulic scheme see Figure 2) consists of a solar collector loop which is hydraulically decoupled from the hot water store with an external heat exchanger. Two heat pumps are connected to the store: a high temperature heat pump provides heat for domestic hot water preparation using water at a medium temperature level of about 40 °C from the middle part of the hot water store as heat source. The condenser of the high temperature heat pump is connected to the upper part of the store. The second, ground coupled heat pump provides heat at medium temperature level for space heating to the middle part of the store. The evaporator of this heat pump is connected to the helical ground heat exchangers, which – if applicable – will be operated with water as heat transfer fluid. Surplus heat from the solar thermal collectors which cannot be stored in the hot water stores is used to heat up the ground. In addition to the effect of the regeneration of the earth, stagnation of the system can be avoided in summer.

The hot water store is the central component of the heat supply systems where all system circuits meet. For domestic hot water preparation, hot water is drawn from the upper part of the store to heat up domestic hot water in an external fresh water station. The space heating loop is connected to the middle part of the store.

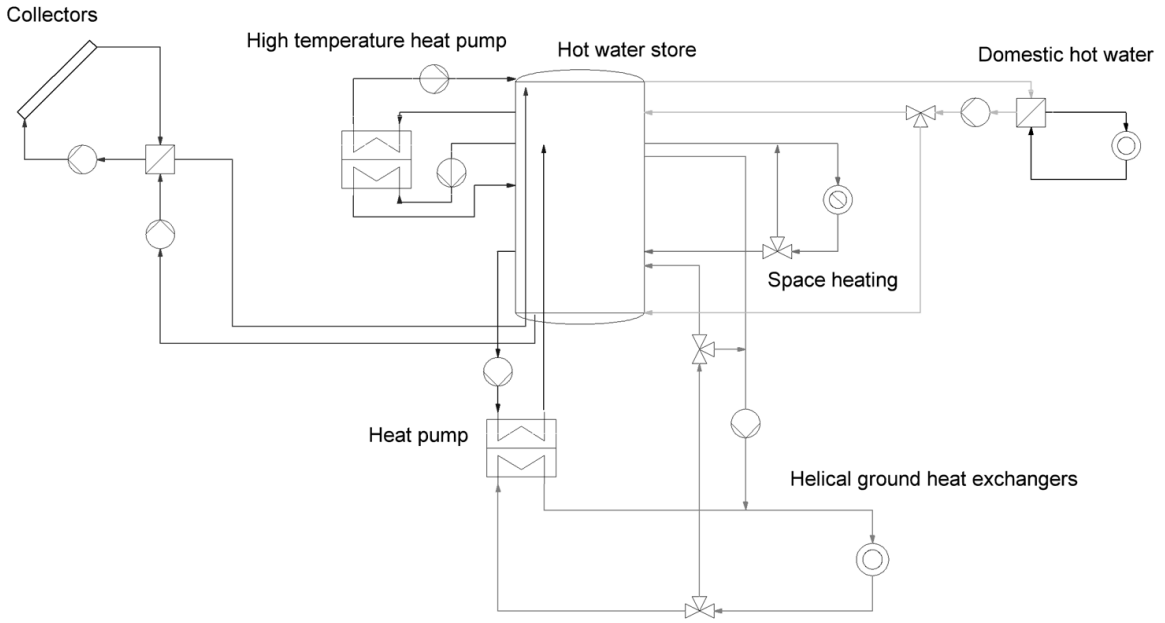

Figure 2: General hydraulic concept

Building characteristics

The building complex in Crailsheim, which is foreseen as pilot plant, consists of three multi-family houses with a total of 40 apartments. The annual heat demand for space heating is 135 000 kWh/a, the heat demand for domestic hot water preparation is 44 200 kWh/a, while half of the heat demand for domestic hot water is needed to provide a constant temperature of 65 °C in the circulation system. The orientation of the roof areas is south-west for two of the

buildings and south-east for the third building. The flow temperature of the low temperature space heating system is 37 °C.

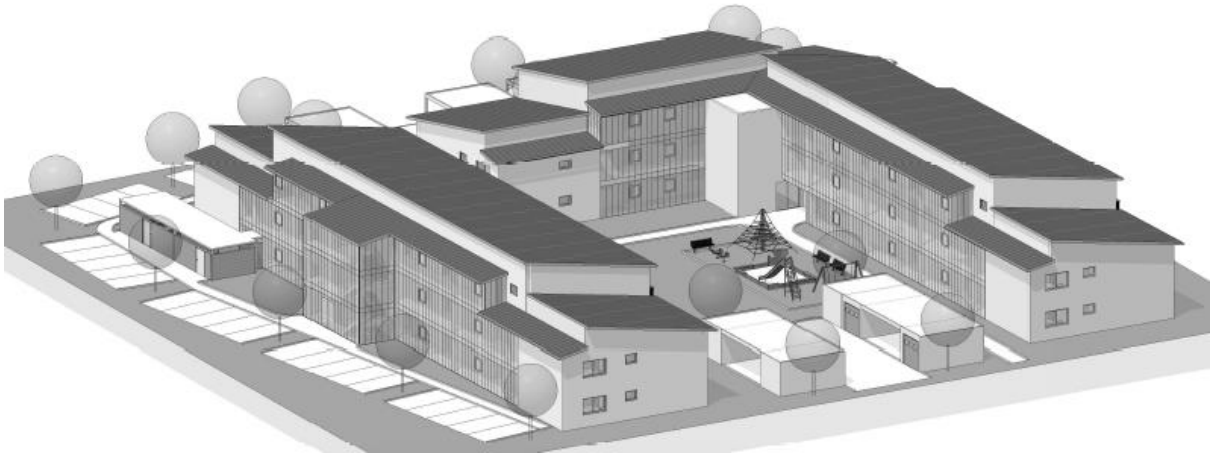

Figure 3: Building complex in Crailsheim, Germany. © Fessel Architekt GmbH

System components

Solar thermal **vacuum flat plate collectors** with a total gross area of about 250 m² will be installed on the roofs of the building complex. Due to the fact that the mono-pitched roofs of the buildings have a very small slope of 10°, it is necessary to raise the solar thermal collectors to a slope of 60° in order to increase the collector gain in winter and during the transition months with low sun positions, while at the same time reduce the solar gain in summer and therefore reduce stagnation times of the system. Additionally, reflector plates as displayed in Figure 4 on the left are planned to be realized in order to further increase the solar gain in times of low sun levels. The right side of Figure 4 shows the solar irradiation on the collector plane for collectors with a slope of 60° with and without reflector plates. As intended, the solar irradiation on collectors with reflector plates is significantly higher in the winter and transition months and in the same range or even less in the summer months.

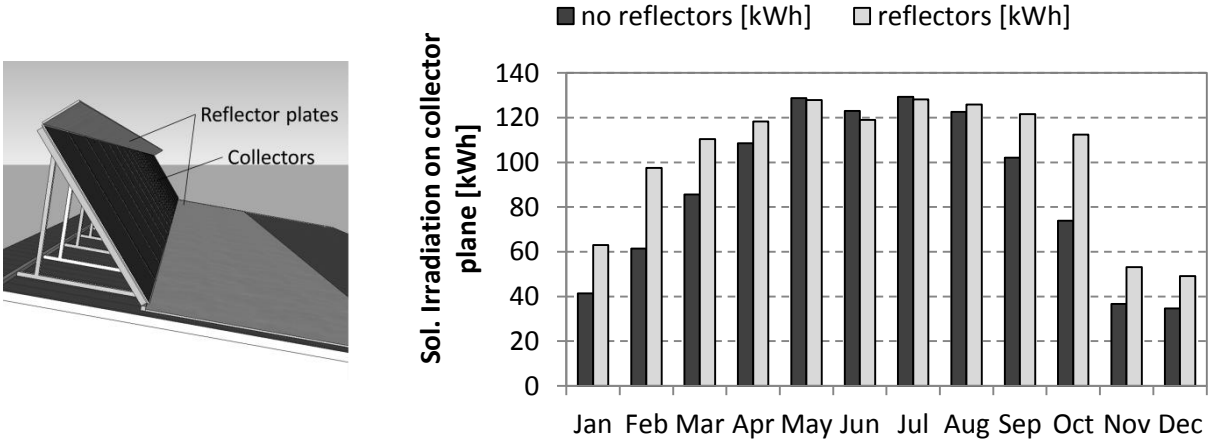

Figure 4: collector installation design with reflector plates (left) and the resulting irradiation on the collector plane (right; collector slope: 60°)

Two **heat pumps** will be installed in order to provide heat for space heating and domestic hot water. The first heat pump with a condenser power of about 50 kW_{th} is a ground coupled heat

pump whose evaporator is connected to the ground heat exchangers. The first heat pump provides heat at a temperature level of about 40 °C to the middle part of the heat store. The second heat pump works at a higher temperature and provides hot water at a thermal output of about 4.5 kW_{th} and a temperature level of about 65 °C for domestic hot water preparation to the upper part of the store. Heat source of the high temperature heat pump is warm water from the middle part of the heat store.

The **helical ground heat exchangers** will be installed in the courtyard between the three buildings. About two hundred helical ground heat exchangers will be installed on a total area of 1 200 m². The **hot water store** will be positioned outside the buildings and is planned to be immersed partly in the ground in order to reduce the heat losses to the environment in winter. An innovative vacuum insulation additionally minimizes the heat losses of the hot water store to the environment. The hot water store has a volume of about 40 m³.

SIMULATION RESULTS

Table 1 contains the results of a first simulation setup which will be the basis for the planning of the system that will be realized at the site in the city of Crailsheim. In this system configuration, 1 kWh_{el} of electricity for the heat pumps ($W_{el,HP1} + W_{el,HP2}$) is used to generate 9.23 kWh_{th} of heat for space heating (Q_{SH}) and domestic hot water (Q_{DHW}) including the additional heat that is needed due to the heat loss of the store ($Q_{loss,sto}$). The solar fraction f_{sol}, which is defined as

$$f_{sol} = \frac{Q_d - Q_{evap,HP1} - W_{el,HP1} - W_{el,HP2}}{Q_d} \cdot 100 = \frac{Q_{sol,net}}{Q_d} \cdot 100 \quad (1)$$

is 58.3 %, where the heat demand Q_d is defined as the sum of the heat demand for space heating and domestic hot water and the heat loss of the store $Q_{sol,net}$ is the difference of the total collector gain and the surplus heat that is transferred from the store to the helical ground heat exchangers and $Q_{evap,HP1}$ is the low temperature heat provided by the helical ground heat exchangers. The fraction of the heat demand that is covered by the two heat pumps f_{HP} is 41.7 % and is defined as

$$f_{HP} = \frac{Q_d - Q_{sol,net}}{Q_d} \cdot 100 \quad (2)$$

Q_{SH} [MWh_{th}]	Q_{DHW} [MWh_{th}]	$Q_{sol,net}$ [MWh_{th}]	$Q_{evap,HP1}$ [MWh_{th}]	$Q_{loss,sto}$ [MWh_{th}]	$W_{el,HP1}$ [MWh_{el}]	$W_{el,HP2}$ [MWh_{el}]
135.24	44.20	109.18	57.97	7.88	17.91	2.38

Table 1: Annual heat balance of the 1to10 system, simulation results

The monthly heat balance of the system, which is displayed in Figure 5, shows that from May to September, almost the whole heat demand is covered by the gain of the solar thermal collectors and the heat pumps only provide a marginal share of the heat demand. In the winter months from November to January, the heat demand covered by the heat pumps is 71 –74 %. According to the simulations, during the transition months March, April and October, 65 – 80 % of the heat demand is covered by the solar thermal collectors.

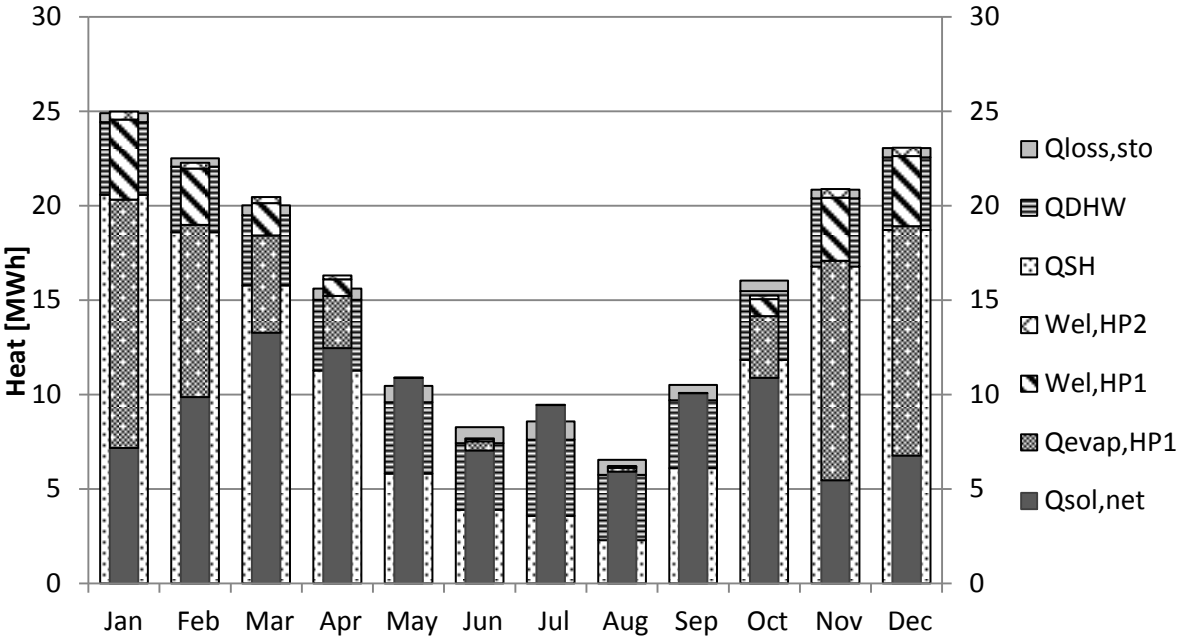

Figure 5: Monthly heat balance of the 1to10 system, simulation results

CONCLUSION

The presented simulation results are the starting point for the planning and dimensioning of the heat supply system to be realized in Crailsheim. Based on these results, the heat supply system with its site-dependent boundary conditions will be planned in an iterative process in collaboration with the architect and the contractor of the building project.

However, these first simulation results allow for the appraisal that the goals of the concept 1to10 can be achieved in this first pilot application.

ACKNOWLEDGEMENTS

The project 1to10 (reference number: BWE 15001) is supported by the Project Management Agency Karlsruhe (PTKA) on behalf of the Ministry of the Environment, Climate Protection and the Energy Sector of Baden-Württemberg (UM). The authors are grateful for the support and take the full responsibility for the content of this publication.

REFERENCES

1. Directive 2009/28/EC of the European Parliament and of the Council on the promotion of the use of energy from renewable sources and amending and subsequently on the repealing Directives 2001/77/EC and 2003/30/EC, April 2009
2. Stryi-Hipp, G., Drück, H., Wittwer, V., Zörner, W.: Forschungsstrategie Niedertemperatur-Solarthermie 2030 für eine nachhaltige Wärme- und Kälteversorgung Deutschlands; Deutsche Solarthermie-Technologie Plattform (DSTTP), c/o BSW-Solar, Berlin, 2010

CORRELATION OF MEASURED WIND DATA

M. Haase[1]; K.S. Skeie[1]

1: SINTEF Building and Infrastructure, Alfred Getz vei 3, 7491 Trondheim, Norway

ABSTRACT

The overall aim of the project is to develop new knowledge, integrated solutions, and technologies of small/micro wind turbines. Different measurement devices were used for measuring wind velocity, wind direction, power output and vibration in 5 minute intervals on the rooftop of a test building. Wind data was also collected from two weather stations nearby. The results were collected by a data logger on the roof and periodically tracked out on a computer. The wind performance was investigated and documented followed by an analysis of the correlation between measured climate data at the installation site and the two nearest meteorological stations. The results show that wind speed on top of the building was much less than measurements from two meteorological stations nearby.

Measured wind conditions on the roof of the building were very different from expected wind conditions. The location of the measurement devices and the wind turbines in the case study were not optimized. Much lower wind velocities were measured on the rooftop than at the other measurement stations. Correlations show a 40% lower wind velocity on the roof than at the measurement stations. The equivalent wind speed would be even lower if the height of the wind turbine is considered (in accordance with the wind shear power law). This should be taken into consideration when planning to install wind turbines in the built environment.

Keywords: wind measurements, correlation, data analysis

INTRODUCTION

Wind power can be used to generate electricity in an urban environment. This trend has mainly been seen in Europe, where the integration of small/micro wind turbines in the built environment is being actively discussed [2]. New wind turbines are under development for this application, which is looking mainly for quiet and efficient devices under turbulent and skewed wind flow [5].

The overall aim of the project is to develop new knowledge, integrated solutions, and technologies of small/micro wind turbines. As well as the installation of wind turbines around and on buildings, there is also interest in 'building-augmented' wind turbines, where the turbine is part of the building structure or façade. The design of the building in this case is augmented in order to get the optimum out of the wind power. Comprehensive monitoring of pilot installations and analysis of the measurement results are used to demonstrate the technology and concepts developed in the project and serve as a testing ground for the design of construction and operation of building integrated or even building augmented wind turbines. Investigation of a number of existing state-of-the-art building augmented wind turbines realised in Norway and abroad was conducted with respect to building design, technologies applied, and resulting energy performance, cost and other significant experiences. The problem is to get good data about wind conditions on and around buildings. Thus pilot installations of vertical axis micro wind turbines were installed and measured on top of a building during the project period of one year.

METHOD

Different measurement devices were used for measuring wind velocity, wind direction, power output and vibration in 5 minute intervals. Since vibration was not considered the vibration measurements were not calibrated. The results were collected by a data logger on the roof and periodically tracked out on a computer. A web-based software that works with the HOBO Remote Monitoring System was used to collect the measured data [4]. The results document discrepancies between the theoretical and the actual performance of the systems, including both system solutions and management.

Figure 1 shows the measurement device installed next to the North facing row of wind turbines. The schematic representation of the whole measurement setup is shown in Figure 2.

Figure 1 – Wind measurement devices [3]

Wind data was also collected from two weather stations nearby. The following parameters were examined:

- Actual local wind speed and direction [4]
- Actual temperature and rain/snow fall
- Actual wind speed and direction at next meteorological station [6]
    - mean wind speed last 10 minutes before observation (FF)
    - highest 10 minute average wind for the last hour (FX_1)
    - maximum gust (3 seconds) last hour (FG_1)

This monitoring campaign allowed to collect and compare wind availability on-site and at two meteorological stations within the city centre [6]. The wind performance was investigated and documented followed by an analysis of the correlation between measured climate data at the installation site and the two nearest meteorological stations (Blindern and Alna). The wind measurements (velocity and direction) were performed continuously for one year. Measurement results from 5 minute intervals were processed; wind direction was vectorised, and summarized to hourly, weekly, monthly and annual data.

Correlations between wind measurements from different sources were calculated.

$$Correl(X,Y) = \frac{\sum (x-\bar{x})(y-\bar{y})}{\sqrt{\sum (x-\bar{x})^2 \sum (y-\bar{y})^2}} \qquad (1)$$

where

X is sample array 1, Y is sample array 2

x and y are the samples, $\bar{x}$ and $\bar{y}$ sample means AVERAGE(array1) and AVERAGE(array2).

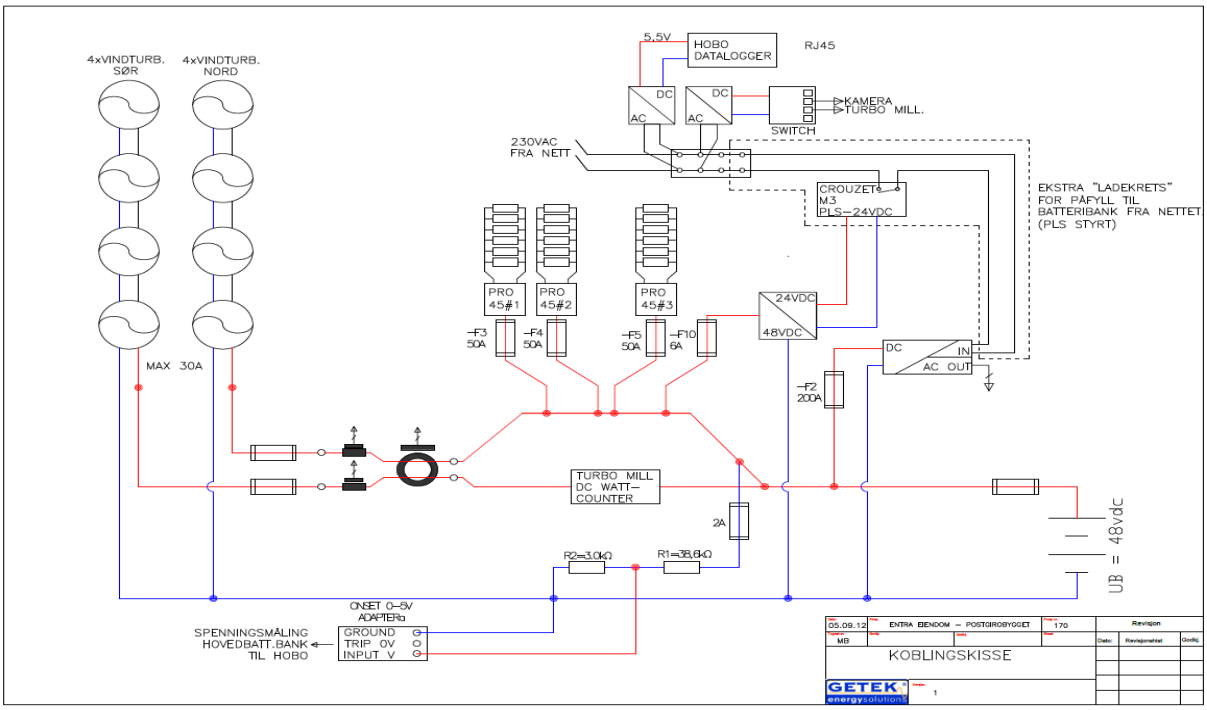

Figure 2 – Monthly wind velocities of different measurement stations [3]

RESULTS

Wind velocity

The results shown in Figure 3 illustrate that wind speed on top of the building was much less than historic data of nearby meteorological stations in Alna and Blindern.

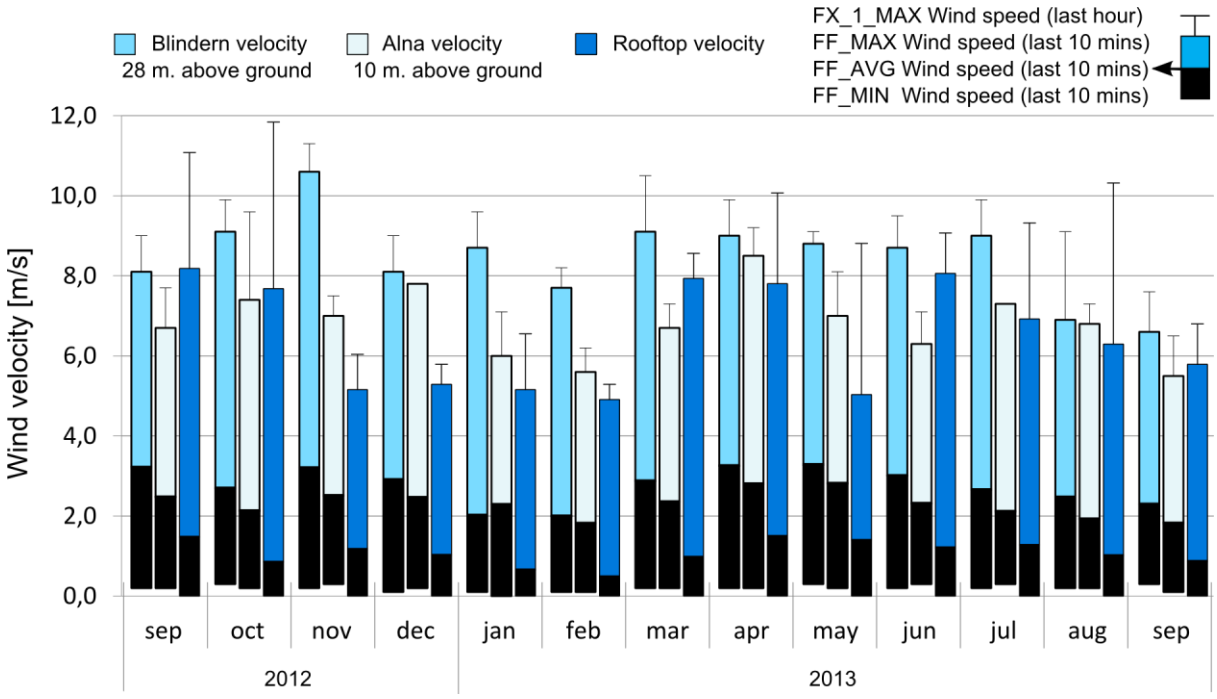

Figure 3 – Monthly wind velocities of different measurement stations

Figure 3 illustrates that mean wind velocity on the roof was much lower than measured at other the stations at Blindern and Alna in Oslo. In average, wind velocities on the roof were only 42% of the average measured at Blindern and Alna.

Wind direction

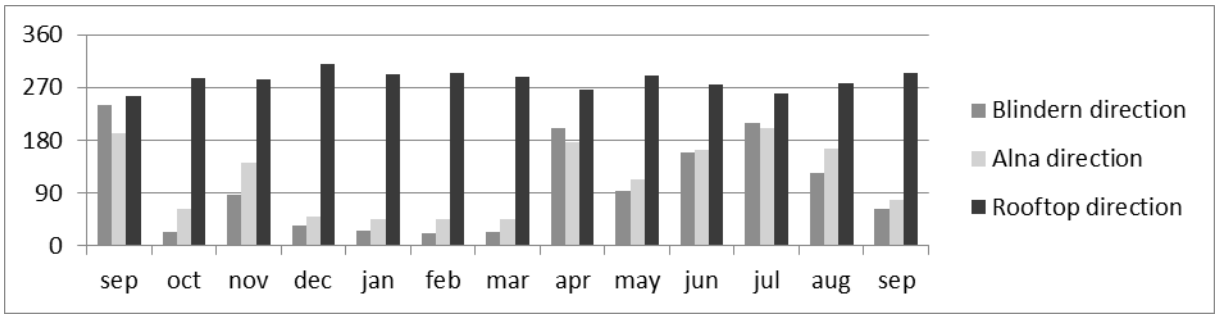

Figure 4 – Monthly wind direction for different measurement stations

Figure 4 illustrates the main wind directions for three different locations in Oslo. Measurements results on the roof of the test building show very different wind directions than those registered at Alna and Blindern weather stations. There were distinct differences in wind direction between summer (April–August) and winter (October–March). This difference in wind direction was not registered by the measured location on the roof of the test building. Here, the prevailing wind direction remained the same throughout the year.

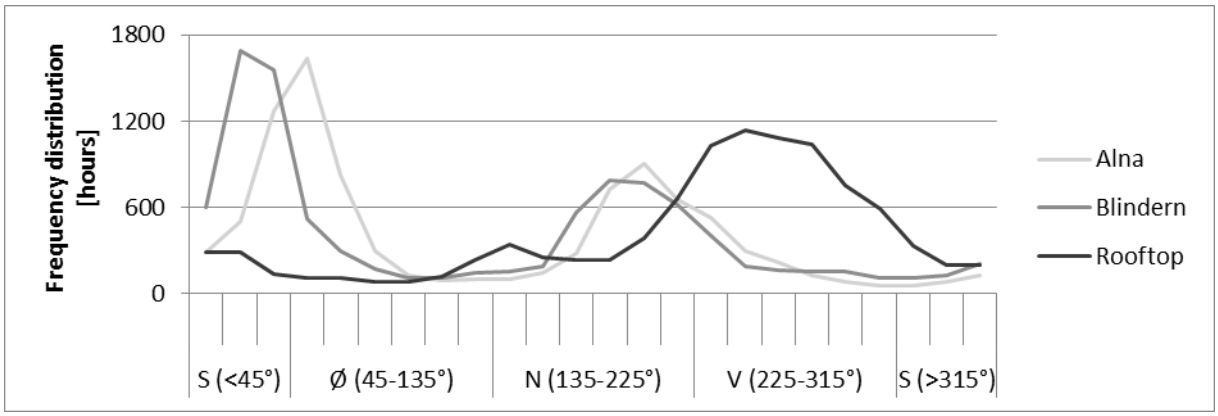

Figure 5 – Annual wind direction for different measurement stations with frequency distribution (year)

It can be seen in Figure 5 (frequency distribution, below) that measured wind directions from the weather stations at Alna and Blindern were dominating from North and North-North-East (30–60'). The measured wind direction on the test building shows dominance from South-West (270 '). This is difficult to explain. One reason for this mismatch could be local «conditioning» and redirection of wind due to the building geometry and the surroundings.

What might have a major impact is turbulence around the building which would lead to higher gut velocities but lower average wind velocities. The different wind directions support the presumption that turbulent wind conditions affect the results.

The measurements of wind velocity and direction were taken in periods from September 2012 to September 2013. Table 1 shows the monthly correlation factors between Alna/Blindern, Blindern/rooftop and Alna/rooftop. It can be seen that correlation between the weather stations is higher than rooftop. Wind gusts have a higher correlation than average wind speed.

date		Alna/Blindern velocity			Blindern/rooftop velocity			Alna/rooftop velocity		
year	month	FF	FX_1	FG_1	FF	FX_1	FG_1	FF	FX_1	FG_1
2012	sep	0.794	0.855	0.875	0.690	0.694	0.843	0.678	0.664	0.866
	oct	0.755	0.805	0.831	0.672	0.692	0.866	0.630	0.677	0.827
	nov	0.737	0.771	0.775	0.742	0.739	0.855	0.714	0.731	0.805
	dec	0.656	0.697	0.766	0.657	0.694	0.768	0.692	0.735	0.822
2013	jan	0.441	0.541	0.657	0.588	0.638	0.744	0.583	0.638	0.788
	feb	0.667	0.733	0.789	0.674	0.713	0.841	0.657	0.711	0.846
	mar	0.714	0.787	0.843	0.665	0.722	0.846	0.674	0.694	0.839
	apr	0.788	0.831	0.863	0.738	0.767	0.883	0.785	0.766	0.875
	may	0.715	0.792	0.844	0.657	0.720	0.845	0.732	0.731	0.821
	jun	0.746	0.815	0.854	0.758	0.715	0.848	0.706	0.719	0.845
	jul	0.769	0.835	0.868	0.709	0.748	0.870	0.664	0.703	0.840
	aug	0.736	0.814	0.837	0.708	0.742	0.861	0.689	0.722	0.833
	sep	0.635	0.741	0.825	0.666	0.693	0.838	0.667	0.697	0.821

Table 1: Monthly correlation coefficients for measurement period. FF is the mean wind speed last 10 minutes before observation. FX_1 is the highest 10 minute average wind for the last hour and FG_1 is maximum gust (3 seconds) last hour.

DISCUSSION

The measurement of wind conditions were continuously monitored between the 4th of September 2012 and end of September 2013. Wind conditions on top of the test building were compared with measured wind data from weather stations nearby. The wind velocity and direction differ greatly from measurements taken at weather stations in Oslo (Blindern and Alna).

Wind conditions were measured at different heights. Alna weather station is measuring 10m above ground, while Blindern is measuring 28m above ground. The rooftop measurements were taken at 89m height. To compare these wind speeds there are some correlation equations where the height and the roughness of the surroundings has to be measured and considered (wind shear power law). This has not been done because the roughness of the surroundings could not be measured. In addition, the test building influenced the local wind conditions so that the wind speed at that height was obstructed and thus lower. The results with such adjustments would lead to lower correlations for the rooftop (since it is much higher than the weather stations).

The roughness of the terrain remains an important parameter as it shows high sensitivity of the wind speed. More detailed measurements are necessary in order to be able to confirm actual roughness of the surroundings (terrain factors). Local wind conditions on top of the high-rise building test building must be greatly influenced by the building and its surroundings. More detailed measurements are necessary in order to be able to explain this.

Measured wind conditions in Oslo (in all three locations) show average wind speeds that are much lower than what is required for electric operation from the wind turbines. The wind turbine product showed good results on the data sheet (power curve). Since these data depend on standard test conditions it is advisable to be careful with transferring them to local situations. It is very important to make local measurements of wind conditions (velocity and

directions) prior to installation. This can help to select wind turbines that fit to the local wind profile.

After a couple of weeks of testing the product failed to function during strong wind gusts. The producer had to retrofit the windmills with a brake unit in order to solve this problem. Unfortunately it turned out to be a long and tedious process to receive these retrofit units. The first units delivered did not fit. This was a major setback in the testing, and it took many months to get the windmills up and running again.

CONCLUSION

Measured wind conditions on the roof of the building were very different from expected wind conditions. The location of the measurement devices and the wind turbines in the case study were not optimized. Much lower wind velocities were measured on the rooftop than at the other measurement stations. Correlations show a 40% lower wind velocity on the roof than at the measurement stations. The equivalent wind speed would be even lower if the height of the wind turbine is considered (in accordance with the wind shear power law). This should be taken into consideration when planning to install wind turbines in the built environment.

Accurate prediction of the wind velocity represents the basis for economic performance and is essential to calculate the electricity output of small and micro wind turbines (MWT). Wind evaluation presents challenges due to the expensive wind measurement tools in urban environments.

The shading and turbulence effect of surrounding obstacles produces inconsistent and unpredictable wind patterns below 30 m. Traditional wind resource maps are rarely available or are inadequate as wind conditions are evaluated at an altitude of 50 m (or 80 m) [1].

The following aspects of the wind resource in the built environment are poorly understood:

- Turbulence and directional variability
- Wakes, eddies, and separation zones
- Three-dimensional wind velocity profile and distribution
- Existing wind resource maps do not translate to the built environment.

As a result, the urgent demand for inexpensive and efficient methods of predicting and collecting local wind data is another key driving factor that requires further development and cost reduction.

REFERENCES

1. As, 2003. Norwegian Wind Atlas. NVE / ENOVA.
2. BLANCH, M. J. 2002. Wind energy technologies for use in the built environment. Wind Engineering, 26, 125-143.
3. Haase, M., Skeie, K.S., Tronstad, T.V., 2014. Building integrated vertical wind turbines: Experiences from the roof of Biskop Gunnerus gate 14 in Oslo. Oslo: SINTEF akademisk forlag (ISBN 978-82-536-1383-3) 59 s. SINTEF Fag(19)
4. HOBO: Remote Monitoring System, http://www.onsetcomp.com/live_systems, Access date: September 2012
5. MERTENS, S., (2006). Wind Energy in the Built Environment - Concentrator Effects of Buildings, PhD thesis, TU Delft.
6. Weather station data from the climate database of the Norwegian Meteorological Institute. http://eklima.met.no/

SUMMER FREE COOLING VENTILATION POTENTIAL OF ROCK-BED HEAT STORAGE

E. Habib

DIAEE – Sapienza Università di Roma, via Eudossiana, 18 - 00184, Rome, Italy

ABSTRACT

In many mild climates, during most part of summer, night-time temperatures are much lower than comfort temperatures. That is the case of most parts of Italy, where monthly mean temperatures in July and August are lower than 28°C. Nonetheless, daytime temperatures are higher, thus air-conditioning is widely used even in buildings with low inner gains, like dwellings.

It is obvious that it would be possible to have free cooling by storing night-time "cold" in order to provide it during daytime. On the other hand, as dwellings are usually occupied during nights, indoor temperature cannot be lowered as much as possible, without limiting comfort. So, rock-bed heat storage will let time shifting of temperature peak. Yet, even though it is not brand new, no design procedure is readily available. Moreover, the heat storage is very bulky so its integration in the architecture is a barrier.

Rock-bed heat storage is numerically simulated in order to figure out its actual behaviour and the relevance of geometrical parameters on its effectiveness. A Schumann two-phase model is used to simulate a free-cooling ventilation system with rock-bed heat storage for a new building, to be built in Pesaro, Italy.

Results show that for time shifting of temperature peak, heat storage volume is relevant rather than its length. This makes it possible to realize low energy demand ventilation systems by reducing pressure drop through the heat storage. Besides, when optimizing system use, its length becomes relevant again.

Keywords: heat storage, rock bed, ventilation, free cooling, dwellings

INTRODUCTION

During summer, in buildings without air conditioning systems, ventilation provides cooling, too. That is the case in many dwellings. Moreover, to accomplish the forthcoming Net Zero Energy Buildings limit, alternative passive cooling systems to traditional air-conditioning should be adopted. Actually, in many mild climates, mean daily outdoor air temperature are lower than comfort temperatures for people with low activity and summer clothes. According to [1], PMV would be lower than 0.5 as long as operating temperature will be lower than 28°C, for 1 met activity with 0.2 m/s air speed at 0.5 clo (common values for residential buildings). Thus, as long as mean daily outdoor air temperature is lower than 28°C, a proper ventilation with adequate heat storage is potentially able to provide cooling. This is close to ASHRAE-55 Standard comfort zone [2].

Much work is being done in the field of thermal energy storage for buildings and many review articles have been published on the subject, as recently reviewed by Heier et al. [3]. Most of the newly proposed techniques focus on the use of PCM either directly embedded in the building or in some system [4].

Moreover, mandatory insulation for envelope of new buildings makes heat transfer through it almost negligible. So cooling load in dwellings is usually low, being due only to internal

gains, occupants' heat and solar radiation through windows. This makes it possible to control ambient temperature by ventilation with 2 h^{-1} air change rates.

The present study focuses on a new residential building currently at design stage, to be built in Pesaro, Italy. It is three levels high, 60 meters long, as sketched in Fig. 1. According to climate data, in July, that is the hottest month, the monthly mean daily average outdoor temperature is 23.2°C, even though the actual maximum temperature is 35°C. As stated above, cooling load is due only to: inner gains, that are evaluated to be 72 Wh/m^2 per day, occupants' heat, equal to 42 Wh/m^2 per day, and solar gain through windows (meanly $1m^2$ per 8 m^2 of floor area), that is equal to 458 Wh/m^2 per day in July. Thus, the daily cooling load is 212 Wh/m^3 per day. The daily cooling potential (DCP) per unit volume from ventilation, for a 2 h^{-1} air change, with 28°C ambient reference temperature, is calculated from typical mean year data by Meteonorm, assuming that ventilation will be off when outdoor temperature is higher than ambient reference temperature, as stated by eq. (1).

$$DCP = \int_{0am}^{12pm} n \cdot c_{p,a} \cdot \rho_a \cdot \max(T_r - T_o, 0) \cdot d\tau \quad (1)$$

where n is air change rate, c_p is specific heat, ρ is density, T is temperature and τ is time, while subscript a is for air, r is for room and o is for outdoor.

DCP is always higher than daily cooling load per unit volume. Thus, ventilation could be adequate for temperature control. Nonetheless, eq. (1) slightly overestimates cooling energy as no lower limitation is set to inlet air temperature.

In order to level inlet temperature, a heat storage could be used. The simplest system is a rock-bed heat storage with one-way continuous ventilation. It could be set in a specifically dedicated basement. Similar systems has been proposed and used in the last decades, but no design tool is readily available in the open literature. Currently, such systems are yet to be investigated, as reported by Brun et al. [5].

In this framework, the present paper aims to study the relevance of the main rock-bed parameters on its performance. Different mass flow rate per unit cross area are evaluated from 0.25 $kg/s \cdot m^2$ to 2 $kg/s \cdot m^2$, and different rock-bed lengths from 5 m to 60 m.

METHOD

The two-phase Schumann's model [6] is used for the rock-bed heat storage. The assumptions of the model are:

- temperature in each storage element T_b is homogeneous and independent of cross-section;
- the arrangement of the rocks is independent of cross section and along the length of the system so that air flow and heat transfer coefficient are homogeneous, too;
- axial heat transfer is negligible as well as through rock-bed envelope.

Figure 1: Sketch of reference building.

Imposing that heat transfer rate of rock phase is equal to air phase, eqs. (2-3) are given:

$$\frac{\partial T_b}{\partial \tau} = \frac{h_v}{(1-\varepsilon)\cdot \rho_b \cdot c_{p,b}}\left(T_a - T_b\right) \tag{2}$$

$$\frac{\partial T_a}{\partial x} = -\frac{h_v}{G \cdot c_{p,a}}\left(T_a - T_b\right) \tag{3}$$

where ε is void fraction, G is mass flow rate per unit cross area, x is abscissa along the rock-bed, subscript b is for rocks, and all other symbols are as stated above. h_v is convection heat transfer coefficient per unit volume given by eq. (4) by Löf and Hawley [7], in which d is rock equivalent diameter:

$$h_v = 651.7 \cdot \left(\frac{G}{d}\right)^{0.7} \tag{4}$$

Equations (2-3) are solved through a control-volume formulation of the finite-difference method. An explicit forward scheme is used for time stepping. The linear equations are readily solved using short enough time step and axial mesh through a specific code in Matlab.

The code is validated against the analytical solution given in [5] with very good agreement with 60 seconds time steps and uniform 0.1 m mesh.

RESULTS AND DISCUSSION

Numerical simulations have been performed for different lengths and mass flow rate per unit cross area in the above stated ranges. 2400 kg/m^3 rock density, 40% void fraction, 5 cm rock equivalent diameter, and 1 kJ/kg·K specific heat of both rock and air has been assumed.

The outlet temperature for two values of mass flow rate and three lengths of rock-bed are plotted in Figs. 2 and 3 together with outdoor air temperature. In the first figure, related to 0.25 kg/s·m^2 time shift between outdoor air temperature peak and rock-bed outflow temperature peak is some hours for 5 m long system, while it is more than a full day for 20 m long and about 4 days for 60 m long rock-bed. On the other hand, in Fig. 3, where temperature values for systems of same length with a four times higher flow rate per unit cross section are plotted, just the 60 m long rock-bed reaches a full day time-shift.

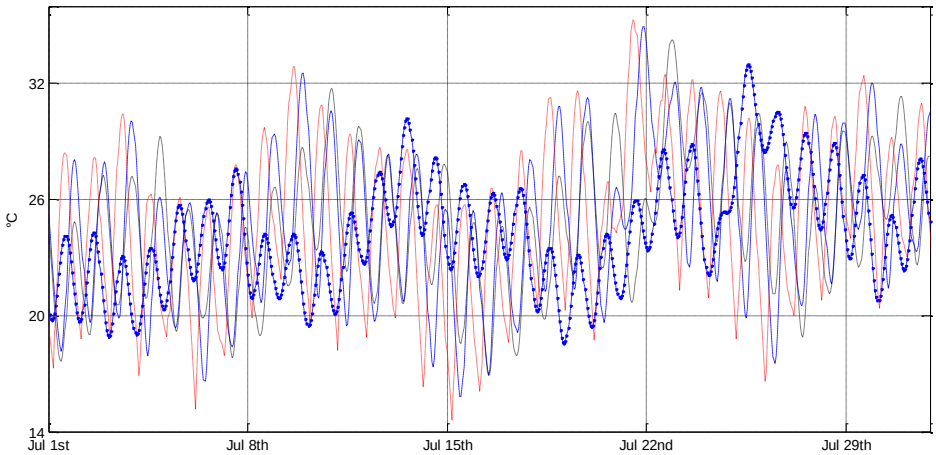

Figure 2: Outflow air temperature with 0.25 kg/s·m^2 for 5 m (blue long-dash), 20 m (black short-dash) and 60 m (blue dot-dash) long rock-bed heat storage and outdoor air temperature (red continuous).

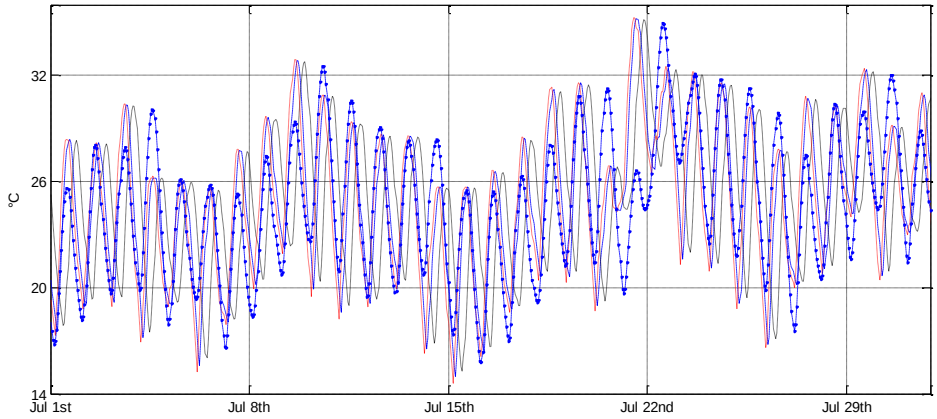

Figure 3: Outflow air temperature with 1 kg/s·m^2 for 5 m (blue long-dash), 20 m (black short-dash) and 60 m (blue dot-dash) long rock-bed heat storage and outdoor air temperature (red continuous).

Actually, at a given flow rate, heat storage volume is proportional to the ratio of system length to its flow rate per unit cross area. Thus, the systems in Fig. 2 have four times the heat storage mass of systems in Fig. 3 with same lengths. Similar plots are provided in Fig. 4 for 10 m^3/(kg/s) heat storage realized with 5 m, 10 m, 20 m and 40 m long rock-bed. It is clearly seen that temperature response of these systems on a 24 hours solicitation is related uniquely to storage mass. Time-shift of temperature peak for all calculated systems has been graphically evaluated and plotted against volume per flow rate, as depicted in Fig. 5, showing a linear correlation, given by eq. (5).

$$Time-shift = 0.4052 \times \mathrm{v}\,[h] \tag{5}$$

To evaluate energy performance of systems, for each bed length and each mass flow rate the daily cooling potential with thermal storage (SCP) have been calculated, using eq. (1) with rock-bed outlet air temperature (T_f) instead of outdoor air and 28°C as room air temperature. Then the ratio of SCP to DCP for each day has been calculated. During summer, outdoor air is often lower than reference temperature, thus, actual hot days has been found in order to make comparisons on actual cooling periods. Therefore, hot days are defined as those days in which outdoor air temperature exceeds reference temperature even for just an hour. The overall effectiveness (Φ) of the heat storage for free cooling is thus the sum of the ratio for each day, divided by the number of hot days, and could be directly found by eq. (6).

$$\Phi = \frac{1}{N_{hotdays}} \sum_{hotdays} \frac{SCP}{DCP} = \frac{1}{N_{hotdays}} \sum_{hotdays} \frac{\int_{0am}^{12pm} \max(T_r - T_f, 0) \cdot d\tau}{\int_{0am}^{12pm} \max(T_r - T_o, 0) \cdot d\tau} \tag{6}$$

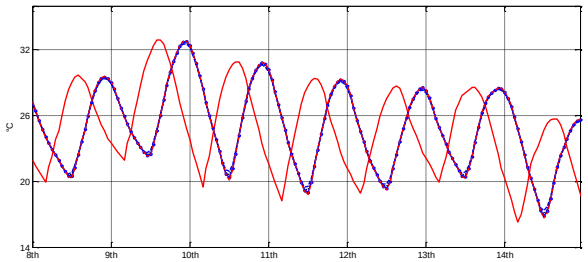

Figure 4: Outflow air temperature with 10 m^3/(kg/s) for 5 m (blue long-dash) and 20 m (blue dot-dash) long rock-bed heat storage and outdoor air temperature (red continuous).

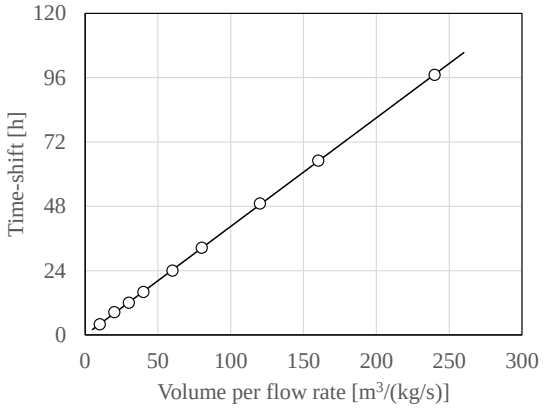

Figure 5: Time-shift of temperature peak vs. System volume per mass flow rate.

Plotting system effectiveness versus system volume per unit mass flow rate shows again a straight correlation, as reported in Fig. 6.

The above stated effectiveness implicitly presumes that ambient supply air will be provided only from the heat storage, that is: ambient cooling will be available only when rock-bed outflow temperature is lower than reference temperature. As the main effect of thermal storage is time shifting of outdoor temperature wave, there will be many periods in which outflow temperature is higher than outdoor temperature. As shown by Brun et al. [5], optimization of heat storage systems for free cooling may provide a significant improvement in its effectiveness. The simplest improvement could be provided presuming that air flow in the heat storage is constant, while ambient ventilation could be provided either by rock-bed outflow or by outdoor air directly, whichever is lower. Therefore, an optimized effectiveness (Φ_o) may be defined as in eq. (7):

$$\Phi_O = \frac{1}{N_{hotdays}} \sum_{hotdays} \frac{\int_{0am}^{12pm} \max(T_r - T_f, T_r - T_o, 0) \cdot d\tau}{\int_{0am}^{12pm} \max(T_r - T_o, 0) \cdot d\tau} \tag{7}$$

Plotting system "optimized effectiveness" versus system volume per unit mass flow rate, as reported in Fig. 7, shows that system length becomes relevant for high heat capacity storage systems but in a non linear way, as 40 m long system performs better than both 60 m and 20 m systems.

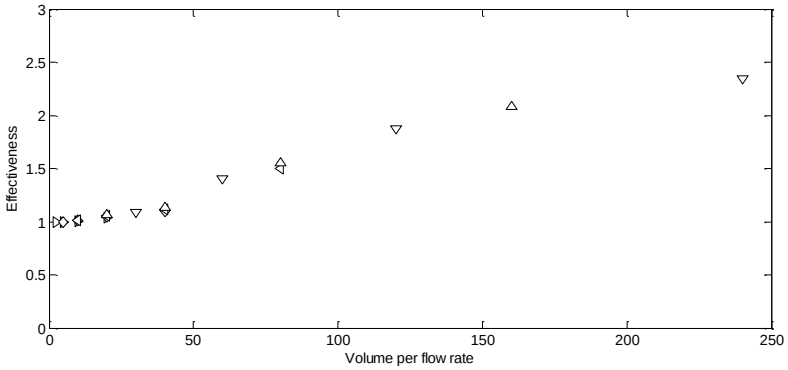

Figure 6: System effectiveness versus system volume per unit mass flow rate.

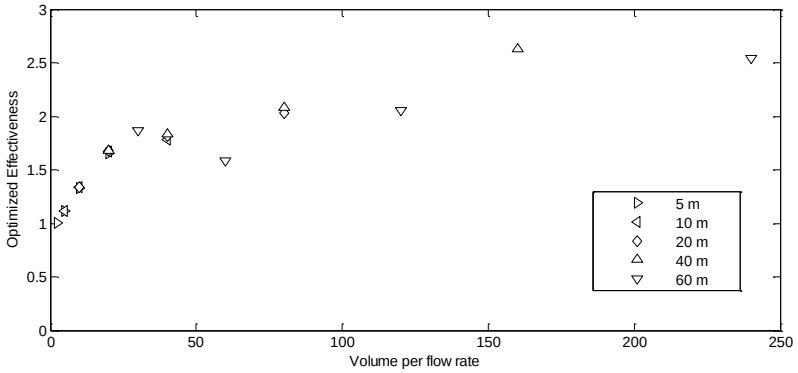

Figure 7: System "optimized effectiveness" versus system volume per unit mass flow rate.

CONCLUSION

The two-phase model of rock-bed heat storage has been numerically solved for dwelling ventilation with typical mean year data for Pesaro, Italy. Results show that such systems could be sufficient for cooling in low inner gain buildings like residential ones.

Time-shift of temperature peak is related to heat storage volume per unit mass flow rate and the correlating equation is given. In order to provide a time-shift of 12 hours (that is night-day temperature inversion of supply air for ventilation), 30 m^3 systems per unit mass flow rate would be needed with set parameters. Even though these results has been figured out from a specific climate, they are properly applicable to almost any other climate as they depend only on main solicitation period, that is always 24 hours.

The system will be effective in increasing daily cooling potential of outdoor air. When optimizing free cooling, system length becomes relevant. As system length is straight correlated to energy demand of fan, optimizing the system requires further research.

REFERENCES

1. EN ISO 7730: Moderate thermal environments - Determination of the PMV and PPD indices and specification of the conditions for thermal comfort, CEN, Bruxelles, 1994
2. ASHRAE: Thermal Environment Conditions for Human Occupancy, American Society of Heating Refrigerating and Air-conditioning Engineers, Atlanta, 2004.
3. Heier J., Bales C., Martin V.: Combining thermal energy storage with buildings – a review. Renewable and Sustainable Energy Reviews, pp 1305-1325, 42, 2015.
4. Sajjadian S. M., Lewis J., Sharples S.: The potential of phase change materials to reduce domestic cooling energy loads for current and future UK climates. Energy and Buildings, pp 83-89, 93, 2015.
5. Brun A., Wurtz E., Hollmuller P., Quenard D.: Summer comfort in a low-inertia building with a new free-cooling system. Applied Energy, pp 338-349, 112, 2013.
6. Schumann T.: Heat transfer: a liquid flowing through a porous prism. J Franklin Inst, pp 405-416, 208 (3), 1929.
7. Löf G.O.G., Hawley R.W.: Unsteady-State Heat Transfer between Air and Loose Solids, Industrial and Engineering chemistry, pp 1061-1070, 1948.

2ND YEAR MONITORING SFH SULZER

D.H. Diego Hangartner[1]; M.S. Matthias Sulzer[1]

1: Zentrum für Integrale Gebäudetechnik (ZIG), Technikumstrasse 21 CH-6048 Horw.

ABSTRACT

The single family house (SFH) Sulzer in Schaffhausen has been retrofitted over a period of three years, starting in 2010 with the improvement of the facade insulation and later on by integrating two photovoltaic systems on the roof and a solar hybrid system at the facade. In 2012, the existing gas burner was replaced by a gas driven solid oxide fuel cell unit which produces in addition to heat also electricity. A 1000 litre storage tank enables to buffer heat loads produced from the fuel cell unit. Since the fuel cell unit took up operation in October 2012, all energy flows in the house (electricity consumption, electricity production and heating energy consumption) have been measured on a 15 minute interval basis.

The evaluation of the first year monitored (1rst November 2012 until 31rst October 2013) shows that the scope of reaching a plus primary energy balance over the year could not be achieved, due to the low solar gains and the suboptimal operation of the fuel cell unit [1]. The necessary adjustments were made for the second year monitored (1rst January until 31rst December 2014), and a positive primary energy balance could be reached.

The monitoring of the house not only aims at demonstrating a low primary energy consumption and low greenhouse gas emissions, but also at analysing how the new system affects the electricity grid and compare it with alternative heating systems such as heat pumps. In fact, fuel cells especially relieve the electrical grid during winter season, when the grid overall load is at high level.

In the coming years, the aim of the project is to further develop the internal energy system of the house in order to meet requirements of the local electrical and gas grid, without losses of user comfort. For this purpose, a power storage device will be integrated in addition to the thermal storage tank to regulate the demand from and supply into the electrical grid. According to the daily forecasting of the system services of the electricity grid, the time flexibility between production and consumption (storage) shall be used to meet the grid's requirements. On a small scale, the single family house Sulzer demonstrates a first pilot energy hub.

Keywords: monitoring, plus energy house, load management

INTRODUCTION

The SFH Sulzer located in Schaffhausen, Fernsichtstrasse 20, was constructed in the 1930s. The house was enlarged in the 1970s in its southern part and presents nowadays an overall energy reference area of about 250 m^2. The SFH Sulzer has been retrofitted over the last few years according to the following steps:

1. Increase of the passive solar gains and retrofit of the envelope.

First, the windows facing south-east were enlarged in order to enhance the passive solar gains. Double-glazed windows were replaced by enlarged triple-glazed windows. Thereafter, the newer annex and the basement were insulated and the thermal bridges between the annex and original part of the building were removed. Finally, due to physical constraints, a curtain-type façade was added to the original part of the building to improve the u-value. The u-values of the walls are less than 0.15 W/m^2K and the u-value of the roof is less than 0.12 W/m^2K.

2. Integration of active solar energy systems (thermal and electrical)

A photovoltaic system (5.6 kWp, el), oriented south-east on the roof, and a hybrid solar system (2.4 kWp, el) at the south facade were installed. The two different orientations and inclinations of the solar plants generate diverse production profiles, enabling a maximum of direct use of the produced electricity. Throughout the use of solar energy, the house does not only play the role as a consumer but also as a producer - hence, the building evolves to a 'prosumer'.

3. Substitution of the heating system

The old condensing gas heater and boiler installed in 1990 were replaced by a solid oxide fuel cell unit. Fuel cell heating systems produce heat and electricity by means of a chemical reaction between hydrogen, gained from natural gas and oxygen. The fuel cells cover a base load (1 kW electrical and 2 kW thermal energy) whereas the supplement burner (4- 19 kW heat power) covers the thermal peak load.

Figure 1: SFH Sulzer before the retrofit (left) and after the retrofit (right).

All energy flows (electricity consumption, electricity production and heating energy consumption) were measured on a 15 minute interval basis in the house, since the fuel cell unit started its operation at the beginning of October 2012. The aim of the monitoring was to identify energy saving potentials and to improve the overall efficiency of the house. Furthermore, the designed energy system "fuel cells and solar systems" (FC & Solar) shall be benchmarked with alternative systems; a conventional gas burner with an overall efficiency 0.95 (GB & Solar) and a heat pump system with a coefficient of performance of 2.5 or 4.5 (HP & Solar COP 2.5 – 4.5)[1]. Primary energy consumption and greenhouse gas emissions were evaluated for all systems. The monitoring of the house not only aims at demonstrating a low environmental impact but also at showing how the different technologies affect the electricity grid in terms of peaks loads.

METHOD

Monitoring of the 1st year

The measured energy flows of the 1st year monitored (1st November 2012 until 31st October 2013) were documented and compared with the projected values. The monitoring of the 1st year was used to optimise the energy system and hence improve the operation of the 2nd year. The following statements show the three most important points during the 1st year monitored:

[1] *The range of COP chosen represents the options of heat pumps from air-to-water up to ground-to-water heat pumps [2].*

- The SFH Sulzer could not reach a plus primary energy balance.
- The electrical efficiency of the fuel cell dropped within the first year.
- The production of the hybrid collectors were considerably below the projected values.

Monitoring of the 2nd year

After analysing the results of the 1st year, the following measures for the 2nd year were proposed and implemented:

- The fuel cell unit was replaced by a more powerful unit.
- Once the fuel cells started, their modulation was limited to a 50 – 100% load in order to avoid the negative effects of the intermittent switch-on/off.
- The fuel cells had to operate as long as possible on a maximum load in order to reach maximum efficiency.
- The conflict between the usage of the fuel cell's waste heat and the thermal energy production of the hybrid solar system during the summer season had to be solved by a more effective energy management.

The optimisation measures mentioned above lead to an improvement of the overall energy balance and environmental impact.

RESULTS

Net energy consumption

Before the retrofit, the energy consumption of the SFH Sulzer was around 40'000 kWh/a (160 kWh/m^{2}a), according to the invoices of the local energy supply company [3]. After the retrofit of the building envelope, as a first step, the energy consumption could be cut in half (-49%). Electricity consumption remained constant over the last years at around 2'750 kWh/a (11 kWh/m^{2}a), see figure 2. The net energy demand was still covered by the gas heater and electricity from the grid.

The second retrofit step was to substitute the heat burner by a fuel cell and to integrate solar systems into the building's envelopes. The heat demand could be covered by the fuel cell unit and a smaller part by the hybrid collectors. The produced electricity by the fuel cells and solar systems exceed the consumption by far (460% of the consumption). The excess electricity is supplied into the grid. The gas consumption was reduced by 48%, despite the fuel cells' production of electricity. Due to the operational optimisation, additional 7% reduction of the energy consumption could be achieved in the 2nd year. The new replaced fuel cell unit could reduce gas consumption by 18% compared to the 1st year, due to the higher unit efficiency and the more effective energy management.

Final and primary energy consumption

The final and primary energy consumption of the 2nd year monitored is showed in figure 3. The primary energy consumption was evaluated both according to the Swiss and according to the European electricity mix [4] in order to differentiate the statements of the results.

Gas is mainly used in winter for space heating, hot water and electrical production, whereas in summer, hot water is partly produced with gas and thermal solar energy. The electricity supplied to the grid is fairly constant over the year. The summer peak of supplied solar energy could be flattened out. According to the Swiss electricity mix, the building consumes more primary energy than it produces (+ 1'745 kWh/a, +7 kWh/m^{2}a)). However, the building produces more primary energy than it consumes (-2'313 kWh/a, -9 kWh/m^{2}a) according to the European electricity mix.

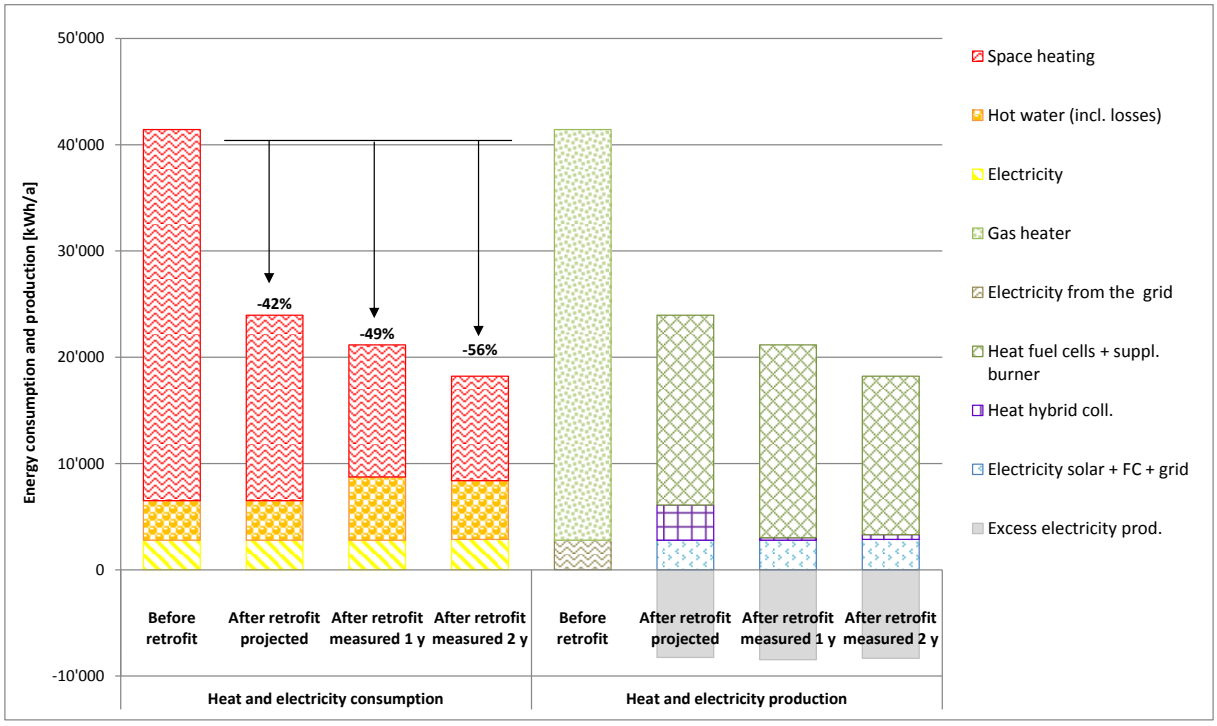

Figure 2: Net energy consumption and production before the retrofit of the house, the projected energy consumption after the retrofit and the measured energy consumption and production of the house after the 1st and 2nd year monitored.

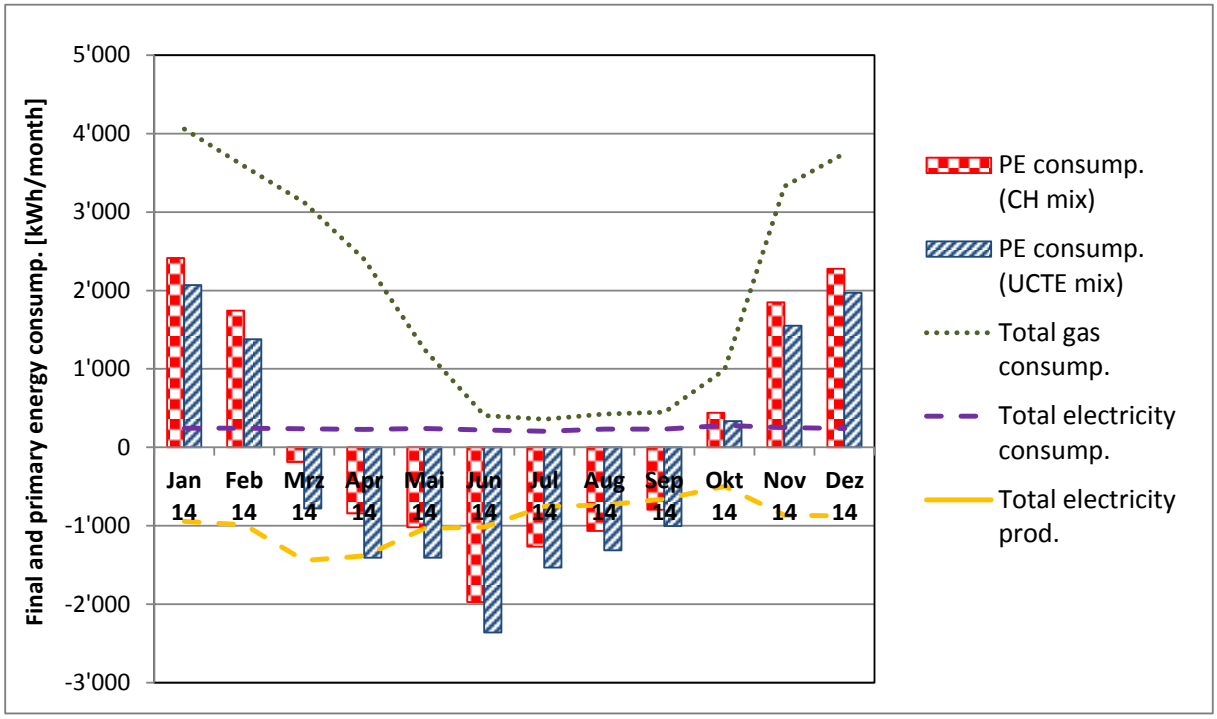

Figure 3: Final (lines) and primary (bars) energy consumption of the SFH Sulzer in the second year monitored.

Comparison: FC & Solar, GB & Solar, HP & Solar (COP 2.5 – 4.5)

The yearly primary energy consumption and greenhouse gas emissions were assessed for the four defined heating systems,: Fuel cell unit and solar systems[2] (FC & Solar), conventional gas unit and solar systems (GB & Solar) and heat pump unit and solar systems (HP & Solar (COP 2.5 – 4.5)), see Figure 4.

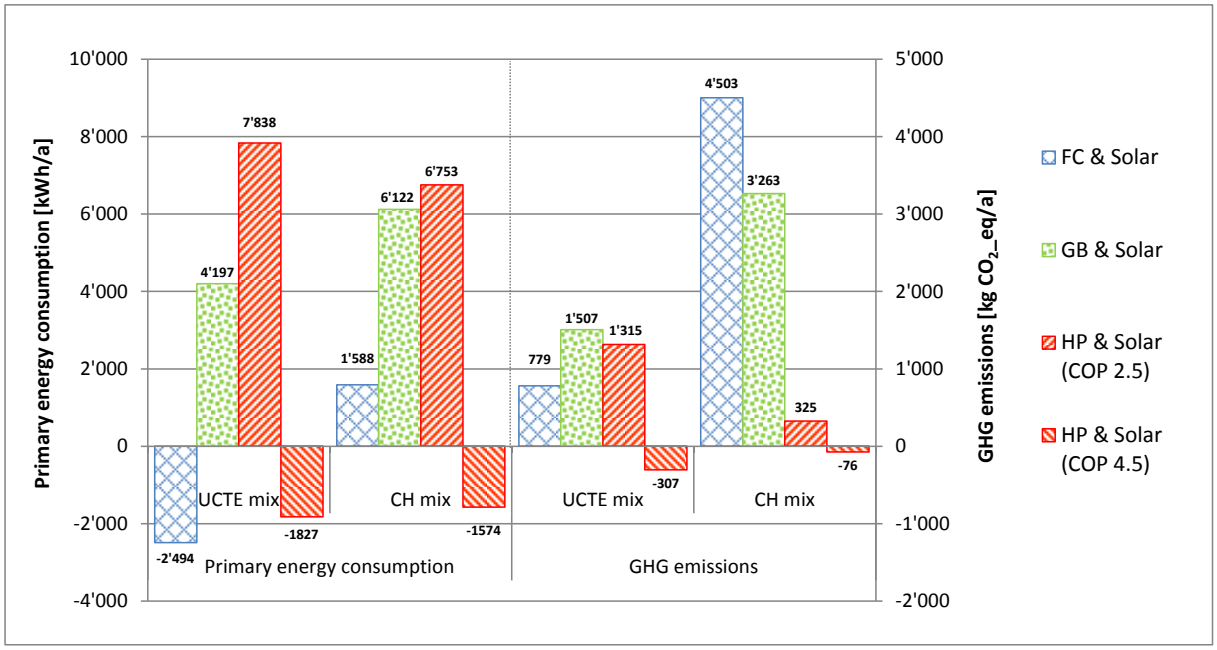

Figure 4: Comparison of different heating systems FC & Solar, GB & Solar and HP & Solar (COP 2.5 – 4.5) for the second year monitored.

The analysis of the different heating systems shows that the impact of the applied environmental factors according to the energy mix is tremendous and influences the statements essentially. According to the European electricity mix, the FC & Solar alternative presents the best option in regards to primary energy consumption and reaches the second best result on GHG emissions. The fuel cells show a low primary energy balance in the Swiss context but high greenhouse gas emissions compared to the other alternatives.

Electricity network load

The building's electrical load profile is characterised by a base load production during the heating season and solar peaks all year long. About 60% of the electricity consumption (1'800 kWh/a out of 3'000 kWh/a) is directly covered by the decentralised power units and 40% is covered by the grid. On the other hand, the grid load profile of a heat pump and solar systems (HP & Solar) is characterised by high electrical peaks during the winter season (heat pumps) and high peaks during the summer (photovoltaic). Assuming the two concepts (FC & Solar and HP & Solar) are combined in a neighbourhood, the electricity grid will benefit from a peak shaving induced by the two houses' concepts. Figure 5 shows the calculated electrical load profile of the combined concepts and indicates the possible peak reduction.

The analysis shows that the combination of the two heating systems possibly reduces the demand peak by 44% and the supply peak by 15%, compared to a sole concept.

[2] The considered solar systems remain exactly the same among the compared heating systems

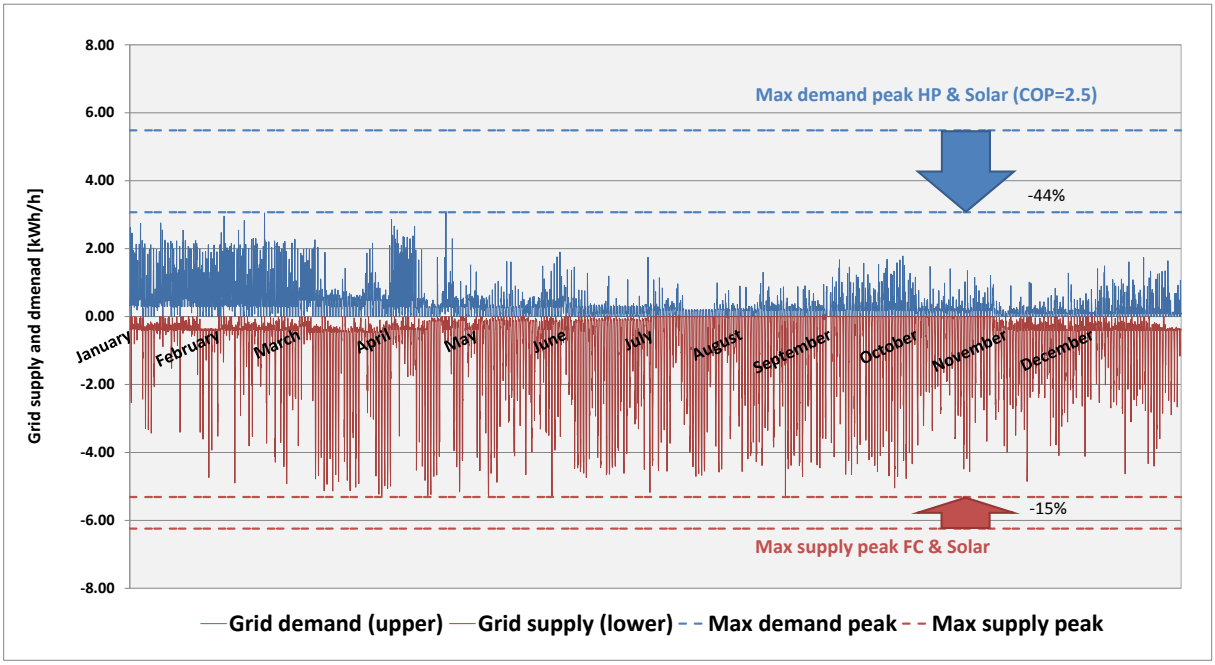

Figure 5: Grid demand (blue) and grid supply (red) of the combination: FC & Solar and HP & Solar (COP = 2.5).

DISCUSSION

The analysis of the 2nd year monitored showed the positive impact of an operational optimisation. The results are satisfying since a negative primary energy balance (considering UCTE electrical mix) could be reached for the retrofitted building. The replacement of the fuel cell unit along with its higher efficiency and more effective energy management were the key measures. This project shows once more the importance of monitoring sophisticated solutions in order to reach the planned and promised goals.

After more than two years of monitoring the building, there are still research questions left unanswered for an effective operation of fuel cells. First of all the environmental impact assessment should be calculated by hourly, daily or monthly factors, according to the current energy mix supplied by the grid. Secondly, buildings shall not only reach a low environmental impact but also be automated to serve the requirements (supply and demand management) of the gas and/or the electricity grid without losses of the user comfort. For further research, a battery pack will be installed in the house in addition to the thermal storage. The building's energy flexibility shall be analysed regarding real technical, economic and ecological benefits, on hourly, daily or monthly basis. The building will be further developed to a small scale energy hub and hence prove such concepts which could be scaled up for quarters and areas.

ACKNOWLEDGEMENTS

This work has been accomplished in the Efficient Buildings & Districts SCCER FEEB&D, funded by The Commission for Technology and Innovation of the Swiss Confederation.

REFERENCES

1. Hangartner, D.: Monitoring EFH Sulzer, Jahresbericht 2012-2013, December 2013
2. Milelli, A.: www.energie.ch/heizungsvergleich, June 2010
3. Sulzer, M.: Einfamilienhaus Sulzer, Schaffhausen – Transformation eines Altbaus in ein Plusenergiehaus, Lauber IWISA AG, Naters, June 2012
4. Frischknecht R.: Primärenergiefaktoren von Energiesystemen, ESU-Services, April 2011

PLUSQUA

D.H. Diego Hangartner[1]; S.B. Stefan Brücker[1]

1: Zentrum für Integrale Gebäudetechnik (ZIG), Technikumstrasse 21 CH-6048 Horw.

ABSTRACT

Buildings in an urban context can hardly achieve positive primary energy balances throughout a year due to the relative high density in the neighbourhood: ratio roof area to floor area (low active use of solar energy) and shading through other buildings (low passive use of solar energy). Depending on their location, plus energy buildings are not even desirable, since they unnecessarily stress the electricity grid [1]. For this reason, renovations on individual buildings shall be assessed in an overall concept at neighbourhood scale, expanding thus the considered system boundary. The aim of the project is to evaluate the additional benefit for the neighbourhood compared to a single house for specific typological, user-specific and technical interventions in terms of maximal thermal and electrical loads.
A typical Swiss urban neighbourhood [2] with a representative utilisation mix has been chosen in Cham in the canton of Zug to analyse the change of its thermal and electrical loads for different scenarios.

- **Networking:** Potential of connecting buildings electrically and thermally.
- **Utilisation mix:** Substitution of 20% and 50% office buildings into residential buildings.
- **Densification:** Increase of 20% and 50% space heating area in the neighbourhood.
- **Efficiency (Renovation):** Renovation of 20% and 50% of the actual building stock.
- **Decentralised production:** Impact of 0% up to 100% roof coverage of photovoltaics and impact of combined heat and power technology.
- **Storage:** Benefit of a daily and monthly thermal or electrical storage.

The scenarios were not set equally in relation with their economic investment, but according to their technical feasibility. The criteria used to define the additional benefits of each scenario were 1) the highest yearly average daily load, 2) the ratio between daily maximum load and daily mean load and 3) the difference between energy demand and energy supply.

The results show that the measures that reduce thermal loads the most are the renovation of 50% of the building stock. In order to reach the energy goals of the SIA 2040, additionally a substitution of the present fossil heating systems is required. If the present heating system based on fossil fuels would be substituted to 100% by heat pumps, the grid loads of the neighbourhood would be increased by at least 34%. Decentralised electricity production of photovoltaics does not additionally stress the transmission lines, although adjustments in the transformation stations would need to be made. Without demand side management, the electricity production from photovoltaic only reduces the grid demand peaks up to a certain point (≈40% of the roof area covered by PV ≈ 50’000 m^2).

The results show that the technical measures clearly have most impact on the peak load reduction, but due to their high costs, resulting in the present low retrofit rates, spatial planning measures present a good option to help mitigate thermal and electrical loads without major effort.

Keywords: Energy strategies at neighbourhood scale, transformation building stock

INTRODUCTION

Buildings in an urban context can hardly achieve positive energy balances throughout a year due to the relative high density in the neighbourhood: ratio roof area to floor area (low active use of solar energy) and shading through other buildings (low passive use of solar energy). Depending on their location, plus energy buildings are not even desirable, since they unnecessarily stress the electricity grid. For this reason, renovations on individual buildings shall be assessed in an overall concept at neighbourhood scale, expanding thus the considered system boundary.

The aim of the project is to evaluate the additional benefit of the neighbourhood compared to a single house for specific typological, user-specific and technical interventions.

METHOD

Choice of the neighbourhood

The following requisites were set in order to define the typical neighbourhood of the suburban agglomeration of Switzerland:

- Frequent typology in urban areas
- High share of residential buildings with a retrofit potential
- Potential to change the utilisation mix in the neighbourhood or in the surrounding area.
- Potential for densification of the neighbourhood.

After analysing more than 10 neighbourhoods, "Cham Ost" near Zug has been chosen (Figure 1).

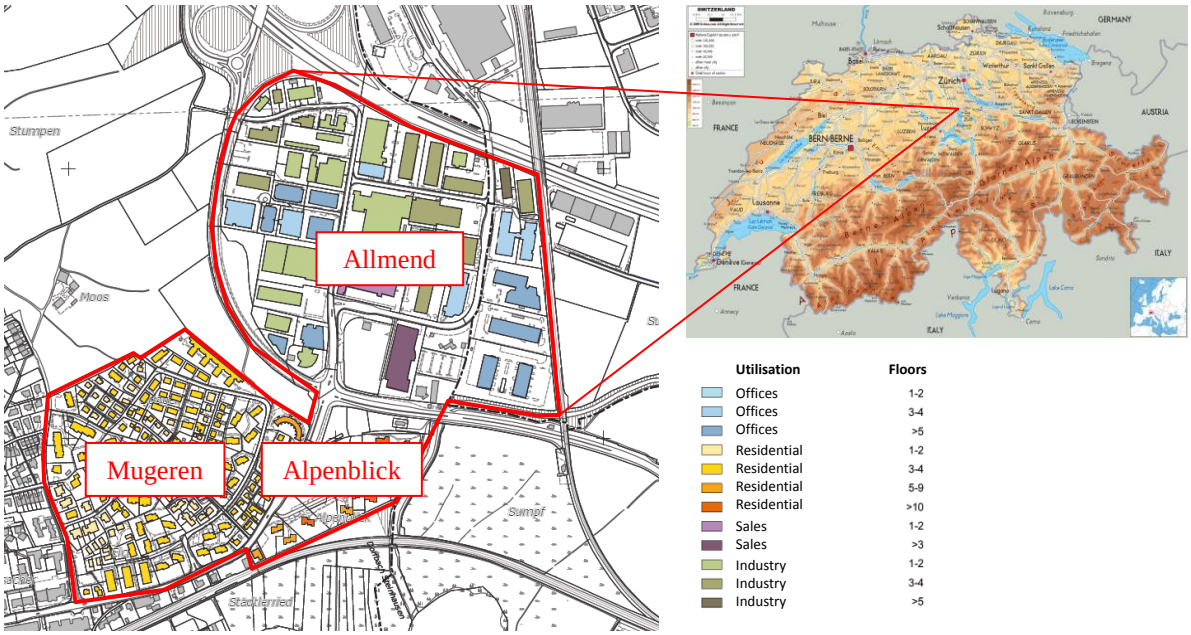

Figure 1: Neighbourhood "Cham Ost" near the city of Zug divided into three subareas, Allmend (offices, sales and industry), Mugeren (residential buildings) and Alpenblick (high-rise buildings).

Criteria for the evaluation

The criteria used to define the additional benefits of the intervention measures were 1) the highest yearly average daily load, 2) the ratio between daily maximum load and daily mean load and 3) the difference between energy demand and energy supply (Figure 2).

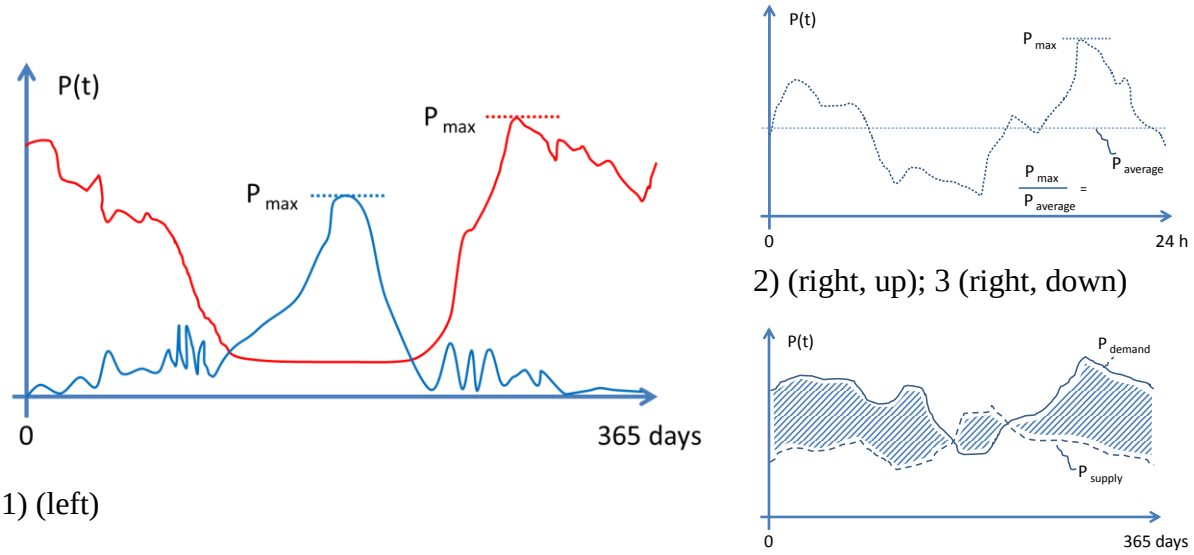

Figure 2: Criteria for the evaluation of the scenarios in the neighbourhood.

Thermal and electrical loads of the neighbourhood "Cham Ost"

The thermal loads of the neighbourhood were determined by means of thermal simulations in IDA-ICE. 16 representative buildings were chosen, modelled and simulated to reproduce the entire neighbourhood. The electrical loads of the neighbourhood were assessed by using measured data on buildings of the same type in the same region. The profiles were then proportionally summed up accordingly to their surface share in the neighbourhood.

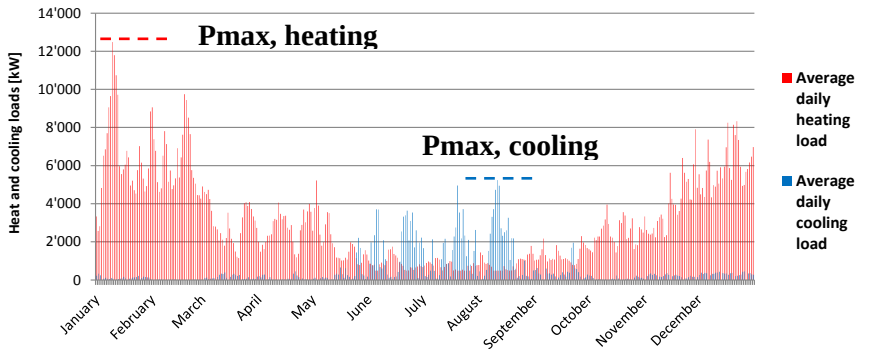

Pmax, heating

12.5 MW

Pmax, cooling

5.2 MW

Heating / Cooling demand

25.8 / 3.5 GWh

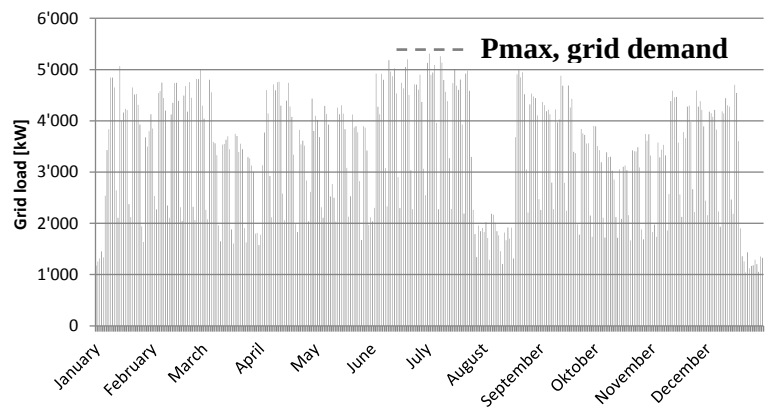

Pmax, grid demand

5.3 MW

Pmax, grid supply

0 MW

Grid demand / supply

27.7 / 0 GWh

Figure 3: Thermal loads of the neighbourhood "Cham Ost" (upper graph) and electrical loads (lower graph) of the neighbourhood "Cham Ost".

Scenarios

Different scenarios were analysed in order to assess their potential according to the defined criteria. The scenarios were not set equally in relation with their economic investment, but according to their technical feasibility in the neighbourhood.

- **Networking:** Potential of connecting buildings electrically and thermally.
- **Utilisation mix:** Substitution of 20% and 50% office buildings into residential buildings.
- **Densification:** Increase of 20% and 50% space heating area in the neighbourhood.
- **Efficiency (Renovation):** Renovation of 20% and 50% of the actual building stock.
- **Decentralised production:** Impact of 0% up to 100% roof coverage of photovoltaics and combined heat and power technology.
- **Storage:** Benefit of a daily and monthly thermal or electrical storage.

RESULTS

The most important results are briefly presented for two scenarios, efficiency and decentralised production of photovoltaic panels.

Efficiency (Renovation)

The results show that in order to reach the goals of the SIA 2040 (target value for operation), 50% of the building stock shall be renovated to actual standard and 100% of the fossil fuel heating system shall be replaced by heat pumps with a yearly COP of at least 3.5 (Figure 5).

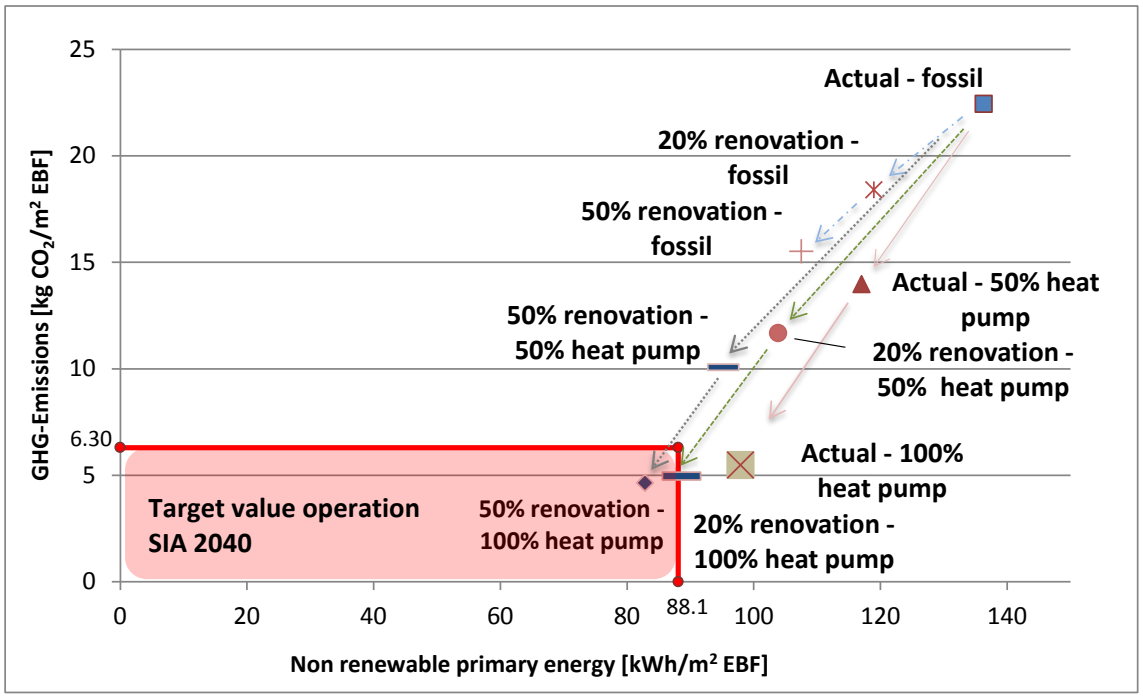

Figure 5: Renovation strategies on buildings for the neighbourhood and environmental impact according to SIA 2040 (target value in operation).

Photovoltaic production

The results show that even if 100% of the roof surface of the whole neighbourhood is covered by photovoltaic panels, the transmission lines not additionally stressed, i.e. the maximum grid

supply load does not exceed the maximum grid demand load. Without demand side management, decentralised production of electricity can only reduce up to certain percentage roof coverage (40% of the roof area = about 50'000 m^2) the grid demand peak.

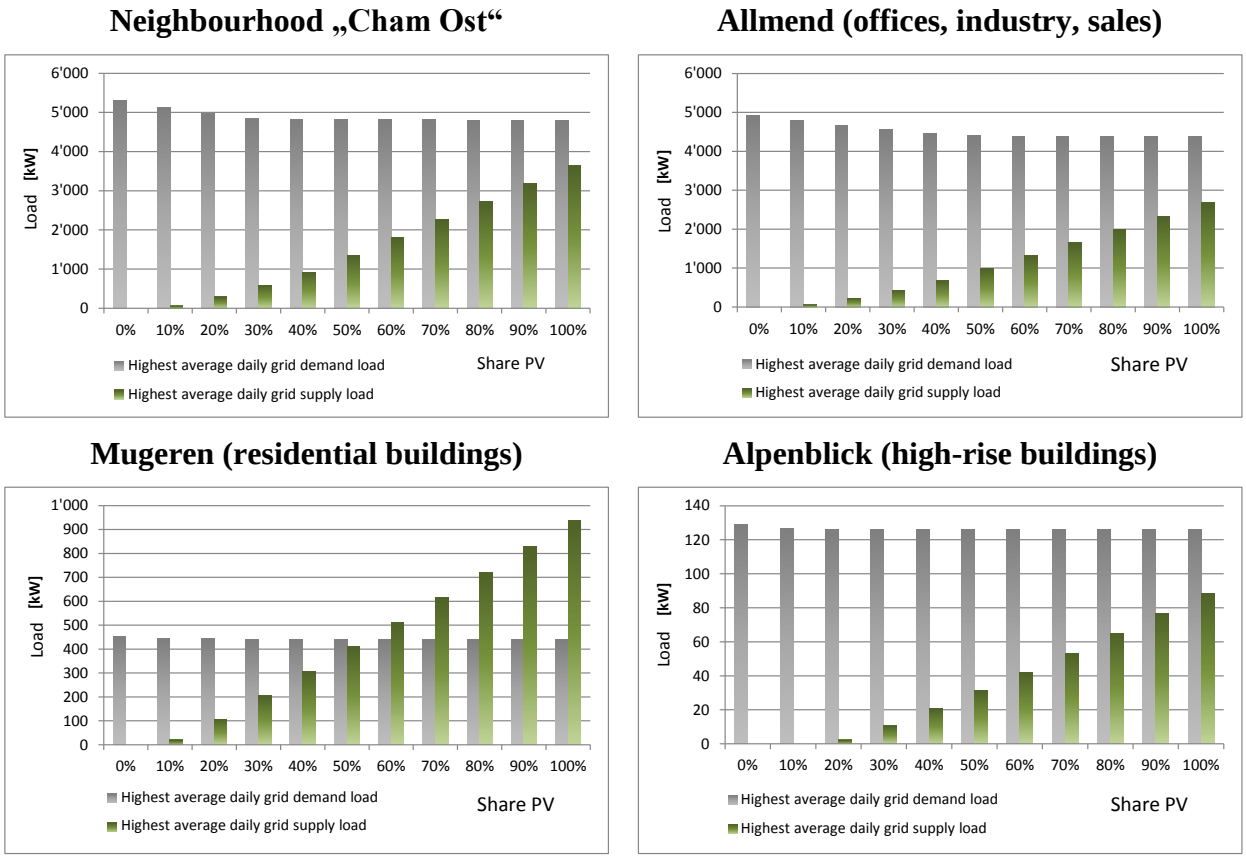

Figure 4: Maximum grid demand (grey) and grid supply peak from PV (green) of the whole neighbourhood and the three subareas when 0% up to 100% of the roof surface is covered by photovoltaics.

Summary of the scenarios

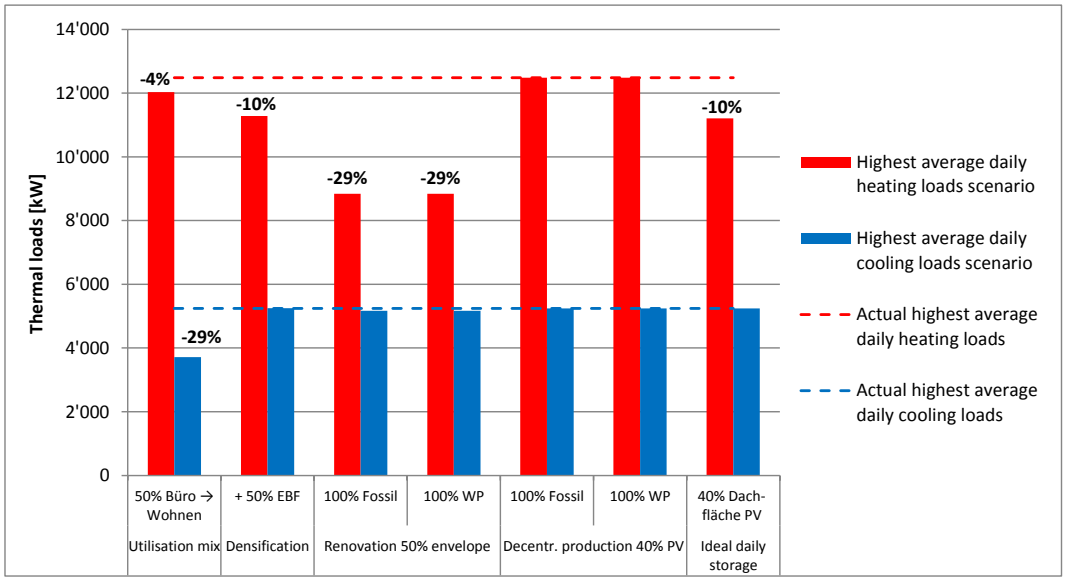

Figure 7: Highest daily average during the year of the thermal loads of the different scenarios (histograms) compared to the actual state (dashed line) by the same surface.

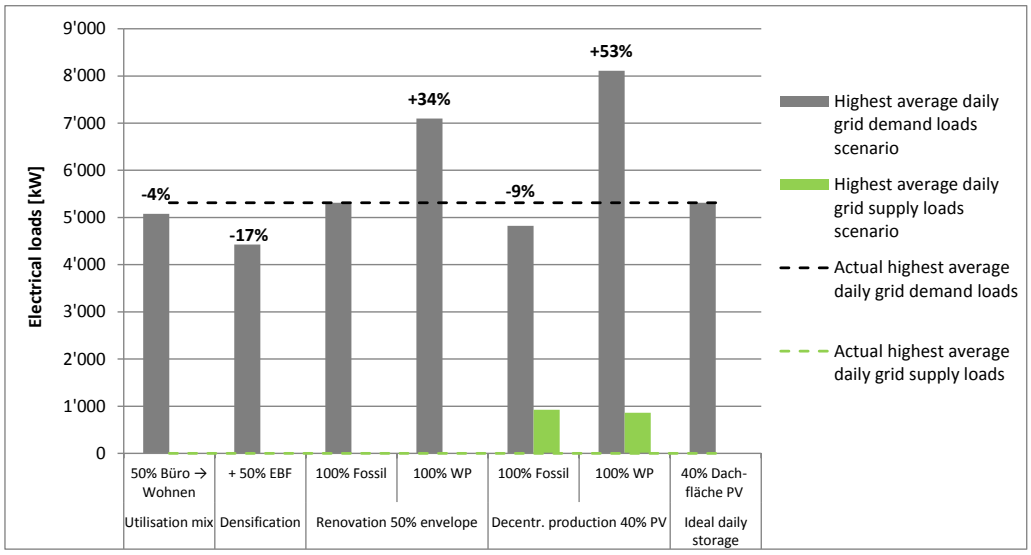

Figure 6: Highest daily average during the year of the electrical loads of the different scenarios (histograms) compared to the actual state (dashed line) by the same surface.

The scenario that has most impact on the thermal loads, without increasing the cooling loads, is the renovation of 50% of the building stock in the area. The conversion of offices into residential buildings reduces both heat and cooling loads, since residential buildings carry a higher specific storage mass than offices. If all internal waste heat would be reused for heat purposes on site, final energy demand could be reduced by 3.5 GWh and maximum heat loads can be reduced by around 10%. Densification of the neighbourhood with residential and office buildings reduces the specific electric loads of the neighbourhood, since the present specific electricity demand due to industry is high. Decentralised production of photovoltaic reduced down to 9% the grid demand peak, while increasing the grid supply. The substitution of fossil fuels with heat pumps increases grid demand load by 34% resp. 53%, according to the renovation state.

DISCUSSION

The peak loads engendered by the use of heat pumps shall be considered as a major issue for the future electricity network capacity and shall be diminished as much as possible, for example by means of demand side management or with the use of high efficient heat pumps. The neighbourhood “Cham Ost” has nowadays an insignificant share of electricity production by photovoltaics. Electricity production by photovoltaic does not present any capacity problems for transmission lines. The only issue of electricity produced by photovoltaic is how to feed back the excess electricity back into the grid’s next level. This can be handled by integrating storage devices or reactive power compensation elements in the local transformation stations. The overall results show that the technical measures on individual buildings clearly have most impact on peak load reduction, but due to their high costs, resulting in the present low retrofit rates, spatial planning measures still present a good option to help mitigate thermal and electrical loads without major effort.

REFERENCES

1. Bucher, C.: Wie viel Solarstrom verträgt das Niederspannungsnetz? Resultate aus hochauflösenden Lastflusssimulationen. Technologie Smart Grid, S. 4., März 2014
2. Göbel V., K. F. (2012). Raum mit städtischem Charakter - Erläuterungsbericht 2012. Neuchâtel: Bundesamt für Statistik (BFS).

ENERGY HARVESTING AND PASSIVE COOLING: A NEW BIPV PERSPECTIVE OPENED BY WHITE SOLAR MODULES

P. Heinstein[1]; L.-E. Perret-Aebi[1] ; J. Escarré Palou[1] ; G. Cattaneo[1] ; H.-Y. Li[1] ;
V. Mussolino[1] ; L. Sansonnens[1] ; C. Ballif[1].

1 : *CSEM PV-Center, Jaquet-Droz 1, 2000 Neuchâtel, Switzerland.*

ABSTRACT

CSEM has developed homogenous white and colored solar panels with conversion efficiencies from above 10% to 15%. This innovative technology is particularly attractive for the building industry as PV elements can blend into any building skin and become a virtually invisible energy source. Aside from completely new possibilities in the design and rendering of active PV façades of any shape and size, notably white PV offers another important feature as a mere side effect: through the reflection of most of the visible spectrum of light the white solar surface will be at a lower temperature than the similar black standard module and therefore improve passive cooling. First tests of outdoor monitoring have shown very promising results and could globally lead to important savings in air-conditioning costs.

Keywords: Photovoltaics, BIPV, architecture, façades

INTRODUCTION

The constant call for colors to stimulate the ambitious market of BIPV products has had no important impact so far [1]. Discussed for more than 25 years, colored photovoltaics cannot yet find its way out from a tiny niche to some broader acceptance by the building industry and most architects. Some identified key reasons are related to poor visual appearance, efficiency losses caused by adding colors to the PV unit and the small series which lead to a mismatch in the targeted price/Wp ratio. Despite many promising attempts at constructing colored PV façades [2] most producers are experiencing difficulties in securing major market shares.

CSEM is proposing a new understanding of the use of color in architecture by broadening the narrow and exclusively design-related perspective according to which colored PV was serving so far to merely embellish the building envelope as a superficial decoration. Colored PV has rather to be redefined as an important added value through its genuine technical properties. To exemplify this technical and intellectual turnaround the attention shall be drawn to the advantage of white PV.

THE MARKET SITUATION FOR COLORED PV

Most PV modules in the market are made of crystalline silicon solar cells, which are interconnected by metallic ribbons, and encapsulated either between two glasses or between a front-glass and a back-sheet. These solar cells, designed to maximize light to electricity conversion and thereby sunlight absorption are characterized by their blueish or black rendering. The overall appearance given by the combination of dark cells, metallic ribbons and very often white back-sheets, is considered by most experts in the building industry and even laypeople to be visually unaesthetic and were a barrier to a more sophisticated use of PV in the built environment. According to many stakeholders in the building industry a homogenous monochromatic colored rendering of PV is in clear demand. White as a “color”

is seemingly of a particular interest: it's not only widely used in architecture and appreciated for its elegance and versatility, but also connoted with adjectives like "clean", "fresh", "classy" and figures sustainably as "modern" throughout the decades despite so many ephemeral architectural trends that passed since the worldwide rise of what is considered to become known as "modern architecture" in the Bauhaus tradition since the 1920's. But despite a clear demand all attempts to ever realize reliable and well performing white solar panels failed due to technical obstacles since it seemed fairly contradictory to the core idea of any PV technology according to which a maximum of light absorption instead of reflection is the aim.

CSEM'S WHITE PV TECHNOLOGY: CHALLENGE AND NEW PERSPECTIVES

The CSEM technology combines two different elements: a solar cell technology based on crystalline silicon able to convert solar infrared light into electricity; a selective filter which reflects and scatters the whole visible spectrum while transmitting infrared.

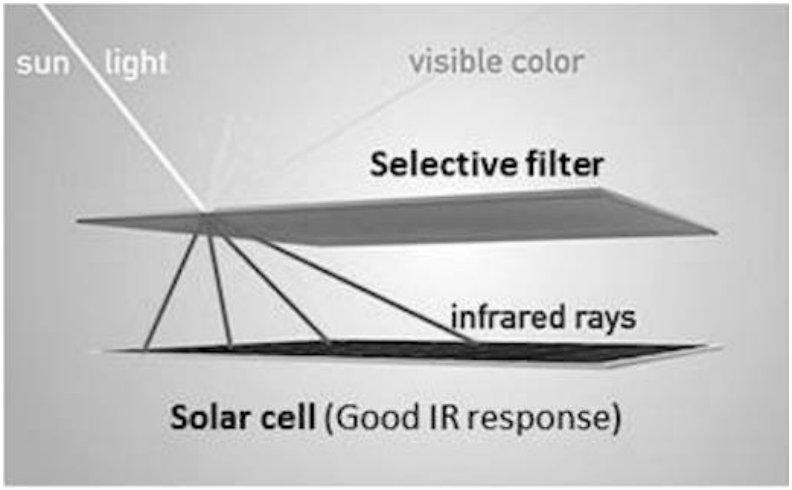

Photo 1: Principal scheme of the CSEM filter technology.

Although any PV technology based on crystalline silicon can be used to manufacture white solar modules, heterojunction crystalline silicon solar cells turned out as the preferred choice. These cells combine open circuit voltages close to 730 mV, i.e. much higher values than the ones measured by standard silicon solar cells (~630 mV), with an excellent response in the infrared part of the spectrum. Approximately 55% of the current generated under standard test conditions comes from the infrared. Thus, even without considering visible light, conversion efficiencies above 10% are possible when using this technology.

The selective filter consists of a plurality of transparent dielectric layers with different refractive indexes, stacked on top of each other, to highly reflect visible light. Moreover, in order to give a white appearance to a mirror-like surface, scattering of visible light is necessary. This effect is achieved either by growing the filter on a micro-structured surface or by placing a foil on top of it with embedded micro particles of different refractive indices. The result is a completely white and homogenous surface which turns the PV wafer structure completely invisible.

Photo 2: The first white PV prototypes developed by CSEM.

The lower temperature of white PV compared to standard dark PV surfaces is an extra advantage. The visible light being reflected reduces the temperature in the module, thus a white solar cell is expected to work at temperatures up to 50° lower than in standard black PV panels. This leads to a clear improvement of performance since in conventional PV the electrical output decreases with rising temperature at rates of 0.3-0.5% per degree Celsius.

This innovative technology can be applied either on top of an existing module or integrated into a new module during assembly. Finally, the white color provides a universal base for a wide range of other possible color variations.

Photo 3: A test module based on the same technology (original picture shows six different colors in the range of terracotta and ochre).

Hence any new building surface could become photoactive, with typical efficiencies in the 10 to 15% range, maximizing the use of space for electricity generation. This virtually invisible energy source offers completely new architectural approaches [3].

Besides its high BIPV potential the CSEM developed optical filter can be applied in many other fields like consumable electronics (laptops), displays, security (cameras), signage,

watch and car industry etc. The next steps for CSEM are to raise the efficiency of white PV modules above 13% and integrate them into new applications.

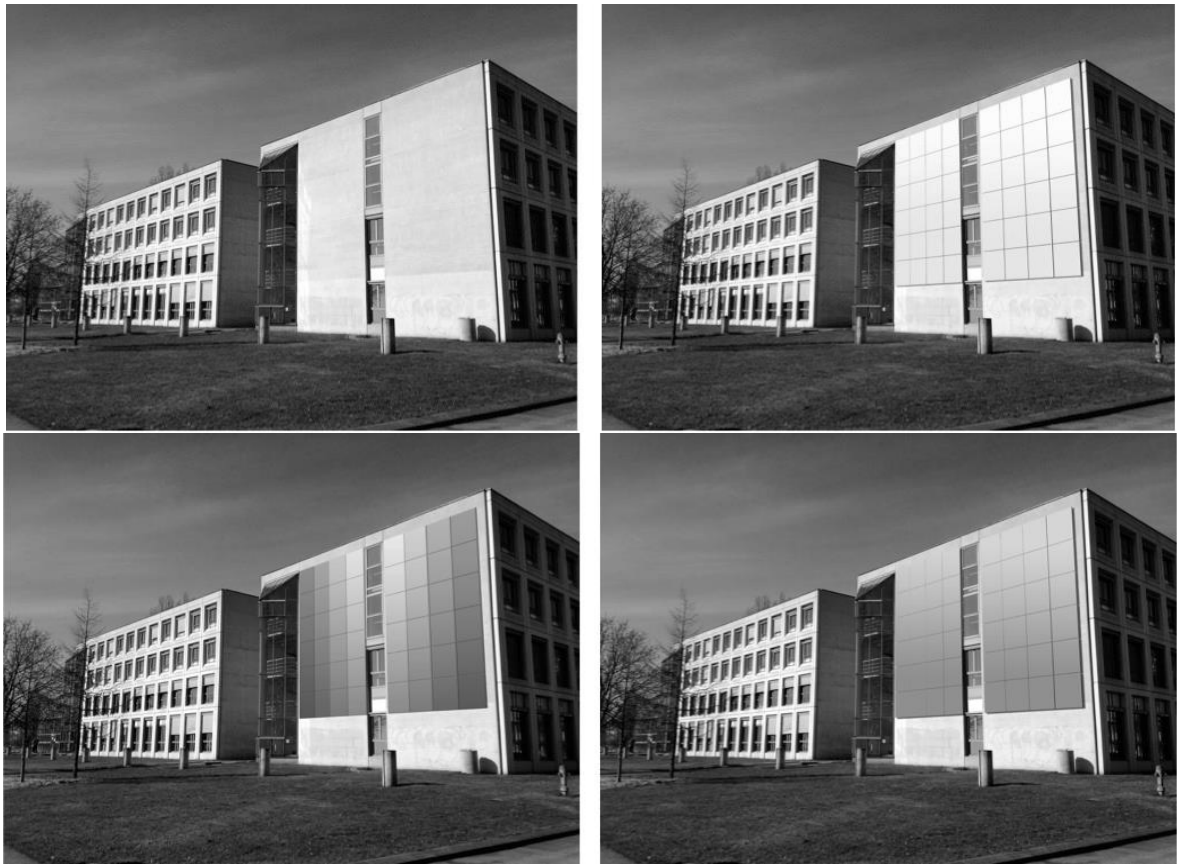

Photo 4a-d: Before and after. The CSEM technology offers virtually an endless variety to design future PV-façades (simulations; original pictures show differently colored PV).

PASSIVE COOLING BY WHITE PV

Targeted to become an industrially manufactured product within the coming year, white PV doesn't only offer a completely new architectural dimension in the so far [as] unlikely considered possibility of constructing homogenous bright white PV building exteriors of any kind by harvesting energy. It could at the same time contribute to energy savings in the building. This additional feature is provided by the color itself: since any white PV-unit reflects most of the visible light by letting through the part of the infrared spectrum important to the PV cell, it could simultaneously operate as a protective sun shield and hence passive cooling component. According to current tests conducted under lab conditions the temperature measured behind a white PV panel is at 10°C lower compared to the temperature behind a black one. This result could be of considerable interest for big cities located in warm climate zones where the "Heat Island" effect takes place but also in any rural zone suffering from hot weather conditions. From this perspective white PV meets an important trend: in most North American cities official initiatives have been launched to improve the urban and indoor climate by turning dark surfaces of the building shell into white ones. Widely known under its name "The cool roofs movement" New York City, Philadelphia, Boston and many other urban communities started to literally paint their flat roofs with ordinary white paint. At first glance a seemingly curious effort to reduce unwanted heat, the result proven by several

independent scientific studies is quite impressive: such treated "white roofs" are at peak temperatures up to 12°C cooler than roofs with aluminium coating and even 17°C cooler compared to roofs covered with a typical black waterproof asphalt layer [4]. This effect clearly contributes to also lower the indoor temperature, which is even more pronounced for buildings with low quality insulation. The decrease of air conditioning output generated by white surfaces could lead according to serious estimations to very promising cost savings in the range of several billion dollars for the US alone. On a worldwide scale the figures would be even more impressive. The additional use of white PV on top of white painted roofs as a façade element could support the effect of outdoor and indoor cooling. The bi-functional solution provided by white PV is worth taking into account in areas with longer periods of peak outdoor temperatures above 30°C: white PV surfaces would hence provide both, energy harvesting on an important scale and the reduction of air conditioning costs by contributing to passively cooling down the building and the urban and rural climate simultaneously. White PV could thus help meet the requirements of any smarter energy concept by reducing the environmental impact of human civilization.

REFERENCES

1. Heinstein, P., Ballif, C., Perret-Aebi, L.-E., Building Integrated Photovoltaics (BIPV): Review, Potentials, Barriers, and Myths, Green, 3, 2, (2013), pp. 22-25.
2. Among others there are very interesting and promising approaches in the field of colored PV by some Swiss PV manufacturers and suppliers like Swissinso and glass2energy.
3. The modules based on the CSEM filter technology are commercialized by Solaxess, Neuchâtel (www.solaxess.ch).
4. See the NYC °Cool Roofs Annual Review 2012, based on studies carried out by Columbia University, NY. There has been measured a temperature decrease even up to 23°C at peak summer outdoor temperatures for NYC.

DC BUILDING NETWORK AND STORAGE FOR BIPV INTEGRATION

J. Hofer; B. Svetozarevic; Z. Nagy; A. Schlueter

Architecture & Building Systems, Institute of Technology in Architecture, ETH Zurich, John-von-Neumann Weg 9, CH-8093 Zurich

ABSTRACT

Electricity loads in buildings are increasingly supplied by distributed renewable generation sources such as photovoltaic (PV) modules or fuel cells. Often these systems are combined with an electricity storage to raise the level of self-consumption in buildings and to reduce the load on the electric grid. PV production and battery storage are both inherently based on direct current (DC) power. At the same time, an increasing number of energy-efficient devices that are part of the building service systems – such as LED's, electronic equipment, or variable speed motors for efficient operation of ventilation units and heat pumps – use DC internally. Consequently, direct coupling of PV generation with electricity storage and DC loads in a local DC network has the potential to avoid power conversion losses arising in conventional alternating current (AC) based systems. In addition to the more efficient use of local generation and storage, an independent building micro-grid can provide system reliability in case of power outage.

In this work, we perform a first evaluation of potential efficiency gains of low-voltage DC versus AC distribution in residential buildings with PV generation and battery storage. We take into account high-resolution electric load and PV generation profiles for a net-zero energy building. We find that relative to a conventional AC system, a DC network improves energy efficiency by approximately 2% without storage and 4% with storage. Moreover, we analyse the sensitivity of the results to variations in PV system size and battery characteristics. We show that the benefit of the DC system becomes more significant with increasing local generation and storage and that energy efficiency improvement and building self-sufficiency are correlated. The theoretical analysis provides guidance for a lab-scale hardware implementation of a small AC/DC hybrid system, which is currently in preparation.

Keywords: Building integrated photovoltaics (BIPV), DC network, energy efficiency, electricity storage, self-consumption, net-zero energy building

INTRODUCTION

In recent years, the installed capacity of building integrated photovoltaics (BIPV) has strongly increased. At the same time, the structure of energy demand in buildings is changing rapidly. This includes a rising share of efficient HVAC technologies and consumer electronics, which use direct current (DC) internally. In fact, all semiconductor electronics for computers, LED, LCD, stereo systems, etc. are DC-based. In addition, the most efficient compressors and fans in heat pumps and ventilation units are using brushless DC motors (BLDC). These motors can operate at variable speed, which increases the efficiency of space heating, cooling, and ventilation by 20-50% compared to simple on/off control [1-5]. An analysis of 32 electricity end-uses shows that energy savings of about 33% are possible by switching the entire load of an average residential building in the U.S. to the most efficient DC-internal technologies [1,2]. While such savings might occur independent of a change to DC power networks, it demonstrates the potential of these technologies to improve building energy efficiency.

Alternating current (AC) allows efficiently transforming voltage for distribution over distance and near the load. However, it seems less attractive for emerging small-scale systems with distributed renewable DC generation, stationary or electric vehicle batteries, and a large fraction

of DC-internal appliances. In this case, a DC bus connection of photovoltaics, battery storage and loads has clear advantages in terms of efficiency, reliability, and cost [6,7]. DC power systems have been successfully implemented in data centers and telecom facilities relying on uninterruptible power supplies with efficiency improvements ranging from 5% to 30% [8,9].

In this research, we estimate potential electricity savings of using low-voltage DC versus AC distribution in a residential building combined with PV generation and battery storage. Only a few studies have analyzed the efficiency gains of DC networks for the integration of local DC power sources, loads, and storage [1,2,6,9]. The reported savings range from 1% to 14%, depending on the assumptions about converter efficiencies, load type and timing, distribution voltage, system size, and the availability of an electricity storage. In this work, we develop a numerical, steady-state model of different AC and DC network topologies with power system conversion efficiencies based on literature data. We take into account a high-resolution electric load and PV generation profile of a single family home located in central Europe. We model the building with a net-zero energy balance between annual electric demand and PV production. We introduce several energy evaluation metrics for the comparison of different systems. The modelling framework is fully parametric and we analyse the sensitivity of the results to variations in component sizes and efficiency.

METHODS

Modelling framework

We analyse four different system topologies for the integration of building electric loads, PV generation and the electric grid: We distinguish between AC and DC distribution, with or without battery storage. Each system is grid-connected to balance electric load and PV production. The components and possible power flows are illustrated in Fig. 1. The model is implemented in Matlab.

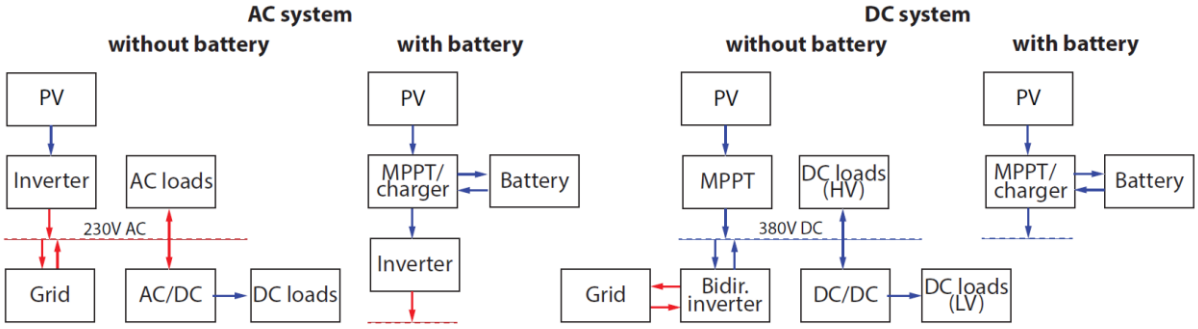

Fig. 1. System setups for AC and DC building network. The configurations with battery are only shown for the part before the main AC and DC bus.

As distribution voltage, we assume 230 VAC or 380 VDC. A 380V standard for DC distribution in data centers and residential buildings is in preparation by the EMerge Alliance [10]. Note that even though distribution losses are not accounted for in this paper, power cable losses are lower when operating with the proposed DC voltage compared with 230 VAC distribution [7]. Alternatively, the cable diameter can be reduced and copper saved, achieving the same efficiency as the AC grid. If the system is modeled with battery storage, four different operation modes are distinguished: a) excess PV production, battery not fully charged, supply of excess to the battery; b) excess PV, battery fully charged, supply excess to grid; c) insufficient PV, battery not discharged, partial or full battery supply; d) insufficient PV, battery discharged, grid backup. The state-of-charge (SOC) of the battery is estimated by integrating the current, and is limited between 10% and 90%. The assumed peak power conversion efficiencies for system components are summarized in Table 1 [1,2,11].

Table 1. Power conversion efficiencies in % (Sources: [1,2,11])

AC system				DC system			
w/o battery		w/ battery		w/o battery		w/ battery	
Inverter (incl MPPT)	95	MPPT/charge control	98	MPPT	98	MPPT/charge control	98
AC/DC appliance	f(P)	Inverter	97	DC house -> AC grid	97	DC house -> AC grid	97
		Battery (round-trip)	90	AC grid -> DC house	93	AC grid -> DC house	93
		AC/DC appliance	f(P)	DC/DC	95	Battery (round-trip)	90
						DC/DC	95

Load profile and PV generation

The building electric load profile is based on a high-resolution stochastic model for domestic electricity consumption developed by Fraunhofer ISE [12]. It has a time resolution of 10 seconds and provides a detailed breakdown by appliance type. The electric load profile used is representative for a single-family home. Ambient temperature and solar irradiation are based on reference weather data file for Southern Germany. It is assumed that the house has an annual heating demand of 50 kWh/m^2, and is equipped with a heat pump for space heating and domestic hot water generation with an annual performance factor of 3.5. The PV modules are oriented south and have an inclination angle of 33°. Fig. 2a shows the assumed annual load and PV generation profile. Fig. 2b shows the electric load by appliance and the power flow between house, grid and battery for one day in summer.

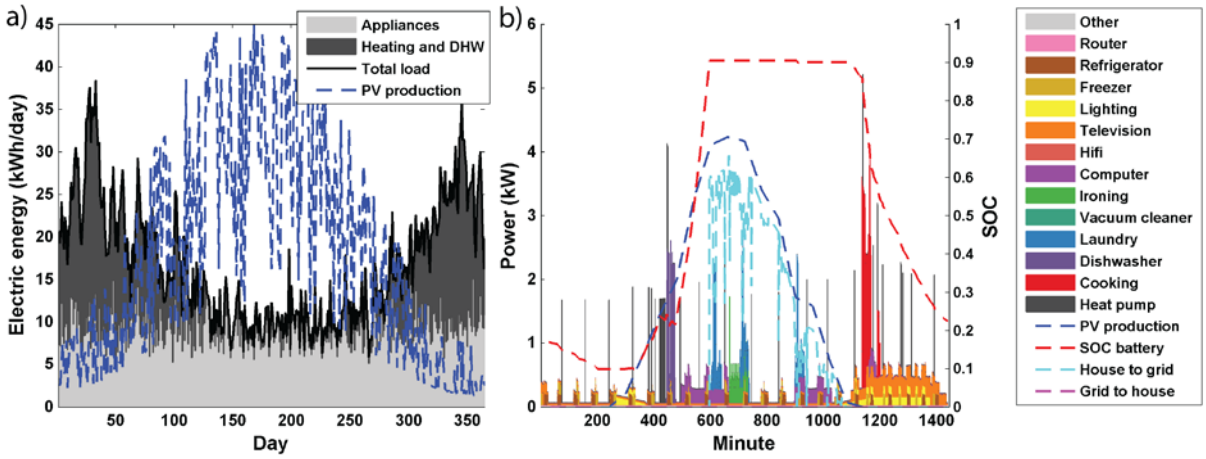

Fig. 2. a) Annual daily load and PV generation. b) Load profile by appliance, PV generation, and battery SOC for one day in summer

Efficiency improvements of DC appliances and power systems

In a conventional building AC network, DC-internal technologies are powered using internal or external rectifiers (e.g. used for laptops, LED, or variable speed DC motors). Direct-DC power systems offer energy savings by avoiding AC/DC conversion losses. Fig. 3 shows the efficiency of certified AC/DC power supplies for 230V input voltage. Based on this data and contact to industry experts we estimate the potential energy savings of using direct DC-coupling. For LED lighting, computers, and other electronic devices we estimate 15-25% efficiency gains, depending on the power level. Furthermore, we estimate 2-5% efficiency improvement for heat pumps, ventilation units, and other devices using variable speed BLDC motors.

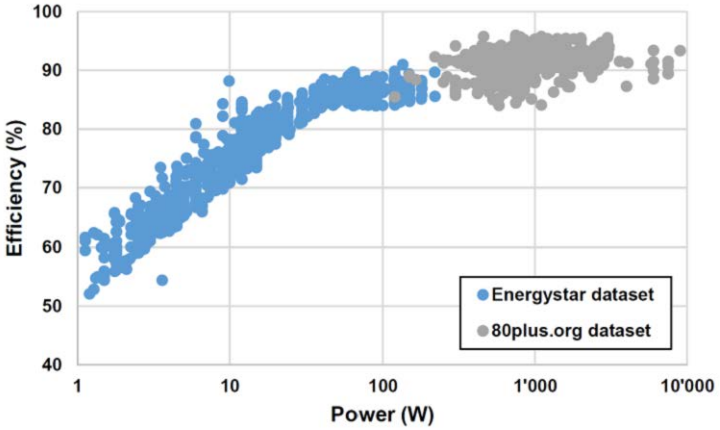

Fig. 3. Efficiency AC/DC power supplies as a function of rated power (Sources: [2,13,14])

Energy evaluation metrics

For the evaluation of different systems, we use four metrics:

- Energy balance: difference between electric energy to and from the grid for a specific house configuration per year
- Efficiency gain of DC over AC system: difference in the energy balance between the AC and DC system relative to the total electric load
- Self-sufficiency: share of the annual electric load covered by PV generation [15]
- Self-consumption: share of annual PV production used directly in the building [15]

RESULTS

Base case

In the base case, we model the building as being net-zero energy and connected to the electric grid. Accordingly, the PV system is sized to produce the total electric demand of the AC house per year (6131 kWh/y, 7.4 kW_{peak}). The battery has a storage capacity of one kWh per kW PV peak power, which is close to the average for grid-connected PV battery systems [15]. Table 2 presents the results for the reference case. For the same installed PV power the energy balance is better for the DC than the AC system, i.e. the DC system uses less energy from and feeds more energy to the grid. This means that the DC system uses the electricity more efficiently. Self-sufficiency and self-consumption increase by approximately 20% for the assumed battery storage size of 7.4 kWh. The efficiency gain of the DC over the AC system is higher with battery storage, as expected, as this configuration incurs additional conversion losses for the AC system.

Table 2. Simulation results in the base case by system

	w/o battery		w/ battery	
	AC	**DC**	**AC**	**DC**
PV to grid (kWh)	4645	4748	3069	3195
Grid to house (kWh)	4645	4606	3177	3053
Energy balance (kWh)	0	143	-107	142
Efficiency gain (%)	-	2.3	-	4.1
PV self consumption (kWh)	1486	1430	2955	2874
Self sufficiency (%)	24.2	25.0	48.2	50.3
Self consumption (%)	23.0	22.2	45.8	44.5

Sensitivity analysis

We analyse the sensitivity of the results by varying the size and efficiency of system components. In particular, we investigate the influence of battery size, battery efficiency, and installed PV capacity on self-consumption and efficiency improvement. Fig. 4 shows how self-sufficiency and the efficiency gain of the DC over the AC system increase with installed PV and battery capacity. This means that the benefit of the DC system becomes more significant with increasing local generation and storage. Self-consumption is reduced with installed PV power and decreasing battery size, because a lower fraction of local production can be used directly in the building.

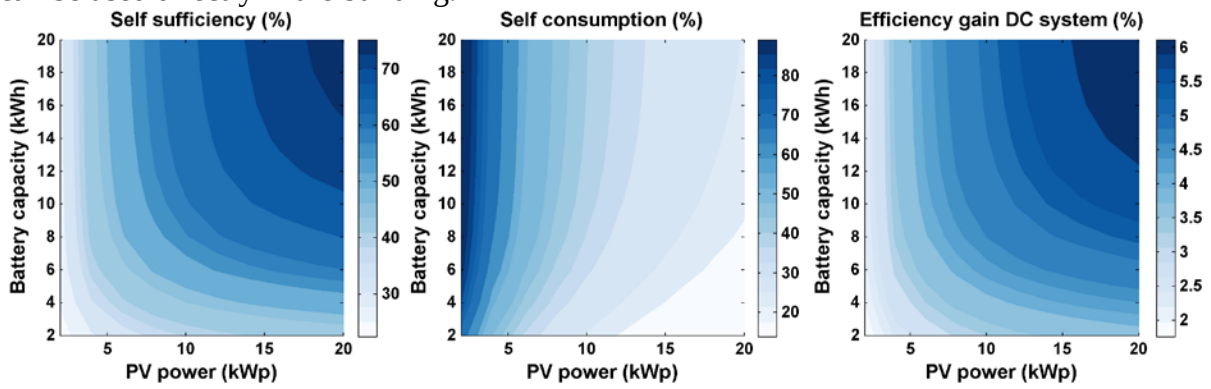

Fig. 4. Self-sufficiency and DC efficiency gain as a function of installed PV power and battery size. The load of the building is constant.

System efficiency with local storage strongly depends on battery performance. In the reference case, we have assumed a round-trip efficiency of 90%, which is realistic for li-ion batteries. However, lead-acid batteries have lower efficiencies about 80% [11]. Fig. 5 shows the dependence of the energy balance of the AC and DC system as a function of battery size and efficiency. In this case, the PV system is sized to meet the annual building electricity demand.

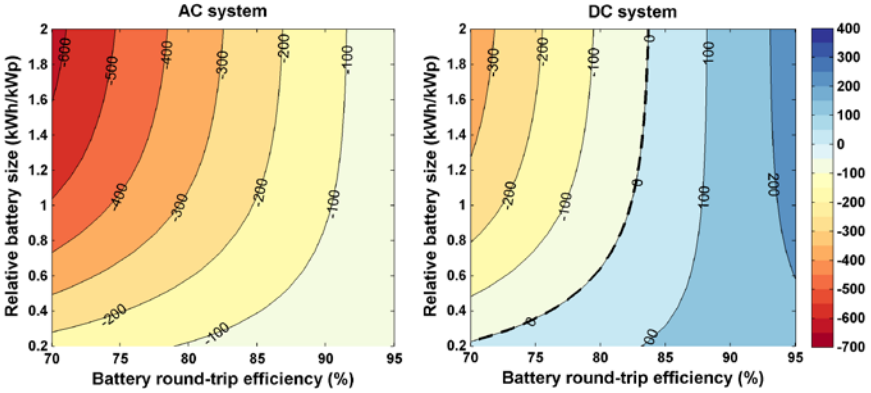

Fig. 5. Difference between energy to and from the grid for the AC and DC system

DISCUSSION

The results presented show that for local PV generation, a DC building network has the potential to improve overall system efficiency. The improvement is particularly high if the PV system is combined with battery storage. The absolute efficiency improvement of 2 to 4% is similar to the results of [7,9], but lower than the values found in [1,2] due to more conservative estimates about potential savings from avoiding AC/DC conversions. The efficiency gains are highest for electronic appliances operating at low power such as consumer electronics or LED lighting. Therefore, it may be most effective to focus on the integration of these devices with PV generation, battery storage, and DC distribution first.

This can be technically also achieved in a hybrid network coupling AC and DC loads simultaneously [16]. Note that electricity savings are greater for commercial than residential buildings because of the higher share of electronic appliances and the better coincidence of PV generation and load.

CONCLUSIONS AND OUTLOOK

In this work, we developed a model for the analysis of DC compared to AC distribution in buildings with PV generation and battery storage. We find that relative to a conventional AC system, a DC network improves system efficiency. Furthermore, we quantified the effect of battery and PV system size on self-consumption and showed that efficiency gains of the DC system correlate with building self-sufficiency.

In the future, we will improve the model by taking into account the variable efficiency of power converters and cable losses. In addition, more advanced battery charging strategies (e.g. peak shaving), demand side management, and additional building DC supplies or loads such as electric vehicles will be considered. Further to the theoretical analysis, a lab-scale hardware implementation of a small AC/DC hybrid system is in preparation to test the feasibility and for validation purposes. The setup is scheduled to be tested in the context of the Adaptive Solar Façade for the ETH House of Natural Resources (http://www.honr.ethz.ch) and the NEST HiLo building at EMPA (www.hilo.arch.ethz.ch).

ACKNOWLEDGEMENT

This research has been financially supported by CTI within the SCCER FEEB&D (CTI.2014.0119) and by the Building Technologies Accelerator program of Climate-KIC.

REFERENCES

1. Vossos, V. et al.: Energy savings from direct-DC in US residential buildings. Energy and Buildings, 68, 223-231, 2014
2. Garbesi, K. et al.: Catalog of DC appliances and power systems. LBNL-5364-E, 2012
3. Saidur, R. et al.: Applications of variable speed drive (VSD) in electrical motors energy savings. Renewable and Sustainable Energy Reviews, 16(1), 543-550, 2012
4. Col, D. et al.: Energy efficiency in a ground source heat pump with variable speed drives. Energy and Buildings, 2015
5. Gasser, L. et al.: Effiziente Luft/Wasser-Wärmepumpen durch kontinuierliche Leistungsregelung. Swiss Federal Office of Energy, 2011
6. Hammerstrom, D. J.: AC versus DC distribution systems: did we get it right? IEEE Power Engineering Society General Meeting, 2007.
7. Sannino, A. et al.: Feasibility of a DC network for commercial facilities. IEEE Transactions on Industry Applications 39(5), 1499-1507, 2003.
8. Fortenbery, B. et al.: DC power for improved data center efficiency. LBNL, 2008.
9. Evans, V.: Why Low Voltage Direct Current Grids? Doctoral dissertation, TU Delft, Delft University of Technology, 2013.
10. Becker, D. J.: DC microgrids in buildings and data centers. International Telecommunications Energy Conference, IEEE 33, 1-7, 2011.
11. Chen, H. et al.: Progress in electrical energy storage system: A critical review. Progress in Natural Science 19(3), 291-312, 2009
12. Fischer, D. et al.: Model for Electric Load Profiles With High Time Resolution for German Households. Energy and Buildings 92, 170–179, 2015
13. EnergyStar database of external power supplies: https://www.energystar.gov/ Accessed: 17.04.2015
14. 80 PLUS database of certified power supplies: http://www.plugloadsolutions.com/ Accessed: 17.4.2015
15. Luthander, R. et al.: Photovoltaic self-consumption in buildings: A review. Applied Energy 142, 80-94, 2015
16. Moix, P. O.: New Trends in Hybrid Systems with Battery Inverter, Studer-Innotec Whitepaper, http://www.studer-innotec.com/ Accessed: 17.04.2015

THERMO-ECONOMIC ANALYSIS OF A HYBRID PHOTOVOLTAIC/THERMAL (PV/T) SYSTEM FOR DIFFERENT CONFIGURATION SETTINGS

W.J.A. Jayasuriya [1], A.U.C.D. Athukorala [1], S. Ragulageethan [1], A.T.D. Perera [1,2], M.P.G. Sirimanna [1]

1: *Department of Mechanical Engineering, Faculty of Engineering, University of Moratuwa, Moratuwa 10400, Sri Lanka*

2: *Solar Energy and Building Physics Laboratory (LESO-PB), EPFL, CH-1015 Lausanne, Switzerland*

ABSTRACT

Solar energy can be harvested thorough solar PV (SPV) conversion as well as solar thermal energy conversion. A hybrid photovoltaic/thermal (PV/T) system has the capability to convert solar energy into both electricity and thermal energy simultaneously. These systems can provide the heating demand of buildings while generating electricity, which becomes ideal for building applications of urban energy systems. Performance analysis of such systems becomes essential to design PVT systems matching with the operating conditions. In this study, a thermo-economic model is developed to evaluate sensitivity of design, operating and climatic parameters for a hybrid PV/T system. Five main configurations of the PV/T system are considered based on the heat transfer fluid and the arrangements of glass and Tedlar layers of PV/T collector. The effect of the packing factor of the PV/T collector on the behaviour of thermal and electrical efficiency and the sensitivity of heat transfer fluids (water and air) were analysed using the thermal model. Subsequently, effect of temperature coefficient on the performance of PV/T collectors in terms of efficiency are studied for five different types of PV cells (i.e. m-Si, a-Si, p-Si, CdTe, CIS, HIT).

Keywords: hybrid PV/T system, thermo-economic model, performance evaluation

INTRODUCTION

The increase of energy consumption related to building applications and its growth rate have resulted in a higher tendency of using efficient and eco-friendly energy conversion technologies. Renewable energy technologies minimize emission levels of obnoxious gasses and global warming. Solar energy is a renewable energy source that can be used to generate both electrical and thermal energy. A PV/T (photovoltaic/thermal) system is a hybrid solar system that combines photovoltaic and thermal systems which produce both electricity and thermal energy simultaneously from one integrated system. Energy requirement of building applications for electricity, heating and cooling can be met through generating electrical and thermal energy from this PV/T system.

A substantial amount of research on PV/T systems has been carried out based on theoretical models which were subsequently validated using experimental setups. Sarhaddi et al. [1] carried out a performance evaluation of a PV/T air collector with a glass to tedlar PV module. A detailed thermal and electrical model was developed to calculate the thermal and electrical parameters of a typical PV/T air collector. The two configurations of air collector with glass to glass PV module, Case I (air flow above the absorber plate) and Case II (air flow below the

absorber plate) were analysed by S. Dubey et al. [2] for five different cities of India. Tiwari et al. [3] have showed that PV/T air collector with glass to glass type PV module can be used to obtain higher efficiency than the glass to tedlar type PV modules. An analytical model was used in this regard which was experimentally validated later. Sobhamayan et al. [4] optimize the exergy efficiency of a PV/T water collector through a similar analytical module coupled with an exergetic analysis. These studies clearly portray the technical feasibility of PVT technology.

Thermo-economic analysis on the parameters that affect the system performances has been an area of interest for a wider research community in the recent past [5]. The PV/T air collector configuration has been analysed considering several types of collectors and it has been concluded that the configuration of a PV/T air collector should be optimized based on the specific priority needs for electrical or thermal output [6]. In addition to the collector configuration, the collector parameters have been analysed to improve the performance. The effect of packing factor of PV/T air collector to electrical and thermal efficiencies has been analysed [7]. A numerical analysis and an experimental validation have been done to evaluate the influence of packing factor of a PV/T water collector on the performance. The performances of three types of PV/T water collectors were determined for different mass flow rates of water and its effect on the operating temperature of the collector bas been analysed [8].

In this study, a mathematical model for the PV/T system is developed and it is used to evaluate sensitivity of design, operating and climatic parameters for the system. The effect of the type of PV module and packing factor on the behaviour of the average annual thermal and electrical efficiency is analysed. Further investigations are carried out by clustering the weather conditions of the year into three sections based on the solar irradiation and wind speed. The three clusters of weather conditions are sectioned considering the weather distribution throughout the year. The clusters considered based on the solar irradiation and wind speed are;

- Case 1 - High solar irradiation and low wind speed
- Case 2 - High solar irradiation and high wind speed
- Case 3 - Low solar irradiation and low wind speed

MATHEMATICAL MODEL FOR PV/T SYSTEM

A summary of the developed model is shown in Figure 1 including the PV/T collector configurations. Hourly solar irradiation, wind speed and ambient temperature are taken using TMY2 climate file as the input for the model.

Energy flow model

The energy analysis of the PV/T system is carried out to develop the mathematical model. A concise description about the mathematical model is presented in this study. Analytical expressions for thermal energy production and thermal efficiency of PV/T collector are obtained by formulating energy balance equations for each component i.e. PV module, absorber plate and heat transfer fluid flowing through the duct. An expression for the fluid outlet temperature ($T_{f,out}$) is derived using the energy balance equations. The rate of useful thermal energy for a heat transfer fluid having a specific heat capacity C_f flowing at a mass flow rate of $\dot{m}$ is calculated. $T_{f,in}$ is the fluid inlet temperature and G is the solar irradiance which are input parameters. The thermal efficiency (η_{th}) of the PV/T collector with length L and width W is obtained as Eq. 1;

$$\eta_{th} = \frac{\text{Rate of useful thermal energy}}{\text{Rate of solar energy incident on the panel surface}} = \frac{\dot{m}C_f\left(T_{f,out} - T_{f,in}\right)}{WLG} \quad (1)$$

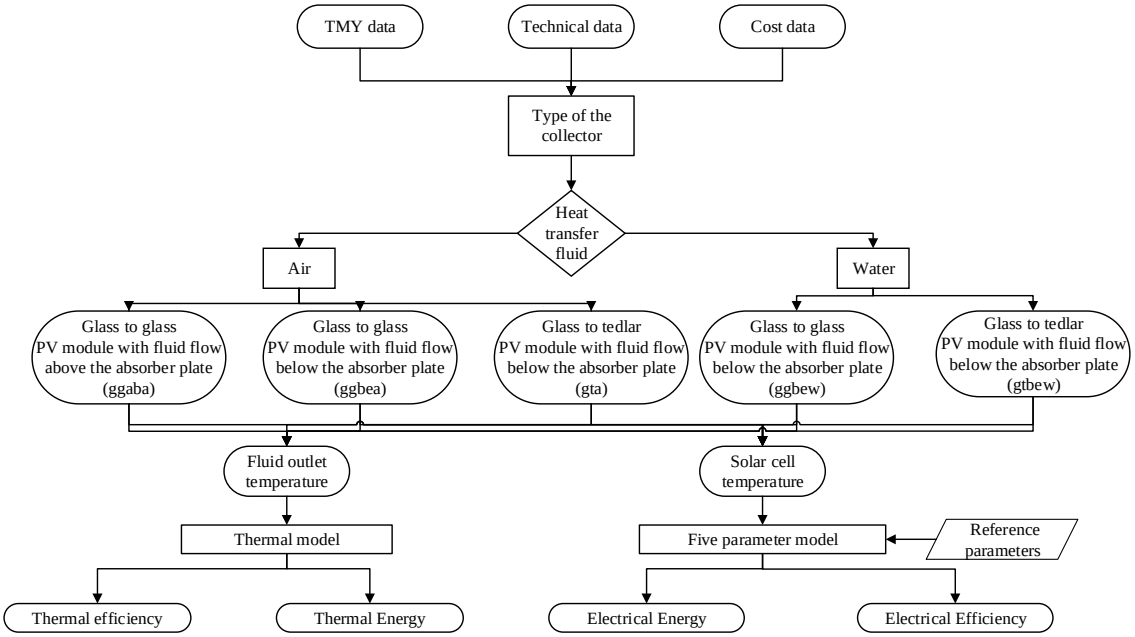

Figure 1: Overview of the mathematical model

The electrical efficiency of the PV/T collector is derived using five-parameter photovoltaic model. A set of nonlinear equations that can be solved with numerical methods are derived to plot the I–V characteristic curve. The values of maximum power point voltage and maximum power point current (V_{mp}, I_{mp}) are obtained from solved I–V characteristic curve. The electrical efficiency (η_{el}) of the PV/T collector is obtained as Eq.2;

$$\eta_{el} = \frac{\text{Actual electrical output power}}{\text{Rate of solar energy incident on the panel surface}} = \frac{V_{mp}I_{mp}}{WLG} \quad (2)$$

RESULTS AND DISCUSSION

The objective of this study is to analyse the effect of the parameters on the performance of PV/T system.

Type of PV module in the PV/T collector

Six types of PV modules (m-Si, a-Si, p-Si, CdTe, CIS, HIT) which are mostly used by researches are taken into consideration to analyse the effect on the performance of the PV/T collectors. The thermal, electrical and overall efficiency variations are considered with respect to type of PV module. Overall efficiency variation is shown in Figure 2.

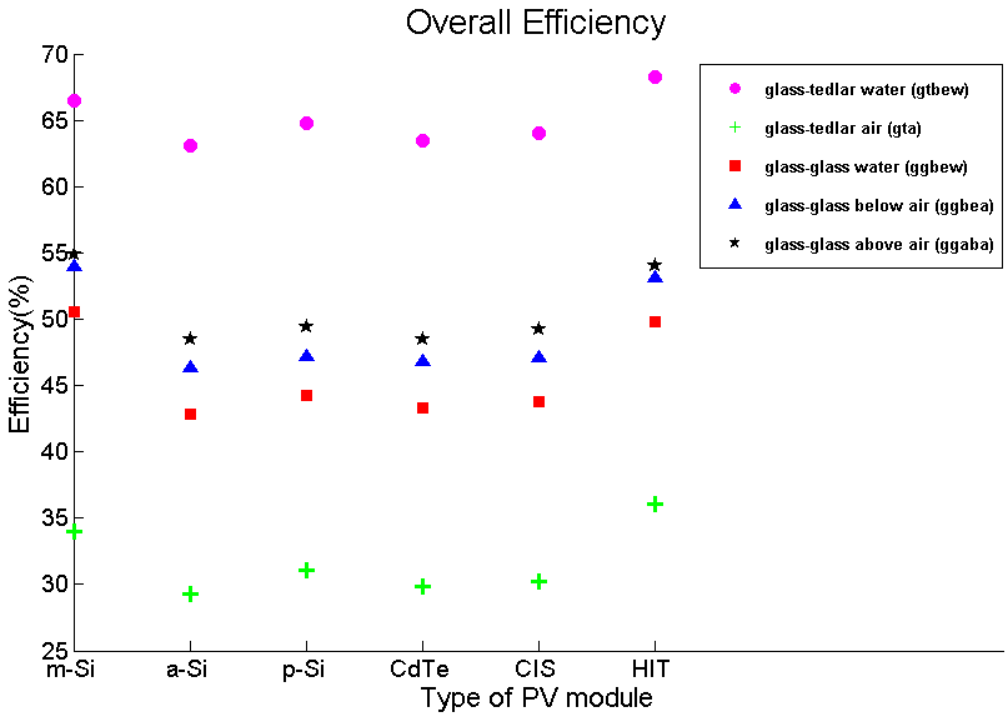

Figure 2: Overall efficiency

It is observed that a PV/T collector with an amorphous silicon (a-Si) PV module has given the highest thermal efficiencies for both glass-tedlar type collectors (gtbew, gta). However, the electrical efficiency is very low for a-Si for all the collectors. The temperature coefficient of a-Si is low, which can be taken as the main cause for lower efficiency levels. For the three types of glass-glass collectors (ggbew, ggbea, ggaba), the PV/T collector with a mono crystalline (m-Si) PV module has shown the highest thermal efficiency. The electrical efficiency varies in the range of 12%-14% which is due to the higher temperature coefficient of m-Si. With respect to the electrical efficiency it can be concluded that any configuration type of collector with hetero junction with thin layer (HIT) PV module has a higher electrical performance. The maximum electrical efficiency of 16.8% is witnessed for glass-tedlar water type configuration (gtbew), which is a promising rate of electrical performance. However, HIT results reductions in thermal efficiency. HIT has shown the lowest rates of thermal efficiency for all the configurations of collectors. At standard test conditions HIT technology has very high module efficiency which is 17%. This has resulted in high electrical performance for HIT. However the higher temperature coefficient of HIT has resulted in hampering its thermal performance. The overall performances of the collectors are investigated by analysing the overall efficiencies. Due to the higher electrical performance of HIT, for all configurations HIT PV type has resulted highest overall efficiency. The m-Si with relatively higher performance in both electrical and thermal factors, all collectors with m-Si has shown higher overall performance.

Packing factor

The packing factors of 25%, 38%, 62.8%, 75%, 83% and 98% are considered for the analysis. Further investigations are carried out for the three cases which consider the weather distribution of the year. The evaluation of overall efficiency of the five collectors in a range of packing factor can be presented in Figure 3.

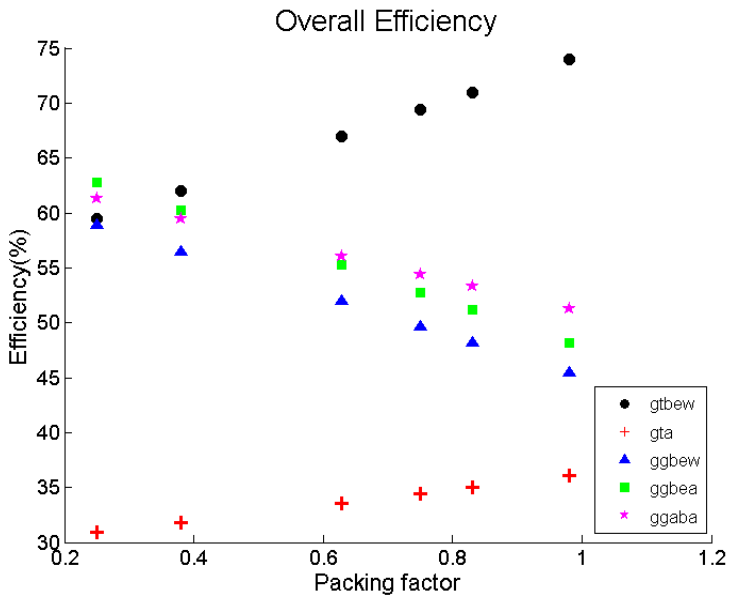

Figure 3: Overall efficiency

For all three types of glass to glass collectors (ggbew, ggbea, ggaba), the thermal efficiency has decreased with the increment of the packing factor. This is because the radiation absorber area from the thermal segment of the collector reduces due to the covering of the PV panel. However, for the glass to tedlar collectors (gtbew, gta), the thermal efficiency has increased with the packing factor increment. The tedlar layer effectively absorbs the heat from the PV module and transfers it to the thermal element and thermal efficiency increases. If the packing factor is raised too much the thermal exit temperature will get higher due to absorbing high amount of thermal energy so it will increase the cell temperature, which causes the decrease in the electrical efficiency.

Further investigations showed that the lower wind speeds and higher irradiation levels have resulted in lower electrical efficiencies. When wind increases with lower irradiation, electrical efficiency increases. Higher wind speeds with high-medium irradiation levels has produced the best electrical efficiencies. Low wind and higher irradiation have resulted in the best thermal efficiencies. Higher wind with high-medium irradiation levels has reduced the electrical efficiencies. When wind increase with lower irradiation, thermal efficiency decreases drastically.

CONCLUSION

The results showed that a PV/T collector with an amorphous silicon (a-Si) PV module has given the highest thermal efficiencies for both glass-tedlar type collectors (gtbew, gta). However, the electrical efficiency is very low for a-Si for all the collectors. For the three types of glass-glass collectors (ggbew, ggbea, ggaba), the PV/T collector with a mono crystalline (m-Si) PV module has yielded the highest thermal efficiency with an average level of electrical performance. With respect to the electrical efficiency it can be concluded that any configuration type of collector with hetero junction with a thin layer (HIT) PV module has a higher electrical performance.

For all three types of glass to glass collectors (ggbew, ggbea, ggaba), the thermal efficiency has decreased with the increment of the packing factor. However, for the glass to tedlar collectors (gtbew, gta), the thermal efficiency has increased with the packing factor

increment. If the packing factor is raised too much, the thermal exit temperature will get higher due to absorbing high amount of thermal energy resulting to an increase the cell temperature, which causes the decrease in the electrical efficiency.

REFERENCES

1. F. Sarhaddi, S. Farahat, H. Ajam, A. Behzadmehr, M. Mahdavi Adeli, "An improved thermal and electrical model for a solar photovoltaic," Applied Energy, vol. 87, pp. 2328–2339, 2010.
2. Swapnil Dubey, G.S. Sandhu, G.N. Tiwari, "Analytical expression for electrical efficiency of PV/T hybrid air collector," Applied Energy, vol. 86, pp. 697–705, 2009.
3. G.N. Tiwari, Swapnil Dubey, "Thermal modeling of a combined system of photovoltaic," in Solar Energy, p. 602–612, 2008.
4. F. Sobhnamayan a, F. Sarhaddi a, M.A. Alavi b, S. Farahat a, J. Yazdanpanahi, "Optimization of a solar photovoltaic thermal (PV/T) water collector," Renewable Energy, vol. 68, pp. 356-365, 2014.
5. A.U.C.D.Athukorala, W.J.A.Jayasuriya, S. Ragulageethan, et al "A techno-economic analysis for an integrated solar PV/T system with thermal and electrical storage — Case study" , MERCon-15, Sri Lanka, PP. 182-187 2015
6. Kanchan Vats, Vivek Tomar, G.N. Tiwari, Effect of packing factor on the performance of a building integrated semitransparent photovoltaic thermal (BISPVT) system with air duct, Energy and Buildings, pp. 159–165, 2012.
7. Feng Shan, Fang Tang, Lei Cao, Guiyin Fang, Dynamic characteristics modeling of a hybrid photovoltaic–thermal solar collector with active cooling in buildings, Energy and Buildings, pp. 215–221, 2014.
8. M. Farshchimonfared, J.I. Bilbao, A.B. Sproul, Channel depth, air massflow rate and air distribution duct diameter optimization of photovoltaic thermal (PV/T) air collectors linked to residential buildings, Renewable Energy, pp. 27-35, 2015.

PV DOMESTIC HOT WATER SYSTEM

A. Lindsay; R. Le Berre[1]; J.F. Doucet[1]; G. Kwiatkowski[1]; P. Dupeyrat[1]

1: EDF R&D, ENERBAT, Avenue des Renardières, Ecuelles, 77250 Moret-sur-Loing, FRANCE

ABSTRACT

PV production and the consumptions of the building on which the PV is installed are not always in phase. In such a context, a coupling between PV production and local thermal systems can be an interesting solution to convert produced electricity into heat, thus storing it locally more easily than in electrochemical devices.

The PV Domestic Hot Water System (PV DHWS) presented here is a direct coupling (DC) between a PV installation and the heating element of an electric hot water tank. The main advantage of such a system is to provide hot water to a building from renewable resources by storing intermittent solar energy as heat.

The technical feasibility of PV DHWS is demonstrated through experimental and numerical considerations, both of these being complementary. A prototype of PV DHWS has been designed and installed in our outdoor test facilities near Paris, and a model of PV DHWS was developed under Modelica / Dymola and validated with collected experimental data.

2.2 kWp of PV panels (mono-Si) tilted at 30° and facing south cover 70% of the hot water needs of a 4-person household over a year. 33% of the annual PV production was lost (percentage of PV production that could be generated but is not due to the temperature of the water tank being at the upper limit), mainly due to vacations during which the hot water is not used. These promising results were achieved with an existing PV power plant. It would be possible to reduce the PV losses while maintaining a high solar fraction by down-sizing the installation.

System performances were simulated under various configurations and compared to the performances of more conventional hot water systems (solar thermal). Given the low prices of PV modules, and although thermodynamically PV DHWS makes less sense than solar thermal, an economic assessment seems to prove that this new concept could be competitive.

Keywords: Photovoltaic, Domestic Hot Water, Integration of Renewable Energy in the Built Environment, Storage

INTRODUCTION

PV modules cost around 60 c€ per Watt peak nowadays, tumbling down from above 3€/Wp back in 2007 and above 1€/Wp in 2011 [1]. Such a striking fall in prices encourages the development of residential photovoltaic systems. In the meanwhile, feed-in-tariffs for PV have decreased all over Europe and are sometimes in the same range or below the price of electricity from the grid. In this context, it will be in the interest of the owner of rooftop PV to keep for his own use as much of the generated electricity as possible rather than sell it back to the grid.

Unfortunately, PV production and the consumptions of the building on which the PV is installed are rarely in phase, especially in the residential sector. An obvious solution is to

store the PV electricity for later use. However electro-chemical devices can be very costly and will probably not be deployed massively in the near future.

Also, whereas the energetic performance of building envelopes increases continuously with the evolution of regulations and standards, the primary energy dedicated to hot water needs remains sensibly the same for standard electric Domestic Hot Water tanks.

Storing the electricity generated by a PV array in a Domestic Hot Water tank would be a way of:

- Increasing the use of self-generated PV electricity without investing into extra equipment such as batteries
- Alleviating the primary energy needed for hot water production

The system described in this paper is a PV Domestic Hot Water System (PV DHWS) with a direct coupling (DC) between the PV installation and the heating element of an electric hot water tank, as represented on Figure 1. The main advantage of such a system is to provide hot water to a building from renewable resources by storing intermittent solar energy as heat.

Figure 1: Concept of a PV domestic hot water system

METHOD

The technical and economic feasibility of PV DHWS were evaluated through real-life testing as well as numerical considerations.

Experimentations

An existing PV installation comprising 2.2 kWp of PV panels (mono-Si) tilted at 30° and facing south was used for the experimentations on our outdoor test platform near Paris. The power output of the array was maintained at the Maximum Power Point (MPP) by DC-DC converters and then injected into a 300L water tank with a resistive element of 3 kW. This resistive element was powered with DC current when the solar panels produced electricity or with AC current when the PV energy was not sufficient to cover hot water needs. The control strategy was implemented on an electronic card that regulates the thermostat. Every day, the hot water consumption of a 4-person household was withdrawn from the water tank, which totals to 100L of hot water at 60°C (M324 profile). The whole PV DHWS was instrumented and monitored. The experimental configuration is described in Figure 2.

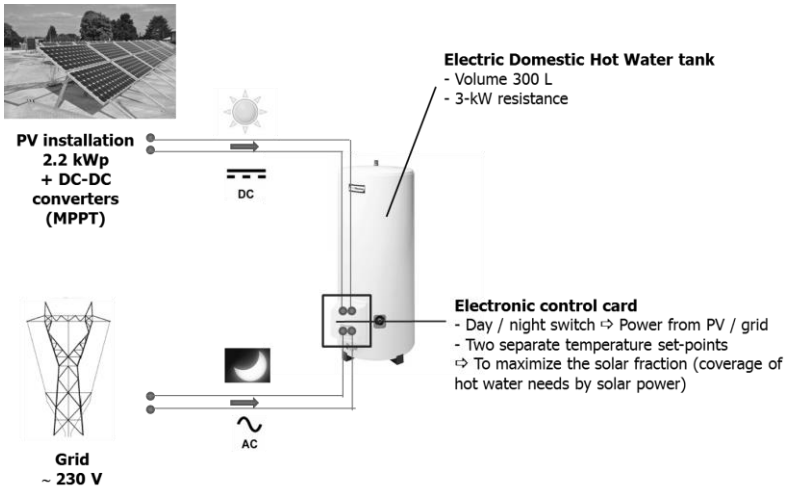

Figure 2: Experimental set-up to evaluate the concept of PV DHWS

Simulations

The prototype was modelled with Dymola, a dynamic energy simulation tool provided by Dassault Systems, using BuildSysPro [2], a Modelica library for modelling buildings and energy systems that is developed by the department of Energy in Buildings and Territories (EnerBaT) of EDF R&D. The graphical assembly of sub-models is presented in Figure 3.

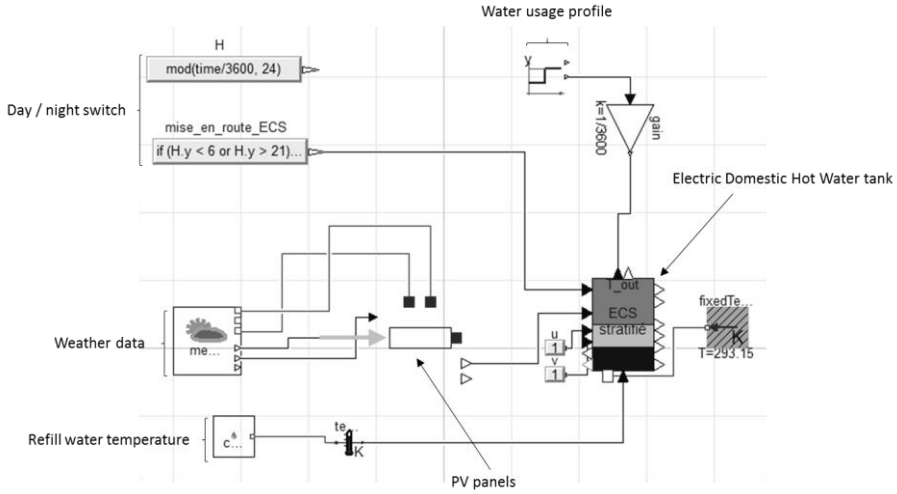

Figure 3: Numerical representation of PV DHWS under Dymola using BuildSysPro models

The model was validated and calibrated with experimental data collected from our prototype of PV DHWS. It was then used to extrapolate the behaviour of PV DHWS to different weather conditions, sizes of tanks, hot water consumption profiles, temperature set point control algorithms and sizes of PV installations.

Economic assessments

The economic evaluation of PV DHWS was done in comparison with solar thermal. In each case, the sizing of PV DHWS was adjusted in order to cover the same percentage of hot water needs as solar thermal by energy coming from the sun, should it be as heat or as electricity.

RESULTS

Our experimental results for the PV DHWS prototype are reported in the Table 1 below in terms of solar fraction, which is the percentage of hot water needs covered by solar:

$$Solar\ \ fraction\ (\%) = \frac{PV\ \ electricity\ \ used\ \ (kWh)}{Energy\ \ used\ \ by\ \ DHWS\ \ (kWh)} = \frac{PV\ \ electricity\ \ used\ \ (kWh)}{Water\ \ heating\ \ (kWh) + Thermal\ \ losses\ \ (kWh)} = \frac{PV\ \ electricity\ \ used\ \ (kWh)}{PV\ \ electricity\ \ used\ \ (kWh) + Electricity\ \ from\ \ grid\ \ (kWh)} \quad (1)$$

	Solar fraction
Spring 2014	80%
Autumn 2014	79%

Table 1: Solar fraction achieved by the prototype over two experimental periods

Over a standard sunny day (Figure 4 below), the temperature in the hot water tank increases from the night temperature set point (45°C) to the day temperature set point (65°C) once the sun has risen. When the day temperature set point is reached, the PV installation is disconnected, explaining the jagged aspect of the "Electric power from PV curve". Overnight, power is taken from the grid in order to maintain the temperature of the water at the night level.

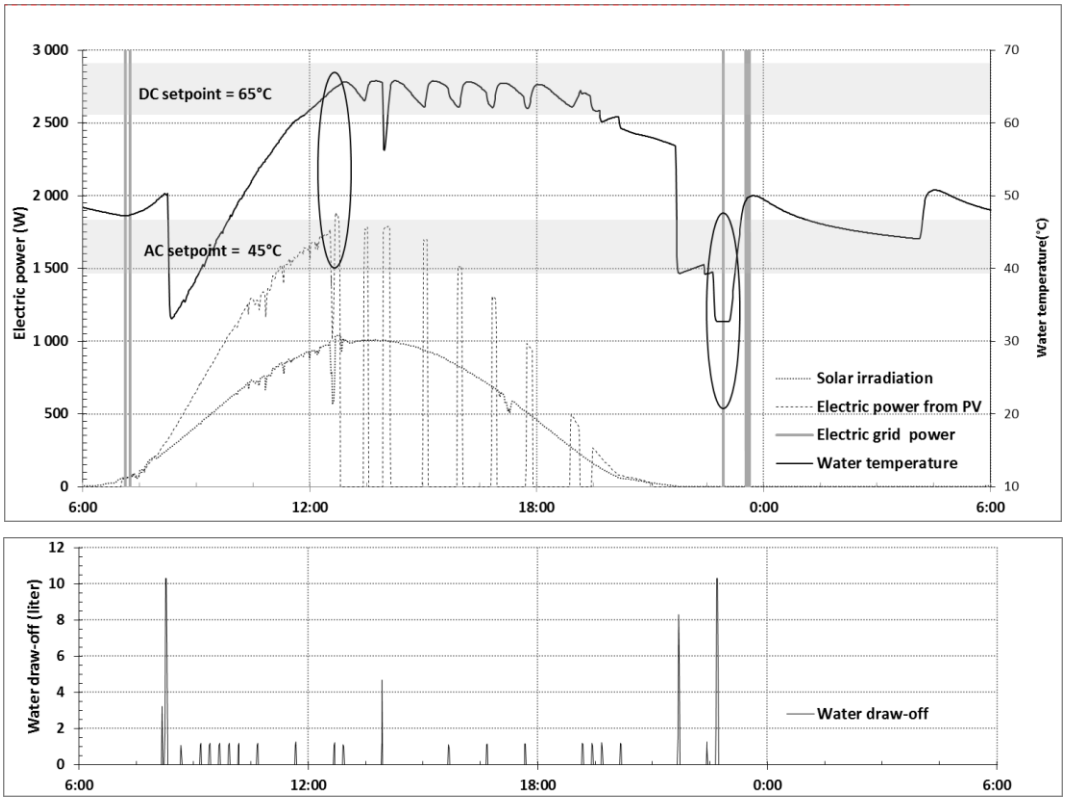

Figure 4: Experimental results of the prototype of PV DHWS for a sunny day

With the dynamic model of PV DHWS in Modelica language, calibrated with the experimental data, the solar fraction and PV losses can be estimated over a whole standard meteorological year. The PV losses correspond to the electricity that could have been generated by the solar panels but is not due to the temperature in the hot water tank being at the set point (see equation 2). Over a standard meteorological year near Paris, given the sizing

of the PV installation and the hot water tank of the prototype and with a M324 water withdrawal profile, the solar fraction would be 70% and the PV losses would sum up to 33%.

$$PV\ \ losses\ \ (\%) = \frac{Potential\ \ PV\ \ \ electricity\ \ (kWh) - PV\ \ \ electricity\ \ used\ \ (kWh)}{Potential\ \ PV\ \ \ electricity\ \ (kWh)} \quad (2)$$

In a second part, the sizing of a PV DHWS with a 300L tank was carried out in Paris and in Nice with the goal of achieving the same solar fraction as a standard solar thermal installation.

In Paris, a conventional solar thermal system would consist in 4 m² of absorbers for an annual solar fraction of 63%. In order to cover the same percentage of hot water needs by solar, this would be equivalent to 1650 Wp of PV for the PV DHW system, which would take up about 12 m² of roof surface.

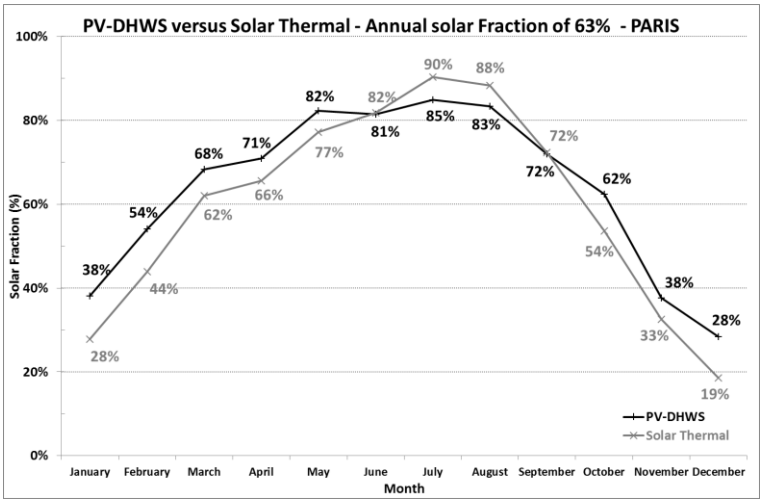

Figure 5: Solar fraction over a year for PV DHWS and solar thermal, in Paris

In Nice, a conventional solar thermal system would consist in 2 m² of absorbers for an annual solar fraction of 55%. In order to cover the same percentage of hot water needs by solar, this would be equivalent to 760 Wp of PV for the PV DHW system, which would take up about 6 m² of roof surface.

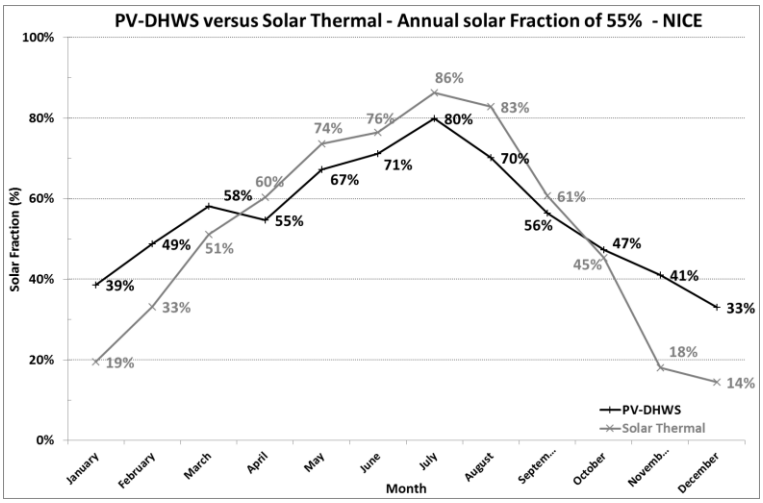

Figure 6: Solar fraction over a year for PV DHWS and solar thermal, in Nice

One can notice by looking at the previous figures that the seasonality of the solar fraction for PV DHWS is less than that of solar thermal. This is due to the fact that the electrical

performances of solar panels increase when the temperatures are lower whereas the performances of solar thermal decrease in such cases. Furthermore, the collector surface is roughly 3 times superior for PV than for solar thermal.

For the economic assessment, the prices published by the ADEME in 2013 [3] for residential rooftop PV installations of less than 3 kWp can be used. These were estimated in the range of 3.3 to 3.7 €/Wp, i.e. 9900€ to 11100€ for a 3 kWp installation. 1000€ are necessary for the connection to the grid, which means that a non-connected residential PV installation costs on the lower side 2.97 €/Wp and 3.37 €/Wp on the higher side (without taking into account the further price reduction due to the absence of an inverter in the PV DHWS). The cost of a hot water tank can be conservatively judged at 1000€. The estimations for solar thermal are issued from a report written by the ADEME in 2013 [4].

With the same sizing of PV DHWS in Paris and in Nice presented previously, the following economic assessment can be drawn:

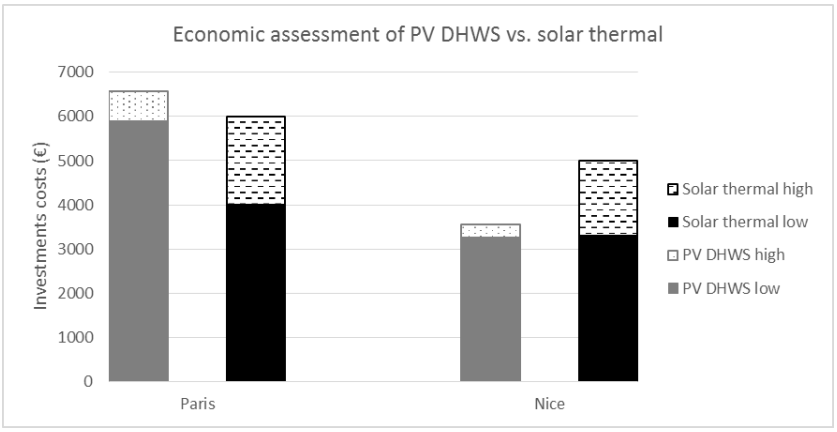

Figure 6: Investment costs of PV DHWS and solar thermal in Paris and in Nice

This figure points out the economic viability of PV DHWS with regards to solar thermal, both in the North and the South of France, on the basis of a conservative estimation of the costs.

CONCLUSION

The technical feasibility of the direct coupling of a PV installation with an electric DHW tank has been proven through the development of a prototype tested for several months on our experimental platform near Paris. With a dynamic model calibrated on experimental data, various simulations have been carried out in order to evaluate the costs of such a system. Although thermodynamically PV DHWS is less efficient than solar thermal, the economic assessments seem to show that PV DHWS is competitive all over France, with a sizing that achieves the same solar fraction as solar thermal.

REFERENCES

1. PV-magazine module price index issued from pvXchange data, website http://www.pv-magazine.com/investors/module-price-index/
2. Plessis, G., Kaemmerlen, Lindsay, A., BuildSysPro: a Modelica library for modelling buildings and energy systems. Proceedings of the International Modelica Conference 2014
3. ADEME, Le photovoltaïque en France en 2013. Version June 2014
4. ADEME, Analyse de la compétitivité et du développement de la filière solaire thermique en France. Version October 2013

REDESIGN OF THE INTEGRATION OF BUILDING ENERGY FROM METABOLISMS OF ANIMAL: THE *RIMA* PROJECT

C. Martín-Gómez[1]; J. Bermejo-Busto[1]; A. Zuazua-Ros[1]; R. Miranda[2]; E. Baquero[2]

1: Building Services and Energy Section. Universidad de Navarra (Spain).

2: Environmental Biology Department. School of Sciences. Universidad de Navarra (Spain).

ABSTRACT

Buildings are a very special kind of machine. In terms of hygrothermal conditioning, it can be said that they switch on and off to maintain a regular temperature in relationship with the activities carried out inside of them. It is a strategy very similar to that developed by the 'warm blooded' animals, which maintain their temperature with a high metabolism rate.

There are numerous passive strategies in architecture that allow to have an effective control over the indoor conditions in order to maintain the levels of comfort needed for human habitability with a lower energy consumption. In the same way, animals have several methods for thermal regulation. Some of them are the *rete mirabile* structure in tuna, the regulation of the temperature in a bee hive or the control of the gases inside a silkworm cocoon.

With these precedent ideas, the researchers will explain a project funded by the Spanish Economics and Competitiveness Ministry. The project tries to explore new design strategies for the energy and building services systems in buildings from biomimicry concepts. The main source for this research will be a thorough analysis of the 'cold blooded' animals' metabolisms, although other temperature control methods of other living beings will be taken into consideration. The project proposal is to create a new way of thinking how energy and building services are integrated and designed in a building, taking into consideration the knowledge imported from a different area of knowledge.

Therefore, the project proposes a reassessment of the paradigm established of the methodology used for design the energy systems in buildings, with an approximate technical view from other areas of knowledge.

Keywords: Integration, energy, metabolism rate, building services, architecture

INTRODUCTION

Below, 'What' is the project and 'Why' the researchers have chosen this working path is exposed.

- What? The architect members in the project are involved in the design, calculation and execution of building services and energy systems in singular buildings since 2000 [1]. These singular projects also require singular solutions with alternative point of view, and in this **highly innovative solutions searching framework** is where it must be understood what it is sought in the project.
- Why? The dynamism of the current society and the requirements demanded to the architecture and construction make essential theoretical and technical reformulations. These may be obtained from the architecture itself or based on the existence of consolidated knowledge in other areas.

Solving these requirements from the knowledge platform representing biology, involves the use of already optimized models during thousands of years that own extraordinary operation systems in regard to the energy optimization. Even though, they require a 'technological' translation for their application in the architecture that is not always neither evident nor direct.

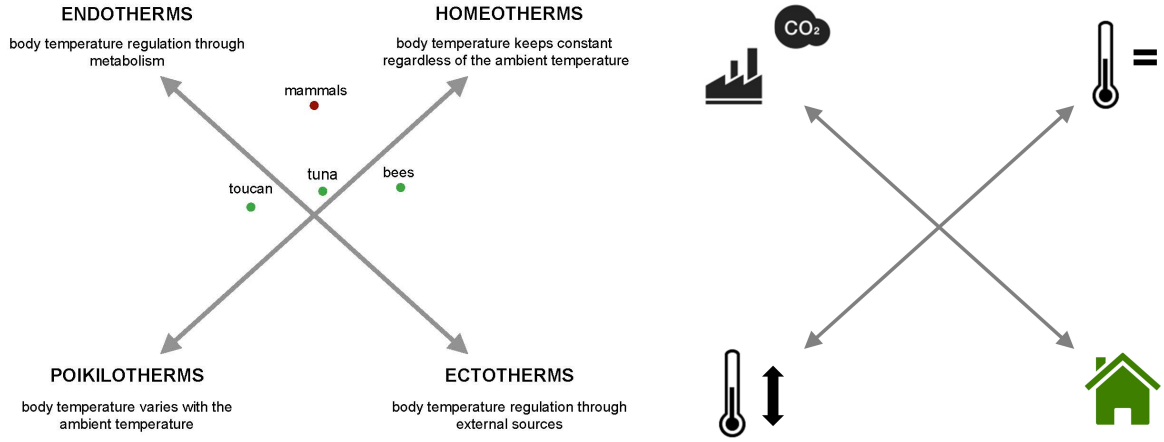

Figure 1: These images show the parallelism between animals and buildings. On the one hand, animals can be classified regarding their mechanism for heat gains; this concept in buildings is extrapolated to the classification regarding the CO2 emissions. On the other hand, animals can be homeotherms or poikilotherms in regard to their temperature variation in relation with the ambient temperature, in buildings is assumed as well the indoor temperature variation depending on the use of the spaces.

METHODOLOGY

How is a project of this nature conceived? Given its singularity, it has also been necessary an alternative approach different from 'traditional' projects developed by the team of architects and biologists.

- Firstly, it has been necessary a knowledge compilation from biology that was understandable for architects. So that, numerous technical datasheets have been created in order to compose an analysis basis from which to make proposals development. It has drawn the attention of the researcher the lack of existence of biology database from an engineering point of view [2]. In this case, the data sheets generated in the project gather the technical data from the animals that could be relevant for architects such as body and ambient temperatures or climate and location. In a brief summary the main strategies of the animals are described and the possible application ideas related with the architecture are listed. In order to facilitate a deeper analysis the datasheet includes the references used for the descriptions.
- Communication (meetings, emails, telephone…) between the team of biologists and architects has been abundant and flowing.
- Given the staff and economical limitations, only the possibilities that could be completed within the timeframe of the project were selected to develop.
- The main references in the world of biology that would apply in architecture were selected from the analysis and working meetings. The extrapolation of results to architecture was performed with the modelling, simulations, and scale-models of architects.

This analytical data sheets have been the absolutely necessary starting point for the development of the project and several months of work were required for their execution. However, they require longer work path that would necessitate additional time and personnel.

RESULTS – 3 EXAMPLES

The researchers have proposed several working plans, always with cold-blooded animals since that was the basis of the project. However, this paper collects the three most developed strategies so far, given the limitations of the space for their exposition:

Tuna's *rete mirabille*

These large fishes own a characteristic that only a few fishes share: the counter current heat exchanger also known as *rete mirabile*. This system allows tuna to achieve and maintain higher body temperatures than ambient temperatures, so that, tunas tolerate to swim in deep seas.

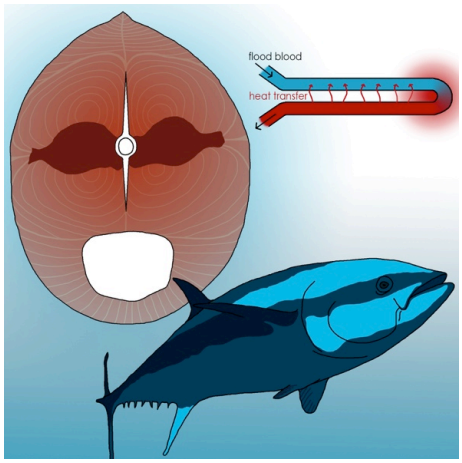

Figure 2 (left): Tuna's thermal behaviour in water. Despite the cold environment where it lives, tuna's body temperature is higher and stable thanks to the inner disposal of dark muscles and the redistribution of heat in the rete mirabile*. / Figure 3 (right): The researchers are currently developing heat recovery system for office buildings optimized from Tuna's thermal behaviour.*

The heat is generated in the central tissues, muscles and organs, named red muscles. This is distributed throughout the blood vessels net to the areas with direct contact with the external ambient. Here, since the blood vessels are in parallel, the heat is transferred to the coldest blood current, thus maintaining an optimal temperature for its operation [3].

The tunas are a perfect example of heating storage, distribution and optimisation. According to architectonical application there are several questions that may be studied such as, what if the high thermal load spaces are located in the center of a building? And what if a heat recovery system is designed/installed to use this heat for other locals? Given the relation between the red muscles percentage of the total volume and the efficiency of the *rete mirabile* [4], can we obtain the optimal relation between the ratio high thermal load space-to-whole building?

First approaches of the researchers have shown that a 'tuna organisation' in office buildings guarantees lower heating demand than other spaces distributions, merely attending to the space distribution.

Toco-toucan and the heat dissipation

In the opposite side of tuna's heat storage and distribution is the heat dissipation. Like other birds, the toucan uses its bill for heat dissipation. In this case, toucan has the largest bill in relation to the body volume [5].

The toucan is able to regulate its heat loss through its bill due to the blood vessels grid on it. This system allows the loss of the excess heat generated by the toucan (during flight) or by high ambient temperatures. It can dissipate 400% of the generated heat when it is beneficed from favourable airstreams [6].

Nowadays in buildings, the use of cooling towers in cooling systems is widespread. Unlike the toucan, the heat dissipation in cooling towers is achieved due to evaporative cooling, carrying legionella risk and high maintenance costs [7]. So that, it may be ask, what if we avoid the use of cooling towers? Is it possible to replace the cooling towers in buildings by a cooling system based on natural convection?

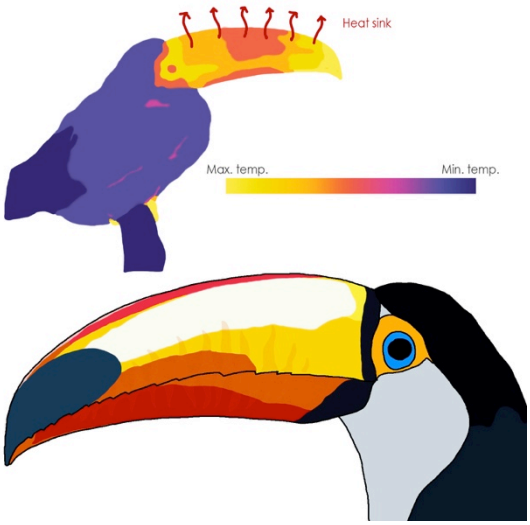

Figure 4 (left): Toco – toucan heat sink. The bill of the toucan is not only a sexual attraction item. It also has thermal properties. Thanks to its large surface, it works as a heat sink, releasing heat and maintaining body temperature lower. / Figure 5 (right): The researchers are working on a heat dissipation system in buildings that will allow the deletion of cooling towers. The solution involves larger machines (like the tuna case) but will eliminate the complex maintenance easements of cooling towers.

Bees

Bees and other social insects are well known because of their good organization within hives. Some of the specimens may work focused on foraging, other ones on defending the colony, some others take care of larvae.

In terms of thermal regulation, automated functions and strategies are also implemented within a hive. The case of the beehive is remarkable as bees can both regulate their temperature when the ambient temperature is high and low.

The most important place of the beehive is the brood comb where larvae are engendered. There, the temperature must be constant and within some tight limits: 32º C to 36º C [8]. In order to achieve these temperatures, bees show up three different strategies: one for heating and two for cooling.

Heating. Bees leave empty some places amongst larvae. They make use of these 'holes' to locate themselves and generate heat by contracting their thoracic muscles. In this way, heat is released ensuring a good brood development.

Cooling. In order to achieve a general cooling process inside the beehive, some specimens try to catch some water droplets and spread them within the colony. Some other individuals place in the entrance of the hive and flap their winds to produce wind mimicking a fan. This combination of facts creates an evaporative cooling effect within the hive.

If bees want to avoid heat from entering into the hive, they can do it locally. Using a technique called 'heat shield', bees are placed between the 'walls' of the hive and the larvae catching the external heat. Once they cannot absorb more heat, they go away and cool themselves flying or even regurgitating the nectar. [9]

This strategies, may lead to a different way of designing building services. Could be more effective to place autonomous machines than a big one to supply heating or energy? Could some spaces be isolated by using removable thermal cushions?

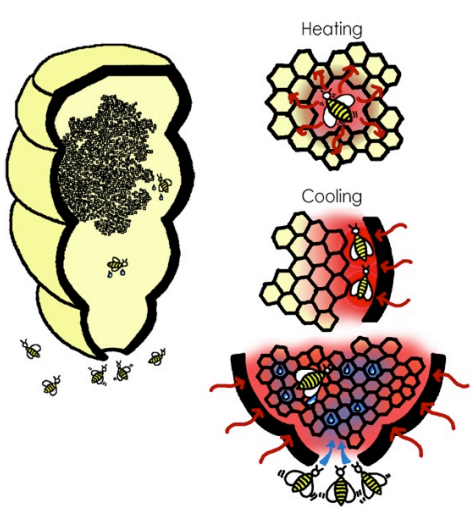

Figure 6 (left): Beehive thermal regulation. Bees are able to control the inside temperature within their hive. Both for cooling and heating, bees develop strategies to increase or decrease temperature. / Figure 7 (right): The researchers have developed two prototypes of HVAC equipment with Peltier cells that would allow an autonomous HVAC system without a central 'brain'.

CONCLUSION

Even though the initial intuition that originated the project was optimistic about the results that could be achieved, the project has demonstrated the possibilities:

- The possibilities of future projects cover a wide spectrum, from the temperature and humidity control by passive measures (without machines) to the redesign of control networks based on nature's neuronal networks. Architects and engineers will be who would select 'what' according to their lines of work.
- The multidisciplinary collaboration with biologists, is comprehended as essential as neither architects nor engineers know sufficiently in depth this subjects, but it is also true that biologists do not know the full potential of applying their knowledge in other areas [10].

The information exposed here will have a greater development in the technical papers that are being prepared right now. However, the exposition of these data in a forum like CISBAT intends to insist on the importance of the extrapolation of this working methodology to other projects and researchers.

ACKNOWLEDGMENTS

This project was funded by the Ministry of Economy and Competitiveness of the Spanish Government under the research project BIA2013-49838-EXP.

REFERENCES

1. Martín-Gómez, C., Eguaras, M., Mambrilla, N., & Lacilla E.: Advanced technologies importantion to architecture. I European conference on energy efficiency and sustainability in architecture and planning, pp 149–53, 2010.
2. Bar-Cohen, Y. : Biomimetics-using nature to inspire human innovation. Bioinspiration & biomimetics, Vol 1, pp 1–12, 2006.
3. Stevens, E. D., Lam H. M., & Kendall J.: Vascular anatomy of the counter-current heat exchanger of skipjack tuna. Journal of experimental biology, Vol 61, pp 145–53, 1974.
4. Morrissey, J., & Sumich J.: Introduction to the biology of marine life. Jones & Bartlett Publishers, 2011.
5. Symonds, M., & Tattersall, G.: Geographical variation in bill size across bird species provides evidence for Allen's rule. The American naturalist, Vol 176, pp 188–97, 2010.
6. Tattersall, G., Andrade, D., & Augusto S.: Heat exchange from the toucan bill reveals a controllable vascular thermal radiator. Science, Vol 325, pp 468–70, 2009.
7. Walser, S. et al.: Assessing the environmental health relevance of cooling towers-a systematic review of legionellosis outbreaks. International journal of hygiene and environmental health, Vol 217, pp 145–54, 2014.
8. Stabentheiner, A., Kovac H., & Brodschneider, R.: Honeybee colony thermoregulation-regulatory mechanisms and contribution of individuals in dependence on age, location and thermal stress, Vol 5, 2010.
9. Bonoan, R., Goldman, R., Wong P., & Starks, P.: Vasculature of the hive: heat dissipation in the honey bee (apis mellifera) hive. Die Naturwissenschaften, Vol 101, pp 459–65, 2014.
10. Pawlyn, M.: Biomimicry in Architecture. RIBA Publications, London, 2011.

EVALUATION AND OPTIMIZATION OF RENEWABLE ENERGY IN THE "QUARTIER NORD": OBJECTIVE ZERO-POWER

D. Mauree[1,*]; Y. Yao[1]; J. Kämpf[1,2]; J-L. Scartezzini[1]

1: Ecole Polytechnique Fédérale de Lausanne, Solar Energy and Building Physics Laboratory, Station 18, CH-1015, Lausanne, Switzerland
2: kaemco LLC, Corcelles-Concise, Switzerland

*dasaraden.mauree@gmail.com, +41 21 693 55 56

ABSTRACT

Buildings account for almost 40% of energy consumption in European countries and hence are responsible for a significant part of greenhouse gas emissions. Recent regulations and standards (Minergie, Minergie P, etc.) are strongly encouraging more sustainable buildings by decreasing energy consumption and integrating more renewable energy sources. It is essential, in such a context, to evaluate the performance of buildings and to determine how relevant are the integration of renewable energies and how their implementation can be improved in order to give full autonomy to such a district (towards zero power districts).

In order to achieve this, it is here proposed to use building energy simulation tools to simulate the heating and cooling energy demand. First Energy Plus is used to simulate the demand with a detailed geometrical model of the STCC. Although the results did not give good agreement when compared with a set of measured and recorded data, they corresponded to what has been expected from the Minergie standards. The geometrical model is then simplified and used as input for simulations with both CitySim and Energy Plus. The differences between both models are considered to be acceptable (15%). Finally, the evaluation of the potential for the integration of renewable energy and storage capacity is done with CitySim.

This work is expected to provide a methodology which could be used in the evaluation of building energy use and help with the integration of renewable energy at a neighbourhood scale along with the dimensioning of the energy storage. Furthermore we gave a quantitative analysis of the differences between the two models. It is thus proposed in future work to couple both models using a co-simulation technique, to take advantage of the performance of CitySim and Energy Plus models and to include processes at different scales.

Keywords: building energy simulation, CitySim, Energy Plus, renewable energy, storage, zero-power district

INTRODUCTION

The recent Intergovernmental Panel on Climate Change[1] again highlighted the need for a drastic change in national and international policies regarding the mitigation of climate change due to greenhouse gas emissions. Buildings account for almost 40% of energy consumption in European countries and hence are responsible for a significant part of greenhouse gas emissions (around 23% for France[2]). Recent regulations and standards (Minergie, Minergie P, etc.) are favouring more sustainable buildings by decreasing energy consumption and with the integration of more renewable energy (RE) sources.

New strategies are however needed to develop and build more sustainable quarters / neighbourhoods. In order to reduce the energy consumption and greenhouse gas emissions,

which usually comes from centralized energy system, communities are encouraged to install more RE. However these RE are often intermittent and are not available when most needed (e.g. heat from the sun during winter months). Storage should thus be used as a complement to reach these requirements. Determining the size of the storage and the RE installation capacity is a tedious process which can only be handled by using numerical software.

Such tools are often used, before renovation and construction, to determine what kind and type of strategies are needed to achieve the desired objectives (both for demand and installation of RE). Models working at different spatial scale have been developed and used in the past. On the one hand at the building scale, models such as Energy Plus[3] are frequently used. However these models do not consider the surrounding neighbourhood which can have a significant influence on the energy balance of the building. On the other hand at the neighbourhood scale model such as CitySim[4] or Envimet[5] have been used. These models give a more realistic representation of the surrounding but however do not have a very detailed description of the considered building.

We hence propose to evaluate with a quantitative analysis the difference between two models working at different spatial scales. We used the Energy Plus model and the CitySim software for the simulations. The idea is to prepare both models for a future co-simulation, as multi-scale modelling could be used to simulate a building at both scales in order to improve results.

In the framework of this study, we focused on one of the landmarks of the Ecole Polytechnique Fédérale de Lausanne (EPFL): the SwissTech Convention Center (STCC). In a first step, we collected data / information on this building. We then developed a detailed model representing the real geometrical and technical characteristics of the STCC to be used as input for simulation with Energy Plus. These results are then compared with measured data. In a third step, we then "simplify" this model so that it can be used in both CitySim and Energy Plus. CitySim is then used to evaluate the renewable energy integration capacity as well as the need for storage, to decrease the dependence on centralized energy systems.

This paper is divided as follows. In this Method section, we give a brief overview of how we used the Energy Plus Open Studio plugin to draw the detailed model of the STCC and how we then simplified it. We also describe how we use a simple methodology to calculate the storage need. In the Results section, we describe the results obtained from both models, the storage need and renewable energy integration in the Quartier Nord. Finally, we discuss the results and conclude on the main outcomes of this study.

METHOD

Geometrical data

To build a coherent model and as close as possible to the actual STCC building, we collected data from the Department of Infrastructure of the EPFL (DII). The data obtained corresponded to the technical details of the building as described by the architects and engineer. However, due to some discrepancies between some of the administrative documents, part of the data (total volume, window glazing / frames …) was considered to be incomplete or incorrect.

Energy Plus

Energy Plus[3] is a software developed by the Department of Energy, USA. It works at the building scale and is widely used in the building energy sector both in the private and research industry. One of the main advantages of Energy Plus is that it is has a low simulation time while having a very detailed description of the building. It also contains an exhaustive

database for construction materials as well as for the heating, ventilation and air-conditioning (HVAC) systems.

Another one of its advantages is that it has a wide range of compatibility with designing software, including Open Studio. This plugin was used to design the STCC building with as much details as possible corresponding to the actual characteristics of the buildings (see Figure 1).

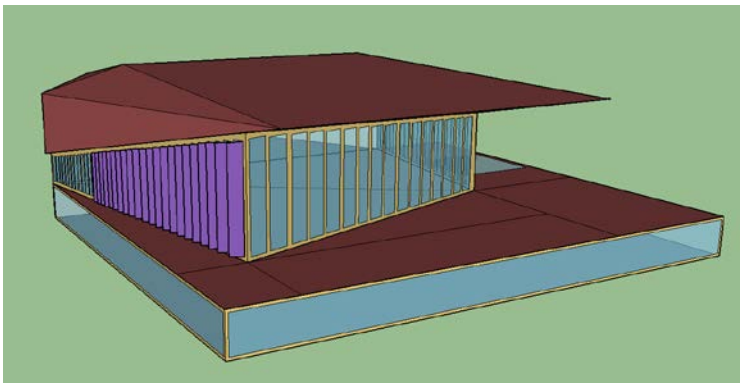

Figure 1: Representation of the STCC with Open Studio

One of the aspects that we have simplified in this representation is the complete description of the HVAC system. The energy system used here is very complex as it uses waste heat water from the EPFL site and also from solar thermal panels installed on nearby buildings. A simplification is thus proposed in the heat network designed for the STCC.

CitySim

CitySim[4,6] is a large-scale dynamic building energy simulation tool developed at the EPFL. The tool includes an important aspect in the field of many buildings simulation: the building interactions (shadowing, light inter-reflections and infrared exchanges). Furthermore, CitySim is based on simplified modelling assumptions to establish a trade-off between input data needs, output precision requirements and computing time.

This thus requires a simplification of the geometrical characteristics of the building under consideration. Based on the first model, we built for Energy Plus, we removed some of the technical details (window frames, Graetzel cells on the west side…) which can be considered to have a minimal impact on the energy consumption or which can be described otherwise. Any simplification done for the CitySim software is also applied to the model used in Energy Plus.

Methodology to evaluate the storage need of the Quartier Nord

The typical building energy consumption and production profiles for a northern European country does not allow for an easy complete integration of RE. It can be noted that during summer months there is a higher production and that if this production can be stored for a couple of months, then it would be possible to use it for the beginning of the winter season as a heating source. The storage thus has the potential to shave off peak RE productions and also decrease the constraints linked to the intermittency of renewable energy sources.

The evaluation of the storage is done as follows. First, we calculate the energy demand and the energy consumption for a whole year. Second, we include renewable energy in the building using only PV panels. We then evaluate what is the surplus electricity (produced – consumed) and how this can be used to heat a water tank ($5m^3$) to store energy for use in future months as a heating source considering heat losses in the tank (to the ground). This is a simplified version of the method used in Guadalfajara et al. (2014)[7].

Monitored data and experiments

For this study, we collected monitored data from the DII regarding the heating and cooling demand. As the STCC has been operational for since July 2014, we run our detailed simulation for only 6 months. These months should be representative of a summer and winter period of a typical year.

As mentioned previously, we run a set of simulations. The first one is done with Energy Plus using the detailed geometrical model and the results are compared with the monitored data. Then we run both CitySim and Energy Plus using a simplified model and when comparing both models, we only use the ideal load, to give a quantitative analysis of the differences between the models. Finally, we include solar PV panels to evaluate the RE integration potential and use a simple methodology to determine the implication of using seasonal storage.

RESULTS AND DISCUSSIONS

Energy Plus simulation comparison with measurements

For EnergyPlus, ideal loads for heating and cooling needs were computed, and the values were divided by 0.8 to get the real consumption as an energy system of 80% efficiency was assumed. The simulation here are done for only 6 months from July to December 2014, as this is the first monitoring period of this newly constructed building.

	DII	**Energy Plus**	**Error (%)**
Heating (GJ)	1395.1	443.9	-68.2
Cooling (GJ)	907.9	1054.2	16.1
Total (GJ)	2303	1498.1	-34.9

Table 1 Difference between Energy Plus and monitored data for 6 months (July to December)

From Table 1 it can be noted that there are significant differences (68%) between the results from the DII and the Energy Plus simulation particularly concerning the winter period whilst during the summer period there is a difference of only 16%, which is slightly above other comparisons done with Energy Plus[8].

However, if we look at the energy consumed per m^2, over one whole year, it can be highlighted that the values obtained from the Energy Plus simulation (39 kWh/m^2) seems to in agreement with the Minergie Standard[9] (40 kWh/m^2). This then raises the question of the behaviour of the control system as well as of the occupants in the buildings. But as mentioned before this was the first 6 months of monitoring and of occupancy of the building and it is hence very likely, according to the DII, that the building is not functioning at its optimal capacity.

Comparison between CitySim and Energy Plus

In this second phase, we simplified the model so that its representation in both CitySim and Energy Plus are as close as possible. The model is then run over a whole year, without internal gains from equipment and occupants and the results and differences between both software are given in Table 2.

It should be noted here that this is the ideal load needed to heat and cool the building. It can be said that over all the precision of the Energy Plus is slightly decreased as there is a slightly higher energy consumption. There is a difference of around 22% between the energy

consumption between CitySim and the Energy Plus simulation. It should also be highlighted that these differences (not shown here) are similar for the both the heating and cooling period. Through some sensitivity analysis that we have conducted we have shown that Energy Plus seems to have higher solar gains inside the building as compared to CitySim. Additional tests are required here to determine the cause of such differences but as this is not the purpose of this paper, it will be addressed in future work.

	CitySim	**Energy Plus**	**Error (%)**
Total (GJ)	2253.8	1837.5	22
Energy Per Area [kWh/m^2]	62.6	51.0	

Table 2: Difference between Energy Plus and CitySim

Renewable energy integration and storage needs

To estimate the renewable energy potential, solar PV panels are integrated to the STCC and a simulation is done over a whole year. From Figure 2, it can clearly be seen that the summer production is much higher than the winter, while the consumption appears mainly during the winter, due to the heating demand.

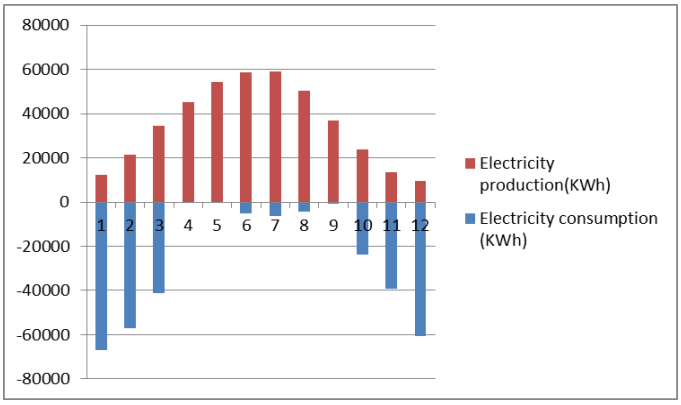

Figure 2: Estimated energy consumption and production

It is thus proposed to use a simple methodology to use this excess summer heat, to heat an underground water tank (with an average yearly ground temperature at 10 °C) of 5m^3 (5000L). In this study, we consider the heat losses to the ground and in the tank but we make the calculation over a whole month. Besides we consider that the accumulated temperature and energy for the first month of the year is equal to the last, so that there is not yearly accumulation.

Table 3 shows the accumulated temperature in a hot water tank. It can clearly be noted that when using such a tank and a system, it is possible to heat a water tank to almost 44 °C. This excess heat can be used thus in the first winter months for heating purposes. It is most likely that additional heating surfaces are needed in order to reach the minimum temperature required for domestic hot water.

Month	1	2	3	4	5	6	7	8	9	10	11	12
Acc. Temp (° C)	30	30	30	32.2	34.7	37.3	39.8	42	43.7	43.7	43.7	30

Table 3 Energy production, consumption and surplus used to heat boiler

CONCLUSION

This study was conducted to analyse the influence of integrating renewable energy in a building to make it autonomous in terms of an energy point of view. Furthermore, we use two distinct models Energy Plus and CitySim to evaluate the energy consumption of a landmark building of the EPFL campus.

First a comparison between Energy Plus simulation and monitored data was conducted. This comparison highlighted the need to account for the user behaviour and other external factors when using building energy simulation tools.

Secondly, we simplified the geometrical model and compared simulation between CitySim and Energy Plus. Although both models gave satisfactory results, it was noted that there could be some significant differences between the ways solar gains are calculated in both models.

Finally, RE sources were integrated and an analysis was conducted to estimate the possibility of using seasonal storage. It was demonstrated that using a simple methodology, the accumulated temperature in the water storage tank can be calculated. More explicit calculation should be done to improve these calculations.

Further works are needed to investigate more in details the reason why CitySim and Energy Plus have some discrepancies. Additional studies should be performed to optimize the actual capacity of the water storage size as well as the possibility to using solar collectors. Besides, this study has now prepared the framework towards co-simulation between the two models working at different spatial scales.

REFERENCES

1. Pachauri, R. K. *et al.* Climate Change 2014: Synthesis Report. Contribution of Working Groups I, II and III to the Fifth Assessment Report of the Intergovernmental Panel on Climate Change. (2014). at <http://epic.awi.de/37530/>
2. ADEME. *Energie et Climat - Edition 2012*. (Agence de l'Environnement et de la Maîtrise de l'Energie, Angers, 2012).
3. Crawley, D. B., Lawrie, L. K., Pedersen, C. O. & Winkelmann, F. C. Energy plus: energy simulation program. *ASHRAE J.* **42,** 49–56 (2000).
4. Kämpf, J. H. & Robinson, D. A simplified thermal model to support analysis of urban resource flows. *Energy Build.* **39,** 445 – 453 (2007).
5. Bruse, M. & Fleer, H. Simulating surface–plant–air interactions inside urban environments with a three dimensional numerical model. *Environ. Model. Softw.* **13,** 373 – 384 (1998).
6. Robinson, D. *Computer Modelling for Sustainable Urban Design: Physical Principles, Methods and Applications*. (Routledge, 2012).
7. Guadalfajara, M., Lozano, M. A. & Serra, L. M. A Simple Method to Calculate Central Solar Heating Plants with Seasonal Storage. *Energy Procedia* **48,** 1096–1109 (2014).
8. Neto, A. H. & Fiorelli, F. A. S. Comparison between detailed model simulation and artificial neural network for forecasting building energy consumption. *Energy Build.* **40,** 2169–2176 (2008).
9. Reglement Marque Minergie 2014-fr.pdf. at <http://www.minergie.ch/tl_files/download_fr/Justificatifs/Minergie/Reglement%20Marque%20Minergie%202014-fr.pdf>

SIZING OF A PHOTOVOLTAIC SYSTEM WITH BATTERY STORAGE: INFLUENCE OF THE LOAD PROFILE

J. Meunier[1,2]; D. Knittel[1,2]; P. Collet[3], G. Sturtzer[2], C. Carpentier[4], G. Rocchia[4], J. Wisse[5], M. Helfter[6]

1: University of Strasbourg, UFR Physique, 3 rue de l'Université, 67000 Strasbourg, France

2: INSA Strasbourg, LGeCo, 24 boulevard de la Victoire, 67084 Strasbourg, France

3: UFR Mathématiques et Informatique, 7 rue R. Descartes, 67084 Strasbourg, France

4: SOCOMEC, rue de Westhouse, 67235 Benfeld, France

5:VOLTEC Solar and VOLTINOV, 1 rue des prés, 67190 Dinsheim-sur-Bruche, France

6: HAGER Electro SAS, boulevard d'Europe, BP3, 67215 Obernai, France

Corresponding author: dominique.knittel@unistra.fr

ABSTRACT

Sizing of an optimal photovoltaic system includes constraints, fitness functions and parameters, which will have more and more importance in the next future: location (and panels direction), autonomy (which is the ratio of the consumed energy covered by the own production), self-consumption (ratio of the produced energy which is consumed by the building), investment capacity, price of the electricity (to buy, to sell), … This sizing depends on the global consumption of the building but also on the associated load profile. For the studied examples, the different load profiles are from the *"Standardlastprofile des Bundesverbandes der Energie- und Wasserwirtschaf", Germany*. The photovoltaic production profile is scaled from a measured production in the Rhine Valley, 2013. The consumption is carried out either by the grid or the battery, and the solar production supplies either the battery or the grid. In the studied application, the battery can only be charged by the photovoltaic energy.

The self-consumption, autonomy and bought electricity are calculated for different PV-storage systems and load profiles. The calculation software has been established in the Matlab environment. In order to obtain significant results, the simulations are conducted over a twenty-six-year period time. The results are analyzed and discussed. For a given configuration, load profile changes may lead to significant self-consumption and autonomy variations.

Keywords: photovoltaic, battery storage, sizing, simulation

INTRODUCTION

With a growing energy demand, renewable energies offer a way to provide energy without draining limited natural resources. But photovoltaic energy is intermittent. To supply at a best level a domestic electricity demand, where the consumption profile differs from the production, there is a need to store the daylight energy production. To satisfy this requirement, batteries are usually used [2, 3, 5]. But the size of the photovoltaic installation (i.e. total PV panel surface) and the size/number of the batteries should be optimized [2, 3, 4, 5, 6, 7, 8, 9, 10].

In this work, a photovoltaic system with batteries is modelled. The influence of different load profiles is then analyzed. The goal is to show that the load profile (and not only the maximum and the average values) has to be taken into account in the optimal sizing of the installation.

METHOD

Simulation model

The modelling software of the photovoltaic system including battery storage, programmed in the Matlab environment, requires electrical load profiles. In this study, the profiles data are from [1], all with a 5000 kWh/year consumption; whereas the photovoltaic production data comes from the Rhine Valley, 2013. All the data have a sampling time of 15 minutes. The studied system uses some photovoltaic panels with a decreasing efficiency of 0.5 % per year and lithium batteries to store the energy. These batteries have a maximum depth of discharge of 75 %, an efficiency of 90 % over a cycle and self-discharge of 1.5 % per day. The different consumption profiles are given below:

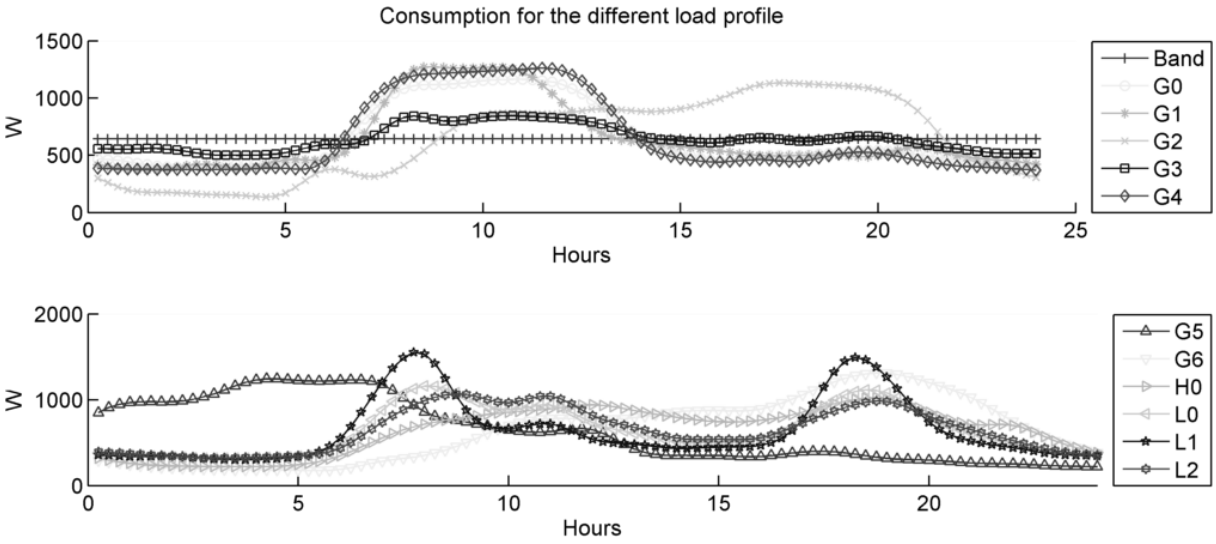

Figure 1: load profiles

Consumption profiles: Band (constant); G0 (Standard commercial); G1 (Commercial weekdays from 8 to 18 hours); G2 (Commercial with severe to predominant consumption in the evenings); G3 (Commercial continuously); G4 (Hairdresser); G5 (Bakery); G6 (Weekend operation); H0 (Household); L0 (Farms); L1 (Farms with sideline animal breeding/ dairy cattle); L2 (Farms without dairy cattle)

The used economic values are realistic values. The installation costs are: 1600 €/kWp for PV panels, 1670 €/kWh for battery storage. Moreover, the power electronic is changed after 13 years with of price of 300 €/kVA. The bought electricity price is 28 cts €/kWh with a rise of 4 % per year and a maximum of 50 cts €/kWh. The sold electricity price is 12.5 cts €/kWh with a lessening of 3 % per year and a minimum of 5 cts €/kWh. The grid subscription is 72 €/kW based on the maximum power required from the grid.

The simulation is conducted over 26 years (25 years warranty period of the PV panels +1 year). For each step time, the load energy is supplied either directly by the photovoltaic panels or by the batteries or by the grid as follow: the solar production is used to supply the load, then to fill the batteries until its maximum state of charge and finally to feed the grid. The

batteries are used to supply the load while it is possible (the minimum state of charge has not to be undercrossed); finally the grid supplies the load.

Criteria : six criteria are used in this study:

- Self-consumption: ratio between produced energy and locally consumed energy (directly by the load or indirectly through the battery to the load). It is calculated over one year and only the first year is plotted.
- Autonomy: ratio between the needed energy and the part of the produced energy that is used locally. It is calculated over one year and only the first year is plotted.
- ROI (Return on investment): number of years for which the cumulated expenses of the PV installation is equal to the cumulated expenses for no installation.
- Number of battery cycles after 26 years (the batteries have 6000 cycles of lifetime).
- Investment: initial cost of an installation depending on the number of photovoltaic panels and the number of batteries.
- Cumulative expenses after 26 years.

RESULTS

The next figures show the six criteria for 3 configurations: 3 kWp of photovoltaic system without any battery (figures 2-3), 3 kWp of photovoltaic system with 3 kWh battery storage (figures 4-5) and 3 kWp of photovoltaic system with 6 kWh battery storage (figures 6-7).

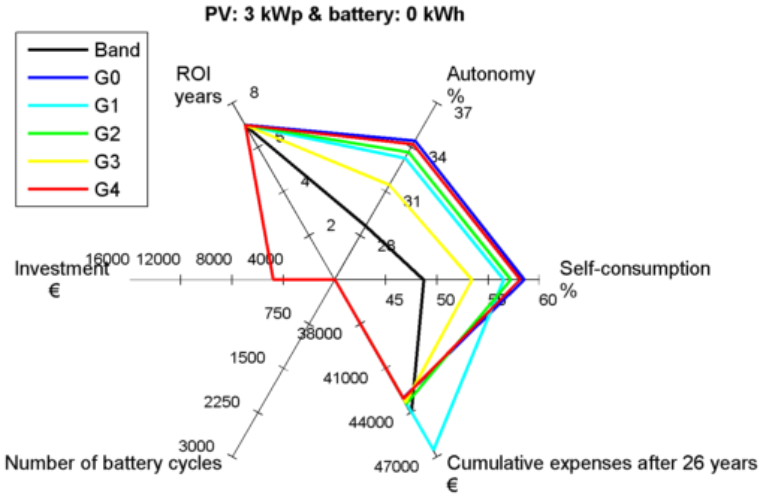

Figure 2: Results for 3kWp- PV, no battery

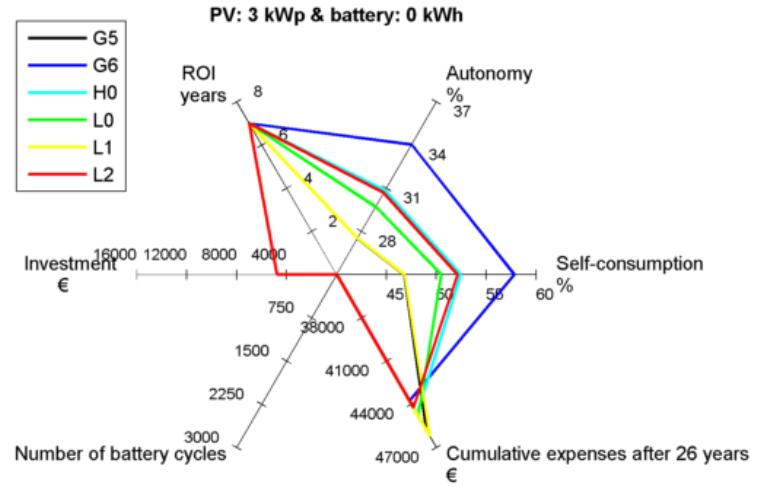

Figure 3: Results for 3kWp- PV, no battery

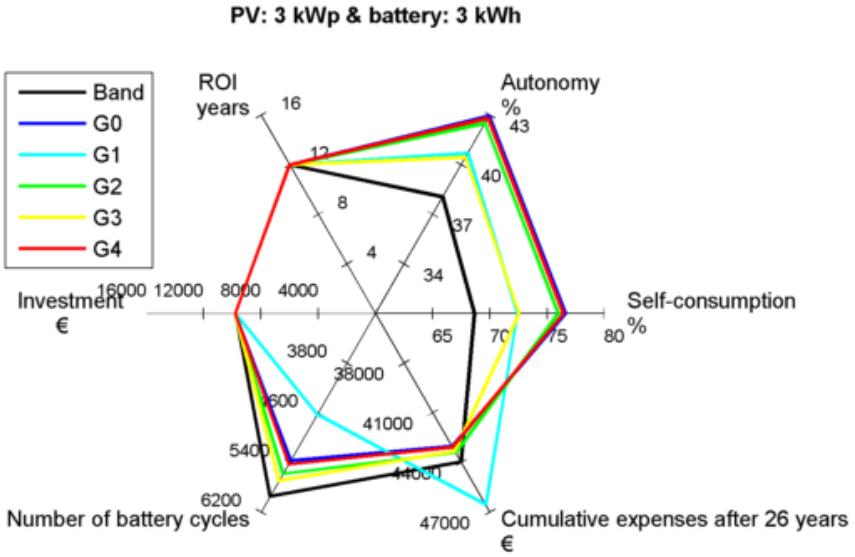

Figure 4: Results for 3kWp- PV, 3 KWh-batteries

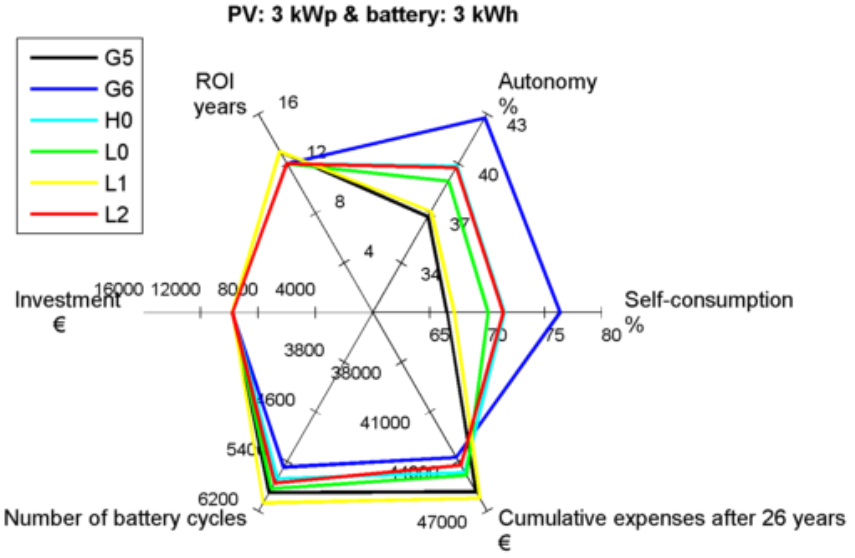

Figure 5: Results for 3kWp- PV, 3 KWh-batteries

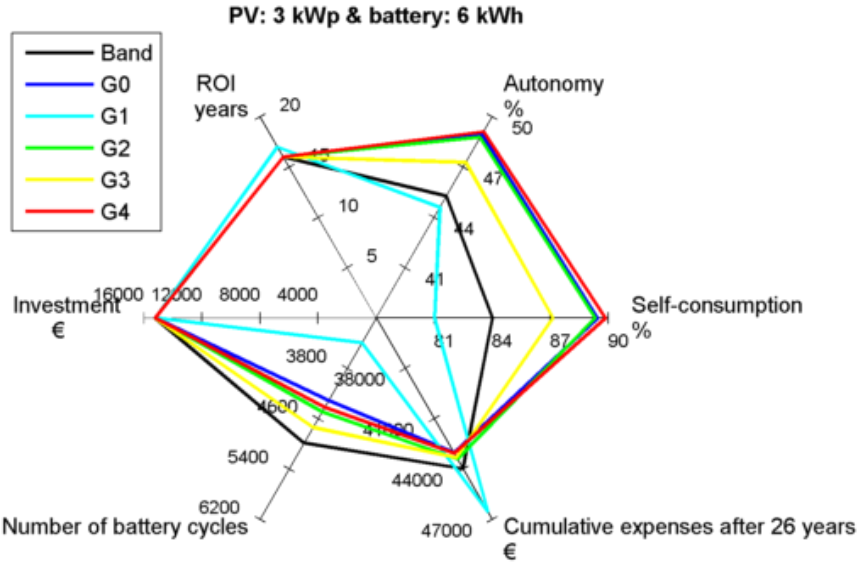

Figure 6: Results for 3kWp- PV, 6 KWh-batteries

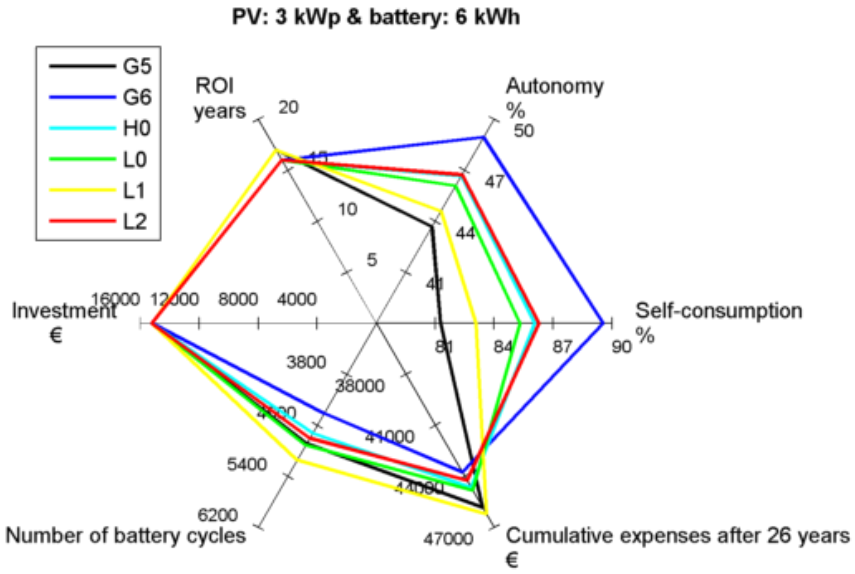

Figure 7: Results for 3kWp- PV, 6 KWh-batteries

DISCUSSION

Configuration 1 : 3 kWp of photovoltaic system without any battery (figures 2-3):

all profiles lead to the same ROI and investment. The cumulative expenses (after 26 years) are quite similar. But there are significant autonomy and self-consumption variations, especially for the band and L1 profiles.

Configuration 2 : 3 kWp of photovoltaic system with 3 kWh battery storage (figures 4-5):

all profiles lead to the same investment, a similar ROI (maximum 1 year difference) and similar cumulative expenses after 26 years. Moreover, the number of battery cycles presents small variations. But there is a wider spreading of the autonomy and self-consumption.

Configuration 3 : 3 kWp of photovoltaic system with 6 kWh battery storage (figures 6-7):

all profiles give the same investment, a similar ROI (maximum 1 year difference) and similar cumulative expenses after 26 years. Moreover, the number of battery cycles presents small variations (except for the profile G1). There are large autonomy and self-consumption variations.

Comparison between the 3 configurations:

- ROI: as expected, the lowest ROI is obtained for configuration 1 and the configuration 3 gives the highest ROI.
- Cumulative expenses after 26 years : quite similar for the 3 cases
- Investment : highest investment obtained for configuration 3
- Number of battery cycles after 26 years : highest value obtained for configuration 2
- Autonomy: highest value obtained for configuration 3
- Self-consumption: highest value obtained for configuration 3

CONCLUSION

This work shows that the load profiles (and not only the maximum or average consumption) play a significant role in different criteria used for PV installation with batteries optimization. For a given configuration, load profile changes may lead to significant self-consumption, autonomy and number of battery cycles variations. But the different profiles lead to small ROI variations (maximum one year of difference).

REFERENCES

1. Standardlastprofile des Bundesverbandes der Energie- und Wasserwirtschaf, http://www.ewe-netz.de/strom/1988.php
2. Yu Ru, Jan Kleissl, Sonia Martinez , Exact sizing of battery capacity for photovoltaic systems, European Journal of Control, vol.20, Issue 1, January 2014, pp 24-37
3. P. Harsha, M. Dahleh, Optimal sizing of energy storage for efficient integration of renewable energy, 50th IEEE Conference on Decision and Control and European Control Conference, 2011, pp.5813–5819.
4. Y.Ru,et al., Storage size determination for grid-connected photovoltaic systems, IEEE Transactions on Sustainable Energy 4 (2013), pp 68–81.
5. G. Shrestha, L.Goel, A study on optimal sizing of stand-alone photovoltaic stations, IEEE Transactions on Energy Conversion 13 (1998), pp 373–378.
6. P. Arun, Rangan Banerjee, Santanu Bandyopadhyay, Optimum sizing of photovoltaic battery systems incorporating uncertainty through design space approach, Solar Energy, vol. 83, Issue 7, july 2009, pp 1013-1025
7. Angel A. Bayod-Rujula, Marta E. Haro-Larrode, Amaya Martines-Gracia, Sizing criteria of hybrid photovoltaic–wind systems with battery storage and self-consumption considering interaction with the grid, Solar Energy, vol. 98, Part C, December 2013, pp. 582-591
8. Luna-Rubio, R., Trejo-Perea, M., Vargas-Vazquez, D., Rıos-Moreno, G.J., 2012. Optimal sizing of renewable hybrids energy systems: a review of methodologies. Solar Energy 86, pp. 1077–1088.
9. Yang, H., Zhou, W., Lu, L., Fang, Z., Optimal sizing method for stand-alone hybrid solar–wind system with LPSP technology by using genetic algorithm. Solar Energy 82 (4), 2008, pp. 354–367.
10. Zhou, W., Lou, C., Li, Z., Lu, L., Yang, H., Current status of research on optimum sizing of stand-alone hybrid solar–wind power generation systems. Applied Energy 87, 2010, pp. 380–389.

ACKNOWLEDGMENT

This work is supported by the French Government (Fonds unique interministeriel, FUI-Solenbat 13), the Hager Company (France), the Socomec Company (France), the Voltec-Solar Company (France), OSEO (France), Région Alsace, Communauté Urbaine de Strasbourg, University of Strasbourg and INSA Strasbourg.

A METHOD FOR GENERATING HOURLY SOLAR RADIATION ON BUILDING ROOFTOPS ACCOUNTING FOR CLOUD COVER VARIABILITY

Miglani, Somil Ajit[1,2]; Orehounig, Kristina[1,2]; Carmeliet, Jan[1]

1: Chair of Building Physics, ETH Zürich, Stefano-Franscini-Platz 5, 8093 Zürich, Switzerland
2: Urban Energy Systems Laboratory, Swiss Federal Laboratories for Materials Science and Technology, Überlandstrasse 129, 8600 Dübendorf, Switzerland

ABSTRACT

Building Integrated Photovoltaic systems (BIPV) are gaining popularity as urban energy systems move towards decentralization. The calculation of the incoming solar radiation for building rooftops at a high temporal resolution is a key input to perform an energy balance of buildings within the larger context of an urban energy planning exercise and to control the supply and demand of energy. Solar radiation on building rooftop surfaces is highly stochastic due to highly variable cloud cover. Hence, for improving the accuracy in calculating the energy potential of BIPV, it is important to incorporate varying cloud cover in the simulation approach. This study presents a GIS based methodology for calculating hourly solar radiation on building rooftop surfaces taking into account the variability in cloud cover. The location of the study is the Fluntern weather station in Zürich, Switzerland. The r.sun module of the open source GIS software suit GRASS is used to calculate the clear sky irradiation (CSR). To account for the cloud cover, a reduction factor called the clear sky index (KC) which is dependent on the cloud cover is applied to the calculated CSR to obtain the real sky radiation. KC is calibrated for different values of cloud cover and time of day using measured meteorological data spanning a time period from 1981 to 2014 from the weather station. The hourly cloud cover is predicted through a discrete state Markov process. KC, the measured cloud cover, the simulated clear sky radiation are then used to obtain the real sky radiation and is validated against the measured values of solar radiation. Results show that the taking into account the cloud cover for calculating radiation reduces the root mean square error and the mean bias deviation by 37% and 86% respectively.

Keywords: Building Integrated Photovoltaics, GIS, Cloud cover, Rooftop solar

INTRODUCTION

As solar technology matures, Building Integrated Photovoltaic (BIPV) systems are becoming more frequently installed. These systems can be installed on building rooftops due to large area availability and be used for the production of a part of a building's electricity and/or heating needs. A detailed energy production profile from the BIPV system is an important input to the design and operation of a building's energy system which consists of multiple energy consuming and producing devices. Hence, it is important to have the knowledge of the amount of solar radiation received by the rooftops at a high temporal resolution. Although the extraterrestrial solar radiation remains constant, the terrestrial radiation exhibits spatial and temporal variability. This variability in solar radiation can be attributed to three factors as listed by Hofierka and Šúri [1]. Firstly, the sun's location in the sky which has a daily as well as a seasonal cycle given a particular geographical location. Secondly, it is affected by the local topography, the orientation of the surface and shadowing effects from neighboring structures. Thirdly, the atmospheric attenuation caused by scattering and absorption by particles and clouds in the local sky cause the radiation to become highly variable. The high intermittency of the solar radiation can be attributed to the stochastic nature of the local atmospheric conditions especially cloud cover. This emphasizes the need for incorporating the cloud cover variability in the calculation of the net solar radiation received by rooftops.

There are several studies conducted in the past that utilize a Geographical Information System (GIS) based approach to calculate solar radiation for building rooftops [2-6]. Chow and Fung [2] use a 2.5D Digital Elevation Model (DEM) to represent the local topography and the building topologies. They use a hemispherical viewshed algorithm implemented in Esri's Solar Analyst plugin, to calculate hourly solar radiation taking into account local terrain effects. Atmospheric conditions are modeled using constant values of transmissivity and diffuse proportions. Kodysh et.al. [3] use the same algorithm using a LiDAR based DEM for daily/monthly averages of solar radiation. Agugiaro et. al. [4] use the *r.sun* algorithm [1] implemented in the GRASS GIS open source software suit for spatial analysis. It is also a DEM based algorithm which takes into account the local terrain and shadowing effects. Local atmospheric conditions are modeled using a parameter named Linke Turbidity. Jakubiec and Rheinhart take in their study [6] a different approach towards computing hourly solar radiation on building rooftops. They use a 3D model of the buildings and a Typical Meteorological Year (TMY) instead of a DEM and a ray tracing algorithm called DaySim. The hourly cloud cover is not modeled in any of the listed studies to calculate the solar radiation.

METHOD

Against this background, a method is developed to compute hourly solar radiation on rooftop surfaces taking a DEM based approach. The *r.sun* algorithm is applied to calculate the clear sky radiation on building's rooftop surfaces. To further compute real sky radiation data taking variations of cloud cover over the year into account, an attenuation factor called the clear sky index (K_C) is used which is calibrated with available measurement data from a nearby weather station. Available past data on cloud cover for the specific weather station location are additionally analyzed and hourly cloud cover values are predicted using a Markov process. The predicted cloud cover values and the calibrated K_C are used in the second step to calculate the real sky radiation on the roof surfaces. The method is deployed at the location Zurich Fluntern and validated using measured data.

Meteorological data from the IDAWEB service hosted by the Swiss Federal Office of Meteorology and Climatology, MeteoSwiss [7] are used. Hourly time series for sunshine duration and Global Horizontal Radiation (GHR) at the Fluntern weather station are extracted from this database spanning a time period from 1981 to 2014, to be used as inputs to this study.

Cloud Cover Prediction

A first order discrete state Markov process is modeled to predict the hourly values of local cloud cover using historical meteorological data from the Fluntern weather station. There have been previous studies conducted using a similar approach [8, 9]. This model assumes that the future state of the cloud cover is dependent only on the current state (memoryless property) and the preceding states have no influence on it. This method of modeling of cloud cover enables capturing historic information of the general cloud cover patterns and using it for prediction rather than using point data from a specific year.

Cloudiness, is a meteorological variable that is most commonly used to represent cloud cover and is measured at most weather stations. Since the cloudiness data was only available at a three hourly resolution it could not be used in this study. Instead, sunshine duration (SD) is used to represent cloud cover (CC). Neske [10] validates the linear relationship between cloudiness and sunshine duration for Hamburg. This linear relationship is as well concluded by Badescu in [11] analytically and validated for Romania. Based on the above studies SD is assumed to be representative of the local cloud cover as described by equation (1). SD is usually measured using a pyranometer which gives an advantage of lower levels of uncertainty as opposed to manually observed cloudiness.

$$CC(t) = 1 - \frac{SD(t)}{60} \quad (1)$$

To generate hourly patterns the state space of the Markov process which consists of ten discrete cloud cover levels ranging from 1 to 10 is used. The cloud cover fraction is classified into ten equal intervals of size 0.1 and allotted the corresponding next higher state (for instance, 0.24 is

allotted state 3). The SD time series data is converted to cloud cover states and is used to construct a first order, monthly state transition probability matrices. These matrices are then used to predict the hourly cloud cover time series.

Solar Radiation Modeling

In the second step the clear sky index (K_C) is calculated. K_C is defined as the ratio between the GHR for a given cloud cover to the CSR.

$$Kc(cc,t) = \frac{GHR(cc,t)}{CSR(t)} \quad (2)$$

Whereby clear sky radiation (CSR) is defined as the radiation received by the surface after scattering from the atmosphere without the presence of any clouds and real sky radiation is defined as the net GHR received by a surface after taking into account the attenuation from clouds.

A GIS based workflow is implemented to calculate the hourly radiation values for the rooftop of the Fluntern weather station building. The workflow is implemented in the open source GIS software suite called GRASS GIS which implements the *r.sun* algorithm. This algorithm takes into account the solar position for each time step, shadowing effects from local terrain features and surrounding topography and atmospheric scattering. The key input parameters for this model are; timestamp (hour, day of the year), DEM (constructed from a 3D model of the building), Linke turbidity and albedo. The monthly Linke turbidity values are obtained for Zürich from the global solar radiation database SoDa [12]. A constant value of 0.2 is used for albedo. To decrease computational time, the DEM consists only of the rooftop area of the weather station and not the surrounding terrain as shown in figure 1. This eliminates the shadow effect from the surrounding terrain. This is justified after the visual observation of the topography on the region reveals a flat horizon and no obstructing topographic features especially in the south direction. The result of this calculation is the CSR value averaged over the whole rooftop for each hour in kWh/m^2.

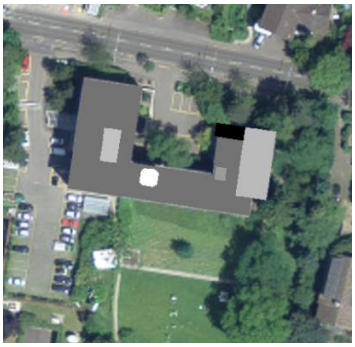

Figure 1: The Fluntern weather station building represented as a Digital Elevation Model (DEM) overlaid on an aerial image

Clear Sky index (Kc) calibration

The hourly time series of the measured GHR, the calculated CSR and the measured cloud cover are used to calibrate the Kc values. The entire dataset is split into two parts; for calibration (1981-2013) and for validation (2014). Kc is calculated for each hour of the calibration dataset. There are some data entries for which the value of the clear sky index exceeds 1, infinite or is negative. These values are eliminated from the calibration process. The rest of the dataset is then used to calculate monthly means of K_C for each cloud cover state and hour of the day. The seasonal variation of KC is taken into account by defining seasons as winter (December, January, February), spring (March, April, May), summer (June, July, August) and autumn (September, October, November).

Real sky radiation

The real sky radiation is obtained using equation (2) for a given cloud cover and hour of day using calibrated K_C. Two hourly datasets for the real sky radiation are created. One each from measured cloud cover and predicted cloud cover. The real sky radiation dataset calculated from measured

cloud cover is used for validation of GHR and eventually K_C. Since the predicted cloud cover is stochastic direct validation of real sky radiation values produced from it is not performed.

RESULTS & DISCUSSION

Cloud cover prediction

The hourly cloud cover as predicted by the Markov process is compared with the hourly cloud cover measured at the weather station in figure 1. A perfect match of the cloud cover is not expected since it is predicted through a stochastic process. However, visual observation suggests a general agreement of the measured and predicted values.

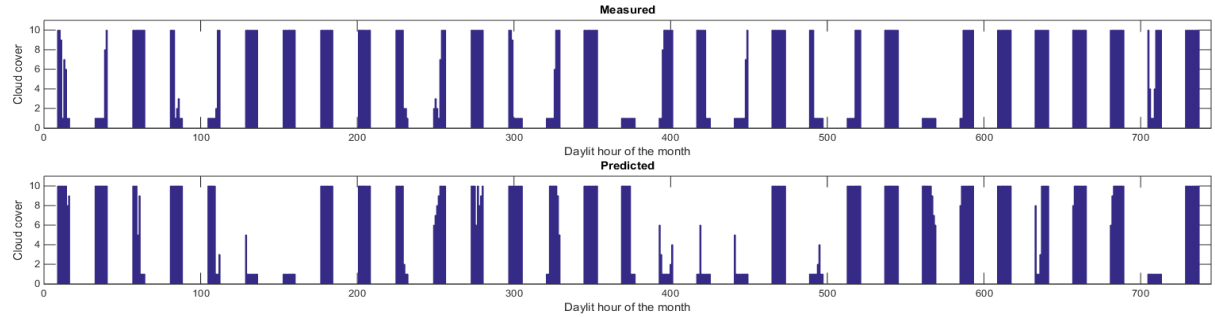

(a)

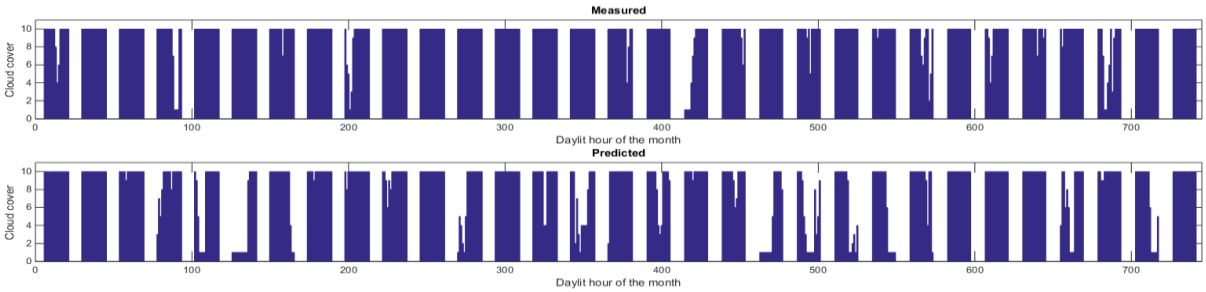

(b)

Figure 2: Measured vs predicted cloud cover (discrete states 1-10) for (a) January 2014 and (b) July 2014

Clear Sky Index (K_C)

The comparison of the mean K_C values obtained from the calibration procedure is shown in figure 3. The clear sky index exhibits variations with cloud cover, time of day as well as seasonal variations.

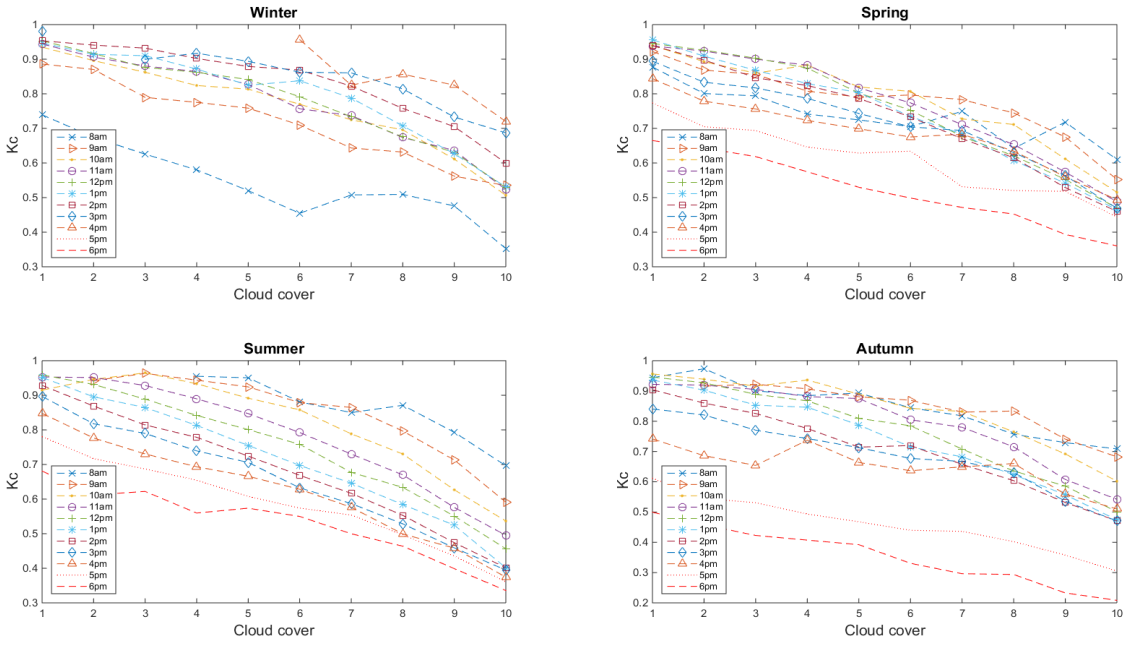

Figure 3: Comparison of clear sky index mean values as a function of cloud cover state and time of day for different seasons.

Validation

The real sky radiation calculated using the measured cloud cover and calibrated K_C is validated against the measured GHR obtained from the weather station database. A comparison of the measured vs predicted GHR is shown in figure 4. The root mean square error (RMSE) and the mean bias deviation (MBD) of the predicted values are 42.62% and 18.54%.

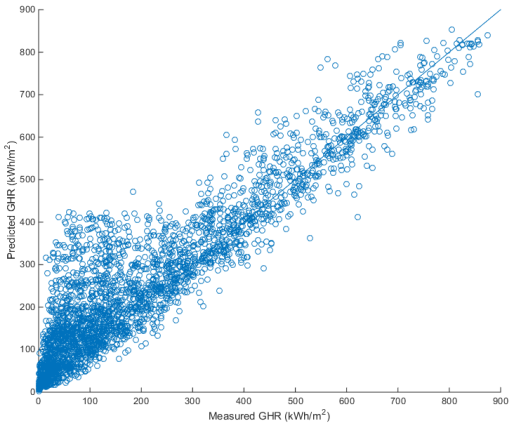

Figure 4: Measured vs predicted GHR in kWh/m^2

Real sky radiation

Figure 5 (a) shows a comparison of the measured GHR and the clear sky radiation calculated using the GIS workflow without taking cloud cover adjustment into account for January 2014. . The percent RMSE and the MBD of the CSR and the real sky radiation is 119.75% and +47.68% respectively It is observed that the CSR over predicts the real sky radiation. Hence, cloud cover attenuation must be applied. Figure 5(b) shows the real sky radiation using the predicted cloud cover from the Markov process for the same month. The RMSE and MBD for this case are 74.64% and +6.73%. The values of RMSE and MBD are not expected to be low because the predicted cloud cover is stochastically generated. However, the reduction in RMSE and the MBD shows that the incorporation of cloud cover reduces the error. The MBD is still positive indicating an overprediction but it is considerably reduced.

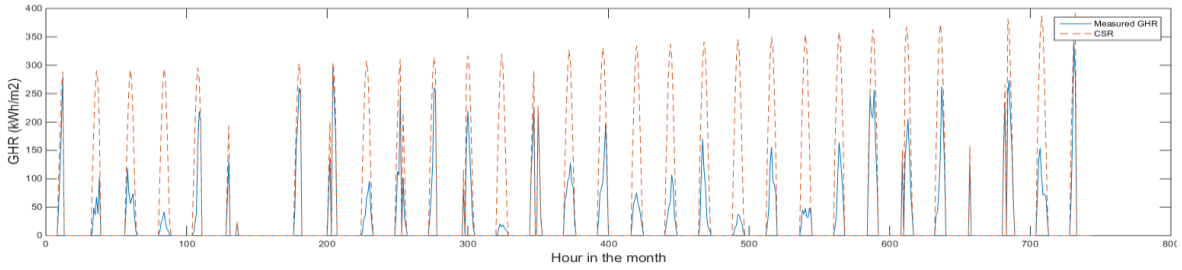

(a)

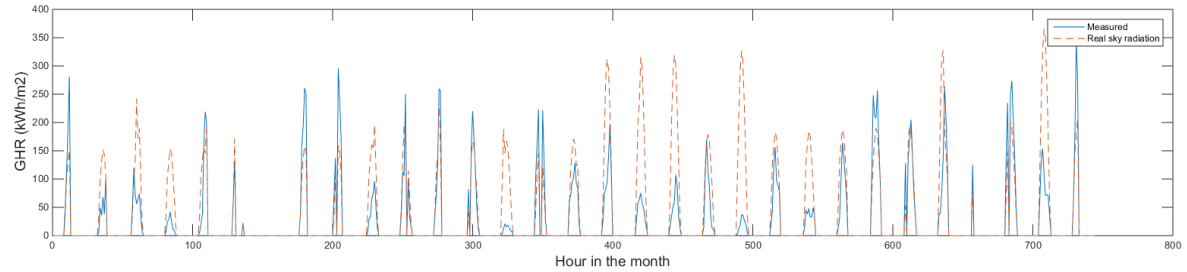

(b)

Figure 5 Comparison of the measured GHR with (a) Clear sky radiation (No cloud cover) (b) Real sky radiation (cloud cover from Markov process)

CONCLUSION

A GIS based method for solar radiation calculation combined with a cloud cover prediction model is used in this study to calculate the incoming solar radiation on a building rooftop on an hourly basis. The data generated is useful for applications such building control system in order to manage the mismatch of energy supply and demand in a building if decentralized energy technologies are integrated. The results show that the solar radiation calculated without the consideration of clouds over predicts the actual radiation received by the rooftop. However, taking into account the cloud cover the error in prediction reduces.

ACKNOWLEDGEMENT

This research in the present contribution was funded in part by SCCER "Future Energy Efficient Buildings and Districts".

REFERENCES

[1] Hofierka, J., & Šúri, M. (2002). The solar radiation model for Open source GIS : implementation and applications. Computing, (September), 11–13.

[2] Chow, A., Fung, A., & Li, S. (2014). GIS Modeling of Solar Neighborhood Potential at a Fine Spatiotemporal Resolution. Buildings, 4, 195–206.

[3] Kodysh, J. B., Omitaomu, O. a., Bhaduri, B. L., & Neish, B. S. (2013). Methodology for estimating solar potential on multiple building rooftops for photovoltaic systems. Sustainable Cities and Society, 8, 31–41.

[4] Agugiaro, G., Nex. F., Remondino, F., De Filippi, R., Droghetti, S., & Furlanello, C. (2012). Solar Radiation Estimation on Building Roofs and Web-Based Solar Cadastre. ISPRS Annals of Photogrammetry, Remote Sensing and Spatial Information Sciences, I-2(September), 177–182.

[5] Hofierka, J., & Kaňuk, J. (2009). Assessment of photovoltaic potential in urban areas using open-source solar radiation tools. Renewable Energy, 34, 2206–2214.

[6] Jakubiec, J. A., & Reinhart, C. F. (2013). A method for predicting city-wide electricity gains from photovoltaic panels based on LiDAR and GIS data combined with hourly Daysim simulations. Solar Energy, 93, 127–143.

[7] IDAWEB, Swiss Federal Office of Meteorology and Climatology, MeteoSwiss.

[8] Morf, H. (2011). The Stochastic Two-State Cloud Cover Model STSCCM. Solar Energy, 85(5), 985–999.

[9] Morf, H. (2014). Sunshine and cloud cover prediction based on Markov processes. Solar Energy, 110, 615–626.

[10] Neske, S. (2014). About the Relation between Sunshine Duration and Cloudiness on the basis of data from Hamburg, 2014.

[11] V. Badescu, "Use of sunshine number for solar irradiance time series generation," in Modeling Solar Radiation at the Earth Surface, pp. 327–355, Springer, Berlin, Germany, 2008.

[12] Wald, L., 2000, SODA: a project for the integration and exploitation of networked solar radiation databases. European Geophysical Society Meeting, XXV General Assembly, Nice, France, 25-29 April 2000, http://www.soda-is.com/.

NEW GENERATION OF A HIGHLY COMPACT SOLAR HEAT PUMP SYSTEM WITH BOOSTED ENERGETIC EFFICIENCY

I. Mojic[1]; M.Y. Haller[1]; B. Thissen[2]; F. Hengel[3], A. Heinz[3]

1: Institute for Solar Technology SPF, HSR University of Applied Sciences, Oberseestrasse 10, CH-8640 Rapperswil, +41 55 222 41 62

2: Energie Solaire S.A., Rue des Sablons 8, Case postale 353, CH-3960 Sierre

3: Institute of Thermal Engineering IWT, Graz University of Technology, Inffeldgasse 25B, A-8010 Graz

ABSTRACT

In this work a new highly compact solar thermal heat pump system for space heating and domestic hot water preparation will be presented in detail. It was developed within the European project "MacSheep". The aim of the project is to build four different solar heat pump systems, which achieve 25 % electric energy savings compared to the state of the art solar heat pump heating systems, while still being cost-competitive. Within the MacSheep project, four different developing groups developed different system concepts to reach this project goal. The system, which is presented in this paper, was developed and designed by the following partners; Energie Solaire SA (industrial partner), Institute of Thermal Engineering (research partner) and the Institute for Solar Technology SPF (research partner).

A key component of the system is a novel brine-to-water heat pump prototype with a speed controlled compressor, an economizer refrigerant cycle and a desuperheater. The heat pump was optimized for low source temperatures, in order to be compatible with concepts that use only unglazed selective collectors as heat source. A key element was the integration of heat pump, storage, and hydraulic connections into one compact system design. Further developments are: a combi-storage, which is optimized for heat pump use, and selective unglazed collectors with a new selective coating. The compact designed heat storage, heat pump and hydraulic solution is placed under one high performing insulating shell built of vacuum insulation panels.

The annual simulation results, which were validated with component tests in the lab, show very promising results for the whole system. The electric savings compared with the state of the art system are expected around 28 % and the improvement of the seasonal performance factor (SPF) of the whole system is around + 40 %. These values will be compared with a whole system hardware in the loop benchmark test in autumn 2015.

Keywords: Solar, Heat Pump, Vacuum Insulation Panels, Desuperheater, Economizer

INTRODUCTION

Within the European project "MacSheep" four developing groups, made up of different research institutes and private companies, have developed each a solar heat pump system for space heating and domestic hot water preparation. The aim was to achieve 25 % electric energy savings, compared to what was the state of the art for solar and heat pump systems at the beginning of the project in 2012. At the same time, the aim was to achieve this without an increase in system cost. In this paper we will present the developed system of one of the four groups, which is represented by the authors of this work.

The newly designed system consists of the following improved or newly developed components:

- variable speed heat pump (HP) with economizer and desuperheater cycle, developed by IWT,
- unglazed selective solar absorbers with new coating that leads to significant cost savings (heat source for the heat pump), developed by Energie Solaire SA,
- thermal combi-storage optimized for heat pump use, featuring enhanced stratification even with high inlet mass flows, developed by SPF,
- high efficiency storage insulation built with vacuum insulation panels (VIP), by SPF,
- hydraulics and control solution that allows the heat pump to serve directly space heating without using the storage for most of the year – compatible with all kinds of heat distribution systems, developed jointly by SPF and IWT.

Unique on this system is that all hydraulic components such as pumps, valves, heat exchangers and the heat pump itself are under the same VIP insulation as the storage unit. Thus, a very compact system can be built with a high degree of pre-fabrication, resulting in much faster and less fault-prone installation in the field. Figure 1 shows the design concept of the system.

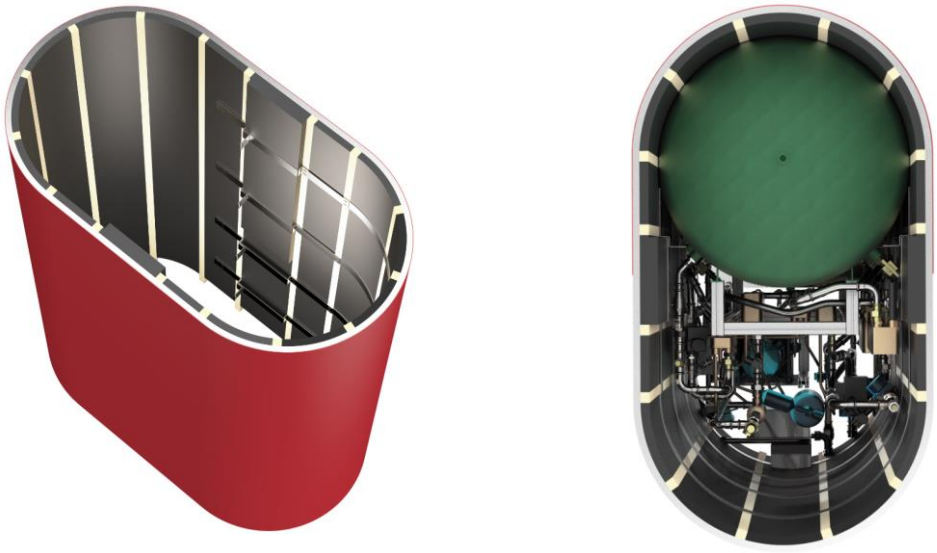

Figure 1: Design of the insulation of the system shown without hydraulic components (left) and with components (right).

Figure 2 shows the square view diagram [1] of the system concept. The main functionality of the system can be described as follows: The heat source of the heat pump - in this particular case - are selective unglazed collectors. If the collector temperature level is high enough and the heat pump is not running, the collectors can load the storage directly. However, it is possible to modify the heat pump source by minor hydraulic changes to a ground source heat pump system, PVT, or ice storage system, alternatively. The heat pump cycle is equipped with a speed controlled compressor and with an additional suction port for vapour injection via an economizer cycle with a plate heat exchanger. A Desuperheater is used to transfer heat from the superheated refrigerant vapor to water for DHW preparation at relatively high temperatures as a by-product of space heating operation. The water side of the condenser is connected to the space heating loop. This is mainly charged directly by the heat pump, without using the storage. Also if enough solar energy is stored in the combi-storage, the

space heating can be loaded directly by the tank. For the hot water preparation a domestic hot water module is used. More details on control and the system concept can be found in [2].

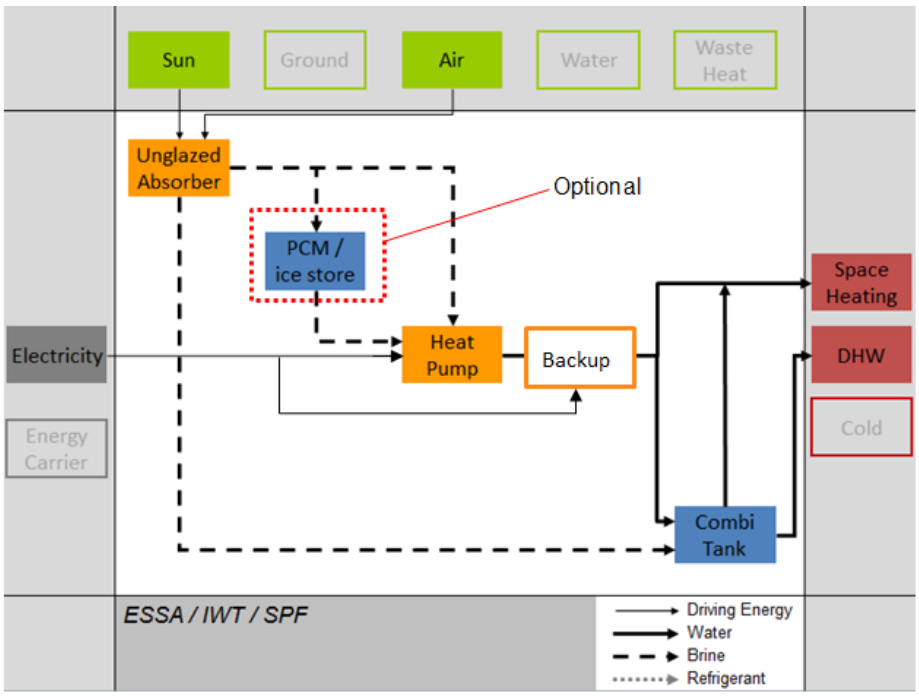

Figure 2: Square view diagram of the concept developed by ESSA, IWT and SPF [1].

METHOD

General

Within the first and second phase of the MacSheep project in the year 2012, breakthroughs for materials, components and control that lead to higher energetic performance and/or lower cost of the system were analysed and selected. The effect of potential breakthroughs on the energetic performance was determined by annual simulations. In phase three of the project (2013-2014) the promising breakthroughs were built into real components and tested in the laboratories. The test results were used to validate and calibrate the component models for the annual simulation. In phase four of the project (2015) a whole system test method will be used to test the complete system and confirm the energetic performance and functionality of the overall system. All performance results are compared with a state of the art solar – heat pump system which is available on the market and which has been tested with the whole system test method in the first year of the project [3].

Simulation

The annual whole system simulation was done with TRNSYS 17. The following components of the system were built and tested in the laboratory separately: unglazed selective collector, heat pump, combi-storage and the domestic hot water module. With the results from the component testing the simulation was validated and calibrated to get realistic results for the whole system. Table 1 shows the main components and their key figures.

Two different climates and two different buildings have been simulated and compared with the reference system. The building heat load (SH) and the domestic hot water demand (DHW) were based on IEA Task44/Annex38 [8] for a single family house (SFH) with 45 kWh/(m^2a)

and a retrofit house with 100 kWh/(m^2a). Details about the boundary conditions and the reference system can be found in [2].

Component	Size	Type	Parameters	TRNSYS Model
Collector	26 m^2	Unglazed Selective Collector	η_0 = 0.954 [-] b_0 = 0.01 [s/m] b_1 = 11.96 [W/(m^2K)] b_2 = 2.904 [W/(m^2K^2)] α = 0.917 [-] ε = 0.26 [-]	Type 202 [4]
Heat Pump	Heating Power 4.9 kW / B0W35 @ 3600 rpm	Variable Speed, Economizer, Desuperheater	COP 4.0 / B0W35	Type 877 [5]
Storage Tank	Volume 750 l	Combi Storage	Heat Losses 3.91 kWh/day (Whole Store at 60°C, not including all hydraulics)	Type 1924 [6]
Solar Heat Exchanger	1.22 m^2	External Flat Plate	U_A-Value 3135 W/K	Type 5b
DHW Heat Exchanger	0.95 m^2	External Flat Plate	U_A-Value 3914 W/K	Type 805 [7]

Table 1: Key components summarized with their key figures.

Testing

A new harmonized dynamic system test method for heating systems was developed and will be applied by the institutes SERC and SP from Sweden, INES from France and SPF from Switzerland. The new method combines the advantages of the different methods that existed before the MacSheep project. The new method is a benchmark test, which means that the load for space heating and domestic hot water preparation is identical for all tested systems, and that the result is representative for the performance of the system over a whole year. Thus, no modelling and simulation of the tested system is needed in order to obtain the benchmark results for a yearly cycle. This is a significant step forward, since the method is now also applicable to products for which simulation models are not available yet. More information and details about the dynamic system test method can be found in [3]. The new developed heat pump was tested under steady state conditions, whereby 58 measuring points were recorded. Additionally to the steady state measurements, dynamic tests with varying operating conditions were carried out. These results were used to validate and parametrize the simulation model of the heat pump.

RESULTS

Heat Pump

Table 2 shows the results of the steady state heat pump measurements for different realistic operating conditions. The results show that with very low source temperatures ($T_{brine,in}$) of −15 °C and condenser water outlet temperature of 34 °C ($T_{cond,out}$) the heat pump still achieves a COP of 2.8. Even at higher condenser water outlet temperatures (48 °C) for DHW

preparation a COP of 2.3 can be reached. These remarkable results can be explained with the implementation of the economizer cycle. However, for the most time of the year much higher brine temperatures can be expected, leading to higher COP's between 4.4 and 5.9. Dynamic test results can be found in [9].

n_{comp}	$T_{brine,in}$	$T_{cond,in}$	$T_{cond,out}$	$T_{DES,out}$	$Q_{cond,sh}$	$Q_{DES,dhw}$	P_{el}	COP
[rpm]	[°C]	[°C]	[°C]	[°C]	[kW]	[kW]	[kW]	[-]
4800 a)	-15	45	48.1	92	3.0	1.9	2.20	2.3
5400 b)	-15	30	34	80	3.9	1.2	1.85	2.8
3000 b)	2	23	28	58	3.9	0.5	0.88	5.0
2400 b)	2	30	33	62	3.0	0.6	0.81	4.4
2400 b)	15	30	34	57	3.9	0.6	0.77	5.9

Table 2: Results of the steady state heat pump measurements for different operating points. a) domestic hot water preparation, b) space heating mode with parallel preparation of domestic hot water (desuperheater)

Whole System Simulation

Table 3 summarizes the results from the annual system simulations with validated parameters of the components. The difference to the reference system is shown in brackets. The key figures here are the seasonal performance factor (SPF) of the whole system, the electricity use ($W_{el,SHP+}$) including the electricity demand of controller, valves and pumps, according to the definitions of the IEA SHC Task 44 [8]. Also the design flow temperature (T_{Fl}) and the design return temperature (T_{Rt}) of the heating distribution are shown. The results show for both climates and heat loads a significant improvement. A further interesting result is that the heat pump in the annual simulation for Zurich SFH45 shows only 21 activations for direct DHW charging (the rest is covered by solar and the desuperheater), which leads to an annual heat pump SPF of 4.03.

	Zurich SFH45	**Zurich SFH100**	**Carcassonne SFH45**	**Carcassonne SFH100**
SPF_{SHP+} [-]	4.48 (+40.5 %)	3.21 (+32.0 %)	5.16 (+34 %)	4.01 (+36.9 %)
$W_{el,SHP+}$ [MWh]	2.52 (-28.8 %)	6.28 (-24.7 %)	1.15 (-30.6 %)	2.82 (-30.5 %)
T_{Fl} / T_{Rt} [°C]	35 / 30	55 / 45	35 / 30	55 / 45

Table 3: Key performance figures for the optimized system, with difference compared to reference system given in brackets (the new system is optimized and designed for Zurich SFH45).

CONCLUSION

The obtained results (HP) from the daily tests (dynamic) and static tests show a satisfying performance of the heat pump prototype and its control. Also the vacuum insulation shell, the storage stratification, the new absorber development, and the hydraulic concept show very promising results. All these components combined and simulated in an annual simulation

show that the goals of the project (-25 % electricity demand) can be achieved or even exceeded. Thanks to the hydraulic concept in combination with the direct solar energy contribution to the storage and the desuperheater loop, exclusive DHW charging by the heat pump can be reduced significantly to 21 times per year, compared to common heat pump systems which have 1 – 2 charging cycles per day. This leads to a very good annual HP SPF because the heat pump does not have to work with high condensation temperatures. The heat losses of the storage system seem high with 3.91 kWh/day, but it has to be considered that the outer insulation surface area is almost doubled compared to common storages, and that this includes at the same time the heat losses of all component of the heat pump, solar pump group, and hydraulics.

While this paper is written the MacSheep system is prepared for the whole system test in the SPF test bench. The final results are expected in autumn 2015 and will be published by end of the year 2015.

ACKNOWLEDGEMENTS

The research leading to these results has received funding from the European Union's Seventh Framework Programme FP7/2007-2013 under grant agreement n° 282825 – Acronym MacSheep.

REFERENCES

1. Frank, E., Haller, Y. M., Herkel, S. & Ruschenburg, J., Systematic Classification of Combined Solar Thermal and Heat Pump Systems. In: Proc. of the EuroSun Conference, Graz, Austria, 2010.
2. Bales, C. et al.: Optimized Solar and Heat Pump Systems, Components and Dimensioning. MacSheep Deliverable 7.3, http://macsheep.spf.ch, 2014.
3. Haberl, R. et al.: Testing of Combined Heating Systems for Small Houses: Improved Procedures for Whole System Test Methods. MacSheep Deliverable 2.3, http://macsheep.spf.ch, 2015.
4. Bertram, E., Glembin, J., Scheuren, J., Rockendorf, G.: Condensation Heat Gains on Unglazed Solar Collectors in Heat Pump Systems. In: Proc. of the EuroSun Conference, Graz, Austria, 2010.
5. Heinz, A., Haller, Y. M.: Appendix A3 - Description of TRNSYS Type 877 by IWT and SPF. In: Models of Sub-Components and Validation for the IEA SHC Task 44 / HPP Annex 38 - Part C: Heat Pump Models - DRAFT - A technical report of subtask C Deliverable C2.1 Part C, 2012.
6. Haller Y. M., & Carbonell, D.: TRNSYS Type 1924 v3.1 - Stratified Plug Flow Solar Combi-Store Model. Institute for Solar Technology SPF, Switzerland, 2014.
7. Haller, Y. M.: TRNSYS Type 805 "DHW Heat Exchanger without Heat Losses". Institute of Thermal Engineering IWT, Austria, 2006.
8. Haller, .Y. M., Dott, R., Ruschenburg, J., Ochs, F. and Bony, J.: IEA-SHC Task 44 Subtask C technical report: The Reference Framework for System Simulations of the IEA SHC Task 44 / HPP Annex 38: Part A: General Simulation Boundary Conditions, IEA-SHC, Paris, www.iea-shc.org/task44, 2012.
9. Heinz, A. et al.: Final Report on Heat Pump Developments in WP 4. Macsheep Deliverable 4.4, http://macsheep.spf.ch, 2014.

DESIGN PROCESS FOR OPTIMIZATION OF BUILDINGS FAÇADES FOR SOLAR IRRADIATION IN THE BRAZILIAN CONTEXT

MORAES, Leticia Niero[1]; PEREIRA, Fernando Oscar Ruttkay[1]

1: Federal University of Santa Catarina, Brazil, letinierom@gmail.com

ABSTRACT

This paper shows the development of a process for solar potential optimization for non residential buildings in a high density urban area in the Brazilian context. Photovoltaic systems are generally installed on roof tops of buildings located in low density areas due to the availability of horizontal surfaces, but the developments of cities with tall buildings have encouraged photovoltaic integration on façades. A parametric solar design optimization is proposed, with the aid of the Rhinoceros 5.0 modelling tool, the plug-ins Grasshopper and Galapagos, which enable geometric transformations and optimized results and solar dynamic plug-in (DIVA for Rhino) for solar radiation analysis. The optimization criterion is based on the economic viability of the installation, through a minimum level of solar radiation that allows the investment return. The approach aims to maximize the solar access of a new building in existing urban area in Florianopolis – SC/Brazil, in the central area of the city. In this area, a reference building is chosen to analyze the influence of urban context on the solar radiation availability. From a reference shape, modelled in accordance with the occupancy limits from current Master Plan, different combinations of parametric transformations were tested: Twist, Slope, Rotation and Taper. The optimization process resulted in a larger area of the envelope with radiation levels above the fitness value.Through this process it was possible to identify the optimized building shape for solar radiation and to verify if façades can be exploited for energy production in dense urban areas in the Brazilian context. Due to the large energy concerns in Brazil and the great potential of using solar energy due to high solar radiation levels, studies that enhance the use of alternative renewable energy are fundamental to the dissemination of this potential.

Keywords: Urban environment, Brazilian context, Solar radiation, Optimization process

INTRODUCTION

In the context of increasing concern with regard to carbon emissions and global warming, interest in renewable energy sources has grown. Due to the significant contribution of buildings energy use, which corresponds to 47% of total electricity consumption in Brazil [1], there is a great interest to promote the use of renewable technologies integrated into buildings. Brazil is a country with high solar radiation levels, higher than those of developed countries, with great potential for solar energy use through photovoltaic systems (PV). With the inevitable verticalization of urban centres, there is a smaller area available on the roof. It is therefore possible to explore the potential of the façades for solar energy production.

Specifically for PV installations on facades, the condition of solar radiation exposure in urban areas is difficult to assess, especially in already established urban contexts. However, the literature discloses a wide variety of analysis tools and methodologies, which contributes to the verification of such conditions. Recent advances in computer science and performance requirements have driven the development of simulation methods to improve building performance, such as the approach known as generative systems, or parameterization and optimization processes. The more than two hundred articles review of major magazines

referenced in the areas of renewable energy and computational optimization revealed that the number of research papers using optimization methods to solve the problems of renewable energy has increased dramatically in recent years, especially in the areas of solar energy and wind [2]. Among the tools available, the plug-in Grasshopper for Rhinoceros [3] allows the generation of parametric models. Simulations of daylight availability and internal loads are performed in Diva-for-Rhino plug-in [4], which integrates thermal simulations of Energy Plus with the daylight availability simulations of Daysim. Within Grasshopper, the optimization process can be performed through the Galapagos Evolutionary Solver [3] which is based on a genetic evolutionary algorithm of random sampling. Several studies have demonstrated the potential use of the tool to perform analyses of envelopes, focusing on optimizing energy or visual aspects [5, 6]; or in solar radiation availability assessments in urban environment [7, 8, 9, 10]. These last studies often use the ECOTEC tools or Diva plug-in for the sun exposure parameter.

In this context, this paper develops a procedure to optimize the building shape considering the impact of the built environment on availability of solar radiation in the Brazilian context, through an innovative parameter of economic feasibility of the installation as fitness value, which differs in optimization studies found in the area.

METHOD

A case study in the city Florianopolis – SC/Brazil is here presented, and an optimization process approach is described, in order to maximize the solar access and solar potential in an existing urban area. A current urban area was selected. The definition of this area considered as the main condition, besides the choice of non-residential areas, the central location area which allows greater height for the building - contextualizing the feasibility of implementation of PV systems on the facades, as more low-rise buildings are more influenced by the surrounding shading. In this scenario a reference building (OI_Reference) was selected to analyze the obstructions impact on solar irradiation levels in the facades. Figure 1 shows the location of the area and the site selected for the reference building. The Master Plan zoning defines much of the area as Mixed Central Area (AMC) - high density, complexity and miscegenation, aimed at, commercial and service. The site selected for the reference building is a corner site with an existing commercial building.

(a) *(b)*

Figure 1: (a) Perspective (b) Master Plan zoning – identifying the Impact Object (OI)

The selected program for modelling of urban setting was Rhinoceros 5.0, mainly due to the integration with plug-ins DIVA, Grasshopper and Galapagos, which will be used in steps of simulation and optimization. The first information used in the construction of scenario is the cadastral map, which features urban dimension information, as lots, streets and blocks. In the

construction process, the height of the buildings is verified through field survey and Google Earth 3D.

The Optimization Process approach

The optimization process consists in consequential and iterative steps, using a combination of design and analysis tools, as shown in Figure 2. The identification, parameterization and optimization processes of the building shapes are composed by consequent stages.

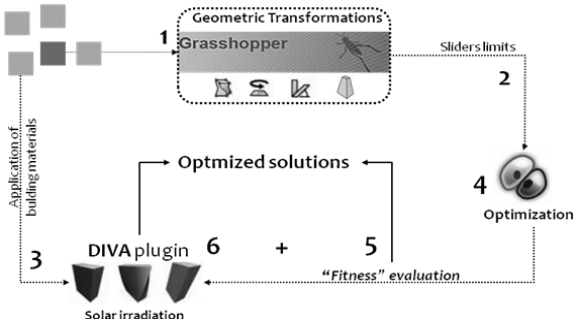

Figure 2: Development of the optimization process

Initially, from the definition and construction of scenario and reference building shape (OI_Reference), geometric transformations tools are applied (variables) within Grasshopper (Step 1), which are correlated with solar radiation levels. The simulations of annual dynamic solar radiation have been carried out using DIVA for Rhino, including the contributions of indirect solar radiation reflected by neighboring buildings. The reflectance of the external surfaces of buildings is set at 43.9%, which is obtained through study of the characterization of an average reflection coefficient for vertical surfaces in the central area of Florianopolis [11]. The reflectance of streets and sidewalks were set at 20%.

From a reference shape, generated in accordance with the occupancy limits from current Master Plan, different combinations of geometric transformations variables were tested: Twist, Slope, Rotation and Scale (Taper). Limits of values are defined for each type of variable, called "sliders", according to the limits observed in the city´s Master Plan (Step 2). Table 1 shows the ranges for each variable. The taper 1 is the normal setting the building, when the roof surface coverage is equal to the base. The length, width and height remain constant (17 x 35 x 42m) as well as the building volume.

	Twis	Rotation	Slope	Taper
OI Height: 42m Volume: 24990 m³	30° (range 5°)	20° (range 5°)	Axis x : -15 a 5° Axis y : -10 a 5° (range 1°)	0.75 a 1 (range 0.05)

Table 1: Summary of building's parametric transformation considered for analyses

The process within Grasshopper starts with modelling the base of OI_Reference, from the ground surface. The second stage refers to the modelling of geometric transformations, which are connected with the initial volumes. The building volume, defined by reference building, is kept constant for all proposed changes. Before the start of each simulation, a scale factor for the maintenance of the building volume is applied through the Scale component. The volume

resulting from the combination of variables, for every interaction, is divided by the desired volume, referring to the initial volume of OI_Reference. This factor is applied twice, due to the modifications resulting of twist variable, as shown in Figure 3.

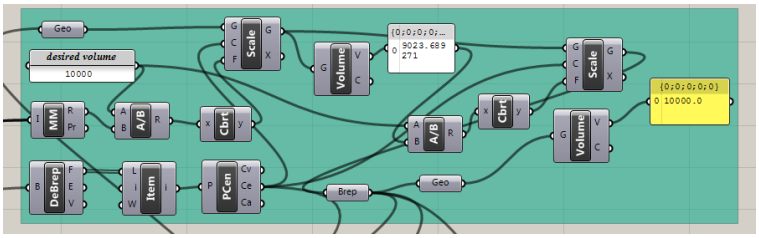

Figure 3: Volume maintenance process in Grasshopper

The limits for each slider are sent to the solver Galapagos, responsible for the optimization process of the building shape (Step 4). This tool allows the combination and evaluation of geometric transformations used from the definition of a value of solar irradiation desired, considered as "*fitness*". The premise adopted is the calculation of the minimum annual solar irradiation amount necessary to ensure an Internal Rate of Return of 6% for 25 years against the option of paying for the electricity distributor, having applied in the financial markets the value of the installation cost of the system [12], in this study regarding the Soliker opaque PV panel with initial installation cost of 1.81 $/Wp for commercial application [13]. The minimum level of solar radiation required for the investment is economically viable is 630kWh/m².year, value adopted as fitness for the optimization process.

The solver Galapagos performs the optimization process by combining the transformations, along with solar radiation simulations with Diva (Steps 5 and 6). At the end of the process, the resulting solutions with the highest number of point analysis higher than in the "fitness" are considered the optimized solutions. The solver Galapagos allows the generation of a set of optimized shapes, defined by the number of stagnation. The configuration adopted considered to maximize the value of the fitness evaluation function, twenty individuals for each generation and the completion of code execution when it reaches the stagnation of twenty generations. Inbreeding rate, was considered 75%, and the individuals of stay from one generation to the other 5%.

For each step, the process starts with an initial shape of reference building. Applying the geometric transformations, together with the simulation of solar irradiation facade is generated a set of optimized shapes. At the end of the process, data is exported to a spreadsheet in Excel format, containing the variables of each transformation, the achieved fitness value (number of points analyses above fitness value) and the percentage of area above this value, for each façade.

RESULTS

This step shows the comparison of solar radiation on the new buildings designed in this case study, with the main objective to analyze formal variability and photovoltaic potential. The first step is related to an assessment of the reference building (OI_base) in Current Scenario, to assess the current urban situation for comparison purposes.

All the optimized results have been compared with the reference building and the percentage of variation has been calculated. The data collecting the ten most significant results of the simulation performed, showing the highest annual solar radiation values for different types of parametric transformation. As shown in Figure 4a, for all optimized solutions there are

increments on the percentage of area above the fitness value, reaching values of up to 29%. In the Figure 4b is shown the main geometric transformations for each optimized result. As can be seen, Rotation and Slope y were the most variable transformations; the transformation twist was not used in this process.

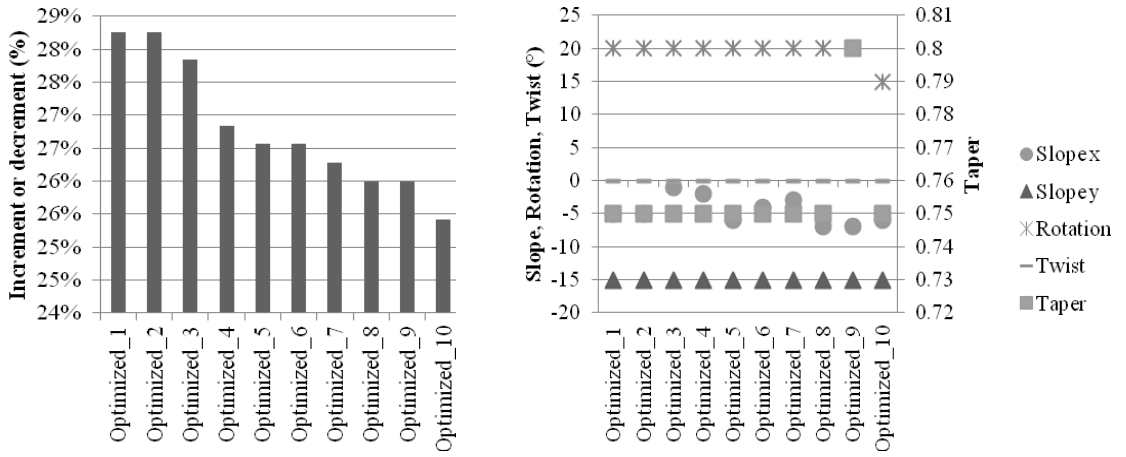

(a) *(b)*

Figure 4: (a) Results of contribution of solar radiation (b) geometric transformations for each optimized solution

The optimization process resulted in a larger area of the envelope with radiation levels above the fitness value, but penalizes the area of facades that already had values above it. Figure 5 illustrates this condition for the Current Scenario. For example, in the North façade, the reference building has a percentage of area above the fitness value of 98%. For an optimized shape, as Optimized_1, these percentage decreases 9.3%, but the fitness value increases 28%.

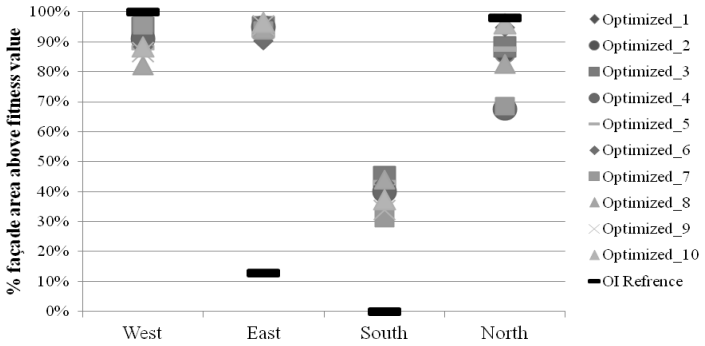

Figure 5: Results of percentage of façade area above fitness value.

Despite this consideration, the optimization process enabled facades that were not exposed to sunlight to increase the exhibition area to the fitness value, such as occurred in the South and East facades. Mainly for the South facade, the reference building did not have any area of the façade above this value. As shown in Figure 5, the optimal solution reached up to 45% of the South façade and 95% for East façade.

CONCLUSION

The analyses performed in accordance with the methodology demonstrate that the optimization process proposed is efficient in terms of achieving the optimized shape of the

buildings according to a radiation amount based on economic viability. One aspect to note is that optimization algorithm can be easily applied to other surrounding conditions and fitness parameters, enabling a variety of analyses.

The results show the improvement of solar radiation envelope in the optimized solutions and the modification of exposure of the façades, increasing the solar irradiation of façades South and East and penalizing façades West and North, in order to increase the total exposed area. Thus, further analysis should be performed to see the influences of this result in the photovoltaic generation potential. Through this process it was possible to identify the optimized building shape for solar radiation and to verify if façades can be exploited for energy production in dense urban areas in the Brazilian context. Due to the large energy concerns in Brazil and the great potential of using solar energy due to high solar radiation levels, studies that enhance the use of alternative renewable energy are fundamental to the dissemination of this potential.

REFERENCES

1. BEN. Balanço energético nacional. [s.l: s.n.].
2. Baños, R. et al. Optimization methods applied to renewable and sustainable energy: A review. Renewable and Sustainable Energy Reviews, v. 15, p. 1753–1766, 2011.
3. Rutten, D. Evolutionary Principles applied to Problem Solving. Available in: <https://ieatbugsforbreakfast.wordpress.com/2011/03/04/epatps01/>.
4. Jakubiec, J. A.; Reinhart, C. F. Diva 2 . 0 : Integrating Daylight and Thermal Simulations Using Rhinoceros 3D , Daysim and Energyplus. Proceedings of Building Simulation, p. 2202–2209, 2011.
5. Gagne, j. M. L.; Andersen, M. Multi-objetive facade optimization for daylighting design using a genetic algorithmSimBuild. Anais...New York City, New York: 2010
6. Torres, S. L.; sakamoto, Y. Facade design optimization for daylight with a simple genetic algorithm. Building Simulation. Anais...2007
7. Giani, M. et al. A Design approach for the solar optimization of built volumesCISBAT 2013. Anais...Lausanne, Switzerland: 2013
8. Lobaccaro, G.; Frontini, F. Solar Energy in Urban Environment: How Urban Densification Affects Existing Buildings. Energy Procedia, v. 48, p. 1559–1569, 2014.
9. Lobaccaro, G.; Masera, G. A digital language for a new sustainable urban planning: Design and Simulation Tools for Solar Architecture. Proceedings of the Building Simulation and Optimization. Anais...London, UK: 2014
10. Vannini, V. C. Otimização geométrica de dispositivos solares de fachada. [s.l.] UFRGS, 2011.
11. Leder, S. M.; Pereira, F. O. R.; Moraes, L. N. Determinação experimental de coeficiente de reflexão médio para superfícies verticais em meio urbano. ENCAC. Ouro Preto: 2007.
12. Jakubiec, J. A.; Reinhart, C. F.. Towards validated urban photovoltaic potential and solar radiation maps based on lidar measurements , gis data , and hourly daysim simulationsSimBuild. Anais...Madison, Wisconsin: 2012
13. EPE. Inserção da Geração Fotovoltaica Distribuída no Brasil – Condicionantes e Impactos. [s.l: s.n.].

EFFICIENCY ANALYSIS OF FLAT PLATE COLLECTORS FOR BUILDING FAÇADE INTEGRATION

Richard O'Hegarty; Oliver Kinnane; Sarah McCormack.

Dept of Civil, Structural and Environmental Engineering, Trinity College Dublin, Ireland

ABSTRACT

A theoretical approach has been used to evaluate the performance of facade integrated solar collectors based on the physical collector parameters such as absorber plate absorptance, transmittance of the glazed cover plate and insulation thickness. A 1D steady state model, based on the Hottel Whillier Bliss equation, was employed to determine the effect of changing parameters to meet façade integration criteria.

Keywords: Solar thermal, building integration, flat plate collectors

FACADE INTEGRATED FLAT PLATE COLLECTORS

Buildings account for 40% of the final energy consumption in Europe [1], Over half of this energy use is associated with building heating, cooling and domestic hot water (DHW) demands [2]. This energy is predominantly provided through the burning of fossil fuels, which can be reduced through the implementation of renewable energy systems. Solar thermal systems, for building applications, make use of an area on the building's envelope to install the solar collectors, which in turn, absorb the solar radiation and convert it to useful heat for the building's heating applications. These solar collectors are usually mounted on the roofs of buildings; however, a limited roof area and a high heating load may require the area of the façade to house these collectors [3]. Architectural integration barriers can become significant when the façade is used to house the collectors.

Solar thermal collectors may be categorised as Unglazed Collectors (UC), glazed Flat Plate Collectors (FPC) or Evacuated Tube Collectors. The FPC is Europe's most popular collector, accounting for 85% of the market share [4]. They consist of an absorber plate with a high absorptance and conductivity, insulated at the back using standard insulating wool or foam and insulated at the front through the use of a transparent cover (typically glass) which provides an air gap between the absorber and cover layer. A 1D steady state mathematical model, based on the Hotel Whillier Bliss equation [5], is used to examine the performance of FPC where the parameters are altered as appropriate for façade integration.

STEADY STATE MODELLING METHOD

The underlying equations for developing the 1D steady state model are based on the following. The instantaneous efficiency, η_i, is used to compare the performance.

$$\eta_i = \frac{Q_u}{A_c G_T} \tag{1}$$

Where A_c is the area of the collector (m^2) and G_T is the solar irradiance on a tilted surface. The theoretical performance of the solar collector is determined using the Hottel-Whillie-Bliss relationship for the useful energy gain, Q_u:

$$Q_u = A_c F_R [G_T(\tau\alpha) - U_l(T_{f,i} - T_a)] \tag{2}$$

Where, F_R is the heat removal factor, $(\tau\alpha)$ is the transmittance-absorptance product, U_l, is the total heat transfer coefficient, $T_{f,i}$ is the fluid inlet temperature and T_a, is the ambient temperature. U_l is found by summing the heat lost through the top, U_t, the bottom, U_b, and the edges, U_e, of the collector. The top heat loss, U_t, is temperature dependent, thus, an iterative process is required to obtain the solution.

The heat removal factor, F_R, is included to allow for the assumption that the plate of the collector is at the inlet fluid temperature, $T_{f,i}$, rather than the actual mean plate temperature, $T_{p,m}$. The inlet fluid temperature is used since the mean plate temperature is difficult to accurately quantify using experimental methods [5]. Rearranging Equations (1) and (2) gives the following:

$$\eta_i = F_R(\tau\alpha) - F_R U_l \left(\frac{T_{f,i} - T_a}{G_T} \right) \tag{3}$$

The instantaneous thermal efficiency, η_i, can be plotted against the reduced temperature difference, $((Tf,i - Ta)/G)$, to determine the collectors performance. Since the top heat loss U_t, is temperature dependent, the relationship is non-linear. The subsequent section of this paper will use this model to plot the efficiency curves of various FPCs.

RESULTS AND DISCUSSION

The model was used to compare the effect of altering three of the primary components of a FPC, cover, absorber and insulation. A standard FPC, with defined parameters (Table 1.) is used as a benchmark. The values used are typical of a FPC [5]. Parameters that are altered as a result of façade integration (highlighted with a **bold** font) will be varied and the resulting efficiency curves can be compared.

Parameter	Value
W (distance between tubes) [m]	0.15
D (Tube diameter inside) [m]	0.01
δ (sheet thickness) [m]	0.0005
k_a (absorber conductivity) [$Wm^{-1}K^{-1}$]	*385*
h_{fi} (convective heat transfer) [$Wm^{-2}K^{-1}$]	300
$\dot{m}$ (flow rate) [kg s^{-1}]	0.03
C_p (heat capacity) [$Jkg^{-1}K^{-1}$]	4190
τ (cover transmittance)	**0.94**
G (solar irradiance) [Wm^{-2}]	1000
α (absorber absorptance)	**0.95**
N (number of glass covers)	1
ε_g (emittance of glass)	0.88
ε (emittance of plate)	**0.95**
h_w (wind) [$Wm^{-2}K^{-1}$]	10
β (tilt angle)	90
σ (Stefan boltzman constant) [$Wm^{-2}K^{-4}$]	5.67037E-08
L_b (back insulation thickness) [m]	**0.05**

Table 1: Design Parameters and benchmark values of a flat plate collector

Cover

One way of achieving architectural integration is by providing a range of colours. Either the absorber plate or the glass cover may be coated to provide a colour that will fit in with the aesthetic of the building. An ideal cover would have a maximum transmittance, τ, value. However, the introduction of colour to the glass cover of a FPC decreases the transmittance value. Work has been conducted on reducing the negative effect of colour on the efficiency of the collector by using thin film layers to produce a colour that is opaque to the human eye (large reflectance in the visible spectrum, R_v), but high transparency to solar energy (large solar transmittance). The idea was proposed by Schüler et al. [6] and then followed up by a number of simulation and experimental studies using different film deposition methods. The efficiency curves for two multilayered coloured coatings are displayed in Figure 1.

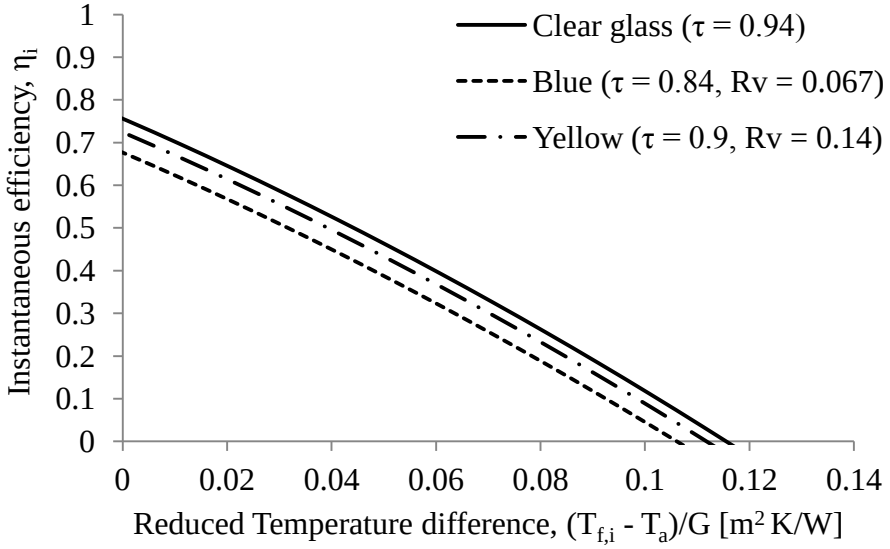

Figure 1: Theoretical efficiency of FPCs with different cover colours (layer properties [7]).

Depending on the number of layers, the refractive index of each layer and the thickness of each layer, a different colour with a different transmittance and visible reflectance would be achieved..

This study investigates how these property alterations affect the performance of a solar collector. Both the blue and yellow coloured thin films have a lower efficiency than that of clear glass, as expected. The thin films are made up of silicon and titanium oxide layers with different thicknesses to achieve these colours. In this case the yellow coloured collector outperforms the blue collector in terms of efficiency. The addition of these yellow and blue layers reduces the efficiency of this collector by 3% and 8% respectively.

Absorber

An alternative approach is to change the colour of the absorber plate. The absorber plate of a solar thermal collector is typically coated with a dark coating that has a high absorptance, α. As with colour coating the cover of a FPC, a reduction in performance is also associated with colouring the absorber [8]. Tripanagnostopoulos et al. [9] used booster reflectors adjacent to the absorber to make up for this reduction in absorptance. To obtain a higher efficiency, spectrally selective coatings may also be applied [10], which have a absorptance, α, for wavelengths between 0.3 and 2.5 μm and a low emittance, ε, for wavelengths greater than 2.5 μm.

The properties of concern for this study are the absorptance, α, and the emittance ε. By adjusting the outlined parameters and applying the model, efficiency curves are produced for three spectrally selective coatings, one black [8] and two alternative colours [11], as well as one non-spectrally selective coating [9]; displayed in Figure 2.

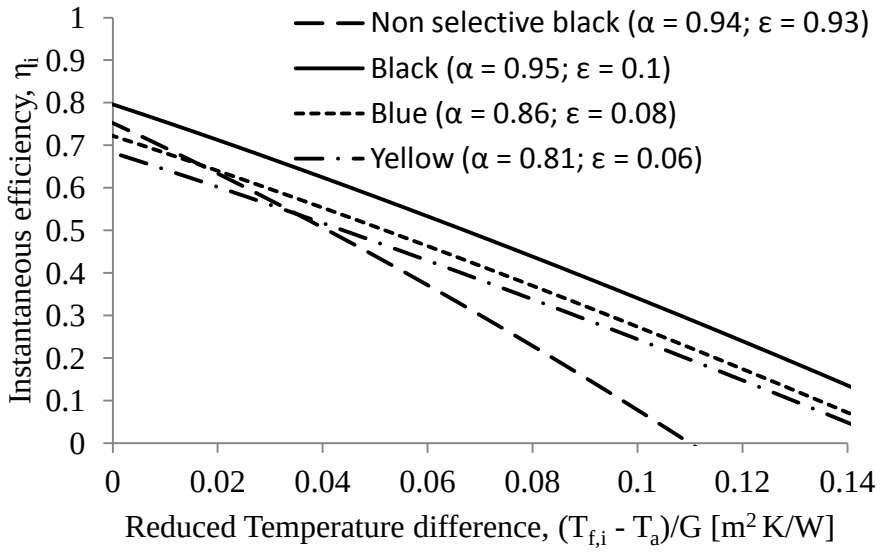

Figure 2. Theoretical efficiency of solar collectors with different absorber colours & spectral selectivity.

The spectrally selective coatings outperform the non-spectrally selective coatings since the emissivity is reduced, reducing the radiative heat losses, particularly as the temperature of the collector increases. A blue and yellow colouring are used again, however, the blue out performs the yellow; this can be attributed to its darker colour and hence higher absorptance. At a low reduced temperature difference (0.01 m^2K/W) the efficiency is reduced by 7% and 11% by changing to the referenced blue and yellow coating respectively; as the reduced temperature difference increases (0.14 m^2K/W) the reduction in efficiency becomes 6% and 9% respectively.

Insulation

The back insulation thickness of a FPC ranges from approximately 0.04 to 0.075 m [12], offering product U-values of between 0.75 W/m^2K and 0.42 W/m^2K (assuming an insulation conductivity of 0.03 W/mK [13]). However, for facade integrated collectors, a thicker insulation layer is required to ensure the envelope abides by building regulation specified U-values.

An insulation thickness of approximately 140 mm would be required to achieve a wall U-value of 0.21 W/m^2K (this is the current standard for the UK and Ireland [14]). On the other hand, considering the high temperature reached by the absorber plate, the resultant radiating heat to the interior space can promote overheating if not appropriately insulated [15] [16]. A negligible increase in the internal temperature of less than 1K has been observed for a variety of wall systems with integrated collectors. The insulation applied to the back of the collectors is used to reduce the heat loss. Figure 3 shows how increasing the insulation at the back of the collector increases the performance, by reducing the heat loss.

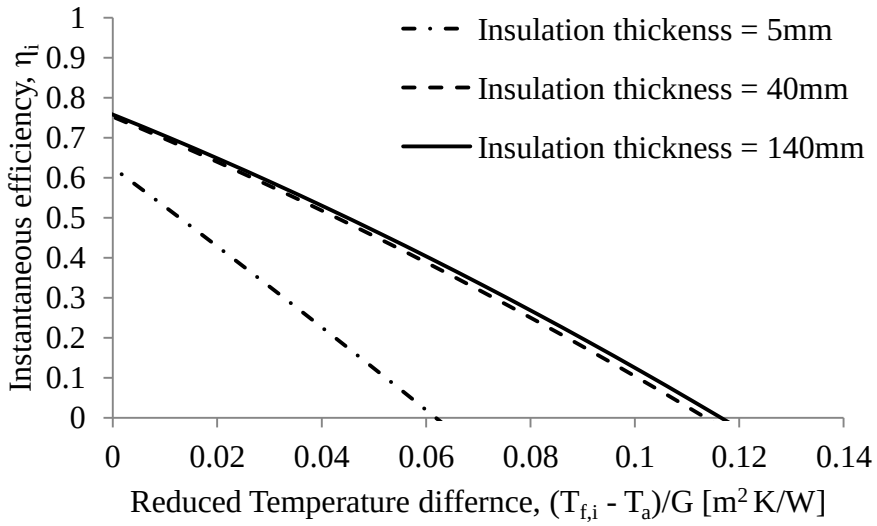

Figure 3. Theoretical efficiency of solar collectors with different back insulation thicknesses.

The results show how an increase in efficiency of no more than 2% is gained by increasing the thickness of insulation by more than 40 mm (typical insulation thickness). The convergence suggests that after 40mm of insulation the majority of the heat is lost through the top of the collector. However, for a facade integrated collector the insulation is also reducing the heat lost from the building's interior, therefore, justifying the increased thickness.

CONCLUSION

The performance of façade integrated flat plate collectors have been evaluated with reference to colouring the absorber and the cover and changing the thickness of the insulation. The effect of integrating a collector into the facade of a building on the efficiency of the collector is, therefore, presented.

It was found that for the colours compared in this study that colouring the glass cover will reduce the performance with the yellow cover considered in this paper having a 5% greater efficiency than that of the blue cover. On the other hand colouring the absorber plate yellow resulted in a lower efficiency than a blue coated absorber, by 2-4%. The effect the insulation's thickness had on the performance of the FPC, perceived for facade integration, was also addressed. The model showed that increasing the thickness past 40 mm resulted in no significant increases in the efficiency, however, if integrated into the facade of a building this would help reduce the unwanted heat losses or gains to the building.

ACKNOWLEDGEMENTS

The Irish Research Council; Firebird Heating solutions; COST Action TU1205.

REFERENCES

[1] IEA, 'Transition to Sustainable Buildings - Strategies and Opportunities to 2050', 2013.

[2] L. Pérez-Lombard, J. Ortiz, and C. Pout, 'A review on buildings energy consumption information', *Energy Build.*, vol. 40, no. 3, pp. 394–398, 2008.

[3] R. O'Hegarty, O. Kinnane, and S. McCormack, 'A Case for Facade Located Solar Thermal Collectors', in *Proceedings of the International Conference on Solar Heating and Cooling for Buildings and Industry*, Beijing, China, 2014.

[4] W. Weiss and F. Mauthner, ‘Weiss, Werner and Franz Mauthner (2012), Solar Heat Worldwide – Markets and Contributions to the Energy Supply 2010, Solar Heating and Cooling Programme, AEE INTEC, Gleisdorf, Austria.’, 2014.

[5] J. A. Duffie and W. A. Beckman, *Solar Engineering of Thermal Processes*, 4th ed. Wiley, 2013.

[6] A. Schüler, C. Roecker, J.-L. Scartezzini, J. Boudaden, I. R. Videnovic, R. S.-C. Ho, and P. Oelhafen, ‘On the feasibility of colored glazed thermal solar collectors based on thin film interference filters’, *Sol. Energy Mater. Sol. Cells*, vol. 84, no. 1–4, pp. 241–254, Oct. 2004.

[7] A. Schüler, J. Boudaden, P. Oelhafen, E. De Chambrier, C. Roecker, and J.-L. Scartezzini, ‘Thin film multilayer design types for colored glazed thermal solar collectors’, *Sol. Energy Mater. Sol. Cells*, vol. 89, no. 2–3, pp. 219–231, Nov. 2005.

[8] S. Kalogirou, Y. Tripanagnostopoulos, and M. Souliotis, ‘Performance of solar systems employing collectors with colored absorber’, *Energy Build.*, vol. 37, no. 8, pp. 824–835, Aug. 2005.

[9] Y. Tripanagnostopoulos, M. Souliotis, and T. Nousia, ‘Solar collectors with colored absorbers’, *Sol. Energy*, vol. 68, no. 4, pp. 343–356, 2000.

[10] Z. C. Orel and M. K. Gunde, ‘Spectrally selective paint coatings: Preparation and characterization’, *Sol. Energy Mater. Sol. Cells*, vol. 68, no. 3–4, pp. 337–353, Jun. 2001.

[11] D. Zhu and S. Zhao, ‘Chromaticity and optical properties of colored and black solar–thermal absorbing coatings’, *Sol. Energy Mater. Sol. Cells*, vol. 94, no. 10, pp. 1630–1635, Oct. 2010.

[12] F. A. Peuser, K.-H. Remmers, and M. Schnauss, *Solar Thermal Systems - Successful Planning and Construction*. Earthscan, 2010.

[13] BS ISO 10456, *Building materials and products - hygrothermal properties - Tabulated design values and procedures for determining declared and design thermal values*. 2009.

[14] TGD Part L, ‘Conservation of Fuel and Energy - Dwellings’, in *Technical Guidance Document Part L*, Dublin: Environment, Heritage and Local Government, 2011.

[15] T. Matuska and B. Sourek, ‘Façade solar collectors’, *Sol. Energy*, vol. 80, no. 11, pp. 1443–1452, Nov. 2006.

[16] T. Salem and M. Pierre, ‘Experimental Study of Active Solar Thermal Collectors Integrated in Building Facade’, in *Solar World Congress*, Beijing, China, 2007.

INTEGRATION OF RENEWABLE DISTRICT HEATING IN LAGUNA-VALLADOLID

Carol Pascual[1]; Asier Martinez[1] , Iñigo Urra[1] , Javier Martin[2]; Oscar Hidalgo[2]

1: Tecnalia, Energy and Environment Division, 20730 Azpeitia, Spain

2: Veolia, servicios LECAM, Avenida del Euro 7, Edificio B, 47009 Valladolid, Spain

ABSTRACT

This paper presents an evaluation of the most suitable renewable sources of energy for Laguna-Valladolid considering the different alternatives of the location, and a detailed design of a demonstrator based on TRNSYS simulations developed in the framework of a European project, CITyFiED (repliCable and InnovaTive Future Efficient Districts and cities).

The overall objective of CITyFiED project is to develop a replicable, systemic and integrated strategy to convert European cities and urban ecosystems into smart cities of the future, focusing on reducing the energy demand and GHG emissions and increasing the use of renewable energy sources by developing and implementing innovative technologies and methodologies for building renovation, smart grid and district heating networks and their interfaces with ICTs and Mobility.

One of the main goals of this project is the development of a deep retrofitting of the buildings, and innovative district heating solutions in three large scale demonstrations, at Laguna-Valladolid (Spain), Soma (Turkey) and Lund (Sweden) in order to achieve powerful models suitable for replication across Europe.

Keywords: District heating, renewable energy, demonstrator, TRNSYS, CITyFIED.

INTRODUCTION

Energy efficiency in new buildings is important, but existing building stock is the main target. Existing buildings, however, are characterized by particular requirements and constraints that are not present in new buildings and that require new developments and adaptation of existing technologies. In order to fulfil the most recent EU directives, solutions for a drastic reduction in primary energy consumption are required. Space heating and domestic hot water preparation (DHW) represent the largest part of energy use in buildings nowadays [1].

Despite these existing initiatives and even though many of them focus on buildings retrofitting, the systemic renovation strategies at district or city level are still not generalized enough in Europe and even less in Spain, where the difficult current economic situation and social aspects do not help to spread the benefits of this approach. It is clear that some general barriers are holding back the massive deployment of such interventions, even if the technology is available and currently some business models such as ESCO are serving as catalysts. Thus, a strong effort is required to spread the benefits of the integrated refurbishment, to overcome the existing barriers and to provide innovative and effective solutions to address the current technical and financial challenges

This paper presents the main results obtained in CITyFIED project, in the evaluation of the most suitable renewable energy sources (such as solar energy, biomass, geothermal and wind energy) of Laguna de Duero (Valladolid, Spain) considering different alternatives of location, and a detailed design of the demonstrator based on TRNSYS simulations.

The intervention aims to drastically reduce the energy consumption by means of passive measures (façade retrofitting) and advanced control and distribution systems implementation, able to control temperature levels building by building. This will result in a good coverage of the energy demand and avoiding heat losses. Besides, an innovative district heating facility will be installed not only for heating but also for domestic hot water supply.

DISTRICT AND SYSTEM DESCRIPTION

Laguna de Duero is a little town located in the middle of Spain, fully integrated in the metropolitan area of Valladolid. Laguna's climate is Mediterranean-continental. Temperatures are very extreme, with big differences between day and night. Winters are cold, with frequent foggy days and frosts around 60 days per year. Summers are hot and dry but present low minimum temperatures during the night. According to this, heating is the principal energy demand of the buildings, as cooling devices are not usually present in dwellings.

Torrelago District:

The demo site, whose representative data are summarized in Table 1 involves 31 residential buildings, split into two phases (1488 dwellings and more of 4.000 residents) which are in use nowadays. Phase 1 has 12 buildings of 12 floors, with 4 apartments per floor of an average area of 100 m^2. These buildings were constructed in 1977. On the other hand, Phase 2 has 19 buildings (identical to buildings in Phase 1). 11 buildings were constructed in 1979 and 8 buildings were constructed in 1981.

Nº of buildings	31 buildings
Nº of dwellings	1488 dwellings
Nº of beneficiaries	> 4.000 residents
% of beneficiaries/municipality	> 18%
m^2 of constructed area subject of intervention	140.000 m^2

Table 1: Torrelago District general description.

Description of current energy systems:

The energy system of the district was composed of two independent gas-fired boiler rooms, one for each phase. These two District Heating (DH) systems provided thermal energy, covering both space heating (SH) and domestic hot water (DHW), for 19 and 12 buildings, respectively. In the case of Phase I, two gas-fired boilers with a total capacity of 5.938 kW were installed. Two gas-fired boilers with a total capacity of 9.386kW were installed in case of Phase II.

Table 2 shows the approximate current yearly energy consumption, demand and CO_2 emissions before district retrofitting works:

Summary of the interventions:

The principal actions being performed to improve thermal energy efficiency in the district are:

- Complete renovation of the façades to increase thermal insulation.
- Deployment of a new District Heating concept, to cover the demand by optimizing the production of thermal energy by means of a mix of energy sources. The use of renewables

must be maximized with the biomass-boiler system, which improves energy efficiency, stabilizes prices and reduces CO_2 emissions.

- A new pumping system based on variable flows is being installed, that will allow making an appropriate balance load to adjust production to demands.
- Implementation of a new control system in order to improve the management and efficiency of the installation. Individual thermal consumptions of each building will be considered on the District Heating control system, with the aim of making a better adjustment of production to consumption. Thermal consumptions of each individual dwelling from the building are being considered as well.
- A Combined Heat and Power facility will be installed, for self-consumption, with appropriate smart grid elements to make an adequate control.

OVERALL THERMAL ENERGY DEMAND BY USE		
Total Thermal Energy Demand	13.037 MWh	93,12 kWh·m^{-2}
- Space Heating	9.663 MWh	69,02 kWh·m^{-2}
- Domestic Heat Water	3.374 MWh	24,1 kWh·m^{-2}
OVERALL CO_2 EMISSIONS		
By gas		3,583 tCO_2
By electricity		58 tCO_2

Table 2: Overall demand and CO2 emissions for Torrelago-District.

DESCRIPTION OF DYNAMIC MODEL AND ANALYSIS OF CASE STUDIES

A dynamic simulation model of the district was developed in order to analyse the described system after considering façade retrofitting works as well as solar thermal energy generation implementation in the mentioned system. The results of the simulations performed by CITyFIED partners (ACCIONA and LKS) revealed that the energy demand for SH was in line of the initial conditions (deviation of 8.65%). After that energy simulations of the retrofitted buildings were carried out [1]. Simulations of the retrofitted case were performed using Design-Builder software [2], showing an energy demand reduction of almost 40%.

Biomass District Heating system:

Two district phases were connected to create a a unique district heating system. Installation of biomass boilers in order to substitute existing natural gas boilers was studied. Existing boilers, installed in the second phase's generation-station, were left as backup systems when biomass boiler's generation capacity would not be able to cover instantaneous demand of the district heating.

The described system's performance was studied by transient simulation software, TRNSYS [3]. Figure 1 shows a simplified hydraulic scheme of the modelled system, consisting of a main heating central with biomass boilers in combination with two buffer storages of 12 m^3 each. Close to Phase II a secondary heating plant is located with backup gas fired boilers.

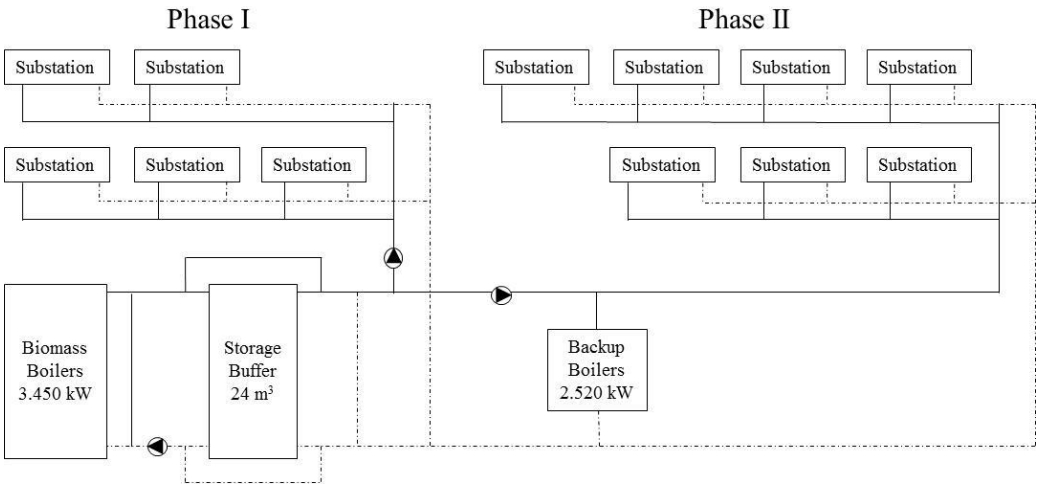

Figure 1: Schematic representation of the hydraulics of the system simulated.

System-performance strategy is divided into different operation modes depending on whole system load capacity and storage charging state. As long as the load stays lower than 3.450 kW, biomass boilers may cover it. When the load is higher than the biomass boilers' capacity they operate at full capacity but delivering in priority to Phase-I. Surplus heat is directed to Phase-II. Besides, in case heat is stored in DH net tanks, this additional capacity is discharged in parallel to biomass boilers.

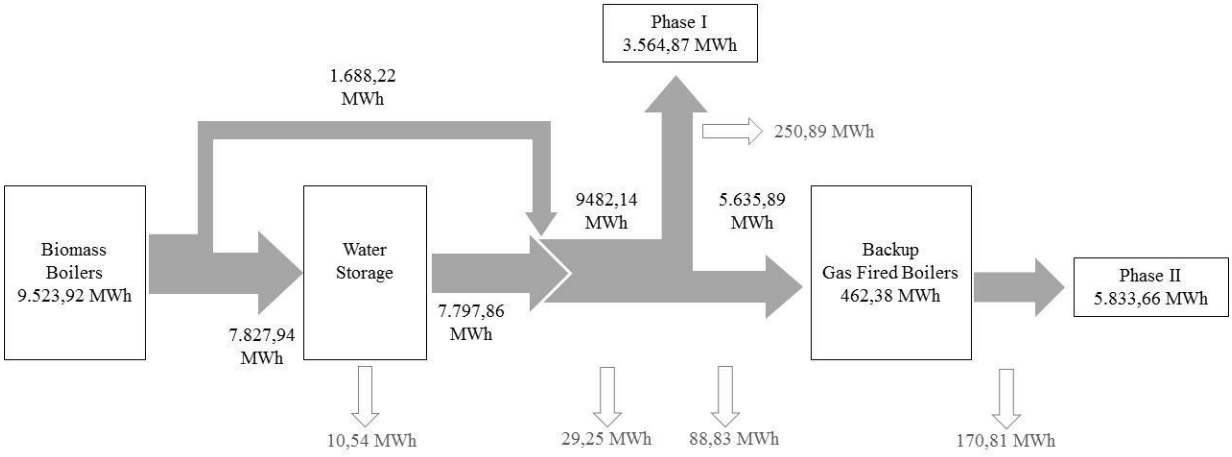

Figure 2: Biomass system simulation yearly energy balance.

Figure 2 shows the analysed system performance. Approximately 95% of heat generation comes from biomass boilers in order to cover demands by Phase I and II, including distribution heat losses along the network, resulting in about 550 MWh. The rest of the heating needed is supplied by gas boilers, covering part of the demand in Phase II.

Substitution of gas fired boilers by biomass boilers in the generation system of Phase I supposes a 78% of primary energy savings and a yearly CO_2 emissions reduction of above 2 tones (see Table 3). Figure 4 shows the monthly distribution of heat generation, by either biomass or natural gas, in the analysed system. It may be shown that the auxiliary system is required during winter months, i.e. from November to March. During winter time both, SH

and DHW are required by DH residents and depending on the hour of the day, installed biomass boilers' capacity does not result enough to cover their necessities.

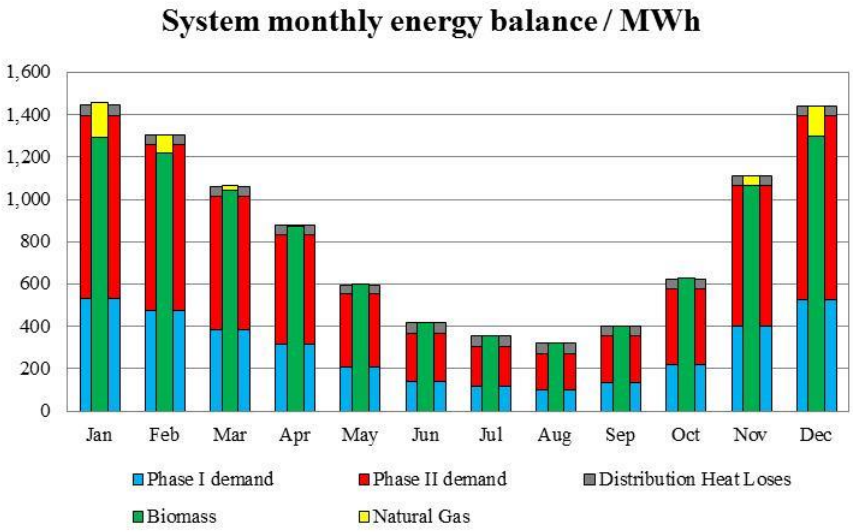

Figure 4: Monthly energy balance of the simulated biomass system.

Solar Generation in combination with biomass:

Solar thermal energy generation in combination with the previously studied biomass generation is proposed. This would be the first DH plant with solar energy contribution in Spain. Solar energy would be used in order to cover DHW demand [4]. Studied and implemented installation for each DH building substation is shown in Figure 5.

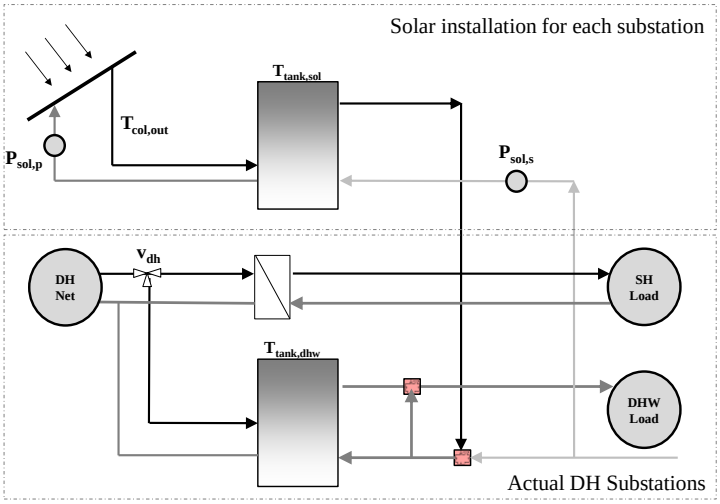

Figure 5: DHW implementation into DH-Substations.

Simulations were performed to estimate the required collector area for different solar fraction values [5]. A total surface of 4.400 m^2 would be needed to get a total solar fraction of 31% (including SH and DHW demand). Figure 6 shows the distribution for covering of the total heat demand, by solar (31,12%), biomass (65,45%) and gas (3,43%).

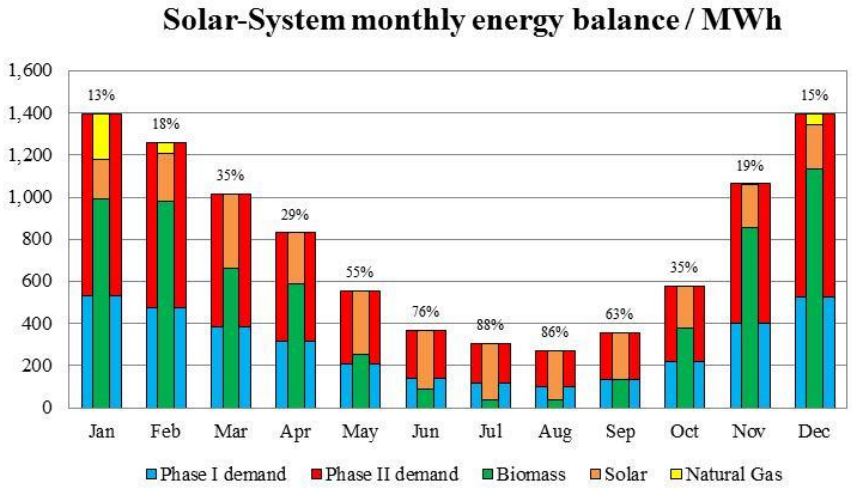

Figure 6: Monthly energy balance of studied system with solar installation.

According to conversion factors summarized in Table 3, installation of solar thermal energy in combination with biomass installation would suppose a reduction of 30.20% in primary energy consumption and a reduction of 114.703 kg CO2 emissions to the atmosphere.

	Primary Energy Factor	CO2-eq emission factor / g·KWh$_{TH}$
Biomass	0,2	7
Gas	1,1	222

Table 3: Primary energy factors and CO_2 equivalent emissions factors.

CONCLUSIONS

This paper presents the evaluation of the most suitable renewable source of energy of Torrelago's DH in Laguna de Duero (Valladolid) considering different alternatives within location and a detailed design of the demonstrator based on TRNSYS simulations developed in the framework of the European project CITyFiED. The results of the dynamic simulations show:

- Heat demand is reduced by approximately 40% after building retrofitting.
- Substitution of gas fired boilers by biomass boilers suppose a reduction of 95% in gas consumption, 78% of primary energy savings and a yearly reduction of CO_2 emissions of 2 tones.
- Solar generation in combination with biomass supposes a reduction of 30,20% in primary energy consumption and 114.703 kg CO_2 emissions. Only 3,43% of the demand is covered by the gas boiler.

REFERENCES

1. European Union Directive on the Energy Performance of Buildings. EPBD 2002/91/CE
2. Design Builder simulation tool. Available online : http://www.designbuilder.es
3. A: Klein, S.A. et al, 2010, TRNSYS 17: A Transient System Simulation Program, Solar Energy Laboratory, University of Wisconsin, Madison, USA, http://sel.me.wisc.edu/trnsys
4. Solar District Heating Guidelines. Collection of factsheets. EU project SDP plus.
5. ASHRAE International Weather Files for Energy Calculations 2.0 (IWEC2). Available online: https://www.ashrae.org/resources--publications/bookstore/iwec2

PHOTOVOLTAIC ORIENTED BUILDINGS (PVOB)

Christian Renken; Prof. Urs Muntwyler, Daniel Gfeller

Bern University of Applied Sciences, Engineering and Information Technology, Photovoltaic Laboratory, Jlcoweg 1, CH-3400 Burgdorf, Switzerland, Tel.: +41 34 426 68 11, Fax: +41 34 426 68 63

christian.renken@bfh.ch; urs.muntwyler@bfh.ch; daniel.gfeller@bfh.ch

www.pvtest.ch

ABSTRACT

The direct use of solar energy by self-consumption in buildings gets more and more important to minimize negative influences on the grid. Therefore, the photovoltaic laboratory of Bern University of Applied Sciences launched the project PVOB – "Photovoltaic oriented buildings" – that will help to improve photovoltaic applications in building envelopes to match the user's energy consumption needs and reduce negative influences on the grid. Creating a database by measuring and evaluating buildings with PV installations on all four façade sides will be one part of the project. Furthermore, cost optimization in planning and realisation processes as well as improvements of fire protection are aspects which will be integrated.

Keywords: BIPV, solar façade, self-consumption, planning processes, fire protection

DIRECT USE OF SOLAR ENERGY

Photovoltaic panels installed in multiple areas of the building envelope increases the self-consumption of solar energy [1], [2]. Through the allocation of the solar panels on façades with different orientations, the electrical production profile during daytime creates a more uniformly characteristic and enables a higher coverage of the energy consumption profile [6]. According to the orientation of the photovoltaic panels and the consumptions profile, the direct use of solar energy will rise up to 50% with roof installations and up to 80% with façade installations.

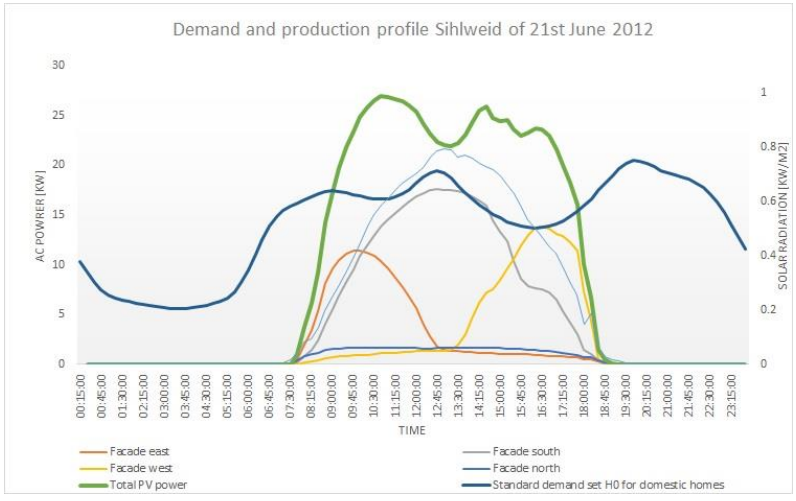

Fig. 1: PV applications for less grid overloads during daytime.

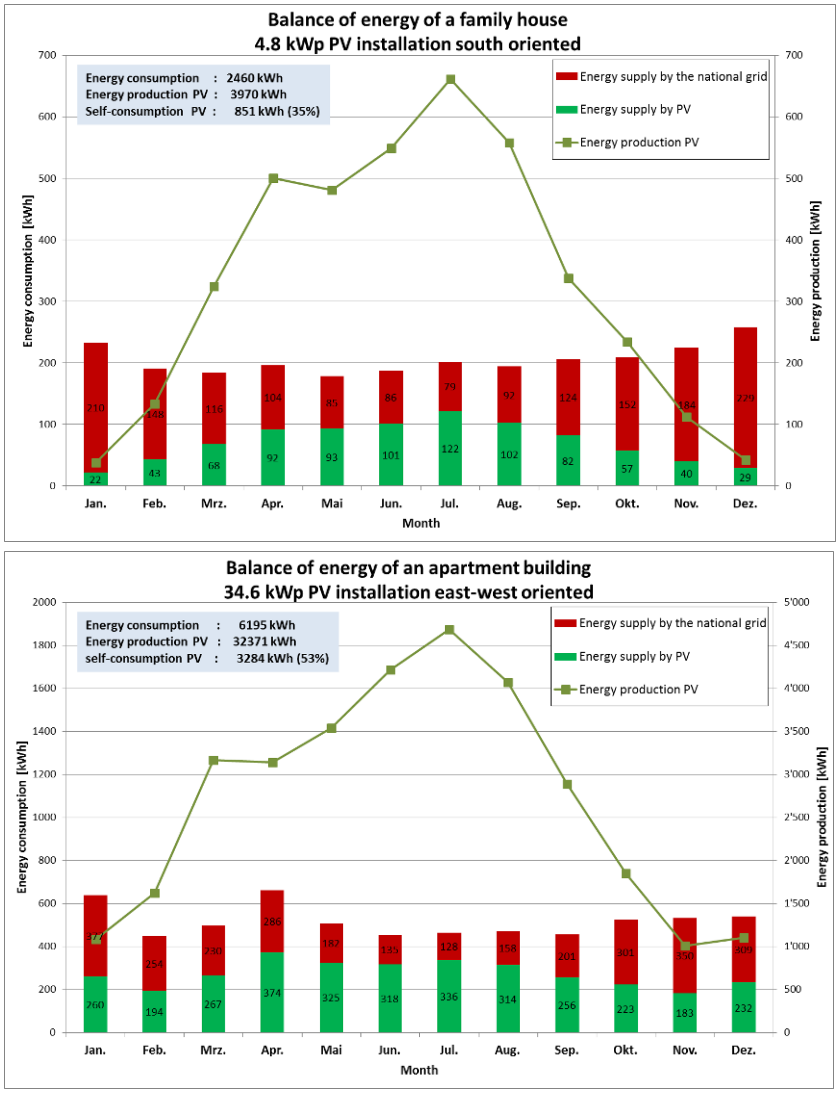

Fig. 2+3: Coverage of energy consumption through PV supply with different oriented PV installations.

For a successful commercialization of photovoltaics in the building envelope, architectural aspects are getting more important. Architects are looking for flexible and aesthetical materials in their design process. Therefore, the solar industries have to offer various solar products which are specified for the integration in the building structure like a building material. Beside aesthetical aspects, the stakeholders have to ensure safety requirements like structural analyses, fire protection and electrical functionality of the photovoltaic application in the planning process.

ECONOMIC INTEGRATION OF PHOTOVOLTAIC IN FACADES

Conventional photovoltaic systems are planned and executed by the solar installer who acts as a general contractor towards the client. In case of implementing the photovoltaic technology in façades, the situation changes completely. Different stakeholders like architect, façade designer, structural engineer, façade- and solar installers are now involved in the project. To prevent uncontrolled increase of the project costs, coordinated planning and realisation processes by the stakeholders are needed. Technical planning tools and specified products for integrated photovoltaic applications helps to reach professional results.

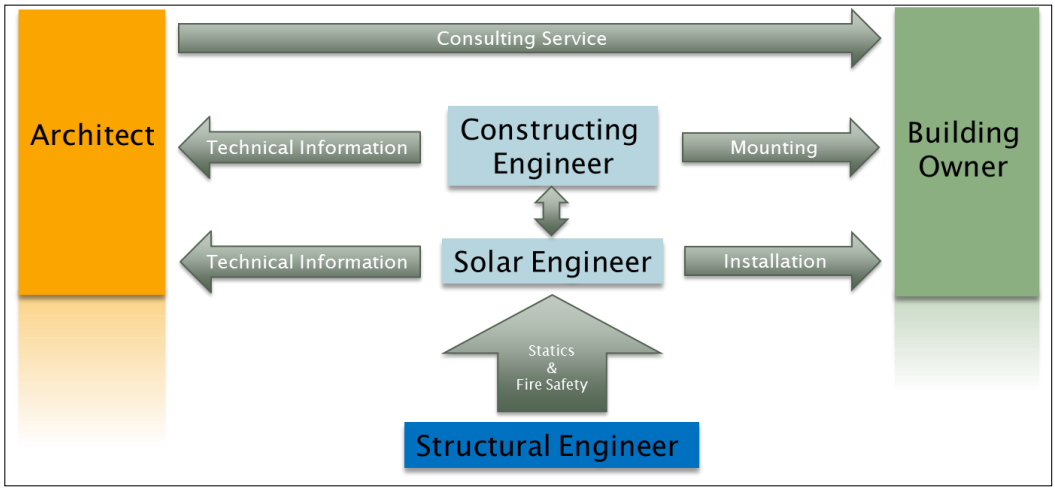

Fig. 4: Stakeholders in the planning and execution processes

DESIGNING OF PHOTOVOLTAIC FACADES

The planning process of photovoltaic facades should start in an early phase of the general project. In this stage, adjustments of the dimensions of the facade, as well as the positioning of windows, doors and balconies in relation to the photovoltaic panels are possible. Furthermore, for each project should be verified if standard panels with common dimensions or custom-made photovoltaic panels simplify the connection to the façade. Cost-effective standard photovoltaic panels can cause significant additional costs in the integration process. In this case, custom-made photovoltaic panels can be an interesting alternative for simplifying the integration and gives more flexibility to the architect while safeguarding the overall costs of the system.

Fig. 5+6: Photovoltaic integration with standard sized panels or custom-made panels.

In order to simplify the processes for architects and increase cost efficiency, the Bern University of Applied Sciences initiated a project between architects and electrical engineers to develop a software-tool as an additional plug-in for CAD software [3]. This tool allows a fast and easy initial estimate of photovoltaic applications in different parts of the façade. The layout of photovoltaic panels can without interruptions be exported to a simulation software like PVSYST to calculate energy yield and shadowing losses. The first results have shown a high potential in cost savings. Therefore, the PVLab targets a continuing project to create a tool for professional applications.

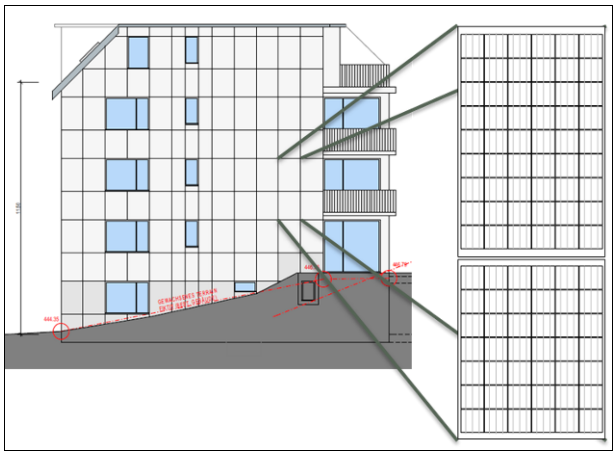

Fig. 7: PV panel modelling in the planning process

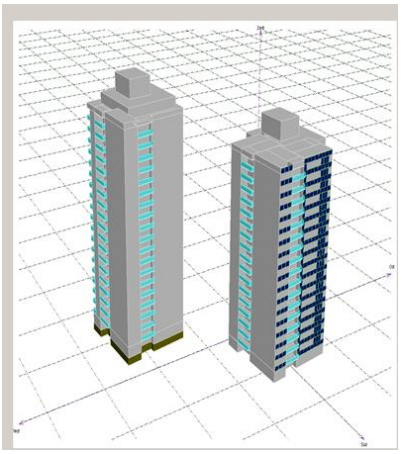

Fig. 8: Data export into PVSYST

STATIC CERTIFICATION OF PHOTOVOLTAIC FACADES

The statics of the photovoltaic system including panels and mounting system have to comply with national standards, such as "SIA261: Impact on supporting constructions". The responsibility for the statics will be taken by the designer of the facade construction. Non-regulated construction products have to be examined individually.

REQUIREMENTS OF FIRE PROTECTION AND MAINTENANCE

The requirements for fire protection according to the regulations for photovoltaic installations by VKF/AEAI (latest version march 2015) have to be verified for each photovoltaic integrated project. Especially the component selection and system configuration of photovoltaic systems in high-rise buildings (in Switzerland from 30 m) have to be specified in all details. Questions about material compositions of the photovoltaic panels or additional safeguards like fire barriers have to be defined in the planning process.

For inspection of defects in photovoltaic modules, the PV-laboratory defined a low priced concept of an IR multi-copter drone to detect hotspots in large free-field and façade photovoltaic installations. The thermography camera installed on a drone records a full-radiometric infrared video. The video, unlike photography, facilitates the evaluation of data. False detections due to reflections and other irregularities can be immediately recognized.

Fig. 9: IR-multi-copter drone of the PVLab

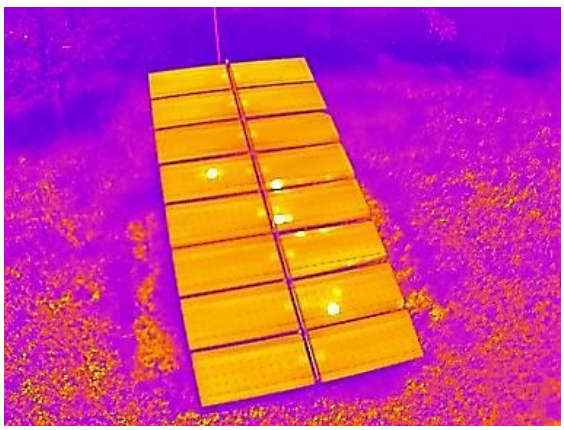

Fig. 10: Hotspot detection of PV panels

REQUIREMENTS OF DC CABLING FOR INTERGRATED PHOTOVOLTAIC

The DC cables in the ventilation space between photovoltaic panels and building have to be protected and a minimum of distance to flammable materials has to be respected. The DC cables have also to be protected against rodents. During the installation of the facade, the solar installer has to take care of the professional treatment of the electrical components.

In a particular ongoing project in the framework of fire protection of photovoltaic installations, the long term behaviour of cross-connections of DC-solar connectors are analysed. In many photovoltaic installations, the DC-connectors of different manufacturers are connected directly together. Usually, the compatibility of connectors of different manufacturers is not guaranteed. Climate chamber tests and testing of the electrical resistance of the connectors should give more insight to this impotent issue of operational safety.

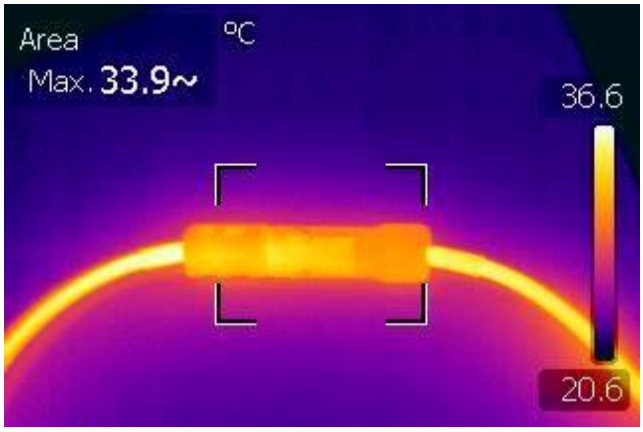

Fig 11: Combination of different DC-solar connectors

CONCLUSION

Standardized planning and implementation processes are one of the main issues to increase the number of photovoltaic installations in façades.

The PV-laboratory of Bern University of Applied Sciences in Burgdorf initiates several projects on this subject in the framework of the competency group PVOB – "Photovoltaic oriented buildings":

In 2014 we started to develop a calculation tool for architects to simplify the designing process of photovoltaics in façades. A new guideline will help architects and installers to perform practical and economic implementation of photovoltaics in façades. Safety requirements, fire protection and the maintenance concept will be included in this guideline. In co-operation with producers, the PV-laboratory will define the necessary specification of the products for easy applications in BIPV. Know-how transfer will be done by organizing workshops for architects and engineers.

ACKNOWLEDGEMENTS

Thanks go to GVB Gebäudeversicherung Bern who gives financial support to this project.

REFERENCES

[1] Christian Renken, Urs Muntwyler, Eva Schüpbach
"Photovoltaic Oriented Building (PVOB)", 1st SCCER-FURIES Annual Conference, December 2014, Lausanne

[2] Urs Muntwyler (Quelle: www.haustech-magazin.ch)
"Photovoltaik erobert die Fassade", Haustech 5/2014

[3] Urs Muntwyler, Duglas Urena
"Rund-um-Solarhaut: BIPV zu PVOB", 12. Nationale Photovoltaik-Tagung 2014, Lausanne / CH, 10. & 11. April 2014

[4] Heinrich Häberlin
"Was tun bei Detektion? Sinnvolle Strategien zum Erreichen eines sicheren Anlagenzustands bei Auslösen des Lichtbogendetektors", 2. Workshop des TÜV Rheinland zu Lichtbogendetektion und -abschaltung sowie Brandrisikominimierung, Freiburg / DE, 2013 Präsentation

[5] H. Häberlin, L. Borgna, D. Gfeller, P. Schärf
"BIPV: Aesthetics alone are not sufficient - Long-term Energy Yield and Safety are Equally Important". 26th European Solar Energy Conference, Hamburg, Germany, September 2011.

[6] H. Häberlin
"Wie viel Solarstrom erträgt das Netz?" [Teil 1 + 2]. Elektrotechnik 8/2011 und 9/2011.

PUMPING POWER PREDICTION IN LOW TEMPERATURE DISTRICT HEATING NETWORKS

Florian Ruesch[1]; Matthias Rommel[1]; Jakob Scherer[2]

[1]*Institute for Solar Technology SPF, HSR University of Applied Sciences, Oberseestrasse 10, CH-8640 Rapperswil, +41 55 222 48 31*

[2]*Amstein + Walthert AG, Andreasstrasse 11, CH-8050 Zürich, Switzerland*

ABSTRACT

A low temperature network providing heat for domestic buildings and cold for a large data centre was modelled in the software Polysun based on simplified loads. The emphasis was set on the electric energy consumption of the decentralized circulation pumps. For this reason, the pump and hydraulic resistance model of the software Polysun was adapted in order to reproduce the characteristics of modulating high efficiency pumps. Energy consumption of the decentralized circulation pumps of less than 1% of the transferred energy was predicted from dynamic simulation with the new models. In order to challenge these predictions, the first four months of operation of a network in Zürich were monitored and analysed. Launched in December 2014, the network is equipped with an extended monitoring system, which records amongst others the network temperature evolution, the heat pump performance and the pumping energy consumption. The main heat pump providing heat to over 400 households at a mean temperature of 68°C reached an overall coefficient of performance (COP) of 3.7 in initial winter operation. This value corresponds to a remarkable overall efficiency factor (including primary and secondary circulation pumps) of 65%. Due to intense usage in winter months, but also slightly higher pressure drops than predicted, the pumping energy reached 1.6 % of the low temperature energy delivered to the heat pump and 1.1% of the cooling energy supplied to a data centre. Even though not all modelled consumers started operation during the monitoring period, the measured data was used to validate dynamic simulations and pump models. By introducing the measured loads and the effective hydraulic resistance to the simulation model, the measured pumping energy fractions could be closely reproduced with the simulation model.

Keywords: low temperature network, pumping energy, decentralized networks, undirected flow, monitoring data

INTRODUCTION

Thermal interconnection has a great potential to reduce primary energy consumption in areas with mixed heating and cooling demands. Several low temperature district heating networks working as heat source for efficient heat pumps in the residential sector as well as cold source for the climatisation of office buildings or other processes with large cooling demands have recently been built in Switzerland (general scheme in figure 1). Large borehole fields connected to the network serve as thermal storages for heat respectively "cold" between the seasons. Thermal losses form the borehole storage as well as in the piping network can be minimized by keeping the temperature of the network close to the average temperature of the surrounding ground. In the contrary to conventional district heating networks with directed flow and central pumping stations, the flow in such networks is generated by decentralized pumps for each connected heat pump (consumers) or "cooling station" (producers). For this reason, the flow in such a network is undirected, meaning that in one piping section the flow can be in both directions depending on the predominant operation mode (heating or cooling).

The interaction between different pumps connected to the network is highly dynamic and difficult to predict. A modelling approach, similar to the one presented in this contribution has been done by Kräuchi et al. in IDA-ICE [1]. However, detailed pump characteristics where not taken into account and pumping energy consumption was not explicitly analysed. Examples, where elevated pumping energy in the same order of magnitude as the energy consumption of the heat pumps based on measured data were reported in [2]. This shows how important an accurate consideration of circulation pump energy consumption is for the overall energy efficiency of low temperature networks.

In order to increase prediction precision, a more detailed pump- and hydraulics model was introduced in the simulation software Polysun [3]. With this model, pumping energy consumption in the range of 0.6...3.4 % [4] of the delivered low temperature energy was predicted for different decentralized heating and cooling units and different pump types of a low temperature heating and cooling network built by a large housing cooperative in the city of Zürich. First parts of this network started operation in the end of 2014 and monitoring data is analysed and compared to preliminary simulations in this paper.

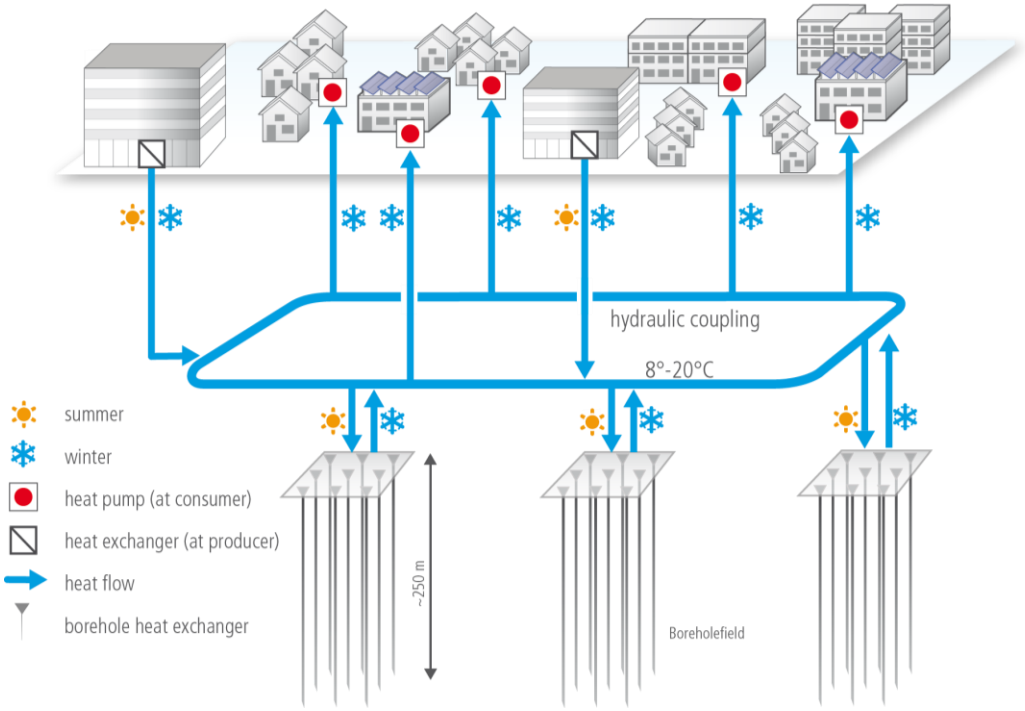

Figure 1 General scheme of a low temperature district heating network.

PRELIMINARY DYNAMIC PUMPING ENERGY MODELLING

The first construction stage of the low temperature network in question was integrated into the software Polysun based on a simplified outdoor temperature dependent load model. It consists of three “heating stations” with large heat pumps (consumer 1, 2 & 3) connected to the cooling unit of a data centre (producer) and a large borehole field for seasonal storage. The simulation scheme is given in figure 2 and the outdoor dependent load modelling in figure 3. A general description of this network is given in [4] and a more detailed description of the pump model and the simplified load modelling in [5]. The simulations of the dynamic pump interactions resulted in pumping energy consumptions reaching from 0.6 to 3.4% of the delivered low temperature energy (for consumer 1 with an efficient pump engine according to IE4 respectively consumer 2 with an intermediate pump engine according to IE2 standard).

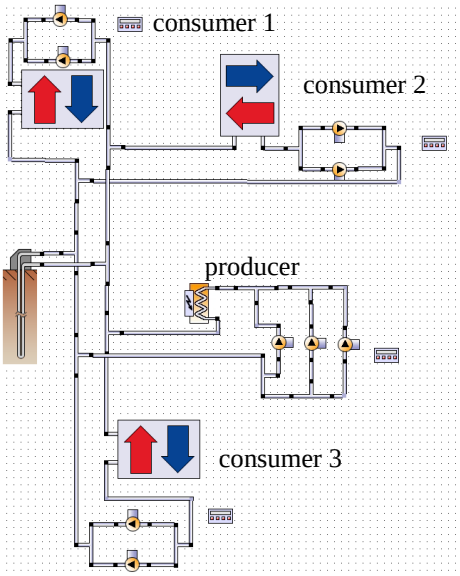

Figure 2 Simplified hydraulics of the first construction stage of the heating and cooling network as implemented in Polysun.

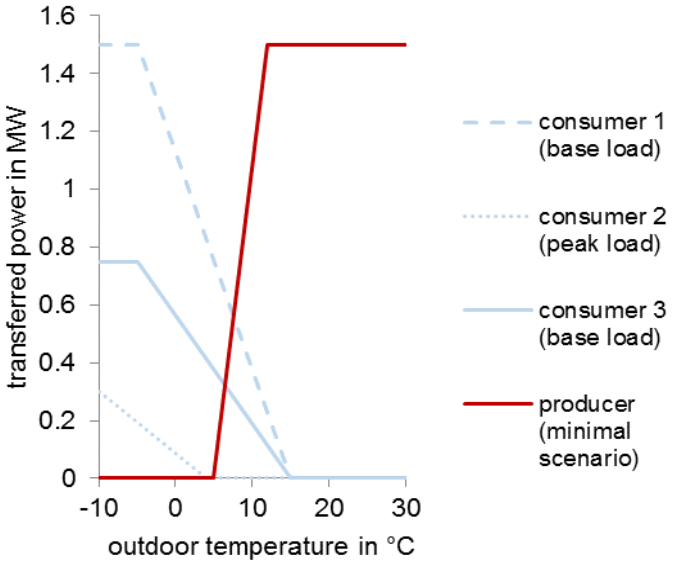

Figure 3 Outdoor dependent power consumption or delivery as used for the simplified dynamic modelling of the first construction stage of the examined network.

MONITORING RESULTS

In autumn 2014 the first consumer started its operation, and from 22.12.2014 on, detailed measurement data with a resolution of one minute is available. In the first winter only two operating units connected to the network were active:

Consumer 1: Large multi compressor heat pump with a nominal power of 2 MW providing domestic hot water (DHW) and Space Heat (SH) for over 400 households. The heat pump is retro fitted to the existing heat distribution system with a mean flow temperature of 68°C.

Producer: Data centre cooling integrated to the primary (direct) and secondary cooling cycle (sink of cooling machines) by heat exchangers.

The other consumers of stage one will start their operation in the heating period 2015/16.

System temperatures and heat pump COP

During the first months of operation, the temperature evolution was dominated by three phases (see figure 4).

Initiation: The heat pump of consumer 1 was working and first tests with the heat delivery from the producer where carried out.

Control adaption: The control algorithm of the producer was adapted. During this time no energy from the producer was transmitted to the network. Temperatures in the borehole field and at the source of the heat pump dropped to nearly 4°C (return).

Regular operation: Pump and mixing valve of the producer are being controlled in order to provide a fixed temperature to the cooling system on the secondary side of the heat exchanger. To this end, the temperature difference between flow and return on the primary side is variable. Temperatures in the system rise as a consequence of the energy input from the producer.

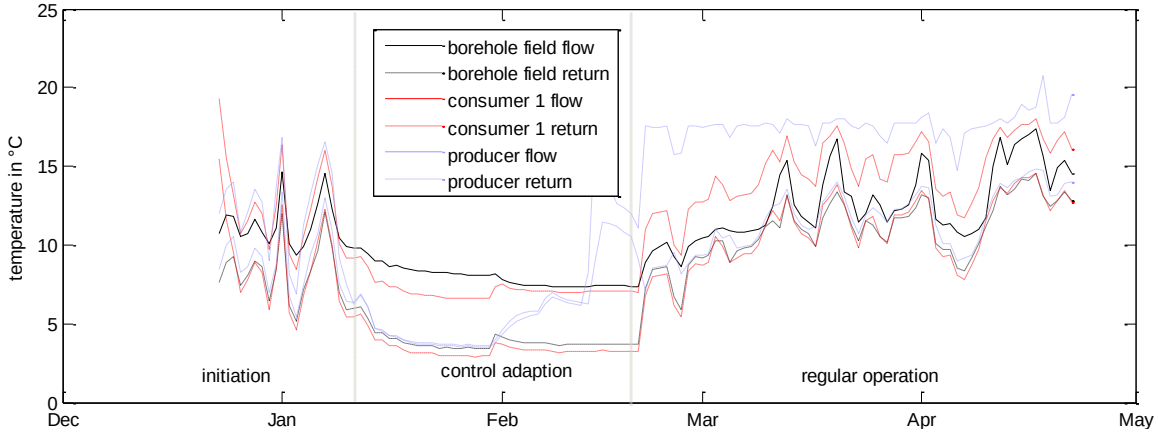

Figure 4 Temperature evolution at different points in the network (daily averages).

The total COP of the heat pump of consumer 1 equals 3.9 (for the heat pump only) and 3.7 (including auxiliary energy from primary and secondary side) during the four months of evaluation. The overall COP depends on the source temperature and varies between 3.2 and 4.3. In the contrary, the overall heat pump efficiency factor is less variable and remains between 62% and 67% (daily values, with two exceptional days). Because of the elevated supply temperature needed for the conventional housings (68°C) the heat pump COP is limited to values below 4 despite of the high efficiency factor.

Circulation pump energy consumption

The decrease in COP by taking auxiliary energy into consideration is mainly due to decentralized network pumps. However, during the measurement period of four months, only a quantity of electric energy corresponding to 1.6% of the low temperature energy delivered to the source side of the consumer heat pump (evaporator) and 1.2% of the energy delivered to the user (heat pump condenser) was needed for the network pumps. At the producer, the network pumps only used an electric energy equal to 1.1% of the transferred energy. Differences in the control strategy of the producer and consumer 1 can be seen in figure 5, where the electrical power consumption from the pumps is compared to the transferred thermal power (at the low temperature level). For consumer 1 the pumping fraction increases with the delivered thermal power. This pump is controlled in order to provide a fixed temperature difference between flow and return. For such a control strategy, part load operation is favourable for the needed pumping power fraction.

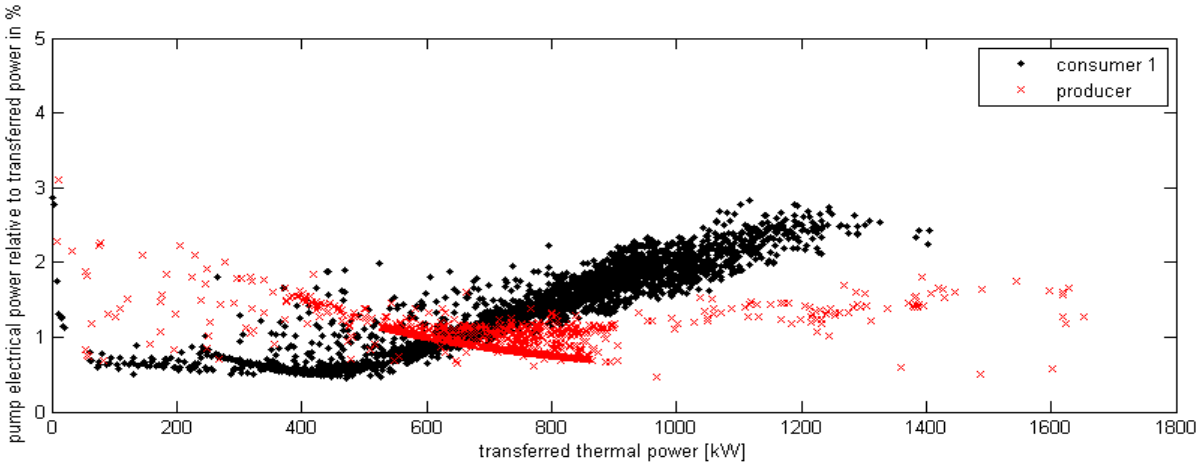

Figure 5 Electrical pumping power as a function of the transferred thermal power (hourly mean values).

The control strategy of the producer provides a constant temperature at the secondary side. For this reason, the temperature difference between flow and return is variable. With a high temperature, elevated thermal power can be transferred with relatively low flow rates. These operation states result in low relative pumping energy fractions. When the temperature difference decreases, less thermal power can be transferred with the same flow rate or pumping power. Consequently, the fraction of pumping power (relative to the transferred thermal power) increases.

VALIDATION OF PUMP MODEL

Even though only one consumer and producer were running during the measurement period, the measured data could be used to validate the simulation model. The measured heating and cooling loads were integrated into the simulation on a one minute time step base in order to test the pump- and hydraulic resistance model. Pumps were controlled in the software in order to provide the desired temperature difference. However the temperature difference was adapted to account for changes in the real control strategy. This affected mainly the control of the producer pumps in the third phase of operation (fixed temperature at the secondary side). Consumers 2 and 3, which are not yet operational, were also deactivated during simulations. From the simplified annual load modelling with all three consumers in operation, an annual electricity consumption of only 0.7% (consumer 1) respectively 0.6% (producer) of the transferred energy was estimated. However there where major differences between the simplified load prediction and the monitored operation:

1. The difference of only one consumer in real operation and three parallel consumers in the simplified model results in lower flow rates in the network and borehole field during winter operation. An even lower pumping energy fraction of 0.6% (consumer 1) of the transferred energy results from disabling consumer 2 & 3 in the simplified load model.
2. The simplified annual load consists of more part load operation than in the measurement period (winter). The pumping energy fraction increased to 1.0% (consumer 1) respectively 0.9% (producer) by introducing the measured winter loads into the model.
3. The measured pressure drop at the in- and outlet of consumer 1 where higher than predicted. By adapting the hydraulic resistance of the connection piping in order to reach the same pressure drop as measured, the modelled pumping energy fraction of consumer 1 further increased to 1.5%.

Table 1 Pumping energy fraction in % of the transferred energy of measured data and model outputs from different loads and hydraulic resistances.

	Consumer 1	Producer
Prediction from annual simplified load	0.7 %	0.6 %
Prediction from simplified load, consumer 2&3 disabled	0.6 %	0.6 %
Simulation with measured load (winter)	1.0 %	0.9 %
Simulation with adapted hydraulic resistance (winter)	1.5 %	0.9 %
Measured (winter)	1.6 %	1.1 %

The remaining difference to the measured 1.6% (consumer 1) respectively 1.1% (producer) pumping energy fraction is assumed to result from modelling of the pumps and their control. Here, mainly the starting and stopping strategy of the pump control could not be reproduced

correctly in the software. However, the effect of not well known hydraulic resistances and thermal loads is considerably higher than the deviations caused by pump modelling. The flowrate of the two users in operation is provided by several parallel and independently modelled circulation pumps. For this reason, the modelling approach is supposed to be valid also for more complicated networks with several consumers and producers in parallel. In order to validate this, further comparison will be done once other consumers are operational.

CONCLUSION

The first months of operation show that the examined low temperature network is well planned and dimensioned, thus working properly and providing low temperature energy for heating and cooling efficiently. The low auxiliary energy consumption results in a high overall heat pump efficiency of 65%. The overall COP in initial winter operation reaches a value of 3.7 at a mean secondary flow temperature of 68°C given by the retrofit heat delivery system. This COP-value is expected to increase, as mean annual network temperatures will be above the ones observed in the initial winter operation phase. For heat pumps to be built in future stages, serving modern buildings with a lower heating temperature level, significantly higher COP-values are anticipated. Only 1.6 % (consumer) and 1.1 % (producer) of the transferred energy is needed for circulation pumping. However, these measured values exceed the predicted values from annual loads. The deviation is mainly due to the measurement period in the winter months and to higher pressure drops than predicted. However, by introducing measured loads into the simulation and by adapting the hydraulic resistance, the simulated pumping power closely matches the measured data. This shows, that the model allows calculating the dynamic pumping power in such a network close to reality. Although only input data from one consumer and one producer were available, the model is supposed to be valid for more consumers, as the interaction of several pumps at two locations with independent flowrates in the opposite direction was considered. Deviations are caused rather by the estimation of the hydraulic resistance and loads than the simulation model.

ACKNOWLEDGEMENTS

Full access and support to the code of Polysun was provided by the company Velasolaris AG. The support of the Swiss Federal Office of Energy (SFOE) for the presented investigations within the TARO project is also gratefully acknowledged.

REFERENCES

1. Kräuchi Ph, Kolb M, Gautschi Th, Menti U-P, Sulzer M, Modellbildung für thermische Arealvernetzung mit IDA-ICE, BauSim2014 Fifth German-Austrian IBPSA Conference, Aachen, Germany, 2014
2. Vetterli N, Brücker S, Monitoring Suurstoffi – Monitoring einer thermischen Arealvernetzung in Kombination mit einem Erdsondenfeld, Jahresbericht 2014, Bundesamt für Energie BFE, Bern, 2015
3. Ruesch F, Kolb M, Gautschi T, Rommel M. Heat and cold supply for neighbourhoods by means of seasonal borehole storage and low temperature energetic cross linking, Proc. of CISBAT 2013, Lausanne, Switzerland. 2013
4. Ruesch F, Scherer J, Rommel M, Wärme- und Kälteversorgung mit Erdsondenfeldern – Vergleich von Messdaten und vereinfachter Abbildung in Polysun,18. Statusseminar brenet, Zürich, Switzerland, 2014
5. Velasolaris AG, Polysun - Simulationstool für Energiesysteme mit Schwerpunkt auf Solarthermie, Available from: www.polysun.ch, Winthertur, Switzerland, 2014

Building Simulation

SERVICE-ORIENTED ARCHITECTURE FOR DATA EXCHANGE BETWEEN A BUILDING INFORMATION MODEL AND A BUILDING ENERGY MODEL

Hu Zhao; Zoltán Nagy; Daren Thomas; Arno Schlueter.

Architecture and Buildings Systems, Institute for Technology in Architecture, ETH Zürich, John-von-Neumann-Weg 9, CH-8093 Zürich

ABSTRACT

Building energy simulation has become an important method for reducing energy use and carbon dioxide emissions in sustainable building design. In the last decade, we have witnessed the employment of building information model (BIM) and internet technologies to be harnessed for energy-efficient building design.

In this research the data exchange between a Building Information Model (BIM) and a Building Energy Model (BEM) is investigated. In previous research energy simulation engines are integrated into the BIM application for BIM users to evaluate the design directly at the conceptual design stage. After the conceptual design stage the energy analysis task is shifted to professional engineers. In a conventional process, engineers analyse the BEM, which has been previously exported manually from the BIM, and optimize the parameters in the BEM. These results are then used to manually update the BIM used in design. However, this process is cumbersome and error-prone as it is hard to keep the BEM up-to-date with the BIM, and the optimization of the parameters on the BEM cannot be easily synchronized back to the BIM model. The increasing uses of the internet for data exchange and new database technologies have the potential to change this. We employ service-oriented architecture (SOA) to connect the components of services in each side of BIM and BEM. Based on a critical study of data and schema in the BIM and the BEM model, we propose a SOA based BIM and BEM exchange framework that can be used to support the collaboration and information synchronization among the participants in a sustainable design project. This framework is exemplified using a case study.

Keywords: Data Exchange, Building Information Model, Building Energy Model, and SOA

1. INTRODUCTION

Building energy simulation has an increasingly important role in the design and optimization of buildings. Using simulation can help the design team to consider many different parameters and design options from an early stage to the construction [1]. As the architectural design is always changing, it is hard to keep the energy model up-to-date. By employing a Building Information Model (BIM), project teams can use the information contained in the models to perform visualization, construction simulation and energy analysis. There are two ways of acquiring Building Energy Models (BEM) from BIM applications: one is by exporting intermediate exchange files such as DXF, GBXML and IFC files; another one is through the application program interface (API) of the BIM modelling editor directly.

Each simulation program uses its own document format. The GBXML file format was developed to facilitate the transfer of building information stored in BIM. The GBXML file can be exported from BIM by the architect and then sent to the engineer by email or other document transfer methods. The engineers or professional users import the GBXML to their simulation program, then after the simulation is completed, the results and the opinions from

the engineer to modify the design is sent to architect by meeting, email and telephone etc. (Figure 1). However, the aforementioned process is inefficient while the BIM is changing, and the architect need export an adequate GBXML in every coordination with engineer, moreover, the round-trip of the design optimization from the engineer side is manual and not fluent. The design coordination requires an efficient optimization process to realize a round-trip of data flow.

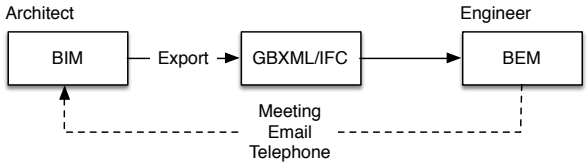

Figure 1 Conventional BIM and BEM communication

As the use of BIM is increasingly adopted in the AEC (architect, engineer and construction) domain and BIM application developers provide APIs for third-party programmers, some researches have built simulation plugins hosted in BIM software (Figure 2). As an example, an IFC based method for semi-automated building energy performance simulation is proposed to facilitate data exchange for BEM. A geometry simplification tool, a space boundary tool and Simergy were developed to realize the simulation in EnergyPlus [2]. However, the IFC file, which contains all information of the BIM, can only be exported manually from within the BIM applications. Generating and transferring IFC are time-consuming and cumbersome. Since 2009, the Design Performance Viewer (DPV) has been developed to calculate and visualize the energy performance of BIM [3].

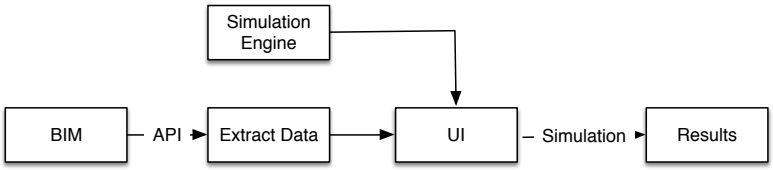

Figure 2 Integrated Building energy simulation Process

Some vendors also have built energy simulation services on BIM; the rising of cloud computation techniques are embedded in their services. Autodesk builds interfaces on their BIM application (Autodesk Revit) to connect to Green Building Studio, which is a cloud-based energy-analysis software that enables architects and designers to perform whole-building analysis and optimize energy consumption earlier in the design process (Autodesk, 2014). Sefaira integrates Autodesk Revit to extend the capabilities of the BIM users to make design decisions collectively using latest performance data. These above-mentioned researches aim to benefit the BIM users in the early concept design process. Algorithms are utilized to form a single-zone BEM model with the information extracted from BIM. However, in the further design development and construction design stages, the building energy performance strongly depends on the heating and cooling zone divisions and HVAC (heating, ventilating, and air conditioning) systems, so the models generated by algorithms are often inaccurate and over-simplified [4].

In this research, we introduce a method that allows considering the coordination of both BIM during design and BEM in a round-trip digital design process. This means the engineers can not only request the BEM from the BIM, but they can also update the BEM related parameters directly in the BIM. This simplifies the sustainable design process considerably and supports the integrated design processes. We present a SOA based framework to support

the model exchange and we implement this framework in a BIM application and an energy simulation application. Finally, we perform a case study to demonstrate the applicability in the design process.

2. METHOD

2.1 FRAMEWORK

In this research, we develop a service-oriented architecture based BIM collaboration framework (SBCF) to handle the round-trip exchange between BIM and BEM (Figure 3). Our goal is to execute efficient data flow and management.

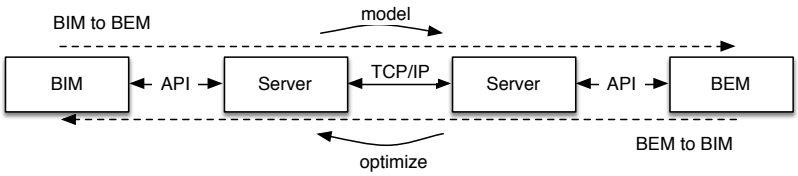

Figure 3 Round-trip between BIM and BEM

The users of the framework can share model information through application server on the internet. Each participant of the framework plays both server and client roles, so it provides flexible access services [5]. The aforementioned coordination process is achieved by integrating various modules to a server on each side of design participant's applications (Figure 4). The basic functions of the BIM application service are to extract models on request and apply modification requests to the BIM. And the basic functions of the BEM services are to send request to BIM and conduct simulation.

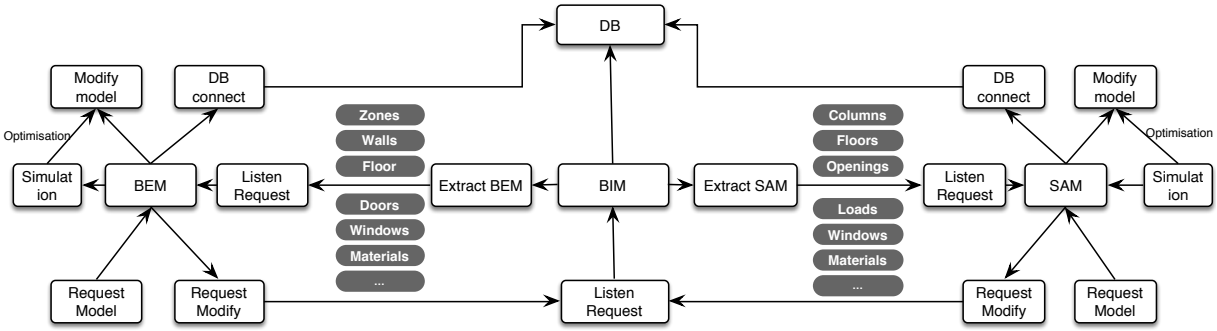

Figure 4 SBCF, coordination with BEM and Structural Analysis Model (SAM)

2.2 IMPLEMENTATION

In this research, we implement SBCF with Autodesk Revit (BIM application) and EnergyPlus (BEM application). It should be noted that BIM and BEM model data have different data formats and hierarchical structure, so we have to build an intermediate representation for the information. On the BIM side, we extract geometrical and physical properties of zones, surfaces and openings using the Revit API [6]. On the BEM side, EnergyPlus uses the open-source format called IDF that contains the simulation model as geometries, systems, schedules etc. Apart from the model data, the intermediate representation transferred between two servers should carry additional information such as the data type, version, warning and error messages etc. In this research we utilize the JSON syntax to represent the data extracted from BIM based on the structure and relationship of BEM data. The ID information of each BIM element is contained in the JSON representation in order to be able to modify the BIM model.

The application services built on the BIM side (Figure 5) receives request and sends model. Once it received a JSON message from a remote participant, it reads the request and informs the BIM user to choose whether he approves the request. If the request is granted, the services will commit the request operations such as extract the model and modify the model.

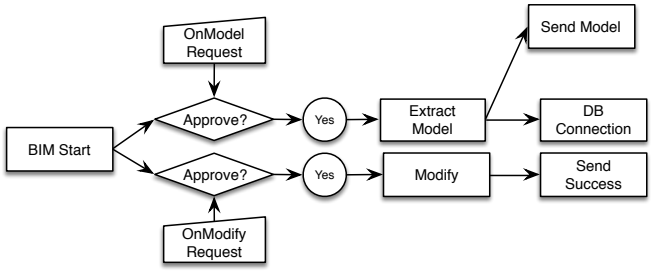

Figure 5 Workflow on the BIM side services

The BIM application chosen (Autodesk Revit) can store not only geometry related information, but also HVAC and MEP related model and information such as zones, systems, occupants etc., which enables the users to fetch more detail information about the project.

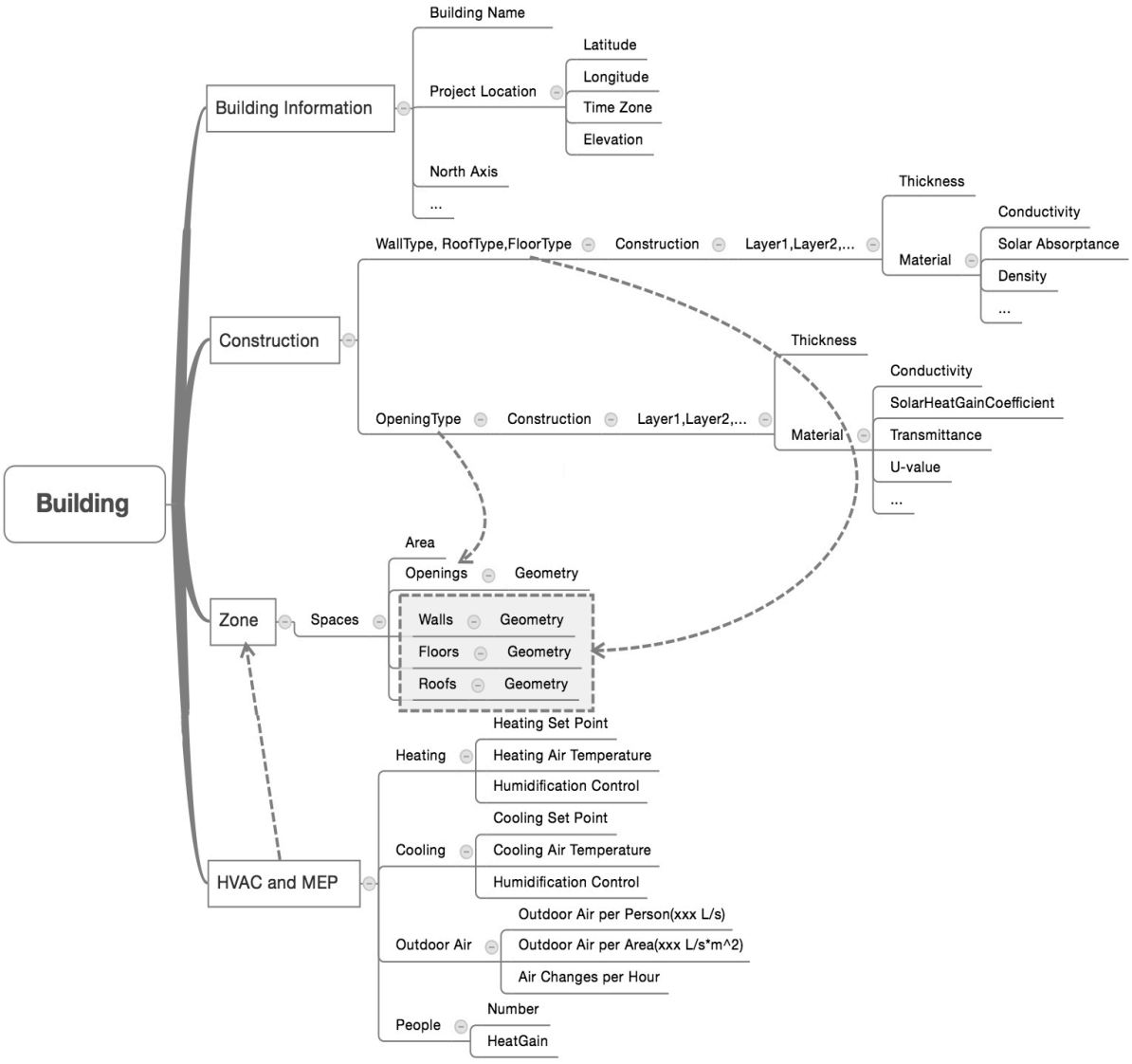

Figure 6 Multi-zones based model extraction structure from BIM model

Different from other methods that use algorithms to form a single-zone BEM from BIM in the concept design stage, in this research, the zones are manually defined in the BIM model and then we extract the geometrical and physical properties around the predefined zones using the API. A multi-zones BEM model with a typical IDF data structure (Figure 6) is generated after the extraction. The model is stored in JSON model and ready to be exchanged over the internet.

On the BEM side, the application services convert the JSON model to IDF, and run the simulation. Model modification request could be sent to the services on BIM side if some model parameters are changed.

3. CASE STUDY

To demonstrate the aforementioned framework (SBCF), we apply it to a case study building design. The object is a two-story office building (Figure 7) with 6 thermal zones. By implementing the SBCF, we realize a design process for determining the window size of the building. We separate the thermal zones in the BIM (Autodesk Revit). On the BEM side, we receive the BEM in JSON syntax after we request. Then, the service converts the JSON file to an IDF file (Figure 8, visualized in Open Studio/ SketchUp). In this process, the HVAC system and lighting controls are defined.

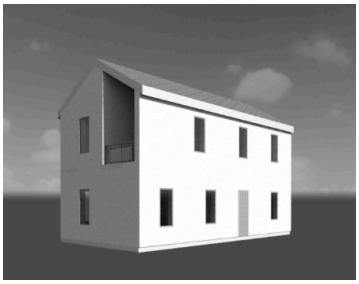

Figure 7 BIM with initial window size

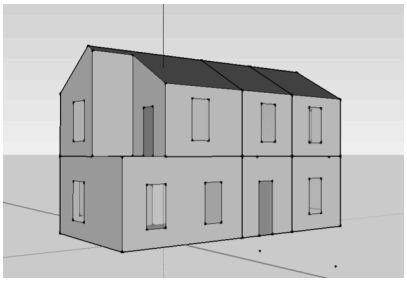

Figure 8 BEM visualized in application

The initial size of the windows is 1.8 by 0.6m and the construction is single-glazed. We change the width of the north, east and west-facing window in BIM from 0.6 to 2.7m in steps of 0.3m, simulate BEM and collect the corresponding results to the result pool. In order to prevent the model from conflicts, the BIM service declines the request of changing the width to above 2.8m. Figure 9 shows the performed round-trip design process.

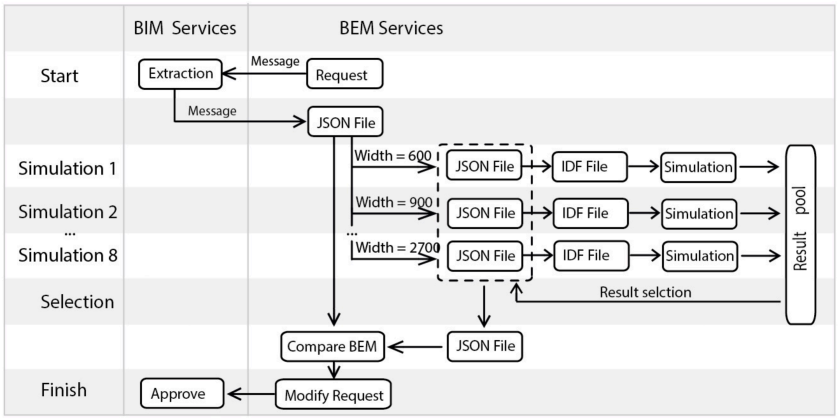

Figure 9 Round-trip design process of determining windows size

As the increasing width of window decreases the lighting energy demand and improves energy demand for heating, we measure the lighting energy uses and heating uses in the results to determine an adequate size.

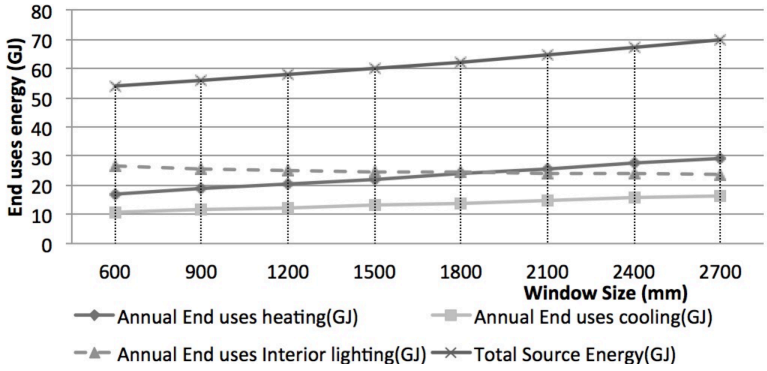

Figure 10 End uses energy performance

In Figure 10, we plot the simulation results from the result pool. In the practical BIM-BEM collaboration, engineers can have a clear understanding of the building energy performance with different window sizes, and then they can select a certain size for the windows based on their goal, which can be sent back to BIM. We compare the selected BEM with the initial BEM, and then the modification of windows are found, at last we send the IDs with their modified parameters to the BIM services.

4. CONCLUSION

This paper illustrates a SOA based method that simplifies the data exchange between a BIM and a BEM. With a case study we test a building with 6 thermal zones using the framework developed. We execute multi-zone model extractions and remote operations on application services. We present BIM-to-BEM and BEM-to-BIM data exchange in a design process, and we have seen benefits of this efficient and accurate model exchange method. This research simplifies the process of BIM-BEM data exchange, enables engineers to be efficient up-to-date with BIM and benefit architects to receive the feedback from engineers. We are currently working on improving the applicability and user interaction on the BEM side as well as extending the data types for exchange.

REFERENCES

1. Ritter F., Schubert G., Geyer P., Borrmann A., and Petzold F.: Computing in Civil and Building Engineering. pp 2023-2031, 2014

2. O'Donnell, James T.: Transforming BIM to BEM: Generation of building geometry for the NASA ames sustainability base BIM. http://eetd.lbl.gov/sites/all/files/publications/lbnl-6033e.pdf, 2014

3. Schlueter A., Thesseling F.: Building information model based energy/exergy performance assessment in early design stages. Automation in Construction, Vol 18, pp 153-163, 2009

4. Daniel C., Paul R., Marcus K.: A review of methods to match building energy simulation models to measured data, Renewable and Sustainable Energy Reviews, Vol 37, pp 123-141, 2014

5. Piyawan K., Duangduen R., and Hassan K.: Current Trends and Future Directions in GIS. CAD and GIS Integration, pp 23-49, 2009

6. Miller C., Thomas D., Irigoyen S. D., Hersberger, C., Nagy Z., Rossi D., Schlueter A.: BIM-extracted EnergyPlus model calibration for retrofit analysis of a historically listed building in Switzerland. In Proceedings of SimBuild, 2014

ECO-ENERGETIC ANALYSIS AND SIZING OF CHP/PV ENERGY SYSTEM IN RESIDENTIAL APPLICATION

Lucien Dorthe[1]; Ralf Dott[1]; Thomas Afjei[1]; Bernd Hafner[2]
1: Institut Energie am Bau, Fachhochschule Nordwestschweiz FHNW, St. Jakob-Strasse 84, CH-4132 Muttenz, Switzerland
2: Viessmann Werke GmbH & Co KG, D-35107 Allendorf, Germany

ABSTRACT

Economic, energetic and environmental concerns foster the development of clean and efficient solutions for residential energy systems. Combined heat and power (CHP) systems allow covering the heat and electricity demand simultaneously. Micro-CHP systems are expected to spread in building application during next years. Thus, finding an optimal size and configuration between micro-CHP, PV module and battery could help to improve the energy saving potential of such systems.

The goal of the study is to identify and understand the influence of some key parameters like PV size, CHP power or battery size on CHP/PV system eco-energetic profitability in residential application with focus on the interactions between components. A parametric study is performed to find an optimal trade-off between objective functions like electricity self-sufficiency, electricity self-usage, CO_2 impact or costs. The heating system of the building is modelled and simulated in a Simulink/Carnot model and analysed. The system is composed of a micro-CHP plant (Var.I: 2.3 kW_{th} / 1 kW_{el} ; Var.II: 9 kW_{th} / 5 kW_{el}), a gas fired burner (19 kW_{th}), a PV system (dif. sizes: 0-10 kW_p), a battery bank (dif. sizes: 0-10 kWh) and a thermal storage. Two buildings were evaluated, a new built (45 kWh/m^2/a) and an existing non-retrofitted (150 kWh/m^2/a). The control strategy is primarily designed to satisfy the heat demand of space heating and DHW.

For both buildings, a configuration was found with a very low need for grid electricity (< 20 kWh/a). Nevertheless, this configuration does not correspond to the best solution from an economical point of view. Therefore, a trade-off solution is proposed to minimize the annual costs and the electricity imported from grid. As example, for the retrofitted building, a 10 kW_p PV system and a 2.5 kWh battery gives an annual cost of 2'280 CHF with a grid electricity import of 198 kWh/a.

Keywords: Micro-CHP, Residential energy system, Photovoltaic, Battery storage

INTRODUCTION

CHPs are very efficient systems able to cover the heat and electricity demand of buildings. By coupling PV modules and CHP, the electricity demand, on an annual basis, is easily covered. Nevertheless, to cover the entire electricity demand, particularly during the night (no PV production), a battery system is needed to store the electricity produced during the day and to restore it, when needed. Having a building which is completely autonomous can also be interesting from an economical point of view. Indeed, the electricity selling price is expected to drop while the buying price will increase. Thus, it is interesting to maximize the amount of electricity produced on site and to minimize the importation. In this study, it is tried to identify the influence of parameters like PV size and battery size on CHP/PV system eco-energetic performance. Additionally, the existence of an optimal configuration, between costs

and electricity self-sufficiency is evaluated. The environmental impact is also highlighted using the CO_2 emissions as indicator.

METHOD

This study is simulated dynamically in Matlab/Simulink using the Carnot Blockset. The energy system consists of a CHP, a backup gas boiler, a PV installation and a battery bank. The produced heat is stored in a 750 l tank, from which heat is taken for the space heating and the DHW. The buildings are based on the SFH45 from the IEA HPP Annex 38 / SHC Task 44 "Solar and heat pump systems" (A38T44) [1] and are located in Strasbourg (moderate climate).

Building model

The first building (B1) represents a newly built single-family house with a good thermal envelope. Its space heating demand is 45 kWh/m^2/a. The second building (B2) represents an existing non-retrofitted building with a space heating demand of 150 kWh/m^2/a. Both buildings have an energy reference area of 150 m^2. Figure 1 depicts the schematic of the building energy system. Some conditions and parameters are applied for all simulations:

- The hot water tapping profile was simplified to three tapings per day (7:00 / 80 l; 12:00 / 40 l; 19:00 / 80 l) corresponding to a total need of 200 l/day at 45°C (2'970 kWh/a).
- The heat is generated by the CHP (and the backup heater) and stored in a 750 l tank, which serves for the DHW and for the space heating.
- The electricity demand profile was generated with the tool Load Profile Generator® [2]. It represents a typical usage of households (kitchen, multimedia, lighting,…), where two adults and two children are living. This represents an annual consumption of 3'247 kWh.
- Two types of internal heat gains are considered in the simulations. One occupation profile corresponding to a yearly value of 1'350 kWh and a waste heat profile from electrical equipment corresponding to a yearly value of 2'010 kWh. Both profiles are taken from the building definition in IEA HPP Annex 38 / SHC Task 44 [1].
- For all cases, the PV panels are south oriented with an angle of 20° from horizontal.
- For the space heating, the heat delivery system is a floor heating (35°C) and a radiator (60°C) for the building B1 and B2 respectively.
- A natural gas burner of 19 kW, with an efficiency of 98%, is used as backup heater.
- The battery is modelled like an integrator with a charging/discharging efficiency of 95% (roundcycle efficiency of 90%). A power limitation of 4kW is applied. No self-discharge rate is considered.
- The CHPs are modelled in a simplified way, taking into account the total gas consumption and the efficiencies to evaluate the heat and the electricity generated.
- For the electricity self-usage, the CHP electricity has always the priority over PV when CHP and PV are producing at the same time.
- The CHP and backup burner control strategy is only based on the heat needs. The tank temperature is maintained at the desired level (with a hysteresis) during the entire year.

Energetic analysis

Two indicators are used to evaluate the energetic performances, the electricity taken from or fed to the grid. It represents on one side, the level of electricity self-sufficiency of the building and on the other side, the part of electricity produced and not used on-site.

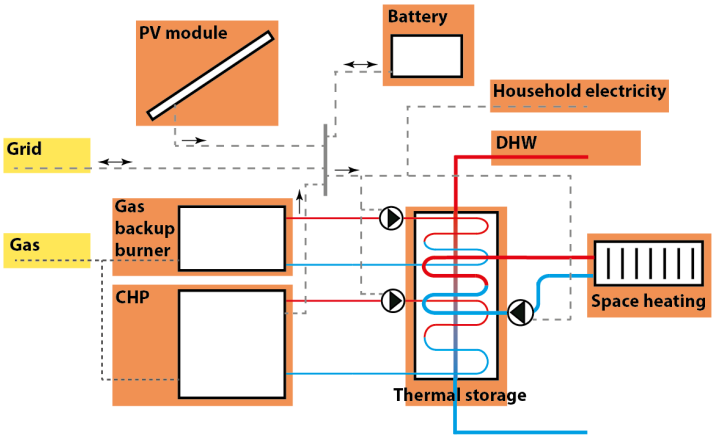

Figure 1: Schematic of the energy system

Economic analysis

The following components are considered for the investment: PV system, battery bank, micro-CHP and backup heater. The currency chosen is the Swiss Franc (the inflation was not considered). At the time of the study the currency change CHF-EUR was 1.03 CHF/EUR. The parameters used for the investment cost calculation are recapitulated in Table 1. For the PV system, the Swiss government offers a contribution of 1'400 CHF + 680 CHF/kW_p to foster the installation of PV modules (new installation built between 04.2015 and 09.2015). All components have a lifetime of 20 years except the battery, for which the lifetime is only 10 years. Thus, the battery is replaced once during the entire lifespan. The economic indicator used in this study is the annual cost (CHF/a). It is composed of the operation costs and of the annualized investment, assuming that this investment is a loan repaid over the entire lifespan (20 years with an interest rate of 6%).

Category	Value	Source
PV system (incl. inverter)	1.08·(1.56 EUR/W_p)	Hoppmann et al. [3]
Battery bank	1.08·(171 EUR/kWh+242 EUR/kW) (lead-acid)	Hoppmann et al. [3]
Micro-CHP	3'400 EUR/kW_{el}	Brandoni et al. [5]
Backup heater	115 EUR/kW	Kapsalaki et al. [6]

Table 1: Economic parameter for investment cost calculation

Category	Value	Source
PV system (maintenance)	1.5% of PV costs per year	Hoppmann et al. [3]
Battery bank (maintenance)	19 EUR/kW per year	Hoppmann et al. [3]
Micro-CHP (maintenance)	0.021 EUR/kWh_{el}	Brandoni et al. [5]
Backup heater (maintenance)	80 EUR per year	Tronchin et al. [7]
Gas price	0.1031 CHF/kWh	IPC / energy [8]
Electricity buying price	0.2149 CHF/kWh	IPC / energy [8]
Electricity selling price	0.1455 CHF/kWh	Groupe E [9]

Table 2: Economic parameter for operation costs calculation

The operation and maintenance costs are presented in Table 2. The electricity and gas prices are taken from the actual Swiss market. In this study, the electricity and gas prices were considered constant over the 20 years lifespan.

Environmental analysis

The environmental analysis is based on the energy system CO_2 emissions. For the electricity, based on the Swiss mix, the CO_2 specific emission of 0.091 kg/kWh is taken from the information given by the "Federal Office for the Environment" [10]. For the gas amount consumed a specific emission of 0.202 kg/kWh is also considered [11].

Decision variables

For the analysis, some parameters are changed to see their influences on the eco-energetic performances:

- The PV panel peak power is varied between: 0 kW - 2.5 kW - 5 kW - 7.5 kW - 10 kW.
- The battery capacity is varied between: 0 kWh - 2.5 kWh - 5 kWh - 7.5 kWh - 10 kWh.
- Two different micro-CHPs are evaluated. The first one (CHP1) has an electric power of 1 kW_{el} and a thermal power of 2.33kW_{th} with efficiencies of 0.27 and 0.63 respectively. The second one (CHP2) has an electric power of 5 kW_{el} and a thermal power of 9 kW_{th} with efficiencies of 0.33 and 0.6 respectively.

RESULTS AND DISCUSSIONS

The results are presented in Table 3. The solution with the lowest investment cost is presented as reference. For each indicator, the best solution is presented with the corresponding value of the decision variables. An additional trade-off point is presented, which is defined as follow: minimal annual cost possible with a maximal electricity import of 200 kWh/a (about 10% of import without PV and battery).

Some general comments can be made:

- All configurations have a positive annual electrical balance.
- Heat demand of the building is always covered, including domestic hot water.
- For all cases, the reduction of CO_2 emissions is relatively low (-3%).
- Since the priority is made on the electricity produced by the CHP, the PV electricity is mainly fed to the grid (60-90%). For the CHP, the part being fed to the grid varies between 40 and 55%.
- The degree of electricity self-sufficiency reaches quickly 90% with a battery. The battery bank has the biggest impact than the PV size. It works mainly as a daily storage.
- PV modules size has an important effect on operating costs since the overproduction is sold to the grid.
- Since the electricity can be exported and sold to the grid, the operation costs decrease quickly with the PV size: about 50% reductions when having a 10 kW_p PV system compared to no PV system.
- As reference, for building B2, if all electricity was bought and all heat produced by the gas burner, the annual cost would be 3'630 CHF/a (investment included).
- It can be seen that for both buildings, the small CHP (CHP1) has better performances. It has lower costs and the peak power heat demand is covered by the backup gas burner.

For the building B1, the configuration with the lowest amount of electricity taken from the grid is the one with a 10 kW_p PV system and a 10 kWh battery. In this case, the building is almost autonomous, only 16 kWh are imported per year, which are mainly due to maximum peak power demand. This is also the solution with the lowest CO_2 emissions. For the lowest annual cost, the configuration is a 10 kW_p PV system and no battery. The total costs are 2'060 CHF/a. It corresponds to the solutions with the biggest electricity export. The tradeoff point was found with an electricity importation of 198 kWh and an annual cost of 2'280 CHF. With

10 kW_p PV, it can be seen that already a small battery (2.5 kWh) can reduce the amount of grid electricity the import considerably (from 1'130 to 198 kWh). Figure 2 shows the imported electricity and the annual costs for the building B1 with the CHP1. Without PV system, the imported amount of electricity is already reduced by about 75% with a 2.5 kWh battery. For the trade-off point of building B1, 50% of the initial investment is the PV system. The CHP represents 20% and the battery bank 17%.

		LIC	LGI	LCO2	LYC	TO
New building B1	CHP model	CHP1	CHP1	CHP1	CHP1	CHP1
	PV size [kW_p]	0	10	10	10	10
	Battery size [kWh]	0	10	10	0	2.5
	Grid import [kWh/a]	2'030	16	16	1'130	198
	Grid export [kWh/a]	2'720	10'000	10'000	11'230	10'200
	CO_2 emissions [kg/a]	3'620	3'430	3'430	3'530	3'450
	Annual costs [CHF/a]	2'560	2'520	2'520	2'060	2'280
Existing building B2	CHP model	CHP1	CHP1	CHP1	CHP1	CHP1
	PV size [kW_p]	0	10	10	10	10
	Battery size [kWh]	0	10	10	0	2.5
	Grid import [kWh/a]	1'780	14	14	950	110
	Grid export [kWh/a]	3'500	11'050	11'050	12'100	11'160
	CO_2 emissions [kg/a]	7'080	6'920	6'920	7'010	6'930
	Annual costs [CHF/a]	4'190	4'170	4'170	3'710	3'930

Table 3: Indicators and decision criteria for each scenario (LIC: lowest investment costs / LGI: lowest grid import / LCO2: lowest CO2 emissions / LYC: lowest annual cost / TO: trade-off point)

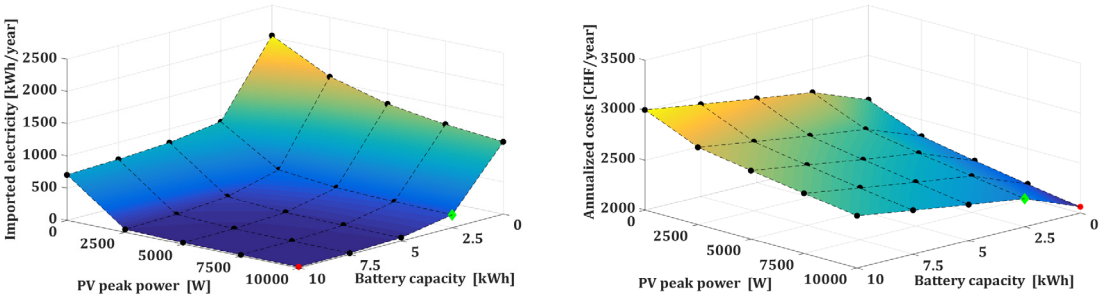

Figure 2: Imported electricity and annualized costs for building B1 with CHP1 (diamond/green point: TO point)

For building B2, the lowest grid import solution corresponds also to a 10 kW_p PV system and a 10 kWh battery. The configuration giving the lowest annual cost is a 10 kW_p PV system without battery. It gives an annual cost of 3'710 CHF. In comparison, for the same building but all the electricity imported and all the heat produced from the gas burner, the annual cost would be 3'630 CHF (investment of gas burner included). Once again, a big PV system allows selling a lot of electricity (up to 12'000 kWh/a), thus reducing the operating costs considerably (~30%). A good tradeoff solution is the one with a 10 kW_p PV system and a small battery of 2.5 kWh. It allows to reduce the grid import to 110 kWh/a and to limit the yearly costs to 3'930 CHF.

A sensitivity analysis was made to evaluate the impact of the inputs like investment costs, maintenance costs or gas and electricity buying price. It turns out that the most influencing parameters are the PV investment costs, the gas buying price and the electricity selling price.

For example, for the trade-off point of building B1, the annual cost is increased by 23.4% when the PV investment cost is increased by 30% and by 23% when the gas price is increased by 30%, which shows the big impact of PV purchasing price and electricity selling price on an economic analysis over 20 years.

CONCLUSION

This study showed that a CHP/PV system combined with battery storage can clearly reduce the building dependency on the grid. It was found that a small battery (2.5 kWh) helps already to improve electricity self-sufficiency of the building (+30%) without increasing too much the annual cost (+10%). A bigger battery is not needed since the battery works as a daily storage and it would only increase the investment cost without reducing the operation cost or increasing considerably the level of self-sufficiency of the building. From a point of view of electricity imported, a big PV system (10 kW_p) is not needed but such an installation is profitable from an economic point of view since the electricity produced can be sold. For both buildings the small CHP seems to be more profitable. Both CHPs are able to cover correctly the needs but the high investment cost of the CHP2 yield to high annual costs. In this study, the regulation scheme was not optimized. A new control strategy based on both heat and electric demand could reduce the costs and the electricity importation or allow minimizing the gas consumption (depending on the objective function to minimize / maximize).

The electricity and gas prices were considered constant over the entire lifespan. It was shown in the sensitivity analysis that a modification of those costs in the future can have a big impact on the economic analysis and profitability. Thus the energetic indicator should be taken with more weight that the economic indicators in case of design decision.

REFERENCES

1. M. Y. Haller, R. Dott, J. Ruschenburg, F. Ochs und J. Bony: The Reference Framework for System Simulations of the IEA SHC Task 44 / HPP Annex 38, 2011.
2. Universität Chemnitz: https://www-user.tu-chemnitz.de/~noah/index.php, 09.02.2015.
3. Hoppmann J., Volland J., Schmidt T.S., Hoffmann V.H., The economic viability of battery storage for residential solar photovoltaic systems – A review and a simulation model. Renewable and Sustainable Energy Reviews, Vol. 39, pp. 1101-1118, 2014.
4. Révision de l'ordonnance sur l'énergie au 1er janvier 2015, Swiss Federal Office for the Energy SFOE, Confédération Suisse.
5. Brandoni C., Renzi M., Optimal sizing of hybrid solar micro-CHP systems for the household sector. Applied thermal engineering, Vol. 75, pp. 896-907, 2014.
6. Kapsalaki M., Leal V., Santamouris M., A methodology for economic efficient design of Net Zero Energy Buildings. Energy in Buildings, Vol. 55, pp. 765-778, 2012.
7. Tronchin L., Fabbri K., Tommasino M.C., On the cost-optimal levels of energy-performance requirements for buildings: A case study with economic evaluation in Italy. International journal of sustainable energy planning and management, Vol. 03, pp. 49-62, 2014.
8. IPC Indice suisse des prix à la consommation 2014; prix moyen de l'énergie, Federal Statistical Office, Confédération Suisse.
9. Tarif de reprise pour installations de production < 10 kW, Groupe E
10. Umweltbilanz Strommix Schweiz 2011, Federal Office for the Environment FOEN, Confédération Suisse.
11. Facteurs d'émission de CO2 selon l'inventaire des gaz à effet de serre de la Suisse, Fiche d'information, Federal Office for the Environment FOEN, Confédération Suisse.

PERFORMANCE CONFRONTATION BETWEEN PARAMETRIC ANALYSIS AND EVOLUTIONARY ALGORITHM TO ACHIEVE PASSIVE HOUSES IN WARM CLIMATES

António Figueiredo[1]; Jérôme Kämpf[2], Romeu Vicente[1]

1: RISCO - Department of Civil Engineering, University of Aveiro, Campus Universitário de Santiago, Aveiro, 3810-193 Aveiro, Portugal

2: Solar Energy and Buildings Physics Laboratory, École Polytechnique Fédérale de Lausanne, Switzerland

ABSTRACT

Passive House (PH) is a concept that serves as a starting point for future zero balance energy houses. With its particular technical and constructive features adapted to specific climate zones and their corresponding climatic boundary conditions, the application of the concept is a necessary strategic condition to support and promote high-energy efficient dwellings. The latter is important to fulfil the main objectives established by the recast of the Energy Performance of Buildings Directive (2010/31/EU, EPBD) for 2018. Acknowledging that the PH concept was established and adopted mostly in cold climate context, the present study investigates how this approach can be extended to warmer climates, in particular to Portugal Mainland climate. In such south-western European climates, in addition to meeting the heating requirements, it is necessary and crucial to provide comfortable conditions in summer, due to a high risk of overheating in the case of fairly glazed dwellings. In this study, a comparison between two approaches: i) a parametric analysis, and an ii) optimisation with a hybrid evolutionary algorithm is proposed to achieve the PH requirements in terms of energy demand imposed by the PH concept (15 kWh/m^2.a). The base case, a representative contemporary architecture dwelling of concrete frame and masonry infills was modelled resourcing to dynamic thermal simulation with Energy Plus software as the energy-modelling tool. The paper presents the optimal solutions obtained by resorting to the parametric study and the evolutionary algorithm (EA), together with an analysis of their performance. The paper compares, taking into account the advantages and disadvantages of the use of an evolutionary algorithm to standard trial and error practice approach.

Keywords: Energy Efficiency, Optimization, Evolutionary algorithms, Passive House

INTRODUCTION

In the recent decades the primary energy demand has increased exponentially, mainly due to the impact of the building sector. It is estimated that this sector is responsible for consuming 40% of the total energy use of the European Union (EU) [1]. In Portugal, the General Division for Energy and Geology (in Portuguese: Direção Geral de Energia e Geologia (DGEG)) collected data that revealed a significant impact on the global energy demand. Approximately 17% of the energy in 2009 is used in residential buildings [2]. On one hand in recent years (2000-2009 period), the energy consumption in EU buildings has not changed significantly, but on the other hand, in the South western European countries it increased, due to the cooling energy demand [3]. Therefore, it is important to highlight the need to thoroughly understand and assess the external envelope constructive solutions adopted in those countries by optimizing insulation thickness, windows solutions, shading protections, etc. for mitigation of the cooling demand without undertaking high overheating risk in summer. To fight against these numbers, the PH concept is foreseen as the way to reduce the

annual energy demand in buildings and to provide high comfort level. Acknowledging that this concept was born in Germany and is well been established mostly in central Europe, other studies in South European zones should be developed. In these zones the summer interior temperature is ever more reliant on window size and orientation, shading devices, interior heat sources and ventilation rate, since there are concerns in respect to overheating risk. As a consequence, the construction technology and detailing has to be adapted to the specific climate zone location and specific climatic boundary conditions. The goal of this work consists in the definition of envelope solutions to apply in buildings located in Mediterranean zones that comply with the PH requirements, comparing parametric and evolutionary optimisation methods.

METHODOLOGY

Dynamic thermal simulation of a detached building was accomplished using EnergyPlus® 8.2.0 (EP) software. EP was used as calculation engine to support the parametric and evolutionary optimization analyses. The first step starts by a hygrothermal monitoring campaign of the building, used to validate the numerical model. The second step was accomplished resourcing to a parametric analyse. Many features were assessed and evaluated, such as glazing type and orientation, bypass air flow rate, and insulation thickness in order to assess the building thermal response. A comparison between parametric analyses and evolutionary approaches was performed. An EA for minimization of a multi objective function, heating and cooling demand was used and the results were presented and compared. Once, the improvements achieved, as third step was defined, a set of new simulations were carried out in order to define the best Passive House solution for other regions of Portugal mainland. The parameters from the best solutions found in the parametric analysis were used as restrictions (upper limit) in the optimized parameter approach. In this way a comparative survey was developed, to find new optimized solutions and to compare parametric versus evolutionary optimization results.

CASE STUDY OF A DETACHED BUILDING

Building characterization

The building is located in Aveiro at about 5 km from the centre city and 12 km from the Atlantic coast, in North central Portugal. This building is situated at latitude of 40.613427ºN, a longitude of -8.652487ºE and 17 m of altitude. Two floors define the proposed architectural solution. The ground floor entails the common part of the building and the first floor comprises the bedrooms and bathrooms (Figure 1). The building has 163 m^2 of treated floor area with a 405 m^2 of exterior surface area and the global percentage of glazing is about 21% of the opaque facade area. The glazing oriented to the North represents a relative percentage of the total glazed area of 26%, 47% to South, 25% to East and finally 2% to West.

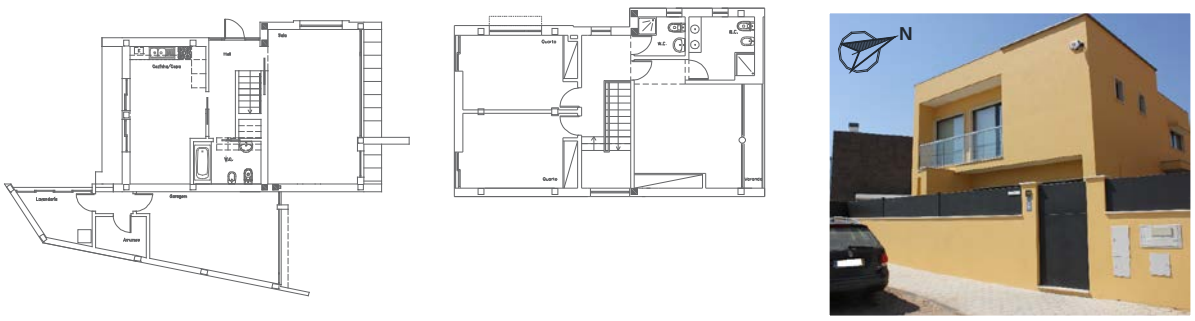

Figure 1: Architectural blueprints (no scale): ground floor level on the left, elevated floor level on the centre and a real 3D view on the left

The building's envelope walls are composed of a double leaf horizontally hollow clay brick with an air gap, partially filled with 4 cm of XPS insulation. The thermal properties of the adopted constructive solutions were (in W/m^2 °C): ground floor slab U_{value} = 0.693; façade walls U_{value} = 0.454; flat roof U_{value} = 0.332. The value of thermal transmission coefficient used for windows ($U_{w,\ installed}$ = 1.77 and solar heat gain coefficient = 0.56) and external glazed doors ($U_{w,installed}$ = 1.40), taking into account the thermal bridges (linear thermal transmittance, Ψ) from the frame, spacer and the window installation. In order to optimize the parametric analysis, an average value, $U_{w,installed}$, was calculated, according to the Passive House Planning Package data Sheet (PHPP).

Numerical modelling: monitoring and validation

The numerical model was validated with data provided from a hygrothermal monitoring campaign developed during some periods in 2013. To record temperature and relative humidity it was used sensors with a temperature probe with 0.5ºC error and a resolution 0.1ºC and with a humidity probe with 3% error and 0.1% resolution. The deployment of *in-situ* sensors, inside of the compartments was done in accordance with ISO 7726 [4]. The numerical model was validated with weather data collected from a local weather station (7km from the local site). The comparison between measured and simulated results was done for the indoor air temperatures during the last week of August without occupation and during December with occupation to validate the numerical model with a real occupancy profile and internal gains. The overlapped results shows a fairly good agreement between the numerical model and *in-situ* measurements with differences between both curves of 1°C maximum.

Thermal building simulation

SkectchUp® tool with OpenSudio plugin, with a graphical interface, were used to reproduce the geometry of the model and define features related to thermal zoning and constructive solutions. The annual thermal behaviour of the building was simulated and calculated resourcing to EnergyPlus® software. A detached multi-zone model was assembled using nine thermal zones (TZ), corresponding to internal compartments of the building. The ground floor has five TZ including the garage (unheated space), and the first floor has another five TZ. One of these five zones is common to both floors levels, including the corridors and the staircase.

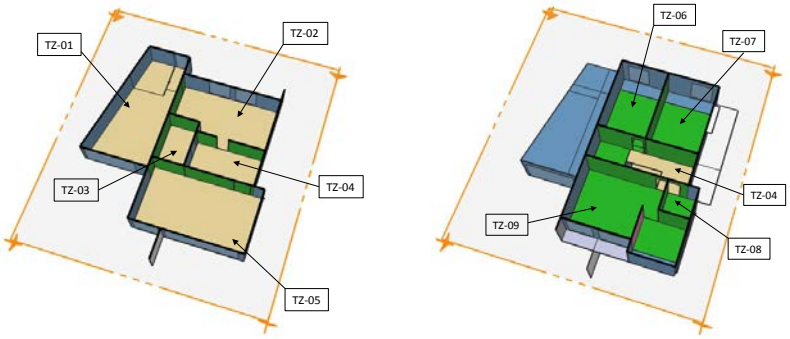

Nomenclature:
TZ-01 – Garage
TZ-02 – Kitchen
TZ-03 – Bat_GF
TZ-04 – Hall (2 floors)
TZ-05 – LivRoom
TZ-06 – BedR_1N
TZ-07 – BedR_2N
TZ-08 – Bat_1ºF
TZ-09 – BedR_1S

Figure 2: Indoor space thermal zone layout

RESULTS AND DISCUSSION

Building characterization

The original building which constitutes our reference case was modelled with an HVAC system to determine the annual energy consumption for heating and cooling as a first approach. In a second approach, the dwelling was modelled without the mechanical ventilation system for heating or cooling. However 0.6 h^{-1} was ensured as a natural ventilation

mode. The second approach without a mechanical system allowed a passive comfort assessment in accordance with standard EN 15251 category II [5]. The overall energy demand for heating the dwelling was 34.39 kWh/m^{2}a and for cooling was 6.96 kWh/m^{2}a considered that the temperature setpoint range was 20-26ºC for all thermal zones. In the passive approach four thermal zones were selected as representative of the overall dwelling behaviour.

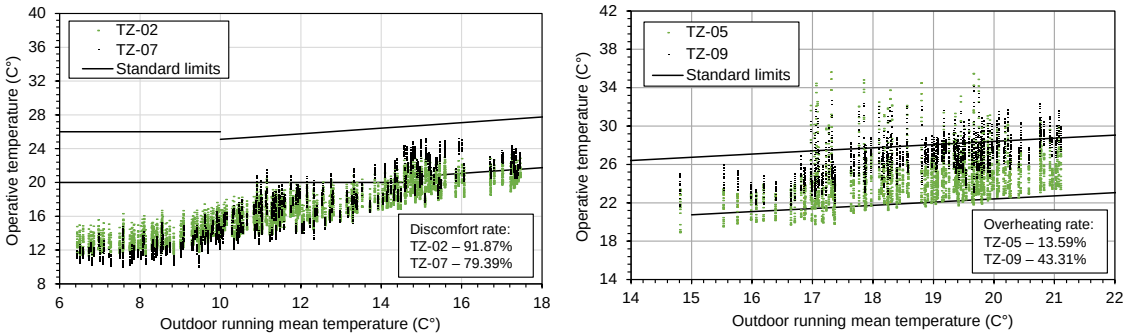

Figure 3: Indoor air temperature for heating (left plot) and for cooling (right plot) seasons

Analysing Figure 3, it is possible to verify an exceedance of the adaptive comfort limits below the lower limit curve for indoor air temperature in heating season and above the upper limit for the summer, indicating long periods of discomfort in winter and overheating in summer.

Parametric simulations - improvements

A series of numerical simulations were carried out in order to analyse the effect and improvement of passive techniques. Different scenarios were defined to evaluate the thermal behaviour. The simulations, were performed combining the following parameters: a) rotation of the building with 0° (original position) 90°, 180°, and 270°; b) additional air flow rate from 0 to 2.4 (bypass capacity is expressed in h^{-1}); c) insulation thickness (walls, roof and floor) between 4 and 12 centimetres; d) original windows solution with double glazing (characterized in section “Building characterization”) and another solution with triple glazing with thermal transmission coefficient of $U_{w,installed}$ = 1.18 and a solar heat gain coefficient value SHGC = 0.5. Summing up, a total of 72 models ran and analysed.

Selected scenarios and results

Parametric analyses

From the simulations performed, the best scenarios were discussed in terms of energy demand for heating and cooling for the comfort range defined (20º - 26°C). Figure 4 lists the best simulations that lead to the best performance. This is the lowest combined heating and cooling energy demand for an annual simulation. The best scenario corresponds to a solution resourcing to a triple glazing, 12cm of insulation for walls, roof and floor, ACH equal to 0.6 with additional bypass rate (ACH = 2.4h^{-1}), and, with the dwelling rotated from the North to 180°C. Comparing with the original solution (34.39 kWh/m^{2}a), a reduction of 42% of the heating energy demand is obtained and the reduction in the cooling demand was 64%.

Multi-objective evolutionary optimization definition

Optimization is an ongoing process of searching and comparison of feasible solutions to a given problem, until no better solutions can be found [6]. In this study four types of decision parameters were used concerning the alternative combinations. The parameters used in the optimization process were the same used in the manual trial and error process. The alternative input parameters considered, and correspondent input method are shown in the Table 1.

Parameter id.	Designation	Box Constrains	Step
x0	Insulation Thickness	0.04 – 0.12 (mm)	0.01
x1 – x8 (by TZ)	Bypass Air flow	0.00 – 2.40 (h^{-1})	0.01
x9	Dwelling Orientation	0 – 360 (º)	1
Strings			
x10	Window Solution	U_{value} = 1.77 (W/m^2 °C) and SHGC = 0.56	
x11		U_{value} = 1.18 (W/m^2 °C) and SHGC = 0.50	

Table 1: List of parameters and constraints

As objective functions a multi-objective optimization was used to minimize the opposite functions: heating and cooling demand.

Multi-objective evolutionary optimization results versus parametric results

The results in this sub-section contain the points of the Pareto front that represents a set of optimal solutions and the points which represent the best solutions from parametric analysis.

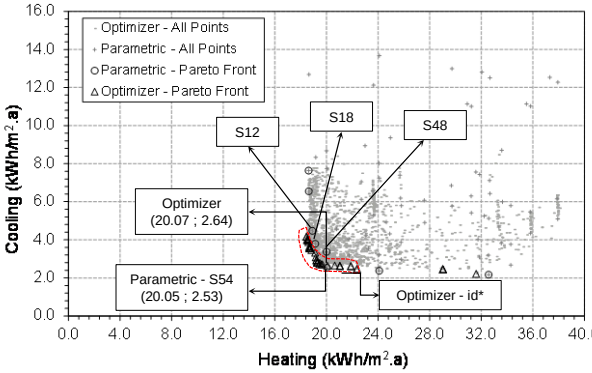

Simulation id.	Insulation Thickness (cm)	Building Orientation	Windows type	By pass air rate h^{-1}
Parametric solutions				
S12	12	0º	TG	1.2
S18	12	0º	TG	2.4
S48	12	180º	TG	1.2
S54	12	180º	TG	2.4
Evolutionary optimization				
Id5811	12	270º	TG	1.98
Id3808	12	241º	TG	2.02
Id8682	12	101º	TG	2.18
Id6773	10.5	271º	TG	2.09

[a] TG – Triple glazing | DG – Double glazing

Figure 4: Comparison between multi-objective optimizer and parametric analysis

Comparing the results from the parametric analysis with the results from the optimizer (Figure 4) differences between 2% to 3% were observed for heating demand and differences between 3.5% and 17% were observed for cooling demand. The results were always better in the optimizer with the exception of the scenario S54 that represents a solution with all the parameters in the upper limit of the defined constraint range. The difference observed between this scenario and the closest non-dominated scenario from the optimizer, was 0.1% for the heating demand and 4.1% for the cooling demand.

PASSIVE HOUSE ASSESSMENT FOR DIFFERENT REGIONS

In this section the PH adaptability measures are assessed for different regions in Portugal mainland. To broadly characterize the different climatic regions of the country, two regions, representative of the interior North and South (Bragança and Évora) and two other near to the coast (Aveiro and Faro) were chosen. As the original building model definition does not comply with the PH requirements as well the improved solutions, a mechanical ventilation system with heat recovery (80% efficiency) was used in turn of the conventional HVAC system used in the first approach.

Results and discussion

The same parameters ranges were used in the attained parametric solutions for each region and were also adopted as the upper limit restriction in the optimizer parameters. The

following plot (Figure 5) shows the best solutions provided from the parametric analyses versus Pareto front from the optimizer approach.

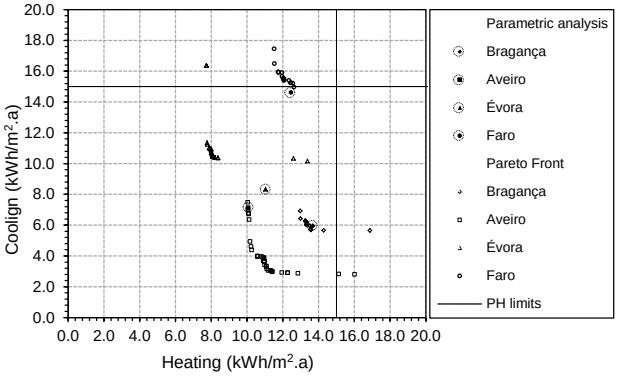

Simulation id.	Insulation Thickness (cm)	Building Orientation	Windows type*	By pass air rate h^{-1}
Parametric solutions				
Bragança	12	180º	TG	2.40
Aveiro	8	270º	DG	2.40
Évora	8	180º	DG	2.40
Faro	4	180º	DG	2.40
Evolutionary optimization				
Bragança	12	85º	TG	1.77
Aveiro	8	262º	DG	1.79
Évora	8	87º	DG	2.16
Faro	4	90º	DG	1.91

[a] TG – Triple glazing | DG – Double glazing

Figure 5: Attained solutions for different zones (Pareto Front with 10.000 evaluations)

Analysing the results the major advantage in use the evolutionary optimization is a wide range of possible solutions assembly. In this particular study and because the attained solutions were always in the upper frontier of the range proposed for the four parameters, the parametric analysis solutions are always near to the best configured solution form the EA approach. The best obtained solution from the parametric analysis for Évora and Faro present less cooling demand, however from the optimisation approach, some solutions attained in the Pareto front show optimised results for these regions by the sum of cooling and heating demand. The optimizer works to finding the best commitment between the both objective function defined.

CONCLUSION

A comparison between two different approaches (optimization and parametric analysis) was applied to a detached dwelling case study. Regarding the results, the parametric analysis is always dependent on the previously defined parameters increment chosen. A parametric analysis can be useful to test an individual set of parameters to understanding the impact of an improvement measure package defined. Multi-objective evolutionary algorithms produce a wide range of non-dominated solutions. The final decision can therefore be based on a real understanding and can be taken by the owner or the designer. In sum the proposed approaches shows a great potential for the evolutionary algorithm approach to solve problems related to retrofit or improvement package solutions. EA can be used as an aid to decision-making in the context of a design project definition.

REFERENCES

1 Buildings Performance Institure Europe.: Europe's buildings under the microscope. 2011.

2 Directorate General for Energy and Geology.: Residential Energy Consumption Survey 2010, in *Statistics Portugal, Lisbon, Portugal, 2011*

3 Balaras, C. Grossman, G. Henning, H. Infante Ferreira, A. Podesser, E. Wang, *L.:* Solar air conditioning in Europe, an overview, *Renewable and Sustainable Energy Reviews*, vol. 11, pp. 299-314, 2// 2007.

4 Ergonomics of the Thermal Environment, Instruments for measuring physical quantities, I. 7726, 1998.

5 EN 15251:2007-08.: Indoor environmental input parameters for design and assessment of energy performance of buildings addressing indoor air quality, thermal environment, lighting and acoustics. CEN, Brussels, Belgium, ed, August 2007.

6 Kalyanmoy, D.: Multi-Objective Optimization using Evolutionary Algorithms, ed. Chichester, England: John Wiley & Sons, Ltd, 2001.

NON-LINEAR THERMAL NETWORKS – HOW CAN A MESHED NETWORK IMPROVE ENERGY EFFICIENCY?

T. Schluck[1], P. Kräuchi[1], M. Sulzer[1]

1: Lucerne University of Applied Sciences and Arts, School for Engineering and Architecture, Competence Centre for Integrated Building Technology (HSLU ZIG), Switzerland

ABSTRACT

A promising mean to realize the integration of decentralized thermal energy sources in districts and urban areas are low-temperature-networks (LTN). However, the general modus operandi of LTN can differ greatly. A very common approach in district heating is to supply consumers with heating and cooling power on the bases of unidirectional mass and energy flows. These systems consist of supply and return ducts. On the other hand, more recently designed networks operate on bidirectional mass and energy flows between a warm and cold duct. The underlying concept is inherently non-linear in character and still bears some challenges and open questions to research.

The question addressed here is what conceptual system design is more energy efficient. With reference to already realized systems, namely "ETH Hönggerberg" and "Brig-Naters", two simulation models were developed and equally parametrised to compare their conceptual designs in regard to their exergetic efficiency. One system operates on unidirectional, the other on bidirectional mass and energy flows. The simulation models consider consumers with heating and cooling demands and a source. For both systems the energy and exergy flows as well as the auxiliary powers were calculated.

Keywords: low-temperature networks, energy efficiency, exergy analysis, modelling, simulation

INTRODUCTION

Low-temperature networks (LTN) are characterized by their reduced operating temperature of approximately 8°C – 20°C. At this temperature level energy transportation losses are significantly reduced and by far less an issue when compared to district heating and cooling networks, which are operating at higher (or lower) temperature levels. A further benefit of LTN is the possibility of freecooling, which is especially advantageous when a seasonal storage is implemented within the LTN. However, these benefits are accompanied with the necessity of heat pumps that provide a sufficient temperature level. The heat pump's efficiency directly depends on the temperature spread and it follows that the building standard of the LTNs customers is a crucial factor. But in the case of a well-defined surrounding, how important is the modus operandi of thermal networks itself?

To approach this question, we compared two different conceptual designs of thermal networks. Each of them comprised the same heating unit (H) drawing heat from the system, the same cooling unit (C) feeding heat into the system and an ideal source, which heats up the system, respectively cools it down if necessary according to simple control regulatories. The first type of system refers to the thermal network of "Brig-Naters" and operates on unidirectional mass and energy flows and is equipped with a centralized circulation pump. The network's source keeps the temperature of the supply duct within a certain bandwidth. The second system refers to the thermal network of "ETH Hönggerberg" that consists of a

warm and a cold duct having circulation pumps located at each costumer of the LTN. In contrast to the unidirectional approach, each costumer conveys the amount of water bidirectional for himself, i.e. from whatever duct that fits his temperature demand best. In a first step focus was set on the annual operational performance of each system. Therefore the heat flux and exergy flow were quantified and all exergy flows across the LTN systems were calculated.

METHOD

The two thermal networks were built-up using in-house developed simulation modules, which are described in [1, 2]. Input data are heat flux profiles for each consumer as shown in Figure 1 and the annual curve of the ambient temperature (not shown here). The heating input profile corresponds to the room heating demand of a greater domestic building with floor heating. On the consumers' side a mean temperature of~35°C was assumed. The cooling demand profile refers to a modern office building using cooling ceilings with an assumed mean temperature of~15°C (freecooling). Each unit draws heat form the LTN with a fixed temperature spread of 4 K. Domestic hot water was not considered in these simulations as it is roughly constant throughout the year and thus only results in an offset.

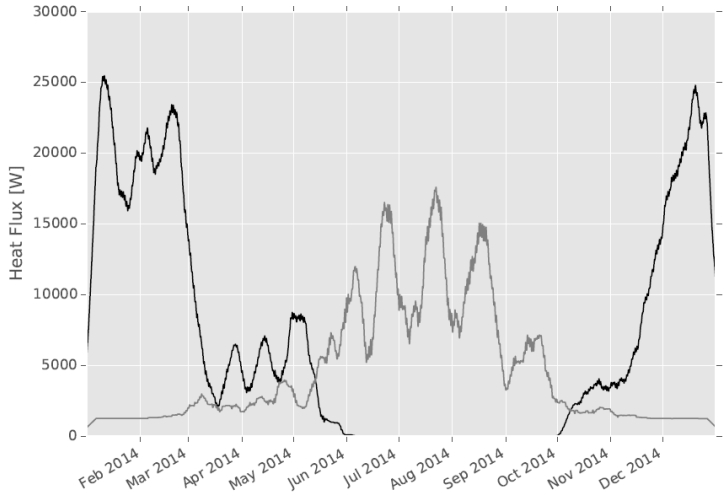

Figure 1: Input data for the simulations. Data frequency is "hour". The profiles were smoothed by a simple moving average (N = 250). The black line is the heat flux demand for heating of a residential building (60 MJ/a). The grey continuous line shows the cooling demand of an office building (40 MJ/a). The overlap of the profiles is 9.8 MJ/a in total.

Figure 2 represents the unidirectional system, which is temperature controlled and driven by the centralized circulation pump. The bidirectional system shown in Figure 3 is more self-regulated in the sense that the consumers' total conveyed mass flows drive the system [1, 2].

The models contain each one cooling unit and one heating unit. To allow for a comparison of both thermal networks, the systems were identically parameterised and kept as simple as possible. Heat fluxes into the LTN are considered positive and negative when leaving the system. The heat pumps were idealized and considered with their highest theoretical efficiency; all heat exchangers were taken into account without losses. Based on the heat fluxes crossing the systems' borders the exergy flows were calculated with reference to the ambient temperature [3]:

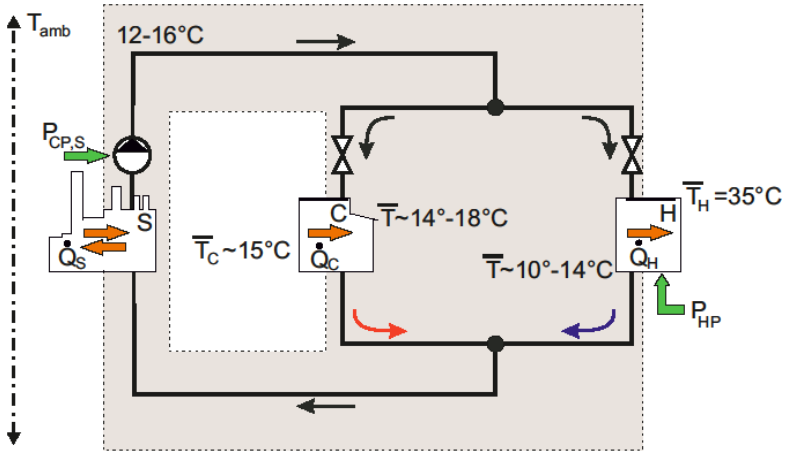

Figure 2: Synoptic presentation of the considered unidirectional thermal network. Mass flow passes the source in one direction. The supply line's temperature is kept in a band of 12-16°C. The coloured background represents the system and its boundaries. Heat and exergy flows cross the system at the source, the cooling and the heating unit. The consumers must throttle down the overall system pressure to achieve the demanded mass flow.

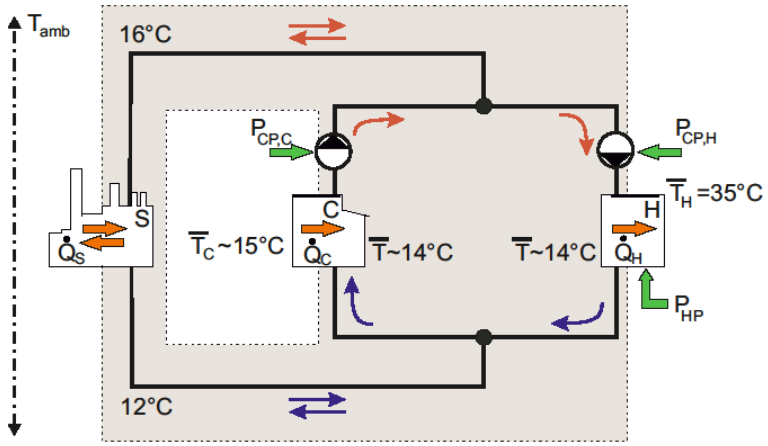

Figure 3: Synoptic presentation of the considered bidirectional thermal network. Mass flow passes the source in both directions. Warm and cold ducts are kept at 16°C/12°C. Each consumer conveys the necessary mass flow from the duct suiting its demand.
(S: Source, C: Cooling unit, H: Heating unit, P_{HP}: Power uptake heat pump, P_{CP}: Power uptake circulation pumps, T_{amb}: ambient temperature, T_C: mean cooling temperature consumer side, T_H: mean heating temperature consumer side)

$$\dot{E} = \left(1 - \frac{T_{amb}}{\overline{T}}\right) \dot{Q}, \quad \text{with } \overline{T} = \frac{T_{in} - T_{out}}{\ln\left(T_{in} / T_{out}\right)}. \tag{1}$$

Temperatures	Source	Heating	Cooling
(T_{in} / T_{out}) – unidir	(T_{supply} / T_{return})	($T_{mean,LTN}$ / $T_{mean,heating}$)	($T_{mean,LTN}$ / $T_{mean,cooling}$)
(T_{in} / T_{out}) – bidir	(T_{warm} / T_{cold}), (T_{cold} / T_{warm})	($T_{mean,LTN}$ / $T_{mean,heating}$)	($T_{mean,LTN}$ / $T_{mean,cooling}$)

Table 1: Different temperature pairs used to calculate the exergy flows

Table 1 gives the temperature pairs used to determine all considered exergy flows. The listed mean temperatures were aggregated values from typical supply and return temperatures at the respective unit and kept constant during the simulations. The used ambient temperature was

the outdoor air temperature, which alike all further network temperatures was variable.
In addition, all auxiliary powers of the heat and circulation pumps were determined as well.

RESULTS

Major simulation results are presented in Figure 4 – 6.

Figure 4 shows the heat fluxes crossing over the source (S) and the belonging thermal exergy flows. 55 MJ/h (unidirectional LTN), respectively 56 MJ/h (bidirectional LTN) of the total necessary 60 MJ/a of heat are delivered from the thermal networks. About 84% of these (55 MJ/a / 56 MJ/a) are fed into the system by the source. The total amount of energy fed into, respectively taken out of the systems differs by 5%, at which the bidirectional system shows the higher total energy flow. It also shows the higher exergetic intake: The unidirectional network yields 60% of the exergy uptake compared to the bidirectional system (annual total energy was normalised for comparison).

Figure 5 gives the exergy flows into the heating unit (H), i.e. the exergy used up by the consumer for its heating purposes. As the consumers in both models are identically, their needs for exergy is identical as can be seen in subplot#3. About 10% of the annual heat consumed is exergy (6 MJ/a) of which in the unidirectional system 76% must be provided by the heat pump and only 65% in the bidirectional system. This reflects in the exergetic efficiency ($\eta_{ex} = \dot{E}_{H,LTN} / P_{WP}$). The bidirectional system yields a mean annual exergetic efficiency of ~ 40%, while the unidirectional system only reaches 24%. Thereby the bidirectional system saves about 0.7 MJ/a of electrical energy when directly compared to the unidirectional system.

A similar result was found for the circulation pumps when only ~ 40% of electricity was needed for the circulation pumps in the bidirectional LTN. However, this auxiliary energy was rather minor in magnitude and range from 29 kJ/a to 78 kJ/a, which is partially due to the fact that during the parametrisation of the model other aspects were more focused on.

Figure 6 shows the exergy flows that accompany the heat fluxes during freecooling (C). The figure gives the exergy flows in regard to the consumer and the network, whereas the leading sign was always chosen in reference to the network (positive sign towards, negative sign from the network away). However, a direct comparison of the systems exergy fluxes is in this case not possible. During the framed period (March - November) the mean temperature of the unidirectional system (~ 23°C) is higher than the temperatures necessary for freecooling (~ 15°C) and thereby not available.

DISCUSSION

In Figure 1 the overlap of the two input profiles is about 17%, i.e. ideally only 84% of energy must be fed into the system by the source from outside. The simulations showed such an ideal reuse of the available waste heat coming from the cooling unit. This is due to the fact that thermal losses of the pipes, losses of the heat exchanger and heat pumps were neglected and the components idealized. But this also gives a first albeit simple validation of this approach.
The finding in subplot#3 of Figure 5 is another indication as it shows that the additional amount of exergy flow gained in the bidirectional thermal network is equal to the additional power uptake of the heat pumps in the unidirectional system. Thus it becomes obvious that the choice and design of the system has a profound influence on the exergy efficiency and can be estimated with the help of simulations. A further important aspect besides the principle design of a system is how the system is operated on. The results in Figure 6 are an example how specification of the source turns freecooling for a long period of the year into unwanted

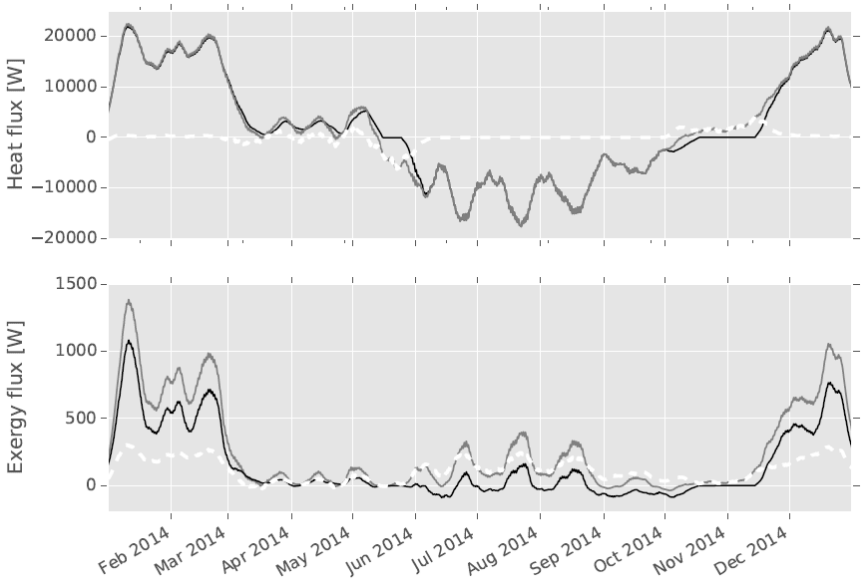

Figure 4: Heat flux (subplot#1) and exergy flows through the source (positive: into, negative: out of system). In black the results for the unidirectional, in grey for the bidirectional system. The difference is shown in white (dashed) line.

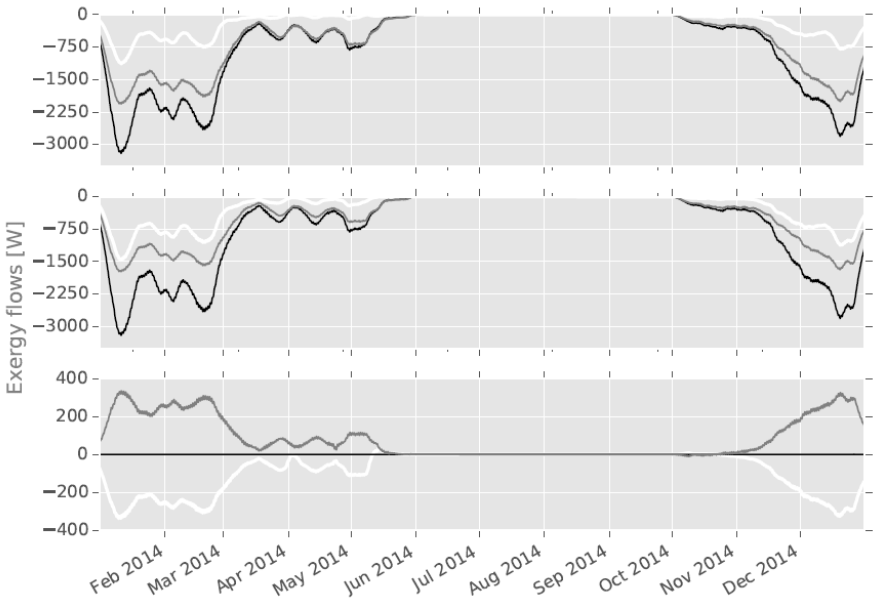

Figure 5: Exergy flows into the heating unit. Subplot#1 describes the unidirectional system; subplot#2 the bidirectional system; subplot#3 the difference subplot#1 – #2. The necessary total exergy flow for heating (black) is equal in both network typologies. Thermal exergy flows from the LTN are depicted in white and the exergy rose by the heat pump in grey.

"free-heating". This result does not affect the simulation by itself at large, because the exergetic calculations were done in a post-processing process and as long as it is presumed that the heat is fed into the system by an alternative (mechanical) cooling process. A further aspect of Figure 6 is the inherent loss of exergy alone due to the different mean temperatures of the LTN and consumer, which offers another chance for optimisations and the study of interfaces.

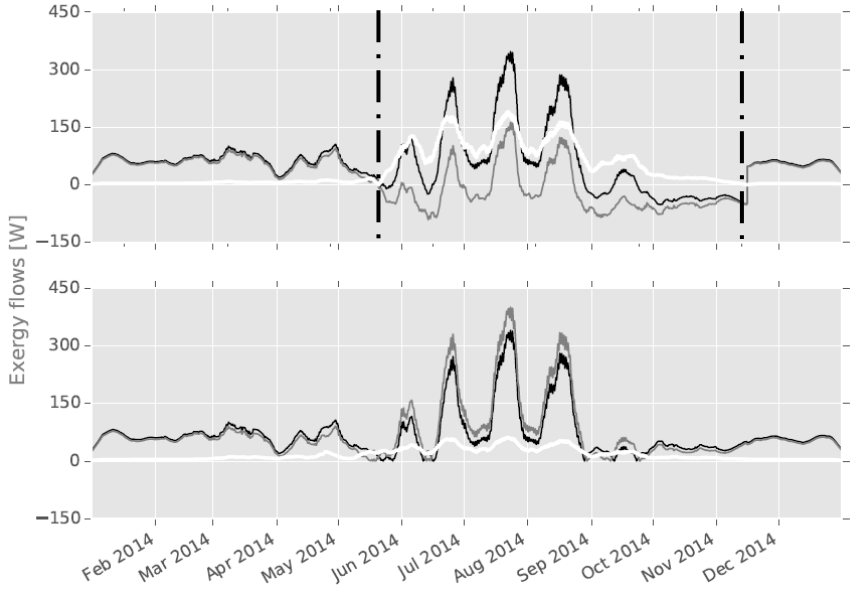

Figure 6: Exergy flows in the cooling unit. Subplot #1 shows the results for the unidirectional system, subplot #2 for the bidirectional. In black the exergy flow from the consumer is shown, in grey the exergy flow to the LTN. The white dashed line is the absolute loss of exergy due to different mean temperatures. The period framed by the dashed lines is explained in the text.

CONCLUSION

In this study two simulation models of LTN with different modus operandi were compared. The first system relies on the regulation of temperature and unidirectional mass flow, while the second allows bidirectional mass flows, but keeps two separate temperature levels. For equal parametrisation the simulation showed a clear advantage of the LTN operating with separate temperature levels and bidirectional mass flows. It outperforms the other in terms of exergetic receptiveness and economy and clearly allows the saving of electricity of significant magnitude.

To improve the model and to provide a tool for the conceptual design process some extensions should be thought of. Among others a more detailed model to describe the interplay of the LTNs and the consumers' temperatures would be certainly of great benefit. But equally important is a systematic sensitivity analysis to gain a better understanding of both system and to allow for a more balanced assessment, which then finally could result in recommendations of best practice.

REFERENCES

1. Kräuchi, P., Kolb, M.: Simulation thermischer Arealvernetzung mit IDA-ICE. BauSIM, Berlin, 2012.
2. Kräuchi, P., Kolb, T. Gautschi, U.-P. Menti, M. Sulzer: Modellbildung für thermische Arealvernetzung mit IDA-ICE. BauSIM, Aachen, 2014.
3. Bargel, S. : Entwicklung eines exergiebasierten Analysemodells zum umfassenden Technologievergleich von Wärmeversorgungssystemen unter Berücksichtigung des Einflusses einer veränderlichen Außentemperatur, Dissertation, Bochum, 2010.

A SUPPLY/DEMAND DECISION MAKING-TOOL FOR THE REGIONAL COORDINATED PLANNING OF THERMAL NETWORKS

L. Girardin[1]; L. Lepage[1]; F. Doppenberg[1]

1: BG Ingénieurs Conseils SA, Av. de Cour 61, Case postale 241, CH-1001 Lausanne

ABSTRACT

The development of urban areas by densification of the existing urban infrastructure and setting up of new dwellings raises the question of spatial and temporal distribution of energy supplies to provide thermal comfort. Urban development projects are indeed not necessarily coordinated and may unexpectedly appear, either through new building projects or by opportunistic study of key area, or by motivation of public or private actors.

The aim of the proposed methodology is to generate optimum scenarii matching, in a long term perspective, the load and temperature levels of heat supply sources and thermal demand of urban areas. It uses energy integration techniques to simulate the thermal energy portfolios, taking into consideration the possibility to increase the supply temperature levels of energy supply sources using heat pumps. The results from simulation are expressed as thermal load curves and a network-diagram connecting urban areas, energy supply sources and heat pumps.

Although many points of view might be considered for the correlation between urban thermal energy supply and demand, some criteria, such as exergy losses, CO_2 emissions, costs and the amount of renewable energy, are strictly quantitative and can be optimized by mathematical programming.

The associated tool is validated on a simple case study and applied for the regional coordinated thermal energy planning of an urban area in Geneva, using six temporal horizon up to year 2100.

Keywords: urban simulation, energy integration, thermal networks, multi-period optimisation

INTRODUCTION

Given the growing demand of heterogeneous powers and temperatures, the establishment of a territorial-coordinated strategic vision 2050-2100 of the thermal energy supply requires the development of a decision-making tool based on the simulation of spatial and temporal evolution of the urban energy system. The method contributes to the better integration of district heat network, renewable energy sources and waste heat in correlation with the evolution of urban demand.

METHODOLOGY

The developed methodology is based on current and future urban hourly heat-temperature demand profiles, generated either with a typological approach [1] or using more advanced urban simulation software, such as CitySim [2]. The initial urban demand is updated, horizon by horizon, using refurbishment rates and considering new developments, in order to predict the evolution of the heat and temperature demand. The sizing temperatures of the heating demands are set to 80/65°C for existing buildings, 65/45°C for refurbished ones and 45/20°C for the new ones.

Given the urban energy demand and the boundaries of the energy supply loads, the use of energy integration techniques [3, 4], with spatial [5] and temporal restriction, optimally

allocates heat loads throughout urban zones considering the temperatures constraints. The method's originality lies in the use of temporal horizon in which the operational planning of the heat supply [6] are performed, considering the possibility of heat sources temperature upgrades. This method linking together time horizons, brings the long term vision needed to perform the coordinated planning of thermal network.

The decision-making process relies on parametric multi-objective optimisation [7] to identify feasible alternatives. A first loop generate a fixed number of sub-optimal solutions between the min. and max. of a single objective and a second one repeats the procedure for each objective, namely exergy losses of heat exchanges, CO_2 emissions and operating costs. The outcome is a cloud of points with a "Pareto front" showing the trade-off between the objectives.

MODEL

The model is composed of streams sets (s), either variable supply or constant demand, geographical zone (z), temporal horizon (h) and time steps (t) with a distinction between operational and sizing conditions.

Annual load profile are made of ordered time series of heat streams ($Q,T_{in},T_{out},\Delta T_{/2}$)[z,t,h] with fixed inlet (T_{in}), outlet (T_{out}) and minimum temperature difference ($\Delta T_{/2}>0$) of the heat exchanges. Streams (s) are grouped within zones (Z_s), temporal horizon (H_s) and units (U_s) which comprise heat supply sources, demand and heat pumps. The heat load (Q) of heat supply is modulated by a multiplication factor (f_s[z,t,h]). In a same unit, all the streams share a common multiplication factor (f_u[z,t,h] = f_s[z,t,h], $\forall$ t, s$\in U_s$, Z_s, H_s) which is bounded by user defined limits (F_{min}[u] and F_{max}[u]). Moreover binary shut on/off variables (y_{uzth}) allow to set time and space restrictions to the heat supply distribution.

Energy balance

Heat supply ($T_{out}>T_{in}$) and demand ($T_{out}>T_{in}$) streams define variable hot, respectively fixed cold streams with flow ($Mc_p=Q[s,t]/(T_{in}[s,t]-T_{out}[s,t])$).

The mathematical mixed integer linear program (MILP) solves, in each zone (z) and for every time horizon (h), the energy balance (2) on each temperature interval (T_k,T_{k-1}) derived from all the streams.

$$\begin{aligned}&\forall z,t,h,T_k : R_k[z,t,h,T_k] = \\ &\sum_{s\in hot,T_{out}[s,t]\geq T_k} f_s[s,z,t,h]\cdot Mc_p[s,t]\cdot\left(T_{in}[s,t]-T_{out}[s,t]\right) - \sum_{s\in cold,T_{in}[s,t]\geq T_k} f_s[s,z,t,h]\cdot Mc_p[s,t]\cdot\left(T_{out}[s,t]-T_{in}[s,t]\right) \\ &+ \sum_{s\in hot,T_{out}[s,t]<T_k,T_{in}[s,t]\geq T_k} f_s[s,z,t,h]\cdot Mc_p[s,t]\cdot\left(T_{in}[s,t]-T_k\right) - \sum_{s\in cold,T_{in}[s,t]\leq T_k,T_{out}[s,t]\geq T_k} f_s[s,z,t,h]\cdot Mc_p[s,t]\cdot\left(T_{out}[s,t]-T_k\right)\end{aligned} \quad (2)$$

The series of positive residuals R_k(z,t,h,T_k) define, for each time step (t), a heat cascade schematically depicted in Figure 1, which ensures that the thermal exchanges between hot (offer) and cold (demand) streams are all made with a positive temperature difference. The continuous variables of this problem are the residuals (R_k), the multiplying factor (f_s and f_u) of stream (s) and unit (u).

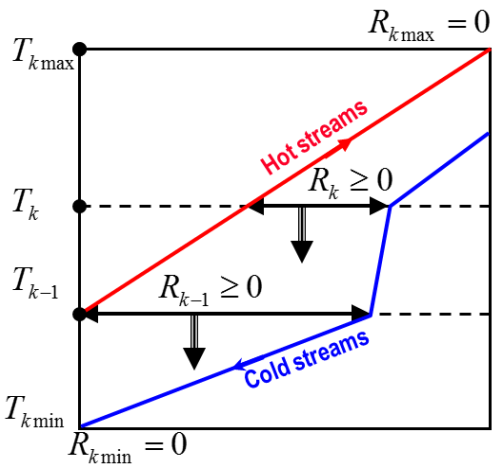

Figure 1: Schema of the heat cascade with balanced supply stream on the top.

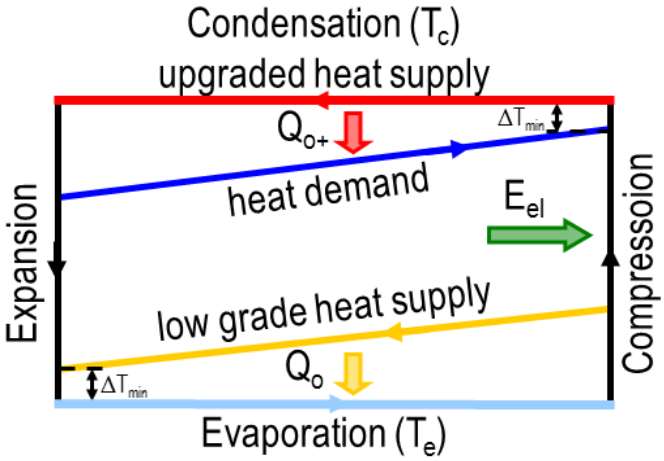

Figure 2: Schema of heat pump integration for the upgrade heat supply temperature.

The closure of the global thermal balance, meaning the sum of hot streams equals the sum of cold streams, is achieved with the bounds constraints $R_k=0$ at the two ends of the heat cascade, at $\max_k(T_k)$ and $\min_k(T_k)$.

Temperature upgrade

The temperature levels of low grade heat supply sources may be upgraded using heat pumps (HP) which add a new electric demand and two streams: a new high grade heat supply above the condensation level (T_c) and a new demand at evaporation levels (T_e), just under the upgraded heat supply (Figure 2). These two new streams are linked together by a common multiplication factor (f_u), which preserves the ratio of the streams and represents the sizing factor of the HP unit (u).

The coefficient of performance ($COP= \eta_{COP}.COP_{th}$) is computed based on the theoretical cycle of the HP ($COP_{th}=T_c/(T_c-T_e)$) using an efficiency factor (η_{COP}), of typically 0.4 for decentralized HP and 0.6 for more efficient centralized HP. The relation between the heat (Q_e) withdraws from upgraded heat supply and the amount of heat (Q_c) delivered at the higher temperature (T_c) is given by ($Q_c=Q_e\cdot(1+1/COP)$), and the amount of required electricity by ($E_{el}=Q_e/COP$).

VALIDATION CASE

The network-diagrams of Figure (3) show the heat load distribution minimizing the CO_2 emissions of three supply sources (Table 3) to two urban zones during horizon 2016-2030 (14 years). It is shown that 3'219 GWh are distributed to zones "PAV" and 1093 GWh to "Semailles" with a heat supply share of 2'948.2 GWh (Backup gas boiler at 120/90 °C), 1'028 GWh (Waste heat from Cheneviers at 120-106/75 °C) and 180.3 GWh (Waste heat from ZIPLO at 30/15 °C).

The optimal integration of heat pump allows to upgrade 165.7 GWh from "ZIPLO" adding 321.2 GWh to "Cheneviers" (1'028 GWh) which can then redistribute 1349.2 GWh to the urban zones. Using the heat pump maximises the usage of the low temperature and low emission "ZIPLO" heat source.

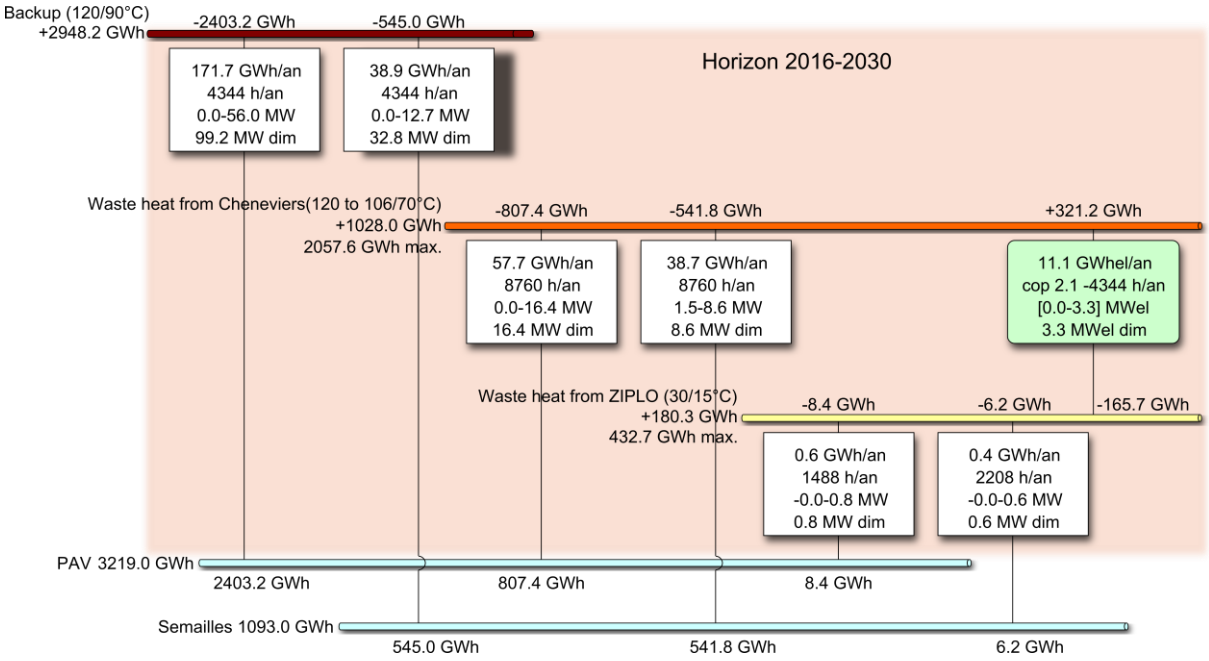

Figure 3: Network diagram of the validation case with heat upgrade.

The indicators, reported in Table 1 are well estimated with monthly time step, but daily simulation, with 12 typical days within a year, is required for the accurate detection of temperature upgrades and charges.

Minimisation of CO_2 emissions	**Indicators**				**Supply load [GWh/year]**				
	Exergy losses [GWh/year]	CO_2 emissions [gCO_2/kWh]	Operating cost [cts/kWh]	ReS share [%]	ZIPLO	Cheneviers	Backup	PAC Th.	PAC El.
Annual	48.3	103.1	8.6	47.0	30.9	147.0	102.6	58.4	27.5
Seasonal	44.0	169.5	8.7	27.2	18.6	84.5	191.6	27.4	13.3
Monthly	**43.1**	**183.9**	**8.7**	**22.9**	**12.9**	**73.4**	**210.6**	**22.9**	**11.1**
Daily (12x24h)	41.6	184.5	8.6	22.0	11.0	70.6	212.2	20.6	10.0

Table 1: Indicators and supply load distribution with different simulation's time steps.

CASE STUDY

The case study comprises nine geo-localized heat supply sources and nine urban zones (Figures 4 and 5), representing more than 500 hectares of heated surface. Daily, monthly and seasonal simulations are performed, up to horizon 2100, using six temporal horizon. A refurbishment rate of 1% per year is applied to the existing building stock. The result of the minimization of exergy losses, using monthly time step without heat upgrade, are shown in Table 2.

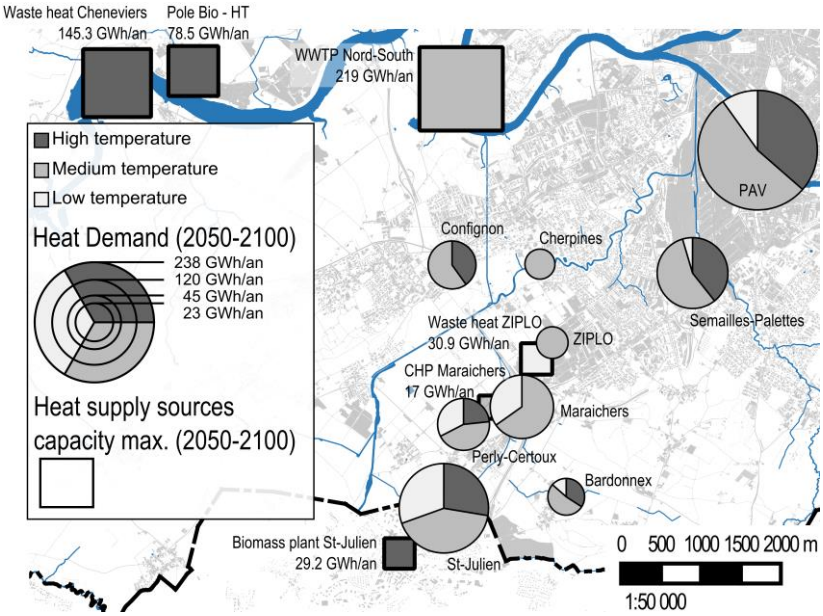

Figure 4: Map of heat supply (square) and demand (point).

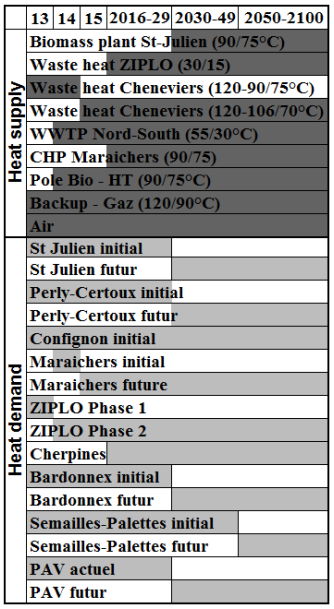

Figure 5: Gantt diagram.

Minimisation of exergy losses	Time horizon duration	**Indicators**				**Supply load [GWh/year]**							
		Exergy losses	CO_2 emissions	Operating cost	ReS share	Backup	Biomass plant St-Julien	CHP Maraichers	Waste heat Cheneviers	Pole Bio	Waste heat ZIPLO	WWTP Nord-South	Total
2013-2014	1	58.67[GWh/year]	54.17 [g/kWh]	7.68 [cts/kWh]	21.50 [%]	457.3			120.7				578.0
2014-2015	1					283.8			67.7	55.0		153.1	559.6
2015-2016	1					308.4			41.8	67.6		160.3	578.1
2016-2030	14					265.3	25.4	14.3	37.3	65.3	25.1	164.5	597.2
2030-2050	20					310.4	29.2	15.7	37.9	64.0	27.1	167.0	651.3
2050-2100	50					277.2	25.4	14.3	37.7	64.4	26.4	166.1	611.5
2013-2100	87					285.4	25.4	14.1	39.0	63.6	25.4	163.9	617.0

Table 2: Minimization of the exergy losses using monthly time step, without heat upgrade.

DISCUSSION

The results show that, with the given refurbishment rates and increase of the building stock, the heat demand is expected to grow between 2014 (578 GWh/year) and 2050 (650 GWh/year), with peak in 2030-2050. By the horizon 2050-2100, the demand will fall back to the level of 2016-2030 (600 GWh/year). Moreover, at least 45% of the studied urban area will not be covered by the planned network infrastructures, due to integration of backup technologies at a minimum level of 277.2 GWh/an (see table 2). However, the use of decentralized extra heat is expected to be reduced by more than one-third up to 2100, due to the lowering of heating temperature and the confluence of new supply capacities. Moreover,

due to excess of heat supply in summer (e.g waste incineration plant "Cheneviers" 2013-2014, see Table 2 & Figure 4), the full potential of thermal sources will require the implementation of seasonal thermal storages. It also has been found that, even if the use of twelve typical days of 24h within a year gives suitable simulation results, the definition of about seven typical day [8] would generate even faster results with a more accurate placement of HPs.

CONCLUSION AND PERSPECTIVES

The heat supply/demand multi-period and multi-horizon decision-making tool is demonstrated at the scale of dwellings up to regional urban areas. By optimal supply/demand correlation, it helps energy planners to prepare future infrastructure investment and policy options to organize the energy transition with the best compromise between operation cost, technical efficiency and low CO_2 emission. The method is forecasting the decreases of temperature in the urban environment which, in turn, reveal the potential of renewable energy sources and reduce investments and heat losses of heat distribution networks. Furthermore, the integration of intermittent renewable sources, such as solar thermal energy, as well as the interaction with cold requirements with temperature downgrade for cooling, can be fulfilled with the proposed approach.

However, the integration of thermal storage will require new programming strategies and a supplementary module for the design of the thermal network [1] would provide decision-makers with the distribution costs needed to make the best investment choices.

ACKNOWLEDGMENT

The authors would like to thank the "Services industriels de Genève" (SIG) and the "Office cantonal de l'énergie" (OCEN) for their support.

REFERENCES

1. L. Girardin, F. Marechal, et al., ENERGIS : A geographical information based system for the evaluation of integrated energy conversion systems in urban areas, in Energy, The International Journal, 2009.
2. D. Robinson, F. Haldi, J. Kämpf, et al., CITYSIM: Comprehensive Micro-Simulation of Resource Flows for Sustainable Urban Planning, Proceedings of the 11th IBPSA Conference, Glasgow, 2009.
3. F. Maréchal, D. Favrat, Combined exergy and pinch analysis for optimal energy conversion technologies integration, in: The 18th International ECOS Conference, Trondheim, Norway, vol. 1, 2005, pp. 177-184.
4. C. Weber, F. Marechal and D. Favrat, Design and optimization of district energy systems, in Computer Aided Chemical Engineering, vol. 24, p. 1127-1132, 2007.
5. H. Becker, L. Girardin and F. Maréchal. Energy integration of industrial sites with heat exchange restrictions. - ESCAPE20, Ischia, Naples, Italy, 6-9 June 2010.
6. R. Iyer, and I. Grossmann, Synthesis and operational planning of utility systems for multiperiod operation, Computers & Chemical Engineering, 22(7-8):979-993, 1998.
7. S. Fazlollahi, et al., Multi-objectives, multi-period optimization of district energy systems: I. Selection of typical operating periods, in Computers & Chemical Engineering, vol. 65, p. 54-66, 2014.
8. S. Fazlollahi, et al., Methods for multi-objective investment and operating optimization of complex energy systems, Energy, Volume 45, Issue 1, September 2012, Pages 12-22.

ASSESSING THE CHALLENGES OF CHANGING ELECTRICITY DEMAND PROFILES CAUSED BY EVOLVING BUILDING STOCK AND CLIMATIC CONDITIONS ON DISTRIBUTION GRIDS

Andreas Ulbig[1], Silvia Coccolo[2], Jérôme Kämpf[2],

1: Power Systems Laboratory, ETH Zürich, Switzerland
2: Solar Energy and Building Physic Laboratory, EPFL Lausanne, Switzerland

ABSTRACT

The buildings sector in Switzerland accounts for more than 40% of the country's overall energy demand and CO_2 emissions. The predicted future weather conditions, according to the Intergovernmental Panel on Climate Change (IPCC), will even reinforce this trend.

Due to the foreseeable further electrification of heating and cooling demand in buildings their electric load demand will likely increase. For these reasons it is essential to reduce the energy demand of buildings, and optimize it by using renewable energy sources (RES) in conjunction with suitable storage elements, such as thermal energy storage (TES). These two factors will, however, drastically change today's observed "typical" building load demand profiles. Higher peak load demand during cold and hot weather conditions as well as significant PV power production on sunny days will induce new challenges for electric distribution grid operation and planning such as more frequent and higher power spikes. These challenges will be assessed and possible mitigation options, i.e. the usage of storage elements, discussed in this paper. The paper presents the energetic analysis of an office building, the Solar Energy and Building Physics Laboratory (LESO-PB), located in the EPFL campus in Lausanne. The building's energetic model was realized with the software CitySim, and validated with on-site monitoring for the time period 2011 to 2013. Further analysis shows its thermic behaviour in future climatic scenarios (IPCC model for the year 2100, scenarios B1, A1B and A2).

The electrical load demand of the building and the electricity production by the BiPV system can be optimally matched, during the different months and hours of the day, by means of thermal and/or electrical energy storage. This enables the maximization of the building's self-consumption from PV power production.

An assessment of the challenges for the electric distribution grid due to changing electric load demand patterns is presented for a residential as well as an office usage profile.

Keywords: Electricity grid, climate change, renewable energy, storage systems

INTRODUCTION

Impacts of changing electric load demand patterns on distribution grids

One the one hand, there is a notable shift from fossil fuel usage to electricity, notably substituting natural gas for heating needs by using heat pumps and liquid fossil fuels for mobility by means of electric vehicles. These additional electric load units will lead to a significant increase in electricity consumption, inevitably leading to higher average load demand as well as higher peak load events in the electric distribution grids. On the other hand, PV installations for instance on building roof-tops and facades will lead to significant decentralized electricity production within distribution grids. Both trends create new challenges for distribution grid operation and planning. Both peak load demand and peak

PV power feed-in can create local voltage problems and, potentially, also line overloading within the distribution grid topology. In this paper we assess these challenges by looking at the LESO building. Typical residential and office load patterns, as derived by representative occupancy profiles are analysed.

The LESO building is located in the EPFL campus in Lausanne, and its thermic behaviour was well documented in previous researches [1] [2]. The object of this paper is to create a dynamic thermic model of the building, showing the heating demand and the photovoltaic production in actual and future climatic scenarios. Weather data for future climatic conditions are realized with Meteonorm [3], and are based on IPCC's climatic scenarios [4].

METHOD

Energetic model of LESO-PB

The solar energy and building physic laboratory (LESO-PB) was built in 1981 and refurbished in 1998, as test building for experimental anidolic facades and indoor climatic monitoring by intelligent microprocessors. The object of the renovation was to reduce the use of non-renewable sources, by creating a performant envelope, increasing the availability of natural light, improving the summer comfort by night cooling and using photovoltaic to produce electricity. The thermic envelope, defined according to [2], is summarized in Table 1. The South facade presents a performant envelope, externally covered by wood, with anidolic windows on the upper layer of each room, and double glazing windows on the lower part.

Element	U-value (W/m²·K)
Wall South	0.3
Wall North	0.2
Double windows with infrared coating	1.4
Anidolic windows	1.4

Table 1 – Thermic envelope of LESO-PB building

Photovoltaic panels are integrated in the rooftop (BiPV), a total area equal to 28 m, oriented south and with a peak power of 3.2 kW. According to previous monitoring, the total energy demand of building is equal to 287 MJ/m², and the net demand is equal to 75 MJ/m², by removing the useful gains by occupants, lighting, devices and solar gains [1].

LESO building presents an unobstructed South facade, facing a garden, and is connected to a second building on the North side. In the energetic model, realized with the software CitySim, the internal temperature is set at 20°C during the winter time, and the occupancy profile is defined according to SIA 2024 [5], including occupants and electrical devices. A hypothetical refurbishment according to actual Minergie and Minergie P scenarios is proposed, increasing the thermal efficiency of envelope (U-value lower then 0.2 W/m²·K) and windows (by replacing the actual windows with triple glazing windows). The energetic model is realized in actual and future climatic scenarios; for the energy behaviour in the year 2100, three different scenarios (provided by Meteonorm [3]) are envisaged according to the IPCC studies [6] [4]:

- **Scenario 2050-B1**: rapid growth of population (8.7 billion) and use of new clean technologies (30% share of zero carbon energy sources in primary energy).
- **Scenario 2050-A1B**: rapid economic growth, rapid population growth (8.7 billion), new efficient energy technology (36% share of zero carbon energy sources in primary energy).
- **Scenario 2050-A2**: continued increase of population (11.3 billion) and reduced research in new technologies (18% share of zero carbon energy sources in primary energy).

The future energetic behaviour of the LESO building is analysed according to two different occupancy profiles: office and residential, showing the impact of the occupancy profile in the energy demand of buildings, and in the grid optimization. The occupancy profile is defined according to SIA 2024/2006 [5]: the number of occupants and their presence during the day is added to internal gains related to appliances; the profile is based on the liveable surface of the building and its function (office and house). Figure 1 shows the occupancy profile (ranging from 0 – unoccupied, up to 1 – maximal occupancy) during a typical day for an office and a house: the house is occupied during evening and night-time; on the contrary the office has the highest occupancy during day-time.

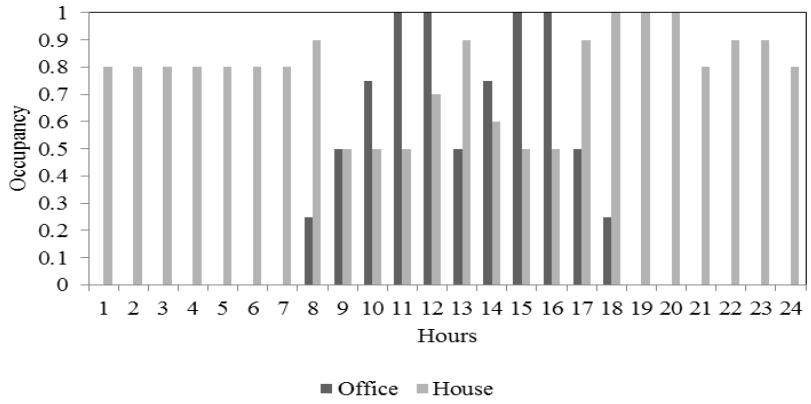

Figure 1 – Typical daily occupancy profile for an office and house building, as sum of people presence and internal gains related to appliances.

RESULTS AND DISCUSSION

Energetic model of LESO-PB

On-site monitoring, realized by ENERGO [7] (average heating demand of LE buildings, 2009-2011), are compared with the simulations, showing a difference of 3% between them.

Figure 2 shows the heating demand of LESO building, expressed in kWh/m³, using the average climatic data provided by Meteonorm (average solar radiation for the period 1991-2010, and average temperature for the period 2000-2009). The South part of LE building (LESO building) has the lowest energy demand compared to the Northern part (LIPID building), completely glazed but without a performant envelope. The warehouse between LESO and LIPID present the highest heating demand, as it is shadowed by bordering building, it has a light metallic structure present no windows.

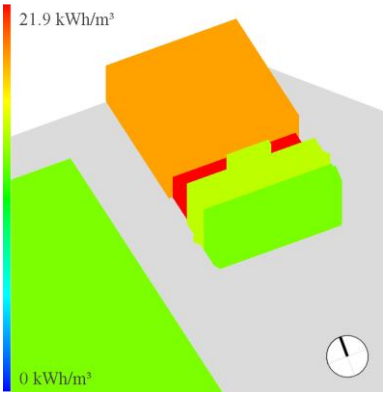

Figure 2 – Heating demand of LE buildings: LESO building (South) and LIPID (North).

In the building simulations, two house types are considered: the existing LESO building setup (E) and an upgraded Minergie Plus building setup (MP) in conjunction with new electricity generation unit (PV) as well as new load consumption types, i.e. heating and cooling demand as provided by heat pump and air-conditioning units. The BiPV production, according to the CitySim model, is equal to 3'350 kWh_e/y (difference of 1% compared to monitoring [1]).

This leads to a change in electric energy demand and, more importantly, the resulting electric load consumption profiles.

Resulting Electric Load Demand Profiles

One the one hand, the shift from fossil fuel usage to electricity, notably substituting natural gas for heating needs by using heat pumps and liquid fossil fuels for mobility by means of electric vehicles, will inevitably lead to higher average electric load demand as well as higher peak load events in the electric distribution grids.

On the other hand, PV installations for instance on building roof-tops and facades will lead to significant decentralized electricity production within distribution grids albeit with a strong seasonal and daily pattern, i.e. peak production during summer noon hours and almost negligible production during winter days, as is exhibited by Figure 3.

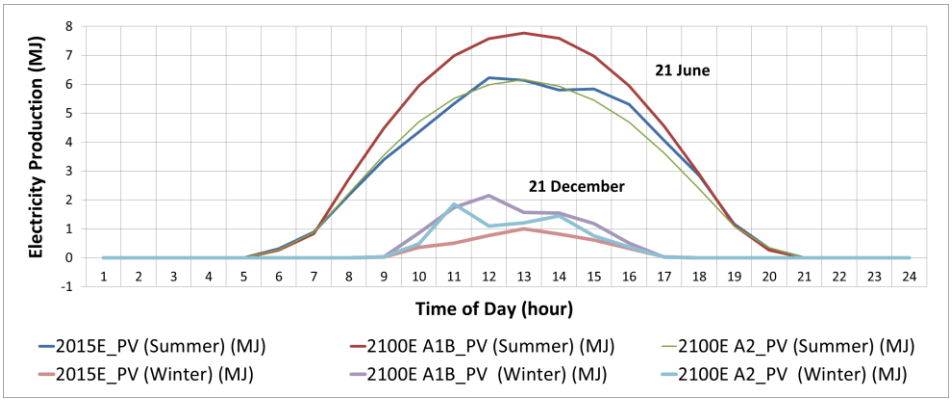

Figure 3 – LESO building's PV production (Summer – 21 June, Winter – 21 December).

Residential Building Load Profile

Figure 4 shows the daily electric load profile of a typical summer day (21 June). The additional load demand for all future building setups, mostly electric cooling, would significantly increase the load demand during day-hours with respect to the nominal setup (2015E). For the most extreme scenario (2100E A1B), the peak load demand (at 18-19h) doubles. Load increase is much lower for Minergie and Minergie Plus building setups.

In case a PV unit is present, a significant net electricity production occurs during noon hours (12h) in all setups – depending on the building setup, this can have about the same magnitude as the peak load demand. Also, a sharp load ramping happens in the afternoon when PV production is rapidly falling while load demand is increasing at the same time.

Figure 5 shows the daily electric load profile of a typical winter day (21 December). Contrary to the summer, overall load demand for all future building setups would be significantly lower than in the nominal setup (2015E). Also, PV feed-in is significantly lower and leads only in some building setups to a net power feed-in into the distribution grid.

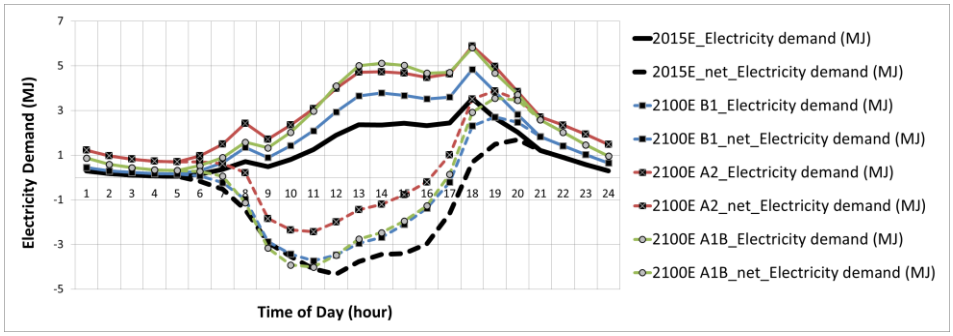

Figure 4 – Residential LESO building's (net) load demand & PV profile (21 June).

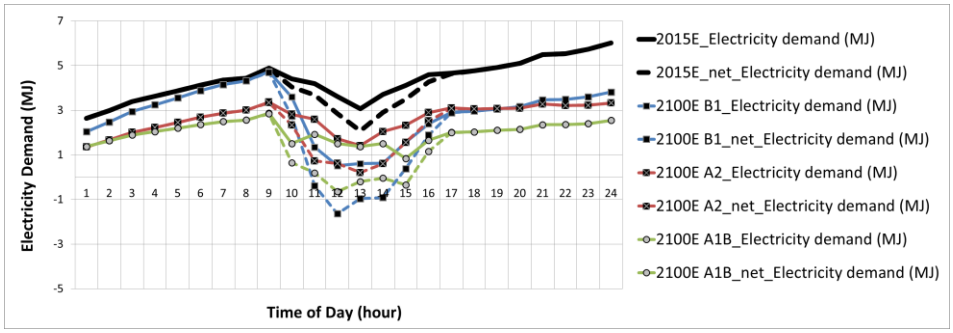

Figure 5 – Residential LESO building's (net) load demand & PV profile (21 December).

Office Building Load Profile

Figures 6 and Figure 7 show the daily electric load profile of a typical summer day (21 June), respectively winter day (21 December). This occupancy mode creates qualitatively similar load demand patterns as in the residential building case. The evening ramping is however less pronounced, i.e. people return home when the sun sets thus not creating additional load demand in the office environment – this happens instead in the residential dwellings.

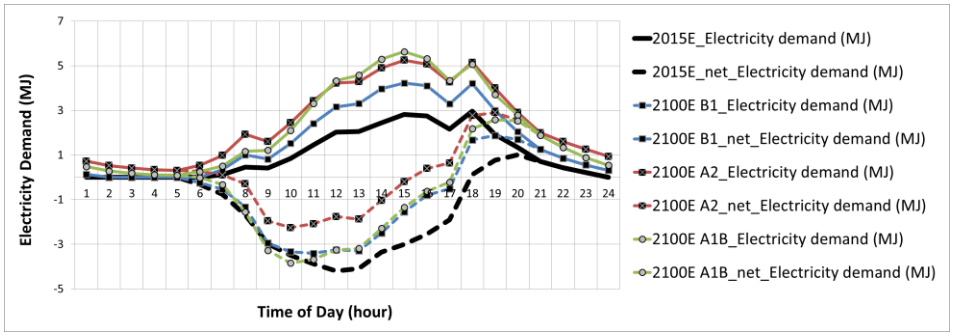

Figure 6 – Office LESO building's (net) load demand & PV profile (21 June).

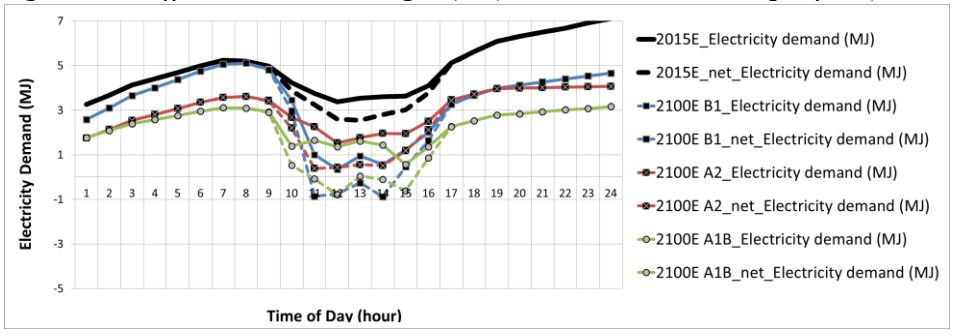

Figure 7 – Office LESO building's (net) load demand & PV profile (21 December).

Impacts for Distribution Grid Operation and Planning

Of the two LESO building usage profiles presented above, the LESO residential summer profile exhibits both the highest peak load demand as well as the highest (positive) power ramping over all studied IPCC scenarios. Compared to the reference case, i.e. today's building setup without PV unit, peak load may increase by up to 65% (2100 A1B) and power ramping increases three-fold for all scenarios with PV unit (up to 349%, 2100E A1B), Table 2.

Scenario	Peak Load Demand (18:00 or 19:00)		Power Ramping (16:00 – 18:00)	
	with PV unit	without PV unit	with PV unit	without PV unit
2015E	48	**100 (= Reference)**	305	**100 (= Reference)**
2100E B1	77	137	307	110
2100E A2	110	167	309	118
2100E A1B	101	165	349	95

Table 2 – Quantification of peak load and peak ramping (LESO residential usage, 21 June).

Such drastic changes in electric load demand profiles inevitably have impacts on the distribution grid to which the building stock is connected to. Rising electricity consumption and higher peak load demand are eventually necessitating upgrades of the distribution grid infrastructure. Net power in-feed created by the roof-top PV units creates reverse power flows from the lowest voltage levels of the distribution grid up to medium voltage levels and, eventually, also the transmission grid. Peak load demand and peak PV power feed-in create local voltage problems and, potentially, also line overloading within the distribution grid. This requires additional grid upgrade investments. The larger load demand ramping notably in the afternoon hours needs to be covered by sufficiently flexible backup generators (for the characteristic load profiles given by the results in Fig. 4–7, compare also with [8]). In case these backup units are not available, coordinated PV curtailment would be necessary in order to reduce the load demand ramping trajectory. This, however, would result into significant energy losses, i.e. the curtailed PV feed-in, leading to an inefficient power system operation. Energy storage technologies, be it direct electricity and/or thermal storage units, can be used to smoothen the load demand profile. Peak events, both of load demand and of PV power feed-in, can thereby be effectively reduced. The optimal choice of the storage technology (thermal, chemical and electricity), storage unit sizing and placement will be decisive for an efficient distribution grid operation.

REFERENCES

[1] R. Altherr, J.B. Gay, A low environmental impact anidolic facade, Build. Environ. 37 (2002).

[2] N. Morel, Description of the LESO Building, (2004).

[3] C.- Bern, J. Remund, S. Müller, S. Kunz, Meteonorm. Global metereological database, (2013).

[4] IPCC, IPCC special report. Emissions scenarios, 2000.

[5] SIA 2024 Conditions d'utilisation standard pour l'énergie et les installations du bâtiment, 2006.

[6] G. Meehl, T. Stocker, Global Climate Projections, In: Contrib. Work. Gr. I to Fourth Assess. Rep. Intergov. Panel Clim. Chang. 2007, 2007.

[7] ENERGO, Energy consumption EPFL, (2014).

[8] CAISO (California ISO), What the duck curve tells us about managing a green grid, URL: www.caiso.com/Documents/FlexibleResourcesHelpRenewables_FastFacts.pdf.

BUILDING ENERGY DEMAND AGGREGATION AND SIMULATION TOOLS – A DANISH CASE STUDY

P. Gianniou; A. Heller; C. Rode

Department of Civil Engineering, Technical University of Denmark, Kgs. Lyngby

ABSTRACT

Nowadays, the minimization of energy consumption and the optimization of efficiency of the overall energy grid have been in the agenda of most national and international energy policies. At the same time, urbanization has put cities under the microscope towards achieving cost-effective energy savings due to their compact and highly dense form. Thus, accurate estimation of energy demand of cities is of high importance to policy-makers and energy planners. This calls for automated methods that can be easily expandable to higher levels of aggregation, ranging from clusters of buildings to neighbourhoods and cities. Buildings occupy a key place in the development of smart cities as they represent an important potential to integrate smart energy solutions. Building energy consumption affects significantly the performance of the entire energy network. Therefore, a realistic estimation of the aggregated building energy use will not only ensure security of supply but also enhance the stabilization of national energy balances.

In this study, the aggregation of building energy demand was investigated for a real case in Sønderborg, Denmark. Sixteen single-family houses -mainly built in the 1960s- were examined, all connected to the regional district heating network. The aggregation of building energy demands was carried out according to typologies, being represented by archetype buildings. These houses were modelled with dynamic energy simulation software and with a simplified simulation tool, which is based on monthly quasi-steady state calculations, using a visual parametric programming language (Grasshopper) coupled with a 3D design interface (Rhinoceros). The estimated heat demand of the examined houses from both simulation tools is compared to actual measured data of heat consumption. An assessment of the two different types of tools follows, which will indicate the suitability of each tool depending on the desired accuracy of results and on the purpose of analysis.

Keywords: Building energy, Heat demand, Archetypes, Energy Simulation Tools

INTRODUCTION

Aggregation of building energy demands is key to depicting national building stocks, while supporting urban development decisions and Smart Cities development. In particular, it is considered to be one of the most efficient methods for analysing stock performance due to its bottom-up approach [1]. The building sector within the European Union (EU) accounts for 35%-40% of the final total energy consumption and 25%-40% of the associated CO_2 emissions [2]. Thus, it can play a pivotal role on Smart Cities development. Especially the residential sector has received extended political attention and so, better statistics and knowledge exist for it, which facilitates its analysis. According to [3], building stocks can be represented by sample buildings and archetypes. Their difference lays in the fact that the former require knowledge about the actual building parameters and measurements, while the latter are statistical composites of features of a specific building type [2]. The methodology of archetype buildings can cope with the lack of physical description of buildings which is very common at a large scale.

Building energy simulation software is widely used for load modelling and building energy estimations. Simulation methods are categorized upon their energy balance calculation to dynamic and quasi-steady-state methods. According to dynamic methods, heat balance is calculated with short time-steps (e.g. hourly) considering the thermal inertia of the building. In particular, their main characteristic is that an instantaneous surplus of heat during the heating period results in an increase of the indoor temperature above the set-point, while it removes the surplus heat by extra transmission, ventilation and accumulation, if no mechanical cooling exists [4]. Furthermore, changes in room temperature highly depend on the heat stored in or released from the mass of the building. On the contrary, quasi-steady-state methods calculate heat balance for a long time (e.g. monthly/seasonal) considering dynamic effects through correlation factors. Regarding heating, a utilization factor is introduced, which considers that only a part of the internal and solar heat gains can reduce the heat demand, while the rest of the heat gains result in an increase of the room temperature above the set-point. In this study, both dynamic and quasi-steady-state energy simulation tools were used. The objective is to investigate their suitability and accuracy at an aggregated level of building energy demands, while using archetypes.

METHOD

Sixteen single-family houses located in Sønderborg, Denmark were investigated upon their heat demand. All of them were connected to the local District Heating (DH) network. No mechanical ventilation or auxiliary heating sources were installed in the houses. These were classified into five building types based on their construction age, following changes in building traditions and energy requirements according to the Danish Building Regulations [5]. Some characteristics of the examined buildings are illustrated in Table 1.

Building type	Construction Period	No. of incl. buildings	Total floor area [m^2]
A	1931-1950	2	238
B	1951-1960	2	180
C	1961-1972	10	1,530
D	1973-1978	1	117
E	1979-1998	1	122

Table 1: Characteristics of archetype buildings

One archetype building was created to represent each type. The characterization of the archetype buildings was based on information gathered by national building databases, TABULA Webtool and on statistical values applied by the Danish Building Research Institute on a national evaluation of the energy demand for the Danish building stock in total. This included information about the median floor and glazing area, U-values of the thermal envelope and glazing, internal gains, as well as infiltration. In particular, the window area of single-family houses is 16% compared to the floor area for those built in the 1930s [6], 22% for those built in the 1960s [6] and 15% for those built in the 1980s and 1990s [7]. Some houses had undergone usual energy refurbishments mainly affecting the U-values of the thermal envelope and glazing, which was taken into account in the building models.

The examined sixteen single-family houses were modelled initially with IDA-ICE. This required extensive information about the building parameters. Multi-zone models were created for all five archetypes according to the standardized parameters. Their space heat and

domestic hot water (DHW) demand was simulated for one whole year. Afterwards, a simplified simulation tool was implemented, Termite, which required a much smaller amount of inputs in the models. Termite is a newly-developed parametric modelling tool, which uses Rhinoceros design interface, Grasshopper parametric options and Danish building performance simulation engine Be10 for energy performance calculations according to EN ISO 13790 [8]. Be10 calculates the energy needs of buildings in accordance with the energy requirements of the Danish Building Regulations BR10 and DS418, based on steady state monthly calculations [9]. For the calculation of energy consumption it uses only a whole building approach (single-zone building models). Be10 includes both static and non-static parameters in the energy performance calculation [10], but it does not enable the change of the input weather data, which are based on the Danish Design Reference Year (DRY) [11]. During the energy performance calculation with Termite, input lists were created to enable the fast modelling of all sixteen houses while using only one model setup. Analytical description of the model setup in Termite can be found in [12]. The results of both tools were compared to hourly heat consumption measured data obtained from the examined houses.

RESULTS

Figure 1 and Figure 2 present monthly heat demand (DH and DHW) as calculated by IDA-ICE and Termite for the five building types, being represented by the respective archetype buildings. These are compared to the measured data of heat consumption, which were averaged for each building type.

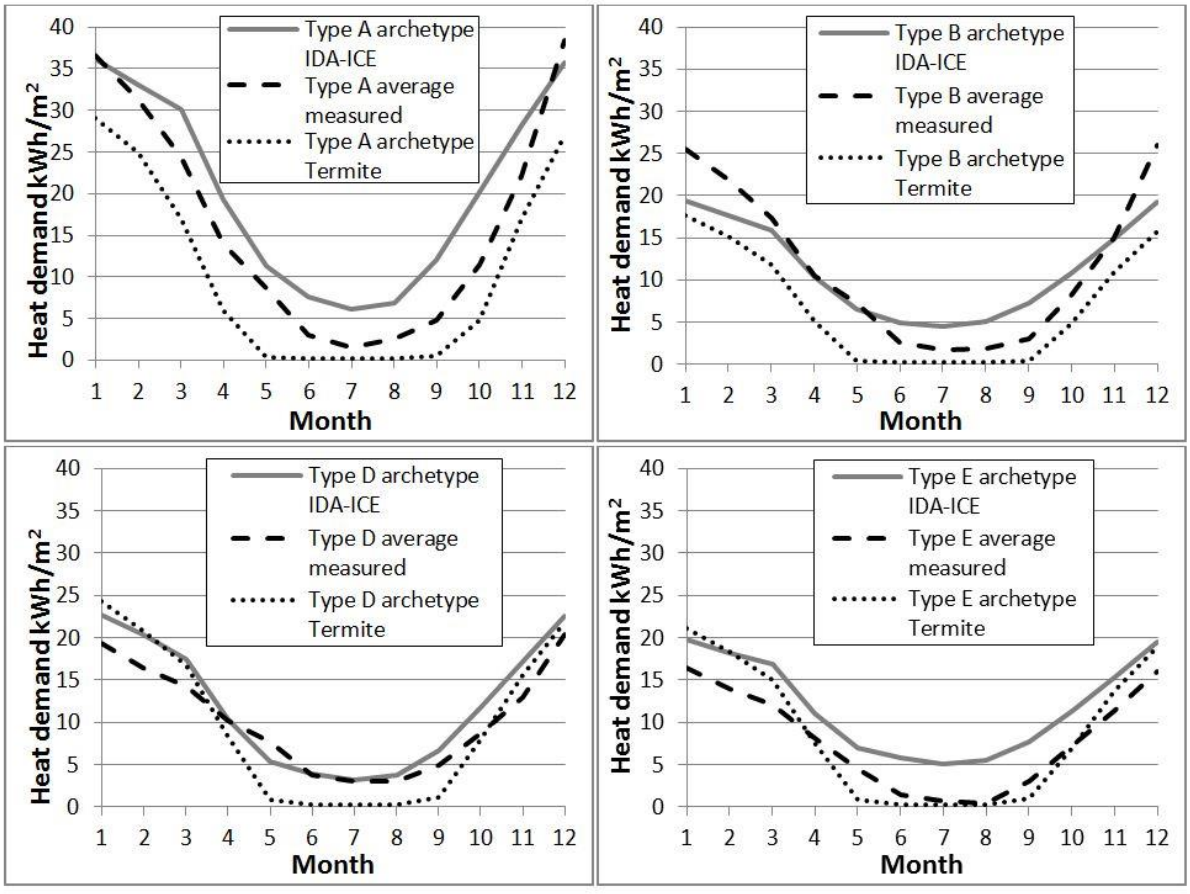

Figure 1: IDA-ICE and Termite monthly results of heat demand for building Type A, B, D and E compared to average measured data

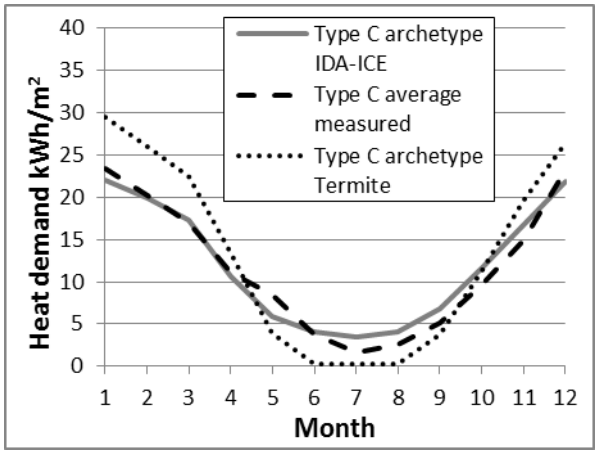

Figure 2: IDA-ICE monthly results of heat demand for building Type C (most representative) compared to average measured data

The calculated heat demands presented in Figure 1 and Figure 2 generally follow similar trends with the measured consumption for all types. The heat demand of the houses reduces as the construction age decreases, as expected. Type C, presented in Figure 2, is considered to be the most representative since the highest number of the examined houses are classified to this type. The rest building types consist only of one or two houses. The deviation between IDA-ICE heat demand and measured heat consumption is quite low for Type C. On the other hand, Termite heat demand differentiates more from the measured heat consumption during both winter and summer period for this type. This may be attributed to the fact that Be10, which is the energy simulation core of Termite, uses DRY climate data that are characterized by very low temperatures in winter and very high temperatures in summer. On the contrary, IDA-ICE makes use of real weather data. The estimated DHW demand by both simulation tools was not estimated accurately, which is due to no information about occupant behaviour.

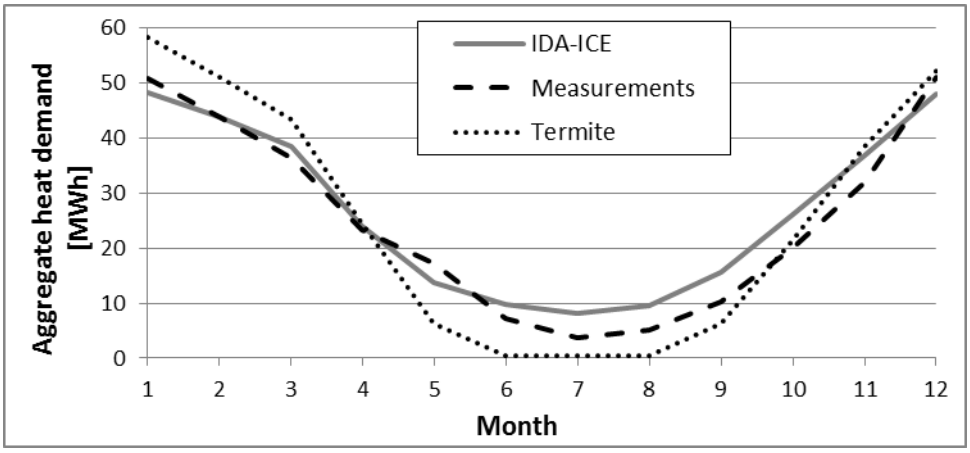

Figure 3: Monthly aggregated heat demand results from IDA-ICE and Termite compared to measured data

Afterwards, the monthly Energy Use Intensity (EUI) [kWh/m^2] estimated by IDA-ICE and Termite for each archetype building was multiplied by the total floor area of all houses classified in the specific type. This aggregated heat demand is illustrated in Figure 3 as calculated by IDA-ICE and Termite for a whole year and is compared to the measured total

heat consumption for the specific year. It is observed that IDA-ICE led to slightly more accurate estimation of the heat demand at an aggregated level compared to Termite. Especially during the winter period, IDA-ICE seems to result in more realistic calculations than Termite. However, it still does not match fully the measured aggregated heat consumption.

DISCUSSION

The lack of information about the building physical properties as well as the occupants' behaviour is a common problem met at large-scale analyses. This was overcome to some extent through the use of archetypes. Even though the sample of the examined houses was small, the methodology described in the present study aims at city-scale projects. For that reason, the values of many building parameters were assumed according to statistical data and national building databases. However, information about the occupants of the houses was not known which would be useful to draw realistically their profiles. The uncertainty in describing physically the examined houses affected the accuracy of results of both IDA-ICE and Termite. Furthermore, the monthly time-step was selected to enable the comparison between these two energy simulation software. Thus, the ability of IDA-ICE to produce hourly results was not exploited. If a yearly time-step had been selected instead, the results would be quite different, but no detailed analysis could be made. Type C was the most representative one, as it included the highest number of houses. The rest of the building types including only one or two houses could not lead to very representative archetypes.

CONCLUSION

The reported results indicated that the estimation of heat demand of clusters of building is a demanding procedure, where uncertainty plays an important role. The latter affected both simple building models, which require fewer inputs and more advanced models, where the number of parameters increases and therefore, the demand for detailed insight into the building construction and user behaviour increases. At aggregated level, it was found that IDA-ICE archetype models represented slightly better the heat demand of the sixteen single-family houses than Termite. Even though the energy calculations conducted by IDA-ICE were more advanced than Termite, the uncertainty in several model parameters counterbalanced its accuracy. However, its estimation of heat demand still remained the closest to the actual measured heat consumption.

Moreover, it was expected that the application of standardized parameter values would lead to rather exact results which was not the case for the current very limited sample of buildings. This could be attributed to the fact that the current buildings were not representative of Danish buildings, or it could be due to the fact that the variability is a dominating factor. The next step of the present work would be to expand the sample of examined buildings, which likely will lead to a more representative case.

The suitability of simulation tools depends highly on the purpose of analysis. If the purpose of this work was to study energy demand shifting in residential buildings, then dynamic simulation software would be the only way to go, since high resolution results would be needed. As the scale moves from building level to district or city level, simplified energy simulation tools may be seen as more preferable. Nevertheless, the methodology of building typologies and archetypes enables the use of advanced dynamic simulation tools, which in any another case would have vast and thus, restrictive computation times. Lastly, the combination of quasi-steady-state and dynamic energy simulation methods could be the solution towards fitting measured consumption data.

ACKNOWLEDGEMENTS

This study has been a part of the Danish strategic research project CITIES (Centre for IT-Intelligent Energy Systems in cities).

REFERENCES

1. International Energy Agency: Annex 31 - Stock aggregation: methods for evaluation of the environmental performance. Ottawa, Canada: CMHC, 2001.
2. Mata, É., Sasic Kalagasidis, A., Johnsson, F.: Building-stock aggregation through archetype buildings : France, Germany, Spain and the UK. Building and Environment, Vol 81, pp. 270-282, 2014.
3. Swan, L. G. & Ugursal, V. I.: Modeling of end-use energy consumption in the residential sector: A review of modeling techniques. Renewable and Sustainable Energy Reviews, 13(8), pp. 1819-1835.
4. ISO13790: Energy performance of buildings - Calculation of energy use for space heating and cooling. CEN, European Committee for Standardization, Brussels, 2008.
5. Wittchen, K. B., Kragh, J.: Danish building typologies. Participation in the TABULA project, SBi, Danish Building Research Institute, Aalborg University, Hørsholm, 2012.
6. Aggerholm, S.: Cost-optimal levels of minimum energy performance requirements in the Danish Building regulations. Danish Building Research Institute, SBI 2013:25, 2013.
7. The Danish Ministry of Housing: Building Regulations 1982, BR82. The National Building Agency, Copenhagen, 1983.
8. Negendahl, K.: Parametric City Scale Energy Modeling - Perspectives on using Termite in city scaled models. iiESI European Workshop 2014, DTU, Copenhagen, 2014.
9. Danish Building Research Institute: SBi anvisning 213 - Bygningers energibehov.
10. Christensen, J. E., Schiønning, P., Dethlefsen, E.: Comparison of simplified and advanced building simulation tool with measured data. Proceedings of BS2013:13th Conference of International Building Performance Simulation Association, Chambéry, 2013.
11. Danish Ministry of Climate, Energy and Building: 2001-2010 Danish Design Reference Year. Technical Report 13-19. Danish Meteorological Institute, Copenhagen 2013.
12. Gianniou, P., Heller, A., Sieverts Nielsen, P., Negendahl, K., Rode, C.: Aggregation of building energy demands for city-scale models, 2015 (submitted).

COMPARISON OF BUILDING TECHNOLOGIES FOR NEARLY ZERO ENERGY BUILDINGS

Carsten Wemhoener; Roman Schwarz

Institute of Energy Technologies, HSR University of Applied Sciences Rapperswil, Oberseestrasse 10, CH-8640 Rapperswil, carsten.wemhoener@hsr.ch

ABSTRACT

Political targets in Europe focus on nearly zero energy buildings (nZEB) to be introduced by 2020. In Switzerland, cantonal energy strategies define a similar target for 2020. While much experience with high performance building envelopes according to MINERGIE-P® exist, a large variety of concepts and standards for nearly zero energy buildings have been defined, making it difficult to compare realized nZEB. In Switzerland an nZEB definition is given by the MINERGIE-A® label. Annex 40 in the IEA Heat Pump Programme (HPP) entitled "Heat pump concepts for nearly zero energy buildings" is investigating heat pump system solutions for nZEB. Task 2 is dedicated to simulation work in order to evaluate performance and cost of different system concepts and to improve design, control and system integration.

As starting point an analysis of system concepts for different demand structures (single-family house (SFH), multi-family house (MFH) and office buildings) is accomplished. Residential buildings are modified from the reference building used in IEA HPP Annex 38/SHC Task 44, while for the office building typical layouts of a three and five storey building are used. For each reference building, building technology and specific consumption of energy were varied by simulations in the software Polysun®. The analyzed criteria are annual costs, energy balance and load match. For the evaluation variable insulation standards are used to enquire the limitation of nZEB balance. Different technology options and combinations are used: air-to-water (A/W) and ground-source brine-to-water (B/W) heat pumps, district heating, solar thermal collectors, boilers and cogeneration (CHP) with heating oil, biomass, biogas or natural gas. For meeting the nearly zero energy balance, photovoltaic panels are used on the roof and façade area.

Simulation results under the chosen boundary conditions confirm that heat pump concepts with photovoltaic panels to balance the energy consumption have the lowest costs to reach a zero energy balance in buildings with moderate energy consumption up to 50 kWh/(m^2a). In SFH on MINERGIE-P® level, A/W-heat pumps are more cost-effective as B/W. Solar collectors tend to increase the cost while not necessarily increasing the performance due to competition with the heat pump and PV surface. In MFH heat pumps and district heating as well as biogas CHP can reach an nZEB balance by just using the roof area. However, biogas CHP has higher costs. The other concepts need an extended area by using the façade for PV generation. B/W heat pumps get more cost-effective with increase of specific heat demand. Regarding load match, though, heat pumps increase the deficit of winter electricity. With solar thermal collectors or cogeneration systems, the load match can be improved. For the office buildings possible concepts with the sole use of PV on the roof area are ground-source heat pumps, district heating and cogeneration with biogas. A limit for the nZEB balance is in the range of 4 storeys. For low building energy demands, district heating is most cost-effective, while ground-source heat pumps get cheaper with increasing energy demands. CHP, on the other hand, has the best load match characteristic. Currently, higher integrated concepts as well as retrofit considerations are investigated.

Keywords: nearly zero energy building, building technology, heat pump, system simulation

INTRODUCTION

To reduce energy costs and to achieve greenhouse gas emissions reduction targets, the development of highly energy-efficient buildings is essential. Low-energy buildings are encompassing a high level of insulation and air tightness as well as ventilation with very efficient heat recovery to reduce space heating needs. This leads to the creation of nearly or Net Zero Energy Buildings (nZEB or NZEB, respectively). The main concept of an nZEB is that weighted renewable energy yields generated at the building site have to compensate the amount of the weighted energy use on an annual basis. There are different possibilities to realize an nZEB by using renewable energy sources, such as biomass, heat pumps, solar thermal or solar photovoltaics.

In Europe there is a large variety of concepts and voluntary standards for highly energy efficient buildings or climate neutral buildings. Therefore, it is often difficult to compare realized nZEB. In Switzerland an nZEB definition is given for instance by the MINERGIE-A® standard. The MINERGIE-A® standard considers only the building technologies (e.g. space heating, DHW, ventilation and air conditioning) and uses so-called national Swiss weighting factors for the energy balance.

IEA HPP Annex 40 gives an international research framework for research projects on heat pump systems for nZEB. In Task 2 the focus is developed to the simulation work:

- Simulation of promising system concepts for different applications
- Improvement of concepts regarding performance and cost
- Evaluation of the design and control of the systems
- Assessment of options of building and system integration

METHODS

Reference Buildings

The single family house (SFH) is modified from the reference building used in IEA HPP Annex/SHC Task 44 [1]. For the multi-family house (MFH) a typical layout of realised MFH in Switzerland is used. As a model for an office building the company head office of "Marché Restaurants Switzerland" is used as example [2]. The building is certified according to the MINERGIE-P-ECO®- standard.

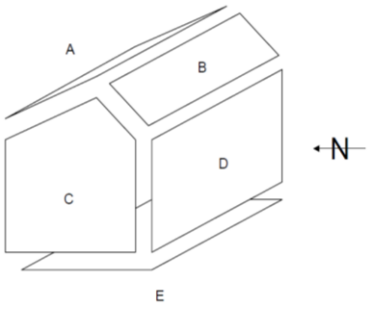

	building	A =d*a	B =d*b	C =c*(e+r/2)	D =d*e	E =d*c
net (inside) area (m^2)	all	54.6	26.4	45.7	56.0	70.0

Figure 1: SFH reference building IEA HPP Annex 38/SHC Task 44

Figure 2: Head office of Marché Restaurants Switzerland

General characteristics

For the energy balance the weighting factors of MINERGIE-A® are used, corresponding to 0.0 for solar and geothermal energy, 0.7 for biomass, 0.6 for district heating with minimum 50% of renewable share, 1 for fossil fuels and 2 for electricity. The balance for all concepts is evaluated for a whole calendar year to equalise the seasonal differences. For the evaluations different balance boundaries are used for residential (SFH, MFH) and office buildings. The balance for SFH and MFH includes only the building technology according to MINERGIE-A®, for the office buildings the energy use of devices is included, as well. Table 1 shows the general characteristics of the different building types which were used for the simulation.

	SFH	**MFH**	**Office A**	**Office B**
Energy reference area (ERA)	164 m^2	1500 m^2	960 m^2	1680 m^2
DHW	50 l/(pers.*d)	50 l/(pers.*d)	5 l/(pers.*d)	5 l/(pers.*d)
Roof area	54.6 m^2	196 m^2	400 m^2	420 m^2
Slope of roof	40°	40°	35°	35°
South façade for PV	-	312 m^2	101 m^2	168 m^2
Orientation	south	south	south	south
Number of storey	2	5	3	5
Number of person	4	30	78	137

Table 1: General characteristics of SFH and MFH and the two types of office buildings

The energy data for the office buildings are calculated with the default values of SIA 2024 [3]. The electrical expense for the cooling demand is determined by typical EER values of SIA 382/2 [4]. In Table 2 the specific and annual energy demand is given.

	per ERA	**Office A**	**Office B**
Air conditioning	4.7 kWh/(m^2a)	4’512 kWh/a	7’896 kWh/a
Electricity for Cooling	1.1 kWh/(m^2a)	1’067 kWh/a	1’800 kWh/a
Electricity for lighting	16.3 kWh/(m^2a)	15’677 kWh/a	27’434 kWh/a
Devices	12.9 kWh/(m^2a)	12’384 kWh/a	21’672 kWh/a

Table 2: Energy requirements of the office buildings (ERA – energy reference area)

System simulations

The different concepts are simulated with the software Polysun® and are analysed regarding the criteria uniform annual cost [1000 CHF/a], energy balance [kWh/a] and load match [-]. For the evaluation different insulation standards denoted as space heating energy needs of 15 kWh/(m^2a) for MINERGIE-P®, 35 kWh/(m^2a) for MINERGIE® and 55 kWh/(m^2a) for a standard new building are used to find limitations of nZEB balance. Different technology options and combinations of them for providing the space heating and domestic hot water (DHW) energy are used: air-to-water (A/W) heat pump, ground-source brine-to-water (B/W) heat pump, district heating, solar thermal collectors, cogeneration of heat and power with heating oil, biogas or natural gas and boilers with fuel oil, biomass (wood pellets), biogas or natural gas. In this study no integrated system solutions are considered, but all systems are installed side-by-side. For meeting the energy balance, photovoltaic panels are used on the roof area or in the building façade. The cost balance includes the investment cost, the running cost and the interest rate for a uniform time period of 25 years.

RESULTS

Single-family-house

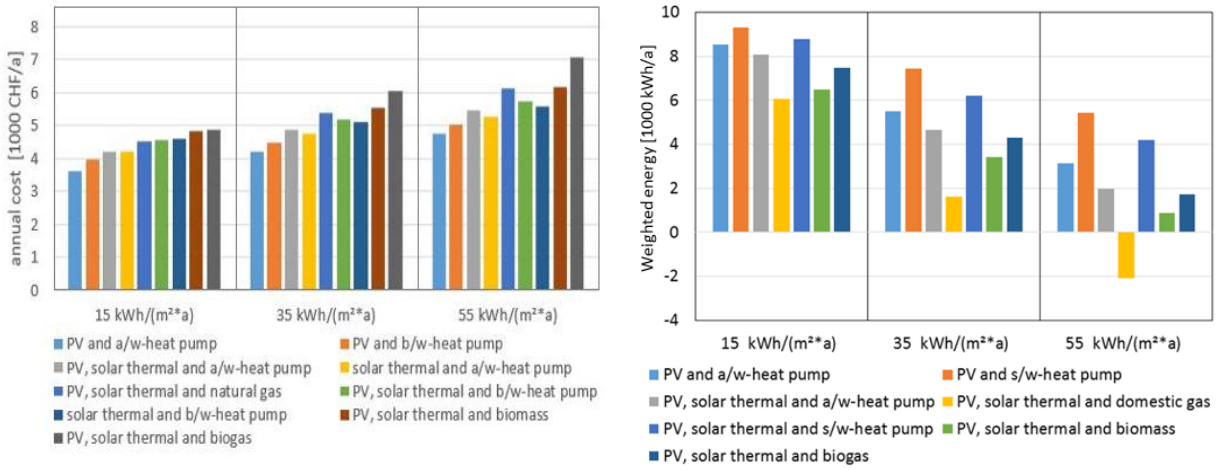

Figure 3: Cost balance (annual cost) and energy balance for SFH

The SFH concepts are simulated with a solar thermal collector area of 8 m^2 corresponding to a DHW design with higher solar fraction. The PV area is designed to use the remaining roof area. The concepts without using PV panels achieve the zero energy balance with electricity purchase from renewable sources. Figure 3 shows the annual cost and energy balance for SFH for different insulation standards expressed as space heating needs 15/35/55 kWh/(m^2a) as described above. In SFH buildings heat pump systems combined with PV have the lowest annual costs. In small buildings with low heating demand A/W are cheaper than B/W heat pumps. Systems with biomass or biogas generate higher annual costs due to higher investment and the high energy costs especially for biogas, which is at current prices about double the price of natural gas. Solar collectors tend to increase the cost while not necessarily improving the performance substantially, which is due to higher cost for storage and piping, decrease of the seasonal performance factor (SPF) of the heat pump, since the heat pump increasingly runs at worse operation conditions, and competition with the PV area. The energy balance in Figure 3 right depict the surplus after energy weighting and confirms that the MINERGIE-A® balance can be reached by most of the concepts up to an insulation standard of a space heating energy need of 55 kWh/(m^2a).

Multi-family-house

In MFH for most concepts a solar thermal collector area of 50 m^2 is chosen corresponding to a system for DHW support. Only for the "PV-solar thermal-A/W heat pump" concept the whole roof area is used for solar thermal collectors and a seasonal storage of 50 m^3 is installed (self-sufficiency for space heating and DHW). The PV area is sized to meet the MINERGIE-A® balance. The results for the cost balance in MFH in Figure 4 left are similar to the results of the SFH. A difference, though, is that the B/W-heat pump gets more cost-effective compared to A/W-heat pumps with the increase of the specific heat demand. Besides the heat pump concepts, district heating and combined heat and power (CHP) on the basis of natural gas offer low-cost solutions with nearly the same cost as the heat pump systems for higher insulation standards (space heating needs of 15-35 kWh/(m^2a)). For low space heating needs the seasonal storage concept has the highest cost, while with increasing space heating needs, the combinations with biogas get the highest cost. Fig. 4 right depicts the percentage of roof area needed to meet the balance. In buildings on passive house level (15 kWh/(m^2a)) the MINERGIE-A® nZEB balance is reached by only using the roof area with all concepts.

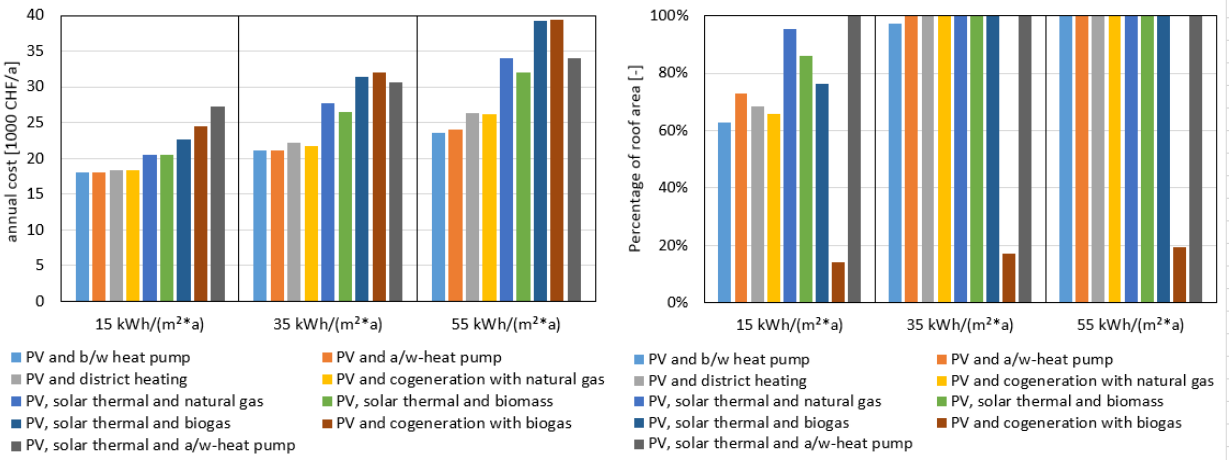

Figure 4: Cost balance (annual costs) and fraction of PV roof area for MFH

With higher specific space heating needs (35-55 kWh/(m^{2}a)) it is necessary to use the façade for additional PV panels. Only CHP with biogas can achieve an nZEB without using the façade area, but biogas has the highest energy cost. An advantage of solar collectors or CHP, though, is to improve the load match, since heat pumps increase the electricity demand in winter, when the PV yield is lower. Therefore, the combination of PV and CHP has a good load match characteristic with winter electricity by CHP and summer electricity with PV.

Office buildings

For the office buildings two buildings with 3 (Building A) or 5 (Building B) storeys were considered to find the limitations of nZEB concepts in office buildings. Besides the roof, also the façades (south, east and west) are used for the PV installations. Different to MINERGIE-A®, the building technologies and also the energy demand for lighting and devices are included in the balance. The cost balance of building A and B are similar, and the number of storeys has only a small impact on the system order regarding annual costs. With low space heating needs, district heating is most cost-effective. B/W and A/W heat pumps get cheaper with increasing needs. CHP with biogas has the highest cost as in the residential buildings.

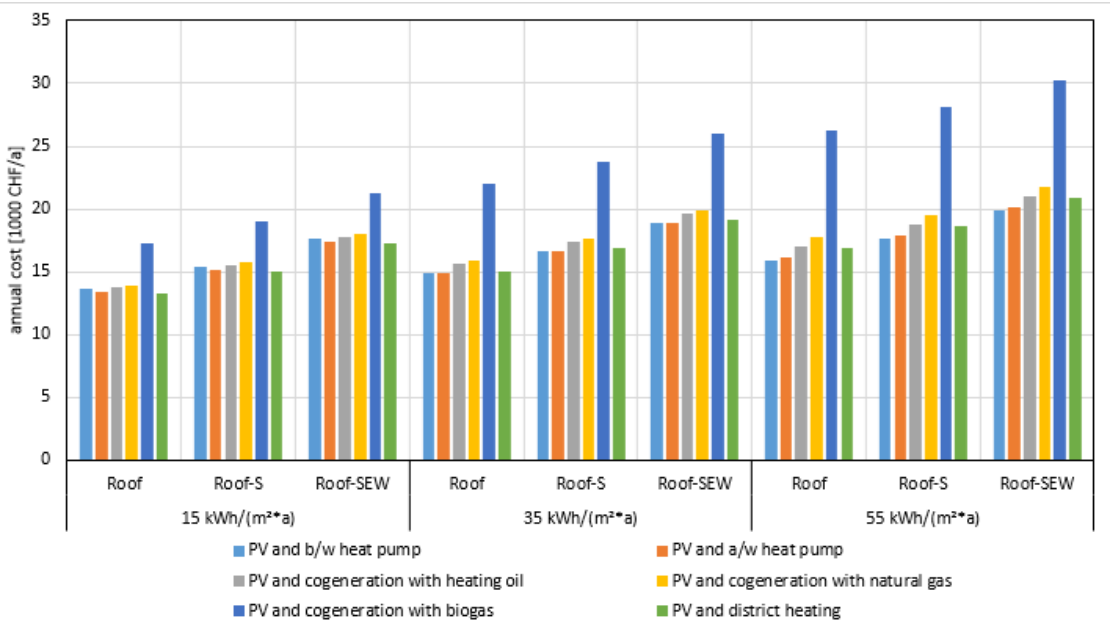

Figure 5: Cost balance (annual costs) office building A

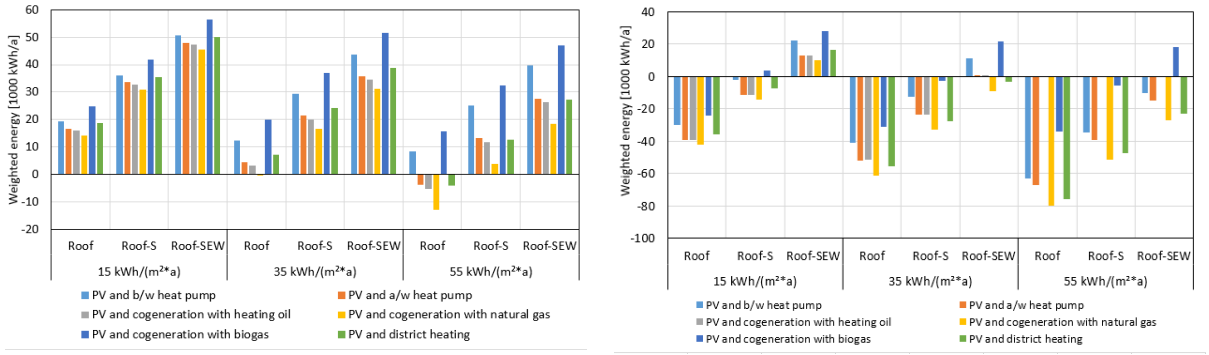

Figure 6: Energy balance of office building A (left) and office building B (right)

CONCLUSION

The heat pump solution is for all building types cost-effective with regard to the annual cost and energy efficient, even though SPF of the heat pump is rather conservative with 2.7 for A/W-heat pump and 3.3 for the B/W-heat pump. Only district heating can compete with the similar annual cost for low space heating needs. With increasing heating needs, ground-coupled heat pumps get more cost-effective due to the better performance and less necessary PV area to meet the nZEB balance. With decreasing heating needs, though, higher investment cost cannot be compensated by the better SPF, so A/W-heat pumps are the cheapest solution. Side by side combinations with solar thermal tend to increase the cost without substantial increase of energy performance due to competition with PV area on restricted overall roof area. Moreover, PV has a weighting factor of 2, while solar thermal energy simply reduces the needs. The only drawback of heat pumps is the limited load match due to the increase of winter electricity. In that sense, CHP has the best load match characteristic, since PV deficits in wintertime are compensated due to CHP operation for winter heating needs resulting in a good load match.

ACKNOWLEDGEMENTS

The study has been performed as national contribution to the Annex 40 in the IEA Heat pump programme (HPP) on “Heat pump concepts for nearly Zero Energy Buildings”. Information on the IEA HPP Annex 40 can be found on http://www.annex40.net. The funding and advice of the Swiss Federal Office of Energy for the IEA HPP Annex 40 is highly acknowledged.

REFERENCES

1. Dott, R., Haller, M.Y., Ochs, F., Reuschenburg, J., Bony, J.: The Reference Framework for System Simulations of the IEA SHC Task 44 / HPP Annex 38, Technical report of subtask C, Report C1 part B, Muttenz, 6.9.2013
2. Naef, R., Stemmler, S.: Marché international support office, Kemptthal, Zürich, Final report SFOE research project, Zurich, 2010.
3. Swiss Society of Engineers and Architects : SIA 2024 Standardnutzungsbedingungen für die Energie und Gebäudetechnik, Zurich, 2006
4. Swiss Society of Engineers and Architects : SIA 382/2 Klimatisierte Gebäude – Leistungs- und Energiebedarf, Zurich, 2011

DEVELOPMENT OF PROTOCOL FOR SUB-METERING FOR SIMULATION MODELS OF SHOPPING CENTRES

M. Haase[1]; K. S. Skeie[1]; R. Woods[1]

1: SINTEF Building and Infrastructure, Alfred Getz vei 3, 7491 Trondheim, Norway

ABSTRACT

The study investigates the efficiencies and inefficiencies associated with the everyday management, operation and use of shopping centres and aims to identify the drivers, barriers and potentials associated with the operation of shopping centres. Its main focus was to track inefficient use and user implications in complex buildings (shopping centres). First, the main predictor variables and performance indicators were identified.

A protocol for sub-metering of energy consumption and flows (mainly heat and electricity, but also other sources and common services) was defined as necessary basis in order to be able to track inefficient use and user implications. User profiles were split into sub-categories, owners, tenants (shop owners, differentiating by size and type) and end-users (shopper, with appropriate differentiation) are three minimal differentiations.

The proposed method provides a solid basis for performance based economic models that have to be introduced in order to be able to apply cost-effective refurbishment investments. The results of key performance indicators provided valuable input in the decision making process for deep retrofitting plans. Different proposals for visualization of results (feedback to managers, tenants, customers) were investigated and are discussed.

Keywords: shopping mall, sub-metering, energy flows

INTRODUCTION

Shopping centres are not interchangeable with other kinds of complex buildings, such as office blocks, hospitals or schools. The character of shopping centres, form, function, usage, and users has implications for energy use. To support the understanding of what causes the main inefficiencies in energy usage and how to develop the best solutions sets, a definition of shopping centres was developed, based on existing literature. The definition chosen in this study describes a shopping centre as "*a formation of one or more retail buildings comprising units and 'communal' areas which are planned and managed as a single entity related in its location, size and type of shops to the trade area that it serves*" [1]. The definition gives an indication of the main form and function in shopping centres. In addition, location, type of development, the size and the GLA, the type of anchor stores and the trip purpose are all aspects that have been used to indicate the needs that a shopping centre serves within social and physical context, these are presented in Table 1. Climate and regional differences have implications for retrofitting practice and the definition and supporting table present climatic and regional differences and are registered in the description of ten representative reference buildings [1].

In general the shopping centre industry is used to key performance indicators (KPIs). Example of KPI for a Shopping centre real estate company are: Total property return, Occupancy, Like-for-like, NRI (net rental income) and Growth in EPS (earnings per share). This work will identify the main predictor variables and performance indicators found in shopping centres in a context with user and occupant expectations and requirements. Form

follows function to a large degree in shopping centres. However, the needs of retail activity and the requirements associated with the different stakeholders and their typical functional patterns actively influence shopping centre architecture and energy consumption [3].

METHOD

Sustainable shopping centres are more than simply energy efficient, they are environments that are accessible to all sides of society irrespective of buying power, social class or disability. This paper therefore opens with a discussion of architectural qualities in shopping centres, because architecture at its best is often understood as a combination of technology, functionality and aesthetics. The paper develops performance indicators based on the technical functionality of shopping centre architecture, for example flexibility and universal design, in short meeting user needs. Subsequently, predictor variables and performance indicators associated with several aspects were examined.

RESULTS

Architecture, typology and layout of shopping centres

Architecture encompasses technology, functionality and aesthetics. In this section, architectural form has been considered in context with user and occupant expectations and requirements to build a basis for energy performance indicators that relates to shopping centre form, layout, users requirements and cultural context. There are different types of shopping centres (see **Erreur ! Source du renvoi introuvable.**) and there is a typology associated with the usage that different areas in shopping centres are put to, functional patterns and stakeholder groups are associated with the areas. The different shopping centre types and typologies may vary according to for example size and use, for example it may be expected that speciality centres will have smaller circulation areas and less storage space than regional centres, and some centres do not have restaurants, staff rooms or atriums [2]. However, if we take into account the variations found within the main shopping centre types, there are certain areas that may be considered standard for all shopping centres. The table describes the five main areas in shopping centres, their usage and different locations within a centre and shows an overlap in usage, for example not all retail takes place in clearly defined retail units; some take place in common areas in temporary or permanent units. Restaurants, food courts and cafes may be found within retail units and on occasion stores may be found in restaurants and cafes. In addition, centres that offer leisure activities, or specialised functions like conference facilities, are typologies not covered in this overview. Typical examples which impose other usages include cinemas, bowling alleys, or swimming complexes. Hotels or apartments may also be located within shopping centres. For these typologies additional performance indicators apply which are not covered.

Energy use and flows in shopping centres

Table 1 offers insight in the broad range of activities which take place in shopping centres, giving customer satisfaction requires a broad range of services from shops, toilets and deliveries, to technical rooms, child minders, cafes and car parks. The range of activity requires a complex and flexible physical structure, one that allows for, amongst other things, changing retail, demographic and technical needs.

Shopping centres are complex buildings with specific needs. The use that different areas are put to affects energy consumption, whereas the different functional patterns and stakeholder

groups influence energy use. They are also associated with specific requirements that make it relevant to consider different types of performance indicators.

Typology	Main usage				Location			
					Common areas	Shop/ retail areas	Behind the Scenes	Outdoors
Common Areas	Circulation	Main horizontal circulation	Vertical circulation	Emergency exits	**Main usage areas**	Within retail units and stalls	None	Benches paths, play areas and other
	Entrance	Main entrance	Side entrance	From car park				
	Sanitary	Toilets	Child care					
	Parking	Entrance	Circulation	Parking				
Restaurants/ cafes/ Food courts	Entrance	Seating	Service	Food preparation	Atrium location	Food serving in-store and restaurants	Kitchens, prep, storage	Pavement cafes
Shops/ Retail/ Other	Entrance	Sales	Service	Staff rooms / storage	Atrium, corridors	**Main retail areas**	Storage, staff rooms	Temporary/ permanent
Behind the Scenes	Entrance	Trolleys	Trucks		None	Storage, staff rooms and waste in some units	**Main usage areas**	Delivery waste storage
	Storage	Services	Waste					
	Technical rooms	Pathway	Shafts	Sanitary				
	Circulation	Horizontal circulation	Vertical circulation	Emergency exits				
Outdoors	Restaurants/ cafes	Entrance	Seating	Service	Benches, paths, play areas and other	Temporary or permanent retail units, or stalls	Delivery and waste storage	**Main usage areas**
	Parking	Circulation	Parking lot	Service				
	Leisure	Resting/ Recreation	Seating	Other				
	Delivery area	Containers						

Table 1: Typical Areas in Shopping Centres [2].

In the scope of this analysis both indicators and requirements with a direct or an indirect effect on energy consumption in shopping centres are identified. When defining the relevance of performance indicators; legal requirements (i.e. for work environment), ownership or authority over parts of the centre, and cultural context also come into play. Therefore, six performance concepts are identified which form the structure of the next sections, all with contextual relevance to energy use and supply of energy in SC:

- Energy follows function
- Energy follows form
- Energy follows user needs

} Functional element sub-division

- Energy follows stakeholders
- Energy follows organization
- Energy follows availability

} Organizational element sub-division

As a result of the underlining complexity of performance requirements in SC, it may also be useful to distinguish between causes of energy use within a functional sub-division, meaning energy divided by the functions which it is used (by end use or supply system), and organizational sub-divisions of energy use distinguished by who pays for the energy and thus is related to billing practice, tenant agreements, and contracts with energy supply carrier companies.

The first three are mainly linked to the demand side and indicators that represent the requirements that can be found in norms, standards and the like. While different stakeholder groups, organisation and contextual aspects like climate and energy availability, also define the relevance of performance indicators, and suggest which priorities should be given when performance requirements are in conflict. The latter interest groups and contextual aspects also form billing practices, sub-metering and indicators for dividing the operational energy costs.

Protocol for sub-metering

Figure 1 illustrates a functional sub division of energy end use within a shopping centre. Starting with the energy supply and the technical services in place, the energy use associated with heating, cooling and electricity are structured by end use. The diagram is easiest to comprehend for centralized HVAC systems, but in principle the structure is the same for all installations localized in tenants' retail space. In a typical shopping centre there will exist several heating, or cooling loops and many electrical subdivisions (distribution boards) on top of various end uses of energy.

The illustrated processes are usually in the control of facility managers and technical staff. A multitude of performance indicators can be related to this structure. Some performance indicators are important in the design and commissioning of the systems, other are of use in the day-to-day running of the centre. Reading the diagram from left to right, the potential of increasing energy efficiency lies both in production, distribution and end-use.

Energy can be considered to follow function because energy in the end is used to meet requirements defined by the activities that take place in a shopping centre. In a SC, requirements are diversified by the type of tenants (shops, retail, restaurants, cafes, etc.), by the size of tenants rental space (stalls, retail units, independent anchor stores etc.), or by the type of spaces (common areas, offices, storage etc.). The different activities can be characterized by functional patterns for various groups; – opening hours for customers will differ from operational hours for technical services and lighting. Facility operation has to meet the requirements of staff before the shopping centre opens to the public. In shopping centres many tasks are performed outside of opening hours which require maintaining health and safety for the workers. Examples are cleaning, sanitation, loading and re-stocking of goods. In relation to this, the ratio of full operation of HVAC and lighting vs. opening hours or service hours is one index that could be used as a performance indicator.

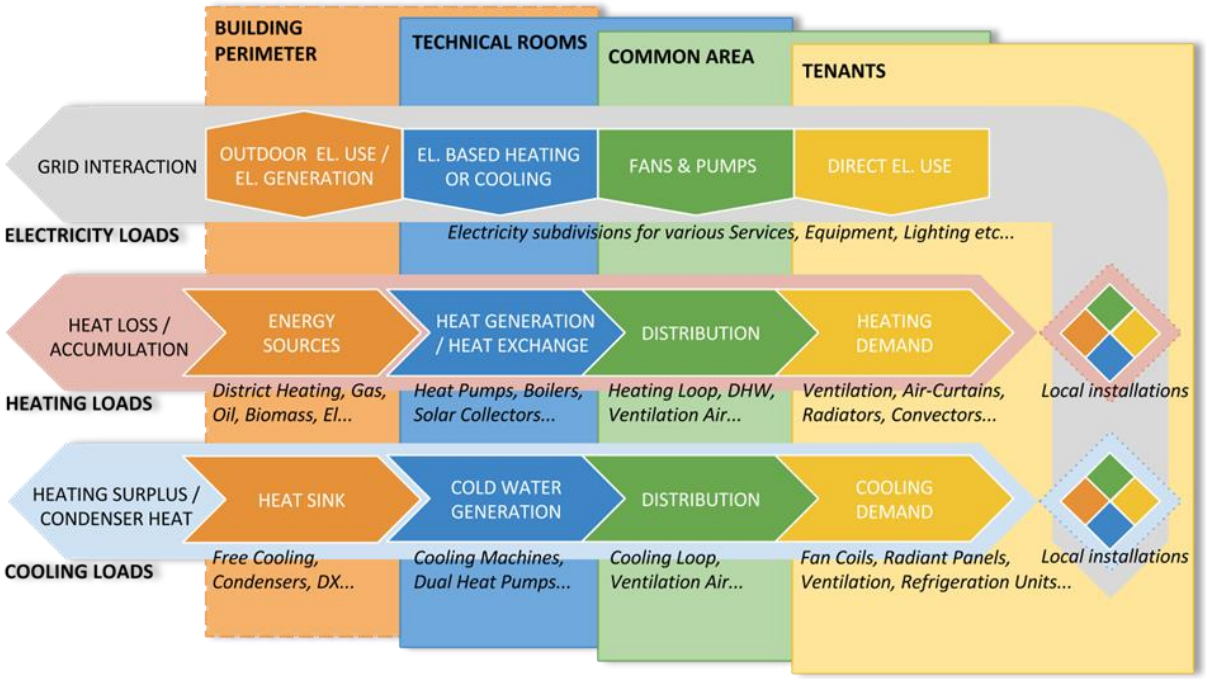

Figure 1 – Monthly wind velocities of different measurement stations

DISCUSSION

The shopping centre market has changed from a fairly homogeneous, mass consumption market to one that is fragmented according to for example taste and lifestyles, reflecting a diverse and changing society. Shopping centre architecture therefore needs to meet needs of consumers who are more sophisticated and demanding. During the rehabilitation process it is important to keep in mind the four main stakeholders groups, namely customers, management, tenants and community. An integrated design process is needed that takes into account the goal to develop future markets where good architecture contributes to low-energy use, attractive trading jobs and meeting spaces, and thereby supporting the activities of all four groups.

Energy follows form

In typical shopping centres the retail units are often heated, cooled and ventilated separately from the common areas. The same retail units are often also connected to the central spaces by large open doorways through which air, odours, light, and noise exchanges occur, effectively linking the different spaces.

Energy follows user needs – workers & customers

It is challenging to meet performance requirements, to keep within accepted limits of comfort and meet retailer needs in such an open indoor environment, where different spaces inside the shopping centre are effectively linked (as described in the previous section). However even with greater energy use focus on accessibility and a wide range of issues will remain of primary importance, not only because of retail needs, but also because, as mentioned earlier, sustainable shopping centres should be accessible to all sections of society.

Energy follows stakeholders – decision makers

Comfort needs, however, are also socially constructed. In the design process, operation, meetings between tenant associations and management, labour meetings performance indicators can be important quantitative statements to meet user needs with regard to comfort and ensure high energy performance.

Energy follows organisation

Organisational forms can be observed in Real estate companies, property companies, management companies, facilities companies (outsourcing or within the same owner company) and tenant associations. Contracts between those organisations and the indicators used in those agreements are often based on KPIs which offers potential for introducing energy intensity related KPIs.

Energy follows availability

Nowadays, it is a challenge to transform the current energy system into modular power generation in order to improve the quality and the reliability of the electricity supply. The renewable energies and efficient solutions can overcome the oversizing problem of the electrical infrastructure for meeting the energy demand peaks as well as the energy transmission losses. However, the incorporation of renewable system in shopping centres must take into account that some problems in the supply can appear given its dependence of the climate conditions as well as the affections in the quality of the grid since they can generate frequency and voltage fluctuations and outages. Furthermore, any interaction in the grid must consider the grid capacity for admit new compounds.

CONCLUSION

In the scope of this analysis both indicators and requirements with a direct or an indirect effect on energy consumption in shopping centres were identified. When defining the relevance of performance indicators; legal requirements (i.e. for work environment), ownership or authority over parts of the centre, and cultural context also come into play. Six performance concepts were identified which have contextual relevance to energy use and supply of energy in SC. As a result of the underlining complexity of performance requirements in SC, it may also be useful to distinguish between causes of energy use within a functional sub-division, meaning energy divided by the functions which it is used (by end use or supply system), and organizational sub-divisions of energy use distinguished by who pays for the energy and thus is related to billing practice, tenant agreements, and contracts with energy supply carrier companies.

A possible task for the future could be to identify if and how relevant energy performance indicators can be incorporated in contracts, or other forms of agreements between the stakeholders.

ACKNOWLEDGEMENTS

The work presented is financed by the European Community Seventh Framework Programme (FP7/2007-2013) under grant agreement n. 608678.

REFERENCES

1. Bointner, R., Toleikyte, A., Woods, R., Atanasiu, B., De Ferrari, A., Farinea, C. and Noris, F. (2014), Deliverable 2.1 report - Shopping malls features in EU-28 + Norway, EU FP7 project CommONEnergy – Reconceptualizing Shopping Malls,
2. Haase, M., Skeie, K.S., Woods, R., Mellegård, S., Schlanbusch, R.D., Homolka, S., Gantner, J., Schneider, S., Lam-Nang, F., (2015) Deliverable 2.3 report - Typical functional patterns and socio-cultural context, EU FP7 project CommONEnergy – Reconceptualizing Shopping Malls, , access date: April 2015
3. Woods, R., Mellegård, S., Schlanbusch, R.D., Haase, M., Skeie, K.S., Deferrari, A., Cambronero Vazquez, M.V., Ampenberger, A., Bointner, R. (2015), Deliverable 2.2 report – Shopping mall inefficiencies, EU FP7 project CommONEnergy – Reconceptualizing Shopping Malls, , access date: April 2015

DYNAMIC THERMAL SIMULATIONS FOR DEVELOPING EARLY-STAGE ASSESSMENTS FOR OFFICE BUILIDINGS

A. Degens; F. Scholzen; C. Odenbreit

University of Luxembourg, Faculty of Science, Technology and Communication,

6, rue Richard Coudenhove-Kalergi, L-1359 Luxembourg

ABSTRACT

Office buildings account for a large portion of the total energy consumption in Europe because due to increased comfort requirements almost all recent buildings are air-conditioned. This project is focused on the influence of thermal storage capacity of commonly used structure types of office buildings and different technical strategies on energy efficiency and thermal comfort. The technical parameter ventilation strategy is essential compared to the parameters structure type or window-to-wall ratio. Additionally a lighting control system based on solar radiation shows a high influence on the internal gains and in consequence on the overheating hours. The slab type respectively the accessibiltiy of the thermal mass has a significantly higher influence than the differences of "massivity" between solid and light weight structures.

INTRODUCTION

A tendency towards highly glazed facades for office buildings can be noticed despite their sometimes bad reputation for being a cause of comfort problems. In contradiction to that trend, current scientific research results recommend a lower window-to-wall ratio and structure types with a high proportion of thermal mass to reduce energy consumption and overheating hours. On the other hand, light weight composite structures are an interesting alternative because of pre-fabrication possibilities and higher design flexibility. Due to this conflicts and dependencies in the early design phase the aim of this project is to develop guidelines and planning recommendations for office buildings with different window-to-wall ratios of facade glazing and light weight composite structures.

METHOD

All the evaluations of this project are based on a representative reference zone with typical input parameters of office buildings. A reference zone method has been used for the parametric study of the main features of the building concerning energy demand and thermal comfort. The advantage of this method lies in the fact that a rather simple simulation model allows to quantify directly the influence of constructional and technical design parameters [1].

Office building and reference zone

The reference zone can be applied to different types of building geometry and the commonly used office organisation concepts. It is located in an intermediate storey of a low- or medium-rise building of three to seven stories. The exterior wall is highly insulated. The floor area is 110 m^2, which provides a work space for about ten persons (typical occupancy rate), see Figure 1. The thermal conditions of the boundary zones are identical to those of the reference zone. The climate is equivalent to the moderate Western European climate of Saarbrücken, Germany.

Figure 1 Floor plan and cross section of office building and reference zone

Structure and Facade

Two structure types of office buildings are defined for this study: one solid structure (SOLID 1) and one steel composite structure (STEEL 1), see Table 1. Both are already optimised with regard to structural and material efficiency.

Structure type	Definition	Image
SOLID 1	280 mm reinforced concrete, 70 mm screed and suspended ceiling	
STEEL 1	steel beam, profiled sheeting C77 + 130 mm concrete slab, floating screed and suspended ceiling	

Table 1 Structure types of office building

The facade system of the reference zone consists of a curtain wall structure as commonly used in office buildings. Three selected window-to-wall ratios represent a punctuated facade with a ratio of 48% (F 48), a band window facade with a ratio of 77% (F 77) and a fully glazed facade (F 100). The window-to-wall ratio calculation is based on the inside surface of the exterior wall and each window area consists of 80% glazing and 20% frame.

Parametric study

Reliable building dynamic thermal simulation tools are required to assess energy efficiency as well as environmental and thermal comfort performances [2]. In this project the transient simulation tool TRNSYS 17 has been selected to determine the energy demand and the overheating hours of the reference zone. A further objective is to analyse the influence of new technologies for example electrochromatic glazings or phase change materials.

In an office building the number of input parameters that influence the energy consumption is very high and it is necessary to identify and concentrate on the most important parameters in order to reduce the number of parametric studies [3] and parameter combinations. Several parameters are fixed or defined as categorical in the course of this project like the window-to-wall ratio and the structure type. Additionally some technical parameters, like the schedule, the set points and the control strategies for heating and cooling, are fixed. Heating has a set point indoor temperature during daytime of 22°C and during night time of 16°C. Cooling starts with a set point indoor temperature of 26°C during USE time (7h-18h). The categorical parameters for glazing types, shading devices, ”Lighting control” and “Ventilation strategy” are variable.

RESULTS

Lighting control system

Lighting control systems are currently used in many new office buildings in order to save energy for electricity. Thewes illustrates that a lighting control system can reduce the energy consumption used for lighting by 50% and additionally it can improve thermal comfort in summer [4].

In the standard 3D building project of TRNSYS 17 the lighting control system depends only on the global solar radiation on the horizontal outside. The light is turned on respectively turned off according to switching values suggested by default of 120 W/m^2 respectively 200 W/m^2. For a daylight factor of 2% these values correspond to the illuminance values of 300 lx and 500 lx [5]. The installed power is 10 W/m^2 including 40% fluorescent tubes which are commonly used in office buildings. This control system leads to 1.500 work light hours a year for the reference zone. However, neither the orientation of the facade nor the window-to-wall ratio, the glazing and shading type have been considered. As a consequence, a new lighting control system was developed, which is based on the short wave solar radiation through the external windows of the reference zone. The illuminance values correspond to the same radiation values as in the standard model. The switching values are defined as 5 W/m^2 respectively 10 W/m^2. This design approach depends on the amount of work light hours and leads to reasonable results in case of a triple glazing and a radiation controlled external shading device, see Figure 2. It allows to consider the influence of the work light hours on the internal gains of the reference zone.

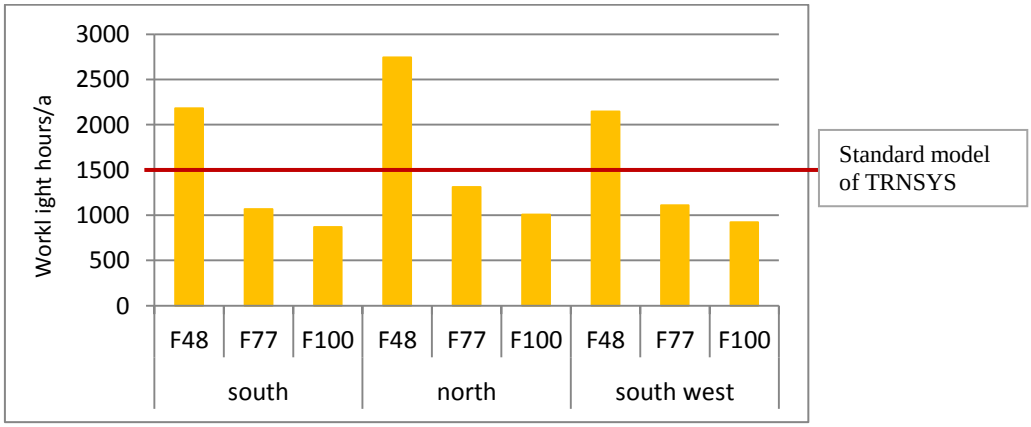

Figure 2 Work light hours/a of the new model based on solar radiation of reference zone compared to the standard model of TRNSYS

Simulation results

A previous analysis has shown that the south west orientation of the reference zone is the most critical orientation concerning thermal comfort and that the design challenges lie in cooling demand and not in heating issues. Any other simulation results present the overheating hours of the south west orientation and consider the new lighting control system.

Shading devices and glazing types

The electrochromic switchable glazing technology allows the variation of visible light transmission and solar heat gain coefficient to adjust heat and light in relation to interior comfort requirements [6]. The system works with a thin solid electrochromic film, sandwiched between two layers of glass which can be activated with low voltage to change transparency [7]. The tool WINDOW 7.2 and the International Glazing Data Base (IGDB) has

been applied to simulate such a system in TRNSYS. A control signal algorithm depending on solar radiation on the facade regulates the glazing state from very transparent with a radiation level of 0 - 120 W/m^2 to fully tinted with a level higher than 420 W/m^2. An electrochromatic glazing (ELEC) and a triple glazing (EW 1) with and without external shading devices have been analysed, see Table 2. The analysis is based on the window-to-wall ratio of 77% and the defined ventilation strategy VENT_NAT, see Table 3 below.

Shading and glazing types	Definition
SHON	External, radiation controlled, shading factor 0.7
SHOFF	Without external shading
EW1	Standard triple glazing, Ug = 0.6 W/m^{2}K, g = 0.584
ELEC	Electrochromatic triple glazing, Ug = 0.78 W/m^{2}K, g = 0.407 - 0.05

Table 2 Shading and glazing types of reference zone

The application of a radiation controlled external shading device in combination with the triple glazing (EW 1_SHON) has an enormously positive effect to reduce overheating hours. The electrochromatic glazing (ELEC) shows approximatively the same performance and a combination of both would lead to another small improvement (ELEC_SHON), see Figure 3, but of course costs for two systems will arise.

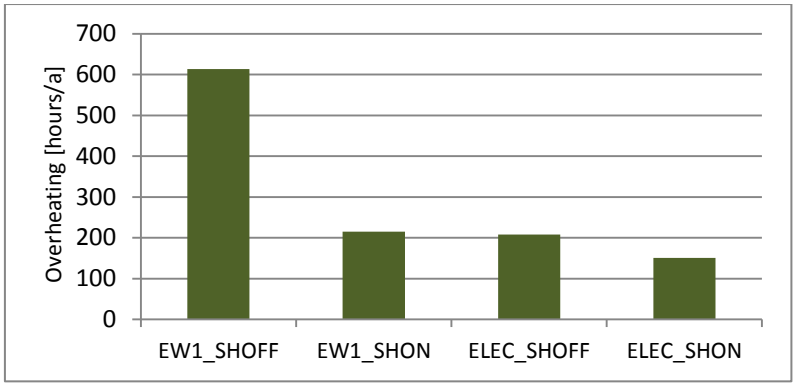

Figure 3 Overheating hours of different shading devices

Ventilation strategy

Three different ventilation strategies have been analysed: a mechanical system with a constant air supply during USE time (VENT_MECH) and a system with enhanced night time ventilation (VENT_NIGHT). The latter benefits from the cooling effect of outside air during periods of overheating risk. The third system is a natural ventilation system (VENT_NAT) with a similar air change rate as the other two systems and an enhanced day- and night time ventilation, see Table 3.

Ventilation strategy	Definition
VENT_MECH	Mechanical ventilation, constant air flow during USE, air change rate 1 h^{-1}, constant supply temperature of 18°C, heat recovery 70%
VENT_NIGHT	VENT_MECH + optional enhanced night ventilation, air change rate 4 h^{-1}
VENT_NAT	Natural ventilation, base rate 0.7 h^{-1} + enhanced daytime, air change rate 2 h^{-1} and night ventilation, air change rate 4 h^{-1}

Table 3 Ventilation strategies of reference zone

The results show that the ventilation strategy has a significantly higher influence compared to the parameters window-to-wall ratio and structure type, see Figure 4.

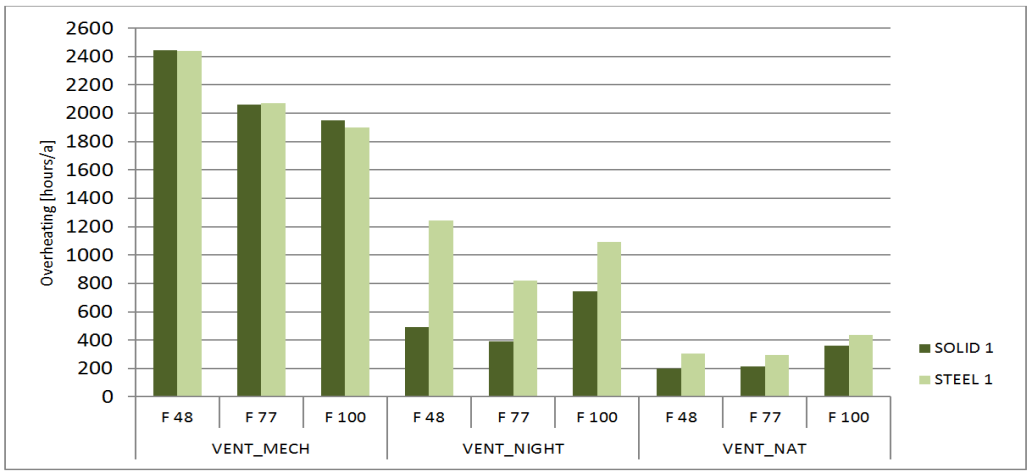

Figure 4 Overheating hours of different types of ventilation strategy

The system VENT_MECH without enhanced ventilation for heat removal causes the most overheating hours. The strategy VENT_NIGHT with enhanced night time ventilation improves the situation but an acceptable range of overheating hours can only be reached if a consequent day- and night time ventilation during periods of overheating is applied. In this case the reference zone complies almost with general comfort requirements, if a lower window-to-wall ratio is selected. The steel composite structure causes more overheating hours in case of an advanced ventilation strategy. Whether the structure type or the slab type is decisive will be discussed in the next chapter.

Influence of structure and slab type

The solid structure (SOLID 1) and the steel composite structure (STEEL 1) are analysed. First both slabs are covered with a suspended ceiling, which has been removed in the next step (marked in Figure 5 with "WCS"). The evaluation is based on the ventilation strategy VENT_NAT, a window-to-wall ratio of 77%, a triple glazing and an external shading device.

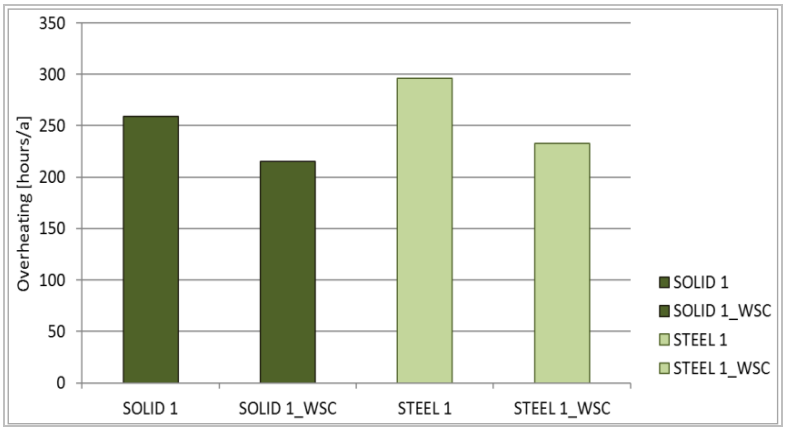

Figure 5 Overheating hours of different slab types

The differences between the solid and the steel composite structure are not as striking as expected. For both structures types it is beneficial (in terms of overheating hours) to renounce on a suspended ceiling as the thermal storage capacity of the slabs can be used more effectively, see Figure 5.

DISCUSSION AND CONCLUSION

The study has been focused on the influence of the main technical parameters lighting control, ventilation strategy and shading devices. The results presented have shown that an adequate ventilation strategy is more important for energy demand and thermal comfort than other building-related design parameters like the window-to-wall-ratio or the structure type. However, in addition to an adequate ventilation strategy the accessibility of the thermal mass and an external radiation-controlled shading device are essential to improve thermal comfort. An electrochromatic glazing is an interesting alternative to conventional shading devices because it shows a similar performance.

A lighting control system which is based on the solar radiation of the reference zone allows a more realistic presentation of the work light hours in future simulations and shows their influence on the internal gains of an office building. Phase change materials will also be integrated in further research because it is assumed that they can increase the thermal capacity of light-weight systems to improve thermal comfort.

A design optimisation and a systematic sensitivity analysis by means of an optimisation tool [8] will be carried out due to a growing amount of input parameters and thus a large number of thermal simulations required. The aim is to rank the parameters according to their impact and importance on energy demand and thermal comfort and to give easy applicable design guidelines for the early planning phases.

ACKNOWLEDGEMENT

The authors wish to thank ArcelorMittal for co-financing this research and the Chair of Steel and Facade Engineering at the University of Luxembourg for the support of this project.

REFERENCES

1. P881: Report of “Sustainable office and administration buildings in steel and steel-composite construction” of FOSTA (Forschungsvereinigung Stahl e.V.). Germany, 2015.
2. Munaretto, F., Peuportier, B., Guiavarch, A.: Accounting for thermal mass in thermal simulation tools: comparison of several assumptions. MINES Paris Tech – Center for Energy efficiency of Systems. Paris. France. CERIB (Studies and Research Center for the Precast Industries). Epernon. France. Conference BS2013, Chambery, France, 2013.
3. Gratia, E., DeHerde, A.: A simple design tool for the thermal study of an office building. In Energy and Buildings 34, pp. 279–289, 2002.
4. Thewes, A.: Energieeffizienz neuer Schul- und Bürogebäude in Luxemburg basierend auf Verbrauchsdaten und Simulationen. 1st ed, Shaker. Aachen, Germany, 2011.
5. Transsolar Energietechnik GmbH Stuttgart: A TRaNsient SYstem Simulation Program, Seminar II, Gebäudesimulation mit TRNSYS. Stuttgart, Germany, 2014.
6. Meek, Ch., Bruot, A.: Toward Net Zero Energy Buildings with Energy Harvesting Electrochromic Windows (EH-ECWs). University of Washington, Seattle, Washington USA. Conference BS2013, Chambery, France, 2013.
7. Beevor, M.: Smart Building Envelopes. 4th Year Project Report. University of Cambridge, UK, 2010.
8. Cenaero Headquarters, Gosselies, Belgium, 2015. Available online at http:// www.cenaero.be/Page_Generale.asp?DocID=15336&la=1&langue=EN

THE EFFECT OF SUSPENDED CEILINGS ON THERMAL MASS TO REDUCE OVERHEATING

C. Jimenez-Bescos[1]

1: Anglia Ruskin University, Department of Engineering and the Built Environment, Chelmsford, CM1 1SQ, United Kingdom

ABSTRACT

Thermal mass has the benefit of regulating energy in buildings and generates potential savings in energy and CO_2 emissions. The effect of climate change with increasing air temperature intensifies even more the opportunities for the use of thermal mass to reduce overheating in summer and minimize the use of cooling energy, providing savings in energy and CO2 emissions. In most educational buildings, the thermal mass is hidden behind a compressed mineral wool suspended ceiling. The suspended ceiling produces a blocking effect for the use of the thermal mass to regulate the indoor conditions, avoiding the loading and unloading of the thermal mass as a regulatory mechanism for indoor temperature.

The aim of this study was to investigate the impact of suspended ceilings on overheating and the benefits of using thermal mass to reduce overheating.

The approach used in this study was based on dynamic thermal modeling to analyse the overheating performance of a test room with suspended ceiling and with the thermal mass exposed. The testing room was simulated under weather conditions for two locations in Europe, London in the United Kingdom and Munich in Germany.

The test room was modeled and simulated using energyplus in DesignBuilder. The test room was modeled using medium weight construction in accordance with the UK Building Regulations Part L2 2010. All room surfaces were adiabatic apart from the south facing wall, which compromised 50% of glazing. The test room was naturally ventilated and a night cooling ventilation strategy was used to cool down the thermal mass. No cooling was used in the simulations to be able to quantify the benefits provided by the thermal mass to reduce overheating.

An overheating limit of 28 ºC was chosen in accordance with the Building Bulletin 101 Ventilation of School Buildings to assess the performance of the thermal mass during the simulations.

The simulation results show that by exposing and making use of the room thermal mass, the number of hours above 28 ºC can be reduce by at least 33% in Munich and 49% in London. The reduction in overheating hours will consequently minimise the need for cooling energy in summer providing savings in energy and CO2 emissions.

Keywords: thermal mass, suspended ceiling, overheating

INTRODUCTION

Thermal mass has the benefit of regulating energy in buildings and generates potential savings in energy and CO_2 emissions. Previous studies (Marceau et al, 2007) have highlighted the energy cost savings, which could be achievable by optimizing thermal mass in the structural frame of buildings. The effect of climate change with increasing air temperature intensifies even more the opportunities for the use of thermal mass to reduce overheating in summer and minimize the use of cooling energy, providing savings in energy and CO2 emissions. The Energy Saving Trust (2005) and the Building Research Establishment (BRE) (2005) had presented the benefits of coupling thermal mass and ventilation in housing to avoid overheating. According to the Zero Carbon Hub (2012), thermal mass and purge ventilation have a beneficial effect on reducing overheating. This study focus on educational buildings, there mostly the thermal mass is hidden behind a compressed mineral wool suspended ceiling for acoustic reasons, which are outside of the scope of this study. This suspended ceiling produces a blocking effect for the use of the thermal mass to regulate the indoor conditions, avoiding the loading and unloading process of the thermal mass to be used as a regulatory mechanism for comfort indoor temperature.

Overheating is a term used here to describe the undesirable effect of higher than comfortable temperatures, which exceed the target room temperatures. Overheating increases in constructions with no thermal mass or when the thermal mass is insulated from ambient-room temperatures, such as with the used of suspended ceilings. An overheating limit of 28 ºC was chosen in accordance with the Building Bulletin 101 Ventilation of School Buildings (2006) to assess the performance of the thermal mass during the simulations.

The aim of this study was to investigate the impact of suspended ceilings on overheating and the benefits of using thermal mass to reduce overheating.

METHOD

The test room was modeled and dynamically simulated using energyplus in DesignBuilder. The test room was modeled with dimensions 7.5m x 7.5m x 3.5m, as shown in Figure 1, and U-values for internal floors with and without suspended ceilings as presented in Figure 2. The test room was naturally ventilated and a night cooling ventilation strategy was used to cool down the thermal mass. No cooling was used in the simulations to be able to quantify the benefits provided by the thermal mass to reduce overheating.

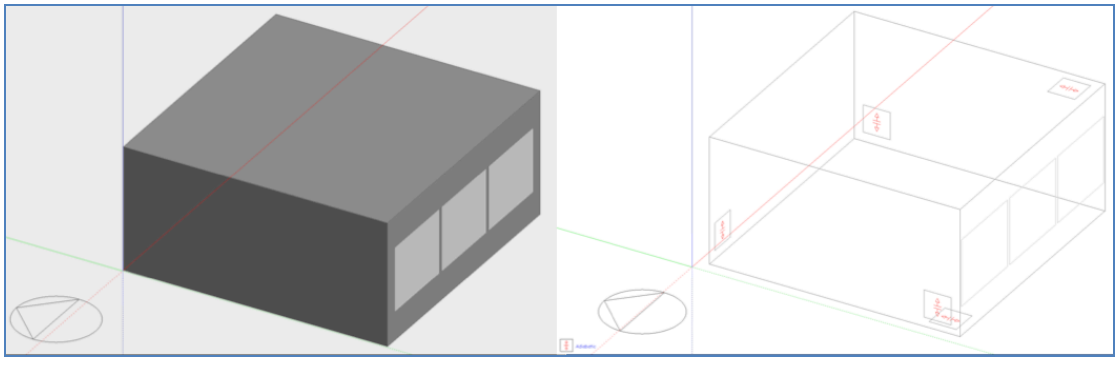

Figure 1: Exemplar room for simulation.

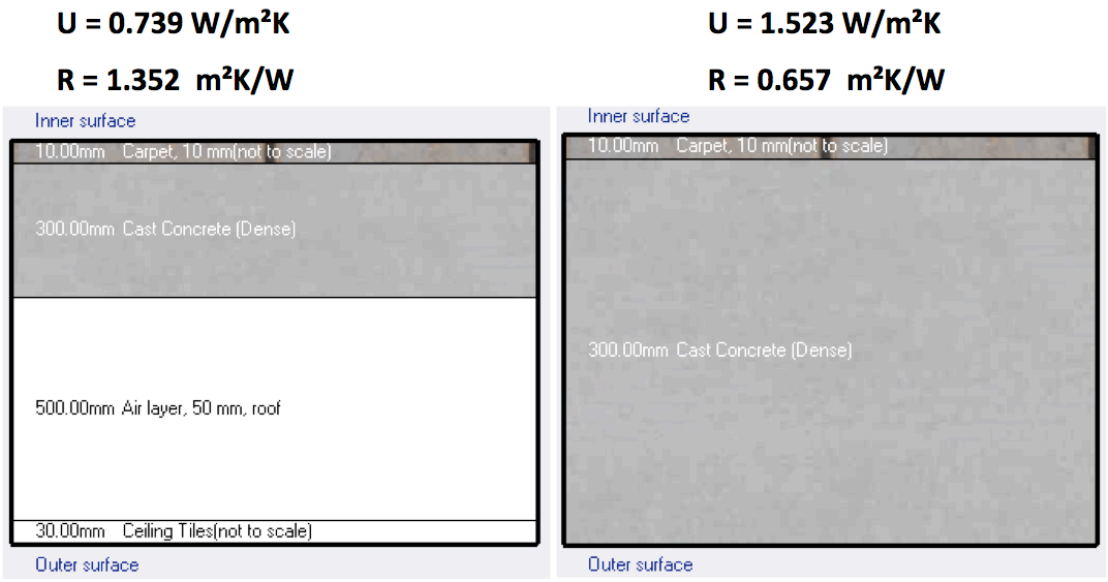

Figure 2: U-values for internal flooring with (left) and without (right) suspended ceiling.

The dynamic computational simulation in DesignBuilder had the following parameters:

- Simulated locations in London (United Kingdom) and Munich (Germany).
- Medium weight construction according to Part L2 2010 (UK).
- All surfaces adiabatic apart from south wall being external.
- 50% glazing in south wall.
- Office equipment load of 10 W/m^2.
- Lighting load of 0 W/m^2.
- People density of 0.111 people/m^2 (well above typical primary teaching spaces according to BB103 Area Guidelines for Mainstream Schools (2014)), following an occupancy schedule from 9:00 to 17:00
- Constant infiltration of 0.5 air changes per hour (acph).
- Natural ventilation rate of 1.5 acph, following a schedule from 8:00 to 19:00
- Night ventilation rate of 6 acph, following a schedule from 24:00 to 6:00
- One year simulation.

Ventilation rates achieved through single side tilted windows following parameters as described in the Building Bulletin 101 Ventilation of School Buildings (2006) for the ClassCool tool.

RESULTS

In terms of assessing the overheating performance (defined in 4.1) with and without the suspended ceiling, four simulations were solved using the dynamic Energyplus engine in DesignBuilder without the use of (simulated) cooling preventing overheating. Two simulations were provided for London location (with and without suspended ceiling) and two simulations for Munich location (with and without suspended ceiling).

Figure 3 shows the temperature distribution results for London with the use of suspended ceiling as an example. Similar results were collected and analysed for the other computational simulations, the final results for overheating hours above 28 ºC are summarised in Figure 4.

Figure 3: Temperature distribution results for London with false ceiling.

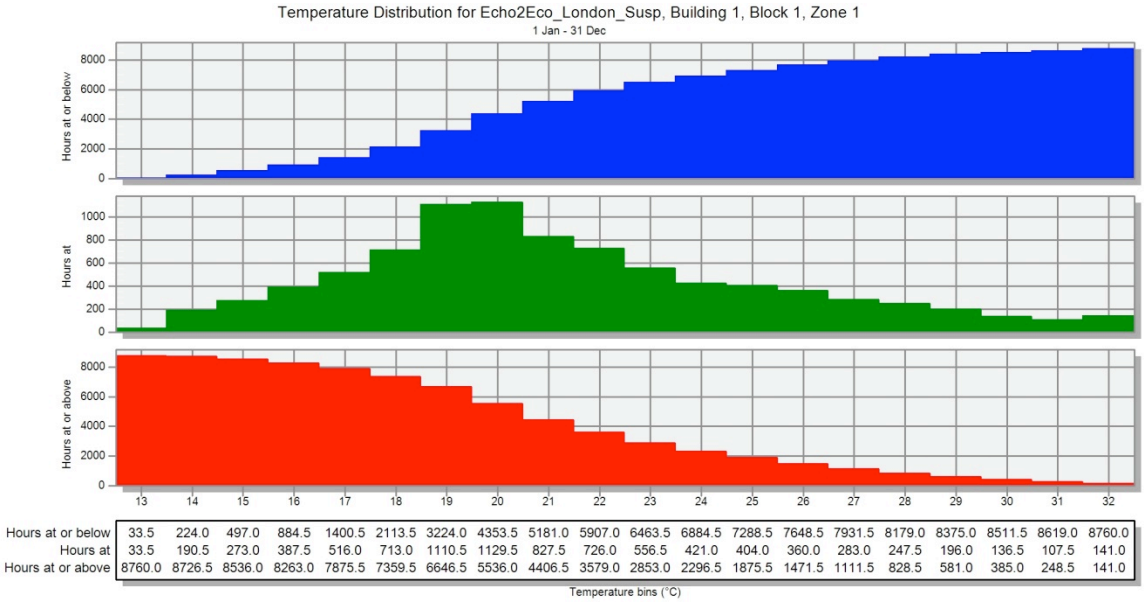

Exposing the thermal mass by elimination of the suspended ceiling reduces the overheating hours above 28^0 C by 33% in Munich and 49% in London compared to the same room featuring a suspended ceiling with accompanying isolation of the thermal mass from ambient temperatures.

The number of overheating hours correlates with the need for cooling in a building and subsequently with the energy use and carbon emissions that cooling would incur. The higher the number of overheating hours, the more energy and carbon emission will be driven by cooling to alleviate the overheating.

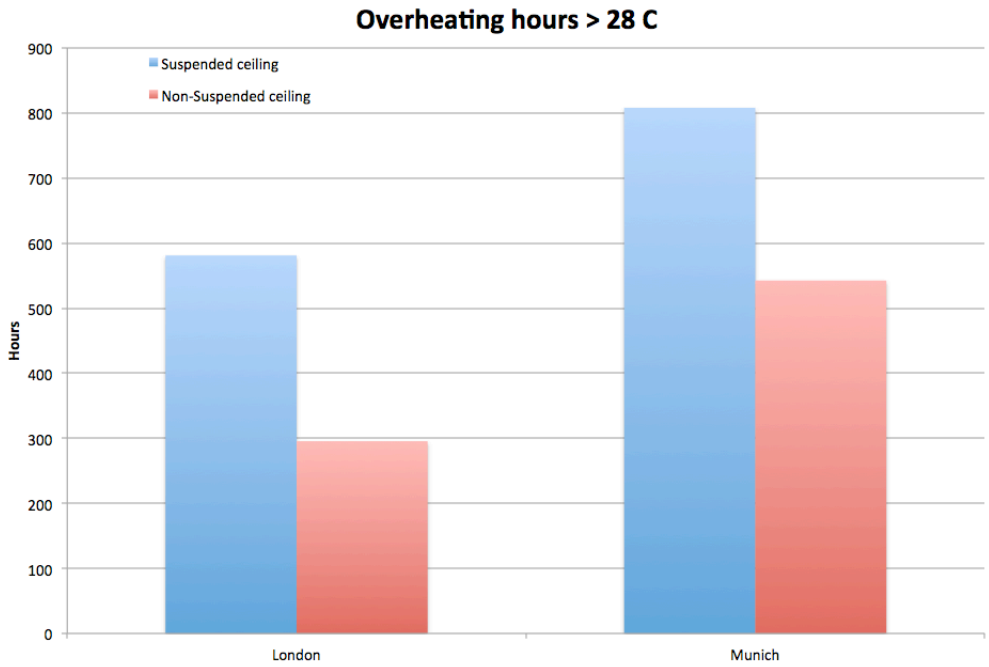

Figure 4: Overheating hours above 28^{0}C for London and Munich, with and without false ceiling.

DISCUSSION

Exposing the thermal mass by elimination of the suspended ceiling reduces the overheating hours above 28^0 C by 33% in Munich and 49% in London compared to the same room featuring a (simulated) suspended ceiling with accompanying (simulated) isolation of the thermal mass from ambient temperatures.

The number of overheating hours correlates with the need for cooling in a building and subsequently with the energy use and carbon emissions that cooling would incur. The higher the number of overheating hours, the more energy and carbon emission will be driven by cooling.

The simulation results show that by exposing and making use of the room thermal mass, the number of hours above 28 ºC can be reduce by at least 33% in Munich and 49% in London. The reduction in overheating hours will consequently minimise the need for cooling energy in summer providing savings in energy and CO2 emissions.

This study agrees with the advise in terms of avoiding overheating from Energy Saving Trust (2005), the Building Research Establishment (BRE) (2005) and Zero Carbon Hub (2012). Furthermore, this study shows that the use of a suspended ceiling can have an unwanted insulating effect on the surface temperature of the overlying thermal mass, impeding energy transfer, and hence reducing the efficacy of the thermal mass's ability to moderate ambient temperatures and consequently lead to overheating.

CONCLUSION

This study shows that the use of a suspended ceiling can have an unwanted insulating effect on the surface temperature of the overlying thermal mass, impeding energy transfer, and hence reducing the efficacy of the thermal mass's ability to moderate ambient temperatures and consequently lead to overheating.

This study shows that the elimination of thermally insulating suspended ceilings could potentially saves energy by exposing the thermal mass of overlying structures, moderating undesirable thermal overheating, and therefore reducing or eliminating the need for artificial cooling.

REFERENCES

1. Building Bulletin 101 – Ventilation of school buildings. Regulations Standards Design Guidance. 2006.
2. Building Bulletin 103 – Area guidelines for mainstream schools. Department for Education. 2014.
3. Building Research Establishment (BRE): Thermal mass and overheating. 2005
4. Energy Saving Trust: CE129 Reducing overheating – a designer's guide. 2005.
5. Marceau, M.L. and VanGeem, M.G.: Modelling Energy Performance of Concrete Buildings for LEED-NC v2.2 Energy and Atmosphere Credit 1. Portland Cement Association R&D Serial No. 2880a, 2007.
6. Zero Carbon Home : Understanding overheating – where to start : An introduction for house builders and designers. NHBC Foundation, 2012.

MODELLING OF LOW TEMPERATURE HEATING NETWORKS WITH IDA-ICE

P. Kräuchi[1], T. Schluck[1], M. Sulzer[1]

1: Lucerne University of Applied Sciences and Arts School of Engineering and Architecture Competence Centre for Integrated Building Technology (HSLU CCZIG), Switzerland

ABSTRACT

This work presents a library for the simulation of low temperature heating and cooling networks for interconnected buildings, heat suppliers and geothermal storage units. Its applications are illustrated by simulating a planned network (case study).

The library was created using the modelling language NMF (Neutral Model Format) and can be used out of the box in the simulation environment IDA-ICE. The library's elements are compatible with IDA-ICE standard elements and therefore integrate easily, such that extensive and project specific models of thermal networks can be generated. The simulation provides information for all aspects of the system. For the hydraulic part of the system, heat and mass flows, water pressure and temperature values within the entire pipeline network are calculated. Information about the soil temperature and the electrical power of the pumps are also provided. Thus, the library allows planning and optimization of thermal networks, especially of low temperature heating networks equipped with geothermal storages.

In the case study the main heat suppliers of the network are photovoltaic-thermal hybrid solar collectors (PV/T), and buildings act as heat consumers and heat suppliers (free cooling), which results in directional changes of the mass and energy flows. We present an approach to such versatile flow systems. Due to the equation system based modelling in combination with the integrated IDA-ICE solver even parallel flows (which are only partially determined by the demand and supply profiles) can be handled.

Additionally, we present selected results of our case study such as the temperature of the geothermal storage and the electrical power consumed by the circulation pumps.

Keywords: simulation, thermal networks, geothermal storage, IDA-ICE, Neutral Model Format (NMF)

INTRODUCTION

Low temperature thermal networks (LTN) are a specific type of thermal networks which are typically fed with waste heat or ambient heat supplied at a low temperature level. Consumers or producers (prosumers) of the LTN either withdraw heat by means of heat pumps (and lift the temperature level to their needs) or supply waste heat (cooling purposes) to the network.

The model components developed at the Lucerne University of Applied Sciences and Arts allow the simulation of two-pipe networks with changing mass flow directions. Typically, the decentralised circulation pumps are located nearby heat users and the geothermal storage serves as a hydraulic balancing of the mass flows between the two pipes.

The results shown in this paper build on the results presented at the BauSIM 2012 [1]. This previous paper described model components for temperature and mass flow as well as an application example. Further developments of the model components were presented at the BauSIM 2014 [2]. The model components were extended to include the variable "pressure" and a modular set-up was realized. This allowed the calculation of the mass flows distribution

in parallel flows, and the gained modularity allowed the modelling of any arbitrary thermal networks. In order to validate the models, the same LTN example presented at the BauSIM 2012 was simulated with the new components.

Auxiliary components were added during later development phases. Functional macros were built up reproducing the typical structures of a LTN. Thermal networks could then be modelled faster and easier. In this work, some of the developed macros were applied to build up a real case LTN with solar heat supply and seasonal heat storage.

METHOD

Development of the models and simulations were performed in the IDA-ICE environment. The components were programmed in the modelling language NMF (Neutral Model Format) [3, 4] which allows to concentrate on the implementation of equation systems and less on programming their solution. The numerical solution was taken over by the commercial solver in IDA-ICE.

SIMULATION

In order to demonstrate the functionality of the main components, the hydraulic network of the study case has been simplified to a combined so called “plant unit” (“GZ”) and a “geothermal storage” (“ES”) (Figure 1, Figure 2). The component „ES“ contains the calculation of the temperature change within the geothermal storage. The model of the geothermal storage is in principle a perfectly mixed tank and thus defined by its volume, an assumed resistance-free heat transfer and resistance-free heat conduction. The ground temperature of the geothermal storage is therefore spatially constant. Heat losses are not considered. The storage capacity is assumed to be ideal in the sense that at any time the full amount of supplied heat is stored. Pressure drops are calculated in a separate component (“pipe”), which is provided in the standard IDA-ICE library. All elements used to model the plant unit are listed in Table 1.

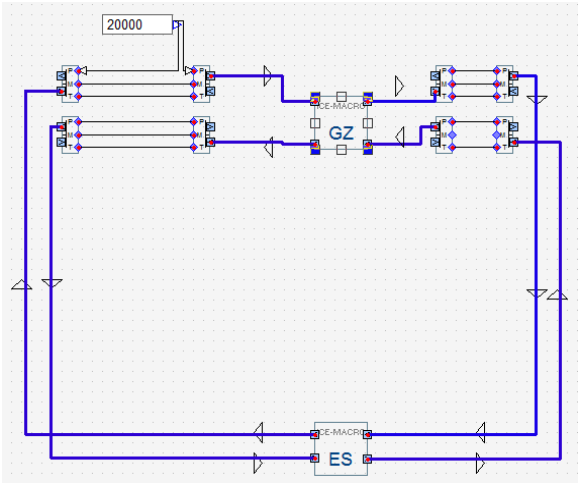

Figure 1: Simplified model of the hydraulic network

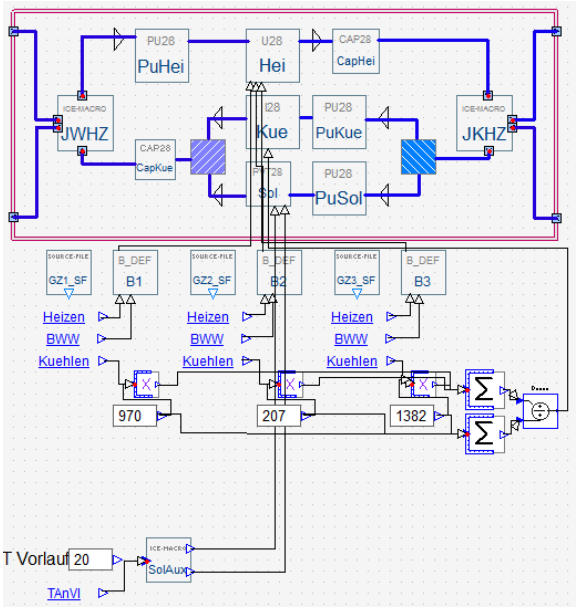

Figure 2: Plant unit (“GZ”)

Element	Description
B1 - B3	Buildings (“B”) require the annual total consumed heat and the normalized profile for space heating and hot water. Therefrom load profiles are calculated and handed over to the component “Hei”.
Hei	Heat demand from the network is modelled by the component „heating unit“. The component aggregates the load profiles of several buildings („B1 – B3“). The resulting total load, in combination with the chosen temperature decrease in the network, is used to determine the massflow in the network. Based on the chosen heating system temperature and the calculated network temperature, the coefficient of performance (COP) of the heat pumps is calculated using the efficiency factor and Carnot-efficiency.
Kue	The component „cooling unit“ calculates, similarly to the component „Hei“, the mass flow in the network. This unit considers free-cooling only, which is typical for LTN. Input data are the annual total heat, a normalized cooling profil, and a constant temperature rise in the network.
Sol	The component „solar supply“ is an adapted version of the component “Kue”. Input data are the heat flux and a normalized profile (instead of the annual heat supply and a normalized profile). Furthermore, the chosen temperature rise is time dependent.
Pu..	The component „pump“ calculates the mechanical and electrical power, using the pressure difference, that results within the network between the inlet and the outlet of the pump. The electrical power is calculated based on the mechanical power and an overall pump efficiency. In case of a pressure decrease from the inlet to the outlet of the pump, the electrical power is assumed to be zero.
Cap..	Thermal inertia by the water mass contained in the network is modelled by the component “Cap”. A perfectly mixed tank is assumed, sized with the inner volume of the duct network.
JWHZ, JKHZ	Junction (T-element with one bi-directional connection and two uni-directional connections).
„Heizen“	Time dependent profile for heating
„BWW“	Time dependent profile for hot water
„Kühlen“	Time dependent profile for free cooling
SolAux	Macro for calculating of the solar supply data (heat flux, temperature rise in the network). These data were calculated using Polysun.
GZ1.. – GZ3..	Linked file with time dependent profiles for heating and cooling
„TAnVl“	Temperature in the network at the entrance of the heat exchanger of solar heat supply
	IDA-ICE library component „WaterMerge“
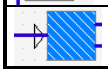	IDA-ICE library component „WaterSplit“

Table 1: Elements of the plant unit

Considered pressure losses in the network were limited to the pressure losses of the geothermal storage. These losses were implemented using the IDA-ICE library component „pipe“. Thermal inertia in the network ducts was considered within the plant unit (components “Cap..” within macro “GZ”).

The configuration of the simulation model is shown in Table 2.

Element	Parameter	Value
Buildings	Annual heat for space heating (B1, B2, B3)	2340, 831, 3179 MWh
	Heating system temperature for space heating	32 °Celsius
	Heating system temperature for hot water	55 °Celsius
	Annual heat for warm water (B1, B2, B3)	793, 260, 1018 MWh
Plant unit	Temperature decrease in network at heating unit	4 °Celsius
	Temperature increase in network at cooling unit	4 °Celsius
	Total efficiency of circulation pumps	0.6
	Efficiency factor of heat pump (COP/COP_{Carnot})	0.5
Geothermal storage	Volume of ground	3'400'000 m^3
	Density of ground	2000 kg/m^3
	Specific heat capacity	1500 J/(kg K)
	Number of probes	746
	Depth of probes	186 m
	Inner diameter of probes	0.032 m
	Roughness	0.045 * 10^{-3} m

Table 2: Configuration of the simulation model

RESULTS

The period of simulation was set to 2 years. Figure 3 shows the temporal development of heat output which is obtained (red) respectively fed into the temperature network by the buildings (blue) and the PV/T plants (yellow). The input time series for heating and cooling loads are normalized and base on measured load profiles [5], such that they can be scaled according to the annual total heating demand. The graphs in grey correspond to the heat flux to the building and the one in blue to freecooling.

The final energy supplied to the buildings (grey) is slightly higher compared to the heat obtained from the LTN (red). This difference corresponds to the electrical power obtained by the heating pumps and thus the red graph depends on the temperature of the network, which in turn defines the COP of the heating pumps.

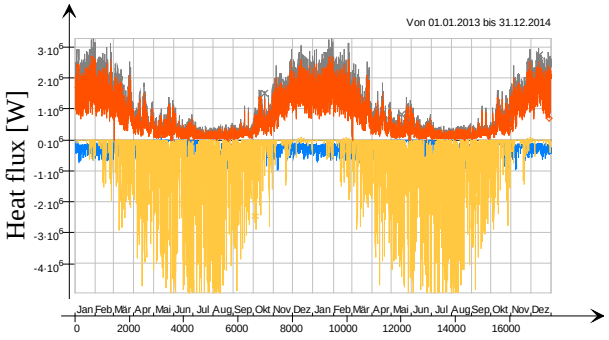

Figure 3: Heat fluxes of the plant unit; supply to the buildings (grey), heat extracted from the network (red), free cooling (blue), solar yields (yellow)

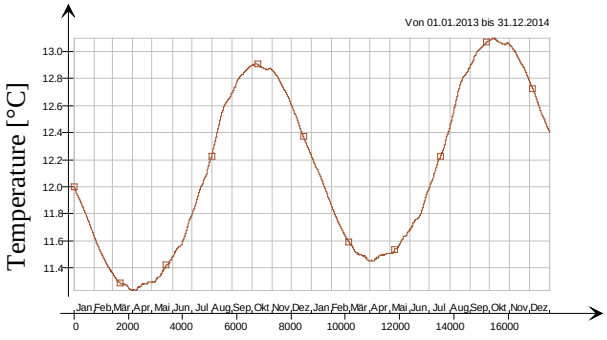

Figure 4: Temperature of the geothermal storage

During the two years the following heat quantities result:

- Heat delivered and consumed by the buildings: 16.86 GWh
- Heat obtained from the network for space heating and hot water: 13.99 GWh
- Heat feed into the network by freecooling: 5.03 GWh
- Heat feed into the network by PV/T plants: 10.12 GWh

This gives a surplus of heat fed into the network of 1.16 GWh. As a result the temperature in the geothermal storage is slightly higher (ΔT 0.4 K) than at the beginning of the simulation (Figure 4). The massflow of the geothermal storage shown in Figure 5 is driven by three decentralised circulation pumps, located at each prosumer. Their pumping power is shown in Figure 6 and clearly illustrates that the pumps alternate over time in sharing their main loads to drive the massflow through the geothermal storage.

To provide the heat of 16.86 GWh the electrical energy of 2.87 GWh were consumed by the heating pumps which equals to an annual coefficient of performance of 5.87. Another 0.013 GWh of electrical energy must be added for the circulation pumps. However, the model only takes into account the pressure drop of the geothermal storage but not the whole thermal network.

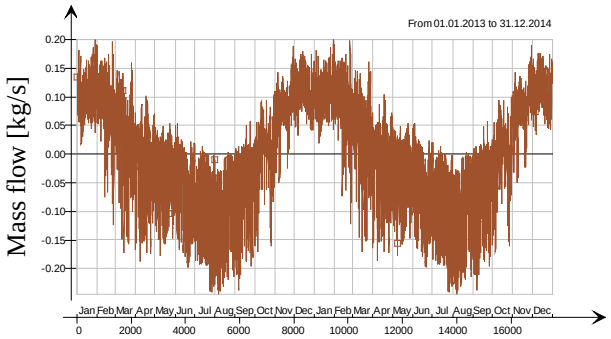

Figure 5: Mass flow in a probe of the geothermal storage

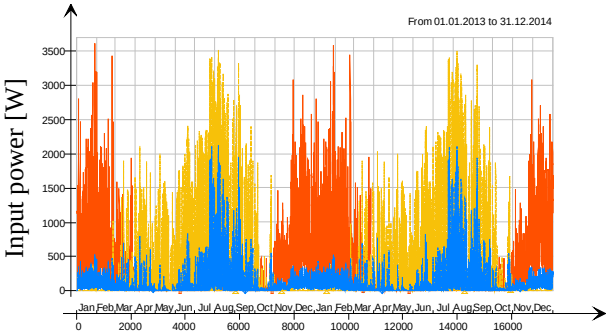

Figure 6: Electrical power consumed by the circulation pumps:
heating unit (red), cooling unit (blue), solar thermal supply (yellow)

DISCUSSION

The developed models allow the assessment of some design and planning issues. For instance the solar yield and the electrical consumption of the heating pumps can be realistically estimated based on the calculated temperature of the hydraulic network. Technical details in construction of hydraulic networks cannot be addressed with the models. However, the possibility is given to incorporate further components or to replace models as long as they have the same interfaces. In particular a 3-dimensional mesh model of the geothermal model is available from the distributer of the simulation platform.

The simulation results of the study case were checked using the energy balance on the heat flux of the geothermal storage. The integral of heat fluxes over the geothermal storage (Q_{ES}) equals the total heat produced and consumed by the plant unit (Q_{GZ}). A further check was investigating the temperature of geothermal storage. The stored heat was calculated using the heat capacity, the volume, the density of the ground, and the temperature change and found

equal to Q_{ES}. Finally, the results of the simulation were found in good correspondence to results derived during the planning phase.

The electrical energy for the circulation pumps were of almost no significance compared to the electric energy consumed by the heating pumps (ratio about 0.5%). However, only the flow resistance of the geothermal storage was considered while all other flow resistances in the network were neglected.

CONCLUSION

A series of component models were developed which integrate with existing IDA-ICE libraries and allows the simulation of arbitrary thermal networks. All necessary and important system variables of a thermal network are calculated (mass flow, pressure, temperature, electrical power).

The components can be grouped in larger functional units (macros), as for instance, the here presented “plant unit”. These macros can be easily used to multiply the same functionality, or be used in new and different models. For instance, in [6] these components are used to simulate a bi-directional thermal network using several simplified plant units.

The study case clearly shows that these self-built model components are suitable for the conceptual design and the optimizing of thermal network in the planning phase. An even higher accuracy and a more detailed planning of the probe field (geothermal storage) should be expected using the 3-dimensional model of the geothermal storage (EQUA Simulation AB).

REFERENCES

1. Kräuchi, P., Kolb, M.: Simulation thermischer Arealvernetzung mit IDA-ICE. BauSIM, Berlin, 2012.
2. Kräuchi, P., Kolb, T. Gautschi, U.-P. Menti, M. Sulzer: Modellbildung für thermische Arealvernetzung mit IDA-ICE. BauSIM, Aachen, 2014.
3. Sahlin, P., Bring, A.: The Neutral Model Format for building simulation. Version 3.02. Royal Institute of Technology, Stockholm, 1996.
4. Sahlin, P.: NMF Handbook. An Introduction to the Neutral Model Format. NMF version 3.02. Royal Institute of Technology, Stockholm, 1996.
5. Vetterli, N., Sulzer, M.: Dynamic analyis of the low-temperature district network «Suurstoffi» through monitoring. CISBAT, Lausanne, 2015.
6. Schluck, T., Kräuchi, P., Sulzer, M.: Non-linear thermal networks – How can a meshed network improve operational flexibility and energy efficiency? CISBAT, Lausanne, 2015.

OPTIMIZATION OF THE HEATING DEMAND OF THE EPFL CAMPUS WITH AN MILP APPROACH

J. Rager[1], S. Coccolo[2], J. Kämpf[2], S. Henchoz[1]; F. Maréchal[1]

[1]*IPESE EPFL Station 9, CH-1015 Lausanne, Switzerland*
[2]*LESO-PB EPFL, Station 18, CH-1015 Lausanne, Switzerland*

ABSTRACT

This works optimizes a heating system including demand side management within two of EPFL's buildings. It combines building simulation with linear optimization providing results at low computational efforts. Overall economies of up 20 % are possible, when the buildings are used as a thermal energy storage within the comfort temperature range of the building in combination with different changes in the energy conversion system.

Keywords: simulation, optimization, demand side management, pinch analysis

INTRODUCTION

The model of the EPFL campus is realized with the software CitySim, calculating the heating and cooling demand of the campus and the electricity produced by the BiPV on the rooftop of buildings. The model was validated with on-site monitoring, showing a good correlation factor between the measurements and the model[1].

In the area of building physics, accessing the thermal mass or capacity impacting the heating or cooling load is a widely discussed field. From here on, only the use of the building mass as a thermal energy storage is considered for the purpose of DSM. Experimental [2] and analytic [3] studies demonstrate that most estimations of the buildings thermal capacity are wrong due to the fact that heat convection is neglected or not correctly calculated.

[4] uses a detailed approach for the modeling of the different heating distribution systems. Then they evaluate different options concluding that DSM shows strong peak shaving potential of up 94% for the heat pump's electricity consumption. [5] proposes a management system enabling the use of DSM. Through the use of HVAC utilities the peak shaving and load shifting in the electric grid is demonstrated. However, both do not show, whether their thermal capacity calculation overcomes the shortcomings [3] showed.

METHOD

For the purpose of using a building as an energy storage, first the thermal mass is calculated with a simplified model based on [3] findings. This result is implemented in an existing mixed integer linear programming (MILP) model minimizing cumulative exergy demand over the life cycle of the equipment used while fulfilling the heating requirements. Combining simulation and optimization allows to quickly find the interest of using a building as an energy storage compared to an only simulation approach requiring frequent runs optimization.

Effective thermal capacity of a given wall

Depending on the length of the storage period, different thermal masses should be considered. The model is based on the hypothesis of one-dimensional heat conduction without internal heat generation and a constant thermal conductivity. In our case, the internal air temperature acts as an excitation source following a sinusoidal function and has a period of 24 hours as in [3]. No heat energy is created in the wall, nor do mass transfers happen. Equation 1 applies an energy balance to a given wall section i with a cross section A. The change of internal energy U over time t equals the difference of the incoming heat load $\dot{Q}_{in}$ and the outgoing heat load $\dot{Q}_{out}$ as the mass M and the specific heat capacity c_p as well as the thermal conductivity λ remain constant. This implies that the temperature change ∂T over time ∂t is proportional to the temperature change over the distance ∂x.

$$\frac{dU}{dt} = \dot{Q}_{in} - \dot{Q}_{out} \implies Mc_p \cdot \frac{\partial T}{\partial t} = A\lambda \frac{\partial T}{\partial x} \tag{1}$$

$$\frac{\partial T}{\partial t} - \frac{A\lambda}{Mc_p}\frac{\partial T}{\partial x} = 0 \text{ with:} \frac{\partial T}{\partial t} = \frac{T_i^t - T_i^{t-1}}{\Delta t} \text{ and } \frac{\partial T}{\partial x} = \frac{T_i^t - T_{i-1}^t}{2\Delta x} + \frac{T_i^t - T_{i+1}^t}{2\Delta x} \tag{2}$$

Equation 2 shows the discrete time derivative of $\frac{\partial T}{\partial t}$ using a first order implicit scheme and the spatial derivative of $\frac{\partial T}{\partial x}$ with a centered finite difference scheme of second order along the direction of x. Δt represents the discrete time t and Δx the discrete width of a slab. Mc_p depends on the mass M and the specific heat coefficient c_p of the considered wall section. Equation 2 can be transformed to Equation 3 that calculates the temperature T of the i-th wall section in the time $t-1$ as function of the surrounding wall sections' temperatures ($i+1$ and $i-1$) and the temperature of the wall section i in the next time step t. λ represents the heat conductivity of the material in wall section i.

$$T_i^{t-1} = T_i^t - \frac{A_i\lambda_i}{M_i c_{p_i}} \frac{\Delta t}{\Delta x} \left(T_{i-1}^t - 2 \cdot T_i^t + T_{i+1}^t\right) \tag{3}$$

For the boundary conditions, the first element of the wall in contact with the air in the room is calculated as follows:

$$U_1 = \frac{1}{\frac{1}{h_{int}} + \frac{x}{2\lambda_1}} \text{ in } \frac{T_1^n - T_1^{t-1}}{\Delta t} = \frac{U_1 A_1}{M_1 c_{p_1}} \frac{(T_{int}^t - T_1^t)}{\Delta x} - \frac{(T_1^t - T_2^t)}{\Delta x} \frac{A_1\lambda_1}{M_1 c_{p_1}} \tag{4}$$

$$T_i^{t-1} = T_i^n - \underbrace{\frac{\Delta t}{\Delta x} \frac{1}{M_i c_{p_i}} \left[U_i A_i (T_{int}^t - T_i^t) - A_i\lambda_i (T_i^t - T_{i+1}^t)\right]}_{\text{excitation vector } \vec{c}} . \tag{5}$$

The indoor convection h_{int} is fixed at $10\frac{W}{kg\ K}$. Replacing the indoor temperature T_{int} and the convection h_{int} with the external ones allows to calculate the wall section temperature on the external side. In order to obtain the thermal capacity of the wall a sinusoidal temperature variation is applied:

$$T_{int}(t) = 21.5 + 1.5 \cdot sin(2\pi \cdot \frac{t}{24h}) . \tag{6}$$

The indoor temperature varies within a defined comfort band of 3° Celsius over the duration of a day based on [6, section 3.1]. All wall section temperatures over the whole 24 hours can be calculated at once using this implicit linear Equation:

$$B\vec{x}_{(t)} + \vec{c} = \vec{x}_{(t-1)} \leftrightarrow \vec{x}_{(t)} = B^{-1}B\vec{x}_{(t)} = B^{-1}\vec{x}_{(t-1)} - B^{-1}\vec{c} . \tag{7}$$

Table 1 – Effective thermal capacity of studying buildings: Polydome, the lightest building on campus based on a wood structure and AAB, the massive building with a concrete structure.

Building	Total Thermal Capacity $[\frac{MJ}{K}]$	Effective Thermal Capacity $[\frac{MJ}{K}]$	Capacity Percentage $[\%]$	Effective Depth $[m]$	Material [-]	Total Building Surface $[m^2]$	Total U-Value $[\frac{W}{m^2.K}]$
Polydome	1583	490	25.6	0.12	Wood	3249	0.22
AAB	2450	627	31.0	0.09	Concrete	2564	0.38

With Equation 7 based on the temperature vector of the previous time step $\vec{x}_{(t-1)}$, the temperature of each wall section at the current time step $\vec{x}_{(t)}$ is expressed with the excitation vector $\vec{c}$ and the coefficient matrix B. This approach is unconditionally stable and thanks to the matrix with constant coefficients only a single matrix inversion is needed leading to computationally inexpensive estimation of the wall's behavior. Over the discharging cycle, when the internal temperature T_{int} is falling, the effective wall thickness x_{eff} used for heat storage can be estimated as a function of the first wall slab $i = 1$ in contact with the internal air:

$$x_{eff} = \frac{\sum_{T_{max}}^{T_{min}} \dot{Q}_1 \ \Delta t}{A_1 \ \rho_1 \ c_{p_1} \ (T_{int}^{t=T_{max}} - T_{int}^{t=T_{min}})} \ . \tag{8}$$

For concrete, this approach yield 10.5 cm, which is the same value as reported by [3] with 10.5 cm. The total effective heat capacity for a building is calculated using the total surface A_{tot} in contact with the heated air within the building:

$$C_{eff} = x_{eff} \ A_{tot} \ \rho_1 \ c_{p_1} \ . \tag{9}$$

Two buildings were analyzed, as they represent a light mass building (Polydome), and a massive one (AAB). Their physical envelope's characteristics are summarized in Table 1. The values of the effective depth are a function of the first internal layer. The heat loss coefficient represents the total weighted average U-value of the building. With the lumped method, the capacity of the AAB Building would have been estimated to 50 % of the building mass in contact with the internal air. In this case, this would have been twice as big as the calculated value.

Linear Optimization Model

The objective function of the MILP model minimizes the overall cumulative exergy demand, the same formulation can be used to minimize the overall costs. The model uses pinch analysis to size the equipment. For this work, two equipment types are available: a gas boiler and a solar thermal collector. The solar thermal collector has the choice to deliver heat at different discrete temperature levels according to the available irradiation calculated by CitySim. Higher temperatures yield lower panel efficiencies. The boiler delivers heat at constant high temperature.

The DSM model can be activated by two mechanisms: either different tariffs for resources are introduced, e.g. day and night tariffs or a stochastic free resource is available during the certain hours of the day. For this case, the second option is chosen: the solar thermal

panels operate for free during the hours where enough irradiation is available. They can be combined with a seasonal storage.

Compared to a typical approach, in this work, the energy demand is introduced as a variable to show the potential of energy storage in a building's wall. More heat is used at a certain moment than the normal heating requirement to store it in the building's wall.

All **variables** within the MILP are printed in **bold**. Equation 10 guarantees the thermal comfort of the building: the room temperature $\mathbf{\Delta T_b} + T_{min}$ should not be higher than the maximal room temperature T_{max} defined as being within the thermal comfort range by the occupants neither lower than the minimum temperature T_{min}. The temperature bandwidth $\mathbf{\Delta T_b}$ can be set for each time step, according to occupation patterns, day and night shifts or seasonal preferences for each building.

$$T_{min} \leq \Delta\ \mathbf{T_b} + T_{ref} \leq T_{max} \tag{10}$$

$$\mathbf{\Delta Q_b} = \mathbf{\Delta T_b}\ C_{eff} \tag{11}$$

The heat energy stored in the building's structure ΔQ_b is a daily energy balance and is calculated via this temperature difference ΔT and the effective heat capacity of the building C_{eff} with Equation 11. The multiplication of the overall heat transfer coefficient U_{tot}, the building's surface A_{tot} and the temperature difference estimate the additional heat losses due to the temperature raise in Equation 12.

$$\mathbf{\Delta Q_b} = \mathbf{\Delta Q_{b,0}} + \sum_{t=1}^{t=nt} d_t \cdot \left(\mathbf{\dot{Q}_{heating}(t)} - U_{tot}\ A_{tot}\ \mathbf{\Delta T_b}\right) \tag{12}$$

$$\mathbf{\dot{Q}_{heating}(t)} = (\mathbf{f(t)} - 1) \cdot \dot{Q}_t \tag{13}$$

They are linked to the reference heat load $\dot{Q}_{heating}(t)$ via the multiplication factor $\mathbf{f(t)}$ in Equation 13: during charging, $\mathbf{f(t)}$ is bigger than 1, during discharging it will be smaller than 1. A value of 1 for $\mathbf{f(t)}$ delivers only the current heating demand. Pinch analysis links the energy conversion technologies with the varying heat demand. When heat should be stored in the building, the heat distribution temperature level T_l is lifted from the standard heating level 0 to a higher level 1 or 2: a combination out of all three streams can be used and is only limited by the user defined maximum value of the multiplication factor f_t. Equation 14 ensures that the building is always heated with the lowest temperature level 0 plus the current building temperature.

$$\forall t \text{ and temperature levels } l \in 0,1,2: \quad \sum_{l=1}^{nl} \mathbf{f_l(t)} \cdot T_l(t) \geq \sum_{l=1}^{nl} \mathbf{f_l(t)} \cdot T_{min}(t) + \mathbf{\Delta T_b(t)} \tag{14}$$

If only the heating requirement needs to be fulfilled, the current level is sufficient. When the building should be heated to a higher internal temperature, also a higher heating level needs to be used. A higher heating requirement leads to a higher demand of utilities that a certain (CExD) price. Therefore the heating requirement will only be increased, if the overall costs can be increased.

In order to run the optimization, the hourly input data, the heat load calculated by CitySim, are clustered/reduced to 10 representative days with 13 time steps per day. The reduction of input date makes running optimization model possible while respecting the power and energy balance.

RESULTS

Table 2 summarizes the different scenarios: using the building's heat capacity plays an important role in reducing the overall cumulative exergy consumption and shaving off the heating peak power for all scenarios. When the DSM is activate (Figure 1), the heat load is shifted delaying the start of the heating system and slightly reducing the maximum required power by preheating: the boiler charges the building during the extreme days while solar panels use it during the rest of the year. During typical summer days, from hour 50 to 90, almost no heat demand is present therefore this storage is not activated. With the same system configuration, but using the building's heat capacity, the objective

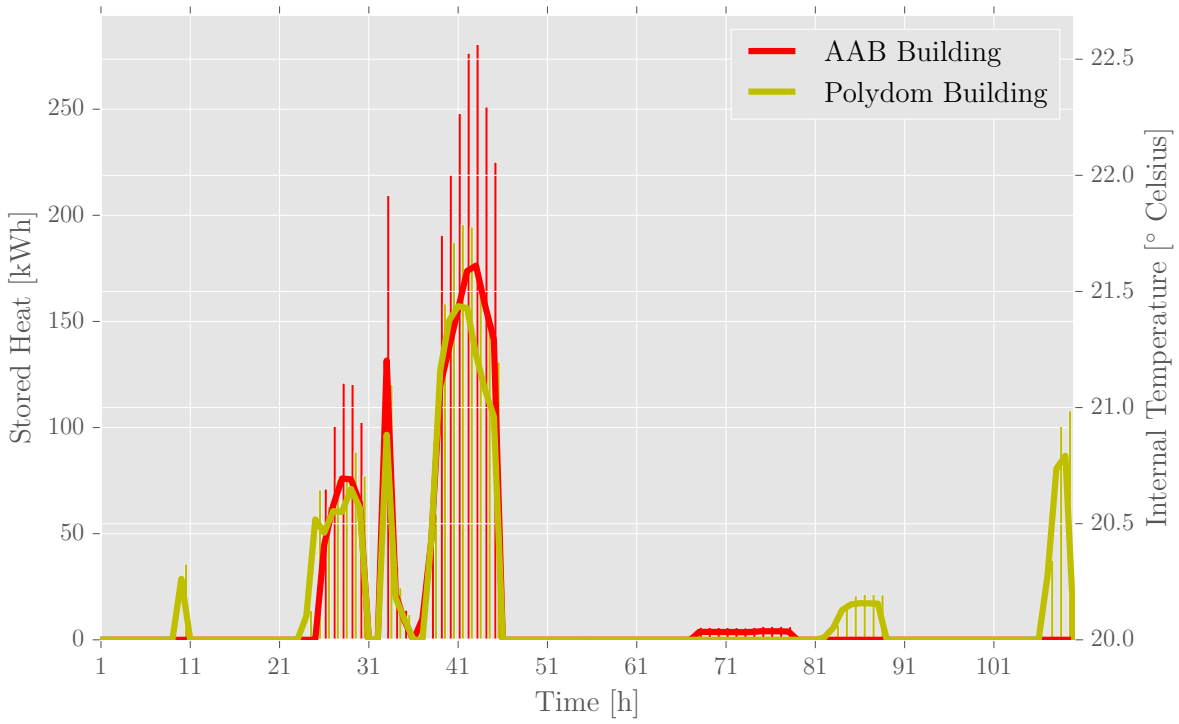

Figure 1 – Internal temperature changes over time in the colored lines and the used stored heat in the bar plots with the

value improves by at least 6 % up to over 20 %. Introducing a seasonal thermal energy storage of 100 m^3 can be of more advantage, when the building's heat capacity is used as well: during the summer, when no heating is required and a high number of solar thermal panels are installed, it can be charged and then discharged during the autumn days into the winter days in combination with the DSM.

DISCUSSION

This simplified two-step approach allows to quickly estimate the effective thermal capacity of a building and its impact on the overall energy system. Instead of searching for optimum temperature while running different simulations, the optimization model uses the effective heat capacity and indicates the temperature range within a single run. This linear optimization model will not give the same result as detailed building model due to the simplification of the building physics. However, it shows whether there is an interest of using a DSM or not and can consider the energy system of interest for further

Table 2 – Results of all scenarios: The storage is always at indicated size, optimal solar panel size indicates the model's choice

#	Scenario Description	Building Heat Storage	Improvement to 1 [%]	Boiler Size [kW]	Solar Panels [m^2]	Long term Storage [m^3]
1	Reference Case	No	-	127.8	201	0
2	Solar as in 1	Yes	6.28%	123.3	201	0
3	Optimal Solar Panel Size	Yes	16.90%	123.3	831	0
4	Solar as in 1	No	4.52%	127.8	201	100
5	Solar as in 1	Yes	8.58%	123.3	201	100
6	Optimal Solar Panel Size	No	6.64%	127.8	449	100
7	Optimal Solar Panel Size	Yes	22.01%	123.3	1098	100

investigation at low computational effort.

CONCLUSION

The proposed method for calculating the effective heat capacity shows coherent results with very few additional efforts compared to the lumped method. Using the building structure as an additional heat storage within a comfort temperature bandwidth shifts peak loads, reducing slightly the equipment size under the condition that the extreme conditions with the highest peak loads are known. The overall economies realizable depend strongly on the system configuration. A final decision of which equipment to deploy at which size requires a detailed study of the energy conversion system already available on site. For EPFL, a study including the already existing heat pump using lake water, two co-generation units with thermal heat storages and PV installation, is planned.

The authors thank the CCEM IDEAS4cities for its financial support and Ben Pfeiffer for his help on the optimization model.

References

1. Coccolo, S., Kämpf, J., and Scartezzini, J.-L.: The EPFL campus in Lausanne: new energy strategies for 2050. Turino, Italy, 2015.
2. Childs, K., Courville, G., and Bales, E. Thermal mass assessment: an explanation of the mechanisms by which building mass influences heating and cooling energy requirements. Technical report, Oak Ridge National Lab., TN (USA), 1983.
3. Ma, P. and Wang, L.-S.: Effective heat capacity of interior planar thermal mass (iPTM) subject to periodic heating and cooling. *Energy and Buildings*, 47:44–52, Apr. 2012.
4. Reynders, G., Nuytten, T., and Saelens, D.: Potential of structural thermal mass for demand-side management in dwellings. *Building and Environment*, 64:187–199, June 2013.
5. Xue, X., Wang, S., Sun, Y., and Xiao, F.: An interactive building power demand management strategy for facilitating smart grid optimization. *Applied Energy*, 116:297–310, 2014.
6. SIA. Standard-Nutzungsbedingungen für die Energie- und Gebäudetechnik 2024, 2006.

Urban Simulation

HUES: A HOLISTIC URBAN ENERGY SIMULATION PLATFORM FOR EFFECTIVE MODEL INTEGRATION

L.A. Bollinger[1,2]; R. Evins[1,2]

[1] *Urban Energy Systems Laboratory, Empa, Überlandstrasse 129, 8600 Dübendorf, Switzerland*
[2] *Chair of Building Physics, ETH Zürich, Stefano-Franscini-Platz 5, 8093 Zürich, Switzerland*

ABSTRACT

Effective design and operation of district multi-energy systems is a complex task necessitating novel modeling and simulation approaches. In this paper, we introduce and describe the *Holistic Urban Energy Simulation (HUES)* platform, an extendable simulation environment for the study of urban multi-energy systems. The platform consists of a growing array of modules and datasets which may be linked in different ways to address different problems in the domain of urban energy systems. Via its combined role as model repository and information management system, the HUES platform facilitates the integration and reuse of constituent modules, opening up possibilities to address the complexity of urban energy systems.

We demonstrate the use of the HUES platform via a case study exploring the relationship between district size and the sizing of the necessary infrastructure, considering realistic variability in heat demand between buildings. We hypothesize that larger districts may more effectively leverage the temporal variation of demand between buildings, reducing infrastructure investment needs. This relationship is explored by linking three modules of the HUES platform – a stochastic demand module, a building energy module and an energy system module – each originally developed for different purposes and adapted for this investigation. The results of the case study indicate that the limited coincidence of demand peaks between buildings means that larger districts require less generation capacity.

The combination of computational modules employed in this case study allows us to extract insights unattainable with any of the modules in isolation – precisely the capability we seek to enable with the HUES platform. Key challenges in the further development of the HUES platform include facilitating model validity, ensuring the development of truly reusable modules and dealing with intellectual property issues.

Keywords: Urban energy systems, Energy hub, Complexity, Modeling platform, Demand variability

INTRODUCTION

The realization of sustainable urban systems requires optimal use of distributed and renewable sources of energy. By serving as loci for the production, storage and consumption of energy in multiple forms, district-scale multi-energy systems (energy hubs) can play an important role in this. Recent work has solidified a set of methodologies for optimizing the design and operation of these systems, considering renewables availability, building energy demands, properties of energy storage and other system characteristics [1, 2, 3].

A significant challenge in this body of work is *complexity*, manifest in the variety and

diversity of system elements and their interactions with the environment. District multi-energy systems may contain a variety of technical components – multiple generation and storage technologies and multiple sources of demand – with numerous interdependences. Furthermore, these systems are inextricably linked with their (dynamic) environment – fluctuating meteorological conditions, changing occupant behavior and a developing urban and institutional landscape. This complexity challenges our ability to sufficiently represent district multi-energy systems for the purpose of optimizing their design and operation. Novel modeling and simulation approaches are essential.

This paper describes the *Holistic Urban Energy Simulation (HUES)* platform [4], an extensible simulation environment for the study of district multi-energy systems. The HUES platform consists of a growing array of computational modules representing different aspects of district multi-energy systems and related domains. In the remainder of this paper, we introduce the core concepts and composition of the platform, and describe a case study employing the platform.

COMPOSITION OF THE HUES PLATFORM

The HUES platform facilitates the linkage of models representing different aspects of energy hub design and control. In designing the HUES platform, we adopt a *multi-model ecologies* approach [5], which entails the cultivation of an evolving set of resources that – with some additional effort – can be recombined and reconfigured for different purposes. Possibilities for model integration are not predefined, but emerge over time from ongoing development efforts.

Our implementation of the multi-model ecologies approach is characterized by the software architecture illustrated in Figure 1. The architecture of the HUES platform is composed of three layers. The first layer consists of the computational elements (models and datasets) that constitute the modules of the HUES platform. These modules are distributed across the computers of different developers working on different projects, and are written in a variety of different computer languages. Each module is developed for a specific purpose, but is designed and packaged such that it may be adapted for other purposes.

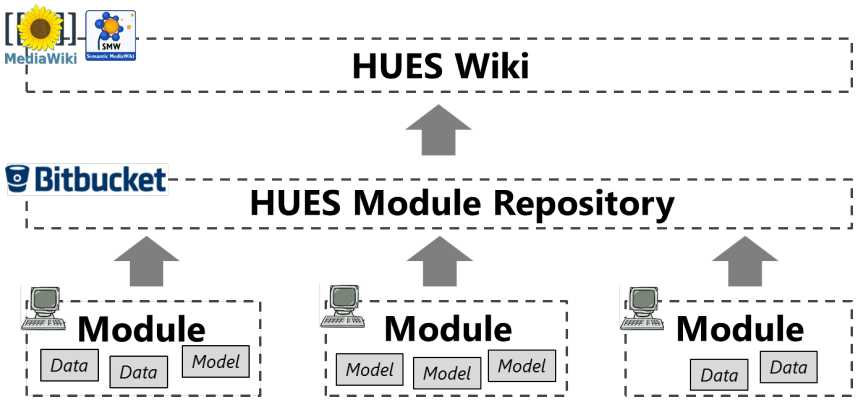

Figure 1: The architecture of the HUES platform consists of three layers.

The second layer is a *module repository*, a cloud-based repository of computational modules. The purpose of this layer is to enable the sharing of modules across diverse platform users. Synchronization of code between the module repository and the files on the computers of individual developers is managed using a Git-based version control system.

The third layer is the HUES wiki[1], a semantic-enabled wiki that acts as an information sharing system for modules in the platform. Each module in the platform is represented by a single wiki page containing key information about the module[2]. Each of the files constituting a module is represented by a separate wiki entry with additional information about that file, allowing platform users to drill down into the precise composition of each module. The wiki also includes *collections*, describing groups of modules that may be used in combination with one another, which enables platform users to understand how modules may be productively combined for different purposes.

The HUES platform has grown around three main types of modules, currently the core elements of the platform. These include: (1) *building energy models* using dynamic thermal simulation to determine the energy demands of individual buildings, (2) *energy system models* which optimize the operation of a district-level system that meets demands by managing supplies through energy conversion and storage, and (3) an *optimization suite* consisting of a range of optimization algorithms that can be applied to any variable or objective present in the platform. In addition, the platform contains many smaller modules that perform specific functions, including stochastic demand models, a longwave radiation model, solar gains calculations, an electricity network model and others.

DEMONSTRATION OF THE PLATFORM

Energy demand may vary significantly between buildings in terms of the magnitude and timing of loads. In the residential sector, this variation is driven by the differing schedules, appliance portfolios, preferences and habits of individuals, as well as the differing physical characteristics of buildings and other factors [6, 7, 8]. When the energy demand of multiple buildings is combined in the context of a district multi-energy system, the energy use patterns of different buildings are aggregated, affecting the sizing and cost of necessary infrastructure. The precise relationship, however, is unclear. Via the set of models described here, we seek to address the following question: *How does the size of a district energy system – in terms of the number of buildings included – influence the optimal sizing of the infrastructure?* To address this question, we link three modules of the HUES platform: (1) a stochastic demand module, (2) a building energy module and (3) an energy system module.

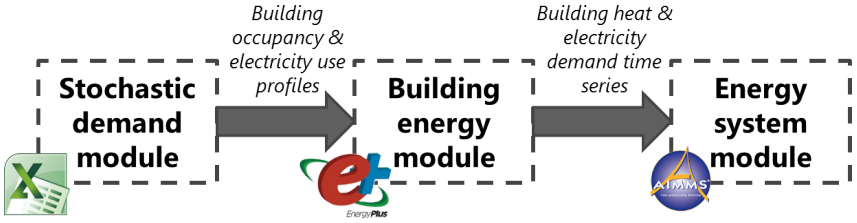

Figure 2: The demonstration model consists of three loosely connected modules.

As illustrated in Figure 2, these three modules are applied in sequence to address the research question above. Each of these modules is represented in the HUES wiki, giving key information about the module and access to the model repository. Likewise, the

[1]The HUES wiki can be accessed at https://hues.empa.ch.

[2]This information includes a description of the module, links to information about the authors of the module, a download link and links to documentation and related publications, the type of license under which the module is released, etc.

combination of modules used in this investigation (and the computer scripts linking the modules) are jointly represented in the wiki as a collection. This information sharing structure is intended to facilitate the future reuse and repurposing of these modules. The computational implementation of the three modules is described below.

Stochastic demand module

This module is based on a model developed by [7][3] that draws from an extensive UK time use survey to stochastically generate residential occupancy and electricity use profiles for households. The model is implemented as a set of Visual Basic scripts run in Microsoft Excel. For a detailed overview of the setup of this model, we refer the reader to [7][4]. A batch run of the stochastic demand module is carried out to generate different occupancy and electricity demand data for 50 identical buildings (with different appliance sets) over a period of one year.

Building energy module

The building energy module takes the results of the stochastic demand module as input, and uses these to generate heat and electricity demand time series for each of building. The physical properties of the buildings are based on those of a hypothetical three-person residence in the Rheinfelden municipality of Switzerland, which is assumed to be connected with a (not yet existing) district heating network. The building energy module uses EnergyPlus. The model is run 50 times to calculate the energy use of a set of 50 hypothetical buildings with identical physical properties. For each run, the model is given a different occupancy and electricity demand profile as input in order to represent the schedule, appliance portfolio, preferences and habits of a different set of occupants. Results for each building are calculated for a period of one year at one minute time resolution.

Energy system module

The energy system module, derived from [9], takes the results of the building energy module as input and calculates an optimal operation schedule for energy hubs of different sizes. It is assumed that each building can be outfitted with solar thermal panels, which (via a district heating network) connect to a centralized heat storage. The aim is to identify a system configuration that minimizes total costs (investment + maintenance + energy) given the goal of cutting carbon emissions to 50% of their baseline level[5].

The energy system module is implemented in the optimization package Aimms as a mixed integer linear program. The outputs of the model include the operation schedule of the energy hub and optimal sizing of the heat storage and solar thermal installations. The calculations account for the investment, maintenance and operational costs of the solar thermal and storage installations, as well as of the grid-connected electric heaters that are assumed to supplement these. A single run of the model represents a timeframe of one week in February at one minute time resolution.

Case study results

Selected results from the energy system module are summarized in Figure 3. As these results illustrate, the maximum heat demand decreases nonlinearly with increasing district

[3]https://dspace.lboro.ac.uk/dspace-jspui/handle/2134/3112

[4]A slightly modified version of the model is used, as described in [8], which enables batch model runs.

[5]The baseline level is defined as the emissions level with no solar thermal or storage installation.

size (left pane) – attributable to the limited coincidence of demand peaks between buildings. On the supply side, the optimal electric heating capacity demonstrates a similar pattern (right pane), as lower peak demand levels translate into lower capacity requirements for heat generation in larger districts. Interestingly, the optimal solar thermal capacity per building exhibits a different pattern (middle-right pane), remaining relatively stable with increasing district size. This may be attributed to the storage, which mitigates the need for higher solar thermal capacity in small districts by covering these demand peaks with stored energy.

While these results are based on a number of assumptions underlying the developed model, they provide an indication of the relationship between district size and infrastructure requirements. Namely, the temporal variation of demand maxima between buildings means that larger districts require less generation capacity to cover these peaks – potentially offering a cost advantage to larger districts. By transferring available energy from times of low demand to high demand, however, energy storage effectively provides the same benefits to smaller districts.

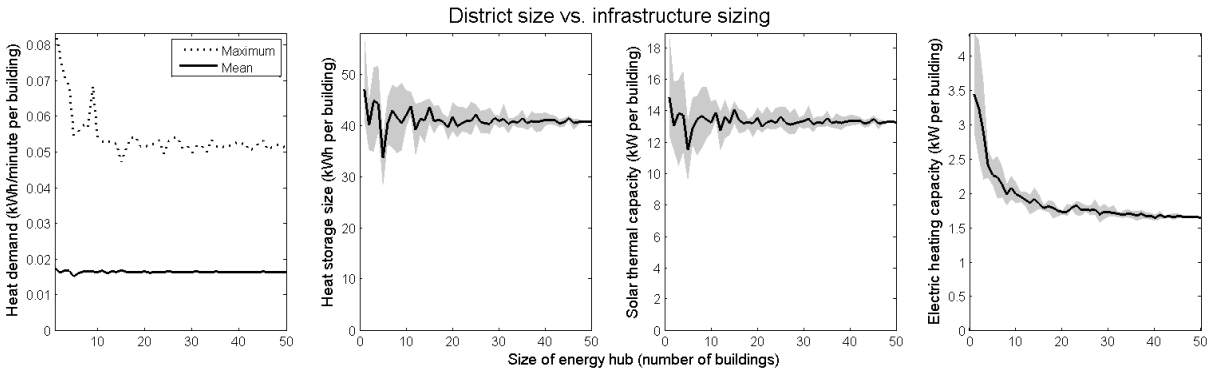

Figure 3: Results of the analysis. Black lines indicate the mean values; shaded areas encompass the range of observed values.

DISCUSSION

Via the combination of modules described in the previous section, we have extracted insights unattainable with any of the modules in isolation. While it would be feasible to construct a single, comprehensive model from scratch to address the same research question, the effort to achieve this would have been considerably larger. By facilitating the sharing, identification and reuse of models, the HUES platform reduces the effort necessary to address research questions such as that above and enhances the complexity of problems that it is feasible to address.

It is important to point out that the modules used in the above investigation were not direct implementations of existing modules. Rather, they were modified – in some cases extensively – to fit the specific needs of our investigation. This process of module adaptation is fundamental to the development of the HUES platform, in which possibilities for module integration are gradually realized through ongoing development efforts.

A key issue moving forward with the HUES platform is *model validity*. The reuse of models beyond the context of their original development risks overstepping their scopes of validity. In general, we leave it to the developers seeking to adapt and integrate modules for specific purposes to understand and accommodate the limitations on module

validity. A prerequisite to this, however, is ensuring that scopes of validity are effectively communicated by the original developers. As cultivators of the HUES platform, we are seeking ways to facilitate this through module development guidelines and via the wiki.

CONCLUSIONS

This paper has introduced the HUES platform, an extensible simulation environment for the study of urban energy systems. We have described the composition of the platform and demonstrated its use via an example case. The platform implements a unique approach to dealing with the complexity of district multi-energy systems, based on the development and cultivation of a set of computational modules that can be combined and recombined in different ways. Many challenges remain, such as facilitating model validity, ensuring the development of truly *reusable* modules and dealing with intellectual property issues. Future work on the platform will address these and other issues, and holds significant promise for advancing the study of district multi-energy systems.

ACKNOWLEDGEMENTS

This research has been financially supported by CTI within SCCER FEEB&D (CTI.2014.0119).

REFERENCES

1. Geidl, M. and Andersson, G.: Optimal power flow of multiple energy carriers. *IEEE Transactions on Power Systems*, 22:145–155, 2007.
2. Evins, R., Orehounig, K., Dorer, V., and Carmeliet, J.: New formulations of the 'energy hub' model to address operational constraints. *Energy*, 73:387–398, 2014.
3. Evins, R.: Multi-level optimization of building design, energy system sizing and operation. *Energy*, In review.
4. Bollinger, L. A. and Evins, R.: Facilitating model reuse and integration in and urban energy simulation platform. In *International Conference on Computational Science*, Reykjavik, Iceland, 2015.
5. Bollinger, L. A., Nikolic, I., Davis, C. B., and Dijkema, G. P.: Multi-model ecologies: cultivating model ecosystems in industrial ecology. *Journal of Industrial Ecology*, 2015.
6. Wilson, C. and Dowlatabadi, H.: Models of decision making and residential energy use. *Annual Review of Environment and Resources*, 32:169–203, 2007.
7. Richardson, I., Thomson, M., Infield, D., and Clifford, C.: Domestic electricity use: A high-resolution energy demand model. *Energy and Buildings*, 42(10):1878–1887, 2010.
8. Evins, R., Orehounig, K., and Dorer, V.: Variability between domestic buildings: the impact on energy use. *Journal of Building Performance Simulation*, 2015.
9. Akomeno, O., Hsieh, S., and Orehounig, K.: Energy hub modelling for the design of solar thermal district heating networks with short-term and seasonal storage. In *CISBAT*, Lausanne, Switzerland, 2015.

INTEGRATED URBAN ENERGY MODELLING APPROACHES TO SUPPORT THE SWISS ENERGY STRATEGY 2050

Ralph Evins[1,2], Kristina Orehounig[1,2], Viktor Dorer[1]

1: Urban Energy Systems Laboratory, Empa, Swiss Federal Laboratories for Materials Science and Technology, Überlandstrasse 129, 8600 Dübendorf, Switzerland.

2: Chair of Building Physics, Department of Architecture, ETH Zürich, Stefano-Franscini-Platz 5, 8093 Zürich, Switzerland.

ABSTRACT

We present a discussion of the combined urban energy modelling research efforts that are being undertaken as part of the Swiss Competence Centres for Energy Research project "Future Energy Efficient Buildings and Districts" (SCCER FEEB&D) as well as other related activities at the Urban Energy Systems Laboratory at Empa. These cover a broad spectrum of topics, from urban microclimate analysis, renewable potential and building demand modelling to multi-energy system design, optimisation and control. The findings are intended to aid in the transition of the Swiss energy system in a more sustainable direction by helping to deliver commercially applicable, real-world solutions.

We give an overview of all topics detailing the contribution to the overall research, along with a report on current and expected progress. We highlight the key interactions and dependencies between research areas, and how these have been addressed. This covers data input requirements, model development efforts and application requirements. Links to the associated Holistic Urban Energy Simulation platform (HUES) are also discussed, though the details of the platform are given in a separate paper. A summary is given of the research findings and how these link to the needs of practitioners and industry. We conclude by summarising the current state of the research topics, and raise discussion points regarding possible future directions and lessons learned.

Keywords: urban, energy, modelling, overview, SCCER, FEEB&D

INTRODUCTION

The Swiss Energy Strategy ('Energiewende') 2050 calls for a reduction of CO_2 emissions to <1.5tCO2/p/a by 2050 (from 4.8t in 2011), and also a reduction in energy demand per capita of 43% by 2035 (compared to 2000). The "Future Energy Efficient Buildings and Districts" (FEEB&D) project will support this by enabling the reduction of the energy demand of the Swiss building stock by a factor of five over this period. This will be achieved through the development of new building-related materials, components and systems, and their combination into holistic concepts for implementation via industry partners. One of the key areas is the exploration of new forms of urban energy system, for example systems with decentralised and distributed elements with large fractions of renewables, and comparison to existing approaches. This paper focusses on the modelling work conducted to support this.

Simulation and modelling can be seen as an emerging paradigm that falls between induction (patterns in observed data) and deduction (deriving statements from established facts): facts are embedded in a model, which is interrogated to give data on optimal solutions, thus providing new information. As our recent review paper [1] has established, there is a huge diversity of models and software tools available in the area of urban energy systems.

Modelling the detailed behaviour of such systems is the only plausible method of obtaining the performance metrics needed to assess their technical, energetic and economic viability.

MODELLING FOCUS AREAS

Energy hubs

At the heart of the urban energy system modelling conducted is the energy hub concept [2]: the use of mixed integer linear programming to optimise the supply, conversion and storage of multiple energy streams. The first major development was the upscaling of the model to neighbourhoods [3] in conjunction with building energy simulations. Different components of the set of energy hub model formulations developed are used in all energy system assessments undertaken. The core model is very simple, but many improvements have been developed, and many more are underway. These include the treatment of part-load efficiency and system start-ups [4], incorporation of sizing and minimum permitted loads [5], [6], and the use of a rolling horizon approach [7]. The model has been validated against with dynamic simulations for integrating thermal energy storage [8]. A bi-level approach to the sizing of energy hub components has also proven successful [9]. Future work will follow the complementary strands of improving the underlying MILP formulations (to improve run times and solution accuracy) and increasing the accuracy of the models in reflecting the real systems under consideration (to increase the relevance and usefulness of the simulations conducted).

Networks

Links between buildings are an essential part of decentralised systems. These can be treated as idealised connections that aggregate many building loads, simplified energy transporters that link different hubs, or complicated systems that require detailed analysis. Heating network layout optimisation can be included in the energy hub models as part of the system sizing process [10]. Constraints on electrical connections are also of importance, particularly when exploring the balance between heat and electricity as the means of energy transport in a district, though their nonlinearity makes integration in an energy hub modelling approach more challenging [11]. Future research will aim to better understand the levels of network abstraction required, improve the modelling of detailed networks and further integrate their various constraints into existing models. Looped low temperature networks with bi-directional flow are of specific interest.

Building demands

Modelling of building energy demands is an established and active research domain, and an emerging focus is the performance and interaction of multiple buildings, ranging from small districts to whole cities. We focus on aspects that are critical to urban energy system design. One is the variability between different buildings caused by occupant behaviour and other factors [12], since this affects the concurrency of the loads and thus the magnitude of the peaks. For large numbers of buildings it is impractical to consider them individually in the urban system, thus clustering and aggregation in spatial and temporal terms becomes an important part of the analysis [13]. In future this will be extended to the issue of how many buildings from a large area must be modelled in detail in order to approximate the demands of the district, and how these archetype buildings should be selected. Together with partners in FEEB&D we work on the geo-dependant representation of building demand data, see also below. Where measured data is available, it’s use in the generation of typical hourly demand profiles has been investigated [14].

Renewable energy generation potential

Alongside the energy demands to be met, the potential to supply energy using renewable technologies must be assessed. PV and solar thermal collectors require careful geometric modelling, since in the urban realm many obstructions can affect the solar radiation available. Borehole systems, used in combination with heat pumps for supply and storage, also present significant modelling challenges. Methods have been developed for the evaluation of renewable energy potential integration in neighbourhoods [15] as well as the evaluation of the trade-off between costs and renewable share maximization [16]. Current work is focussed on the development of a method for generating hourly solar potentials for neighbourhoods [17].

INTERACTIONS BETWEEN RESEARCH AREAS

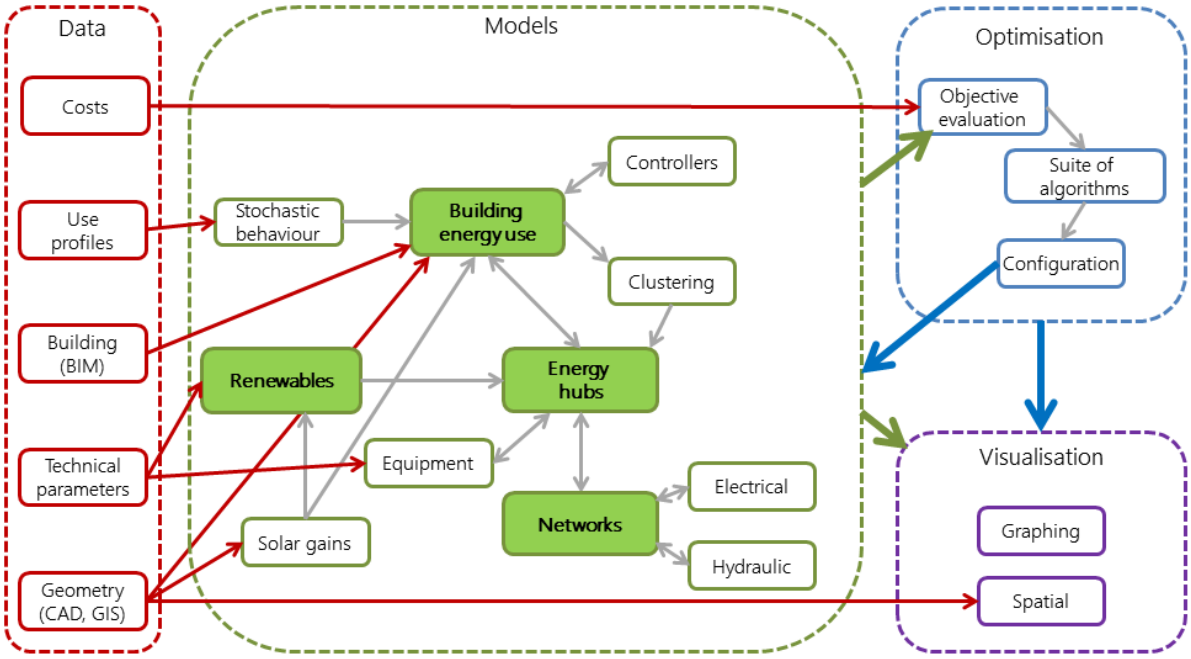

Figure 1: An overview of the interactions between modelling areas (core topics are shaded), and to other key activities. The current state of the HUES platform follows a similar structure.

It is an important part of the modelling philosophy employed here that the urban energy system should be treated as a whole; the interactions that are made explicit in this holistic approach are highly significant. For example, the buildings that make up the urban area must be modelled concurrently with the district energy system so that the exact matching of demand with supply can be established. This is important at a design level when comparing options like the retrofit of buildings against improvement in supply efficiency. Coupling the use of energy in buildings with the supply system model would allow demand-response techniques to be incorporated, however this is computationally much more demanding.

On-going development efforts are focussed on the integration of the modelling areas discussed above as well as the improvement of individual models. The ambition is to facilitate model reuse and integration [18] so that new problems can be addressed more effectively and efficiently. This is achieved via the Holistic Urban Energy Simulation platform (HUES), outlined and demonstrated in [19]. This approach is in contrast to the development of a unified, homogenised program that can assess many domains at once; this may become unmanageably complex and hard to maintain over time, though there are clearly benefits regarding computational integration of the domains.

Common data input requirements determine one aspect of integration between modelling areas, as it is highly desirable to use the same data source for multiple aspects of the system to ensure comparability. For example, the same data on geometries, surroundings, topology and

weather should be used for analysing solar gains to buildings as for analysing the potential for PV generation. This requires a means of accessing common datasets from different models, and the data storage requirements needed to achieve this amongst multiple project partners is an ongoing challenge. The geo-dependence of demands and supplies is another example of this, and the use of GIS tools for both demand and supply aspects is also under development.

The computational optimisation of building designs for low-energy performance is a topic of significant and growing interest [20], and this is now being extended to problems concerning urban-level issues, including energy systems. Recent research in this area has used genetic algorithms in combination with MILP to form a bi-level optimisation process that addresses design and operational aspects using the best tools for the respective problems [9]. Other work in this area includes speeding up the process of finding good building-level parameters by using different resolution models [21], and investigating optimal urban forms for multiple buildings to minimise energy use across the district [22].

APPLICATION EXAMPLES

Typical neighbourhood configurations within Switzerland have been used as application cases to demonstrate potentials and possibilities towards achieving the goals of the Swiss Energy Strategy 2050. The methods and models developed as described above have been specifically tailored to address these research questions, and in a further step are being deployed on demonstration cases. So far demonstration cases include a rural neighbourhood [15], a new city quarter [23], an existing semi-rural neighbourhood [24], industrialized and office areas [25] and more urban locations. The results will be used to make recommendations on how the envisioned goals can be achieved, and in a second step to provide industry and practitioners with guidelines and methods to translate the research results into practice.

Building demands

The current energy consumption of buildings in Switzerland will be reduced by increasing renovation rates. The reference model approach developed [14] has been deployed on various cases (e.g. [24]) to demonstrate the renovation actions (e.g. window replacement, façade insulation, system replacement) and timeline that would be necessary to achieve the goals by 2050. The energy hub approach has also been used for a sensitivity analysis exploring the impact of climate change on building energy demands, and the affect this has on urban energy system design [26].

Renewable energy generation potential

Renewable energy sources available include photovoltaic and solar thermal collectors, biomass based electricity and heat production, and small hydro power installations. However, the potentials vary significantly depending on geographic location and type of buildings and neighbourhoods. As demonstrated for a rural neighbourhood in the mountains, hydro power offers a huge potential for electricity generation for this specific location, whereas photovoltaic installations are limited to those roof surfaces where buildings are not historically protected [15]. The energy hub approach combined with the assessment of hourly photovoltaic potentials can evaluate which roof surfaces are most beneficial for photovoltaic installations in terms of costs and emission reduction; the ideal trade-off between local electrical storage sizes and electrical grid feed-ins are also demonstrated [16].

Update of urban energy systems

Existing energy systems in neighbourhoods offer significant potential for improving energy efficiency, reducing CO_2 emissions and reducing the import of fossil fuels. A study on the

village of Zernez demonstrates to what extent the village can be energy sustainable (with no energy inputs from outside), and how building-related CO_2 emissions can be dramatically reduced [15]. Another study conducted in the city of Rheinfelden demonstrates the potential for integrating local thermal energy storage, and investigates the ideal size, type and location of the storage [8], [24].

Present modelling work has focused on the design and performance assessment aspects of urban energy systems, however, operational aspects are also important. In the energy hub in the presently built NEST[1] building at Empa, control aspects are the main focus.

CONCLUSIONS

We have outlined the significant research contributions delivered so far regarding urban energy system modelling within the FEEB&D project and the Swiss Energy Strategy 2050. We highlight the core modelling activities undertaken, the need for a holistic approach and the critical interactions this exposes, and the assessment cases used. This summary may be of use to others undertaking such a programme of model development in other contexts.

The control of energy hubs poses many challenges, including how to match the different time scales for thermal (years to hours) and for electric microgrids (μs), and will be at the core of future research. NEST will be an important test bed for these issues, and also for the comparison and verification of energy hub results with measured data as well as with more detailed models.

Expected future contributions in line with the roadmap of the FEEB&D project[2] include the further development these models within the framework of the HUES platform. These will support the assessment of new urban energy concepts, their comparison with existing systems, and development of best-practice guidance for their implementation in industry.

REFERENCES

[1] J. Allegrini, G. Mavromatidis, K. Orehounig, F. Ruesch, V. Dorer, and R. Evins, "Buildings as a part of urban energy systems: a review of models and tools," *Renewable and Sustainable Energy Reviews*, 2015.

[2] M. Geidl and G. Andersson, "Optimal Power Flow of Multiple Energy Carriers," *IEEE Transactions on Power Systems*, vol. 22, no. 1, pp. 145–155, 2007.

[3] K. Orehounig, R. Evins, and V. Dorer, "Integration of decentralized energy systems in neighbourhoods using the energy hub approach," *Applied Energy*, vol. in press, 2015.

[4] R. Evins, K. Orehounig, V. Dorer, and J. Carmeliet, "New formulations of the 'energy hub' model to address operational constraints," *Energy*, vol. 73, pp. 387–398, Aug. 2014.

[5] G. Mavromatidis, R. Evins, K. Orehounig, V. Dorer, and J. Carmeliet, "Multi-objective optimization to simultaneously address energy hub layout, sizing and scheduling using a linear formulation," presented at the Engineering Optimisation, Lisbon, 2014.

[6] B. Morvaj, R. Evins, and J. Carmeliet, "Optimal selection and operation of distributed energy resources for an urban district," presented at the Engineering Optimisation, Lisbon, 2014.

[7] J. Marquant, R. Evins, and J. Carmeliet, "Reducing computational time with a rolling-horizon approach applied to a MILP energy hub model," presented at the Simulation of Large-scale Complex Urban Systems, Reykjavik, Iceland, 2015.

[1] http://nest.empa.ch/de/innovationen/energy-hub/

[2] http://www.sccer-feebd.ch/wp-content/uploads/SCCER-FEEBD-Innovation-Roadmap-March-20152.pdf

[8] A. Omu, S. Hsieh, and K. Orehounig, “Energy hub modelling for the design of solar thermal district heating networks with short-term and seasonal storage,” presented at the CISBAT, Lausanne, Switzerland, 2015.
[9] R. Evins, “A bi-level design and operational optimisation process applied to an energy centre,” *Journal of Building Performance Simulation*, 2015.
[10] B. Morvaj, R. Evins, and J. Carmeliet, “The impact of low energy buildings on the optimal design of distributed energy system and networks,” in *Building Simulation*, Hyderabad, India, 2015.
[11] B. Morvaj, R. Evins, and J. Carmeliet, “Bi-level optimisation of distributed energy systems incorporating non-linear powerflow constraints,” presented at the CISBAT, Lausanne, Switzerland, 2015.
[12] R. Evins, K. Orehounig, and V. Dorer, “Variability between domestic buildings: the impact on energy use,” *Journal of Building Performance Simulation*, 2015.
[13] J. Marquant, A. Omu, R. Evins, and J. Carmeliet, “Application of spatial-temporal clustering to facilitate energy system modelling,” in *Building Simulation*, Hyderabad, India, 2015.
[14] K. Orehounig, G. Mavromatidis, R. Evins, V. Dorer, and J. Carmeliet, “Predicting energy consumption of a neighborhood using building performance simulation,” in *Building Simulation and Optimization (BSO 2014), UCL, London, UK*, 2014.
[15] K. Orehounig, G. Mavromatidis, R. Evins, V. Dorer, and J. Carmeliet, “Towards an energy sustainable community: An energy system analysis for a village in Switzerland,” *Energy and Buildings*, vol. 84, pp. 277–286, Dec. 2014.
[16] G. Mavromatidis, K. Orehounig, and J. Carmeliet, “Evaluation of photovoltaic integration potential in a village,” *Solar Energy*.
[17] S. Miglani, K. Orehounig, and J. Carmeliet, “A method for generating hourly solar radiation on building rooftops accounting for cloud cover variability,” presented at the CISBAT, Lausanne, Switzerland, 2015.
[18] L. A. Bollinger and R. Evins, “Facilitating model reuse and integration in the urban energy simulation platform,” presented at the Simulation of Large-scale Complex Urban Systems, Reykjavik, Iceland, 2015.
[19] L. A. Bollinger and R. Evins, “HUES: A Holistic Urban Energy Simulation platform for effective model integration,” presented at the CISBAT, Lausanne, Switzerland, 2015.
[20] R. Evins, “A review of computational optimisation methods applied to sustainable building design,” *Renewable and Sustainable Energy Reviews*, vol. 22, pp. 230–245, Jun. 2013.
[21] C. Waibel, A. Ramallo-Gonzalez, R. Evins, and J. Carmeliet, “Reducing the computing time of multi-objective building optimisation using self-adaptive sequential model assessment,” in *Building Simulation*, Hyderabad, India, 2015.
[22] C. Waibel and R. Evins, “Optimising urban morphology using different variable representations,” in *Building Simulation*, Hyderabad, India, 2015.
[23] S. Hsieh and K. Orehounig, “Evaluation of renewable energy sources integration potential in a new development area,” presented at the Energy for Sustainability Conference, Coimbra, Portugal, 2015.
[24] S. Hsieh, R. Weber, V. Dorer, and K. Orehounig, “Integration of thermal energy storage at building and neighbourhood scale,” in *Building Simulation*, Hyderabad, India, 2015.
[25] M. Hohmann, C. Waibel, V. Dorer, R. Evins, and J. Carmeliet, “Optimisation of urban energy systems: case study of the Empa Areal,” presented at the CISBAT, Lausanne, Switzerland, 2015.
[26] G. Mavromatidis, K. Orehounig, and J. Carmeliet, “Climate change impact on the design of urban energy systems,” presented at the CISBAT, Lausanne, Switzerland, 2015.

CLIMATE CHANGE IMPACT ON THE DESIGN OF URBAN ENERGY SYSTEMS

G. Mavromatidis[1,2]; K. Orehounig[1,2]; J. Carmeliet[1,3]

1: Chair of Building Physics, Swiss Federal Institute of Technology, ETHZ, Zurich, Switzerland

2: Laboratory for Urban Energy Systems, Swiss Federal Laboratories for Materials Science and Technology, EMPA, Dübendorf, Switzerland

3: Laboratory for Multiscale Studies in Building Physics, Swiss Federal Laboratories for Materials Science and Technology, EMPA, Dübendorf, Switzerland

ABSTRACT

The initial step of the distributed energy system design process is the determination of the energy demand that the system needs to cover. Building simulation is often used for this purpose requiring climate data for the examined period. The long lifetime of buildings corresponds to timescales when considerable changes in the climate are expected to occur. Design using historical or current weather data could lead to underperformance of energy systems that cannot meet future peak loads and/or to the introduction of new demands (e.g. for cooling), considering the long-term impact of climate change. The aim of this work is to firstly investigate the impact of climate change on the loads of buildings for a case study urban quarter in Switzerland and subsequently on the design of the urban energy system to meet the quarter's needs. Multi-year weather files are created, ranging from 2020 to 2040, using raw data from selected GCMs and carbon scenarios for the examined location using a statistical downscaling technique known as morphing. The optimal design of the urban energy system is obtained using the energy hub concept, examining simultaneously the design (selection and sizing of the conversion and the storage devices) and operational aspects of the system, with minimization of total cost as the objective. Initially, the buildings' energy demands are calculated for the current and the future climate scenarios and their impact is assessed. Subsequently, optimal energy hub design for the current and future climate scenarios are obtained, and their differences are examined in terms of total cost, but also optimal composition and size of the energy hub. However, since standard practice involves the use of current weather data, the impact of today's design when operating under future climatic conditions is also assessed. The differences between the operation of the future climate optimised system and the today's design in terms of operational patterns and resulting costs are examined and any potential hours when the demand cannot be met by the present-day design are quantified.

Keywords: climate change, morphing, weather files, energy hub

INTRODUCTION

Buildings are a major contributor to anthropogenic greenhouse gas (GHG) emissions that are considered the main driver of climate change. The adoption of distributed generation technologies in order to transform building and urban energy systems into sustainable entities can curb emissions and contribute towards the mitigation of climate change. However, given that a degree of future climate change is now inevitable regardless of mitigation efforts, buildings will also have to operate and adapt to the future climatic conditions.

Buildings are long lasting structures, and they are expected to function properly for decades, meaning they are particularly at risk from climate change. Climate change is expected to affect buildings' differently, depending on the location. The main impacts can be summarized as a

shift in energy use via a decrease in heating energy demand and an increase in cooling demand. Other impacts, according to [1], include a shift in thermal operational conditions of equipment that could lead to passive/natural systems going out of range or HVAC capacity mismatch for the heating and cooling peak loads, resulting in inefficiencies. Thus, the energy systems installed should be designed considering the future climate in order to be able to supply the buildings with the necessary energy services ensuring a comfortable indoor environment.

In the building energy design process, the first step that building and system designers need to take is to evaluate the buildings' energy demands. This task is usually performed using Building Performance Simulation (BPS) tools that use weather files to represent the climate that buildings are exposed to. The current status quo practice includes the use of weather files generated using past weather data. However, climate conditions due to climate change are expected to be different compared to the previous years; thus there is always a risk of an ineffective design leading to bad energetic and economic performance of the system.

Climate change impacts on the building stock's energy consumption and GHG emissions has been the topic of several publications, ranging from country scale investigations (*e.g.* [2]) to specific building case studies (*e.g.* [3]). Moreover, the scope of the studies is not always energy consumption, but studies have also focused, for instance, on thermal comfort aspects [4]. The objective of this paper is to take the next step and investigate how the changes in energy consumption patterns are reflected upon the optimal energy system design. The differences between the optimal designs obtained for the current and the future climate are assessed and the shortfalls of the operation of today's design under future climatic conditions is analysed.

METHOD

Climate change weather files

The first step of the methodology is the generation of weather files that reflect the future climatic conditions. In order to model the global climate, General Circulation Models (GCM) are used in conjunction with Representative Concentration Pathways (RCPs), which denote the cumulative measure of human GHG emissions from all sources. In this work, climate change data have been obtained from the Coupled Model Intercomparison Project, Phase 5 (CMIP5) coordinated by the World Climate Research Programme (WCRP) [5] that have also been the basis of IPCC's fifth assessment report [6].

However, a well-known problem with using the output of GCM models is that they have very coarse spatial (~100-200 km) as well as temporal (typically monthly) resolution. Therefore, in order to use their output with a building simulation software, a technique is needed to downscale the data to the examined location and at the desired, hourly resolution. In this paper, a statistical downscaling approach is used called *morphing*, as introduced by Belcher et al. [7] is used to obtain hourly weather data. The technique transforms present-climate weather files into future climate change weather files by shifting the data to adjust to the future monthly mean of the examined weather variable, applying a stretch to match the monthly variance or a combination of both.

In this work, climate change weather files are created for two different GCM models, namely the *GISS-E2-H* and the *GFDL-CM3*, and two RCPs, namely *rcp45* and *rcp85*, representing an intermediate and a high emission scenario, respectively. Moreover, similarly to the work of Robert and Kummert [8], individual future years for the period of 2020 to 2040 are created to preserve some year-to-year variability and thus the extremes that can be observed during the projected operation of the urban energy system.

Case study

To illustrate the methodology and the impacts of climate change on the optimal energy hub design a case study urban neighbourhood is considered consisting of three buildings of different types, namely an office building, a restaurant building and a multi-family residential building. The buildings' energy demands for heating, cooling and electricity services are calculated with *EnergyPlus* using the generated future weather files for the climate of Zurich, Switzerland.

Energy hub model

For the case study selected, the energy system design is performed using the energy hub model [9]. It is used to select the optimal components, their capacities and calculate their optimal operating schedule. For the case study considered in this paper, the energy hub representation can be seen in Fig. 1. The candidate system is composed of a natural gas fired boiler and a CHP engine for the supply of heating services. For the cooling needs of the buildings, a conventional electric chiller and an absorption chiller are included. To allow flexible usage of the devices hot and chilled water storage modules are added. Finally, the electricity demands of the buildings can be covered by the CHP engine, while connection to the national grid is also maintained.

The objective of this energy hub study is the minimisation of the total cost of the system, composed of the investment required to purchase the equipment and the operation cost during life time of the equipment. The model formulation follows the typical energy hub structure, as presented in other publications (e.g. [10]). This means that the constraints included in the problem are energy balances for the different energy services and the operation of the storage systems, non-violation of maximum capacities for conversion devices and storage during operation, maximum possible storage capacities due to space limitations, and minimum part loads for the operation of the conversion devices.

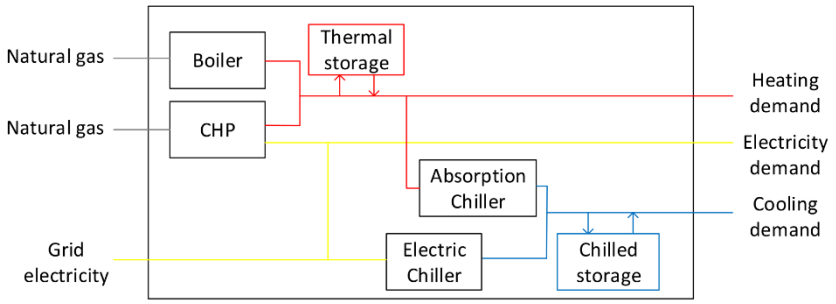

Figure 1: Energy hub representation of the urban energy system considered in this case study

In this paper, the energy hub model is used to perform two different calculations. Initially, the model is run to obtain the optimal energy hub design using the energy demands of the buildings calculated with today's weather and for each climate change scenario considered. The second calculation stream consists of calculating only the optimal operation schedule of the design obtained with today's weather but under the future energy loads change in order to investigate any potential shortfalls in its performance.

Due to the mixed-integer formulation of the problem, performing the design of the energy hub considering all the hourly steps that it is expected to operate (8760h for the current climate and 20 years in hourly steps for the climate change scenarios) would make the problem intractable. For that reason, a two-step approach is considered. Initially, for the considered operational periods, a set of typical days is created following the approach by [11], and the hub's design problem is solved for these typical days only. After the optimal components of the energy hub and their capacities are calculated, they are fixed to their nominal values and the operational schedule is calculated for the complete period.

RESULTS AND DISCUSSION

Climate change impacts on buildings' energy demands

The first step, as was discussed earlier, is the calculation of today's heating and cooling demands using the present-day weather file and for the climate change scenarios during the 20-year period considered. The variation of annual heating and cooling demands against today's benchmark value is presented in Fig. 2.

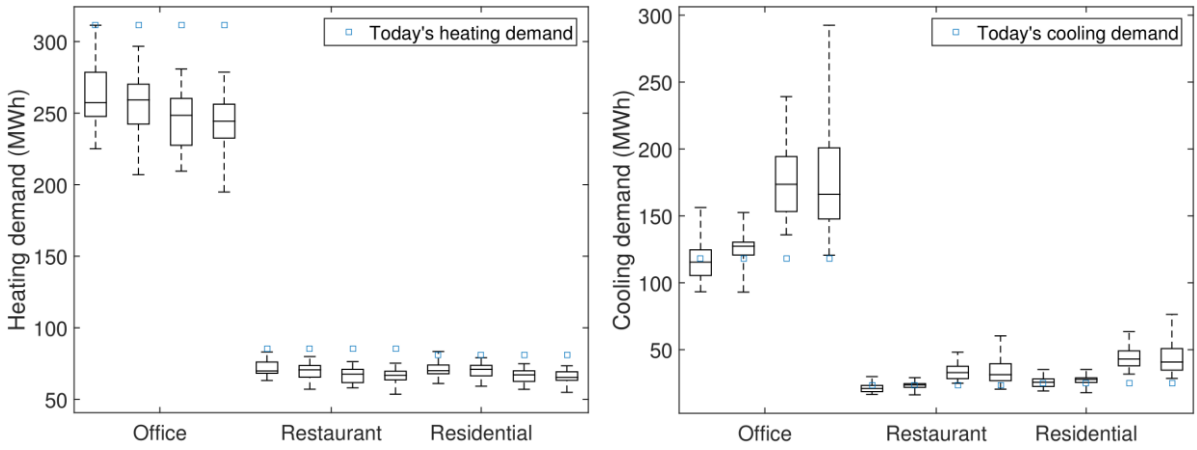

Figure 2: Variation of annual heating and cooling demand of the buildings for the current and the future climate. The four box plots per building correspond to the different models used in the analysis (GISS-E2-H-rcp45, GISS-E2-H-rcp85, GFDL-CM3-rcp45, GFDL-CM3-rcp85).

Regarding the heating demand, it can be seen that for all buildings, the level of energy requirements calculated for today's climate is higher for the majority of the years for all models considered. On the contrary, the mean annual cooling demand for all buildings and for the first two climate change scenarios seem to be relatively close, even though the boxplots' ranges show that there can be warm years when the annual cooling demand is significantly increased. The situation is reversed for the two latter climate change scenarios, where it is seen that the increase in annual cooling demand for all buildings is more dramatic, with the cases of the office and the residential building having for all 20 years, in both models, demands that are higher than the ones calculated with the present climate data. Finally, it can be seen that there is significant difference between the cooling demands predicted by the two different models considered (*GISS-E2-H* and *GFDL-CM3*), but the difference between the two carbon scenarios (*rcp45* and *rcp85*) using the same model is not substantial for the future horizon considered.

Climate change impact on optimal energy hub design

The next step is the comparison between the optimal energy hub designs for today's climate and the future climate scenarios. The variation of the capacities of the elements selected and the resulting investment cost are shown in Fig. 3. It can be seen that in today's design, under the current climate, a simple configuration for the energy system is selected. The CHP engine and the absorption chiller are excluded from the design and only a boiler and an electric chiller are selected. On the other hand, the designs of the climate change scenarios include all possible components. Compared to today's design, the boiler is sized lower for all scenarios and the chiller's capacity is smaller for the first two and larger for the latter two scenarios. Additional heating and cooling capacity are also added in the form of the CHP engine and the absorption chiller. Finally, in all configurations the thermal and chilled storage capacities are maximised and equal to the maximum allowable due to space availability constraints.

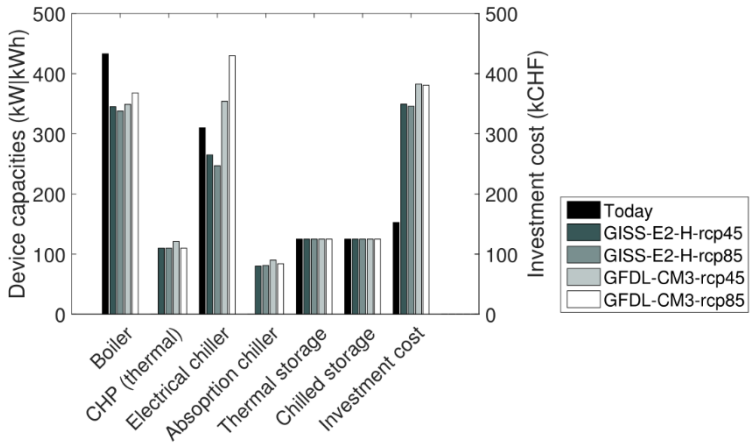

Figure 3: Variation of optimal energy hub design for the current and future climate

The final results discuss the operation of the hub design obtained with today's climate under the future loads. In Fig. 4a, the number of hours that the cooling demand cannot be met for each scenario due to lower installed cooling capacity are presented. For the first two scenarios, the number of hours is limited, due to lower impact on the demands predicted by the GISS-E2-H GCM. However, for the second GCM considered, it can be seen that the number of hours during the lifetime of the system ranges from more than 400 hours to above 600 hours.

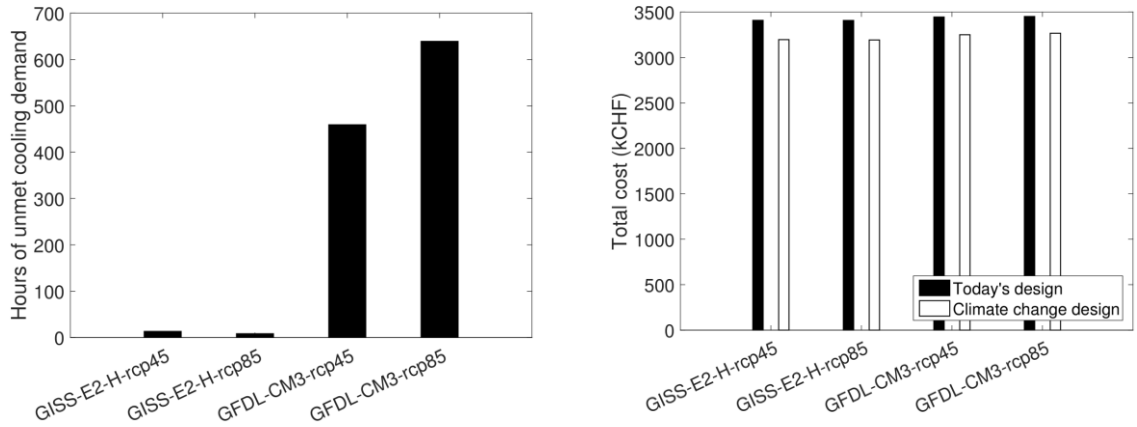

Figure 4: a. Number of hours that today's energy design cannot meet the cooling demand for the future climate scenarios. b. Total cost comparison between the energy hub design obtained with today's climate operating under climate change and the optimal designs for each climate change scenario.

More importantly, though, Fig. 4b presents the total cost of the system when operating under the future loads against the optimal design for each particular case using the future loads. It is seen that in all cases costs are much higher, even though for all cases the investment costs are larger, as presented in Fig. 3. The reason is that the energy hub design obtained when considering the future energy demands is specifically optimised for the future's climate conditions and thus an increased investment cost is compensated by a much lower operating cost. Therefore, not considering climate change when designing an energy system can lead to suboptimal designs both in terms of demand coverage but also in cost terms.

CONCLUSIONS

This paper deals with considerations of climate change and the design of urban energy systems. Initially, it can be seen that even for a few years into the future (2020-2040) the use of weather

files built upon past data can lead to an overestimation of heating and an underestimation of cooling demands for buildings. Extending the investigation on the impact on optimal energy hub design, it became evident that firstly the components selected change as well as their capacities. Moreover, the system design obtained with the current weather file underperforms when subjected to the future energy demands leading to hours of unmet cooling demand, but also a higher total cost compared to the climate change optimised system designs, even though the latter ones have higher investment costs.

As future work, the incorporation of additional models from CMIP5 and projects with higher spatiotemporal resolution, like CORDEX will allow a wider and more accurate view on the possible future outcomes. Finally, the introduction of stochastic programming techniques will allow the selection of an energy hub among the different designs under climate change that can perform optimally for all the possible climate change scenarios.

ACKNOWLEDGEMENTS

Research presented in this paper is supported by funds from CCEM (IDEAS4cities project).

REFERENCES

1. de Wilde, P., Coley, D.: The implications of a changing climate for buildings. Building and Environment 55, 1-7, 2012.
2. Ren, Z., Chen, Z., Wang, X.: Climate change adaptation pathways for Australian residential buildings, Building and Environment 46, 2398-2412, 2011.
3. Taylor, S., Peacock, A., Banfill, P., Shao, L.: Reduction of greenhouse gas emissions from UK hotels in 2030, Building and Environment 45, 1389-1400, 2010.
4. Roetzel, A., Tsangrassoulis, A.: Impact of climate change on comfort and energy performance in offices, Building and Environment 57, 349-361, 2012.
5. Taylor, K.E., Stouffer, R.J., Meehl, G.A.: An overview of CMIP5 and the experiment design. Bulletin of the American Meteorological Society 93, 485-498, 2012.
6. IPCC: Climate Change 2013: The Physical Science Basis. Contribution of Working Group I to the Fifth Assessment Report of the Intergovernmental Panel on Climate Change [Stocker, T.F., D. Qin, G.-K. Plattner, M. Tignor, S.K. Allen, J. Boschung, A. Nauels, Y. Xia, V. Bex and P.M. Midgley (eds.)]. Cambridge University Press, Cambridge, United Kingdom and New York, NY, USA, 2013.
7. Belcher, S.E, Hacker, J.N., Powell, D.S.: Constructing design weather data for future climates. Building Services Engineering Research & Technology 26, 49-61, 2005.
8. Robert, A., Kummert, M.: Designing net-zero energy buildings for the future climate, not for the past, Building and Environment 55, 150-158, 2012.
9. Geidl, M., Andersson, G. 2007. Optimal Coupling of Energy Infrastructures. In: Power Tech, IEEE Lausanne, 2007.
10. Mavromatidis, G., Evins, R., Orehounig, K., Dorer, V., Carmeliet, J.: Multi-objective optimization to simultaneously address energy hub layout, sizing and scheduling using a linear formulation. In: ENGOPT 2014, Lisbon, Portugal, September 8-11, 2014.
11. Domínguez-Muñoz, F., Cejudo-Lópeza, J.M., Carrillo-Andrésa, A., Gallardo-Salazarb, M.: Selection of typical demand days for CHP optimization. Energy and Buildings 43, 3036-3043, 2011.

BI-LEVEL OPTIMISATION OF DISTRIBUTED ENERGY SYSTEMS INCORPORATING NON-LINEAR POWER FLOW CONSTRAINTS

B. Morvaj[1,2]; R. Evins[1,2]; J. Carmeliet[1,3]

1: Chair of Building Physics, ETH Zürich, Zürich, Switzerland

2: Laboratory for Urban Energy Systems Laboratory, EMPA, Dübendorf, Switzerland

3: Laboratory for Multiscale Studies in Building Physics, EMPA, Dübendorf, Switzerland

ABSTRACT

This paper presents a bi-level optimisation process for the design and operation of a distributed energy system taking into account non-linear electrical grid constraints. It includes the optimal selection of various distributed energy resources (micro combined heat and power, photovoltaic, air source heat pump, gas boiler and heat storage) and the optimal operation of the selected resources at the neighbourhood level. The objective is to explore the tradeoff between cost and carbon emissions over the lifespan of the selected resources while satisfying the heat and electrical demands of the buildings as well as avoiding the violation of existing electrical grid constraints. This is accomplished by using two optimisation "levels" within one optimisation process. The main level uses a multi-objective genetic algorithm (GA) to optimise a set of design variables (capacities of technologies in each building). The evaluation of each candidate solution of the GA has two steps. First, the optimal operation of all distributed energy resources is determined using the energy hub approach (a mixed integer linear programming model); the results are passed back to the main level where they are summed to give the objective function value. This is followed by a non-linear power flow calculation to check if the proposed operation violates existing electrical grid constraints. The optimisation framework is applied to a case study consisting of several buildings at the low voltage distribution network level. The optimal design and operation of distributed energy system is determined. The impact of the existing electrical grid in limiting integration of distributed energy resources is shown to be highly significant. The effect on the solutions proposed and how limitations can be decreased are also discussed.

Keywords: bi-level optimisation, power flow constraints, MILP, GA, energy hub

INTRODUCTION

The Swiss energy strategy 2030 set a target of at least 50% reduction of greenhouse gas reduction compared to 1990. Distributed energy systems (DES) that satisfy simultaneously various energy demands (heat and electricity) can be a key enabling factor for meeting the targets. They provide potential for large energy savings but with the downside of energy networks becoming more complex to design and operate. Various authors have looked at the optimal design and operation of DES while taking into account building systems [1] [2] [3]. The models used for optimising DES are largely based on mixed-integer linear programming formulations (MILP). However, they all assume that the distribution grid capacity is big enough to integrate any amount of renewables. This is not always a valid assumption since most of the electrical grids were design before renewables were an influencing factor. On the other hand, a number of publications address optimal power flow and/or placement of

distributed generation in the distribution grid while assuming building systems as predefined [4] [5] [6]. Such optimisations are mostly based on heuristics such as genetic algorithm.
In this paper, we present a multi-objective bi-level optimisation framework for the optimal design and operation of DES which takes into account building systems and non-linear power flow constraints. We analyse how much the existing electrical grid is limiting integration of distributed energy resources and how this limitation can be decreased.

BI-LEVEL OPTIMISATION FRAMEWORK

A bi-level optimisation framework uses two optimisation "levels" within one optimisation process. An overview is given in Figure 1. Here the main level uses a multi-objective genetic algorithm to optimise a set of design variables (equipment capacities) for each building. The evaluation of each candidate solution has two steps. The first is a MILP model, where optimal operation is determined and the cost and emissions calculated. This is followed by a power flow calculation to check if the proposed operation violates existing electrical grid constraints. If the proposed solution violates a grid constraint, it will be penalised in the constraint function of genetic algorithm.

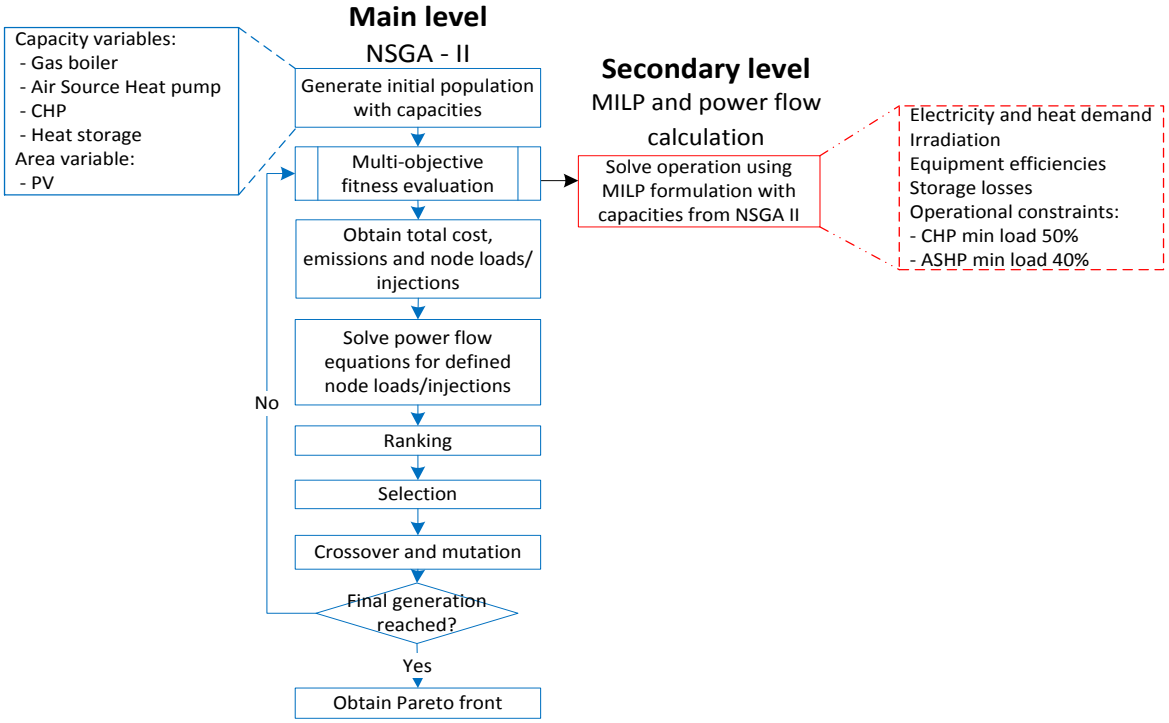

Figure 1: Flowchart of the bi-level optimisation process.

The genetic algorithm – design optimisation

Genetic algorithms are a metaheuristic belonging to the class of evolutionary approaches based on iteratively improving solutions by use of recombination and mutation. Solution population based on their fitness and used to form a new population. In this paper the multi-objective Non-dominated Sorting Genetic Algorithm NSGA II [7] is used. The two objectives used are minimization of total cost and carbon emissions over the lifespan of the technologies. The design variables are the capacities of the considered technologies for each building: combined heat and power (CHP), photovoltaics (PV), air-source heat pump (ASHP), gas boiler and heat storage. There are 5 buildings giving a total of 25 decision variables. If a decision variable is equal to 0 it means that that technology will not be installed. Capacities are passed to the MILP secondary level optimisation model (described below) where optimal operation as well as operating costs and emissions objectives is determined. Proposed

solutions are checked if they violate grid constraint by solving power flow equations (see next section). If they violate grid constraints, they are penalised proportionally by how much limits are exceeded. In the sorting step, solutions without violations are always dominating solutions with violations and solutions with smaller violations dominate solutions with larger violations. This way non-violating solutions are always selected and eventually violating solutions will not be included in the current population.
The optimisation was run for 100 generations with a population size of 100, crossover probability 0.9, mutation probability 0.5 and mutation distribution η_m 10.

Mixed integer linear programming – operational optimisation

Optimal operation for each solution by proposed the main level is solved using a MILP model. The formulation is based on the energy hub framework [8] where each technology is represented by a conversion efficiency between different energy streams. Each building is represented by an energy hub as shown in Figure 2. Additional constraints included are minimum load for CHP (50%) and ASHP (40%), and daily heat storage. For more details about the model, the reader is referred to [9].

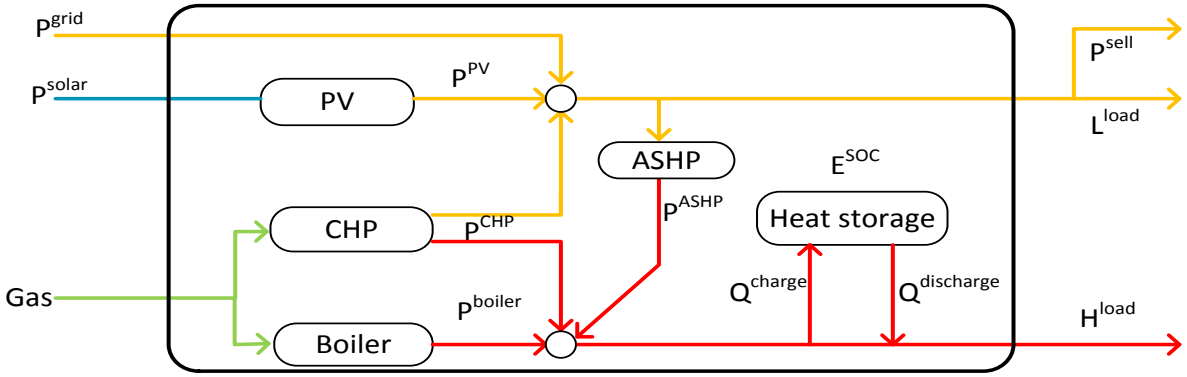

Figure 2: Representation of conversions between various energy streams within one building.

The buildings were modelled in EnergyPlus and simulation was run using weather data for Zürich, Switzerland in order to obtain hourly heating and electricity demand. In the MILP model, electricity and heat demand are represented by 24 hourly demand curves for each month in order to decrease computational time (in total 288 timesteps). The model uses the design variables proposed by NSGA as capacity constraint and aims to minimise total costs (investment and operational cost) while satisfying the electricity and heat demand of each building. Carbon emissions are calculated by applying the following carbon factors: grid electricity 0.5 $kgCO_2/kWh$ and natural gas 0.2 $kgCO_2/kWh$. It is assumed that carbon is accounted for electricity exported to the grid with the same grid carbon factor. This is the reason why negative net carbon emissions can be obtained in the result section. Operational cost and carbon emissions were calculated for 20 years (the assumed lifespan of the equipment). The efficiency, capacity bounds and cost of each technology is shown in Table 1 based on data from [1] [2] [3].

Technology	Efficiency	Capacity bounds	Cost
CHP	η_{el}: 25%. HER: 2	0 -100 kW	500 €/kW
Gas boiler	80%	0-150 kW	70 €/kW
PV	15%	0-150 kWp	600 €/m^2
ASHP	COP: 2.8	0 -100 kW	400 €/m^2
Thermal storage	99% per timestep	0-60 kWh	70 €/kWh

Table 1: Efficiency, capacity bounds and linear cost of technologies used

Non-linear power flow calculation – electrical grid constraint

After solving the optimal operation in the MILP model, it is calculated how much electricity each building is producing or consuming for each timestep. The values are passed to the electric grid model where buildings are represented as nodes with known loads or injections. The network comprises a single 20/0.4 kV distribution transformer with a single one phase feeder supplying the five residential buildings. The data for the network is based on [10] along with cable data shown in Figure 3. The power factor for all consumers was assumed to be 0.85 lagging and for distributed generation 1. For each timestep, steady-state power flow calculation using the Newton-Raphson method is performed in MATPOWER[11]. The solutions are checked to see if they violate grid constraints – voltage higher than ±10% of the nominal voltage and/or line current higher than 250 A. If they violate, a penalty value of difference between calculated value and the needed one is assigned to the solution in the main level.

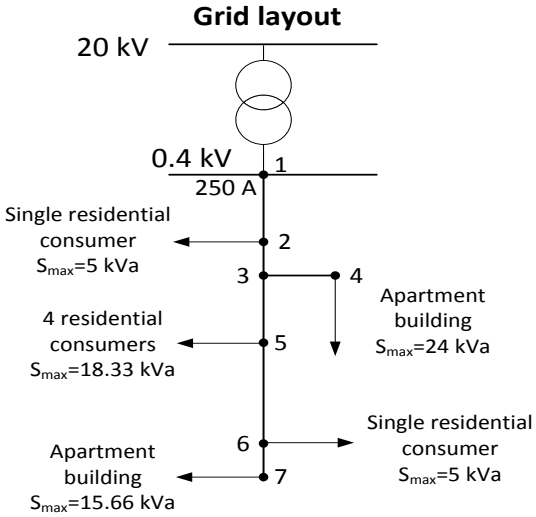

Line data

Sbase	100 kVA		
Vbase	0,4 kV		
Send node	Receive node	Resistance (p.u.)	Reactance (p.u.)
1	2	0,012425	0,00363125
2	3	0,0062125	0,001815625
3	4	0,02174375	0,0037625
3	5	0,012425	0,00363125
5	6	0,0186375	0,005446875
6	7	0,0062125	0,001815625

Figure 3: Electricity grid characteristics and line data.

RESULTS

Figure 4 shows the Pareto front obtained, consisting of 28 solutions (blue dots). In addition, grey dots show all evaluated solutions and red crosses solutions that violated either voltage or current constraints. In total there were 10,000 function evaluations. Looking at solutions that violated grid constraint, they are clustered at the lower part of the Pareto front. Lower carbon emissions optimal designs are not possible without upgrading the electrical grid in order that more distributed generation can be integrated. Also, it shows it is very important to include grid constraints in the optimisation of distributed energy systems.

Variable and objective functions values for all 28 optimal solutions are shown in Figure 5. Variables for each building are summed per solution and solutions are sorted by objective function. An increase of cost by 23% can give savings of 47% in carbon emissions when the cheapest solution (1550 k€, 5201 tCO_2) is compared to the most expensive (1916 k€, 2799 tCO_2). It can be clearly seen that PV capacity influences the objective functions the most. Looking at gas boiler, CHP and HP capacities, a small pattern can be observed. In the solutions where sum of CHP and HP capacity is higher than 140 kW, boiler capacity is lower than 300 kW. The reason is that boiler is not used anymore to cover the peak demand but only demand below the minimum part load of CHP and ASHP. Further decrease in carbon emissions is possible by installing more PV and CHP, but these solutions violate grid constraints. If decreasing emissions is imperative, installing batteries or upgrading the electrical grid is needed.

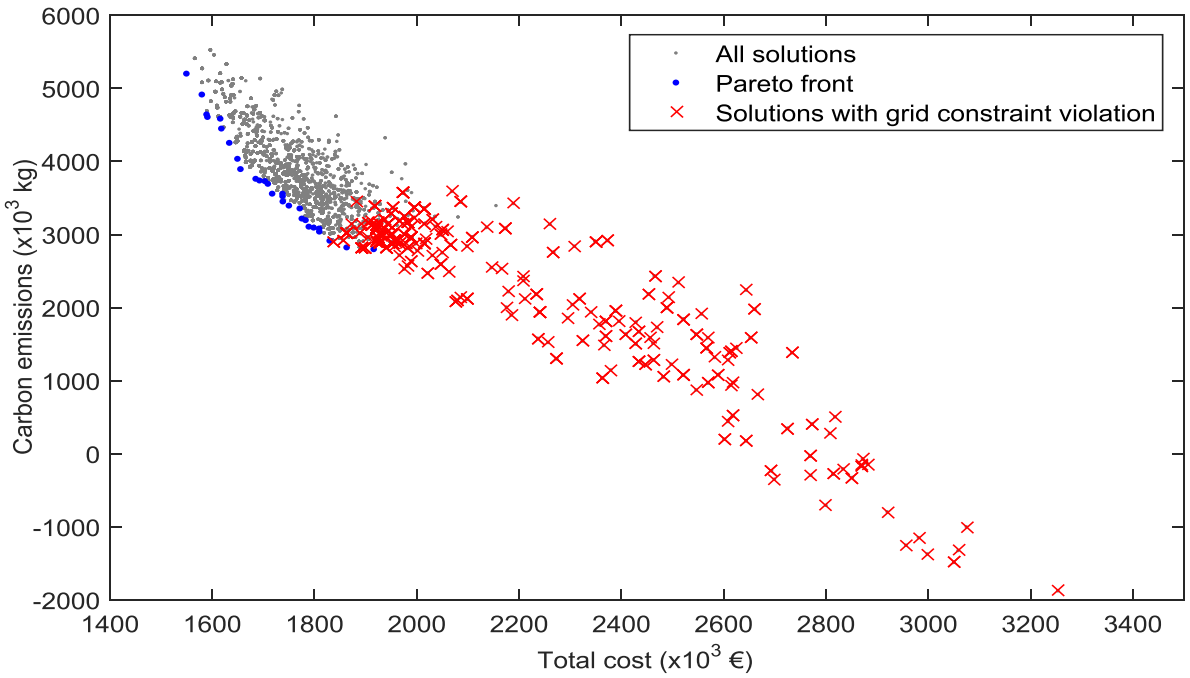

Figure 4: Results of the optimisation showing Pareto front, all solutions evaluated and solutions that violated grid constraint.

Solution	Boiler (kW)	PV (kWp)	CHP (kW)	ASHP (kW)	Heat storage (kWh)	Cost (k€)	Emissions (tCO2)
1	258	195	126	102	142	1916	2799
2	254	192	74	94	131	1863	2824
3	320	189	54	64	82	1830	2915
4	328	176	73	58	127	1809	3040
5	342	177	63	47	178	1809	3082
6	318	177	58	65	117	1798	3094
7	322	173	46	74	88	1789	3108
8	299	167	56	82	52	1782	3197
9	284	164	51	104	96	1775	3219
10	278	154	68	119	92	1771	3357
11	345	152	49	65	60	1750	3396
12	278	145	68	85	122	1738	3452
13	327	142	69	48	124	1738	3525
14	334	141	65	81	128	1737	3558
15	277	136	57	111	114	1717	3559
16	340	135	41	55	157	1709	3694
17	327	129	43	67	159	1703	3731
18	296	127	63	61	109	1692	3739
19	290	122	74	76	121	1685	3763
20	344	111	52	81	167	1655	3895
21	322	102	52	57	123	1649	4036
22	342	85	62	49	123	1633	4255
23	310	69	48	90	92	1618	4450
24	340	63	56	44	109	1616	4585
25	279	51	62	126	137	1591	4609
26	328	56	54	59	71	1589	4643
27	318	32	75	65	75	1580	4915
28	346	10	62	47	167	1550	5201

Figure 5: Capacity breakdown for each technology and objective functions.

CONCLUSIONS

A bi-level optimisation framework for distributed energy systems with the inclusion of non-linear power flow for grid constraints is presented. The framework consists of three interconnected parts: the NSGA-II algorithm for design, a MILP formulation for the optimal operation and steady-state power flow calculations for checking violation of grid constraints.

The results showed that it is important to include grid constraints when optimising DES, especially of low net emissions are targeted. Optimal solutions without violation of grid constraints are possible only down to value of 2799 tCO_2 compared to the overall possible minimum carbon emissions of -1980 tCO_2. Compared to the cheapest, emissions can be decreased by 47% with an increase of cost by 23%, with PV capacity being the most influential parameter. Further decrease in emissions is not possible without grid upgrades or inclusion of batteries.

REFERENCES

[1] E. D. Mehleri, H. Sarimveis, N. C. Markatos, and L. G. Papageorgiou, "Optimal design and operation of distributed energy systems: Application to Greek residential sector," *Renew. Energy*, vol. 51, pp. 331–342, Mar. 2013.

[2] A. Omu, R. Choudhary, and A. Boies, "Distributed energy resource system optimisation using mixed integer linear programming," *Energy Policy*, vol. 61, pp. 249–266, Oct. 2013.

[3] C. Weber and N. Shah, "Optimisation based design of a district energy system for an eco-town in the United Kingdom," *Energy*, vol. 36, no. 2, pp. 1292–1308, Feb. 2011.

[4] T. Gozel, M. H. Hocaoglu, U. Eminoglu, and A. Balikci, "Optimal placement and sizing of distributed generation on radial feeder with different static load models," in *2005 International Conference on Future Power Systems*, 2005, p. 2 pp.–6.

[5] H. Falaghi and M.-R. Haghifam, "ACO Based Algorithm for Distributed Generation Sources Allocation and Sizing in Distribution Systems," in *2007 IEEE Lausanne Power Tech*, 2007, pp. 555–560.

[6] F. Rotaru, G. Chicco, G. Grigoras, and G. Cartina, "Two-stage distributed generation optimal sizing with clustering-based node selection," *Int. J. Electr. Power Energy Syst.*, vol. 40, no. 1, pp. 120–129, Sep. 2012.

[7] K. Deb, A. Pratap, S. Agarwal, and T. Meyarivan, "A fast and elitist multiobjective genetic algorithm: NSGA-II," *IEEE Trans. Evol. Comput.*, vol. 6, no. 2, pp. 182–197, Apr. 2002.

[8] M. Geidl, G. Koeppel, P. Favre-Perrod, B. Klockl, G. Andersson, and K. Frohlich, "Energy hubs for the future," *IEEE Power Energy Mag.*, vol. 5, no. 1, pp. 24–30, 2007.

[9] B. Morvaj, R. Evins, and J. Carmeliet, "Optimal selection and operation of distributed energy resources for an urban district," in *Engineering Optimization 2014*, CRC Press, 2014, pp. 709–714.

[10] S. Papathanassiou, N. Hatziargyriou, and K. Strunz, "A benchmark low voltage microgrid network," in *Proceedings of the CIGRE Symposium: Power Systems with Dispersed Generation*, 2005, pp. 1–8.

[11] R. D. Zimmerman, C. E. Murillo-Sánchez, and R. J. Thomas, "MATPOWER: Steady-state operations, planning, and analysis tools for power systems research and education," *Power Syst. IEEE Trans.*, vol. 26, no. 1, pp. 12–19, 2011.

DISTRIBUTED ENERGY SYSTEMS SCENARIO MODELING FOR A RURAL AGGLOMERATION IN SWITZERLAND: A CASE STUDY

M. Yazdanie[1]

1: Laboratory for Energy Systems Analysis, Paul Scherrer Institute, CH-5232 Villigen PSI

ABSTRACT

Today's electricity generation and distribution systems are characterized by large-scale, centralized technologies. However, as distributed energy technologies become more readily available and affordable, their role in future energy networks must be evaluated. This study assesses the role of distributed energy technologies in a Swiss rural agglomeration using a cost optimization, energy systems modeling approach until 2050. Three main scenarios are considered: a baseline scenario in which future technology options reflect the existing infrastructure; a decentralized scenario which introduces suitable decentralized energy technologies without considering storage; and a decentralized scenario which additionally includes storage. A carbon tax is also applied in a sub-scenario which penalizes oil-based technology investments. In the baseline scenario, it is found that although the energy supply mix does not vary significantly until 2050, there is a technology shift from district heating to more decentralized and efficient wood boilers, as well as heat pumps. The main investment introduced through the decentralized scenario without storage is a run-of-river plant. This plant reduces the dependency of the village on electricity imports from the national grid by 35% by utilizing 43% of the total, local hydro potential. In the storage scenario, the run-of-river plant is replaced by a hydro dam which can achieve an electricity import reduction of 65%, alongside a 6% reduction in system costs compared to the baseline scenario. This is achieved through full utilization of the local hydro potential via seasonal storage. The introduction of a carbon tax to the model results in a significant replacement of oil boilers with heat pumps, as long as electricity network upgrade costs are not prohibitively expensive. Overall, the results indicate that distributed energy technologies (including storage) offer the potential to increase energy independence and achieve system cost savings for rural agglomerations with sufficient, local, natural resource potential in Switzerland.

Keywords: decentralized energy, distributed energy, storage, cost optimization, rural, case study

INTRODUCTION

Centralized generation technologies have long formed the beating heart of power production and distribution systems worldwide. These systems are characterized by large-scale generation, typically requiring the transmission of electricity over long distances. They have offered important benefits in the past, such as economies of scale, which have led to their widespread adoption. However, as new technologies are developed and sustainability goals come into focus on a national scale, decentralized generation strategies must also be considered as part of the design of our future energy networks.

Decentralized energy technologies (DETs) are characterized by relatively small scale applications. They offer modularity and flexibility, and are typically situated close to loads. Distributed energy strategies offer the possibility to design more energy- and cost-efficient networks [1], [2]. Local heat and electricity production may be coupled with storage options and load management, and DETs can also enable increased energy security and independence.

The purpose of this case study is to gain insight into the impacts and potential benefits of integrated, decentralized, energy-adaptive systems for a rural village in Switzerland. Both electricity and heat generation are considered. It is of interest to compare the business-as-usual case with cases introducing decentralized generation technologies, including storage options, through energy system and scenario modeling from 2010-2050.

METHOD

A least-cost optimization modeling approach is applied in this investigation. A number of scenarios are developed, modeled, analyzed, and compared in order to gain insight into the application of decentralized generation and storage systems in a rural setting.

Modeling Framework

The cost optimization model for this case study is developed using the TIMES framework. TIMES is a bottom-up, energy systems, cost optimization modeling tool developed by the International Energy Agency (IEA) [3]. It enables the development of dynamic, perfect-foresight models and determines the cost optimal evolution of capacity allocation and dispatch for specified scenarios over the modeling timeframe. The model captures the entire energy system and conversion chain. For the village in this case study, major sectors include residential and commercial/services. End-use energy demand includes building space heating, domestic hot water, and electricity.

Scenarios

Three main scenarios are developed for the case study. The baseline scenario reflects the existing energy infrastructure of the agglomeration. Only existing technologies are available as investment options. For heat generation, this includes conventional boilers (oil, wood, and electric), heat pumps, solar thermal heating, and district heating using a wood boiler and biogas CHP. Electricity demand is otherwise met by the grid (centralized production) only.

The second scenario, decentralized without storage, introduces decentralized heat and electricity generation technologies in addition to the baseline options. This includes small hydro (run-of-river), photovoltaics, wood micro CHP for individual buildings, and wood and oil CHP for district heating. These technology options have been selected based on their suitability to the agglomeration.

In the third scenario, decentralized with storage, hydro storage is considered in addition to the decentralized and baseline options of the preceding scenarios. A sub-scenario is also included which introduces a carbon tax.

Case Study Inputs and Assumptions

The annual energy demand by energy carrier is depicted in Figure 1 for the rural agglomeration in 2010. End-use energy demand for heating and electricity by sector remains constant in the model. The village is further segmented into six building categories, differentiated by function and age [4]. Hourly load curves for space heating for each building type have been defined for the study; and hydro, solar, and wood resource potentials for the village are also applied according to [4].

Technology parameters and cost input data are defined within the TIMES STEM family of models for Switzerland [5], [6] . Oil prices are adapted for Switzerland according to the IEA 4D scenario [6], and the CO_2 price is zero unless otherwise specified. If applied, CO_2 prices are used from the Swiss Energy Perspectives 2050 study, business-as-usual scenario [7]. Wood prices are based on Swiss statistics and vary with oil price fluctuations [8]. The cost for

electricity from the grid is exogenous to the model and remains constant according to current electricity prices [9].

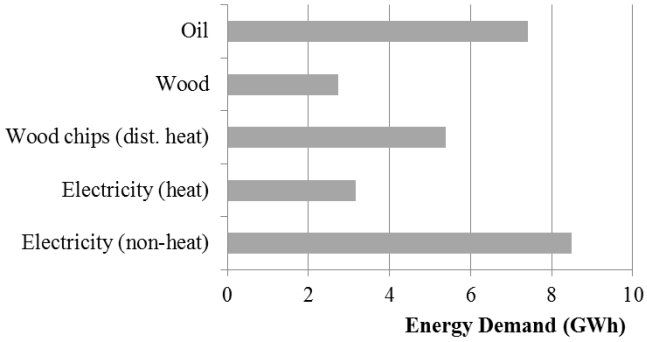

Figure 1: Annual energy demand by energy carrier in 2010 for the rural agglomeration

RESULTS & DISCUSSION

Baseline Scenario

Figure 2 illustrates the total installed capacity across heat generation technologies in the baseline scenario (a), as well as the energy supply mix (b).

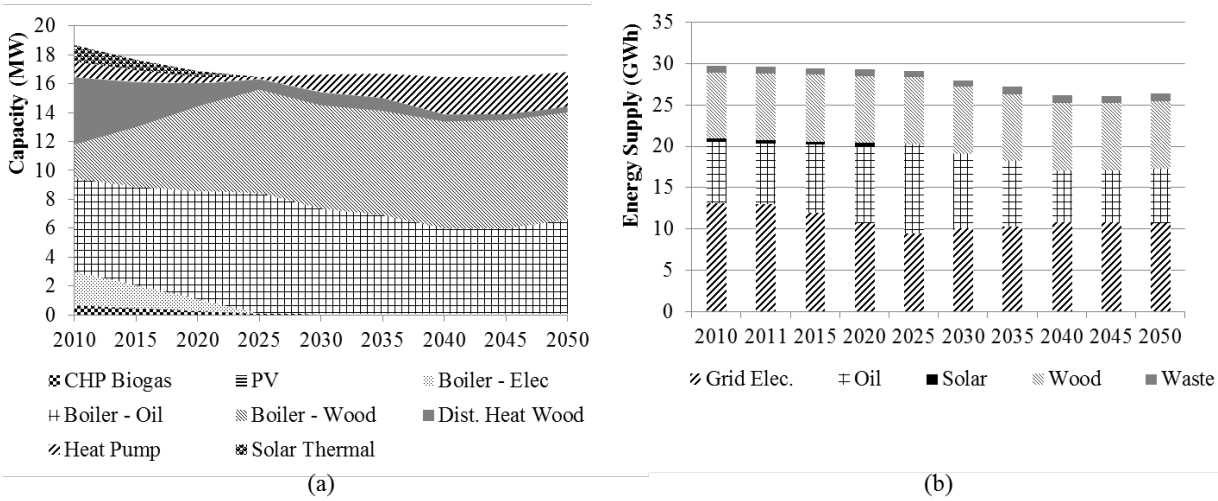

Figure 2: Baseline scenario: total installed capacity (a) and energy supply mix (b) until 2050

In the baseline scenario, oil, wood, and electricity continue to dominate the energy supply mix until 2050 with approximately the same shares as in 2010. However, a significant shift in the technology mix occurs. District heating using wood is replaced with more efficient and less costly wood boilers, electric boilers are replaced with more efficient heat pumps, and solar energy technologies are phased out altogether given the high cost of investment. The waste resource potential, although relatively small, continues to be entirely utilized by CHP biogas from 2010 until 2050. Local wood resources are also entirely utilized over the time horizon.

Decentralized Scenario without Storage

The energy supply mix and total installed capacity across heat and electricity generation technologies is illustrated in Figure 3 for the decentralized scenario without storage.

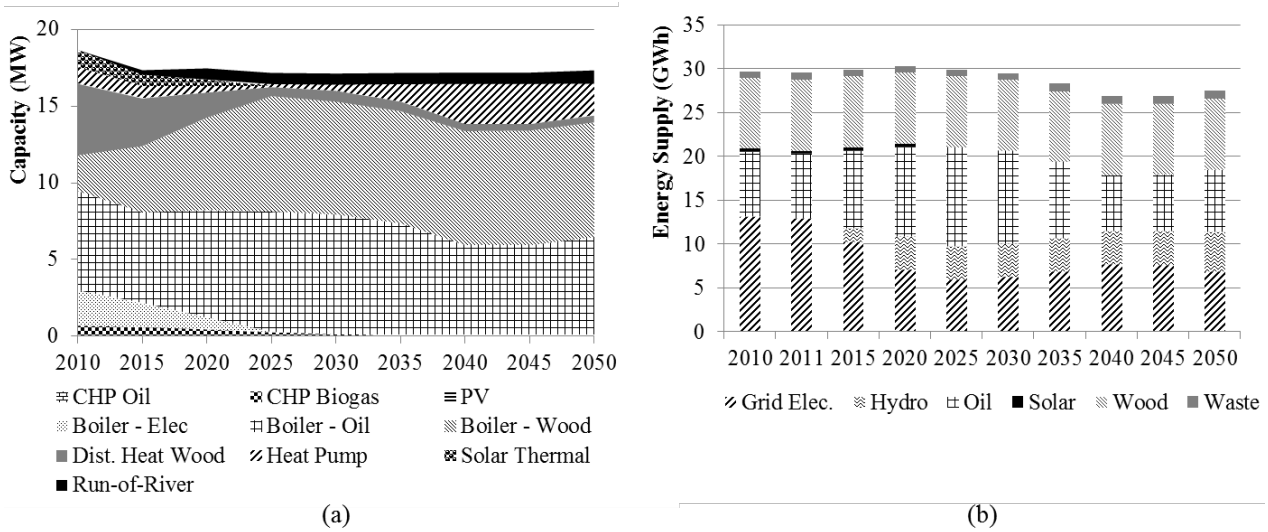

Figure 3: Decentralized scenario without storage: total installed capacity (a) and energy supply mix (b) until 2050

Similar results are found for heating technology investments in the decentralized scenario compared with the baseline case. Newly introduced decentralized heating options (CHP and micro CHP) are not selected given their high investment cost. However, investment in small hydro takes place beginning in 2015 for decentralized electricity generation. The investment in run-of-river enables a significantly reduced dependency on electricity from the grid; electricity imports are reduced by 35% in 2050 for the decentralized case compared to the baseline (centralized) case. The run-of-river plant also enables a small increase in heat pump investment. However, without the possibility of storage, only 43% of the total hydro potential is utilized (as low winter flows occur when heat demand is high, and high summer flows occur when heat demand is low). Therefore, a storage option is considered in the next case.

Decentralized Scenario with Storage

Figure 4 depicts the installed capacity and energy supply mix for the decentralized scenario with an additional hydro dam storage option.

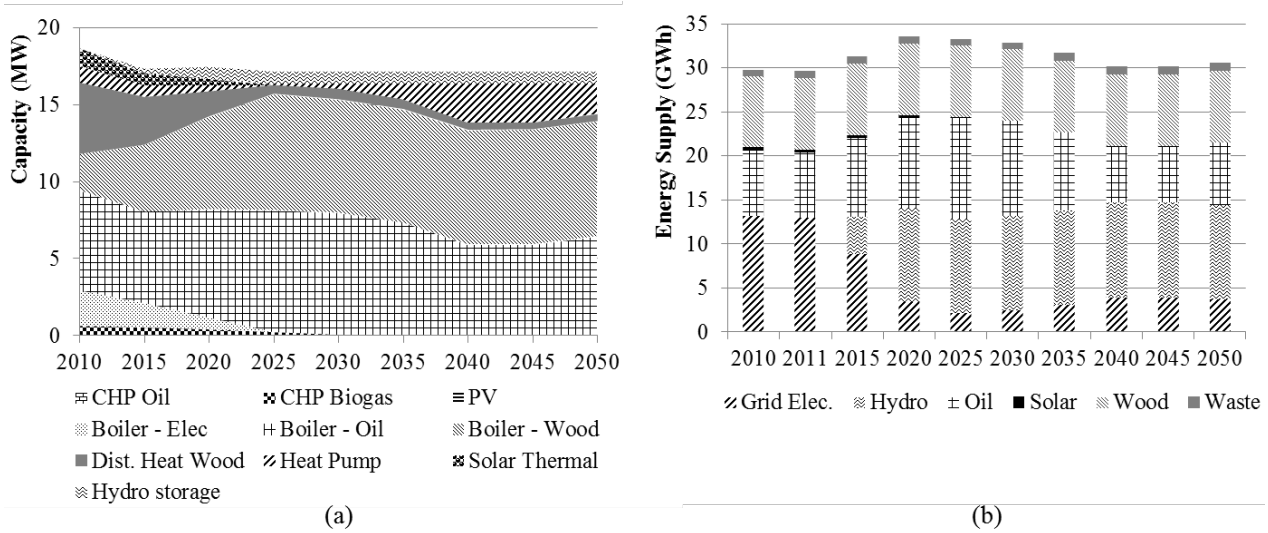

Figure 4: Decentralized scenario with storage: total installed capacity (a) and energy supply mix (b) until 2050

The run-of-river plant is replaced completely by the small hydro storage plant. The ability to store water enables 100% utilization of the local hydro potential (compared to 43% in the previous case). Water is stored over the spring, summer, and fall seasons, and is discharged during winter. The introduction of the hydro dam enables a 65% reduction in electricity grid imports in 2050 compared to the baseline scenario. This translates to a 6% reduction in total system costs. Overall, hydro storage enables a significant increase in the energy independence of the rural agglomeration in conjunction with system cost savings.

Carbon Taxed Decentralized Scenario with Storage

A carbon tax is introduced to the decentralized scenario with storage. This price varies from 15.20 CHF/ton CO_2 in 2010 to 56.70 CHF/ton CO_2 in 2050. The effect of the carbon tax on capacity investment and the energy supply mix is illustrated in Figure 5. A significant decrease in oil boiler investment and use occurs until 2040, when oil consumption is approximately 35% lower compared to the baseline scenario in the same year. Oil is replaced with heat pumps, whose capacity increases 88% by 2040 compared to the baseline scenario.

After 2040, the trend appears to reverse and heat pumps are gradually replaced with oil heating. This occurs due to the gradual retirement of the existing electricity transmission and distribution network. It is more costly to invest in upgrading and maintaining the electricity network than it is to use oil, even with an increasing carbon tax, according to the model parameters. This illustrates the significant role that the cost of network upgrades can play in defining the cost optimal system.

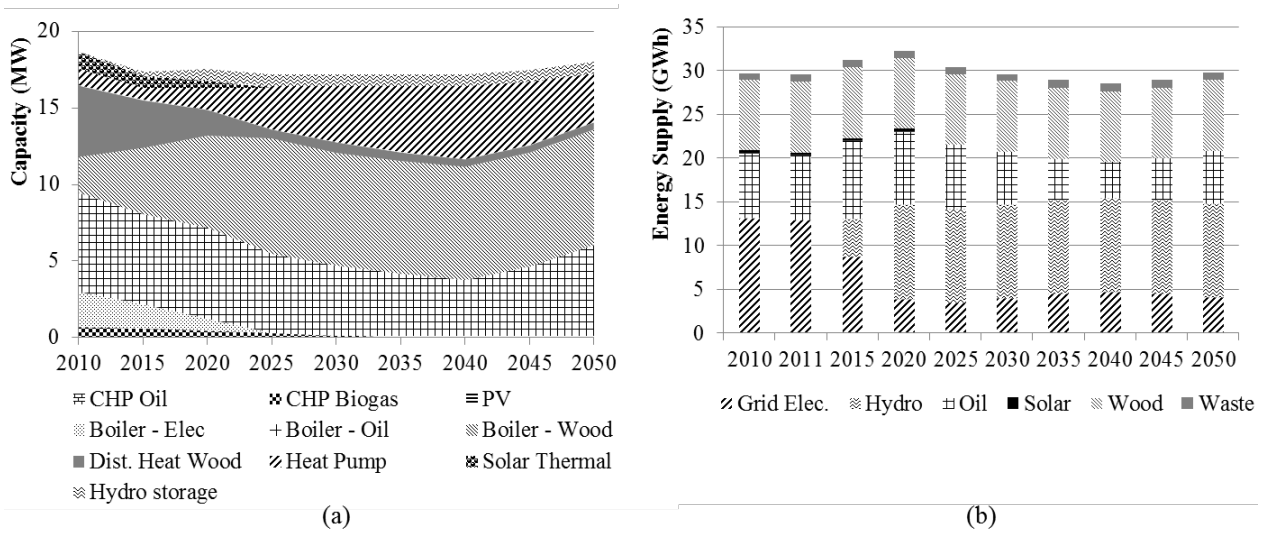

Figure 5: Decentralized scenario with storage and carbon tax: total installed capacity (a) and energy supply mix (b) until 2050

CONCLUSION

The selection of results presented in this study illustrates some of the impacts of decentralized energy technologies on cost-optimal investment decisions until 2050 for a rural agglomeration in Switzerland.

The relaxation of the baseline model to include decentralized electricity and heat generation technology options until 2050 resulted primarily in small hydro (run-of-river) investment for electricity generation. The run-of-river plant enabled a 35% reduction in electricity grid imports in 2050 using 43% of the total hydro potential. CHP and solar technology options

were not selected as cost optimal solutions, indicating that further cost reductions are needed for these technologies.

The relaxation of the decentralized model to further include storage resulted in the replacement of run-of-river with a hydro dam. Seasonal dammed storage enabled 100% utilization of the total hydro potential with a 65% reduction in electricity imports in 2050 compared to the baseline scenario. Additionally, system costs were reduced by 6%, indicating that hydro storage is a financially feasible option even for small, rural agglomerations.

The investment in CO_2-emitting oil boilers was also noticeably reduced under the implementation of a carbon tax. However, an eventual return to oil may occur if electricity network upgrade and maintenance costs are prohibitively expensive for rural applications.

Overall, it is found that system cost savings and increased energy independence can be achieved for the rural agglomeration through the full-scale utilization of local wood and hydro resources to meet energy demand. A deeper sensitivity analysis will be conducted in the next phase of this study, alongside further scenarios introducing additional storage technologies.

REFERENCES

[1] H. a. Gil and G. Joos, "Models for Quantifying the Economic Benefits of Distributed Generation," *IEEE Trans. Power Syst.*, vol. 23, no. 2, pp. 327–335, May 2008.

[2] V. H. Méndez, J. Rivier, J. I. D. La Fuente, T. Gómez, J. Arceluz, J. Marín, and a. Madurga, "Impact of distributed generation on distribution investment deferral," *Int. J. Electr. Power Energy Syst.*, vol. 28, no. 4, pp. 244–252, May 2006.

[3] R. Loulou, U. Remne, A. Kanudia, A. Lehtila, and G. Goldstein, "Documentation for the TIMES Model," 2005.

[4] K. Orehounig, G. Mavromatidis, R. Evins, V. Dorer, and J. Carmeliet, "Towards an energy sustainable community: An energy system analysis for a village in Switzerland," *Energy Build.*, vol. 84, pp. 277–286, Dec. 2014.

[5] K. Ramachandran and H. Turton, "Documentation on the Development of the Swiss TIMES Electricity Model (STEM-E)," Villigen, 2011.

[6] Energy Economics Group, "CHP SWARM 2nd Annual Report," Villigen, 2014.

[7] A. Kirchner, D. Bredow, F. Dining, T. Grebel, P. Hofer, A. Kemmler, A. Ley, A. Piegsa, N. Schütz, S. Strasbourg, J. Struwe, and M. Keller, "Die Energieperspektiven für die Schweiz bis 2050," 2012.

[8] Swiss Forest Owner's Association, "Swiss Forest Owner's Association." [Online]. Available: http://www.wvs.ch/. [Accessed: 22-Apr-2015].

[9] Federal Electricity Commission Elcom, "Basic Data for Tariffs of the Swiss Distribution Network Operators," *2010 Tariffs*, 2010. [Online]. Available: http://www.elcom.admin.ch/themen/00002/00097/index.html?lang=de. [Accessed: 22-Apr-2015].

LONG WAVE RADIATION EXCHANGE FOR URBAN SCALE MODELING WITHIN A CO-SIMULATION ENVIRONMENT

Clayton Miller[1], Daren Thomas[1], Jérôme Kämpf[2]; Arno Schlueter[1]

[1] *Architecture and Building Systems (A/S), Institute of Technology in Architecture (ITA), ETH Zürich, Zürich, Switzerland*
[2] *Solar Energy and Building Physics Laboratory (LESO-PB), Ecole Polytechnique Fédérale de Lausanne (EPFL), Lausanne, Switzerland*

ABSTRACT

This paper describes the implementation of long wave radiation (LWR) exchange as part of a co-simulation process of an urban scale simulation program, CitySim, and a building scale program, EnergyPlus. This coupling process was achieved through the use of functional mockup units (FMU) to exchange various weather, load, and environmental information between the two simulation engines. LWR is an important factor to exchange between the programs as CitySim has more advanced capabilities for radiation exchange calculations from a set of urban buildings and EnergyPlus has a more advanced building heating and cooling load calculation engine. The LWR exchange between surfaces is computed in CitySim by a linearization of the longwave energy balance at each surface around an average between the surface and its environmental temperatures. The environmental temperature for each surface is determined using the simplified radiation algorithm neglecting inter-reflections and is aggregated into a single, global environmental radiant temperature (T_{env}). The LWR exchange process is implemented in EnergyPlus by CitySim sharing the variables T_{env} and h_{env} that are then used to calculate radiation gain or loss through the envelope as well as influence on the conductances of the surfaces. This approach overrides the conventional EnergyPlus ground, sky and air radiation calculations. Solo and coupled simulations are performed on a set of four scenarios and result in up to a 36% discrepancy in heating and 11% in cooling load calculations amongst solo and coupled simulations.

Keywords: Urban-scale simulation, Co-simulation, Long Wave Radiation Exchange

INTRODUCTION

Today about 50% of the worlds population lives in urban areas and is expected to grow to 66% by 2050 [1]. Collectivities, urban planners and stakeholders will therefore have to face major energetic issues during the next decades. Urban energy simulation tools are becoming more common in order to simulate these environments for planning purposes. However, when simulating only one building within an urban district (for a retrofit action for example), actual detailed building simulation engines have the drawback of not taking into account the adjacent buildings in their calculations (obstructions and energy exchange). One way to address this issue is to establish a co-simulation environment between urban and building energy simulation engines to benefit from both advantages - the urban environment and a detailed output for one considered building.

One effort in coupling and co-simulation pairs the widely used building simulation engine, EnergyPlus, with the urban-scale simulation engine, CitySim [2]. This approach establishes a link between the two programs using a functional mockup interface (FMI) and a work-flow automation process. The co-simulation process enables the exchange of outdoor conditions between CitySim and EnergyPlus. This feature enhances EnergyPlus simulations due to CitySim's ability to calculate urban scale conditions in a more detailed means than the conventional typical weather file method. This exchange sends the outdoor air drybulb and wetbulb temperatures, relative humidity, diffuse and direct solar radiation, and wind speed and direction to EnergyPlus at each simulation time-step in exchange for surface outside face temperatures and heating and cooling loads. The last missing step in this effort is to couple environmental long wave radition (LWR) between the engines, a variable that has been shown to have a non-trivial impact on heating and cooling loads [3].

This paper outlines the addition of LWR exchange to the list of variables coupled between the two simulation engines. Coupling this variable enhances the building-scale simulation within EnergyPlus by allowing for radiant heat gain or loss to adjacent surfaces. As is, EnergyPlus does not take these characteristics of adjacent buildings and surfaces into consideration. LWR exchange has been implemented in EnergyPlus previously by implementing new input variables into the engine that specify the radiant heat transfer coefficients of nearby obstruction surfaces [3]. This approach used flat-file schedules and hard-coded variables containing the necessary radiation input data at each time step of the simulation in order to emulate radiation exchange with these surfaces. The novelty in our implementation is the coupling of EnergyPlus with the CitySim program that will provide a comprehensive LWR calculation automatically and in a reusable manner.

METHODOLOGY

Long Wave Radiation Exchange Calculation

In EnergyPlus, LWR exchange for a surface is calculated through the summation of radiation gain from the ground, sky, and air as seen in Equation 1 and Figure 1a [4]. The radiant heat transfer coefficient for each of these environmental variables is calculated according to Equation 2 with σ as the Stefan-Boltzmann constant and ϵ as the emissivity. A major assumption of this approach is that the modeled building's surfaces and those of adjacent buildings are at a uniform temperature and the LWR radiation exchange is negligible; a situation that is an oversimplification in an urban scale domain [3].

$$Q_{LWR,EnergyPlus} = h_{r,grd}(T_{surf} - T_{grd}) + h_{r,sky}(T_{surf} - T_{sky}) + h_{r,air}(T_{surf} - T_{air}) \quad (1)$$

$$h_{r,variable} = \frac{\epsilon\sigma(T_{surf}^4 - T_{variable}^4)}{T_{surf}^4 - T_{variable}^4} \quad (2)$$

In comparison, CitySim calculates LWR exchange by calculating an aggregated equivalent temperature, T_{env}, and radiative heat transfer coefficient, $h_{r,env}$, from surrounding urban surfaces in addition to ground, sky, and air [5]. The calculation for T_{env} is expressed in Equation 3 with the F values being view factors of the surrounding environment including adjacent surfaces $i = 1..n$. $h_{r,env}$ is based on a first order Talyor development of Equation 2 around $(T_{surf} + T_{variable})/2$. $Q_{LWR,CitySim}$ is calculated using Equation 4.

$$\sigma T_{env}^4 = \sigma F_{sky} T_{sky}^4 + \sigma F_{grd} T_{grd}^4 + \sum_{i=1}^{n} \epsilon_i \sigma F_i T_i^4 \quad (3)$$

$$Q_{LWR,CitySim} = h_{r,env}(T_{surf} - T_{env}) \quad (4)$$

In the proposed coupled simulation, EnergyPlus uses the CitySim supplied equivalent $h_{r,env}$ and T_{env} to calculate weighted $h_{r,sky}$, $h_{r,grd}$, and $h_{r,air}$ values using the view factors and the sky-to-air split ratio. Figure 1 illustrates the schematic differences between the solo and coupled simulations on a theoretical example of a target building with two adjacent buildings with surfaces available for radiation exchange.

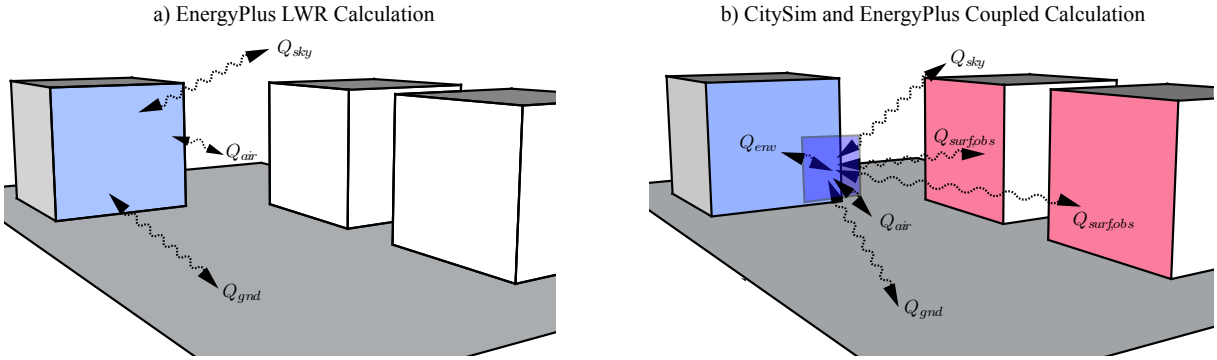

Figure 1: Comparison of the LWR components between a) Solo EnergyPlus and b) Coupled CitySim/EnergyPlus configuration)

Simulation Coupling and Co-Simulation

Simulation engine coupling is accomplished through a work-flow automation process that extracts geometry from a building information model, converts the geometry to EnergyPlus and CitySim simulation models and simulates two solo simulations and two coupled simulations. Figure 2 illustrates the adapted single-zone, theoretical coupling scenario and work flow configuration from previous research that is adapted for the experiments in this methodology [2].

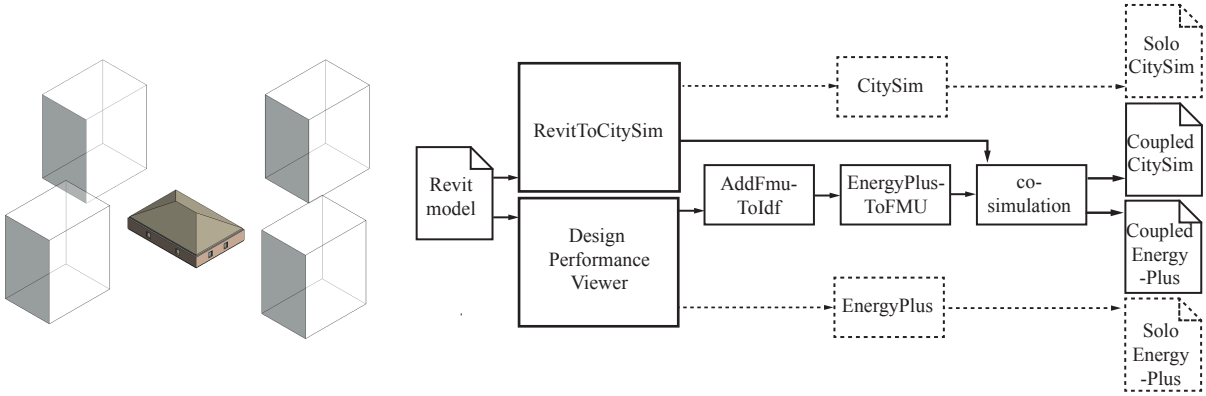

Figure 2: (left) Theoretical, single-zone test model surrounded by four buildings, and (right) overview diagram of the coupling process (adapted from [2])

Experimental Scenarios

Four scenarios, seen in Table 1, are designed in order to illustrate the LWR exchange impact. These experimental scenarios simulate EnergyPlus in four combinations of solo versus coupled and non-surrounded versus surrounded. Scenarios 1 and 2 include the

solo and coupled simulations in the absence of surrounding buildings, while 3 and 4 are the same with the surrounding buildings included. The scenarios all have constant base internal loads and use weather data for Zürich, Switzerland. Infiltration and ventilation loads are not included in any of the scenarios.

Scenario	Label	Description
1_S_NS	Solo No Surrounding	EnergyPlus without neighboring buildings
2_C_NS	Coupled No Surrounding	Co-simulation without neighboring buildings
1_S_WS	Solo With Surrounding	EnergyPlus with all neighboring buildings
4_C_WS	Coupled With Surrounding	Co-Simulation with all neighboring buildings

Table 1: Experimental scenarios for demonstrating co-simulation and LWR exchange

RESULTS AND DISCUSSION

After executing the automated work flow process for the four experimental scenarios, an analysis is presented of the LWR calculation input variables and heating and cooling load impact. Figure 3 illustrates a comparison of the average outside surface temperatures of the target buildings to the sky, ground, and air temperature and the T_{env} variables from the coupled scenarios. The target building surface temperatures are, in general, higher than the T_{sky}, T_{gnd}, T_{air} and T_{env} in the outlined scenarios. This situation results in LWR loss to the environmental surroundings, a phenomenon that could be the opposite in many other practical scenarios when the adjacent building surfaces have high enough surface temperatures or emissivity to produce a T_{env} value that is above the target building's surface temperatures.

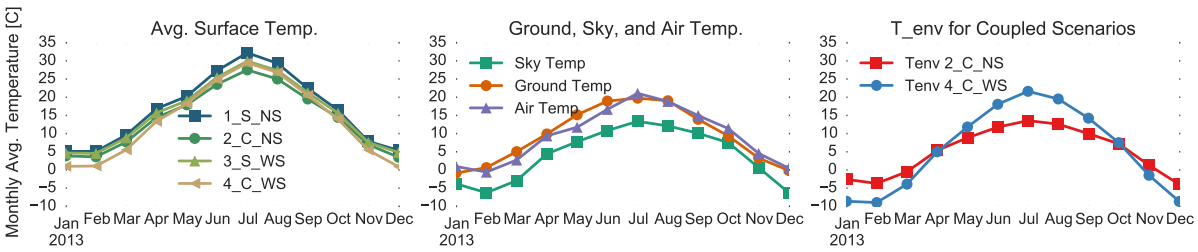

Figure 3: Average annual sky, ground and air temperatures as compared to average outside surface temperatures of targeted building within EnergyPlus

Figure 4 shows a comparison of the radiative heat transfer coefficients. The h_{sky}, h_{gnd}, and h_{air} values for the coupled simulations are calculated within EnergyPlus from the h_{env} value that is passed from CitySim. The coupled simulations result in higher h values due to the surrounding surfaces, resulting in more radiative heat transfer.

Figure 5 illustrates the resultant net thermal radiation summation of all surfaces in the target buildings represented as an average across January, for the heating season, and July, for the cooling season. The higher h values calculated from the CitySim coupling combined with cooler surrounding environmental temperatures results in an increase in LWR exchange in scenarios 2 and 4.

Figure 6 illustrates the impact that coupling has with respect to heating energy consumption. The heating consumption for the coupled simulations is higher by 15 and 36% as

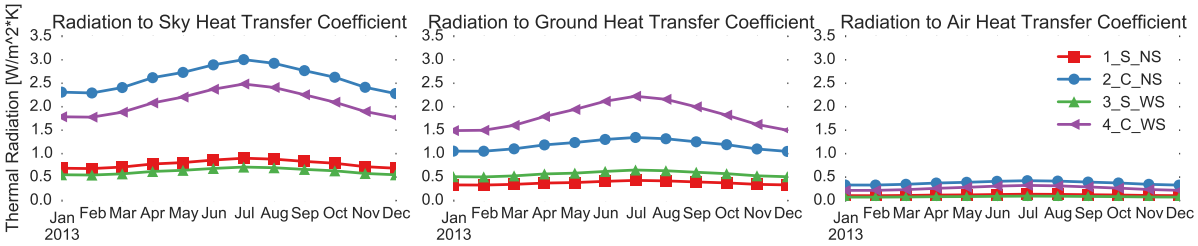

Figure 4: Average annual sky, ground and air radiative heat transfer coefficients within EnergyPlus

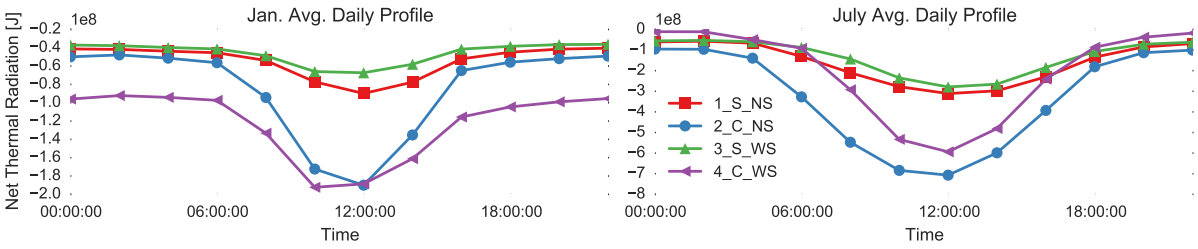

Figure 5: Net thermal radiation summation for all surfaces in target building for January and July

compared to the solo baseline. The emissivities of the surrounding surfaces are 0.9 by default, thus creating cooler radiant temperatures and elevated h values and resulting in net LWR loss to the surroundings, especially at night. These percentages should be interpreted carefully as the scenario developed is envelope dominated and doesn't include ventilation and infiltration loads.

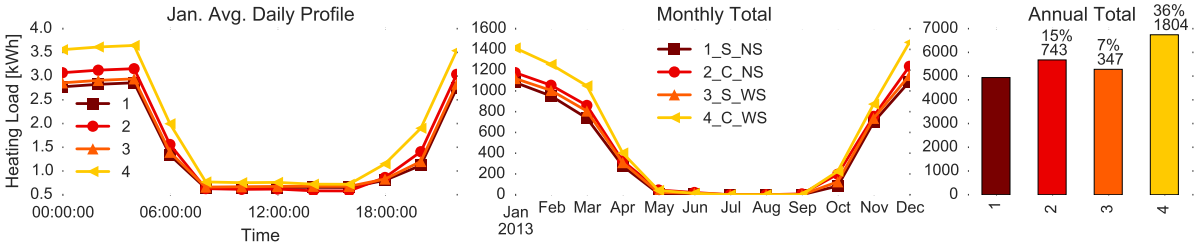

Figure 6: Daily average and monthly and annual total heating load calculation results

Figure 7 reflects the impact that coupling has on cooling energy consumption. The cooling consumption differences show a consistent offset amongst the scenarios across the course of a day and are larger in the summer months. The percentage difference for cooling is lower than heating with a maximum offset of 11%. This decrease in cooling load is also due to the net radiation loss of the target building due to surrounding surfaces emissivities and therefore cooler radiant temperatures and h values. The results of the cooling load calculation should be interpreted only in the context of the scenarios in this study. Scenarios designed with adjacent surfaces that are much warmer than those of the target building could result in a net LWR gain and produce higher cooling loads on hot days.

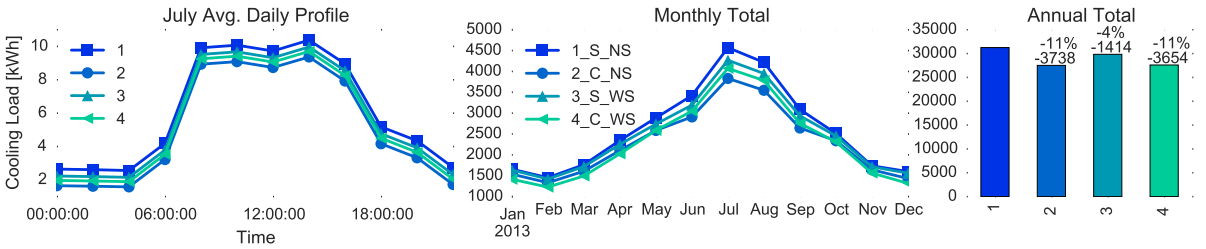

Figure 7: Daily average and monthly and annual total cooling load calculation results

CONCLUSION

This paper describes the addition of LWR exchange within an existing coupling and co-simulation process of two common building performance simulation programs, EnergyPlus at the building level, and CitySim at the urban scale. The exchange of LWR information from CitySim is utilized to overcome the simplification assumptions existent in the EnergyPlus engine, namely that the radiation exchange with surrounding surfaces is negligible. A set of theoretical scenarios illustrates that a coupled EnergyPlus simulation predicts cooling and heating loads that are different from solo simulations by up to 36%. These results are specific only to the scenarios outlined and are not generalizable, however the methodology of LWR exchange in a coupled environment has been validated. The next step within this research effort is to apply the coupled co-simulation environment on a real-world case study project and validate the scenarios using measured data.

ACKNOWLEDGEMENTS

Funding for this project was provided by an ETH Zürich Institute of Technology in Architecture (ITA) Fellowship and the Swiss Competence Center Energy and Mobility (CCEM) through the Urban Multi-scale Energy Modeling (UMEM) project.

REFERENCES

1. United Nations Department of Economics and Social Affairs Popluation Division: *World urbanization prospects: The 2014 revision.* 2014.
2. Thomas, D., Miller, C., Kämpf, J., and Schlueter, A.: Multiscale co-simulation of EnergyPlus and CitySim models derived from a building information model. In *Bausim 2014: Fifth German-Austrian IBPSA Conference*, pages 469–476, 2014.
3. Evins, R., Dorer, V., and Carmeliet, J.: Simulating external longwave radiation exchange for buildings. *Energy and Buildings*, 75:472–482, June 2014.
4. United States Department of Energy (DOE): EnergyPlus Engineering Reference Version 8.2: The Reference to EnergyPlus Calculations. *The Reference to EnergyPlus Calculations*, 2015.
5. Robinson, D., Haldi, F., Kämpf, J., Leroux, P., Perez, D., Rasheed, A., and Wilke, U.: CitySim: Comprehensive micro-simulation of resource flows for sustainable urban planning. In *Proceedings of BS2009: 11th International Building Performance Simulation Association Conference*, Glasgow, Scotland, July 2009.

A BUILDING SPECIFIC, ECONOMIC BUILDING STOCK MODEL TO EVALUATE ENERGY EFFICIENCY AND RENEWABLE ENERGY

C. Nägeli[1]; M. Jakob[2]; B. Sunarjo[2]; G. Catenazzi[2];

1: Department of Civil and Environmental Engineering, Chalmers University of Technology, Sven Hultins gata 8, 412 96 Gothenburg, Sweden

2: TEP Energy GmbH, Rotbuchstrasse 68, 8037 Zürich, Switzerland

ABSTRACT

In developed countries, the residential and commercial building stock account for a considerable share of final energy demand and greenhouse gas emissions. Building stock modeling is an established tool to assess different development paths of buildings on city, region or country level. Current building stock models (BSM) as well as previous works of the authors, however, lack a holistic approach that take technological, economic and ecological factors into account on an individual building scale. There are, therefore, limitations in the conclusions that can be drawn. In order to increase their significance, current research shows trends towards spatial differentiation, representation of individual building and owners as well as economic decision modeling. However, no model combines all three aspects in a more holistic approach. This paper describes a novel approach which combines spatial differentiation with building specific heat demand modeling and an economic decision simulation.

The model developed combines a building specific engineering model with a micro-economic discrete choice approach. Using spatial building data, the engineering model calculates space heat and hot water energy demand on a building level. The alteration of the building refurbishment state is modeled using a discrete choice approach to simulate the decision process of building owners of building envelope refurbish and/or to substitute the heating system. Due to the building specific approach, the decision model is able to take into account building specific information such as size, geometry, room temperature, investment, maintenance and energy costs and achievable energy savings as well as other factors such as local potentials and restrictions on the use of renewable energy.

In a case study of the city of Zürich we demonstrate the feasibility and strengths of the new model approach. The results demonstrate that modeling space heating demand on an individual building scale yields specific heat demand distribution across building clusters (and not simply in average values as in other models). The building level approach enables the model to deliver differentiated results of the heat demand development for the whole building stock, building types building periods or spatially distributed as shown in the results.

Keywords: building stock model, energy efficiency, discrete choice model, energy planning, policy evaluation

INTRODUCTION

In developed countries, the residential and commercial building stock account for a considerable share of final energy demand and greenhouse gas emissions. As a consequence, policy makers in both the European Union and Switzerland are implementing stricter and stricter efficiency standards for new as well as existing buildings [1, 2] and have set ambitious reduction targets. However, especially for urban areas making use of the potentials for energy-efficiency and renewable energy poses numerous challenges. Moreover, clear pathways for the transformation of the built environment to reach energy and GHG reduction targets are lacking.

Building stock models (BSM) are used to develop and evaluate different such pathways and improve the understanding of the specific potentials and challenges in the development of the building stock. BSMs include a variety of different modelling techniques which are used to describe both the energy demand of the current as well as possible development scenarios for the future building stock. [3] gives an overview of the different modeling techniques available. More recent development in the field including previous work by the authors show trends towards spatial differentiation [4, 5], as well as including economic factors for optimal use of local potentials [6].

While the level of detail of BSM keeps increasing, the examples mentioned above, however, still rely on representative building archetypes based on average geometries. This reduces the complexity of these models as well as the computational time, however limits the accuracy of the model on a building level [7], which can affect the development of transformation strategies. Therefore, in order to increase the accuracy of BSM to give more meaningful information for the development of transformation pathways the individual building needs to be considered [8]. The representation of individual buildings not simply increases the accuracy of the energy demand model, but also enables a detailed modeling of refurbishment and heating system substitution processes. Instead of relying on average refurbishment rates, a building specific evaluation of the costs and benefits of different energy efficiency and renewable energy measures can be modelled.

This paper describes the further development of the building stock model previously developed by the authors [4, 9, 10] to combine spatial differentiation with a building specific heat demand model and an economic decision simulation to model the development of the building state.

MODEL CONCEPT

The bottom-up simulation methodology previously developed by the authors [4, 9, 10] to model building stock energy demand and carbon emissions was advanced from a building archetype level to building level. However, building stock level information is still used both to calibrate the initial building state as well as influence the alteration during the model period. Figure 1 depicts the interaction between building level and building stock data as well as the building development model concept.

The model adopts an inverse approach from the previous model developed by the authors [4]. Instead of using individual building data to form building cohorts by aggregating it by building type, construction period, etc., the model uses the individual building level data directly. However, building stock level data is used in order to substitute missing building level data and to determine the initial building state. Thus, building level data from building registers as well as from local utilities is combined with generic data that is known or assumed on the building stock level. The building geometries (wall, roof, floor and window areas) are calculated by matching the building register with a city 3D model. Based on the initial building state the model calculates the space heating and hot water demand based on the Swiss norm SIA 380/1 [11].

Instead of using average refurbishment or diffusion rates the model applies a discrete choice approach to model the refurbishment and heating system substitution decisions for each building. Both decisions are modeled in a two-step approach. In a first step the timing of the refurbishment/substitution is modeled based on the age of the building component using the hazard rate function (equation 1). The hazard rate h describes the probability that a technical system is going to fail in the year t given that it has not failed so far. The models applies the hazard rate of the Weibull function, which is commonly used to model the lifetime of

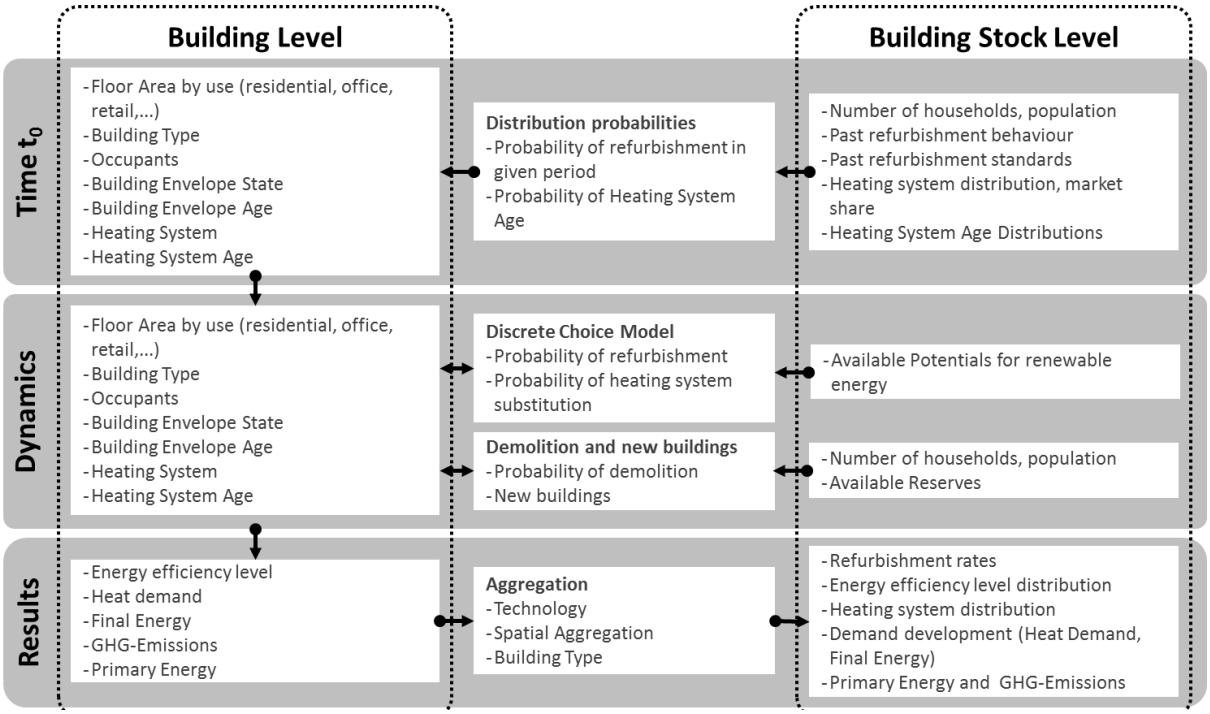

Figure 1: Model concept of interaction between building level and building stock data

technological systems. Based on the hazard rate the year in which a given building component or the heating system has to be refurbished/substituted is determined.

$$h(t,k,\lambda) = \frac{f(t,k,\lambda)}{1-F(t,k,\lambda)} = \frac{k}{\lambda}\left(\frac{t}{\lambda}\right)^{k-1} \quad (1)$$

In a second step the model evaluates different refurbishment or substitution options for each component based on a predefined choice set. In case of the refurbishment the choice is between simply overhauling the building component without efficiency improvement or different levels of predefined refurbishment standards. The resulting U-values are defined based on the current standards [11]. The choice set for the heating systems is defined based on general as well as locally available options (i.e. district heating is only available to buildings close to the district heating distribution network). The choice probability of the different options in the choice set are then calculated based on a discrete choice approach. The discrete choice model calculates the choice probability P_i of a certain option based on the utility U_i of the alternative as well as the utility of the other options in the choice set (equation 2).

$$P_i = \frac{e^{U_i}}{\sum_j^S e^{U_j}} \quad (2)$$

The utility of the different refurbishment options is modeled for each building component individually according to the utility function described in equation 3. It takes into account the annualized investment costs (AC_i), the resulting energy costs (EC_i), the energy savings (dE_i), a factor for comfort improvements (dC_i), the protection status of the building (P_i) as well as the willing ness to pay (WTP_i) of each option in the choice set. The costs of the different options are calculated using cost factors from [12]. The model takes into account results from choice experiments as in [13] and is then calibrated using results from [14].

$$U_{i,BR} = \beta_{AC}AC_i + \beta_{EC}EC_i + \beta_{dE}dE_i + \beta_{dC}dC_i + \beta_{pro}P_i + \beta_{WTP}WTP \quad (3)$$

The utility of the heating system substitution choice is defined similarly to the utility function of the refurbishment choice. However, as can be seen from equation 4, the utility function

differs in certain values. The maintenance costs (MC_i) of the different heating systems are included in the function. Furthermore, a factor for the previous system (PS_i) is included to account for the advantages of replacing an existing system with a system of the same type and the reluctance of the building owner to change system. Both investment and maintenance costs of the different systems are calculated using data from [15].

$$U_{i,HS} = \beta_{AC} AC_i + \beta_{EC} EC_i + \beta_{MC} MC_i + \beta_{dE} dE_i + \beta_{ps} PS_i + \beta_{WTP} WTP \quad (4)$$

Similar to the modelling of the refurbishment and heating system also the demolition probability of each building is modelled individually based on the building age. However, instead of using a Weibull distribution the survival function of the loglogistic distribution shown in equation 5 is used to estimate the demolition year of a building. This was found to give a better fit when calibrating the function based on the building register data of the city of Zürich. Next to the building age also the building type, city district and construction period are included in the statistical fit of the survival function yielding differentiated demolition rates across building types and districts.

$$S(t) = \frac{1}{1+(\lambda t)^{\frac{1}{\gamma}}} \quad (5)$$

The modelling of new construction is linked to the demolition model as especially in urban areas buildings are mainly demolished to make way for new buildings. The size and geometry of the new building is defined based on the available reserves according to the zoning restrictions for the parcel it will be built on. Similarly, the model also includes extensions and additions to existing buildings, if the available reserves on the parcel allow it.

In a final step, the model calculates both the heat demand and the final energy demand of every building based on the current state of the building envelope and heating system installed for each year until 2050. Using emission and primary energy factors the model then estimates GHG emissions and primary energy use. These building level results can then be aggregated according to building type, building age or location depending on the research question.

RESULTS

The following section shows the results for the development of the existing building stock in the year 2010 (excluding new construction) of the district Altstetten of the city of Zürich previously studied in [5]. Compared to the previous model used in [5], figure 3 shows that the building level approach not simply results in average energy consumptions, but that the specific heat demand varies greatly in the building stock. The results indicate that the largest share of buildings shift from having a heat demand from 250 - 450 MJ/m^2 in 2010 to 200 - 350 MJ/m^2 for existing buildings.

Figure 4 shows the spatial distribution of the heat demand based on an aggregation on the individual building data in a hectare-raster. While the results show that the heat demand in general will decrease according to the calculated scenario, they also indicate that the energy demand in the centre of the district will remain high do to the high density of buildings. Such local clusters of high heat demand could therefore be cover by a localized district heating network.

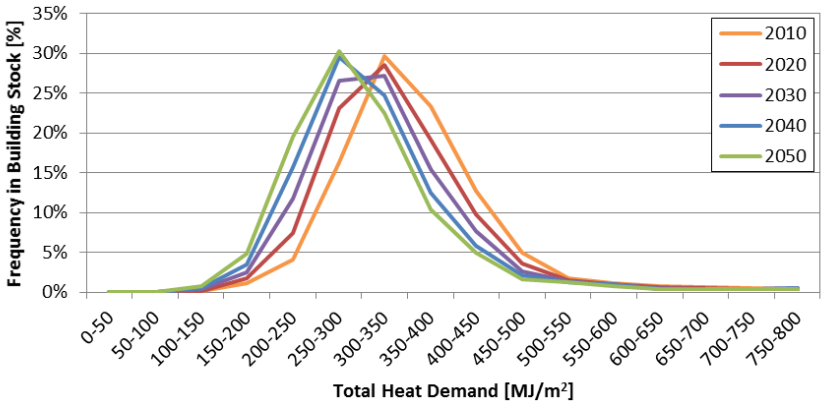

Figure 3: Exemplary results of the development of the distribution of the specific heat demand of the existing building stock from 2010 to 2050 (Reference scenario)

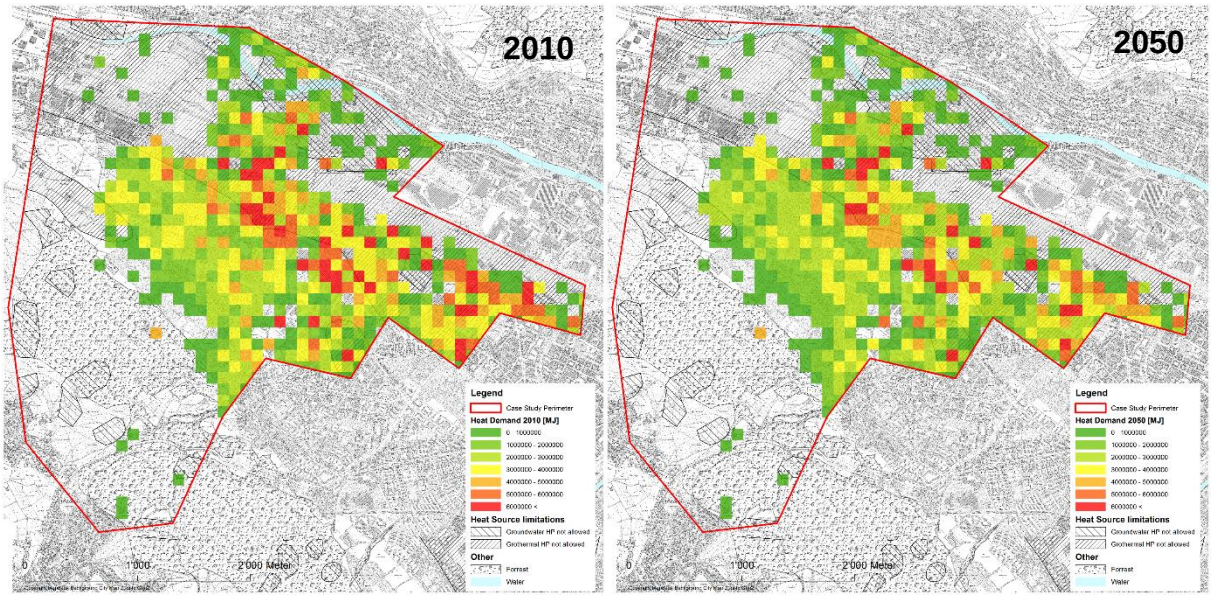

Figure 4: Exemplary results of the spatial distribution of the heat demand of the existing building stock in 2010 and 2050 (Reference scenario)

CONCLUSION

The developed approach of building specific BSM including a discrete choice model make it possible to include building specific information such as the actual building geometry or heating systems. Moreover, the developed discrete choice approach is able to take into account investment, maintenance and energy costs based on that building specific information resulting in individual decision criteria for each building. In addition to this, implemented decision model accounts for locally available energy infrastructure (e.g. district heat) and potentials for the use of renewable energies in the choice set. The developed BSM approach can be used both to evaluate policy measures (e.g. effect of subsidies, taxes and other policy measures) as well as for energy planning on a local scale, enabling a mutually consistent assessment of both. Moreover, if measured energy demand data is available, the building level approach, makes it possible for the model to be calibrated based on actual measurement data, increasing the accuracy even more [16]. Furthermore, the model is currently being extended to include electricity use and the embodied impact of buildings within the project GEPAMOD and therefore include the environmental impact of both construction and use phase of the building.

REFRENCES

1. EU (2010). Directive 2010/31/EU of the European Parliament and of the Council of 19 May 2010 on the energy performance of buildings. June.
2. EnDK. (2015). Mustervorschriften der Kantone im Energiebereich (MuKEn). Ausgabe 2014. Bern, Schweiz: Konferenz Kantonaler Energiedirektoren, January.
3. Kavgic M., Mavrogianni A., Mumovic D., Summerfield A., Stevanovic Z., Djurovic-Petrovic M. (2010). A review of bottom-up building stock models for energy consumption in the residential sector. Building and Environment. 45 (2010) 1683-1697.
4. Jakob, M., H. Wallbaum, G. Catenazzi, G. Martius, C. Nägeli, and B. Sunarjo. (2013). Spatial building stock modelling to assess energy-efficiency and renewable energy in an urban context. In Proceedings of CISBAT 2013. Lausanne, Switzerland.
5. Markus P., Avci N., Girard S., Keim C., Peter M. (2009). Energy demand in city regions – methods to model dynamics of spatial energy consumption. ECEEE 2009 Summer Study.
6. Biberacher M. et al. (2010). Räumliche Modelle als Entscheidungsgrundlage für die Inwertsetzung regional verfügbarer Energiepotentiale zur CO2-neutralen Deckung des lokalen Wärmebedarfs. 56 (2010).
7. Taylor, S., Allinson, D., Firth, S., Lomas, K. (2013). Dynamic energy modelling of UK housing: Evaluation of alternative approaches. 13th Conference of International Building Performance Simulation Association, Chambéry, France, August 26-28
8. Österbring M., Mata E., Jonsson F. Wallbaum H. (2014). A methodology for spatial modelling of energy and resource use of buildings in urbanized areas. SB14, Barcelona, October 2014.
9. Wallbaum H., Jakob M., Heeren N., Gross N., Martius G. (2010). Gebäudeparkmodell – Büro-, Schul- und Wohngebäude – Vorstudie zur Erreichbarkeit der Ziele der 2000-Watt-Gesellschaft für den Gebäudepark der Stadt Zürich. ETH Zürich und TEP Energy i.A. Stadt Zürich, Amt für Hochbauten, Fachstelle nachhaltiges Bauen, Zürich, Mai.
10. Heeren N., Jakob, M., Martius, G., Gross, N., Wallbaum, H. (2013). A component based bottom-up building stock model for comprehensive environmental impact assessment and target control. Renewable and Sustainable Energy Reviews, 20 (April 2013): 45-56.
11. SIA (2009). „SIA 380/1:2009 Thermische Energie im Hochbau“. SIA, Zürich
12. Jakob M., Grodofzig Fürst B., Gross N. (2010). Energetische Gebäudeerneuerungen - Wirtschaftlichkeit und CO2-Vermeidungskosten: Eine Auswertung des Gebäude-programms der Stiftung Klimarappen. Stiftung Klimarappen, Zürich, Juni.
13. Banfi S., Farsi M., Jakob M. (2012). An Analysis of Investment Decisions for Energy-Efficient Renovation of Multi- Family Buildings. Federal Office for Energy, Bern.
14. Jakob M. Martius G., Catenazzi G., Berleth H. (2014). Energetische Erneuerungsraten im Gebäudebereich – Synthesebericht zu Gebäudehülle und Heizanlagen. TEP Energy GmbH im Auftrag des BFE. Zürich, Februar.
15. Jakob M., Kallio S., Nägeli C., Ott W., Bolliger R., von Grünigen S. (2013). Integrated strategies and policy instruments for retrofitting buildings to reduce primary energy use and GHG emissions - Final synthesis for Switzerland. TEP Energy and econcept, Zürich.
16. Booth, A.T., Choudhary, R. & Spiegelhalter, D.J., 2012. Handling uncertainty in housing stock models. Building and Environment, 48(1), pp.35–47.

EXPLORING METRICS ON THE EVALUATION OF THE BIOCLIMATIC POTENTIAL AT EARLY STAGES OF URBAN PROJECT

R. Nahon[1]; G. Besuievsky[2]; E. Fernández[3]; B. Beckers[4]; O. Blanpain[1].

1: Université de Lille 1, Cité Scientifique 59655 Villeneuve d'Ascq, France

2: Universitat de Girona, Campus de Montilivi, 10071 Girona, Spain

3: Universidad de la República, Julio Herrera y Reissig 565, Montevideo 11300, Uruguay

4: Université de Technologie de Compiègne (UTC), Sorbonne Universités, Rue du Dr Schweitzer, 60200 Compiègne, France

ABSTRACT

Understanding and limiting the impact of buildings on their environment while seeking for optimal comfort became a matter of prime concern in urban planning. This important issue brings us to a reflection on the definition of a "bioclimatic urban planning": aiming at minimizing the energy needs while optimizing the luminous comfort on an urban project.

In this paper, we explore different metrics of luminous comfort and daylighting of the literature [1, 2] in an attempt to define an indicator appropriated to the early stages of an urban project. We choose as a case-study an office building regarding its daily occupancy and strong lighting consumptions.

Regarding urban planners practices in France, we can identify three key stages in the design of an urban project: the "*guide plan*", the "*mass plan*" and the "*block plan*". In the *guide plan,* an approximate 2D distribution of the different elements of the urban program is configured. The volumes are represented in the *mass plan*, as mass blocks corresponding to the level of detail LOD1 of the CityGML norm [3]. Finally, architectural details such as openings at windows positions, roof tilts or solar protections are defined in the *block plan*.

The *mass plan* strikes us as a key stage of an urban project regarding its "bioclimatic potential". Works on the search of an optimal geometrical configuration of the urban layout have pointed out the impact of parameters such as glazing ratios and performances or walls characteristics on the final solution [4]. Those parameters are still unknown at this stage of the project. Meanwhile, based on expert opinions, it is possible to emit consistent hypothesis for given climatic zone, use and targeted thermal performances of the building. The architectural details remain unknown but it is possible to have a precise idea of the building envelope and an indication on its interior through those three parameters.

Window positioning, solar protections or balcony are defined by the architects. Meanwhile, the urban planner may explore their impact on the performance of his project to set his architectural guidelines. Using procedural modeling to configure levels of detail may allow a refined analysis of the geometry at the early stages of the project [5].

Keywords: urban planning, bioclimatic potential, daylight penetration

INTRODUCTION

Bioclimatic architecture principles are well known since the end of the twentieth century. For a greater efficiency, those principles should be applied at the urban scale [6] and taken into account at the design phases of an urban project.

An urban project is declined in three main phases characterized by different Levels Of Details (LOD): the "*guide plan*", the "*mass plan*" and the "*block plan*". The volumes are represented in the *mass plan*, which make it a key stage of an urban project regarding its bioclimatic potential. In the present paper, we explore the metrics on the evaluation of the bioclimatic potential of an urban project and their fitting to this peculiar stage.

Bioclimatism is declined in 3 aspects: thermal loads, daylight conditions and thermal comfort in summer. In [4], the authors pointed out the impact of the buildings characteristics such as walls conduction or glazing ratios on the optimal geometric configuration of the urban environment regarding thermal loads. Based on expert opinions, it is possible to emit consistent hypothesis on those characteristics at the mass plan step knowing the climatic zone of the project, the use and targeted thermal performances of the buildings. It is however possible to estimate the heating and cooling loads in the mass plan, which should directly serve as an indicator of the first aspect of the bioclimatic potential of an urban project.

Interviewing urban planners, we identified their needs in terms of daylighting: the estimation of daylight penetration in order to seek an urban geometry which minimizes the dark spaces at the center of the buildings, where artificial lightings will be used most of the year. So, a particular attention should be put on the depth of daylight penetration in the interiors.

The Useful Daylight Indicator (UDI) [1] and the Daylight Autonomy (DA) [2] appear as prime candidates to characterize the daylight penetration in an interior. The UDI is the number of hours in which "useful" daylight conditions are achieved: when sufficient level of illuminance on the work plan is achieved avoiding discomfort due to glare. The DA is the number of hours with sufficient levels of illuminance on a horizontal plane.

Both indicators need a precise description of the interior, which is still unknown in the mass plan. The use of procedural modeling [5] provides the benefit of easily modifying modeling parameters in order to explore with changing element sizes or shapes. This advantage improves simulation application where different elements should be explored in order to analyze the impact of a given configuration.

In the next section of this paper, we present the study case and two different simulation approaches. Then, we explore the impact of the sky vault partition and time step on daylight modeling, through both approaches. In the final section, we explore the impact of architectural details such as solar protections, walls covering or window positioning on daylight penetration and justify their consideration at early stages of an urban project.

TEST CASE

We use as a test case the exact 3D model of a side-lit office space used by [1] (cf. Figure 1).

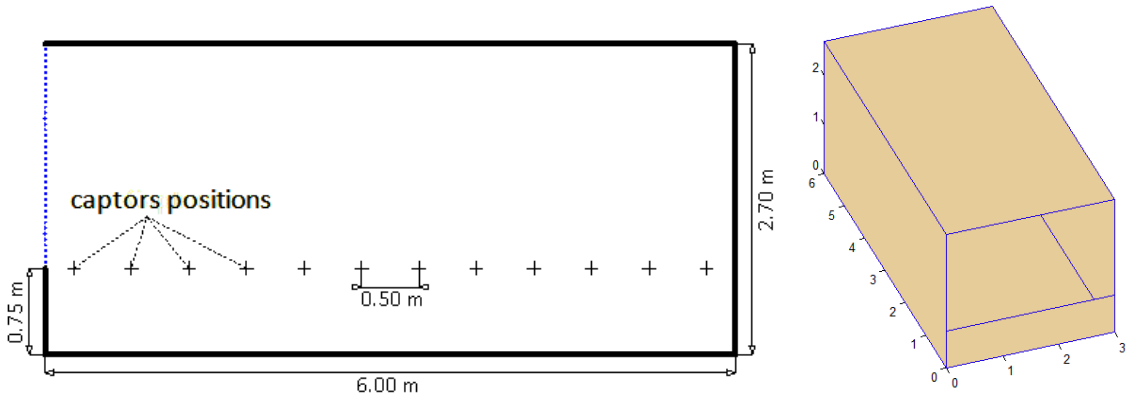

Figure 1 Office model

The same meteorological file is used with both simulation approaches for the city of London, Gatwick (latitude 51.15°) in [7]. We use the sky vault partition described in [8]. The luminance of each sky element is calculated using [9].

In a first approach, the Standard Radiosity (SR), the direct and diffuse illuminances are treated separately. Sun visibility is set for the exact position of the sun at a given time step. Sky tiles visibility is set for each calculation point though the tiles center: if the tile center is visible from one point then we consider that the entire tile is visible.

In a second approach, the incoming light that arrives to the interior spaces is treated with a pinhole model for each patch of the opening, for simplification purposes. In this work, we adapted the method presented in [10], originally intended for opening shape optimization, for daylight computation. The method is referred here as PBLI (Pinhole Based Lighting Incidence). In this case, the sky tile model includes the direct sun incidence. Another difference against the previous approach is that the visibility computed from the sky patches to all the mesh and sensors, considers the fraction of the tile that is visible.

SKYMESH AND TIME STEP

Using a sky partition of 145 elements and a time step of one hour, the SR approach shows significant differences with the reference simulation from [1] while the PBLI shows a strong correlation (cf. Figure 2). In Figure 2, we show the percent of a working year (all days from 9:00 to 18:00) with levels of illuminance inferior to the upper and lower limits of the UDI.

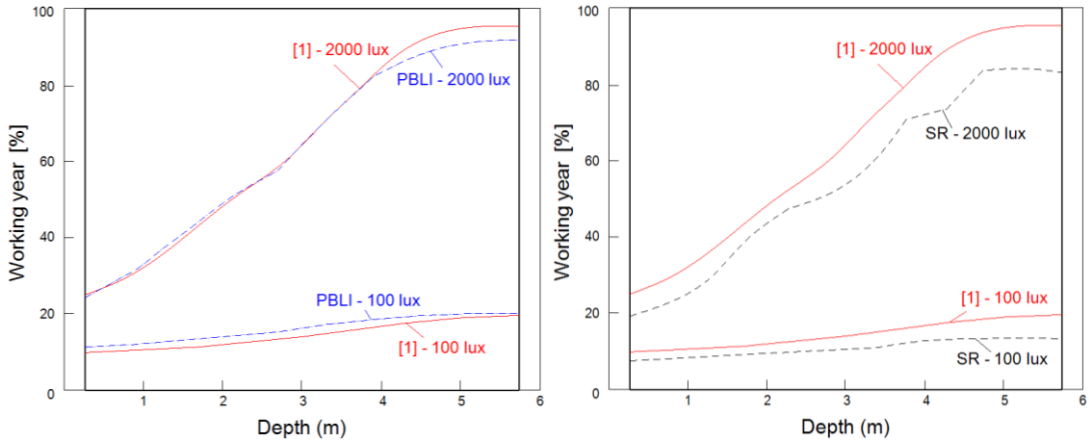

Figure 2 Distribution of Illuminance, comparison between the PBLI (left) and SR (right) methods with the reference simulation in [1]

The SR and PBLI approaches show differences both on the solar and sky direct component. The difference in the sky contribution is due to the assumption in SR that a tile is entirely visible if its center point is visible. In both [1] and the PBLI approaches, the sun luminance is distributed on the closest sky tile while in the SR approach we consider the exact position of the sun; which explains the differences in the sun contribution. As stated in [11], [1] uses a refined partition of the sky in 5010 tiles for the calculations of the direct component to minimize the angular displacement between the sun position and that of the sky tile.

The angular displacement between the sun and sky tile position is significant across a time step of one hour. To discuss its impact, we compute the number of hours with a direct illuminance exceeding 2000 lux using the SR approach. We first compare the values given by 145, 5000 and 20000 tiles with a reference simulation considering the exact position of the sun and a time step of 60 min. We then compare the values given by a time step of 60 and 15 min with the ones given by a time step of 5 min considering the exact position of the sun.

depth (m)	0,25	0,75	1,25	1,75	2,25	2,75	3,25	3,75	4,25	4,75	5,25	5,75
145 tiles	-1,6%	-1,1%	-2,0%	5,7%	13,0%	14,4%	-4,8%	16,1%	-5,0%	20,7%	-3,0%	-30,2%
5000 tiles	0,6%	0,2%	0,4%	0,4%	0,0%	0,4%	2,4%	1,3%	-2,5%	3,4%	-13,4%	3,8%
20000 tiles	0,1%	0,2%	0,7%	-1,0%	-0,6%	-0,4%	0,6%	0,0%	-2,5%	0,0%	3,0%	3,8%

Table 1 Sky vault partition impact on the solar direct contribution

depth (m)	0,25	0,75	1,25	1,75	2,25	2,75	3,25	3,75	4,25	4,75	5,25	5,75
60 / 5 min	-0,5%	1,5%	0,6%	-2,9%	1,8%	-1,9%	8,4%	-6,3%	-13,7%	-6,7%	-16,6%	-4,4%
15 / 5 min	-0,4%	0,0%	-0,3%	0,2%	-0,4%	-1,1%	-1,6%	-0,5%	-0,6%	-1,9%	-3,2%	0,7%

Table 2 Time step influence on the direct illuminance considering a 5000 tiles partition

A partition of 5000 elements appears as a good compromise regarding the precision of the results and the calculation cost, as stated in [8]. Meanwhile, although the meteorological data is set on an hourly basis, a time step higher than 15 min induces significant differences when studying the daylight conditions at the back of an interior.

In Figure 3, we compare the distribution of the illuminance using a sky partition of 5000 elements and a time step of 15 min with the SR and the PBLI approaches to the reference simulation in [1]. The results show insignificant differences and lead to the conclusion that, for this test case, a sky vault partition of 145 tiles and a time step of one hour are sufficient.

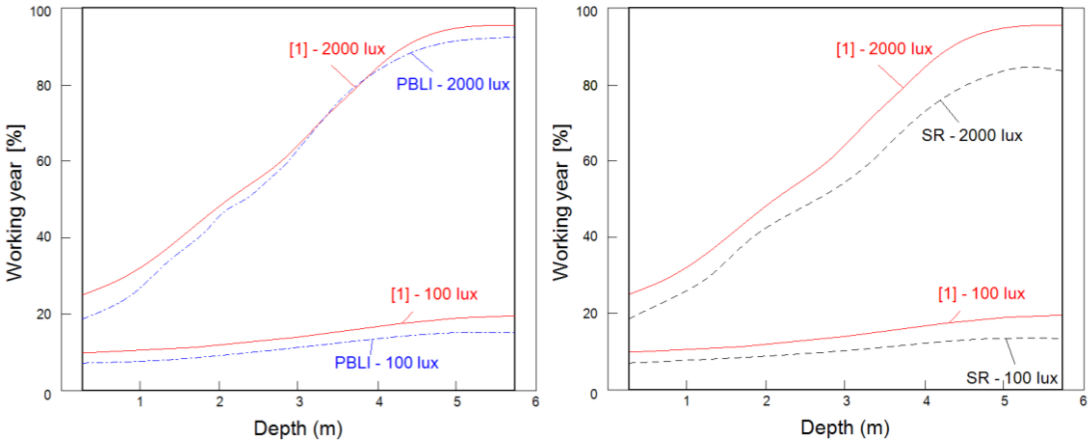

Figure 3 Comparison between the PBLI (left) and SR (right) methods with the reference simulation in [1]*, using a sky partition of 5000 elements and a time step of 15 min*

ARCHITECTURAL DETAILS

Urban planners need to be able to estimate daylight penetration in the interiors when distributing the volumes of a project, in the mass plan. Daylight penetration can hardly be characterized by the incoming illuminances on the external walls of a building. In the mass plan, the glazing ratio is known for the diverse orientations and the partition index may be estimated regarding the use of the building, its target performance and the climatic zone of the project. Architectural details such as solar blinds, walls covering or window positioning come within the know-how of architects and are introduced in the block plan. In this part of the paper, we illustrate their impact on the daylight penetration and justify their consideration as soon as in the mass plan. We use the SR approach with a sky vault partition of 145 elements and a time step of one hour.

Solar blinds

Solar mobile protections are commonly used in building offices and both [2] and [1] have shown their impact on the daylight conditions in an interior. In this part of the paper, we

illustrate this impact trough the following methodology. We use a “no blinds” scenario as a reference simulation to estimate the magnitude of uncertainty due to the user behavior. Such as in [2], we consider two types of user : “passive” and “active”. The passive user keeps the blinds always lowered. The active user lowers the blinds whenever the UDI upper limit is crossed on the point at 0.75 cm from the window. The blinds are modeled as filters that stop the solar direct contribution and reduces the sky direct component by 80%, as in [1]. In Figure 4, we compare the portion of the working year in which the lower limit of the UDI (100 lux) and DA (500 lux) are surpassed for the three scenarios.

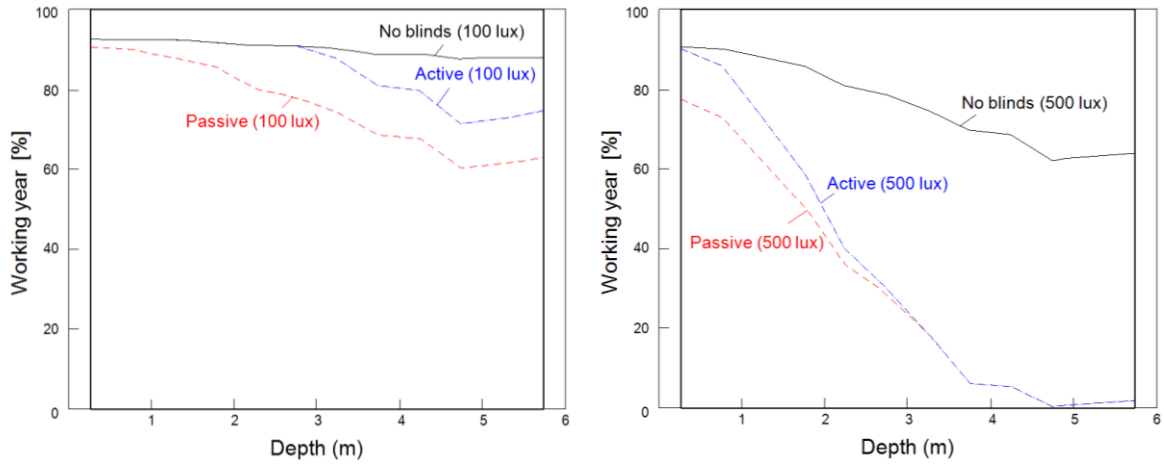

Figure 4 Solar blinds impact on the UDI (left) and DA (right)

Window positioning and wall covering

In a first example (Var1), we compute the daylight penetration in the office test case changing its window from horizontal to vertical, conserving its area. In a second example (Var2), we change the reflectivity of the ground from 0.2 to 0.5. We consider “active” solar blinds for both simulations. In Figure 5, we show the differences in the daylight penetration for both scenarios.

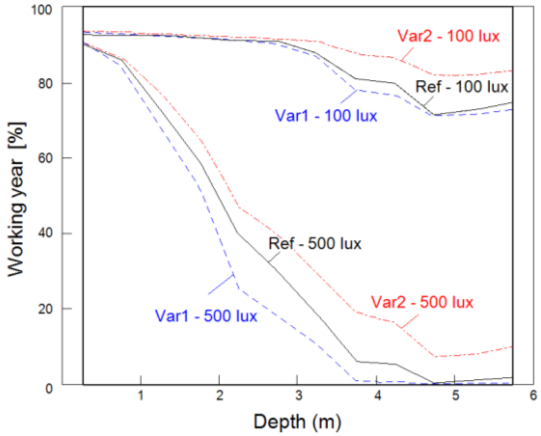

Figure 5 Window positioning (var1) and ground covering (var2) impact on the UDI and DA

CONCLUSION

In the first part of this paper, we study the impact of the time step and the sky vault partition on the UDI in order to define a criterion adapted to the points at the back of an interior, where the sky view is restrained. The results show that, although significant differences on the solar direct contribution are recorded, the impact on the UDI is negligible for this test case and a sky partition of 145 tiles appears sufficient for both the sun and sky direct contribution. The

conclusion might have been different placing the office model in an urban context, were the sky view from a window is partially obstructed, and with a different orientation of the window.

In the second part, we show the strong impact of architectural details on daylight penetration and justify their consideration at early stages of an urban project. Urban planners have a good understanding of those parameters and should be able to easily explore their impact on a project as soon as in the mass plan. Perceptive thresholds and occupants behavior are the main factors impacting the criteria definition and so the final validation of a project. Urban planners can easily assimilate them and choose their optimal values according to the specificities of each singular project.

ACKNOWLEDGEMENTS

Part of this research was conducted by the first author in the context of the SERVEAU project, partly funded under FUI (the Unified Inter-Ministry Fund). The work also was supported by project FSE_1_2014_1_102344 from Agencia Nacional de Investigación e Innovación (ANII, Uruguay) and TIN2014-52211-C2-2-R project from Ministerio de Economía y Competitividad, Spain.

REFERENCES

1. Nabil, A. and Mardaljevic, J.: Useful daylight illuminance: a new paradigm for assessing daylight in buildings. Light. Res. Technol., vol. 37, no. 1, pp. 41–59, Jan. 2005.
2. Reinhart, C. F. and Wienold, J.: The daylighting dashboard - A simulation-based design analysis for daylit spaces. Build. Environ., vol. 46, no. 2, pp. 386–396, 2011.
3. Gröger, G.; Kolbe, T.; Nagel, C. and Häfele, K.: Open Geospatial Consortium OGC City Geography Markup Language (CityGML). Encoding Standard. Version 2.0. 2012.
4. Vermeulen, T.; Kämpf, J.H. and Beckers B.: Urban Form Optimization for the Energy Performance of Buildings Using Citysim. in *CISBAT*, pp. 915–920, 2013.
5. Besuievsky, G.; Barroso, S.; Beckers, B. and Patow, G.: A Configurable LoD for Procedural Urban Models intended for Daylight Simulation. Eurographics Work. Urban Data Model. Vis., pp. 19–24, 2014.
6. Beckers, B.: Solar Energy at Urban Scale, Wiley-ISTE, 2013.
7. U.S. department of Energy, http://apps1.eere.energy.gov/buildings/energyplus/weatherdata_about.cfm. [Online].
8. Beckers, B. and Beckers, P.: Sky vault partition for computing daylight availability and shortwave energy budget on an urban scale," Light. Res. Technol., 2013.
9. Perez, P.; Seals, R. and Michalsky, J.: All-weather model for sky luminance distribution—preliminary configuration and validation. *Sol. energy*, vol. 50, pp. 235–245, 1993.
10. Fernández, E. and Besuievsky, G.: Inverse opening design with anisotropic lighting incidence. Comput. Graph., vol. 47, pp. 113–122, 2015.
11. Mardaljevic, J.: Simulation of annual daylighting profiles for internal illuminance. Lighting Research and Technology, vol. 32, no. 3. pp. 111–118, 2000

SIMSTADT, A NEW WORKFLOW-DRIVEN URBAN ENERGY SIMULATION PLATFORM FOR CITYGML CITY MODELS

Nouvel, R.[1]; Brassel, K-H[1]; Bruse, M.[2]; Duminil, E.[1]; Coors, V.[2]; Eicker, U.[1]; Robinson, D.[3];

1: University of Applied Sciences Stuttgart / Energy Department, Germany

2: University of Applied Sciences Stuttgart / Geo-informatics Department, Germany

3: University of Nottingham, United Kingdom

ABSTRACT

In this paper, we introduce new urban energy simulation platform *SimStadt*, which has been developed to support public authorities and engineering companies in the planning of the energy transition at urban scale. SimStadt design is marked by two particular features: 1- it is based on the open 3D city model CityGML and, 2- its workflow-driven structure is highly modular and extensible. These particularities allow him for a potentially unlimited variety of urban analysis, benefiting from the big geo data possibilities. This first version contains the workflows Solar and PV potential analysis, Energy demand and CO2 emission calculation, and refurbishment scenarios generation and simulation. Other workflows and plug-ins are under way, in particular district network design and simulation.

This paper details these features and workflows, and presents an application on the administrative district of Ludwigsburg, a case study of half a million inhabitants spread over 34 municipalities.

Keywords: SimStadt, urban energy analysis, 3d city model, CityGML

INTRODUCTION

Used for modelling an ever growing number of cities (e.g. Berlin, Lyon), regions and even countries (Germany), virtual 3D city models represents an invaluable support for public authorities and engineering companies to tackle the urgently required energy transition.

They have recently shown huge possibilities in the fields City planning, Environment and Energy, enabling diverse urban studies (solar radiation exchange and shadowing, urban wind flows, district heating network etc.) and combining expert urban simulation algorithms with the richness of the Big Geo Data. Among the 3D city model formats, the open standard CityGML seems to stand out as the reference [1], providing an excellent and flexible spatio-semantic data structure for 3D geospatial visualization, multi-domain analysing, simulation and exploration tool. It is the basis of design of the new urban energy simulation platform *SimStadt*, commonly developed by the departments Energy and Geo-informatics of the University of Applied Sciences Stuttgart during the last 2 years.

This platform aims at supporting urban planners and city managers with defining and coordinating low-carbon energy strategies for their cities, with a variety of multi-scale energy analyses. It shall also allow scientists for developing and testing new simulation algorithms and exploring the potential of new data sources.

SIMSTADT APPROACH

To achieve the above goals, *SimStadt* must be able to integrate (a) large data sets of different kind and at different level, e.g. building geometries and features, heating networks, patterns of energy consumption, production and conversion, (b) third-party simulation systems, and (c) inhomogeneous hardware resources like database servers, simulation engines, web services, graphics cards, and workstations. Moreover, to be considered as a useful working tool, the platform must provide a modern graphical user interface, enable fast parallel computation and help to easily understand given workflows and add new ones.

When looking at these requirements, scientific workflow systems seem to be the natural choice of platform to use. [2] However, no standard for such systems exists yet. To avoid locking into a special software product, we decided to build upon Java and its rich ecosystem. Especially, new language idioms of Java 8 provide features common to scientific workflow systems like high-level support for parallel computing, domain specific languages, functional programming, and generic user interfaces. Last but not least, Java provides industry-proven support for XML processing that comes very handy for the kind of data we have to deal with.

A data structure based on the open city model standard CityGML

The OGC Standard CityGML [1] is the basis of design of the new urban energy simulation platform SimStadt. A considerable asset is its flexible object modelling in 4 different Levels of Details (LoDs), enabling the virtual city model to adapt to local building parameter availability and application requirements. The present release of SimStadt deals with the Level of Details LoD1 and LoD2, consideration of LoD3 is under way.

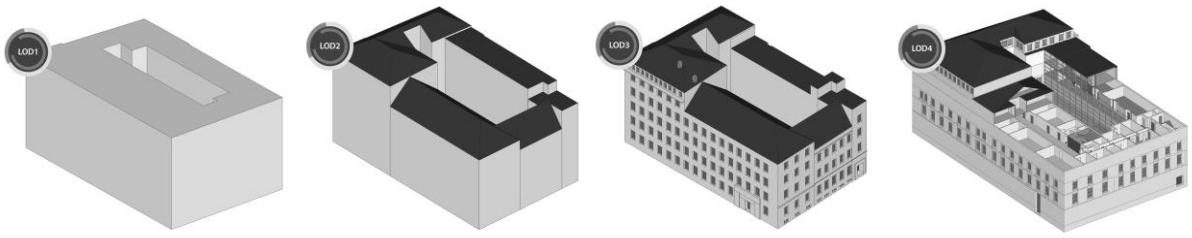

Fig. 1: The four Levels of Detail of CityGML applied to the Building 2 of the HfT Stuttgart.

Presently, the CityGML data model (version 2.0) does not contain any energy-related objects and attributes. To solve this issue, an application domain extension (ADE) for CityGML, called Energy ADE, has been designed and implemented with other European partner institutes. This extension enables the modelling of building thermal zones and boundary surfaces, construction and material properties, occupancy conditions of zone area, energy systems and consumptions. Having the energy-related data integrated into the city models eases the processing of this data through SimStadt.

SimStadt utilizes the library citygml4j [3] to load, process and store CityGML files with Java. This library provides a Java API and Java classes for all standard CityGML types so that a CityGML model can be instantiated in Java applications. Furthermore, citygml4j provides a JAXB-XJC binding compiler (ade-xjc) which conveniently generates Java classes from custom ADE XML schema definitions like the Energy ADE, so that the newly introduced energy-related attributes and types are now able to be loaded and stored together with a standard CityGML model by *SimStadt*.

Modular workflow-driven processing

The structure of computational tasks at hand is considerably simple, and best described as "hierarchical workflow". From a birds eye view, such workflows basically consist of chains of processing steps that create, transform and consume specific data objects step by step. Conforming to the disaggregation of model objects from high-level to low-level (e.g. city > district > building > building zone > wall) often a processing step at a higher level is realized by a chain of steps working on lower-level model objects, thus the term "hierarchical". In some cases, chains of processing steps at one level may be logically independent, and thus be executed concurrently. Note, that in this schema, circular processing of steps is not allowed. Fig. 2 depicts what it looks like to define a hierarchical workflow in SimStadt.

```
Workflow.start(new ImportCityGML("Stuttgart"))
  .next(new WeatherAndPreprocessing("Weather and Preprocessing")
         .par1(new WeatherProcessor("WeatherProcessor"))
         .par2(new Preprocessing("Preprocessing")
                .sub(Workflow.start(new BuildingFilter("Filter"))
                       .next(new GeomPreprocessor("Geometry"))
                       .next(new PhysicsPreprocessor("Building Physics"))
                       .next(new UsagePreprocessor("Building Usage"))
         )))
  .next(new RadiationProcessor("RadiationProcessor"))
  .next(new MonthlyEnergyBalance("DIN18599")));
```

Fig. 2: Definition of a hierarchical workflow to compute monthly energy balance.

While dealing with large-scale models based on different data sources, the risk of errors and incoherent results are generally very high. A Graphical User Interface (GUI) enables to navigate in the different workflows and workflow steps, allowing for the analysis of the intermediary results at each step of the workflow, through charts, tables and other output. The GUI also enables the user to modify the hypotheses and parameters of workflow steps and create scenarios accordingly.

FIRST BUNCH OF SIMSTADT FUNCTIONALITIES

At the redaction date of this paper, the SimStadt Platform integrates the workflows solar potential analysis, heating demand and CO2 emission calculator, based on the main WFS and functionalities detailed below. Due to its modular structure, SimStadt may be extended with new WFS and workflows corresponding to new urban energy analyses, provided that the required data are available in the 3D city model or processed previously by other WFS.

Data pre-processing and probabilistic disaggregation

Urban energy analyses and simulation algorithms are important consumers of geo data. Beside the geometric data, which can be extracted from the 3d city models, semantic data relative to the buildings physics and operation, occupants and local climate are also required. Nevertheless, the diversity of their availability and quality in existing urban areas represents a challenging issue. The use of the flexible city data model CityGML enables to adapt to the available data and their level of details, as described in the previous section. In addition, some data pre-processing modules integrated in the workflow enable to address gaps in information by estimating the missing data and transforming the available ones.

These data pre-processing modules use elementary algorithms to deduce missing parameters from available information (e.g. determination of the building types based on geometrical parameters), as well as different libraries of benchmarking values and archetypes:

- Building typology libraries, containing building physics archetypes referenced by building age and building type
- Building usage libraries, detailing occupancy and operation parameters representative of the different zone usage types (e.g. residential, retail, education).
- Energy System and fuel libraries.

Additionally, if some essential information data are neither available nor deducible at the building level, they can be probabilistically assessed from aggregated data. This method is particularly interesting to deal with energy systems or refurbishment states at urban scale. Although these information data are rarely accessible in private buildings, their distribution per neighbourhood or municipalities may be provided by European census data for instance.

Weather and radiation processing

Urban energy analyses such as the heating demand or solar potential analysis require local weather data, at hourly or monthly basis (e.g. ambient temperature, relative humidity, horizontal global and diffuse radiations). They are imported in the WFS WeatherProcessor from different online/software databases (*PVGIS, Insel*) or weather data files (*Meteonorm*), selected by the user, and if required pre-processed.

The WFS RadiationProcessor allows for the computation of the incoming solar radiations on each building boundary surface. For this purpose, the user may select different radiation distribution models, depending on its precision requirements and allowed computational time:

- A radiation/orientation mapping, based on the Hay sky model. It considers each building as an insulated object without interaction with its surrounding. This model may be preferably used in urban area with low-density.
- A ray-casting algorithm, coupled with the Hay sky model. Programmed to benefit from the full computational power of GPU, it considers the obstruction of surrounding urban objects, but not the mutual reflections (instead, an urban albedo is considered).
- The Simplified Radiosity Algorithm [4], coupled with the Perez sky model. It considers both shadowing and reflexion effects of surrounding urban objects.

Energy demand calculation

The space heating, domestic hot water (DHW), and electrical demands are assessed in SimStadt, allowing for a global energy demand assessment, building per building.

The DHW and electrical demands, which depends mainly on the building usage and occupancy, are calculated by means of a statistical method at yearly basis. For the space heating demand calculation, a monthly energy balance (according to ISO 13790) is applied to each building, allowing for the pre-certification of the building energy-efficiency. In order to calculate additionally the hourly heating loads, the modular implementation of a simplified dynamic simulation is currently under development.

Based on these energy demand analysis and knowing the energy systems of the different buildings and their performances, the primary energy demand and CO2 emissions may be calculated.

Generation of scenarios

Based on the diagnosis of the actual energy state, alternative energy refurbishment and energy supply scenarios may be developed, compared, combined and optimized, with the purpose to plan and coordinate the best energy transition at urban scale.

The platform SimStadt offers a module to quickly generate such scenarios, by means of refurbishment rates (% of floor area per year), time horizon, and priority indexes (either oldest building first, or less-efficient buildings first, or a user-defined index, or randomly). Some reference refurbishment variants and energy-efficient systems to be implemented are predefined in the Building typology and Energy system libraries. The user may create further variants, so as to observe the impact of customized scenarios.

Software plug-ins

Plug-ins interfacing with third-party simulation softwares may be programmed inside WFS. This is the case of the actual workflow development "sizing and simulation of district heating network". Based on the geo-localized heat demand and loads calculated in *SimStadt*, an optimized network layout is automatically generated by means of graph algorithms, and its pipe sizes and heat losses calculated by the utility network calculation software *Stanet.*

EXAMPLE APPLICATION: ADMINISTRATIVE DISTRICT OF LUDWIGSBURG

The administrative district of Ludwigsburg covers a ground area of approx. 700 km² at the South-West Germany and counts 34 municipalities for a total population over half a million inhabitants.

In the framework of the project *Integriertes Klimaschutzkonzept Landkreis Ludwigsburg*, an Energy action plan was conducted to identify and plan CO2 emission savings, based on the available 3D city models (CityGML, Level of Details 1 and 2). For this purpose, different workflows of the urban energy simulation platform SimStadt have been used and combined to assess the actual heating demand and the related CO2 emissions per building, predict energy savings potential following different refurbishment scenarios, and identify the solar energy potential.

For the whole studied area, the total yearly heating demand reaches 3.9 TWh, with an average specific heating demand of 145 kWh/m².yr. Considering the heating system distribution available for each municipality (from census data survey), this corresponds to 0.92 Mega-tonnes equivalent CO_2 per year.

Fig. 3: Specific heating demand calculated with SimStadt, view in a Web browser (originally in color).

In a neighbourhood of Ludwigsburg (Grünbühl) where actual gas consumptions were available, comparison with the calculated consumptions showed deviations varying from 2% to 31% depending on the data availability and quality [5].

For the photovoltaic potential analysis, only roofs with a surface larger than 40 m² and receiving more than 1100 kWh/m².yr solar radiation have been selected. In total, the diffuse power central formed by all these roofs could generate 668 MWh/yr, which would cover 26% of the electric demand (for building electrical appliances) of the administrative district.

CONCLUSION AND PERPECPECTIVES

In the recent years, considerable progresses have been realized in both domains urban energy simulation and 3D Geographical Information System, however without notable cross-domain interactions. The new urban energy simulation platform SimStadt introduced in this paper holds in its DNA both domains, making the best common use of models and geo data.

The first *SimStadt* version integrates workflows, which allow for first city-scale energy demand diagnoses as well as low-carbon scenario simulations. Meanwhile, it remains a great deal of work to model energy flows more precisely, with higher Level of Details, shorter time resolutions (typically hourly loads) and taking into account the whole complexity of urban scale interactions. Integrating optimisation functions supporting decision takers in the definition of their energy strategies is also an exciting challenge.

In any case, based on its extensible modular structure and on the full potential of virtual city models, the new SimStadt platform may provide an adequate and powerful solution to plan and coordinate the energy transition, at the scale of neighbourhoods, cities or whole regions.

AKNOWLEDGMENT

Financial support received for this work from the BMWi German Ministery is gratefully acknowledged. Thanks also to our project partners Drees & Sommer AG (coordinator), Landkreis Ludwigsburg, Ludwigsburger Energieagentur LEA e.V. and Energetikom - Energiekompetenz und Ökodesign e. V. for their support and cooperation.

REFERENCES

1. Groeger, G., Kolbe, T.H., Nagel, C., Häfele, K.H 2012. OGC City Geography Markup Language (CityGML) En-coding Standard. OpenGIS® Encoding Standard, Version: 2.0.0, OGC 12-019, 2012-04-04
2. Curcin, V.; Ghanem, M., "Scientific workflow systems - can one size fit all?," *Biomedical Engineering Conference, 2008. CIBEC 2008. Cairo International* , vol., no., pp.1,9, 18-20 Dec. 2008.
3. Nagel, C., April 2015. Citygml4j [GitHub Markdown Readme file]. Retrieved from https://github.com/citygml4j/citygml4j
4. Robinson, D., Stone, A. 2005. A simplified radiosity algorithm for general urban radiation exchange. In: Building Serv. Eng. Res. Technol. 26,4 (2005) pp. 271/284
5. Nouvel, R., Zirak, M., Coors, V., Eicker, U. 2014. Urban energy analysis based on 3d city model for national scale applications. In Proceeding BauSim 2014, Aachen.

USE OF MICROCLIMATE MODELS FOR EVALUATING THERMAL COMFORT: IDENTIFYING THE GAPS

Tania Sharmin; Koen Steemers
The Martin Centre for Architectural and Urban Studies, Department of Architecture, University of Cambridge, 1-5 Scroope Terrace Cambridge, CB2 1PX2

ABSTRACT

The study identifies the gap between actual thermal sensation and theoretical comfort calculated through simulated microclimate data in different urban configurations in a tropical, high-density, megacity: Dhaka. The methodology stated here could be applied for evaluating outdoor comfort conditions for future urban areas at an early design stage. To apply the concept of theoretical comfort it is important to understand its limitations and degree of deviation from the actual comfort conditions at real scenarios. This study mainly focuses on traditional and formal (contemporary) residential settlements with different urban-geometry features. On-site climatic measurements were carried out during the hot-humid months and were compared with simulation results calculated through ENVI-met 4. Simulation results were found to have good agreement with actual air-temperature, mean radiant temperature (Tmrt) and relative humidity. In terms of windspeed, the simulated model for a complex traditional settlement did not successfully match with the actual scenarios. However, this does not affect the model competency, because, the area has rather unusual wind pattern due to its location and current arrangements of buildings. The simulated results were subsequently used to calculate outdoor thermal comfort using the PET index in RAYMAN Pro. The calculated theoretical comfort was assessed against Actual Thermal Sensation Votes (ASV) obtained through a thermal comfort survey in the case-study areas. Strong correlation (r=.58) was found between theoretical and actual comfort in the formal settlements, while the comparison with the traditional settlements produced rather weak results (r=.238). This leads to the understanding that theoretical comfort can be a useful tool for comparing between regularly planned sites; however, for complex urban geometry, theoretical comfort can deviate from actual comfort levels recorded, in part due to adaptive behaviour.

Keywords: urban geometry, outdoor thermal comfort, actual sensation vote, PET, ENVI-met

INTRODUCTION

Unbridled urbanisation, unplanned growth of built environment, acute energy shortage and elevated air-pollution levels are common problems in the high-density tropical cities located mostly in the developing countries. Such factors have adverse consequences on cities micro-climate, consequently affecting comfort levels in urban outdoor spaces as well as energy performance in urban buildings. Considering the socio-economic context of these cities, the most effective answer to the deteriorating urban micro-climate can be achieved mostly through proper urban planning and urban design. Especially, modification of urban geometry, as an urban planning tool, can play a crucial role in ameliorating the urban micro-climate. Urban micro-climate is largely determined by different components of urban geometry that includes: configuration of the streets, building heights, density and separation, roughness length and urban permeability. The effect of these components will vary according to the local climate and morphological context of the concerned area. The existing knowledge mostly concentrates on the Western (usually colder) countries and thus the strategies applied to improve their urban micro-climate are not suitable for use in tropical cities. Studies concerning tropical cities are still very limited. Therefore, insights from these cities could be

valuable towards making them more liveable and resilient, so that they are able to act appropriately in response to potential challenges.

The study summarises finding from a thermal comfort field-survey and compares this with a numerical analysis. Numerical modelling and computer simulation techniques are playing increasingly important roles in current studies for predicting urban microclimate. Urban microclimate is a complex consequence of different parameters which involves innumerable natural and urban processes. Due to the complexity of diverse processes involved behind different microclimates, numerical methods are becoming more acceptable now-a-days. However, the application of physical data from the models for predicting pedestrian thermal comfort conditions is a rather new area of research and could be a useful tool for comparing between different sites which have variable urban morphology. Therefore, in this study theoretical comfort model has been compared against actual thermal comfort level. Previous studies in this field have compared theoretical comfort index (PMV, PET) with actual comfort, but using on-site microclimate data instead of simulated data [1,2]. The methodology followed in this study could be applicable for understanding outdoor comfort conditions for virtual environments for still unbuilt areas at the design phase.

SITE SELECTION AND METHOD

The study focuses on the tropical megacity Dhaka. The city falls under tropical Monsoon climate with a distinct warm-humid rainy season, a hot-dry summer and a short cool-dry or winter season. The mean annual temperature is 25.8^{0}C with an annual range between 8.2^{0}C to 39.4^{0}C. The mean annual relative humidity is 75%.

Figure 1. Typical formal areas: a)FRA_1_EW, b) FRA_2_EW, c) FRA_2_NS

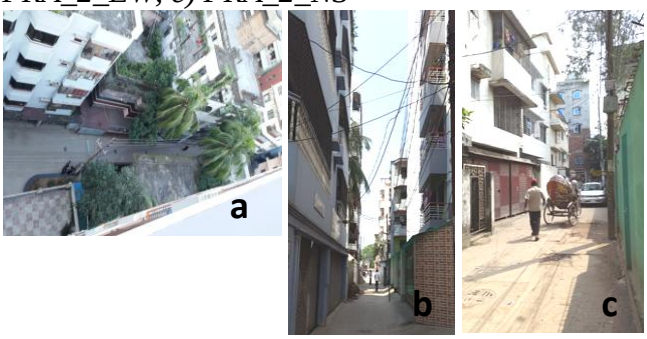

Figure 2. Typical traditional areas: a)TRA_1_EW, b) TRA_1_NS, c) TRA_2_NS

Two sets of residential settlements: traditional and formal, were selected for the study. Table 1 lists the site names, abbreviations and their common geometric characters. In general, formal residential areas, which evolved from urban planning regulations, are characterised with buildings of equal height and width, with roads laid out in a grid-iron pattern (Fig 1). Traditional residential areas on the other hand, mostly resulted from spontaneous developments under loose planning controls; have variable building forms, heights, plot sizes and even different building usage (Fig 2). While both settlements have compact design, high H/W ratio (building height/ street width) and lack of vegetation, the former (formal) is mostly uniform and the latter is quite diverse and variable.

Measurements were carried out in north-south (NS) and east-west (EW) oriented streets in two traditional and two formal sites during the hot-humid month in September. These included air-temperature (T_a), humidity (*RH*), globe temperature (T_g), mean radiant temperature (*Tmrt*) and windspeed

(*V*). Instruments used in the study were: tiny-tag air-temperature and humidity data loggers and OM-CP-WIND101A data logger with a 3-cup anemometer. Globe temperature was measured using Tiny-tag data-loggers with a thermo-couple thermistor probe inserted inside a 40mm (D= dia= 0.04m) globe painted in Humbrol matte grey (ε = emissivity =0.97). Subsequently, Tmrt was measured using the following formula:

$$\text{Tmrt} = \left[\frac{\left(T_g + 273\right)^4 + \left(1.10 \times 10^8 V^{0.6}\right)\left(T_g - T_a\right)}{\left(\varepsilon D^{0.4}\right)}\right]^{1/4} - 273$$

A questionnaire survey was carried out along with physical measurements among 339 people. Pedestrians were asked about their thermal sensation. The actual thermal sensation vote was analysed according to ASHRAE seven point thermal sensation scales [3].

Typical values from site measurements were used to set up the boundary conditions for the micro-climate simulation tool ENVI-met 4. ENVI-met is a numerical microclimatic tool with high temporal and spatial resolution that is able to recreate the major microclimatic processes inside complex urban arrangements [4]. In order to examine comfort conditions in outdoor spaces, this study adopted PET (Physiologically Equivalent Temperature) [5]; a widely used thermal comfort index based on the Munich Energy-balance Model for Individuals (MEMI). The simulated climatic data calculated by Envi-met that included Ta, RH, Tmrt and V was used as an input for PET calculations in Rayman Pro [6].

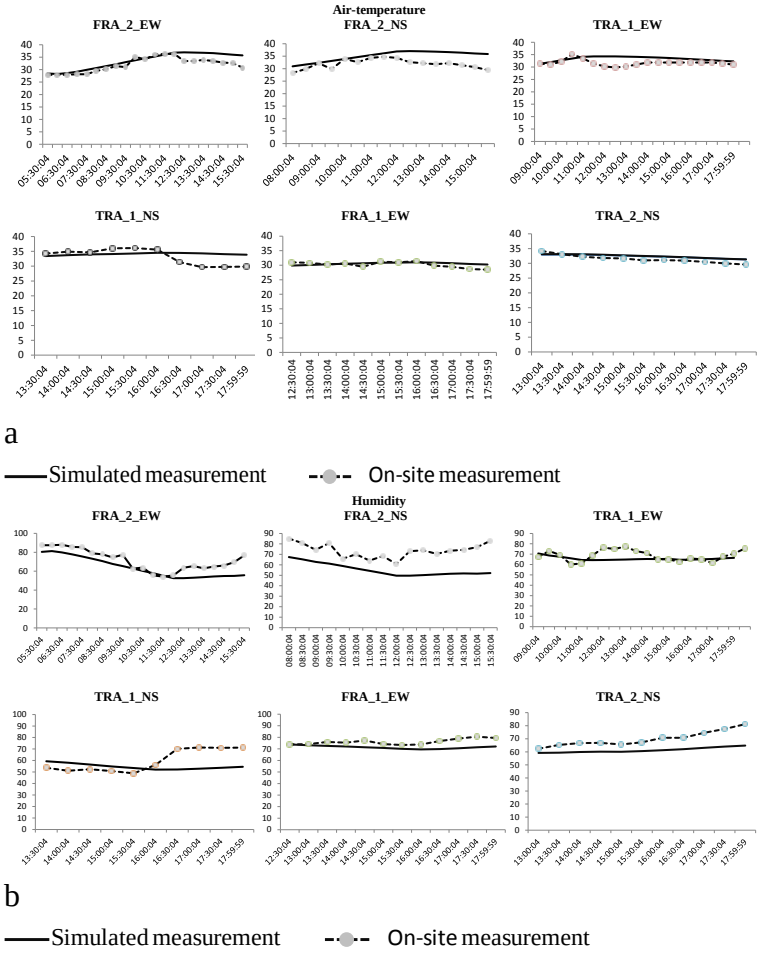

Figure 3: Simulated versus on-site measurements of a) air-temperature, b) humidity

RESULTS

Micro-climatic simulations using ENVI-met for the hot-humid climate of Dhaka is validated through the current study by comparing actual on-site measurements with the simulated measurements of the climatic variables. Comparison of air-temperature, humidity and Tmrt led to the conclusion that simulation results were in good agreement with actual measurements (Fig. 3, Fig 4). Only exception was FRA_2_NS where humidity and Tmrt was over estimated by simulation. This can explained by the fact that simulation models were kept as simple as possible due to their long running time. Therefore, due to their simplicity, the exact character, number and position of plants are not identical to the actual sites. Plant sizes and their positions seem to have affected the humidity and Tmrt levels.

Another anomaly was identified regarding windspeed in traditional areas that are more diverse in character (TRA_1_EW, TRA_1_NS). Simulated results, in this case, deviated quite

extensively from the actual values. It is one of the model limitations that the windspeed and direction at the model boundary remains constant throughout the simulation period although this is modified inside the model depending on the presence of 3 dimensional objects. This indicates the calculation of windspeed using ENVI-met can be somewhat compromised for very complex urban geometry. It is also important to remember that simulations tools are mainly for understanding the trend of microclimate, rather than generating actual numbers. However, the model is not solely accountable for the deviation. Most other micro-climatic sites in the city were found to have very low windspeed, while, the site in question was reported with high turbulence during the survey. Therefore, none of the other sites were affected by the fact. The reason why windspeed was higher in the particular site is due to the fact that the site is located next to an abandoned airport, making the north-west side of the area totally open. This makes the wind-pattern in the area rather unpredictable. Accurate windspeed prediction of the area will mean modelling of entire the urban district in a very high resolution. The necessary modelling time and computer power is beyond the scope of this research.

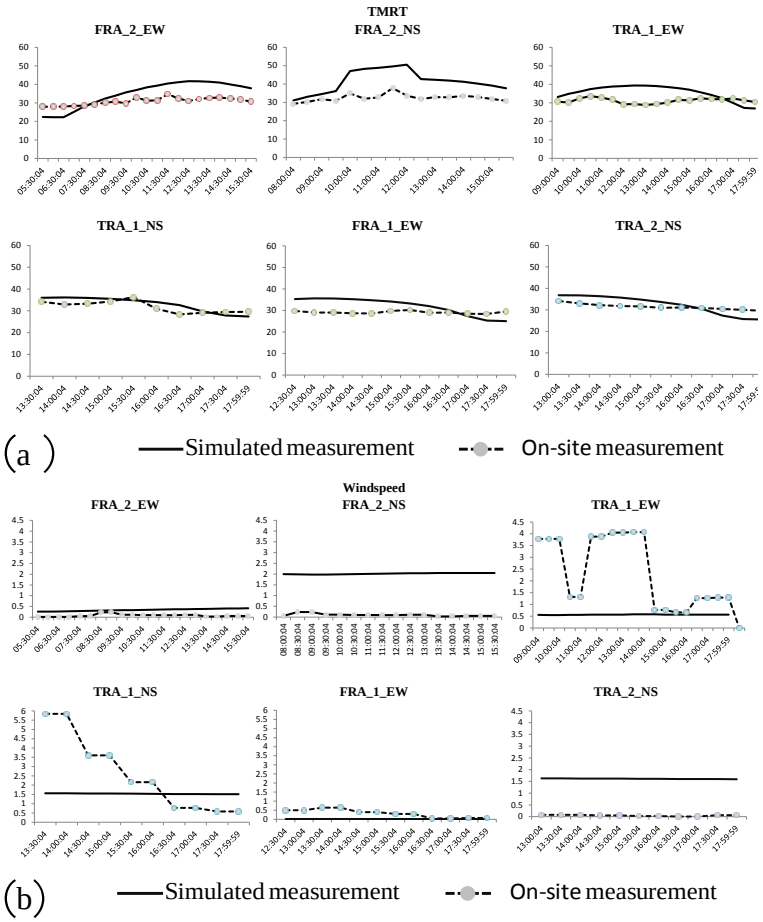

Figure 4: Simulated versus on-site measurements of a) Tmrt, b) windspeed

PET was compared with ASV for all case-study areas and a moderate (spearman's rho = 0.348) but significant correlation (p-value = 4.883e-11) was found. This finding suggest theoretical comfort calculation will follow the similar trend as the actual comfort sensation of the pedestrians, but the latter may not be fully explained by physical conditions only. Afterwards, PET was calculated separately for the traditional and formal areas. For formal areas a stronger (spearman's rho = 0.58) and significant (p-value < 2.2e-16) correlation was seen between PET and ASV. This is due to good agreement between micro-climate variables in simulated models and actual measurements. Also, the comparatively simpler geometry in the formal areas aided analysis and understanding of the outdoor comfort conditions through theoretical calculations.

Within traditional areas, especially in TRA_1_EW, TRA_1_NS, simulation model was still able to predict the micro-climatic variables quite competently except for the windspeed, as discussed previously. Windspeed is an important parameter for outdoor thermal comfort and was somewhat compromised in the micro-climatic simulations. Since, simulated windspeed was lower in case of TRA_1_EW and TRA_1_NS and higher in TRA_2_NS than the actual values (Fig. 4) PET was slightly overestimated in the first two cases and under-estimated in the third case respectively.

	MICRO-CLIMATE SITE NAME	ABBREVIATED NAME	H/W RATIO	SVF
1	TRADITIONAL RESIDENTAL AREA 1 EAST-WEST_ SOUTH1 KAFRUL	TRA_1_EW	2.6	0.177
	TRADITIONAL RESIDENTAL AREA 1 NORTH-SOUTH_ SOUTH KAFRUL	TRA_1_NS	2.5	0.231
2	TRADITIONAL RESIDENTAL AREA 2 NORTH-SOUTH _ MID KAFRUL	TRA_2_NS	3.5	0.149
3	FORMAL RESIDENTIAL AREA 1 EAST-WEST_MAHAKHALI DOHS	FRA_1_EW	2.4	0.201
4	FORMAL RESIDENTIAL AREA 2 EAST-WEST_BARIDHARA DOHS	FRA_2_EW	1.8	0.229
	FORMAL RESIDENTIAL AREA 2 NORTH-SOUTH _BARIDHARA DOHS	FRA_2_NS	1.2	0.259

Table 1. Site names, abbreviations and urban geometry characters

Subsequently, statistical analysis in the traditional sites between PET and ASV produced weak (spearman's rho =.238) but significant (p value = 0.003) correlations. Apart from the physical microclimate, ASV seems to be deviated from PET for the effect from thermal adaptation as well. The roads in these areas being quite narrow and deep were able to cut down large amount of solar radiation. However, other factors like higher traffic and absence of pavements may have affected the ASV in TRA_2_NS, while the other two streets (TRA_1_EW, TRA_1_NS) were not affected due to lower traffic.

Thermal sensation	PET range
Cold	14-18
Cool	18-22
Slightly cool	22-26
Neutral	26-30
Slightly warm	30-34
Warm	34-38
Hot	38-42
Very hot	<42

Table 2. PET range for Taiwan

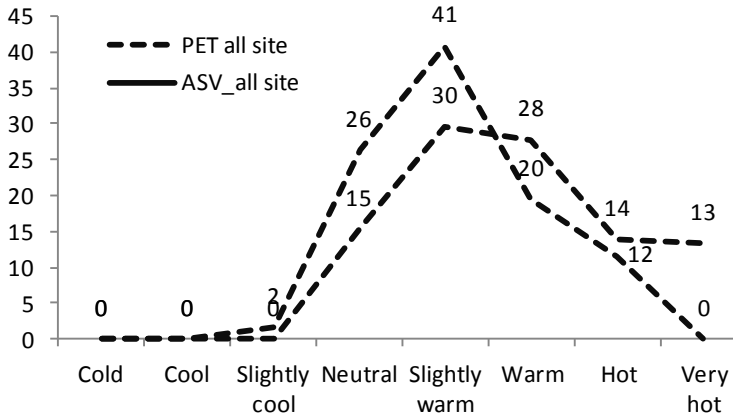

Figure 5: Comparison of ASV and PET (percentage) all sites

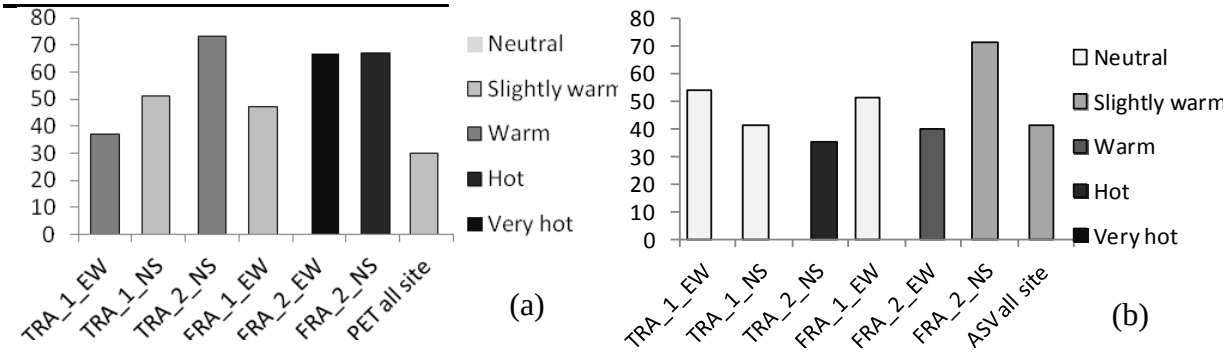

Figure 6: Compare peak thermal sensation in each site for PET(a) and ASV(b) analysis

For the hot-humid climate of Dhaka, comfortable temperatures for outdoor conditions ranges from 28.5^0C to 32^0C at an average relative humidity of 70% under still air conditions for people wearing typical summer clothes (0.4 to 0.5 Clo) and involved in sedentary activities [7]. This comfort range is not categorised for PET index. In the absence of a 'PET range' for Dhaka, the scale developed for Taiwan (warm-humid sub-tropical region) has been used in this study [8]. The PET data was arranged according to the PET range and ASHRAE seven point thermal comfort scale and then compared with the ASV data collected through the questionnaire survey. The comparison of shows that in both analyses most people were found to be feeling 'slightly warm': 41% for ASV and 30% for PET analysis (Fig 5). However, the PET analysis slightly overestimates people feeling 'warm' and 'hot' and highly overestimates

people feeling ‘very hot’. In the actual survey, none of the subjects reported feeling ‘very hot’.

The peak thermal sensation for both ASV and PET analysis on site by basis are also compared to each other (Fig 6). Thermal sensation was over estimated for each of the sites by PET analysis, except TRA_2_NS. For example, the peak thermal sensation for TRA_1_EW, TRA_1_NS and FRA_1_EW were ‘neutral’. But this has been replaced by ‘warm’, ‘slightly warm’ and ‘slightly warm’ respectively. It is anticipated that the road conditions, pavements and traffic, as mentioned before, have further modified the thermal comfort levels apart from the micro-climate. The other formal areas FRA_2_EW and FRA_2_NS were highly overestimated by PET, especially, for the east-west streets, although the micro-climate was quite accurately predicted in the simulated model. The use of a PET range from a different city may have affected the results to some extent. This still indicates, theoretical comfort largely ignores the thermal adaptation level of the pedestrians in a tropical climate.

CONCLUSION

Numerical simulations in this study were found to be in good agreement with actual microclimate measurements. Theoretical comfort calculated using simulated data, on the other hand produced mixed results depending on the site geometry. For simple urban geometry in the formal areas, the results were strongly aligned with actual measurements, although overestimated. For complex geometry in the traditional areas, a poor correlation was reported and the results deviated significantly. This indicates, as long as microclimatic simulations are closely correlated with actual measurements, theoretical comfort (PET) will follow a similar pattern as the actual comfort (ASV). However, this does not mean PET values will be identical to the ASV values. In fact, for most of the microclimates sites PET was overestimated in relation to ASV. Previous studies have also demonstrated that a solely physiological approach is insufficient to understand comfort conditions outdoors [1]. This suggests that theoretical comfort models can be applicable for obtaining a relative understanding of comfort situations at urban outdoors; however, they can vary considerably from actual thermal sensations due to the role of thermal adaptation.

REFERENCES

1. Marialena, N.: Thermal comfort in outdoor urban spaces (Doctoral dissertation, University of Cambridge), 1998.
2. Rajapaksha, I. and Rathnayaka, C. T.: Thermal acceptability for urban parks in tropics: Evaluating the effects of environmental attributes on user perceived controls. Proc. of the 8th Windsor Conference, London, 2014.
3. ASHRAE Standard 55:thermal environmental conditions for human occupancy, ASHRAE Inc., Atlanta, 1992.
4. Ali-Toudert, F.: Dependence of outdoor thermal comfort on street design in hot and dry climate (Doctoral dissertation, Universitätsbibliothek Freiburg), 2005.
5. Höppe, P.: Heat balance modelling. *Experientia*, Vol 49, pp 741-746, 1993
   Matzarakis and Rutz 2006
6. Matzarakis, A. and Rutz, F.: Modelling the thermal bioclimate in urban areas with the RayMan Model. International Conference on Passive and Low Energy Architecture, 2006.
7. Ahmed, K. S.: Comfort in urban spaces: defining the boundaries of outdoor thermal comfort for the tropical urban environments. Energy and Buildings, Vol 35(1), pp 103-110, 2003.
8. Lin, T, et al.: Shading effect on long-term outdoor thermal comfort, Building and Environment, Vol 45 (1), pp 213-221-, 2010.

A METHOD FOR THE GENERATION OF MULTI-DETAIL BUILDING ARCHETYPE DEFINITIONS: APPLICATION TO THE CITY OF LISBON

Claudia Sousa Monteiro[1]; Carlos Cerezo[2]; André Pina[1]; Paulo Ferrão[1]

1: IN+, Center for Innovation, Technology and Policy Research IST - Instituto Superior Técnico, Lisbon University. Avenida Rovisco Pais 1, 1049-001 Lisbon

2: Building Technology Program, MIT - Massachusetts Institute of Technology, Cambridge, MA, United States

ABSTRACT

In Europe, buildings are responsible for 40% of energy consumption and about 35% of the current building stock is over 50 years old. A significant part of this energy consumption is determined by the buildings' characteristics. However, cities are complex systems with a diverse and very large number of buildings and, as a consequence, the quantification of energy consumption in the existing building stock requires the characterization of a set of buildings types that may represent most of the built urban environment.

It is therefore necessary to limit the number of building types to analyse, in a compromise between feasibility and accuracy. As such, there is a need to establish methods that define sets with limited numbers of building archetypes, but that are still able to represent the entire building stock. Furthermore, it is important to understand which restrictions can limit the development of these classifications.

This paper presents a method intended to characterize archetypes for an effective simplification of the modelling of the urban built environment. The method enables the development of different levels of classification of the built environment. This classification is dependent on the available data and documented sources, as well as on the definition of several parameters related with the final model goal.

The result of the method is an archetypal tree-data structure with a set of detail dependent archetype tiers, that allow structuring the building stock typification as a base for the evaluation of urban modelling techniques and their uncertainty.

The method is applied to the city of Lisbon. The results show how much the building stock characterization can be simplified and how many building types should be considered. In particular, it proves how the creation of archetypes depends highly on the level of detail of the considered parameters and the availability of reliable data. As a final product of this work, a complete dataset of building archetypes for Lisbon is provided, as well as a set of recommendations for improving or expanding existing urban information.

Keywords: Building Stock, Building Archetype, Urban Modelling

INTRODUCTION

The opportunity to improve the overall energy performance of buildings through retrofitting strategies is increasing and becoming more important, once the building stock, mainly in developed cities, is getting old and corresponds to a large share of the built environment. Additionally, the Energy Performance of Buildings Directive [1], established clear guidelines

for the promotion of energy efficiency in buildings up to 2020 and further, constituting an opportunity for the existing building stock to become more energy efficient.

The building stock, even at city scale, is very large and diverse, making it necessary to limit the number of buildings to analyse, in a compromise between feasibility and accuracy. Therefore, the classification of a set of building-types which represent the characteristics of large groups of buildings in the stock is required.

The building stock can be described in categories of sample buildings and/or archetypes, and the literature provides several descriptions of the building stock for several EU countries with the purpose of modeling its energy demand [2]. Stock modelling based on archetypes is considered a promising tool for exploring resource and emissions reduction. It is particularly helpful in stock aggregation with the potential of analyzing the existing stock and can be used to make scenarios of energy retrofit measures and future projections [3].

Building archetypes are theoretical buildings created by a composite of several characteristics found within a category of buildings with similar attributes. Therefore an archetype is a virtual representation of a number of buildings that share similar characteristics in the stock.

In this study is proposed a new methodology with a qualitative approach to archetypes' construction for compiling, structuring, validate and representing the information of the existing building stock. This paper describes the building stock typification as basis for urban models, namely a) reviewing the existing methodologies, identifying key issues as data input and sources of information; b) describing a new methodology for building stock typification applicable at different scale levels and for different purposes and c) applying the proposed method to Lisbon city.

METHODOLOGIES FOR BUILDING STOCK TYPIFICATION

Supplementing EPDB, the commission guidelines [4] on the energy performance of the buildings establish that reference buildings should be defined using one of the two following ways: selection of real example building or the creation of a virtual building. According to [5] [6] [7] [8], the typification of the building stock, as reference buildings or buildings typologies, can be summarized by the following three methodologies:

- *Real Building Methodology*: selection of a real existing building representing the most typical building in a specific category. The selection process is performed through a statistical analysis in order to find out the real building with characteristics similar to the mean geometrical and construction features of the statistical sample.

- *Example Building Methodology:* creation of a virtual building which for each relevant parameter includes the most commonly used material and systems on the basis of expert inquiries and other sources of information - no statistical data available.

- *Synthetical Average Building Methodology*: creation of a virtual building which for each relevant parameter includes the most commonly used material and systems using basic statistical data; Statistical composite of the features found within a of buildings in the stock.

Table 1 outlines several publications focusing on the typification of building stock for energy models purposes. The most common methodology used is the Synthetical Average since it relies on statistical data analysis. Still, there are some studies that combine two methodologies in order to overcome the lack of information in some parameters. However, studies that combine all the methodologies applied to the Portuguese case were not found.

Paper	Concept			Method			Parameters				Scale			Scope
	Bld Typology	Reference Bld	Archetype	Real Building	Example Building	Synthetical Average	Climate Zone	Constr. Period	Bld Type	Other Parameters	National	Regional	Urban	
[5]		X			X	X	X	X	X	X			X	residential
[2]			X			X	X	X	X	X	X			resid/non-resid
[9]	X					X	X	X	X	X		X		residential
[7]		X			X	X	X	X	X	X		X		residential
[10]	X				X		X	X	X	X	X			residential
[11]	X			X		X		X	X	X	X			residential
[12]	X			X		X	X	X	X	X	X			residential
[6]		X			X	X	X	X		X	X			office
[13]		X		X		X		X	X	X			X	residential
[14]	X				X		X	X	X	X	X			residential
[15]	X					X		X		X	X			residential

Table 1: Literature Review of Building Stock Typification Studies

Climate Zone, Construction Period and Building Type are usually the parameters that serve as selection criteria for the building stock segmentation. Still, there are other parameters that must be defined and detailed in order to build the energy model. These additional parameters can be divided into four different sets, based on DOE's report [16]: Geometry (form), Construction (fabric), Systems (equipment) and Operation (program). The parameters definition for each set is dependent on the chosen energy model data requirements. For other modelling purposes, other selection and additional parameters sets can be established without compromising the building stock typification process.

Regardless of having several studies applying the methodologies described above, there is no agreement in a common approach between the definition of reference buildings and the existing buildings' data, which is creating several problems at national and European level [6] [7]. As a result, the *TABULA (Typology Approach for Building Stock Energy Assessment)* project effectively made the effort of constructing a European database of building typologies sharing the same approach, by presenting a methodology for the identification of reference buildings focusing on residential building types. Studies 7, 10, 11, 12, and 14 presented in Table 1 follow the *TABULA* approach, which counts with the data of 13 participating countries as part of its building typology database. The proposed *TABULA* methodology is therefore the reference used in Europe for building stock typification in energy demand studies.

This methodology displays the building typologies in a 'building typology matrix' for a specific climate zone and use. The matrix is characterized by two axes, namely the building age class and the building size class. Each cell in the matrix contains a reference building type that is a building considered representative of that specific condition. This categorization procedure may not be most appropriate and can be considered rigid since it is represented by a bi-directional matrix with fixed parameters as the period of construction and building size-class.

The process of categorization is very complex and its accuracy will rely on the level of detail of the building-types. Although *TABULA* does not constrain the methodologies that can be used in simultaneous, the majority of the studies based on this approach rely on one or sometimes two methodologies.

Define buildings-type accurately is important to achieve realistic results and therefore the use of all methodologies in simultaneous allows the access to more data from different sources and can overcome the problem of lack of data in building-types categorization.

METHOD

This paper presents a new method for the identification of building-types, which is innovative in two important points. First, it is a mixed method since it combines all the methodologies described before. For each relevant parameter, it includes as input statistical, empirical and real data. All the sources of information available are considered, allowing a more complete characterization of the existent building stock in archetypes and accurate energy estimation. Second, the information is structured using a data-tree arrangement instead of a matrix, working as decision analysis and giving more flexibility in the building categorization. Important insights can be generated based on experts through changes in the order of the tiers of archetypes, adapting the model to the real case-study and identifying the better strategy to reach a specific goal. It also allows new possible scenarios for archetypes definition through the addition or through different combination of the selection parameters.

The methodological approach is divided into the following steps (Figure 1):
1 – Parameters Definition: All the parameters needed for the model are identified. The parameters used depend on the goal of the study and the chosen model to materialize it.
2 – Categorization: Considering the previous list, define which parameters are considered as Selection Parameters. Selection Parameters are those which will serve as base criteria to define the different tiers in the data-tree. The number of selection parameters corresponds to the number of detail tiers.
3 – Data-Tree: Based on the number of tiers, define the order. Each tier represents the outcome for the selected parameter and each node represents the corresponding archetype.
4 – Characterization: Define all the parameters for each Archetype in the selected tier. Compare the attributes to avoid redundancy between archetypes and eliminate the ones not required before passing to the other tier. As final result, a database of archetypes with all parameters characterized according to the order of selection parameters defined previously is constructed.
5 – Archetypes Frequency: Definition of weighting factors for the archetypes in order to quantify the number of existing buildings applied to each class. A GIS map allocating spatial information and the archetypes characteristics can also be developed.

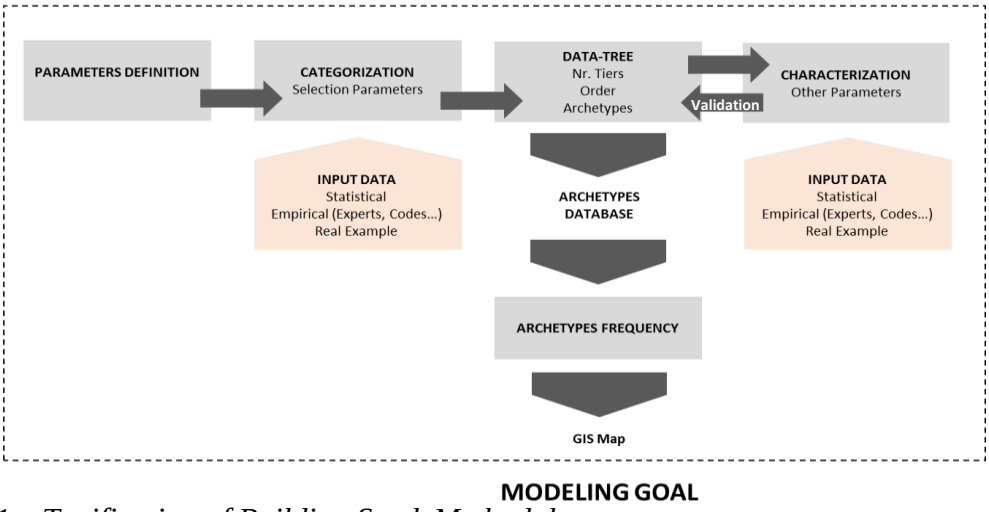

Figure 1 – Typification of Building Stock Methodology

CASE-STUDY

Lisbon City was selected as case-study to demonstrate the methodology. A restricted area within the urban territory was defined here, however the methodology can be applied at urban, regional or national scale. The archetypes characterized will be used for modelling the environmental performance of the neighborhood and city with respect to operational and embodied energy use, walkability and daylighting potential, using UMI – Urban Modelling Interface, a tool developed by the Massachusetts Institute of Technology team.

Considering this tool, the parameters needed for the model were identified. The selected parameters included the climatic zone, the main use, the period of construction and the roof type, since these are the parameters that bring higher variability to the model. After the last tier outcome, the other parameters remain relatively constant not justifying more detail.

RESULTS

The following figure exemplifies the archetypal data-tree for this case-study. For the selection parameters 3 tier of detail were determined resulting in 13 archetypes for this neighbourhood. The data-tree arrangement allows the user to set the boundaries regarding the energy model goals and compare results when considering a specific aggregation of parameters or all of them. Therefore, the presented archetypes are options for decision making allowing the test of different scenarios. Also, the graphical representation enables a better comprehension of the relations between parameters and a critical view of the quality of the outcome. This methodology is flexible enough to integrate more parameters and consequently more detail into the model without compromising the archetypes already set before.

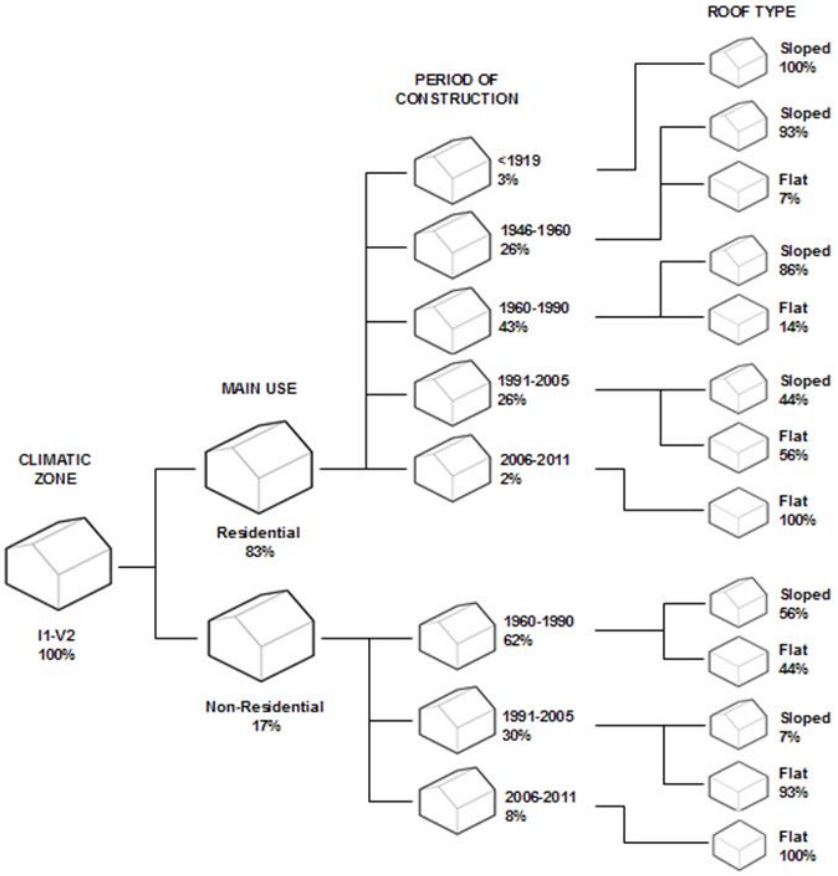

Figure 2 – Archetypal Data-Tree – Lisbon Case-Study

CONCLUSION AND FUTURE WORK

This paper presents a new methodology for the development of archetypes that characterize the existing building stock. This can be used for studies on building energy performance, LCA, risk prevention and policies towards effective refurbishment measures, among others. It is a hybrid method since it combines several methodologies, which results in the use of more complete input data, increasing the model accuracy without compromising its feasibility.

As a result, this new methodology reduces uncertainty related with the building stock typification since it considers several sources of information and several parameters detail. The goal is to provide the most complete and comprehensive framework of the archetypes

able to represent the existent building stock. The data-tree structuration proved to be a useful representation in the typification of a large number of buildings, with different sizes and complex characteristics. The number of archetypes required to accurately represent the building stock differs considering the detailing and differentiation pretended. The final number of archetypes achieved changes with the variation on the selection parameters, depending on how is stablished the cutting criteria line.

Further investigation involves an identification of the most relevant variables which explain energy use through a statistical parametric analysis able to identify and rank the key parameters and the development of archetypes based on that. Thus, it will be possible compare this method with the one presented in this paper and analyse the modelling results when considering a quantitative versus a qualitative approach in archetypes data-tree construction.

REFERENCES

[1] European Comission, "Directive 2012/27/EU of the European Parliament and of the Council of 25 October 2012 on energy efficiency, amending Directives 2009/125/EC and 2010/30/EU and repealing Directives 2004/8/EC and 2006/32/EC," *Official Journal of the European Union,* vol. 55, pp. 1- 56, 2012.

[2] É. Mata, A.S. Kalagasidis, F. Johnsson, "Building-stock aggregation through archetype buildings: France, Germany, Spain and the UK," *Building and Environment,* vol. 81, pp. 270-282, 2014.

[3] A. A. Famuyibo, A. Duffy and P. Strachan, "Developing archetypes for domestic dwellings - an irish case study," *Energy and Buildings,* vol. 50, pp. 150-157, 2012.

[4] E. Comission, "Guidelines accompanying Commission Delegated Regulation (EU) No 244/2012 of 16 Jan. 2012 supplementing Directive 2010/31/EU," *Official Journal of the European Union,* 2012.

[5] A. Vasconcelos, M.D. Pinheiro, A. Manso, A. Cabaço, "A Portuguese approach to define reference buildings for cost-optimal methodologies," *Applied Energy,* vol. 140, pp. 316-328, 2015.

[6] S. Corgnati, E. Fabrizio, M. Filippi,V. Monetti, "Reference buildings for cost optimal analy-sis: methods of definition and application," *Applied Energy,* vol.102, pp 983-993, 2013

[7] I. Ballarini, S. P. Corgnati and V. Corrado, "Use of reference buildings to assess the energy saving potentials of the residential building stock: The experience of TABULA project," *Energy Policy,* vol. 68, pp. 273-284, 2014.

[8] TABULA, "Typology Approach for Building Stock Energy Assessment. Main Results of the TABULA project.," IEE-EPISCOPE, 2013.

[9] L. Filogamo, G. Peri, G. Rizzo and A. Giaccone, "On the classification of large residential building stocks by sample typologies for energy planning purposes," *Applied Energy,* vol. 135, pp. 825-835, 2014.

[10] K. Droutsa, S. Kontoyiannidis, E. Dascalaki and C. Balaras, "Ranking cost effective energy conservation measures for heating in Hellenic residential buildings," *Energy and Buildings,* vol. 70, pp. 318-332, 2014.

[11] J. Kragh and K. Wittchen, "Development of two Danish building typologies for residential buildings," *Energy and Buildings,* vol. 68, pp. 79-86, 2013.

[12] T. P. Team, "Application of building typologies for modelling the energy balance of the residential building stock," Episcope - TABULA Thematic Report, 2012.

[13] G. Dall'O, A. Galante, M. Torri, "A methodology for the energy performance classification of residential building stock on an urban scale," *Energy and Buildings,* vol. 48, pp. 211-219, 2012.

[14] E.G. Dascalaki, K.G. Droutsa, C.A. Balaras and S. Kontoyiannidis, "Building Typologies as a tool for assessing the energy performance of residential buildings - A case study for the Hellenic building stock," *Energy and Buildings,* vol. 43, pp. 3400-3409, 2011.

[15] I. Theodoridoua, A. M. Papadopoulosb and M. Heggera, "A typological classification of the Greek residential building stock," *Energy and Buildings,* vol. 43, pp. 2779-2787, 2011.

[16] M. Deru and e. al, "U.S. Department of Energy Commercial Reference Building Models of the National Building Stock," NREL, National Renewable Energy Laboratory, 2011.

URBAN ENERGY SIMULATION OF THE EPFL CAMPUS IN FRIBOURG USING A NEW PARADIGM: THE CITYGML APPLICATION DOMAIN EXTENSION ENERGY

Silvia Coccolo[1], Jérôme Kaempf[1,2]

1: *Solar Energy and Building Physics Laboratory, EPFL, Switzerland*
2: *kaemco LLC, La Riaz 6, 1426 Corcelles-Concise, Switzerland*

ABSTRACT

Rapid urbanisation and the increasing world population call for a new approach in urban design, favouring energy efficiency and sustainability of the built environment. When focusing on City Energy Modelling, unlike Building Energy Modelling, each urban simulation engine generally has its own tailor-made data-model: municipalities and other urban information data administrators use their own data base structure to collect and manage urban information data, without the possibility to store and share urban models. To address this issue, since May 2014, an international consortium of urban energy simulation developers and users is establishing an Urban Energy Information standard, as Application Domain Extension (ADE) of the CityGML urban information model. This paper presents a methodology to establish a gateway between one of the urban simulation tools CitySim and the CityGML Energy ADE data format. The future EPFL campus in Fribourg is presented as case study, demonstrating the storage possibility of the CityGML Energy ADE of geometrical properties and annual heating and cooling demands for each building. The connection between CitySim and CityGML Energy ADE represents an innovative approach to urban energy analysis: a city model can be simulated, stored and exchanged between the two formats creating a common database of knowledge, in which researchers and municipalities could share their results.

Keywords: CityGML, Urban Energy Simulation, urban data model

INTRODUCTION

Due to a rapid urbanization throughout the planet, planners and decision makers from municipalities are facing important challenges in controlling the growth of the number of shelters and their associated energy consumption. Furthermore, the current densification of city centres demands inevitable planning choices that need to be addressed from the city scale point of view in order to mitigate traffic and building energy consumption but also to increase the use of renewable energy sources. To address these urban scale elements, specific algorithms and software solutions have recently been developed by international research centres and private sector actors.

When focusing on City Energy Modelling, unlike Building Energy Modelling where few well-established building information model standards exist (IFC, gbXML, etc.) and serve as exchange support between different tools and experts, each urban simulation engine generally has its own tailor-made data-model. The situation gets even more complicated as municipalities and other urban information data administrators use their own data base structure to collect and manage urban information data. This leads to multiple import and export features for the different tools that may complicate the life of practitioners and feel like an everlasting starting over.

To address this issue, an international consortium of urban energy simulation developers and users (11 European organisations[1] representing 5 urban energy platform developments[2]) has since May 2014 been working on an Urban Energy Information standard, as Application Domain Extension (ADE) of the CityGML urban information model. CityGML is a XML-based open data model for the storage and exchange of virtual 3D city models, issued by the Open Geospatial Consortium (OGC) [1]. CityGML is organised around a CityGML core model, prolonged by Application Domain Extensions (ADE) for different purposes such as: geometry, construction, occupancy and energy systems. With the Energy ADE under development, the set of ADE will allow adding energy related information to existing CityGML models. The CityGML core is already well established for the modelling of whole agglomerations (Berlin, Lyon) [2] [3], regions and countries (Germany) [4]; it offers possibilities for numerous and varied spatial analyses at city scale, such as noise mapping, urban wind flow studies, photovoltaic potential or flood risk analysis. A considerable asset of CityGML is its flexible object modelling at different Levels of Details [5], enabling the virtual city model to adapt to local building parameter availability and application requirements.

This paper starts with a brief introduction of the specificities of the CityGML Energy ADE standard and presents the first simulation results based on CitySim simulation. CitySim is an urban energy modelling able to quantify heating and cooling demand from a single building to the urban scale with simplified input physical and geometrical data [6]. The aim of this study is to use as a first case-study the project of the EPFL campus in Fribourg to be completely described (geometrically and physically) using the CityGML Energy ADE with a level of detail allowing for hourly dynamic simulations. The first results are visualized with FZKViewer [8], a free program able to read and display geometrical 3D CityGML data. Further results showing the thermal behaviour of the campus today and in future climatic scenarios, according to Institute panels of Climate Change (IPCC) - scenarios A1B, A2 and B1 [7], are stored using the CityGML Energy ADE. The paper concludes with an analysis of the future possibilities offered by the new data model.

METHODOLOGY

The methodology aims to show the gateway between CitySim and CityGML data models. It starts by explaining the paradigms behind the CitySim data model, and follows by detailing those of CityGML Energy ADE. It ends by defining the case-study on which we will shift from the CitySim to the CityGML data model to demonstrate the exchange of information concerning geometrical properties of buildings and their annual energy demand.

CitySim data model

The CitySim data model is based on the XML (eXtensible Markup Language) format and composed of different modules defining each a building in the scene:

- Building thermal zone, which contains the information about volume, set-point temperatures for heating/cooling, infiltration rate and thermal bridges, but also:
    - Occupation (number of occupants, and their profile during the day)

[1] Hochschule für Technik Stuttgart, Technische Universität München, Karlsruhe Institute Technology, RWTH Aachen University, HafenCityUniversität Hamburg, European Institute for Energy Research, Ecole Polytechnique Fédérale de Lausanne, Centre Scientifique et Technique du Batiment, Electricité de France, Sinergis, M.O.S.S Computer Grafil Systeme.

[2] CitySim, SimStadt, Energy Atlas, Modelica library AixLib, Sunshine platform.

    - Description of the Walls (geometrical and physical, together with the characteristics of the windows and photovoltaic systems)
    - Description of the Roofs (same parameters)
    - Description of the Floors (same parameters)
- Energy system for heating and cooling purposes.

The structure is tree-based with objects included in other objects such as Walls inside a Thermal Zone inside a Building.

CityGML with Energy ADE data model

CityGML with Energy ADE is structured by the following four interrelated modules, which are linked to the 3D information in the CityGML core through references:

- Building, Zones and Boundaries: contains information concerning building geometry, thermal zones, opening and schedules.
- Construction and Layers: defines physical characteristics of the envelope, such as materials, and their physical and optical properties (emittance, absorptance, transmittance, and reflectance).
- Occupancy Module: describes the usage of the building, the presence of occupants, and the consequent usage of facilities and appliances.
- Energy System Module: describes the energy demand supplied by different energy systems (conversion, distribution and storage).

The four modules are completely independent of each other, may also not be present and are linked together through references.

The gateway between CitySim and CityGML Energy ADE data model

According to previous analysis, the CitySim and CityGML data model have common data organized in different structures. The structure of the CitySim data model is tree-based, where a district contains buildings, and each building contains thermal zones, which contain further information about the building such as physical and geometrical characteristics. On the other hand, the structure of the CityGML data format is organized in independent modules which may or may not be present for each building. Figure 1 summarizes the idealized structure of CitySim (a) and CityGML Energy ADE (b). In CitySim the building tag contains all information about the building; on the other hand with the CityGML Energy ADE each module is linked with the CityGML core and some modules are interconnected between them: Building, Zones and Boundaries are linked with Occupancy and Energy System modules, and the latter is connected with Construction and Layer.

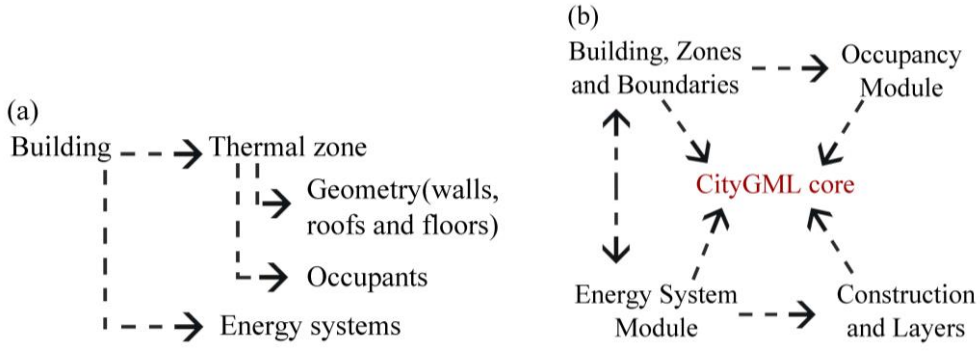

Figure 1 Idealized data structure of CitySim (a), and CityGML Energy ADE (b)

An adequacy between the two data models can be defined: both 3D geometrical and physical data from the CitySim data model can be transferred to the CityGML data model. The same

process can be established for the simulations results: urban models simulated with the CitySim software can be saved using the CityGML Energy ADE including the annual heating and cooling demand of each building.

Case study: the EPFL campus in Fribourg

The EPFL campus in Fribourg will be an outstanding centre of research in technology, construction and sustainable architecture; this centre will be set up in collaboration with the School of Engineering and Architecture HEIA-FR and the University of Fribourg. The scientific pole, called BlueFACTORY, will host academic and private partners, promoting public-private partnerships. The site is under construction and an international design competition drew the masterplan design [9] that is composed of nine new buildings, among which the Smart Living Lab, a smart building able to combine sustainability with human wellbeing.

The numerical model of the campus was established with the software CitySim from geometrical DXF data and completed with physical attributes corresponding to Minergie-P standards. The envelope is designed as a double concrete wall with a central EPS insulation layer and a U-value equal to 0.1 ($W \cdot m^{-2} \cdot K^{-1}$); the windows are made of triple glazing with argon covering 0.5 of the façade, their U-value is equal to 0.7 ($W \cdot m^{-2} \cdot K^{-1}$) and g-value equal to 0.7. The total area of the campus is about 77.000 m² according to original 3D geometry [10]. The buildings are simulated without occupants and electrical devices, under current and future climatic scenarios (IPCC 2100 A1B, A2 and B1).

RESULTS AND DISCUSSION

Using the previously described methodology, we present in what follows the abilities of the CitySim software to export the geometrical information to the CityGML data format, and to further export the annual simulation results for heating and cooling demands using the CityGML Energy ADE.

Geometrical information

The model of the EPFL campus in Fribourg presented in Figure 2 is read and displayed by the FZKViewer. The geometrical data exported maintain a distinction between walls, roofs and floors.

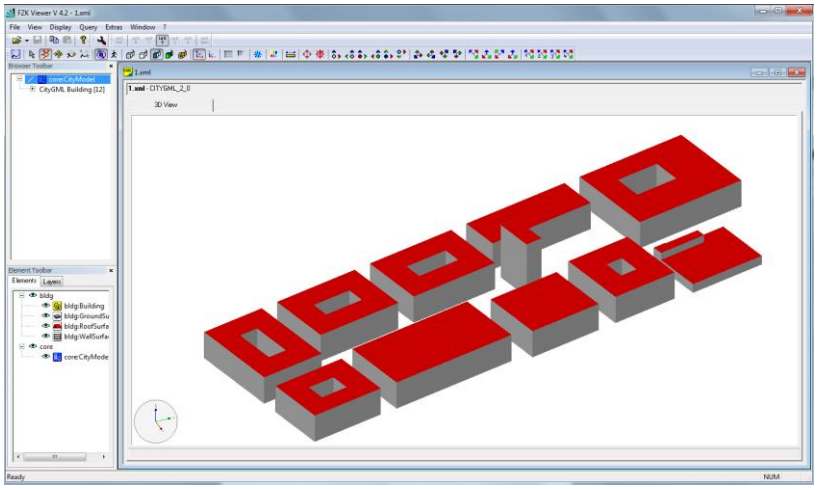

Figure 2 EPFL campus in Fribourg exported in GML format

Annual energy demand for heating and cooling

The results obtained with CitySim are stored using the CityGML Energy ADE. According to last year's averaged weather data, the campus would consume 1300 GWh for heating and 590 GWh for cooling (to maintain a maximum internal temperature of 26°C during summer). In future climatic scenarios the heating demand would decrease by 6% (scenario B1) to 17% (scenario A2) and the cooling demand would increase by 35% (scenario B1) to 140% (scenario A2). In scenario A2 the averaged energy demand for cooling will be 18 kWh/m² slightly higher than the heating demand which is equal to 14 kWh/m². Figure 3 shows the annual heating demand of the site for the current climate scenario (expressed in kWh/m³ per each building) using a 3D representation and a colour scale, and Figure 4 shows an extract of the corresponding CityGML ADE Energy XML file. The energy demand for heating (<energy:id> SpaceHeating_1 </energy:id>) and cooling (<energy:id> SpaceCooling_1 </energy:id>) is defined for each building and expressed in kWh per year, under the tag: <energy:values>156412.8</energy:values>. The tag <gml:TimePeriod> represents the period of simulated results, in this case annual.

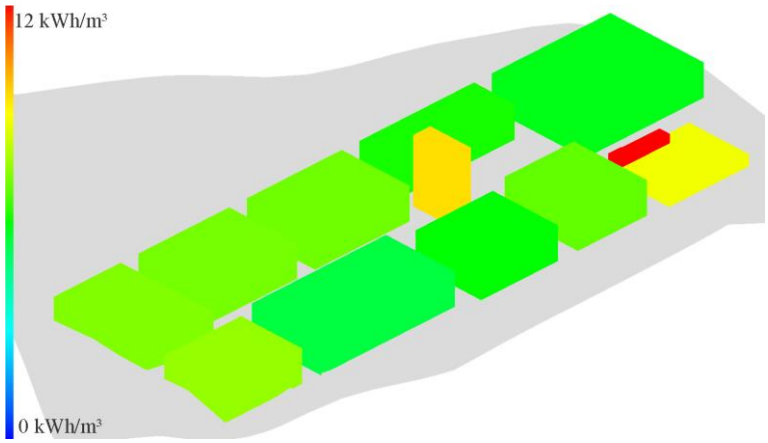

Figure 3 Heating demand of the EPFL campus in Fribourg, today scenario. 3D representation with colour scale

```
<energy:energyAmount>
    <energy:RegularTimeSeries>
        <energy:id>SpaceHeating_1</energy:id>
        <energy:temporalExtent>
            <gml:TimePeriod>
                <gml:beginPosition>01.01.2014</gml:beginPosition>
                <gml:endPosition>31.12.2014</gml:endPosition>
            </gml:TimePeriod>
        </energy:temporalExtent>
        <energy:variableProperties>
            <energy:TimeValuesProperties>
                <energy:acquisitionMethod>Simulations</energy:acquisitionMethod>
                <energy:interpolationType>Continuous</energy:interpolationType>
                <energy:qualityDescription>None</energy:qualityDescription>
                <energy:source>On-site sensor measurements</energy:source>
                <energy:uom uom="kWh"/>
                <energy:variableLabel>Heating demand</energy:variableLabel>
            </energy:TimeValuesProperties>
        </energy:variableProperties>
        <energy:timeInterval unit="year">1</energy:timeInterval>
        <energy:values>
            156412.8
        </energy:values>
    </energy:RegularTimeSeries>
</energy:energyAmount>
```

Figure 4 Heating demand of the EPFL campus in Fribourg, today scenario. Extract of the CityGML ADE XML file

These results show a new paradigm in data format, which can be simulated with the software CitySim and exported in the CityGML ADE data format: this gateway allows the creation of a common database, where data (geometrically and energetic results) are readable by different viewer.

CONCLUSION

Several computer tools quantify the energy demand and thermal behaviour of buildings, from the urban to the edifice scale, but none of them is actually able to convert and exchange information between them different at the urban scale. For this reason, a new paradigm called the CityGML Energy ADE is under development. This paper presents a methodology to establish a gateway between one of the urban simulation tools CitySim and the CityGML Energy ADE data format. The future EPFL campus in Fribourg is presented as case study, demonstrating the storage possibility of the CityGML Energy ADE of geometrical properties and annual heating and cooling demands for each building. The connection between CitySim and CityGML Energy ADE represents an innovative approach for the urban energy analysis: city model can be simulated, stored and exchanged between both format creating a common database of knowledge, in which researchers and municipalities could share their results. Future development of this research topic will focus on displaying results obtained through different software in graphical user interfaces.

REFERENCES

1. G. Gröger, T.H. Kolbe, C. Nagel, K.-H. Häfele, Open Geospatial Consortium OGC City Geography Markup Language (CityGML) En- coding Standard, (2012).
2. U. Eicker, R. Nouvel, C. Schulte, J. Schumacher, V. Coors, 3D-Stadtmodelle fuer die Waermebedarfberechnung, In: Fourth Ger. IBPSA Conf., 2012: pp. 1–7.
3. R. Nouvel, C. Schulte, U. Eicker, D. Pietruschka, V. Coors, Citygml-Based 3D City Model for Energy Diagnostics and Urban Energy Policy Support, Proc. BS2013 13th Conf. Int. Build. Perform. Simul. Assoc. (2013) 218–225.
4. OGC, Open Geospatial, (n.d.).
5. F. Biljecki, H. Ledoux, J. Stoter, J. Zhao, Formalisation of the level of detail in 3D city modelling, Comput. Environ. Urban Syst. 48 (2014) 1–15.
6. D. Robinson, Computer modelling for sustainable urban design. Physical principles, methods & applications, 2011.
7. IPCC, IPCC special report. Emissions scenarios, 2000.
8. Karlsruher, FZK Viewer, (2015).
9. EPFL Fribourg, Smart Living Lab, (2015).
10. T. Jusselme, Personal communication, (2014).

INTERDISCIPLINARY MODELLING OF ENERGY TRANSITION IN RURAL AND URBAN SYSTEMS

M. Freunek Müller, M. Kubli, S. Ulli-Beer

Zurich University of Applied Sciences, Technoparkstrasse 2, 8406 Winterthur, Switzerland

ABSTRACT

The current energy transition towards a rising share of fluctuating and decentrally installed renewable power has introduced new challenges to the modelling of national and regional energy supply systems. More technologies are involved than in centrally designed energy systems, and the physical potential strongly depends on regional context factors. Furthermore, nontechnical factors such as social, economic, and legislative settings, may limit solutions that are technically feasible, and the management of multiple actors with varying interests at the local and national level is required. Empirical studies show the relevance of nontechnical factors, such as delays in the approval and installation of power plants, due to missing acceptance and knowledge [1]. Modelling and scenario analyses tools have a great potential to support such complex decision and management tasks. However, the available modelling and scenario analyses tools are mostly not suited to the needs of the local stakeholders managing the transition of their local energy system. The required simulation time horizon is in the range of decades due to the long planning, construction, and life times of the energy infrastructure, which hinders an intuitive understanding of the system. Additionally, the communication of models of this size and complexity is a barrier for the energy transition [1], as stakeholders in a decentrally organized energy system have very heterogeneous backgrounds, and cannot be expected to have a detailed system understanding. Current models of energy systems are bottom-up or hybrid models, thus often bound to the regions they have been developed for. A simulation model for the transition management of regional energy systems should cover the technical system within its socioeconomic and legal boundaries, and be accessible and comprehensible on the same time. This paper provides a detailed discussion of the available energy system models for Switzerland. Exemplary effects of social and legislative issues are demonstrated. We present the participative modelling environment TREES (Transition of Regional Energy Systems) that consists of a generic interdisciplinary model which is customizable to the specific application case.

Keywords: Urban simulation, modelling, energy transition, interdisciplinary

INTRODUCTION

Existing simulation environments of energy supply systems are based on physical and economic models. Depending on the application scenario, the models are optimized for technical feasibility, least cost scenarios or maximum welfare. The current transition towards energy supply systems with increasing share of fluctuating power and decentrally installed renewable generators increases the required complexity of applied models, and the rising importance of nontechnical factors introduces new challenges to their design. The energy systems to be modelled consist of more technologies than centrally designed energy systems and involve various decisions at the local and national level. Their physical potential strongly depends on regional factors. Local and (inter-)national social, economic, and legislative settings often limit solutions that would be feasible from a technical point of view. Examples of such nontechnical factors are delays in the approval and installation of power plants due to

missing acceptance and knowledge [1]. Empirical studies showed both a technology specific social acceptance and an increased probability of acceptance for existing experience with the technology [1, 2]. Such factors have not yet been added to the classical physical-economical models, which reduces their predictive value. The available research on the development of regional energy systems includes simulation models and, concerning sociotechnical issues, descriptive studies with few empirical data.

This work provides an overview of the state the art of modelling and the current research on nontechnical factors for the development of regional energy system with a special focus on Switzerland. The paper is structured as follows: First, existing general modelling approaches and the available models for Switzerland are presented. The section closes with a discussion of required model extensions following from socio-economic research. In the following part, the interdisciplinary model Transition of Regional Energy System TREES is presented. Finally, an outlook on further research is given.

MODELLING APPROACHES FOR ENERGY SYSTEMS

Energy System Simulation Models

The basic approaches of energy system models can be divided into bottom-up and top-down models. Bottom-up models typically provide a high level of detail in the technical and physical model parts and sometimes their economic properties, such as technology specific interest rates or sectorial demand. Many models include data for the development of technologies concerning their cost and efficiency. Figure 1 depicts the main components of state of the art bottom-up energy system models.

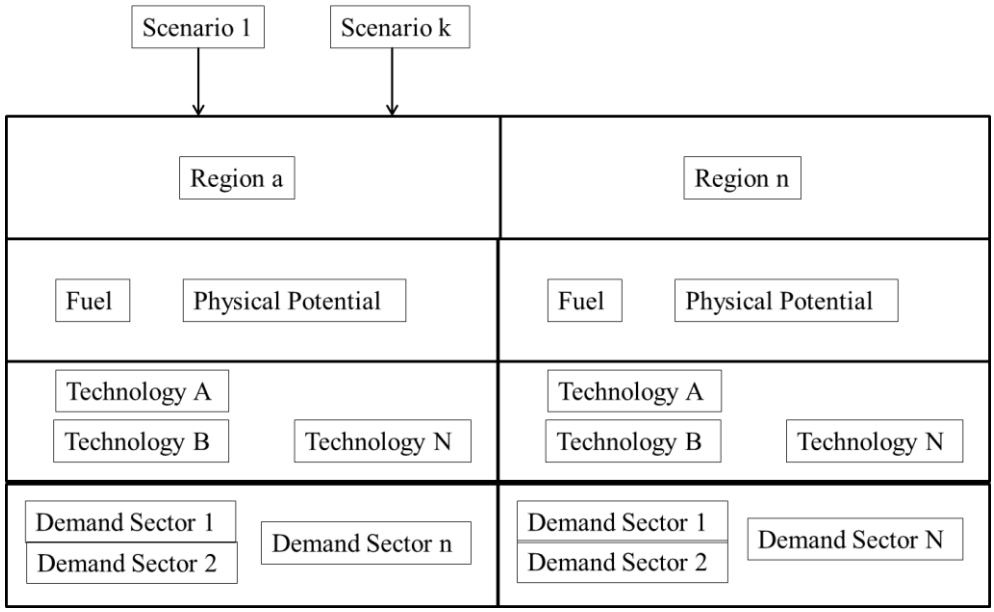

Figure 1: Typical components of bottom-up models for energy systems.

There are two main optimization directions for the bottom-up energy models: Cost and energy supply. The cost optimization models often are based on the economic concept of partial equilibrium models. Here, economic scenarios are modelled as a market, which is limited to the energy market. Equilibrium within this market is reached, when demand equals supply. The price within these models is depending on the demand. The aim of this approach is to assess the policies for a certain energy supply at lowest cost. To that aim, first the model is simulated without policy scenarios and then with possible political constraints. A very

popular example is the *MARKet ALlocation model MARKAL* and its successor, *The Integrated MARKAL-EFOM System TIMES* [3]. Technologies are included from mining over energy conversion to transport for the whole world, which is aggregated to main areas. The demand side covers the domestic and industrial sectors being represented to varying levels of detail. The system dynamic model *Prospective Outlook on Long-term Energy Systems POLES*, a partially equilibrium model with endogenous price models, is another example of this model group [4]. In its structure, *POLES* is similar to the *TIMES* family. The Regional Energy Deployment System model ReEds represents a detailed, GIS-based bottom-up model of the US energy system [5].

The top-down approach provides the macroeconomic view and thus more detail of the economic behavior and system. Top-down models can be separated into two approaches: Computational General Equilibrium (CGE) Models and econometric models based on statistical analysis of historical data, such as linear regression. In CGE models, market equilibrium between demand and supply is calculated from mathematical optimization methods including detailed model of price building and many detailed sectors. As bottom-up models usually include technical models with very simplified financial assumptions, and top-down models include economic mechanisms, some approaches try to combine both [6].

Energy System Models for Switzerland

The available energy system simulation models for Switzerland are mainly bottom-up models focussing on technical and economic aspects. Kannan et. al. developed the *TIMES* model for Switzerland *Swiss TIMES Electricity Model STEM-E*, which models a single region (Switzerland) with approximated models of four neighbouring electricity markets [7]. The follower model *CROSSTEM* includes a more detailed model of foreign policies and their influence on the Swiss electricity market [8]. The overall simulations will be combined with energy system models including heat, storage and mobility in the European environment. The most detailed model of the Swiss energy system, the *Energieperspektiven* with thousands of pages of documentation has been developed by Prognos for the Swiss *Energiestrategie 2050* [9]. Their model is bottom-up with linear optimization and detailed descriptions of cohorts of existing infrastructure, buildings, electrical devices, vehicles, power plants and population based on real data.

Within the 2014 founded Swiss Competence Centers of Energy Research, various modelling activities have been started, and a broad coverage of all relevant technical systems can be expected in the near future. Again, the interdisciplinary models amongst these models focus on technical and economic aspects. For example, the University of Basel presented a bottom-up electricity market model for Switzerland, *Swissmod*, which takes into account the transmission structures, the hydropowered electric supply and the European electricity markets [10]. There are two groups with technical-economic models at ETH: The RESEC group continues its research with their dynamic general equilibrium model with endogenous growth *CITE* (*Computable Induced Technical change and Energy*). A hybrid model consisting of a CGE and a dispatch model is developed at CEPE.

On a local level, energy planning is often done by energy consultants and engineering offices. In this field, the balance sheet tool for Energy regions and the Swiss program *EcoSpeed* are used [11,12]. *EcoSpeed* is a bottom-up energy balancing tool for domestic, transport, industrial and infrastructural demand as well as production. Local potential can be optimized, and scenarios can be calculated. A common bottom-up tool in technical energy planning is the Danish program *Energyplan* [13].

Limitations of existing approaches

The energy transition includes a transition of the energy infrastructure towards a smart grid including decentral and potentially off-grid power structures, that are coupled via communication technologies. New institutions (e.g. standards, pricing mechanisms, regulations etc.) organizations and business models are also required to form secure and efficient smart energy systems. With the increasing level of realization of these new energy systems the nontechnical aspects, such as legal or socioeconomic factors, gain importance. Furthermore, the different actors, their motivations and the interactions between them need to be better understood also in their long term development. This is important since the challenge for practitioners involved in energy transition tasks is to overcome system failure [14] and to enhance their steering capacity in order to achieve policy objectives within acceptable social, economic and environmental limits [15]. This steering challenge is addressed by scientific frameworks of socio-technical transitions [16]. Researchers have applied appreciative theory and narratives to describe path dependency, path creation and circular causation in transitions of energy systems. But causal modeling and simulation frameworks are often missing, for regional settings, in particular. In addition, available research often addresses isolated topics [17]. For example, there has been no systematic approach on the interactions between consumers, grid operators, prosumers, and utilities and the effect of different technical, economic and regulatory grid operation models, although grid operators need to handle the fact, that their traditional business models already begin to fail. A descriptive study has been done by Meeus und Saguan on the often contradictory motivations of utilities and grid operators for three European case regions [18]. Agrell et. al. suggested as a results of their macroeconomic model that due to asymmetric information the reorganization of grid structures should be assigned to the grid operators [19]. However, there has been no systematic modeling approach yet, that takes into account all relevant disciplines. The same is valid for the research on social acceptance and regional installation rates of renewable technologies which is mainly descriptive and in few cases based on surveys, but always part of isolated studies [20, 21].

METHOD

The modelling environment Transition of Regional Energy Systems TREES addresses the challenges outlined above. It consists of a generic model which is customizable to the specific case. Figure 2 shows the settings and definition of boundaries within TREES. Data for exogenous variables are obtained from technical studies, national offices, and climate simulation models (METEONORM). TREES is realized as system dynamics model, as the visual approach enables a quick identification of main causal dependencies (causal loops or feedback processes), and provides an overall system overview as well as an understanding of the system behavior. In addition, scenarios, policies and actor specific strategies can be analyzed and evaluated from different perspectives and development paths. There are four main development priorities that are to be balanced: economy, acceptance of technology, ecology, and security of supply depending also on the degree of autarky or share of renewable energies.

In order to meet the regional boundaries and case specific demand, TREES consists of a base model, which is modified according to the case specific demand in the required level of detail. Figure 3 shows the modelling process. The base model TREES is built on available public data from national sources, the climate simulation program METEONORM, and results from the other SCCER research groups. In a workshop with partners from the specific case and experts, case specific scenarios, variables of analysis and system boundaries are identified.

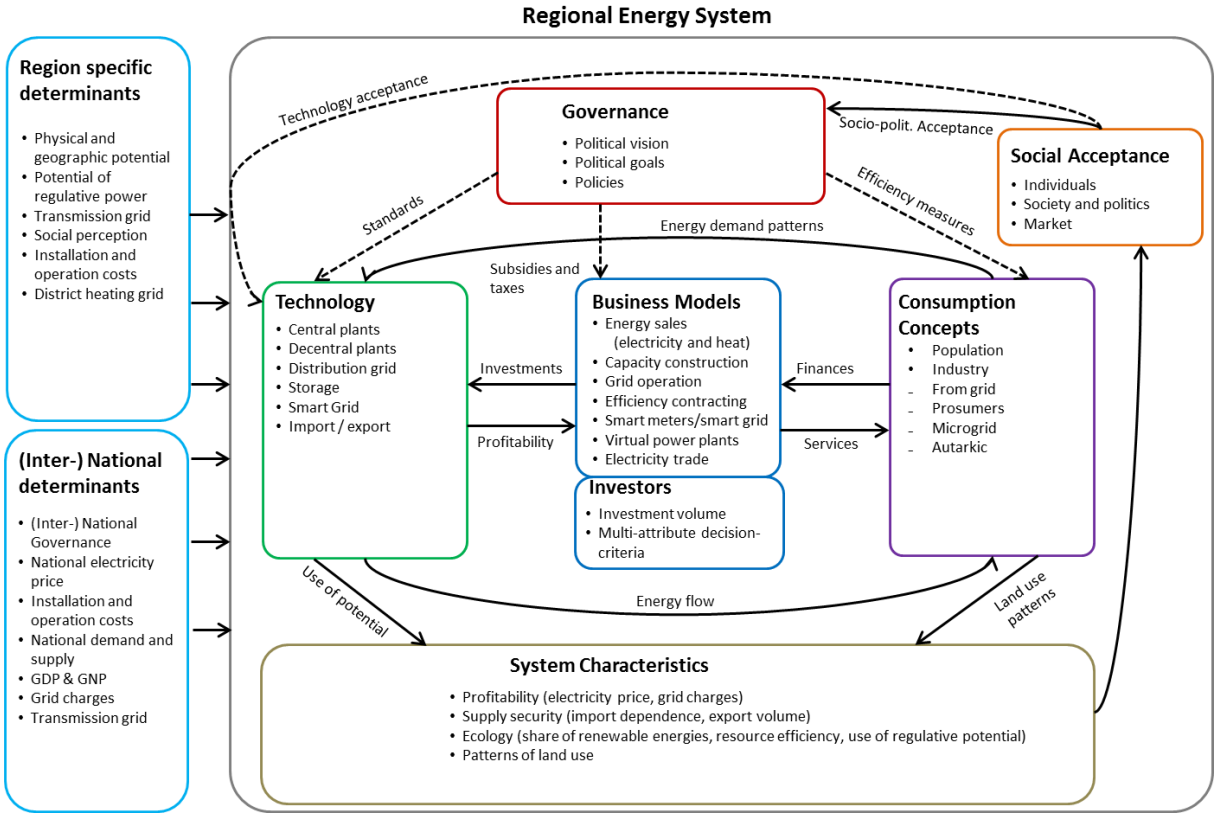

Fig. 2: (Inter-)national and region specific settings and boundaries as well as main interactions and variables in TREES.

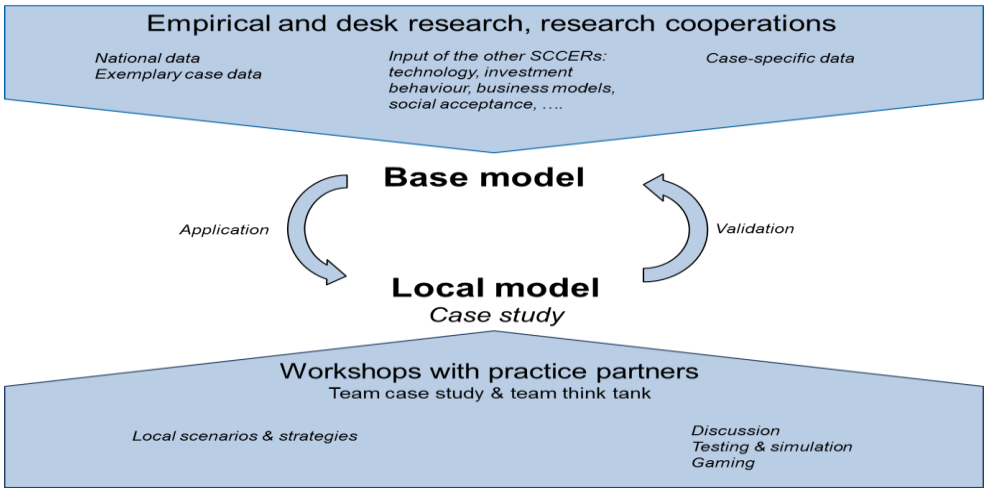

Fig.5: Modelling and data flow in the TREES model.

Besides the model specification, the aim of this participative approach is to include and identify relevant local actors in a very early stage, and to enhance their common system understanding in order to develop feasible strategies close to the real settings with its specific conditions. Based on the workshop results, TREES is adapted accordingly using additional case data. In the final step, simulations and sensitivity tests are performed; typical transition pathways, and robust strategies and policies are identified.

The main scope and implementation is its use as a strategy formation tool for planners of regional energy systems in a complex and uncertain environment. Its users are enabled to test "What if.."-scenarios and develop a sufficient system understanding. In order to allow for

analysis of long term developments and also to be compliant with the Swiss *Energieperspektiven*, the time horizon ranges from 2000-2050.

The planned validation of TREES includes usage of historical data. Currently, there are few data and models available for the nontechnical variables or relations. Here, data are gathered from own research and research cooperation in order to quantify assumed correlations or functions.

CONCLUSION

An interdisciplinary modeling environment for the transition of regional energy systems TREES has been presented. With this model, relevant stakeholders can be involved at the earliest stage of project planning, and sustainable, realistic local energy systems can be developed. While the final design of the identified technical solution will in most cases require further detailed modeling with technical simulation tools, TREES assists in the task of handling a complex system with many uncertainties and individual constraints, and in identifying robust transition strategies for local energy systems.

REFERENCES

1. Federal Office of Energy: Delays of projects for current production from renewable energies [German], Bern, Aug. 2013.
2. C. Wunderlich: Acceptance and public participation of renewable energies [German]. Renews Spezial 60, November 2012.
3. R. Loulou, U. Remme, A. Kanudia, A. Lehtila, G. Goldstein: Documentation for the TIMES Model, PART I, ETSAP, April 2005.
4. B. Schade, A sensitivity analysis to investigate the impacts of oil and gas resources on the energy market, No. 23800126. EcoMod., 2008.
5. Short, W; et al., Regional Energy Deployment System (ReEDS), Technical Report NREL/TP-6A20-46534, 2011.
6. S. Rausch, M. Mowers: Distributional and efficiency impacts of clean and renewable energy standards for electricity, Resource and Energy Economics, Elsevier 36(2), 556-585, 2014.
7. R. Kannan, H. Turton, H., E. Group: The Swiss TIMES Electricity Model (STEM-E) Updates to the model input data and assumptions, November 2012.
8. R. Pattupara, R. Kannan: Exploring uncertainties in CCS – De-carbonization of the power sector & country-wise opportunities, IAEE European Energy Conference, Rome, Italy, 2014.
9. A. Kirchner, et al.: Energy Perspectives for Switzerland until 2050 [German], Prognos AG, Basel, 2012.
10. I. Schlecht, H. Weigt: Swissmod – A Model of the Swiss Electricity Market, 2014.
11. http://www.energie-region.ch/de/bilanzierungs-tool/, accessed 2015/04/29.
12. https://www.ecospeed.ch, accessed 2015/04/29.
13. H. Lund, A. N. Andersen, P. A. Østergaard, B. V. Mathiesen, D. Connolly: From electricity smart grids to smart energy systems – A market operation based approach and understanding. *Energy*, *42*(1), 96–102, 2012.
14. R. Gustafsson, R., E. Autio: A failure trichotomy in knowledge exploration and exploitation. Research Policy, 40(6), 819–831, 2011.
15. Calvert, K., Pearce, J. M., & Mabee, W. E. (2013). Toward renewable energy geo-information infrastructures: Applications of GIScience and remote sensing that build institutional capacity. Renewable and Sustainable Energy Reviews
16. F. W. Geels, M. P. Hekkert, S. Jacobsson; The dynamics of sustainable innovation journeys, Taylor & Francis, 2008.
17. E. C. Ricci: Smart-Grids and Climate Change. Consumer adoption of smart energy behaviour: a system dynamics approach to evaluate the mitigation potential. Nota di Lavoro 71.2013. Milan, Italy: Fondazione Eni Enrico Mattei, 2013.
18. L. Meeus, M. Saguan, Innovating grid regulation to regulate grid innovation: From the Orkney Isles to Kriegers Flak via Italy, Renewable Energy 36, 2011.
19. P. J. Agrell, Smart Grid Investments, regulation and organization. Energy Policy 52, 2013.
20. N.M.A. Huijts: Sustainable energy technology acceptance: A psychological perspective. PhD Thesis, Delft University of Technology, 2013.
21. G. Walker, B. Evans, P. Devine-Wright, S. Hunter, H. Fay: Harnessing community energies: explaining community based localism in renewable energy policy in the UK. Global Environmental Politics, 7 (2). pp. 64-82, 2007.

TRANSITION PATTERNS OF DISTRIBUTED ENERGY GENERATION CONCEPTS CONSIDERING NETWORK EFFECTS

M. Kubli[1]; S. Ulli-Beer[1]

1: Institute of Sustainable Development, Zürich University of Applied Sciences, Winterthur, Switzerland

ABSTRACT

Distributed generation is becoming increasingly important in energy systems, causing a transition of regional energy systems. These decentralisation dynamics are difficult to predict in their scope and timing and therefore become a major challenge for political decision makers, utility companies and technology developers. Network effects are crucial in these decentralisation dynamics, strongly influencing the dominance of the various concepts of distributed energy generation. Network effects emerge between technologies, the installed base of a concept and actor-specific decision criteria.

A System Dynamics simulation model is built, capturing the consumer concepts related to distributed generation as well as arising network effects, to analyse likely transition dynamics in regional energy systems. The direct network effects of grid charge adjustment, learning theory and an effect due to density as well as indirect network effect between storage technologies and combined heat and power systems in microgrids are represented in the model. Preliminary simulation results on the transition of the distributed generation concepts are shown and will be analysed in further research on the specific impact of network effects on the transition patterns. This paper aims to make a contribution to the field of energy transitions by translating theories on network effects of the economic literature to the energy systems simulation and by discussing and simulating relevant network effects as relevant drivers of the dissemination of distributed energy generation concepts and the related consumer concepts.

Keywords: regional energy systems, transition, network effects, distributed generation, simulation, System Dynamics.

INTRODUCTION

Current energy systems show strong decentralisation tendencies [1, 2]. This development is driven by the integration of new renewable energies, which are suitable for local and small scale installation, into the energy system. In this context, prosumer and microgrid concepts become attractive [3-5]. Despite the significance for the energy transition and the growing number of regional initiatives, decentralisation dynamics and network effects in the transition of distributed generation systems has enjoyed little attention in research so far. However, early strategy development and stakeholder engagement is crucial for successful deployment of these concepts and to avoid high costs of late adaptation.

We hypothesise that deployment patterns of prosumer systems and microgrids strongly depend on regional-specific initial conditions; as well as early co-ordinated initiatives in general - and network effects in particular. Network effects are defined as the dependency of the product utility on the network size as well as the positive effect of coalitions with other products [6]. We presume that network effects are decisive for the dominance of a particular concept and can promote distributed generation systems to a breakthrough, which otherwise would not happen on a comparable scale. Hence, a better understanding of evolving network effects is critical for choosing early on the right investment strategy and partners.

We apply System Dynamics [7], a causal modelling approach focussing on feedback mechanisms in a system, to simulate likely deployment pathways of distributed generation systems, integrating five essential network effects. A detailed understanding of likely decentralisation dynamics in a region is essential for production planning, business model development and grid maintenance for utilities, producers of technological components and the political governance of a region. The novelty of this paper is the application of the network theory on the field of energy transitions as well as the combination with the System Dynamics simulation approach.

BACKGROUND

Energy transitions are a widely discussed topic in the scientific literature. Today, new renewable energies that favour the distributed generation of energy are about to transform the energy system [8]. Distributed generation is defined as an "electric power source connected directly to the distribution network or on the customer site of the meter" [9]. Within these decentralisation dynamics, different consumer concepts related to distributed generation emerge and become increasingly attractive. Prosumer systems and microgrids are frequently analysed in a technological manner [10, 11]. Also simulation studies are conducted in the area of distributed generation systems. Hiremath et al. [12] and Manfren et al. [13] provide useful overviews of simulation models applied at various levels of decentralised energy systems and their planning. Hiremath et al. [12] observe that most of these simulation models use an optimization technique to find the ideal constellation of technologies for the specific area. However, these approaches do not provide an explanation and analysis addressing the co-evolution and the diffusion processes of these concepts. This is surprising since in liberalised network industries, such as the electricity sector, a co-evolution between technology and institutions is decisive to avoid incoherence and instability in the system [14]. Network effects are considered as major determinant of diffusion processes [15] and play a crucial role in the co-evolution between technology and institutions. Qualitative discussions of benefits and challenges of distributed generation systems [4, 10, 11] provide valuable insights into relevant aspects of the diffusion. To our knowledge, a formal quantitative analysis of likely diffusion patterns of these concepts has not yet been provided in the literature.

METHOD

A System Dynamics model is built addressing the issue of likely transition patterns of consumption concepts related to distributed generation in energy regions applying a consumer perspective. Analysing processes within in the energy system is essential to consider the consumer perspective due the importance of consumer or households decisions of how to consume and produce electricity [16]. Simulation is useful and essential for this study to support the complex thought experiments that could not just be conducted mentally. With our simulation approach, we address the need highlighted by Manfren et al. [13] for innovative simulation models analysing transition aspects for decentralised energy systems, taking into account the complex interlinkages between technology, actors, the economy and institutions as. We chose System Dynamics as considered the most suitable modelling and simulation technique to address this issue, since multiple feedback processes, delays and the state of the systems are critical to understand the transition patterns of regional energy systems. System Dynamics [7] is a simulation and mapping method based on causal modelling. The most central elements of System Dynamics are feedback loops - chains of causal interlinkages that form a back coupled cycle. The concept of feedback loops also exists in other methods and theories, such as the multi-level perspective or network theory. System Dynamics finds applications as a planning, analysis and policy design method in various areas of the wide field of energy research [17].

The model presented here is generic in its structure. We aim to model typical patterns that can arise from the decentralisation dynamics of regional energy systems. The model captures four distributed energy generation concepts: prosumers, autarkic prosumers, microgrids and autarkic microgrids. Microgrids are a cluster of producer units that are installed close to multiple consumer units and are connected through a small scale grid with a single node to the main grid [11]. Autarkic concepts are assumed to be completely decoupled of the main grid. These distributed generation concepts are compared to the standard consumption concept, here called "grid consumer", which are purchasing the required electricity from the main electricity grid. The investment decision made by consumers is based on a utility assessment of the concept, based on the economic aspects in form of the net present value of the concepts, which is enriched by non-economic factors of learning, practical aspects and a scarcity effect.

The model captures five network effects, three in form of feedback loops and two as simple causalities. Figure 1 highlights the central feedback loops captured in the model.

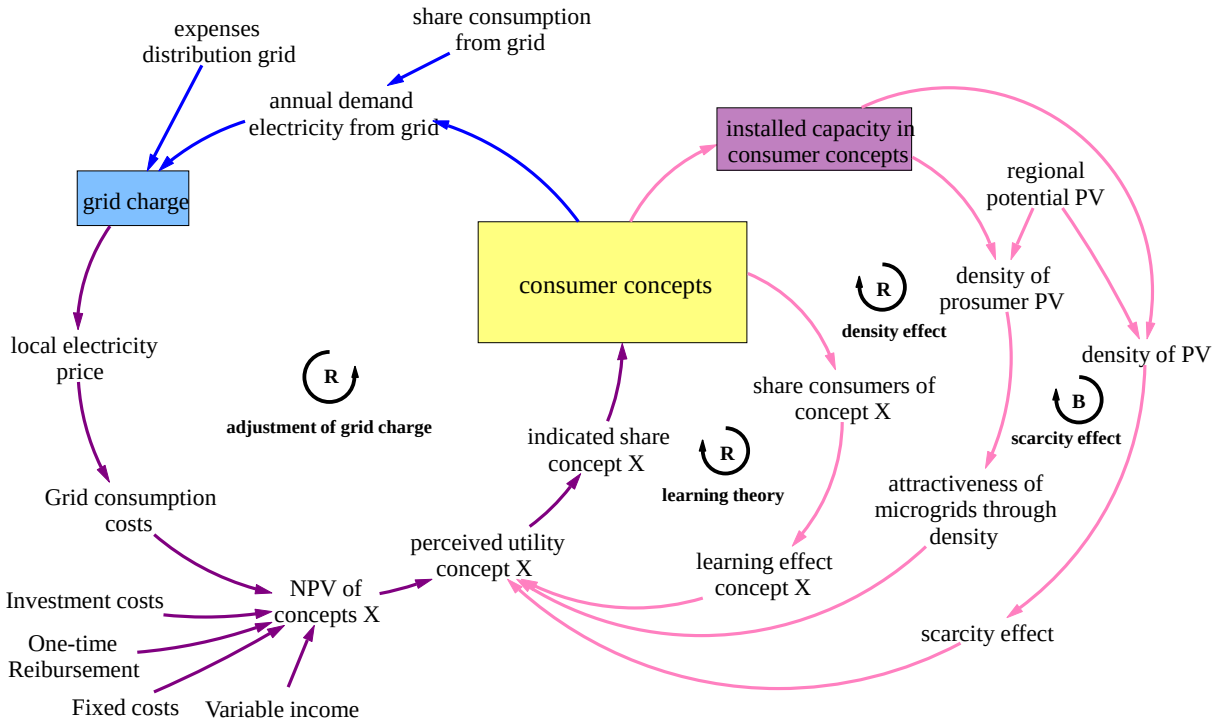

Figure 1: Overview of the feedback loops represented in the model. Underlined variables represent structure elements that are modelled with subscripts.

Feedback loop R1 "adjustment of grid charge" addresses the effect of reduced demand from the main grid, on the grid charge, caused by increased captive power generation, and the feedback to the investment decision. In particular, the number of prosumers is crucial for the tension on the coverage of the transmission grid costs. Prosumers consume less energy from the grid, contributing less to the coverage of the grid cost, but still strongly use the main grid as a buffer. Consequently, the grid charge per electricity unit has to be increased to cover all costs, all else being equal. This closes a feedback loop of a reinforcing character. Grid parity, equal generation costs of captive power systems compared to the total energy costs paid for the electricity consumed from the grid, is considered as the crucial point for the diffusion of prosumer systems [8] and consequently is sensitive for the attractiveness of all other distributed generation systems. In network theory, scholars frequently speak about positive externalities of increased installed base. Gupta et al. [18] define direct network effects as the increase in use of the utility through a larger network. In the case of distributed generation, that type of network effect plays out over the feedback loop of grid charge adjustment (R1). The direct functioning of distributed generation concepts is not altered by an increasing number of prosumers, since the technology remains the same. However, the increase in the grid charge raises the NPV of these concepts, and with this, the perceived utility, which ultimately changes the investment decision. In Abrahamson (1997) this process is categorised under the bandwagon theories as the increasing return theory.

Feedback loop R2 "learning theory" is built based on the insights gained in network theory. The adjustment of perceived utility due to higher awareness and improved information is in network theory called the learning theory [15]. In this model it is assumed that a higher information level leads to more positive evaluation of the concepts. This theory is supported by Basu et al. [10] for the case of microgrids, which mentions a lack of experience and information as a barrier for the deployment of microgrids. In System Dynamics the concept of the word-of-mouth effect [7] is more common. In contrast to the learning theory, the main argument for the word-of-mouth effect is the exposure to advertising, which more referring to awareness rather than the actual information level.

In network theory literature, a set of fad theories are discussed. Fad theories become important in innovation diffusion with ambiguous profitability of the innovation and unclear or no information flows. Therefore, social processes and information on the adopters become more important and affect

the diffusion. Abrahamson et al. [15] distinguish between four types of fad theories. They address the motivation for adoption through the assumption of better knowledge of others, an evaluation bias due to higher share of adopters, the threat of lost legitimacy through emerging social standards, and finally the competitive bandwagon pressure that arises through the pressure to maintain competitive advantage. These types of network effects are not represented in the System Dynamics simulation model. The fad theories would all have a very similar formulation to the learning theory feedback loop, due to the high aggregation level, which would result in redundancies. The analysis of the relevance of fad theories and their impact are still to be explored in future research.

Feedback loop R3 "density effect" is chosen to address the aspect of geographical closeness as a crucial factor for microgrid deployment. If microgrids are formed through the connection of existing prosumer systems, this requires the physical closeness to build a reasonable microgrid. This interconnection is also a network effect. The relation of this effect to existing network-theories needs to be discussed in more detail. On the one hand, the installed base is the driver for this development, but in contrast to the definition of the direct network effect, here the installed base of prosumers affects the perceived utility of microgrids – meaning that the complementary installed base is decisive. Hence, it is related to the concept of complementary goods, although it does not fit its classical definition. Prosumers that move into a microgrid become part of a larger system designed in a more complex manner with several extensions, and do not just increase their own utility through the addition of another product.

Indirect network effects arise through the combination of complementary goods [18]. In our model the indirect network effects are modelled as causal effects and not as feedback loops, since this would require a larger model boundary than desired for our purpose. A network effect of the indirect type emerges in the consumption concept "autarkic prosumer". Autarkic prosumers combine a distributed generation system with a storage system, in our model a photovoltaic plant and a battery. The utility of the autarkic prosumer concept depends on both components. Changes in the price or the technological effectiveness or their compatibility of both technologies alter the attractiveness of this concept. An indirect network effect of a similar manner arises through the combination of several technologies in the microgrid concept. Here, the photovoltaic plants, the CHP plant and the other supporting plants all need to be attractive for an investment. Systems with complementary goods frequently have coordination problems for marketing the products due to the two-way contingency for demand [18]. From a transition perspective, this also raises questions of timing. Here, we hope to make a contribution with the System Dynamics approach by analysing different transition patterns and their interactions. In this model, the indirect network effect between prosumer systems and battery systems is particularly interesting in light of the expected decrease in battery prices.

Feedback loop B1 "scarcity effect" is a typical process emerging from a diffusion reaching its carrying capacity. The rate of growth is reduced through the limitations appearing. In this model, the physical constraint for the diffusion of distributed generation systems is the carrying capacity for PV plants, which is called PV potential in the model. This balancing feedback loop is not a network effect.

RESULTS

We here present some preliminary simulation results of the base run. An extended analysis of the effect of the network effects in the transition patterns is submitted to the journal Energy Research & Social Sciences and will therefore not be presented at the place [19]. The analysis focuses on the generic patterns arising in the transition on regional energy systems and not exact numerous outcomes. The simulation analysis is conducted for an imaginary region with 50,000 households. Initially, all households are assumed to consume their electricity from the main grid and are therefore "grid consumers". The potential for PV plants in this imaginary region is set to 150 MW. The simulation period starts in the year 2010 and ends in 2040.

In Figure 2 the simulation results for the different consumption concepts are presented. The first graph shows the transition of all concepts, while the graph on the right focusses on the distributed generation consumption concepts.

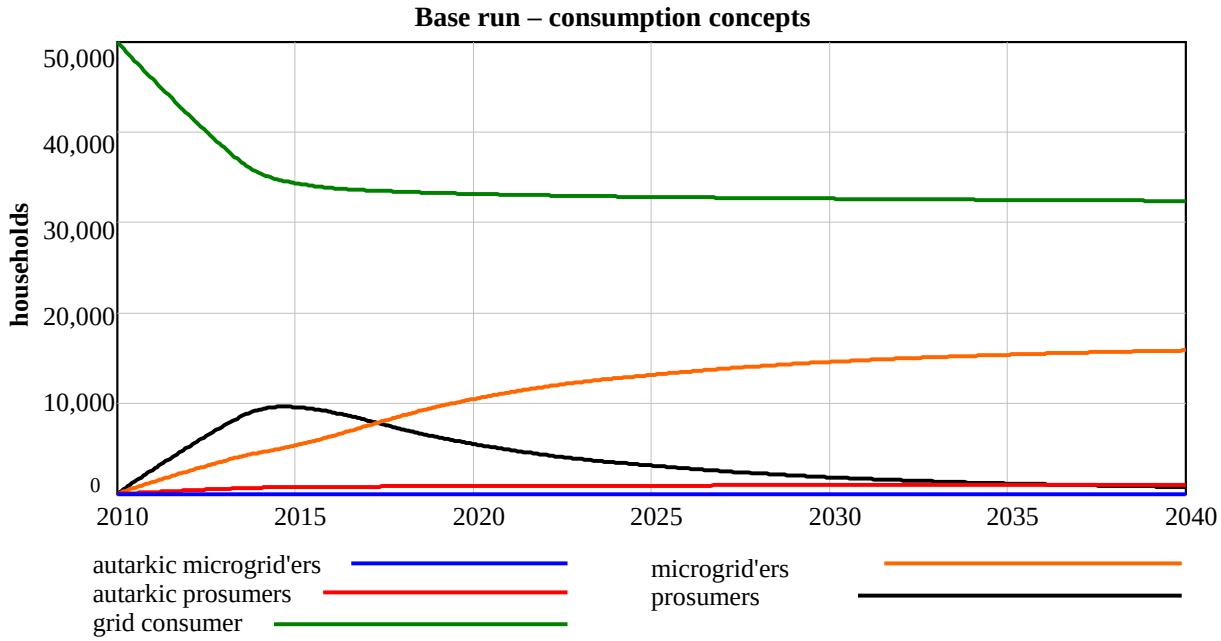

Figure 2: Base run – Simulation results for the number of households in the different consumption concept

In the first phase, we observe a strong increase in the number of households choosing the prosumer concept. This boom is supported by the feedback loop R1 "adjustment of grid charge". The increasing number of prosumer causes the grid charge to increase and makes prosumer systems even more attractive. This development reaches its peak in the year 2015. Already at the beginning of the simulation period, there is a slow increase in households applying a microgrid concept. The slope of the microgrid growth rate increases when the stock of prosumers reaches its peak. Interestingly, the transition towards microgrids is spread over the two deployment pathways – deployment of microgrids from a previous prosumer system and the direct installation of a microgrid. The autarkic concepts – autarkic prosumers and autarkic microgrids – are low in their perceived utility. The concept autarkic prosumer finds some applicants, while the autarkic microgrid seems totally unattractive. The transition towards the autarkic prosumer system shows a similar pattern, with the shift between the two deployment pathways, as observed in the transition to microgrids.

It is important to understand that these dynamic patterns are driven by the network effect and do not emerge from changes in technology prices. These dynamics are all driven by the structure of the system and the network effects gaining on weight and influencing the investment decision by the consumers.

CONCLUSION

Distributed energy generation systems are becoming increasingly attractive and are adopted more frequently. These decentralisation dynamics cause a major transition in regional energy systems. Although increasing shares of prosumer systems and microgrids do have significant impacts on the businesses and strategies of major actors in regional energy systems, decentralisation dynamics and network effects in the transition have not gained much attention in research so far.

A System Dynamics simulation model was built to address the question of likely transition patterns of consumption concepts related to distributed generation. Major drivers for this transition are arising network effects between the installed base of the consumption concepts and the development of complementary technologies. We model the direct network effects: adjustment of grid charge, learning theory and density effect. Indirect network effects between complementary concepts and technologies are addressed between photovoltaics, storage technologies, CHP plant and a network effect between the installed base of prosumers and the deployment of microgrids. Simulation results and the analysis of the impact of network effects, reveal the high impact of network effects on the decentralisation

dynamics of a regional energy system in general and on the different consumption concepts related to distributed generation in particular.

Our paper makes the following contributions. By shedding light on the decentralisation dynamics in regional energy systems, new perspectives and options for strategy development are highlighted. The application of the network effect concept on energy systems research in combination with dynamics simulation is novel. The results obtained will be useful for both practitioners in regional energy systems, such as politicians, energy planners, strategy developers in utility companies or technology developers, as well as for the research in the field of energy transitions.

ACKNOWLEDGEMENT

We gratefully acknowledge the financing by the Swiss Commission of Technology and Innovation (SCCER CREST) as well as by the Zurich University of Applied Sciences.

REFERENCES

1. Alanne, K. and A. Saari, *Distributed energy generation and sustainable development.* Renewable and Sustainable Energy Reviews, 2006. **10**(6): p. 539-558.
2. European Parliament's Committee on Industry, R.a.E.I., *Decentralised Energy Systems*. 2010, European Parliament's Committee on Industry, Research and Energy (ITRE).
3. Kesting, S. and F. Bliek, *Chapter 14 - From Consumer to Prosumer: Netherland's PowerMatching City Shows The Way*, in *Energy Efficiency*, F.P. Sioshansi, Editor. 2013, Academic Press: Boston. p. 355-373.
4. Soshinskaya, M., et al., *Microgrids: Experiences, barriers and success factors.* Renewable and Sustainable Energy Reviews, 2014. **40**(0): p. 659-672.
5. Marris, E., *Upgrading the grid.* Nature, 2008. **454**: p. 570-573.
6. Katz, M.L. and C. Shapiro, *Network externalities, competition, and compatibility.* American Economic Reviews, 1985. **75**: p. 424-440.
7. Sterman, J., *Business Dynamics*. 2000: McGraw-Hill.
8. Schleicher-Tappeser, R., *How renewables will change electricity markets in the next five years.* Energy Policy, 2012. **48**(0): p. 64-75.
9. Ackermann, T., G. Andersson, and L. Söder, *Distributed generation: a definition.* Electric Power Systems Research, 2001. **57**(3): p. 195-204.
10. Basu, A.K., et al., *Microgrids: Energy management by strategic deployment of DERs—A comprehensive survey.* Renewable and Sustainable Energy Reviews, 2011. **15**(9): p. 4348-4356.
11. Chowdhury, S., S.P. Chowdhury, and P. Crossley, *Microgrids and Active Distribution Grids*. 2009, London, United Kingdom: The Institution of Engineering and Technology.
12. Hiremath, R.B., S. Shikha, and N.H. Ravindranath, *Decentralized energy planning; modeling and application—a review.* Renewable and Sustainable Energy Reviews, 2007. **11**(5): p. 729-752.
13. Manfren, M., P. Caputo, and G. Costa, *Paradigm shift in urban energy systems through distributed generation: Methods and models.* Applied Energy, 2011. **88**(4): p. 1032-1048.
14. Finger, M. and R. Künneke, *The co-evolution between institutions and technology in liberalized infrastructures: the case of network unbundling in electricity and railways*, in *1th Annual Conference of The International Society for New Institutional Economics*. 2007.
15. Abrahamson, E. and L. Rosenkopf, *Social Network Effects on the Extent of Innovation Diffusion: A Computer Simulation.* Organization Science, 1997. **8**(3): p. 289-309.
16. Stern, P.C., *Individual and household interactions with energy systems: Toward integrated understanding.* Energy Research & Social Science, 2014. **1**(0): p. 41-48.
17. Ford, A., *System Dynamics and the Electric Power Industry.* System Dynamics Review, 1997. **13**(1): p. 57-85.
18. Gupta, S., D.C. Jain, and M.S. Sawhney, *Modeling the Evolution of Markets with Indirect Network Externalities: An Application to Digital Television.* Marketing Science, 1999. **18**(3): p. 396-416.
19. Kubli, M. and S. Ulli-Beer, *Network effects in decentralisation dynamics of regional energy systems.* Energy Research & Social Science, 2015, in review process.

INDICATE: TOWARDS THE DEVELOPMENT OF A VIRTUAL CITY MODEL, USING A 3D MODEL OF DUNDALK CITY

AM Aidan Melia[1]; EN Eoin Nolan[1]; Ruth Kerrigan[1]

1: Integrated Environmental Solutions, Helix Building, West of Scotland Science Park, Glasgow, G20 OSP, UK

ABSTRACT

According to the United Nations, the World's population currently stands at 7.2 billion people and it is estimated to grow to 9 billion by 2050; as a result appropriate urban development in our cities will become more important. Smart technologies are seen as an important technological step forward with respect to tackling the challenges and improving the efficiency and effectiveness of urban systems, and as a result can have a major contribution to the sustainability of the city and its occupants. The definition of the word 'smart' means that innovative and new approaches are required for urban design, city planning, energy and buildings, low energy & zones for residential, industrial and commercial use, optimal building density etc. Under the EU FP7 INDICATE smart cities project, a decision support masterplanning tool will be developed, which will; plan, integrate and optimize the following sub-systems of the overall city system: buildings, energy efficiency technologies, renewable technologies and the electricity grid. The INDICATE tool will achieve this through the integration of real data from a city with the dynamic simulation software, the IES <Virtual Environment>, 3D Urban CAD modelling tools, the ESRI CityEngine package, and Sustainable Urban Indicators, to create a Virtual City Model. This will provide a 3D model of the city, its networks and its buildings, ready for urban simulation. This paper will discuss the early stage analysis of the 3D dynamic simulation urban model of one of the test sites for the project; Dundalk in Ireland. The model will analyse the impact of refurbishment for a select number of buildings in Dundalk, with metered data available. The aim will be to understand their energy use and optimise their efficiency at building and district level. Indicators developed through the INDICATE project will then be applied to understand the effects of the changes to the individual buildings, the district and also within the overall urban context.

Keywords: masterplanning, sustainable urban indicators, virtual city model, LiDAR, <Virtual Environment>, energy use intensity

INTRODUCTION

Given the challenges and complexity of urban energy systems, and the related challenges for the decision making, the planning and optimisation of the sub-systems of a city, requires appropriate urban modelling and simulation calculation methods to address these following key issues [1]; First, the variety of the building data available and the level of detail in a city area. Second, data pre-processing stage which must take into account a flexible data set which must be always adapted for the district/city-scale to allow for customisable comparison for modelling and simulation calculations. Third, a set of modelling and simulation calculation metrics which allow for good comparison between results [2].

Widely used building simulation tools are only suitable for high-level detailed design analysis of single buildings, or small groups of buildings [3]. A detailed dynamic thermal building simulation for an urban district, over a long period, with a large amount of different modelling input parameters (multiple model objects, solar and thermal inter-relation, shading, HVAC systems, internal gains etc.), often puts strain on simulation tools that are currently available. Because of the complexity of these systems, the smallest changes in their parameters can induce high consequences in the systems' efficiency.

To address these challenges, a Virtual City Model (VCM) will be developed. This will illustrate a city and store the processed output from a dynamic simulation model, created with the <Virtual Environment> (<VE>) software. Results from sustainable urban indicators relating to the city, are also applied to the VCM. This is so that it can be passed to a user interface to inform decision making and determine which is the optimal way of retrofitting the building. Different factors such as; the use of the building, smart technologies, integration into the city and its systems, and the geographic location of the building, would further aid this process.

METHOD

A key element of the VCM, is the development of a 3D model ready for simulation. This model has been created with the use of a masterplanning tool that has been developed by IES. This tool works as a plug-in in conjunction with the popular 3D drawing package SketchUp by Trimble. This allows for rapid extrusion of buildings within a model and also assignment of data to the model.

In the case of the Dundalk model, ordinance survey mapping was provided by Ordinance Survey Ireland (OSI), through the local authority for Dundalk; Louth County Council (LCC). This mapping acted as a base-layer in the model, and ensured that all buildings in the town were accurate in terms of their location relative to each other. Coupled with this base mapping, LiDAR information was also provided, which helped to ensure that all buildings in the SketchUp model were accurate with regard to their height.

Steps in the Modelling Process

The following are the steps used in the modelling process:

1. Importing the OSI mapping

The OSI mapping in AutoCAD .dwg format file was imported into a SketchUp model.

2. Creating and Extruding the Polygons

Once the OSI maps were imported, the boundaries of each building had to be marked in order to activate a polygon around the site of the buildings, which could then in turn be extruded. This was done by using a drawing tool in the SketchUp plugin. Once polygons were drawn around each building, the faces of these polygons could then be selected and extruded.

3. Importing The Lidar Data

The LiDAR data was imported into the SketchUp model using a custom build, with functions that allow us to enter a series of set command codes typed in, using the GDAL (Geospatial Data Abstraction Library) format. The command codes were then created and typed in, to allow the model to read the LiDAR files and obtain the height data for identified object (buildings) in the correct geo-located positions. The model buildings were created inside the polygon area which was modelled with a default height of 2.5m before the LiDAR data height was applied. The command codes were entered into a ruby console and set the building heights to selected objects (model buildings) identified in the SketchUp model, in which resulted in the object heights changing with the respect to the new data available.

Due to unavailability of LiDAR data for some areas in Dundalk, missing areas were applied with a default height of 2.5m per floor of each building. It is expected the model will be updated again when more data is available. It is noted some objects in the model have more than one floor, in which the LiDAR height data was applied and divided equally on the identified objects with more than one floors. Without information on glazing size in the

identified model, most objects were modelled with a general assumption of between 15-30%. All objects are modelled with flat roof and are the same size as the footprint of the building. The following figure shows the result of 3D modelling for a section of Dundalk.

Figure 1: 3D model of Dundalk (Map data: Google)

Some additional building information can be accessed from the model without data assignment to generate the metrics. Examples of these are: footprint of building; building compactness indicators; building height; floor area; number of buildings; density factors Dsurf and Dvol; urban form ratio; urban compactness ratio; elongation ratio.

Information on building typologies in Dundalk was obtained from the Planning Section of Louth County Council (LCC). This allowed us to apply the different building typologies to the identified model buildings. The following figure shows the range of different building typologies in the centre of Dundalk, with each colour representing a different typology. In this case, the main categories were; yellow for residentail, brown for retail, and dark brown for commercial.

Figure 2: Building typologies mapped in Dundalk (Map data: Google)

Building energy rating metrics were built as custom attributes in the model, which allowed us to highlight the energy rating of each building, where information was supplied by LCC.

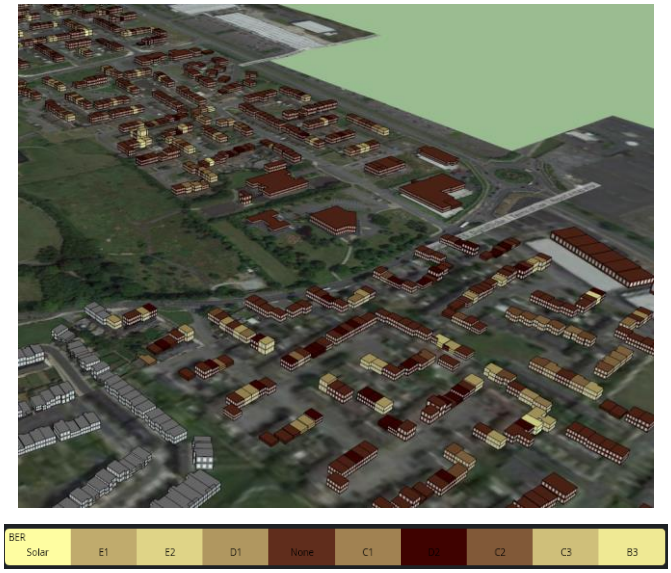

Figure 3: Building Energy Rating mapping of buildings in the Muirhevnamor area (Map data: Google)

THE DYNAMIC SIMULATION MODEL

The SketchUp model of Dundalk was imported into the IES <VE> software. This allowed us to carry out solar and wind analyses of the buildings in the town. The following figure shows the wind analysis result on the centre of Dundalk using MicroFlo; the computational fluid dynamics (CFD) analysis tool within the IES <VE> software. The following figure show the wind speed surrounding the buildings in Dundalk town are in the range between 2 – 5 m/s, where the darker the blue, the higher the wind speed. This was taken at a point in time to provide an indication of what is possible with regard to CFD analysis. Colour is required for a clearer understanding.

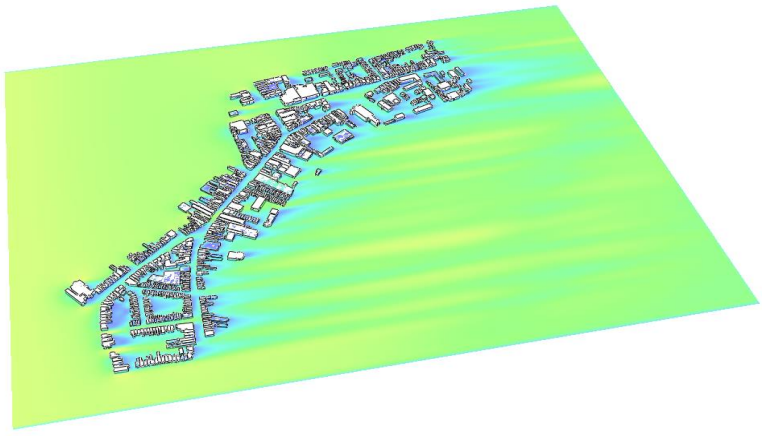

Figure 4: Wind Analysis of Dundalk Town

The following figure shows the solar analysis result on the Vincent Avenue area in the centre of Dundalk, which included solar radiation striking the external walls and roof surface areas of the buildings. The annual number of hours of solar radiation striking the surface of the buildings in Dundalk was calculated and is displayed in the following figure (colour is required for a true understanding). It is noted that an historical weather file was used in the

analysis, so the solar incidence information will be different to the actual values. Nevertheless the solar radiation results generated are encouraging and clearly show the potential use of renewable energy technologies such of PV or solar thermal panels on buildings in Dundalk, with the majority of roof areas receiving over 12 kWh/m^2 of solar irradiance.

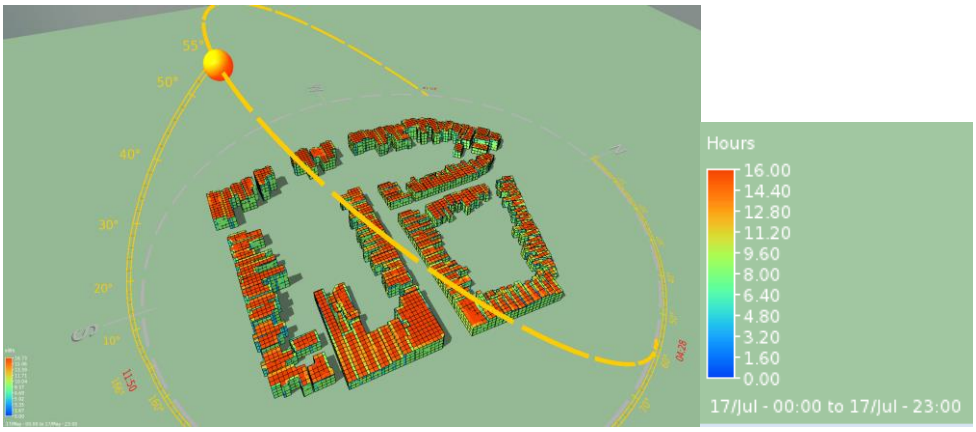

Figure 5: Solar analysis on partial area of Dundalk Town

IMPACT OF RETROFIT ON A SELECT NUMBER OF BUILDINGS IN DUNDALK

The buildings identified in the Muirhevenamor (MM) area which had building energy rating data were selected for a range of building simulation analysis within the IES <VE>. Detailed data input parameters (e.g. construction, internal gain, HVAC systems etc.) was applied to each identified building model in the MM area. The following figures illustrate the energy use intensity (EUI) result from a dynamic simulation run in the <VE> through the SketchUp plug-in, with the darker colours on the right hand side highlighting an improved EUI. This was used to consider the impact on energy with and without the potential retrofit / refurbishment options.

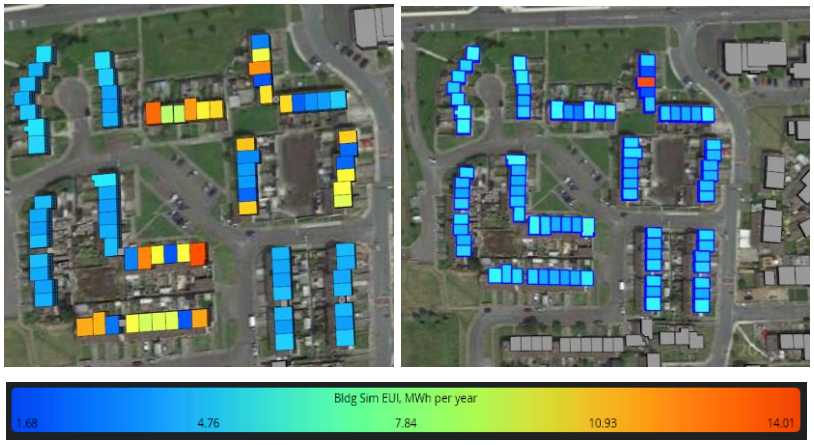

Figure 6: Energy Use Intensity (EUI) on buildings in Muirhevenamor area before and after retrofit implemented (Map data: Google)

The simulation result shows the average EUI on selected building in the area, with different retrofits implemented, is 39.74 kWh / m² per year compared to 55.77 kWh / m² per year without retrofits implemented. The simulation result shows the 28.74% decrease in energy performance between the buildings with the respect to the construction and district heating

retrofit implemented. It is important to note that the urban configuration of Dundalk can facilitate or hinder the viability of different retrofit technology to be implemented.

The variety of the buildings available, and the level of detail in the building information available must be taken into account. Some input data was modelled based on information obtained through a library of building typology templates which IES have already compiled.

CONCLUSION

This paper has highlighted a number of modelling and simulation methods available through the IES masterplanning plug-in and <VE> software. The results clearly show the huge potential impact on energy consumption within the buildings modelled in Dundalk along with implemented retrofits.

The visualisation capability and its results from the masterplanning tool have highlighted the numerous potential solutions which can be utilised in tackling the challenges, and improving the efficiency and effectiveness of urban systems. This includes a set of metrics that it can be constructed within the tool and should prove useful for urban design, city planning, and energy planning and general construction.

Through the use of the tool, it clearly shows how it is easy to compare the renewable energy potential across individual buildings or groups of buildings in a city. This paper has highlighted the method shown to be an effective way of modelling and simulating at the early stage of analysis, and can have a positive impact on areas like Dundalk.

It is one of objectives of the INDICATE project is that the indicators (metrics) should be easily scalable and developed through the project, which will be then applied to demonstrate the effect of the changes within buildings, districts and within the overall urban context. The report has highlighted the key areas of the modelling approach in which will be similar, with the respect to the capabilities to be developed as the project progresses, along with the <VE> software and ESRI CityEngine software.

ACKOWLEDGEMENT

This work was conducted as part of the INDICATE project under the European Union's 7th Framework Programme for research under grant number 608775.

REFERENCES

1. Page, J., Basciotti, D., Pol, O., Nuno Fidalgo, J., Couto, M., Aron, R., Chiche, A., & Fournie, L. (2013). A multi-energy modelling, simulation, and optimisation environment for urban energy infrastructure planning. In: *13th conference of international building performance simulation association, 26-28 August 2013 Chambéry, France.*
2. Nouvel, R., Schulte, C., Eicker, U., Pietruschka, D., & Coors, V. (2013). CityGML-based 3D city model for energy diagnostics and urban energy policy support. In: *13th conference of international building performance simulation association, 26-28 August 2013 Chambéry, France.*
3. Huber, J., & Nytsch-Geusen, C., (2011). Development of modelling and simulation strategies for large-scale urban districts. In: *12th conference of international buildings performances simulation association, 14-16 November 2011, Sydney, Australia.*

GENESIS OF THE CITYGML ENERGY ADE

R. Nouvel[1]; R. Kaden[2]; J-M. Bahu[3]; J. Kaempf[4]; P. Cipriano[5]; M. Lauster[6]; J. Benner[7]; E. Munoz[8]; O. Tournaire[9]; E. Casper[10].

1: HFT Stuttgart, Germany / 2: TU Munich, Germany / 3: EIFER, Germany

4: EPFL Lausanne, Swiss / 5: Sinergis, Italy

6: RWTH Aachen University - E.ON Energy Research Center, Germany

7: KIT, Germany / 8: HCU Hamburg, Germany / 9: CSTB, France / 10: SIG 3D, Germany

ABSTRACT

The current climate and environmental policy efforts require comprehensive planning regarding the upgrade of the energy supply and infrastructures in cities. Planning comprises e.g. the determination of locations for new power generating facilities like photovoltaic, geothermal and decentralized combined heat and power stations, the widespread introduction of e-mobility solutions and hence the grid development as well as large-scale energetic building refurbishments. A holistic approach integrating extensive complex information is essential for the strategic planning of the different measures. In order to establish interoperability and data exchange between the different planners, stakeholders, and tools, an open information standard is required.

To answer this need, an international group of urban energy simulation developers, geo-information scientists and users from 11 European organizations is developing an Application Domain Extension (ADE) Energy for the OGC open standard CityGML. This paper presents the collaborative development of this new open urban information model, including its genesis, objectives, structure and next planned steps.

INTRODUCTION

Urban Energy Modelling and Simulation has seen a substantial development during the last decade, boosted by two factors; the shift of the energy transition paradigm at the city scale level, and the increasingly high computational performances reached by multi-core microprocessors and Graphic Processing Units. In the past few years, international research centres and private sector actors have developed specific algorithms and software solutions (e.g. CitySim, UMI), which provides new digital methods for energy planning and decision support. Decision makers, in municipalities, housing authorities, energy supply companies and other stakeholders are just getting used to the enormous potential of them.

However, contrary to Building Energy Modelling, where a number of well-established Building Information Model (BIM) standards (IFC, gbXML) serves as exchange support between different tools and expert fields, allowing for high interoperability possibilities, no comprehensively applicable model standard exists until now for Urban Energy Modelling. Therefore, developers of new urban energy tools have created their own tailor-made data-models, while municipalities and other urban information data administrators have their own database structure to collect and manage urban information. As such, these models exist without interoperability possibilities, necessitating that each new attempt at developing a comprehensive Urban Energy Model begin from the ground up.

An open Urban Information Model standard namely exists to encode, store and exchange virtual 3D city models and landscape models: CityGML [1], which is developed by the Open

Geospatial Consortium (OGC). This XML-based data model defines classes and relations for the most relevant 3D topographic objects in cities (e.g. buildings, transportation infrastructures, city furniture, water bodies) regarding their geometry, topology, semantics, and appearance. In particular, the representation of buildings includes WallSurface, GroundSurface, and RoofSurface as well as for the description of the roof shape, usage type, number of storeys, construction year, and building height. A considerable asset of CityGML is its flexible object modelling in different Levels of Details, enabling the virtual city model to adapt to local building parameter availability and application requirements (see Figure 1). However, since CityGML is an application independent information model, it does not include specific energy-related elements naturally.

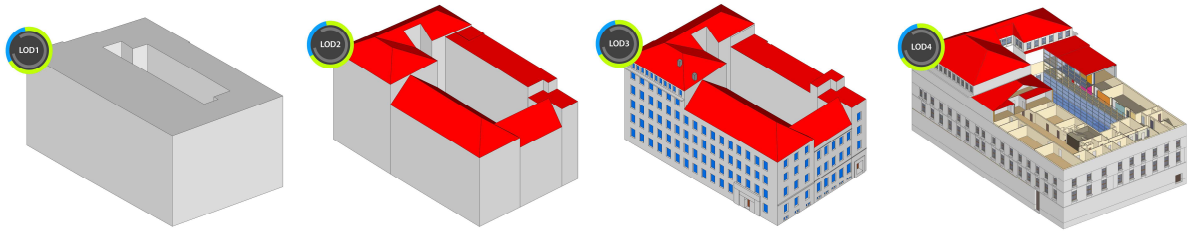

Figure 1 Building 2 of HFT Stuttgart, represented in the four Levels of Detail (LoD) of the OGC standard CityGML (source: HFT Stuttgart)

With the CityGML concept of Application Domain Extensions (ADE), it is possible to incorporate domain-specific entities which are not pre-defined in CityGML standard. Concretely, an ADE is represented by an XML-Schema using a specific namespace (energy in our case), interfacing with the CityGML base schema. The ADE concept supports two different methods for extending the base standard, detailed in the OGC "Best Practices Document" [2]:

- Existing CityGML classes can be extended by additional attributes or relations ("ADE-attributes"). ADE-attributes substitute the CityGML generic attributes and additionally support relations to geometry objects, CityGML or ADE feature classes, and the usage of Enumerations or Codelists.
- In the ADE schema, new classes ("ADE-classes") can be defined, which optionally can be derived from existing CityGML classes using the generalisation concept. In consequence, an ADE-class inherits all attributes and relations of the base class.

Due to the rich information model, its extensibility, and the rapidly increasing data availability all over the world, the combination CityGML + ADEs is a suitable information model for a common engineering data backbone for urban energy, environmental, and mobility planning.

PRELIMINARY WORK

In the past few years, the University of Applied Sciences Stuttgart (HFT) and the Technische Universität Munich (TUM) have developed new urban energy simulation platforms, SimStadt (HFT) and Energy Atlas (TUM), based on the CityGML data model. While their input requirements for the calculation of the building heating demands were going far beyond the available data structure of CityGML, they developed in parallel two different drafts of Energy Application Domain Extensions (ADE).

In order to exchange the models and compare the energy simulation results, HFT and TUM started working together on the harmonization of the ADE models into a unique Energy ADE.

Since that, several international urban energy simulation developers and users have joined this initiative. In May 2014, an international group of experts from 11 European organisations from Germany, France, Italy and Switzerland met to plan together the development of a common Energy ADE for the CityGML urban information model. They were representing six urban energy simulation platform developments: CitySim [3], SimStadt [4], EnergieAtlas [5], Modelica library AixLib [6], Sunshine platform [7] and the Curtis platform [8]. This collaborative work led to a first release of the Energy ADE in February 2015, which this paper introduces.

OBJECTIVES

The objective of this Energy ADE is to store and manage data required for the calculation of the building energy flows and its main results in the CityGML-based virtual 3D city model. The physical boundary of this new data model is the building envelope, including the systems installed on it (e.g. solar panel, shading devices). Small-scale centralized energy systems may also be modelled in this Energy ADE. However, urban centralized energy infrastructures, like district heating system or gas network, are not in the scope of this development, since they are already represented by the CityGML Utility Network ADE [9]. The Energy ADE allows for interfacing with the utility networks through substation node objects.

Following the philosophy of CityGML, this Energy ADE aims to be flexible, in terms of compatibility with different data qualities, levels of details and urban energy model complexities (from monthly energy balance, to sub-hourly dynamic simulation of software like CitySim or EnergyPlus). It aims to be integrated as far as possible within the existing CityGML data model, avoiding the creation of a parallel data structure that would be tailor-made for specific calculation methods. Moreover, this Energy ADE considers the existing international building and energy data specifications, like the INSPIRE Directive of the European Parliament, as well as the recent US Building Energy Data Exchange Specification (BEDES), and integrates their relevant energy-related attributes.

An important issue is also to track and manage the diversity of data sources and data qualities, which highly affects the reliability and precision of the energy calculation results. For this purpose, a concept of metadata is currently under development within the Energy ADE working group. As it seems to be a general concern for many present CityGML developments, we foresee a coordinated work with other CityGML developers in this field.

A MODULAR STRUCTURE

The Energy ADE is presently structured in 3 modules and a core model:

- Construction and materials
- Building Occupancy
- Energy and Systems

This structure enables to potentially reuse and extend some of its modules in other domains and applications, with data exchanges and interoperability opportunities. For instance, socio-economic studies may make use of the Energy ADE module Occupancy, while the module Constructions and Materials could also be applied for acoustics or statics.

Energy ADE core

The Core of the Energy ADE contains the thermal building objects required for the building energy modelling. These thermal building objects are linked to CityGML building objects through the CityGML abstract classes *_AbstractBuilding*, *_BoundarySurface* and *_Opening.*

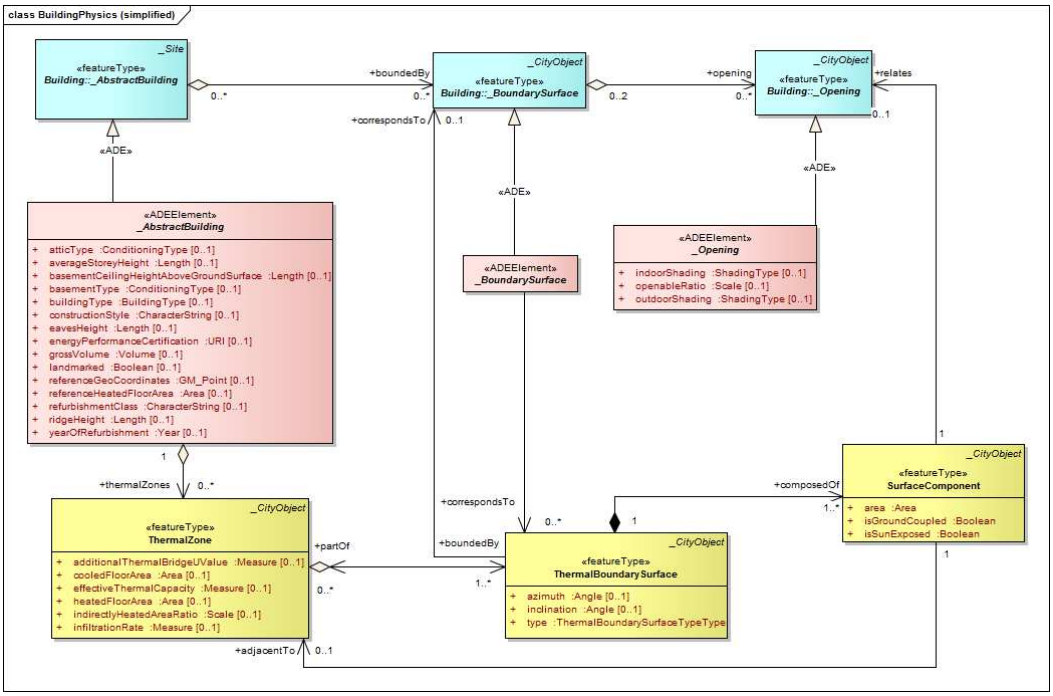

Figure 2 UML diagram extract of Building Energy ADE core

This schema is designed to be compatible with the four Levels of Detail (LoD) of CityGML while modelling faithfully the different thermal zones. A building may have one or more *ThermalZone* objects, which can be linked to a CityGML geometric object (e.g. *Building*, *BuildingPart*, and *Room* in the LoD4 case) or be pure semantic objects (e.g. storey for a CityGML Building whose LoD is lower than 4). Similarly, the *ThermalBoundarySurface* objects may correspond to a CityGML *_BoundarySurface* (e.g. roof, outer wall) or not (e.g. in case of an attic floor bounding the thermal zone for a CityGML Building LoD2-3).

The *_AbstractBuilding* extension contains energy-related attributes relevant for the building energy analysis, partly inspired by the INSPIRE data specification.

Construction and Materials

This Energy ADE module may be used and further extended for multi-field analysis (e.g. statistics and acoustics). It contains the physical characterization of building construction elements and can be flexibly associated with any CityGML *_CityObject* (in particular a *SurfaceComponent*, a *ThermalBoundarySurface* or a whole *Building*).

This module is based on a hierarchical structure *Construction*, *Layer*, *LayerComponent* and *Materials*, inspired by the gbXML format.

Flexibly designed, the data model is applicable for static energy balance purpose (which required the building contruction's U-Values and windows g-Values) as well as for more complex transient heat simulation. For this latter, the data model provides the material thermal characteristics of each construction layer. Thus, the level of detail of these parameters fits the granularity of urban energy models and the data availability.

Building Occupancy

This Energy ADE module may also be used and further extended for multi-field analysis (e.g. socio-economics, demographics and census data). It contains the characterization of the building usage, including HVAC operation set points, ownership and occupancy information

as well as information about the owner and facilities. This module connects to all other elements of the Energy ADE (*_AbstractBuilding* and *ThermalZone*) through the class *UsageZone*, which defines a zone of a building with a usage type considered as homogeneous. One or several *UsageZone* may be associated to a *ThermalZone*, giving the flexibility to model mixed-use buildings with a mono-zone or multi-zone building model. *UsageZone* may have one or several Occupancy and Facilities objects. The object *Occupancy* represents a homogeneous group of occupants (the decision was made not to model single occupants for privacy reasons).

Temporal variables, such as occupancy rate or operation schedules (for heating, cooling, ventilation or any facilities), can be modelled with different levels of details, depending on the modelling purpose and the data availability: *ScheduleLoD0* corresponds to a constant average value. *ScheduleLoD1* distinguishes usage and idle values and set their daily switch time. *ScheduleLoD2* is a collection of typical daily schedules, while *ScheduleLoD3* corresponds to detailed time series.

Energy and systems

This Energy ADE module contains information concerning the energy forms (energy demand, supply and sources) and the energy systems (conversion, distribution and storage systems).

An *EnergyDemand*, which may be associated to any *CityObject* (in particular *Building*, *ThermalZone*, *UsageZone*, *BuildingUnit* etc.). This object represents the useful energy required to satisfy a given end use type such as heating, cooling, domestic hot water etc.. Other energy forms are *EnergySupply*, representing the part of the energy produced by the energy conversion systems, which is supplied to satisfy the energy demand, and *EnergySource*, corresponding to the final energy consumed by an energy conversion system.

All energy form objects are characterized by an *energyAmount*. It corresponds to a regular or irregular time series, containing variable properties such as *acquisitionMethod* (e.g. simulation, metering) or *interpolationType*. Therefore, both simulation results and metering data may be stored in the data model, for instance for a comparison purpose. Moreover, different time steps (sub-hourly to yearly, regular or not) corresponding to different building simulation methods and metering systems may be used.

The *EnergyConversionSystem* objects, which contains general parameters such as *nominalEfficiency* or *yearOfManufacture*, are specified by energy conversion technologies such as *Boiler*, *SolarThermalSystem* etc… These systems may have different operation modes for the needs of the different end uses, e.g. a reversible heat pump may supply during a year the space heating demand, the domestic hot water demand and the space cooling demand, representing three operation modes with different efficiencies, control strategies and operation time. The produced energy (power or thermal) is then supplied to the end users through energy distribution and energy storage systems.

CONCLUSION AND PERSPECTIVES

With the common objective of improving data exchange and tools operability in the urban energy modelling community, an international expert group of research institutes, standardisation organisations and GIS companies has extended the open city model standard CityGML with an Energy ADE. This new development is a long iterative process, which has just delivered its first results with this first XML Schema release 0.5.0.

During the second semester 2015, a test phase will allow confronting the Energy ADE schema with concrete real project and software integration issues. The numerous and diverse urban energy modelling and simulation tools used and developed by the different partners of this

expert group will serve as test applications, in order to verify and optimize the Energy ADE flexible design. The present release is freely accessible on the SIG3D website: http://www.sig3d.org/citygml/2.0/energy/. New active participants are very welcome in this continuing development and test process.

ACKNOWLEDGMENT

We would like to thank all members of the Energy ADE development group who contributes voluntarily to the present development: University of Applied Sciences Stuttgart, Technische Universität Munich, Karlsruhe Institute of Technology, European Institute for Energy Research, RWTH Aachen University / E.ON Energy Research Center, HafenCityUniversität Hamburg, M.O.S.S Computer Grafik Systeme, Centre Scientifique et Technique du Batiment, Electricité de France, Sinergis and Ecole Polytechnique Fédérale de Lausanne. Thanks in particular to the Special Interest Group 3D (SIG3D) who provides the group with its infrastructure and an official framework to our work.

REFERENCES

1. Groeger, G., Kolbe, T.H., Nagel, C., Häfele, K.H 2012. OGC City Geography Markup Language (CityGML) En-coding Standard. OpenGIS® Encoding Standard, Version: 2.0.0, OGC 12-019, 2012-04-04.
2. Van den Brink, L., Stoter, J., Zlatanova, S. (2014): Modelling an application domain extension of CityGML in UML; OCC 12-066, 2014-01-31
3. Robinson, D., Haldi, F., Kämpf, J. H., Perez, D. 2011. Computer Modelling for Sustainable Urban Design, in Computer Modellling for Sustainable Urban Design, 2011.
4. Nouvel, R., Duminil, E., Bruse, M., Brassel K-H, Coors, V., Eicker, U. 2015. SimStadt, a new workflow-driven urban energy simulation platform for CityGML city models. In Proceedings: Conference CISBAT 2015.
5. Kaden, R., Kolbe, T. H. (2014): Simulation-Based Total Energy Demand Estimation of Buildings using Semantic 3D City Models. In: International Journal of 3-D Information Modeling, Volume 3, Issue 2.
6. Lauster, M., Teichmann, J., Fuchs, M., Streblow, R., and Mueller, D. 2014. Low order thermal network models for dynamic simulations of buildings on city district scale. Building and Environment, 73:223–231.
7. Giovanni, L., Pezzi, S., Di Staso, U., Prandi, F., De Amicis, R. 2014. Large-Scale Assessment and Visualization of the Energy Performance of Buildings with Ecomaps. In Proceedings of 3rd International Conference on Data Management Technologies and Applications (DATA 2014).
8. Blin D., Casciani F., Imbert P., Mousseau B., Pasanisi A., Terrien P., Viejo P. A software platform to help Singapore to build a more smart and sustainable city. Energy Science Technology Conference 2015, Karlsruhe, 21st May 2015.
9. Becker T, Nagel C, Kolbe TH (2011) Integrated 3D modeling of multi-utility networks and their interdependencies for critical infrastructure analysis. In: Kolbe TH, König G, Nagel C (eds) Advances in 3D Geo-information sciences, Springer, Berlin.

.

EXTENSIVE GEOTHERMAL HEAT USE IN CITIES – ENERGETIC AND ECONOMIC COMPARISON OF OPTIONS FOR THERMAL REGENERATION OF THE GROUND

P. Persdorf; F. Ruesch; M.Y. Haller

Institute for Solar Technology SPF, HSR University of Applied Sciences, Oberseestrasse 10, CH-8640 Rapperswil, +41 55 222 41 65

ABSTRACT

Geothermal energy as a heat source for heat pumps is increasingly unused in the city of Zürich. However, as indicated by other authors, the renewable potential for shallow geothermal heat use is limited due to the fact that natural regeneration in the absence of ground water flow is slow. Constant heat extractions from dense geothermal heat pump installations continuously cool down the affected ground layer.. In this case boreholes have to be drilled deeper or regenerated in order to avoid freezing around the borehole. The aim of this simulation study is to find the most economic geothermal heat pump concept, which does not lead to borehole freezing after 50 years of operation in areas with dense installations (an exemplary mean geothermal heat extraction of 35kWh/m2/a was supposed for this this study). Therefor a multi-family house with a standard ground source heat pump was simulated for a period of 50 years in Polysun. Various solar concepts, an air heat exchanger concept, a geo cooling concept and also a system without regeneration were added to the system. These concepts were compared under the assumption that all neighboring installations are using an equivalent regeneration strategy as the simulated system

For the different system concepts, highly variable total borehole length were needed to avoid freezing, reaching from 1020m for a system with a large glazed collector field to 2160m for the un-regenerated case. The heat cost of the analyzed system concepts was in the range of 21 - 27 Rp/kWh. The most cost-effective system concepts according to this analysis are the air heat exchanger or unglazed collectors. Increasing the total borehole meters was not only one of the most expensive options, but also the least sustainable, since the continuation of ground temperature decrease after 50 years was more pronounced with this option than for any other option.

Keywords: geothermal potential, borehole regeneration, g-function, borehole interaction, regeneration coasts

INTRODUCTION

According to the energy concept of the city of Zürich in 2050 (EK2050, efficiency scenario A), about 44 % of the total useful energy for heating and domestic hot water will be provided by heat pumps – 38 % or 450 GWh a^{-1} of these will be delivered by geothermal heat pumps [1, 2]. This consumption is 10 times higher than today, with about 44 GWh a^{-1} heat extraction in 2013. According to the study "geothermal borehole potential in the city of Zürich" [3] (in german) a geothermal heat extraction, as provided in the EK2050, is only sustainable if it is actively regenerated at locations with a high density of borehole heat exchangers (BHE). Objects with only one or a few BHE are usually just designed for heat removal. And only the mutual influence of the object's own BHE's is usually considered. In the Swiss guideline (SIA 384/6) it is mentioned, that in the case of local accumulation the mutual interaction has to be considered and the effect has to be compensated by seasonal recharging. However, the established planning tools do not provide means to consider the influence of neighboring installations. In this paper a method for considering neighboring installations in the form of a regular field of equal BHE is introduced. This method was used to compare different

regeneration concepts according to the annual energy extraction, the total needed borehole length and the resulting energy costs.

METHOD

One exemplary multifamily house with a geothermal heat pump was simulated with different regeneration systems. The exemplary system was supposed to be suited in an area with high geothermal energy usage. In order to be able to compare different system concepts that lead to a different degree of regeneration, the following assumptions were made:

1. The probe lengths for each variant were customized to fulfill the SIA 384/6 requirement of ground source temperatures above -3/0 °C after 50 years of operation.
2. All neighboring boreholes are subjected to the same heat extraction and injection rate profile as the simulated system.
3. Neighboring geothermal installations are supposed to be placed in a regular pattern of single boreholes with a distance of 20 m. This is equivalent to a mean geothermal heat extraction of 35 kWh/m2a.

Neighbor G-Function

The software polysun uses the g-function approach based on the work of Eskilson [4] to include long term effects in the simulation of borehole heat exchangers. The influence of the neighboring geothermal installations was included in the form of a neighbor g-function. This was defined as the effect of a regular field of BHE to the BHE in the center. The neighbor g-function was generated using a new semi analytical model [5] with the assumption that all boreholes in are subjected to the same heat extraction rate density. With this assumption g-functions for regular fields with increasing size were generated. This g-functions are plotted in figure REF. It can be seen that an increase from 41x41 to 101x101 BHE has a very small effect on the g-function of the field (deviations can be spotted above log(t/tES)=2 which represents more than 1000 years for typical borehole depths). For this reason the g-function of the 101x101 BHE field is supposed to be representative for an infinite field. Because of the superposition principle, the neighbor g-function can be calculated by subtracting the g-function of a single BHE (with an equivalent heat extraction distribution along the borehole) from the g-function of the entire field. The effect of the neighbors corresponds to an additional temperature drop of the BHE by around 7K after 50 years for the assumptions made above. Because of assumption 2, (all neighboring boreholes are subjected to the same heat extraction and injection rate profile as the simulated system) the neighbor g-function can simply be added to the g-function of the BHE of the exemplary system for long-term simulations.

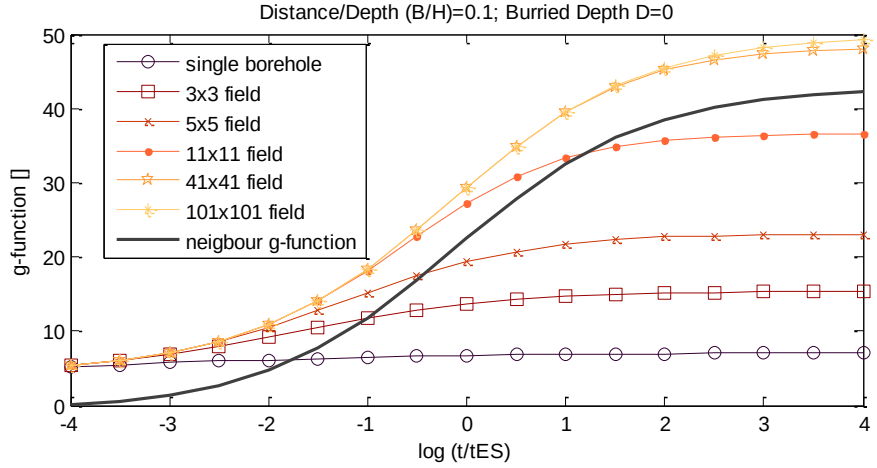

Figure 1: G-functions for increasing field sizes and resulting neighbor g-function.

Simulation

A multi-family house (renovated according to the Swiss energy lable "Minergie") with 12 apartments, 260 m^2 south roof surface was simulated for a period of 50 years in Polysun. The building has an annual heating demand of 72 MWh and a hot water consumption of around 40 MWh. A standard ground source heat pump system (50 kW) extracts 87 MWh heat from the soil within the first year of operation in order to meet the total heating demand.

The following regeneration concepts are investigated:

- No regeneration (basic variant)
- Air heat exchanger (60 kW)
- Geo cooling
- Unglazed absorbers (60 m^2, 260 m^2)
- Unglazed selective absorbers (60 m^2, 218 m^2)
- Glazed collectors (60 m^2, 132 m^2)
- Unglazed PVT-collectors (60 m^2, 260 m^2)
- Glazed collectors with additional solar storage (60 m^2, 138 m^2)

For comparison, all simulations are based on the same hydraulic (basic variant). The regeneration with the air heat exchanger and the solar regeneration are integrated as shown below. The solar regeneration concept is also simulated with an additional solar storage, to demonstrate the utility. The concept geo cooling regenerate the soil with passive solar gains in summer over the floor heating system of the building.

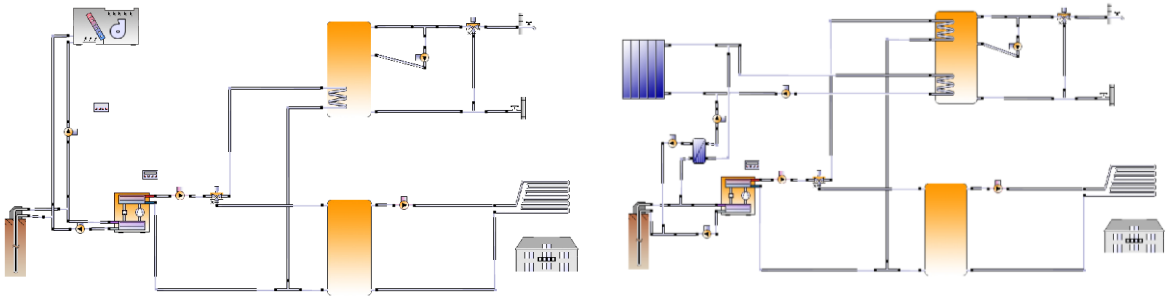

Figure 2: Simulated regeneration concepts with a) an air heat exchanger b) solar collectors.

RESULTS

In this section, the simulation results are presented. The annual net energy extraction of the BHE and the annual regeneration energy are shown in following Figure 3 for the first and the fiftieth year of operation. The sum of net energy and regeneration energy give the gross energy extraction. The difference between gross energy of the concept with glazed panels and gross energy of the basic variant is a result of the direct use of solar energy for water heating. The graph shows that with an additional solar storage significantly more solar energy can be used directly. Regeneration concepts with a strong dependence on the difference between ground and ambient temperature (air heat exchanger, unglazed collectors), show a lower net extraction after 50 years of operation. This is due to the decreasing ground temperature and accordingly a higher efficiency of the regeneration system. None of the variants to the left of the black line reaches a full (100%) regeneration even after 50 years. Thus the soil temperature will still decrease slightly after 50 years. Only the glazed solar collectors (132 m^2) and the selective solar absorbers (218 m^2) are able to regenerate from the first year to 100 % (shown below the black bar). With these regeneration strategies sustainable use of geothermal energy is guaranteed independent of the considered time horizon.

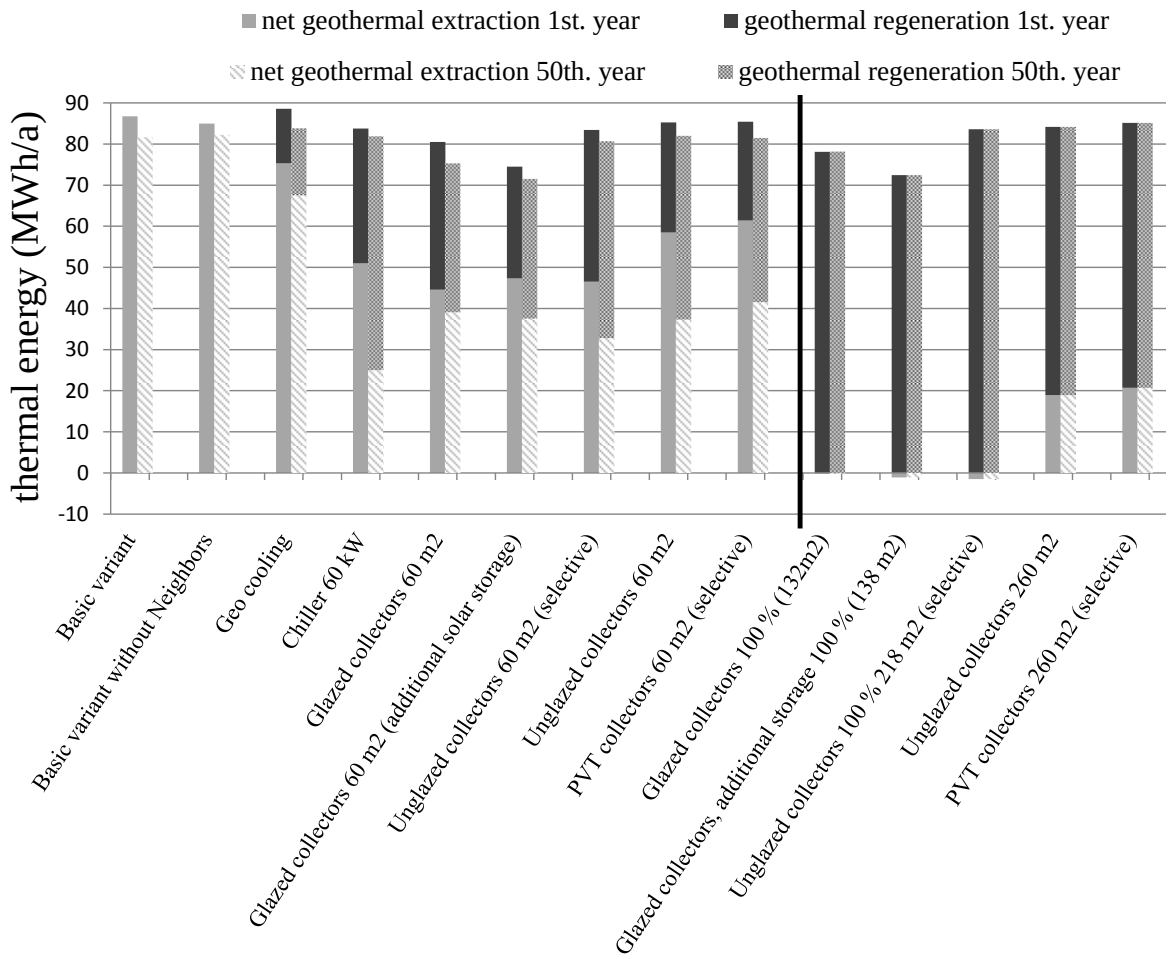

Figure 3: Net geothermal heat extraction and geothermal regeneration in the first and fiftieth year of operation.

Figure 4 shows the entire borehole length of the different regeneration variants to meet the SIA 384/6 requirement of -3/0 °C. By considering the neighboring fields twice as many borehole meters are needed in order to meet the requirements.

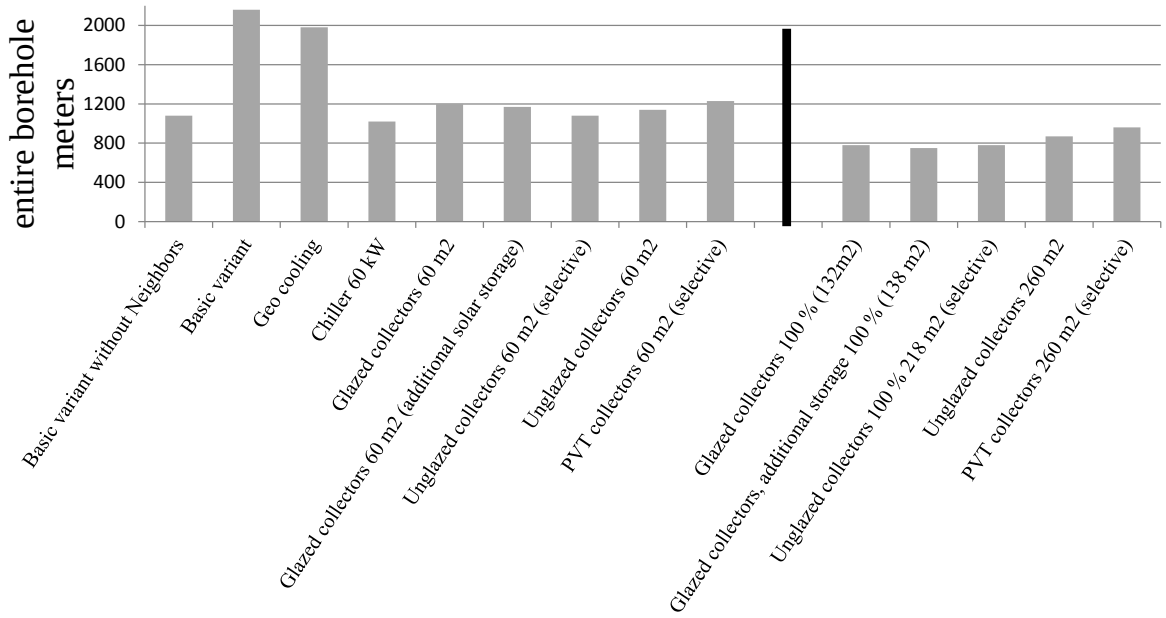

Figure 4: Entire borehole meters of different system concepts.

Figure 5 shows the heat costs of the investigated systems. The costs include the BHE with heat pump, the needed storages, the hydraulics and piping between BHE and system. The extra investments in the air heat exchanger or the collectors are taken into account with piping, hydraulic and heat exchanger in the respective regeneration concept. It has been calculated using the current electricity price of 23.4 Rp/kWh. The annual price increase in the electricity is estimated with 1.4 %, according to the information of the City of Zürich. The effect of neighboring objects leads to additional costs in the range of 2,200 – 4,500 Fr/a. This means an increasing in costs of 10 – 21 % compared to a single object (without neighbors). With the assumptions made in this work the most cost effective concepts are the air heat exchanger or unglazed collectors. However, both techniques are not suitable to achieve complete regeneration. A complete regeneration is possible with glazed collectors or selective absorbers, but it requires a collector area of 132 m^2 or an absorber area of around 218 m^2, which increases the costs up to 25 or 27 Rp/kWh.

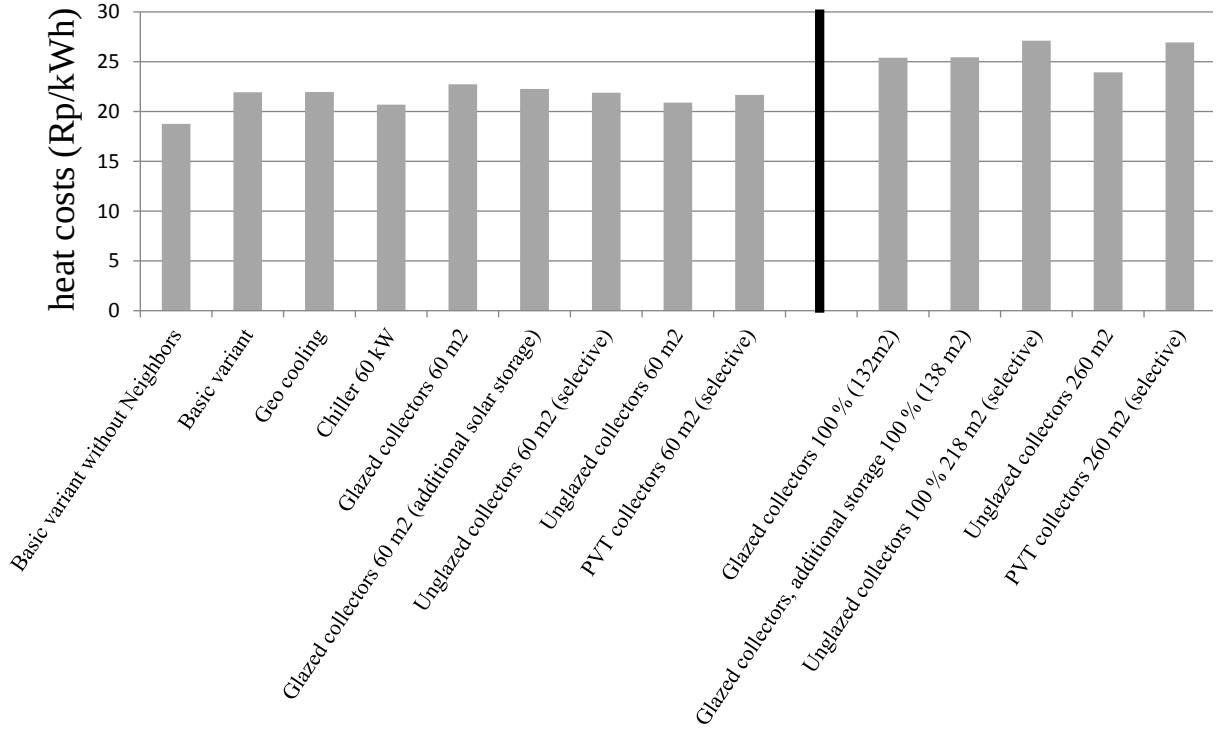

Figure 5: Heat costs of different system concepts.

CONCLUSION

This study was done to compare different methods for the regeneration of BHE from an energetic and economic point of view. The following statements can be made with the results of this simulation study:

- With the assumptions made in this study (geothermal energy extraction of 35 kWh/m2/a) neighboring installations lead to an additional drop of the ground temperature by 7K when not compensated by longer boreholes or BHE regeneration.
- Already by partial regeneration, the long term cooling can be counteracted. This allows higher density of BHE and / or a longer operating times.
- Total regeneration is possible with large area of glazed or unglazed selective collectors. But this leads to higher heating costs compared to concepts with partial regeneration.

- Extending the entire probe length instead of regenerating is both, economically and from the perspective of sustainability one of the worst options.
- The differences between the heating costs with different methods of regeneration are low. Therefore none of the regeneration methods are favoured. The regeneration method can be chosen depending on the specific situation.

The systems with partial regeneration and with consideration of the neighbor effects need a similar total borehole length than the unregenerate system without considering the neighbors. For this reason a change in BHE design is not urgently needed, also for areas where a high geothermal heat extraction density is foreseen for the future. However, new and existing ground source heat pump systems have to be equipped with (at least partial) regeneration systems when a critical extraction density is reached in the neighborhood.

REFERENCES

1. Jakob, M., Flury, K., Gross, N., Martius, G. & Sunarjo, B.: Kurzbericht – Konzept Energieversorgung 2050 – Szenarien für eine 2000-Watt-kompatible Wärmeversorgung für die Stadt Zürich, Zürich, 2014
2. Schmied, F.: Dichter Einsatz von Erdwärmesonden, ungelöste räumliche und rechtliche Fragen. Seminar Erdwärmesonden / Grundwassernutzung für Bewilligungs- und Vollzugsbehörden, Schweizerischer Nationalfonds (SNF), Bern, 24. April 2014.
3. Wagner, R., Weisskopf, T.: Erdsondenpotenzial in der Stadt Zürich. Im Auftrag des Amtes für Hochbauten der Stadt Zürich, 2014 (Download www.stadt-zuerich.ch/egt).
4. Eskilson, P., 1987. Thermal analysis of heat extraction boreholes. PhD Thesis, Department of Mathematical Physics, University of Lund.
5. Cimmino, M. & Bernier, M., 2014. A semi-analytical method to generate g-functions for geothermal bore fields. International Journal of Heat and Mass Transfer, 70(0), p.641–650.

URBAN DENSIFICATION AND ENERGY PERFORMANCE OF EXISTING BUILDINGS: A CASE STUDY

C.S. Polo López [1]; F. Frontini [1], S. Bouziri [1]

1: Institute for Applied Sustainability to the Built Environment (ISAAC), SUPSI, University of Applied Sciences and Arts of Southern Switzerland, Trevano, CP 105, CH-6952 Canobbio, Switzerland

ABSTRACT

Urban densification and preservation of soil are a much discussed topics on which there is still little detailed research. In Switzerland these concepts are also acknowledged by visions and regulations at the federal level together with the importance of increasing energy supply by renewable energy sources and reducing the energy demand in-primis of existing building. The scientific community is however well aware of the need to enlarge the scale of analysis and to move to urban planning and design scales, which would better allow to take into account buildings shape, orientation and density and to detect possible cumulative effects limiting both the access to sunlight or solar gains and the possibility of equipping buildings with solar renewable systems. Moreover the impact of solar energy availability on existing buildings (in particular historical buildings) during urban transformation is still not well understood and is a matter of research. High-urban densification plans expect a complex environment, where self-shading and the overshadows of adjacent buildings can dominate solar energy potential and daylight availability, but also the imposition towards greater energetic production of PV for new buildings would compromise the visual perception of existing settlement under transformation. But how do these urban revolutionary changes towards densification appear and impact? What are the implications for existing buildings during the process? What does solar energy mean for new/existing urban areas with protected heritage buildings? The aim of this research is to delve into these questions by analyzing a real case study in the city of Lugano Paradiso (Ticino). The City Centre district is currently undergoing a profound change towards densification of the urban environment with a new urban master plan and new zoning regulations.

Keywords: urban densification, energy efficiency, solar PV potential, protected buildings

INTRODUCTION

From the Aalborg Charter (May 1994), further on the Leipzig Charter and the Toledo Declaration (June 2010), the importance of implementing effective policies in land use and planning was recognized, involving a strategic environmental assessment. The emphasis was put on the opportunities offered by dense urban concentrations to provide public transport services and more efficient energy supply, while at the same time reserving the human dimension of development. In Switzerland urban densification has being supported and emphasized through strategies and regulations at a national and federal level. The need for high quality densification of urban settlements is gaining momentum also in the public opinion, as recently stated by Schweizer Heimatschutz, the Swiss Heritage Society, which agreed for a reasonable and sustainable use of the land [1]. On the other hand, Swiss federal energy policies emphasize the importance of incrementing the supply of energy from renewable resources, while also reducing the energy demand, with specific focus on the construction sector. Furthermore, the future obligation to install at least 10 Watt/m^2 of PV in new buildings, today only voluntary, as reported in the new *"Model for energy* requirements

at Swiss Cantonal level" (Swiss Federal Council, Sustainable Development Strategy 2012-2015, January 23, 2012) presumes changes in the visual perception of dense neighbourhoods and in the cities themselves. Furthermore, many European and Swiss research projects also reflect on the cities with substantial and valuable heritage with the aim to overcome the aspect linked to the too rigid protection regulations in urban areas that do not allow even the most needed adaptation of historic buildings and areas to the requirements of recent times by reaffirming the key role of energy efficiency and the integration of renewable solar energy (RES) to propose new solutions and promote new policies for the sustainable renovation of existing cities [2-4]. The effects of urban densification, anyway, are important if new measures are implemented quickly and without a careful study of the boundary conditions that serve to meet with the qualitative and architectural culture of the place, affecting mainly the cultural protected heritage in the area. The interest is also to avoid the opposition of the population towards this transformation.

PURPOSE OF THE WORK

Urban planning determines significantly the possibility to exploit solar irradiation. In densely built-up areas it is important to consider factors such as the buildings' geometry and height, the materials and colours, as well as the distance between the buildings themselves (size and morphology of the roads), as factors that can affect the solar radiation absorption and reflection. In the same way, urban shape also depends on the specific conditions of the local place and the climate. To prevent an arbitrary use of solar energy technology, it is necessary to assess the solar potential in relation with its immediate environment and the constructive and typological features. For this reason SUPSI in 2014 started a research project (VerGE) that focus on a real case study in Ticino with the aim to investigate how urban modifications, in particular urban densification policies, can influence the solar availability but also the impact on the heritage protected and on the energy demand of existing building. Only the first points will be addressed by this paper.

METHODOLOGY

In order to assess solar access in urban planning it is important to consider the interaction of multiple parameters and factors. The solar energy potential in urban is also a key factor that affects the energy consumption and the behaviour of existing and new buildings.

The starting point of this research is the analysis of a real case study in Ticino (Switzerland), in the Paradiso municipality, part of Lugano's settlement. It is a district that is undergoing a very fast urban densification process, by changing the open urban sprawl towards infill with closed and compact urban fabrics, as defined in the new master plan regulation.

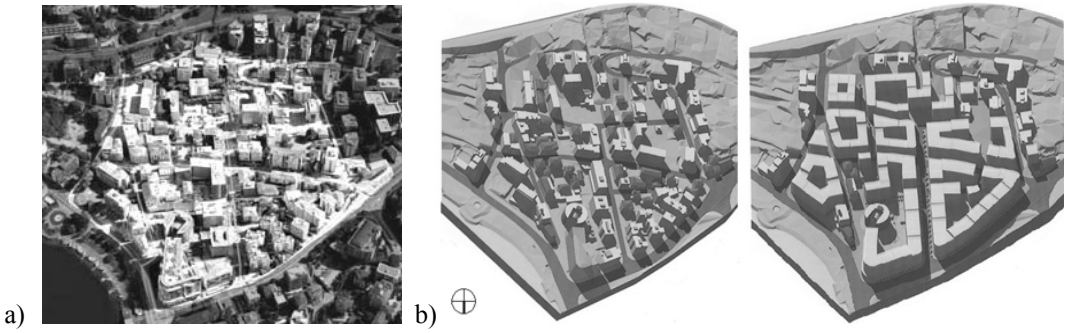

Figure 2: Lugano-Paradiso City Centre district: a) Aerial view (google earth, 2013); b) Spatial urban planning, current and future urban development (new Master Plan).

The study includes the analysis of the current situation and the urban transformations envisaged by the municipality with the entry into force of the new Master Plan. The project workflow presented in Fig. 2, shows three level of analysis from the general aspects (urban level) to particular and detail aspects (building and energy levels). For each level of the analysis some parameters that influence energy aspects and the energy balance of a building (consumption and production) are identified together with the relevant phenomena highly influenced by urban morphology.

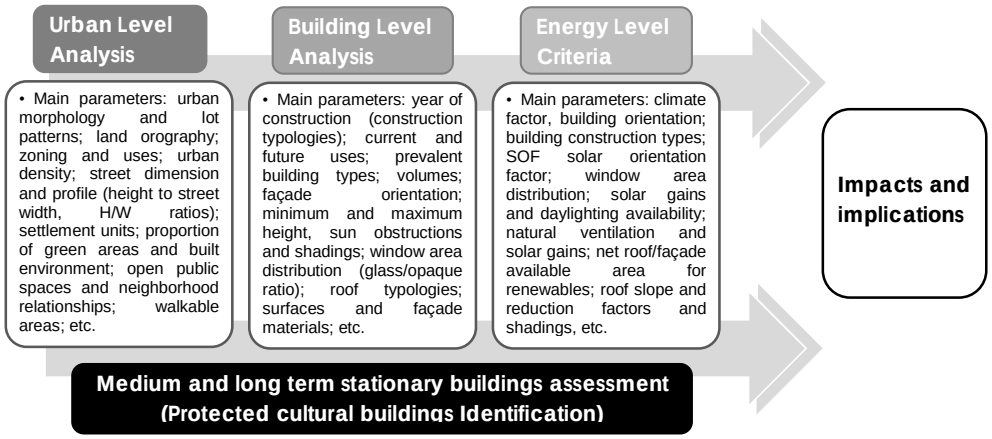

Figure 2: Workflow diagram of VerGE project methodology.

The specific urban planning significantly determines the possibility to harvest solar irradiation in buildings. At the same time, solar energy exploitation on existing buildings could be compromised during urban transformation. To shift the detail at a building level, but always referring to the urban environment, it is necessary to examine the existing and under transformation architectonical situations. This will be done by analysing the distinctive elements of the surroundings according to building techniques, year of construction, materials used, morphology of the buildings and so on. All these aspects will finally complete the assessment at the energy level. All levels have a direct impact on medium and long term stationary buildings (i.e. heritage buildings). Compare the current situation with the future one (when the New Master Plan will be completely implemented) allows to establish the main impacts of densification, such as the solar potential for renewable solar energy installations (RES). The main focus of the methodology proposed is to measure the impact and repercussions of the urban changes on the solar availability and also the effects of these measures in the existing historical buildings and cultural monuments.

ANALYSIS

The analysis has been done with three levels of detail: Urban, building, energy.

Urban Level Analysis

As result of this analysis, the City Centre area (CC) of Paradiso was selected to investigate the main key parameters mentioned above, regarding phases 2 and 3 as stated in the methodology process because an important urban transformation is expected in this area towards densification by increasing the percent of buildable area and the public walkability of the streets, with tallest closed blocks of buildings up to nine floors. The new master plan sets out for a minimum of 40% primary residence and a maximum of 30% on secondary residences, 30% offices. The downtown area of the municipality has an urban setting with "*warped parallel*" roads as street pattern and currently buildings are freely positioned on the plot where

façade orientation in this case is less determined by the street layout that are equally divided on North-South and East-West. The geography of the place does not have much slope varying from 16% to 1% next to the lake. It is the most densely built area of the territory of Paradiso. It is the area with the largest number of protected cultural buildings. Currently, the proportion of buildings with respect to open spaces (public and private) is important, near to 40% of buildings and 10% for roads, and 50% of open spaces (mainly private 28%).

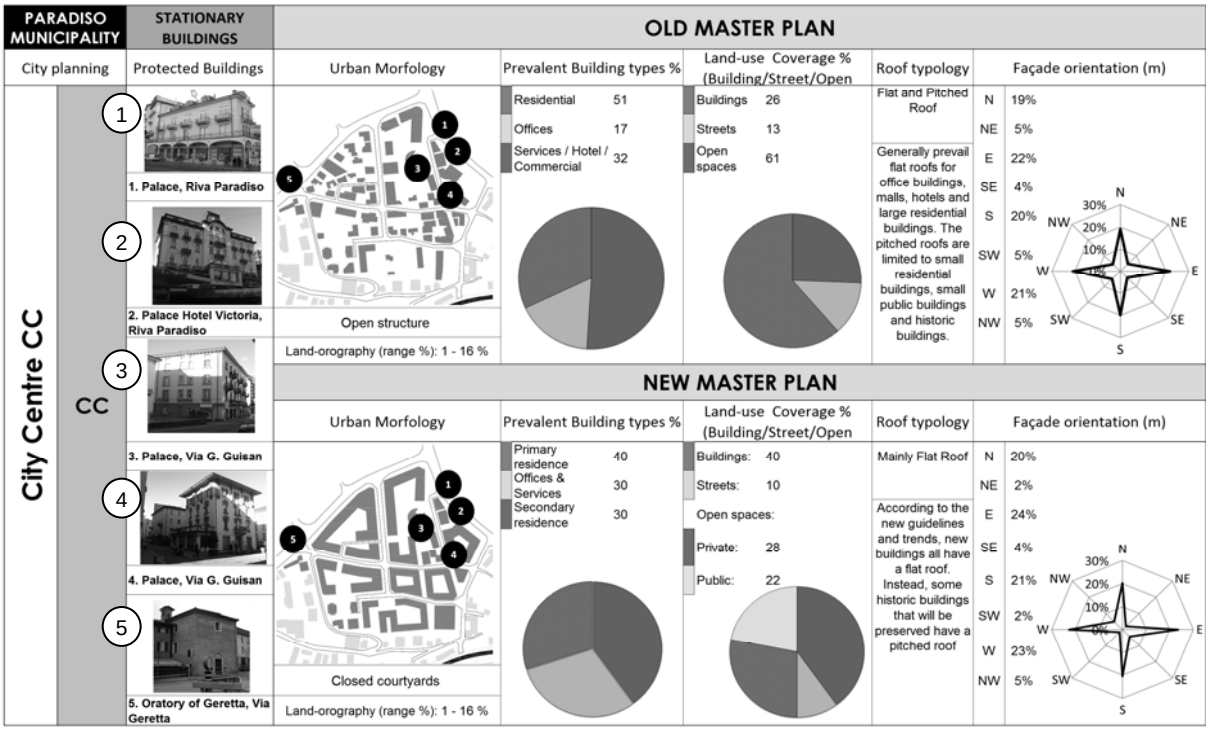

Figure 3: Comparative table of the New Master Plan regulatory status and the current situation status for the whole City Centre area.

Building Level Analysis

Different aspects have been analysed from the urban level to the building level for each of the sectors of the selected area (the Master Plan divides the City Centre core in different building areas, named from A to G), which are: Aspects regarding urban morphology: *street patterns and street profiles, settlement unit, the height to street width ratio (H:W) and the urban density (%)*; Aspects regarding building configuration and design: *prevalent building types (uses and construction typologies, year of construction, etc.), orientation, building heights*; Aspects regarding building shape and façade materials: *roof and façade typologies and building envelop features.*

As outcome of this analysis it has been found that street profiles significantly change in the new configuration of the Master Plan with building heights reaching up to 29,5 meters from the level of the street. Due to the relationship between the heights of buildings in the area on each side of the streets, for all cases the H:W, height to street width ratio, is quite high, which mean, a poor balance in solar access terms with shading effects on surrounding buildings. This situation is significantly accentuated in the case of the new plan with building heights up to nine plants with H:W ratios up to 2,5 in some cases. There will be a reduction on the potential use of solar passive strategies and will limit the use of façade surfaces for integrated solar photovoltaic systems. Besides, air circulation in the urban area could be reduced significantly due to the configuration of these urban canyons. Building orientation remains

predominantly oriented along N-S or E-W axis which means that well-oriented façades are proportionally equal to those not well-oriented. It would be necessary to adequately differentiate openings in the different orientations to maximize passive energy gains minimizing energy losses at the same time.

Energy Level Analysis

At this level, a first estimation of the total energy balance in the area was performed considering a full exploitation of the solar potential for renewable systems (solar photovoltaics). This PV potential, in the present status, assumes the use of all the roofs surface available in the area while in the future scenario it has been necessary to consider also the facade surfaces well exposed to solar radiation (to comply with the obligation of 10 Watt/m^2 of PV), due to the high densification. The scope of this analysis is to verify whether it is possible to reach the objectives suggested by future Swiss policies in a high dense urban area, while at the same time, to know the impacts also in terms of visibility and changes of the urban perception when these technologies are in proximity to buildings protected.

The total thermal energy consumption (thermal/DHW) of the buildings has been roughly estimated in the current state and future state based on statistical information collected and developed at SUPSI [5] by applying average coefficients [kWh/m^2yr] of thermal consumption indices as a function of year of construction for new and existing buildings. In the study, the annual heat requirement [MWh/m^2yr] of each sector it has been calculated building by building, considering the category of the building and use relative to each (i.e. residential, commercial, offices, schools, etc.), type of building based on the year of construction (more than 50 years; from 20 to 50 years; max. 20 years; new or renovated buildings) and the energy reference surface [m^2]. In case of future buildings, to quantify an equivalent electrical amount of energy, the heating and cooling energy demand has been converted in an equivalent electric load. Considering the hypothesis that these new buildings will be more efficient, it has been supposed the generalized use of heat pumps for thermal conditioning (equivalent coefficient of performance, COP equivalent equal to 3). The total electrical energy consumption [MWh/m^2yr], i.e. annual electricity needs in the area, sector by sector for the current state and the future one, has been estimated also by applying the Swiss regulation SIA 380/1:2009 and the SIA 380/4:2006. The solar irradiation estimation and solar potential analysis for renewable solar systems (RES) has being conducted by using the solar Cadastre of Ticino provided by OASIS platform (*http://www.oasi.ti.ch/*) for the current situation and also by using simulation tools like PVSOL for the new (*considering PV modules of multicrystalline technology with Nominal Power of 270 Wp and module efficiency η_m 16.5%, for simulations).

		CURRENT SITUATION (ACTUAL URBAN PLAN)						FUTURE SITUATION (NEW URBAN PLAN)					
Sectors		GROSS FLOOR AREA [m^2]	THERMAL DEMAND [MWh/yr]	ELECTRICAL DEMAND [MWh/yr]	ESTIMATED ANNUAL PV PRODUCTION [MWh/yr]	(1) PV ELECTRICAL CONTRIBUTION [%]	(2) PV ELECTRICAL CONTRIBUTION [%]	GROSS FLOOR AREA [m^2]	PRIMARY THERMAL DEMAND [MWh/yr]	ELECTRICAL DEMAND [MWh/yr]	ESTIMATED ANNUAL PV PRODUCTION [MWh/yr]	(1) PV ELECTRICAL CONTRIBUTION [%]	(2) PV ELECTRICAL CONTRIBUTION [%]
Paradiso Municipality - City Center Area (PRG CC)	A	20'437.0	1'696.5	544.7	257.0	47%	11%	70'822.0	1'010.5	2'051.6	683.5	33%	22%
	B	48'366.0	3'364.1	1'170.1	324.0	28%	7%	77'461.0	1'119.3	2'271.6	627.3	28%	18%
	C	14'624.0	1'158.8	401.9	100.0	25%	6%	33'171.0	491.8	976.8	285.4	29%	19%
	D	3'199.0	188.0	87.8	53.0	60%	19%	2'947.0	52.6	84.7	24.3	29%	18%
	E	15'730.0	1'522.9	432.5	112.0	26%	6%	40'302.0	549.1	1'169.3	400.0	34%	23%
	F	21'162.0	1'900.1	602.4	202.0	34%	8%	41'175.0	561.0	1'194.6	391.1	33%	22%
	G	42'336.0	2'612.2	1'176.0	192.0	16%	5%	64'997.0	934.5	2'145.4	580.6	27%	19%
Total urban area		165'854.0	12'442.7	4'415.5	1'240.0	28%	7%	330'875.0	4'718.8	9'894.1	2'992.2	30%	20%

(1) Considering only the electrical demand
(2) Considering electrical demand plus thermal demand

(1) Considering only the electrical demand
(2) Considering electrical demand plus thermal demand

Table 1: Energy demand, PV solar potential and global energy balance. The table shows the PV percentage contribution to meet the objectives of a Net-zero Energy settlement.

RESULTS AND CONCLUSION

The paper shows the impacts of urban densification and solar RES implementation policies in a case-study (Lugano-Paradiso). The simulated scenarios consider solar photovoltaic systems fully integrated in the City Centre (CC) district area, where there are several protected buildings. The results highlighted that the estimated PV percentage for electrical supply is almost equal for the current and the future situations when the new urban Master Plan will be completed (28% and 30%, respectively). The main differences in the two scenarios are that a high PV density (Wp/m^2) in the second case impacts on PV system visibility while transforming the complete urban area appearance. In the hypothesis of covering also the thermal buildings demand, the future situation is better if considering a high-efficient built stock (future average thermal energy density index of 14 kWh/m^2yr compared with 77 kWh/m^2yr calculated for the present status). These results show how important is the proper integration of PV technologies in future buildings, especially in dense urban areas through the use of BIPV (Building integrated Photovoltaics) products. The proposed methodology foresees that the energy impacts of the densification policies, must to be quantified to enable new approaches for urban planning alternatives. Further aspects affecting solar access in dense urban areas will be developed within the project and presented in future.

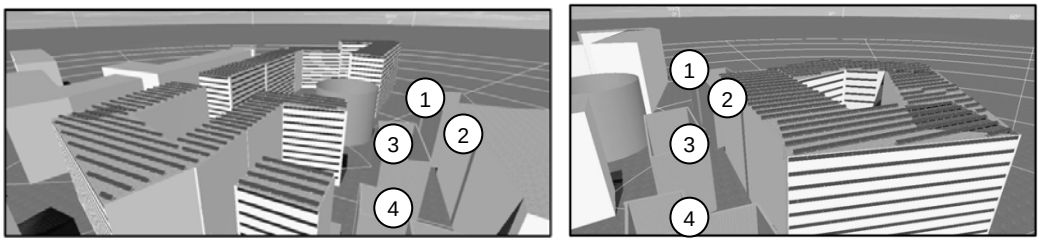

Figure 4: PV in the future scenario, B-C sectors (numbers are protected buildings).

ACKNOWLEDGEMENTS

This project was funded by the Stiftung zur Förderung der Denkmalpflege (Foundation for the Promotion of the Conservation of Historical Monuments). We are also grateful to Lugano-Paradiso Municipality and Planidea SA which provided the 2D/3D drawings of the new urban development planning. Moreover we thank also the colleagues from ISAAC-SUSPI and other contributors (in particular, Pampuri Luca and Sala Mariaemma).

REFERENCES

1. Swiss Heritage Society position paper: L'aménagement du territoire face à de grands défis / Raumplanung vor grossen Herausforderungen. Densificare con qualità (2010).
2. URBACT III European Territorial Cooperation programme (2014-2020). http://urbact.eu/
3. EnSURE Project: Energy Savings in Urban Quarters through Rehabilitation and New Ways of Energy Supply. INTERREG IV B Central Europe (2007-2013).
4. Polo López C. et al.: ENBAU, Energie und Baudenkmal. Energy Conservation Practices on the Historic Heritage Buildings. Proc. of the BRENET Status-Seminar, Zürich, 2012.
5. Bianchi P., Pampuri L., Crivelli G., Cellina F., Mobiglia, M.: Quanto calore consumano gli edifici residenziali in Ticino? Aggiornamento della metodologia di stima dell'indice energetico per il fabbisogno termico. Dati - Statistiche e società, A. XIV, n. 2, pp 81-85, 2014.

DEVELOPMENT OF A CITY INFORMATION MODEL TO SUPPORT DATA MANAGEMENT AND ANALYSIS OF BUILDING ENERGY SYSTEMS WITHIN COMPLEX CITY DISTRICTS

Jan Schiefelbein[1], Amir Javadi[1], Moritz Lauster[1], Peter Remmen[1], Rita Streblow[1]; Dirk Müller[1]

[1]*RWTH Aachen University, E.ON Energy Research Center, Institute for Energy Efficient Buildings and Indoor Climate*

ABSTRACT

Urbanization causes increasing energy demand within cites. To identify energy saving potentials on city district scale, integral planning approaches are necessary. This paper describes the development of a city information model (CIM) with focus on buildings and energy systems. It accounts for different building and energy system types plus geometry, building physics as well as occupant information. The CIM structure has been implemented on a PostgreSQL database (DB), which has been linked to a geographic information system (GIS) to enable graphical data analysis and modification. Considering data uncertainty, the CIM structure supports a simplified city district modeling. Within a case study, DB and a Python tool are used to parameterize buildings for dynamic simulations to estimate the state of retrofit.

Keywords: City district, CIM, GIS, energy systems, PostgreSQL

INTRODUCTION

The megatrend urbanization causes increasing needs within cities. Especially rising energy demands have to be covered. This concentrated energy demand leads to high greenhouse gas emissions within cities. Urban areas are responsible for around 70% of emissions, but only cover 2% of land mass [1]. Therefore, they offer great potential for emission reduction. However, the identification of options for greenhouse gas emission reduction on city district scale is challenging. A single building already holds a multitude of parameters, such as building age, type or geometry attributes. A city district can consist of a plurality of heterogeneous buildings. Therefore, the number of relevant objects and their attributes rises tremendously. The city complexity can complicate data handling, which is necessary for the analysis of city districts. Thus, the data management should be simplified to support the identification of greenhouse gas emission options.

This paper describes the development of a city information model (CIM) with focus on energy systems. It accounts for different building and energy system types. The demand side is mainly represented by buildings and their user behavior. Therefore, the CIM takes building geometry, building physics as well as occupant or attendee information into account. On the generation and distribution side diverse thermal and electrical energy supply systems are included. The CIM structure has been implemented on a PostgreSQL-Server. The relational database (DB) is linked to the GIS software QGIS, which combines entity location and further object data. This enables graphical data analysis and modifica-

tion. Based on a Python tool, named TEASER, building parametrization is automatized. The generated building models can be used for further analysis or dynamic simulations.

METHODOLOGY

For the CIM as well as its implementation into a database, the following requirements are defined:

- Data management simplification (Dealing with large number of objects; GUI usage)
- Account for diverse building and energy system types (High flexibility)
- Account for data uncertainty (Simplified modeling approaches; estimation methods)
- Good interconnectability (Interfaces for data interchange)
- Enable use cases (e.g. support generation of city district models)

In the following, CIM and its related entity-relationship (ER) scheme are described. Second, the DB infrastructure is explained. Third, a Python tool for building parametrization is elucidated.

City information model

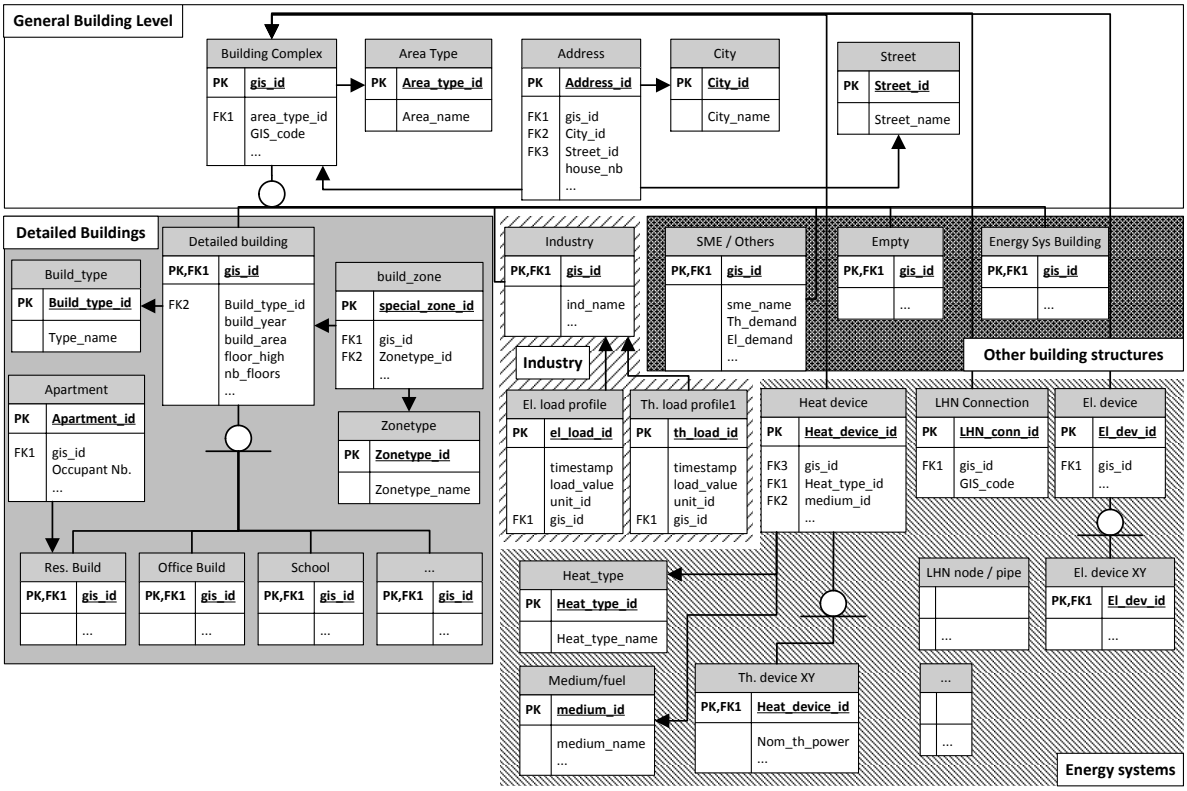

Figure 1: Simplified Entity-relationship scheme of CIM

The simplified version of the developed ER scheme is shown in Figure 1. The general building complex builds the scheme core. It can hold address and area type information. Furthermore, it includes a 'GIS_code', which can be interpreted as position data in a specific reference system by GIS. Possible area types are:

- Detailed buildings (with higher quality of data; comparable installed appliances and user behavior; e.g. residential or office buildings)
- Industrial buildings
- Small and medium sized enterprises or other buildings with energy demand (low level of knowledge about internal processes)
- 'Empty' area (placeholder, e.g. for buildings under construction)
- Energy system buildings (main function is energy generation; e.g. power plants)

Industrial buildings are mainly taken into account via measured load profiles. SME and other buildings with less information about internal processes are primarily modeled via estimation of annual thermal and electric energy demands, for instance, with Fraunhofer ISI statistics about specific energy demands per SME type [2].

Buildings with comparable structure or higher data quality (respectively sufficient estimation methods) are taken into account as 'detailed buildings', such as residential or office buildings. There are two main reasons for this modeling concept. First, appliance and user profiles of the same building type are comparable. Therefore, a few modeling approaches can be used to model multiple profiles. Second, necessary data, such as building ground area or building height, can be extracted from different sources, such as openStreetMap, BingMaps or CityGML datasets. If further information about internal building structure is available, special building zones can be defined. Furthermore, apartments with number of occupants are set into relation with residential buildings. Every building complex can hold a number of thermal and electric supply units as well as storage systems. Moreover, local heating network (LHN) connections are taken into account.

Database infrastructure

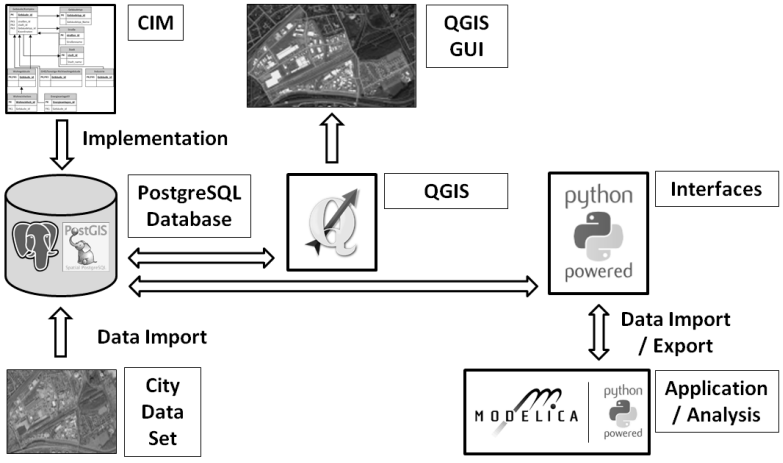

Figure 2: Database infrastructure and interfaces

The CIM has been implemented into a PostgreSQL database with PostGIS. The PostGIS plugin supports usage of geometrical types in PostgreSQL [3]. To simplify handling of geographical data, the open source software QGIS is connected to the database. It enables the visualization of the city district as well as modification of geographic and semantic data. Furthermore, a Python interface enables data import and export for further analysis or applications, such as dynamic simulations of city districts. Figure 2 shows the database infrastructure.

Building parametrization tool

A possible application for the city database is the support of building model generation. Therefore, a Python tool named 'TEASER' (Tool for Energy Analysis and Simulation for Efficient Retrofit) has been developed. It is based on a Python tool originally developed by Hillebrand [4]. The tool is able to parameterize building models based on IWU building typology [5]. The modeling workflow is shown in Figure 3.

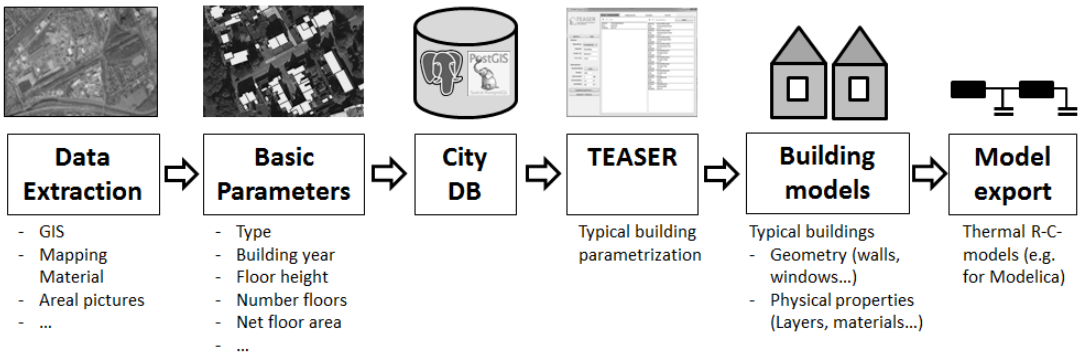

Figure 3: Building parametrization workflow

TEASER generates typical building geometries (outerwall, window, rooftop and basement areas) as well as typical layer structures (such as wall layers with material properties, e.g. specific heat capacity, density, heat transition coefficient and layer length), based on some elementary building parameters:

- Building type (e.g. residential)
- Year of construction
- Floor height
- Number of floors
- Net floor area

Most basic parameters can be extracted from or estimated with GIS sources or local authority datasets. TEASER can import necessary datasets via DB connection. The parameterized model sets can be saved for further modification or be exported for further usage, such as Modelica building model generation.

CASE STUDY

A case study has been performed with an existing residential district with 248 buildings, which have mainly been constructed before 1950. The final thermal energy demand is known by statistics of local authorities. However, the state of retrofit is unknown. Therefore, the aim is to estimate the state of retrofit for the residential district. Thus, dynamic simulations within Dymola/Modelica have been performed.

Modeling and simulation setup

DB and TEASER are used to parameterize 248 buildings of the residential district with different retrofit years (1960, 1970, 1980, 1990). To simplify the modeling of retrofited buildings, the recent retrofit year is set as building year of construction. Therefore, a retrofited building is modeled as newly constructed building within the retrofit year. This

simplification might lead to wrong layer structures and parameters. However, under the assumption, that the overall heat transfer coefficient of retrofited and newly constructed buildings are comparable, due to defined building efficiency standards, the approach is valid to estimate the state of retrofiting. The buildings are exported as Modelica record files, which are used to parameterize thermal zone models of Modelica AixLib [6]. Boiler heating devices are installed in all buildings. Annual occupancy, appliance and lighting profiles are generated with a modified version of the Richardson tool [7]. The desired indoor temperature is defined as 20 °C. The test reference year (TRY) for region 5 of German weather service (DWD) is used as input for external loads [8]. Within Dymola, annual simulations are performed for the residential district with different retrofit years. The final thermal energy demand is weather adjusted with climatic factors of DWD [9], the amount of energy for domestic hot water is cleared out (64 liters per person and day with a temperature increase of 35 Kelvin [10]) and the boiler efficiency has been taken into account to generate a reference value for net thermal demand of space heating.

Results

Figure 4 shows the normalized thermal energy demand of the city district for the different years of retrofiting (Ratio of simulated to measured space heating energy demand).

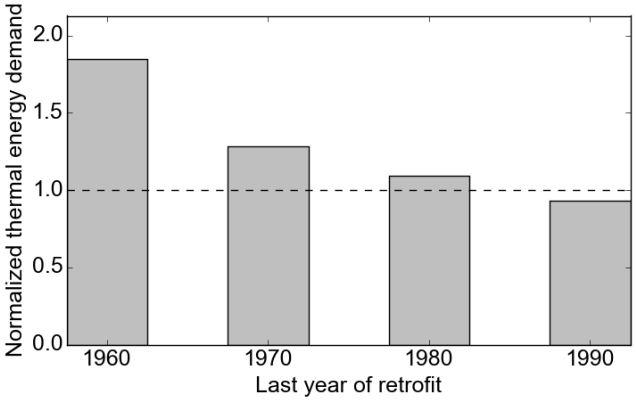

Figure 4: Normalized thermal energy demand of city district

The total thermal energy demand decreases regressively with higher years of retrofit, due to better building standards and shorter heating periodes. There is a good fit with an 'average' retrofit year between 1980 and 1990. Within the scope area a minority of buildings has been retrofited in 2003. Therefore, for all other buildings a reference model with mean building construction class G, respectively 1980 as last year of retrofit, is chosen (according to building class G of IWU [5]). Still, the analysis can only provide an orientation about the retrofit state. Further parameters, such as desired indoor temperature, air exchange rate or occupancy periodes, are uncertain. However, the city district DB structure and its TEASER interface enable a simplified modeling of multiple buildings and are, therefore, supportive for city district analysis.

CONCLUSION

This paper describes the development of a city information model (CIM) with focus on energy systems. It accounts for different building and energy system types. The CIM structure has been implemented on a PostgreSQL database. The relational database is

linked to the GIS tool QGIS, which combines entity location and semantic data. This enables graphical data analysis and modification. A Python tool, named TEASER, allows the automatized parametrization of building models. A database connection enables the export of necessary building data to TEASER. Within a case study, this interface is used to generate building models of a reference city district with different retrofit years. All models were simulated with Dymola/Modelica. Results show a good fit between measured thermal energy demand data and simulated thermal demand for retrofit year 1980. The usage of relational database concepts for city district data management and analysis is promising, especially in combination with GIS, which enables visualization and modification of city objects and their attributes. Though, the developed CIM scheme is not meant to be universal. Its primary goal is the simplified data handling of complex city districts. Therefore, it might not account for every possible application. Standardization on city district level will play a larger role for future applications. However, experiences show that the current CIM structure has been sufficient for the analysis of mixed city districts as well as the generation of building models for dynamic simulations.

ACKNOWLEDGEMENTS

We gratefully acknowledge the financial support for this project by BMWi (German Federal Ministry for Economic Affairs and Energy) under promotional reference 03ET1138D.

REFERENCES

1. United Nations. Cities and Climate Change: Global Report on Human Settlements 2011, 2011.
2. Fraunhofer Institut für System- und Innovationsforschung ISI. Energieverbrauch des Sektors Gewerbe, Handel, Dienstleistungen (GHD) in Deutschland für die Jahre 2007 bis 2010, 2013.
3. PostGIS. PostGIS — Spatial and Geographic Objects for PostgreSQL, 2015.
4. Hillebrand, G., Arends, G., Streblow, R., Madlener, R., and Mueller, D.: Development and design of a retrofit matrix for office buildings. *Energy and Buildings*, 70:516–522, 2014.
5. Institut für Wohnen und Umwelt - IWU. Deutsche Gebäudetypologie: Beispielhafte Maßnahmen zur Verbesserung der Energieeffizienz von typischen Wohngebäuden, 2011.
6. RWTH-Aachen University, E.ON Energy Research Center, Institute for Energy Efficient Buildings and Indoor Climate. Modelica AixLib, 2014.
7. Richardson, I., Thomson, M., and Infield, D.: A high-resolution domestic building occupancy model for energy demand simulations. *Energy and Buildings*, 40(8):1560–1566, 2008.
8. Deutscher Wetterdienst. Testreferenzjahre, 2015.
9. Deutscher Wetterdienst. Klimafaktoren (KF) für Energieverbrauchsausweise, 2013.
10. Knight, I., Kreutzer, N., and Manning, M. European and Canadian non-HVAC electric and DHW load profiles for use in simulating the performance of residential cogeneration systems, 2007.

ENERGY EFFICIENCY OF RAILWAY VEHICLES

Nadège Vetterli[1]; Prof. U.P. Menti[1]; F. Sidler[1]; E. Thaler[1]; Prof. G. Zweifel[1]

1: Zentrum für Integrale Gebäudetechnik (ZIG), Technikumstrasse 21 CH-6048 Horw.

ABSTRACT

The railway vehicles in Switzerland consume, in addition to the traction energy, a high share of electricity for comfort purposes. About 20% to 40% of the electricity consumed by the vehicles is used for **h**eating, **v**entilation and **a**ir-**c**onditioning (HVAC). The goal of this project was to optimise the HVAC system of the vehicle EWII of the Swiss Rhaetian Railway (RhB) to reduce overall energy consumption without any detrimental impact on passenger comfort.

The project was originally initiated by the Physics Department of the University of Basel with financial support from the Federal Office of Energy and the Federal Office of Transport. Over the last three years, six vehicles of four different railway companies were monitored by the University of Basel. The Center for Integral Building Technology of the Lucerne University of Applied Sciences and Arts (HSLU) has built up models of the rail vehicles in a simulation program and carried out additional measurements (heating-up experiments, air tightness measurements and thermographic imagery) in order to assess their energy demand and to calibrate the model. Once the models were calibrated, the optimisation measures for the HVAC system and the vehicle hardware of the EWII could be defined and calculated.

By means of simulations, the highest heat losses in the vehicles could be identified. Two substantial reasons for the high energy demand in rail vehicles turned out to be the poor insulation of the wagon envelope and the lack of heat recovery in the ventilation system. Both are challenging to improve due to on-board space requirements for additional systems as well as the high expenses. The most feasible measures identified to reduce the energy demand were the reduction of the outdoor air flow rate by means of CO_2 control or the temperature setback at night and during high occupation periods. Measures of this type are considerably easier to implement and, result in important energy savings, especially the CO_2 control when no heat recovery is installed in the ventilation unit.

Simulation results have shown a saving potential for heating demand as important as 40% for railway vehicles in case of the combined implementation of the measures, control of the air flow rate as a function of the CO_2 concentration, the reduction of the wagon temperature set point by 2K and the night setback of the vestibules. For the whole EWII fleet of the RhB this would represent a possible energy saving potential of about 840 MWh/a.

Keywords: railway vehicles, energy efficiency, heating demand of HVAC systems, CO_2-control, measurements, simulations.

INTRODUCTION

The passenger railway vehicles in Switzerland consume, in addition to the traction energy, a high share of electricity for comfort purposes. Relevant factors influencing this share are the thermal properties of the housing, the implemented controls and the operational parameters such as the distance of travel and the immobilisation time. Three years ago, a research project was initiated by the Physics Department of the University of Basel with the objective of improving the energy efficiency of HVAC systems in public transports. Several vehicles of

different railway companies were examined and a monitoring system was developed and placed in the train to measure temperature, heating and cooling energy, position (GPS) and meteorological data. The main objective was to define and quantify measures to reduce energy consumption of the HVAC without compromising the comfort quality for the passengers.

METHOD

The Center for Integral Building Technology of the Lucerne University of Applied Sciences and Arts (HSLU) has built up models of the rail vehicles in a simulation program. The following additional measurements were carried out in order to assess their energy demand and calibrate the models: heating-up experiments, air tightness measurements and thermographic imagery.

Heating-up experiment

The scope of the heating-up experiment was to define the active thermal mass and the heat coefficient of the vehicle housing. The vehicle was put in a railway depot with a constant ambient temperature and the inside heated up to about 40°C . The cool down behaviour of the vehicle was then analysed in order to extract the necessary information. Measurements of the heating-up experiment were used to correct the parameters such as thermal bridges or coefficients in the simulation model and calibrate the model up to the point of matching simulations results with data of the heating-up experiment.

Tracer gas measurements

Previous experiments had shown that the outdoor air flow rate of the ventilation system has a high impact on the accuracy of the simulation models of the vehicles. In order to assess precisely this variable, tracer gas measurements were performed. Basically, a room in the vehicle was filled up with a tracer gas, i.e. SF_6 until saturation was reached. The decay of concentration was then observed, when ventilation system was turned off. The decay is caused by either wall infiltration or by the supply of outside air through the ventilation system. Knowing the volume of the wagon and the gas concentration decay, the outdoor air flow rate can be calculated.

Internal heat gains

All internal heat sources need to be known as a function of time. In the case of railway vehicles, the gains from lighting and from people need to be considered. Heat flow of electronic devices used by the passengers can be neglected. Lighting in the wagons is always switched on during operation and was assumed to be constant. Passenger occupancy strongly varies during the day and was not available as measured values for the whole time. For this reason, the occupancy was calculated by means of the measured CO_2 concentration in the wagon and the outdoor supply flow rate of the ventilation. This consideration improved the accuracy of the simulation model a lot against the assumption of a constant number of people over the operation period.

Simulation models

The vehicles were modelled and simulated in the software program IDA ICE. This software originates from the building sector and is widely used in research and engineering applications. The input data to the model consist in the geometrical and physical properties of the wagon, (especially the housing), the HVAC equipment including its control, the internal heat gains and the outside climate (temperature, solar irradiation and wind). The final model

was calibrated with the help of the long term measurements by the University of Basel in combination with the stationary heating-up and tracer gas measurements and passenger countings. Once the models were calibrated, the optimisation measures for the HVAC units and the vehicle hardware could be defined and the highest energy saving potential in the vehicles could be identified.

Definition of Measures

In a first step, the energy flow diagram was generated. Ideas on how to optimise the wagon envelope and the operation of the HVAC system were gathered and evaluated in collaboration with the railway companies (Figure 1). The analysed measures were assigned to three categories: envelope, HVAC and operation. The measures were examined according to their energy saving potential and to the expenditure needed to implement the measures on an existing vehicle. The measures were classified into three levels, low, medium and high according to their expenditure. The lowest expenditure represents measures with small adjustments such as control and regulation of the HVAC systems. These measures can rapidly be implemented and are cost-efficient. Measures with medium expenditure affect additional or different HVAC components. The third category with the highest expenditure concerns the improvement of the opaque and transparent parts of the envelope.

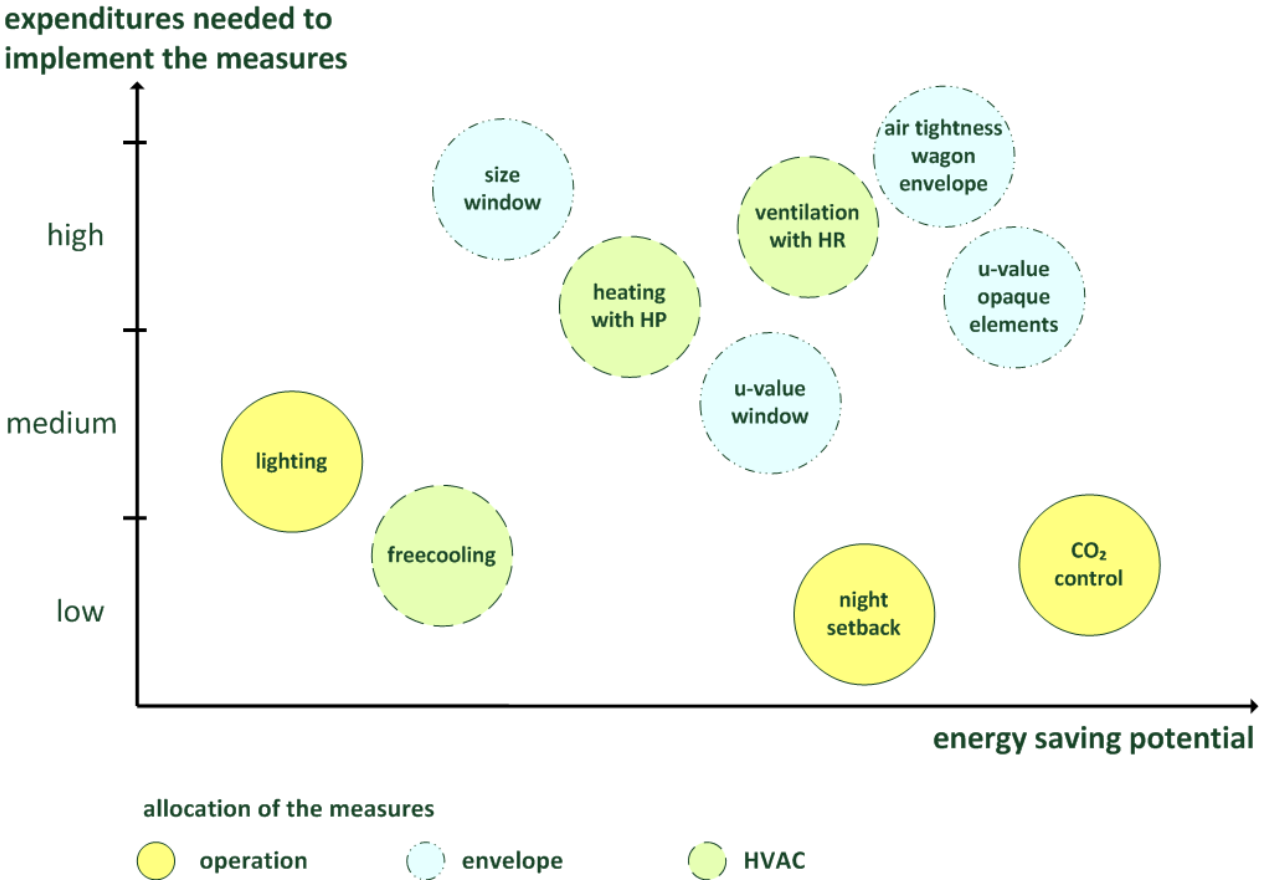

Figure 1: Qualitative cost-benefit assessment for the different measures (the assessment was performed by railway experts).

In a second step, defined measures were tested on the model of a specific wagon, the EWII of the Swiss Rhaetian Railway (RhB), and their energy saving potential was assessed.

RESULTS

Energy flow diagram

The energy flow diagram in Figure 2 shows the energy balance of the EWII of the Swiss Rhaetian Railway (RhB) on the base of the climatic data of the year 2011, i.e. the total heat gains (on the left) and heat losses (on the right) of the wagon for comfort purposes without considering the traction energy. “Solar” stands for solar heat gains through windows, “Light” the heat gains from lighting and “People” for heat gains from the passengers. The passenger room is conditioned by heating of the ventilation supply air, whereas the vestibules at the entrances are heated by radiators. The radiators have a three-stage manual control without temperature sensor. For this reason, the effective heat input of the radiators lead to a high uncertainty in the simulations.

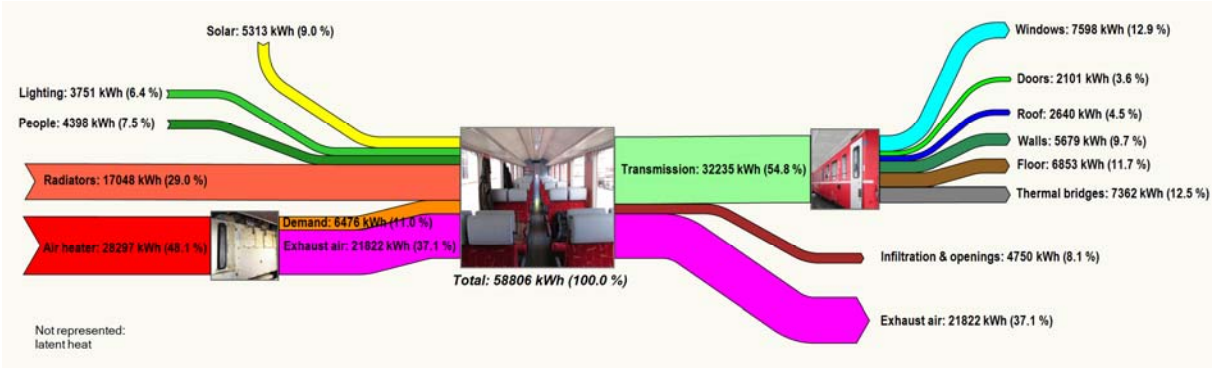

Figure 2: Energy flow diagram of the EW II (RhB) based on the simulations.

The results show that 55% of the heat losses are going through the envelope of the wagon (transmission losses) and 37% through the exhaust air of the ventilation system. Infiltration (incl. door openings) are responsible for 8% of the total heat losses. This shows that two substantial reasons for the high energy demand are the poor insulation of the wagon itself and the high outdoor air flow rate with a lacking heat recovery of the ventilation system. Not represented in figure 2 is the energy saving potential due to the reduction of the internal temperature set point and to the reduced operation times, inducing a proportional reduction of the energy flows.

Possible measures with their energy saving potential

A total of seven different measures were simulated for the EW II and the energy saving potential of each measure is shown in Figure 3. The five options represented on the left side are single measures (not cumulated), whereas the two options on the right side are a combination of left hand measures. Since the heat gains from lightning, people and solar irradiation are identical in all options, only the heat demand of the radiators and air heaters are represented.

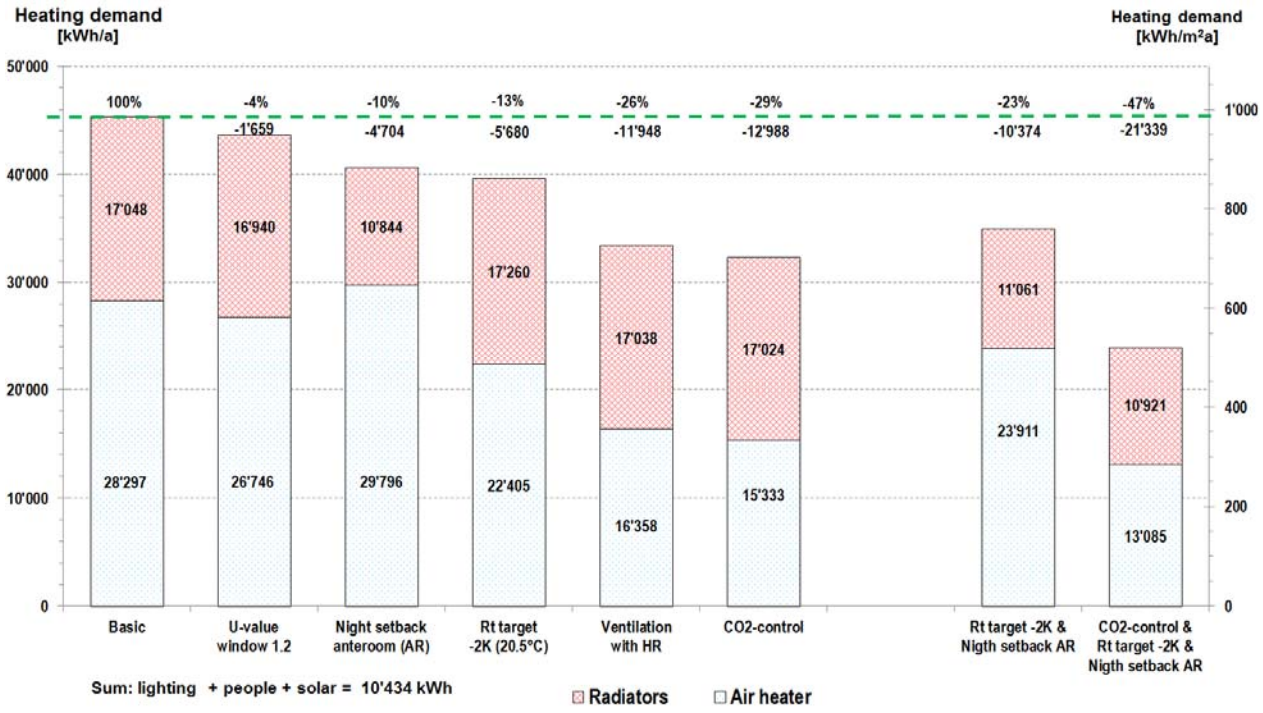

Figure 3: Heating demand of the EW II (RhB) after implementing different measures. The five options represented on the left side are single measures (not cumulated), whereas the two options on the right side are combined measures.

In the basic case, the U-value of the windows equals 3.1 W/m^{2}K. In the first option, this was reduced to 1.2 W/m^{2}K. This measure results in a 4% reduction of the heating demand.

In the second option, the air temperature of the two vestibules is reduced the same way (night set back) as in the passenger room. An anti-freeze protection to a set point of 6°C is assumed. This measure saves up to 10% of the heating demand.

The reduction of the indoor air temperature in the wagon from 22.5°C to 20.5°C (option 3) reduces the heating demand by 13%.

Another possibility to diminish heating demand is to implement a heat recovery (HR) in the ventilation system. The antifreeze protection for the HR was considered by limiting the exhaust air temperature to 1°C. The installation of a heat recovery system would allow 11’948 kWh or 26% of the heating demand to be saved.

The demand control of the outdoor air flow rate as a function of the CO_2 concentration (option 5) has shown even a slightly higher potential than the HR system. The set point has been set to a maximum of 1’000 ppm CO_2 concentration. This way, the heating demand can be reduced by around 29%.

The heating demand can be reduced further if more than one measure is implemented. The combination of the reduction of the wagon temperature by 2 K (option 2) and the night setback of the vestibules (option 3) can reduce heating demand by 23%.

If these two measures are combined with the CO_2 control of the air flow rate (option 5), the heating demand can be reduced by 47%, which corresponds to a saving potential of 21’000 kWh per year.

DISCUSSION

By means of a heating-up experiment and tracer gas measurements, a simulation model that reproduces the thermal mass, the heat losses through the envelope and the HVAC system of trains could be built up and validated. The heat demand of the specific railway vehicle (EWII of the RhB) could be represented and several improvement measures could be simulated.

The results have shown that the single measure which reduces the most the heating demand (-29%) is the demand control of the outdoor air flow rate as a function of the CO_2 concentration. This can be implemented at relative low expenses by integrating CO_2 sensors and a fan speed control in the ventilation system. The installation of a heat recovery in the ventilation system has fairly the same reduction potential as the CO_2 control, but leads to much higher expenses, since it requires the installation of additional components, which is difficult on existing wagons due to shortage of space. The improvement of the envelope insulation was not further analysed since this measure is only feasible in a total revision of the wagon. This measure is costly and requires space inside the wagon, which is hardly available.

By the simulations it could be shown that the simultaneous implementation of three relative easy and cost-effective measures in the wagon (the CO_2 control of the air flow rate, the reduction of the wagon temperature by 2K and the night setback in the vestibules), can reduce the heating energy demand by more than 40%. The implementation of these measures to all 40 EWII wagons of the RhB in operation would reduce their annual heating energy consumption by 840 MWh. The annual electricity consumption of the entire SBB passenger fleet is about 1’200 GWh [4]. Assuming that about 20% of this energy is used for the HVAC system, and 30% of it can be saved by the presented measures, about 70 GWh of electric energy could be saved annually for the SBB passenger fleet.

There are several other types of public transportation vehicles like buses, trams, air planes or ships, which presumably present a great energy saving potential for their comfort installations. These will also have great importance in future electric cars, since the heating and cooling demand highly affects the distance range of the vehicle. By means of thermal simulations, it is possible to calculate the energy demand of the comfort facilities of these transportation vehicles in detail and to assess different energy efficiency measures.

ACKNOWLEDGEMENT

This project is supported by swisselectric research, the Swiss Federal Office of Energy (SFOE), the Federal Office of Transport (FOT) as well as by personal contribution of the involved project partners.

REFERENCES

1. Sidler F. et al.: Energieeffiziente HLK-Technik bei Schienenfahrzeugen, brenet Status-Seminar Zürich, September 2014
2. Wellstein J.: Komfort in Zügen braucht Energie, energieRundschau, September 2012
3. Brunner U. C. et al.: Energiesparen bei Reisezugwagen, Messungen am erneuerten B 20-73 - Bericht 5, BFE, März 2000
4. Oral communication by Mr. Tuchschmied from SBB

Information and Communication Technologies

TOWARDS DATA-DRIVEN BUILDING RETROFIT

Mario Frei, Zoltán Nagy and Arno Schlueter

Architecture and Buildings Systems, Institute for Technology in Architecture, ETH Zürich, John-von-Neumann-Weg 9, CH-8093 Zürich

ABSTRACT

Due to the relatively low construction rate of new buildings in Europe, the energetic performance of the building stock can mainly be improved by retrofitting existing buildings. Current methods to derive and assess retrofit measures require either on-site inspection by an expert consultant and code based approaches, or numerical simulations using a building energy model that needs to be first developed. Since the former is rather inaccurate and prone to overestimating the retrofit measures (prebound effect), and the latter is time and cost intensive, in this work we propose a data-driven-retrofit (DDR) approach to derive optimal retrofit measures. The approach uses wireless sensor networks (WSN) for the determination of building characteristics, energy consumption and occupancy patterns. Building models in the broadest sense can be extracted from the collected data. Retrofit scenarios can be incorporated in these buildings models in order to estimate the future energy consumption of the building, and to choose the optimal measures. The approach is presented as a chain-like framework. The deployed WSN can remain installed to verify the retrofit execution, and to perform continuous long term monitoring for fault-detection and optimal performance of the installed building systems. This work extends our previous research in this area, and presents the DDR framework, and results from a case study on a listed building in Zurich, Switzerland.

Keywords: data-driven retrofit, in-situ measurement, system identification, building modelling, zero-emission retrofit

INTRODUCTION

Energy related carbon dioxide emissions in building account for 25% of the total global carbon dioxide emissions. Therefore, optimizing building performance offers a big leverage to face the challenges of climate change [1]. Due to the relatively low construction rate of new buildings in Europe, the performance of the building stock can mainly be improved by retrofitting existing buildings. Typically, to decide what measures to apply, first the current building performance has to be assessed. This is usually done by experts performing code-based calculations, e.g., the SIA 380/1 for heating demand in Switzerland. However, results from such code-based calculations may differ significantly from measurements, as the pre-retrofit performance of buildings tends to be underestimated (pre-bound), and the post-retrofit performance tends to be overestimated (rebound) [2]. This results in an overestimation of the effect of the retrofit measures. Another method to assess the performance of a building is by simulation. However, building simulations require a lot of effort to accurately reproduce the thermal behaviour of the building. Also, detailed information about the properties of an existing building is often difficult to obtain.

Therefore, in this work, we propose the data-driven retrofit (DDR) approach as a non-intrusive and cost-effective method to determine actual buildings parameters and energy performance. Based on this data, better assessment of the current state of the building can be

made, and more effective retrofit measures can be determined. Finally, the same techniques can be applied as a quality control measure, to validate the performance after retrofit.

The paper is structured as follows. In the next Section, we detail related research. Then, the proposed data-driven retrofit approach will be outlined in the "Methods" Section. In the "Results" section, we will show examples of a verification case study in terms of the DDR approach. Finally, we conclude the paper by discussing our results.

RELATED RESEARCH

In this Section, we briefly review current building performance assessment methods, building modelling approaches and data acquisition methods.

Typical procedures for the energy performance assessment of a building require on-site inspection by an expert. Recently, decision aid tools for retrofits have been proposed [5, 6]. The current deterioration of building elements is based on visual inspection and comparison. Based on the assessment cost and energy performance of a retrofit a refurbishment is assessed. A survey may include visual inspection of the building, gathering energy bills, occupant questionnaires, and individual measurements [7]. The end result is usually a heat loss coefficient (in W/K) or normalized energy consumption in a standard year. However, only the performance of the whole building can be assessed, and compared against each other. There is no insight on individual components of the building and their respective performance.

The energy consumption of future buildings can be estimated by performing a building energy simulation (BES). Usually BES is not available for existing buildings facing a retrofit. In this case the BES would need to be developed from scratch, which is cost and time intensive, prone to errors and requires validation with real data to be useful for retrofit predictions.

Papafragkou et al. presented a simple and inexpensive method for building performance assessment, without the need of on-site inspection [3]. A small USB-temperature logger is sent to the customer, who places is near the thermostat. Based on the measured data, the building in question can be qualitatively classified into four categories. However, no quantitative data is obtained, and the method is only applicable for specific cases, where the heating system has a night setback mechanism.

Thermal RC models for buildings have been used since the 1970s [8], and are often applied for model predictive control of building systems [9]. The verification, i.e. parameter fits, of such models is often based on the error of predicted temperature and not on comparisons of the physical entity represented by the RC-components. This does not ensure the physical meaningfulness of these models, and therefore sub-components of the models cannot be altered, such as needed for the prediction of retrofit measures. Other models, e.g., neural networks, ARMA models or statistical models are difficult to physically interpret as they may even completely ignore the internal physics of a building. This is acceptable for control tasks. However, it is virtually impossible to predict changes in building performance due to retrofit measures.

All these assessment methods have in common, that, because lack of data, they rely on a variety of assumptions. There are a lot of applications of building models, mainly in building control and energy performance estimation of planned buildings. Techniques from this fields applied to building retrofits are not satisfying, as they lack the possibility to appropriately reproduce the physical details of the thermal behaviour of a building, or they lack the possibility to project changes to the building.

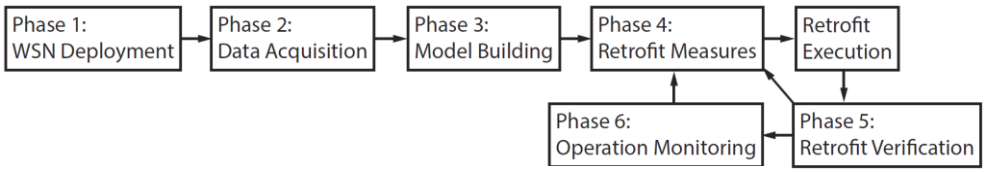

Figure 1: Data Driven Retrofit approach

METHOD

In this section we introduce the Data-Driven-Retrofit (DDR) approach shown in Figure 1. In brief, in phase 1 a wireless sensor network (WSN) is deployed as a necessary basis to gather data on the thermal behaviour of the building in phase 2. Then, in phase 3, the data is fused into a building model. This model can be used to derive and analyse retrofit measures in phase 4. After refurbishment, the effect of the implemented retrofit measures can be verified with another measurement period in phase 5, which can potentially be extended to a permanent operation monitoring in phase 6. In the following, we detail each of these phases:

Phase 1 is dedicated to improving the available data on the building by in-situ measurements. First, building plans can be completed by in-situ U-value, and energy consumption measurements, such as electricity, oil or gas. Energy consumption measurements yield high-resolution data, and also allows for an insight on energy usage patterns, and building dynamics. Secondly, a reference baseline for the temperature set points and comfort of the occupant can be established by measuring the room temperature, air humidity and outdoor temperature. Monitoring the outdoor conditions allows for normalization of the energy consumption using the actual local data rather than measurements from a potentially far away weather station. This normalization in turn allows for comparisons, especially before and after the retrofit.

The main key for success of DDR is a quickly deployable, modular, online wireless sensor network (WSN) for building performance assessment, which is not available up to this date. Quick deployment requires a full wireless operation for both energy supply of the WSN, as well as data transmission to a central server for further analysis. Modularity is needed because each building is individual, and the installed building systems and energy meters do not have a unified read port. In brief, the process of data gathering must be as fast as possible, saving both time and money.

Phase 2 incorporates, online data acquisition, i.e., the data is sent to a central server via the mobile network, which is key for a fast assessment. This centralized data acquisition allows to constantly monitor the quality of the data, and, thus, perform the measurements just as long as needed for the required data quality. This minimizes the duration of the measurement installation. Further, online monitoring allows for fault detection and correction. This is not possible with offline data loggers, which are typically used [2,3].

In phase 3, a building model is built. This model shall be able to incorporate the measured building characteristics and it should be able to incorporate retrofit measures, in order to predict the performance of the building after the retrofit. Most probably, simple RC models which reflect the physical properties well can be employed successfully, as we have shown in an earlier example [4]. In addition to the building, models for the behaviour of the occupant can be extracted from the data as well, which is important as occupancy patterns are significant for the energy consumption of a building [10]. Our approach is more time efficient than a traditional BEM simulation, and preserves the ability to determine the thermal behaviour of the building.

In phase 4, possible retrofit measures are incorporated into the previously established building model. This allows to analyse and choose the optimal combination of retrofit measures for the desired result. This phase is followed by the execution of the selected retrofit measures.

For the verification of the retrofit procedure, the WSN is deployed again in phase 5. This enables quality management of the newly installed measures. Re-measuring energy consumption indoor and outdoor conditions allows for consideration of multiple effects, such as possibly altered occupancy patterns, outdoor conditions and occupants behaviour. A data based verification allows for an objective confirmation that the performance goals of the building were reached or allows, if necessary, for further improvement.

In a potential phase 6, the verification can be extended to a continuous operation monitoring by simply leaving the WSN in place. This enables fault detection in operation, which ensures that the building systems operate as designed.

We note that the DDR process chain does need do to be applied completely from beginning to end. For example only phases 1 through 3 could be applied, improving the data quality. Then a traditional retrofit process could follow. Also, phase 5 could be applied on its own, verifying the result of a performed retrofit. The sensing hardware could further be used for single applications such as U-value measurement or energy-metering, without the surrounding framework. The versatility of the framework allows for an application tailored to the need and resources.

RESULTS

In this section we present results from a DDR for phases 1,2 and 5 focusing on retrofit verification. The employed WSN, shown in Figure 2, is a further development of our previous work [4], and is able to measure, temperatures, air humidity, heat-fluxes, electric pulses, solar radiation, luminosity and mains-current. The input for electric pulses was used to read out an oil flow meter of a heating system and an electricity meter. The main focus during the development of this version of the WSN was modularity and fast deployment. For robustness reasons, we choose to have wired power for each sensor node; data transmission between the nodes and to the central server was done wirelessly.

The WSN was installed in a listed building in Zürich. It is the same building as in [4]. The measurements performed with the current iteration of the WSN took place after the refurbishment, which consisted of replacing the windows and the application of insulating plaster. This case study is an example for a retrofit verification (phases 1,2 and 5). We measured the U-value of one office wall, air temperature and humidity of the same office, as well as oil consumption and electricity consumption of the building. It took about 45 minutes in average for each sensor node to install. The measurements started on October 16, 2014 and ended partially on the January 22, 2015.

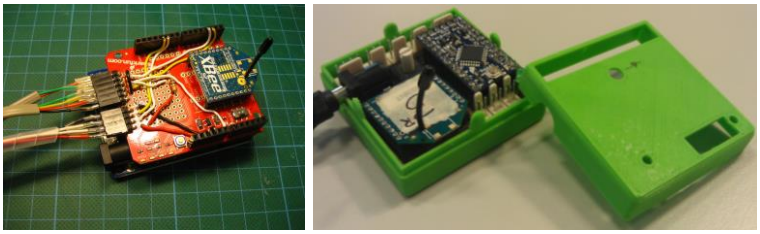

Figure 2: Wireless Sensor Node, left v1 [4], right: v2 (this work)

The heating energy demand was calculated for the building before as well as after the refurbishment, according to SIA 380/1. These calculations included estimations of U-values according to SIA 279.

As shown in Table 1, the measured U-value after the retrofit agrees well with the predicted value. Thus, we can conclude that the retrofit measure of the insulating plaster has been performed adequately.

Method	**U-Value (**W/m^2K**)**
Calculation pre-retrofit	1.43
Calculation (prediction) post-retrofit	0.71
Measurement post-retrofit	0.67

Table 1: Comparison U-Value Calculations vs Measurements

The heating system was monitored by an oil-meter, connected to the WSN. This allowed for a monitoring of the oil-consumption of the heating system, with high temporal resolution (5min data). Further, the supply temperature and return temperature of the heating system was monitored. Paired with the indoor and outdoor temperature measurements already taken with the U-value setup the following detailed analysis was performed.

We calculate the total thermal loss per heating degree day as 14.1 kWh/(K·d) for 2014 after the retrofit. This is an improvement compared to 16.8 kWh/(K·d) before the retrofit [4]. Next, as shown in Table 2, we find the annual energy consumption to be 172 MJ/m^2a, a clear improvement to the 204 MJ/m^2a from before the retrofit. While a clear improvement of the retrofit measures can be seen, it is also clear, that the code-based calculation overestimates the improvement effect of the retrofit by over a factor 2. This is a strong pre-bound effect and is mostly likely due to the fact that retrofit measures are financially incentivised for a predicted improvement rather than actual improvement.

Method	**Pre-Retrofit** (MJ/m^2a)	**Post-Retrofit** (MJ/m^2a)	**Improvement (%)**
SIA 380/1	408	251	38
Oil Consumption Measurement	204	172	16

Table 2: Overview Heating Demand Calculations and Measurements

Finally, Figure 3 shows the time series of air temperature and humidity of the monitored office after the refurbishment. The set-point room temperature after the retrofit is on average 23.01°C, in comparison of 22.89 °C during the same time a year earlier. Thus, we can not identify a rebound effect. However, the gathered data clearly shows that the air conditions in the room are always out of the comfort zone. While this may be typical for the heating season (especially the low humidity levels), it is also an indication that the retrofit did not yield any improvement for the comfort of the occupant.

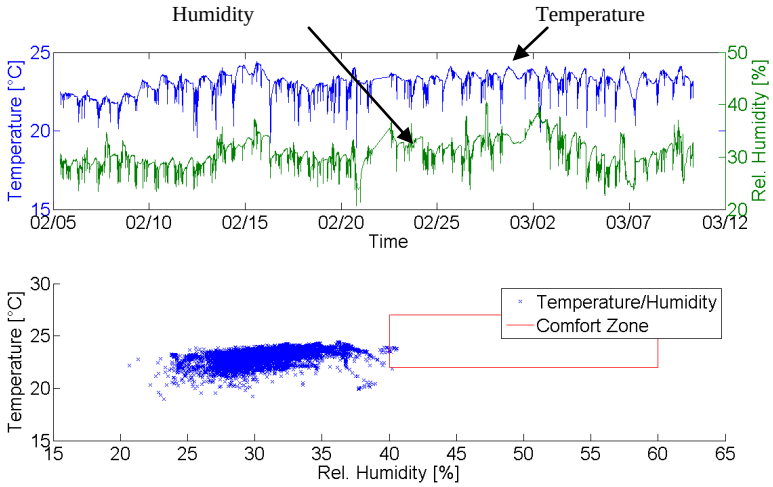

Figure 3: Comfort Measurement Data

Conclusion

We have presented an overall scheme for data driven retrofits (DDR), and we have shown practical application of a wireless sensor network. In our case study, the sensor network was deployed quickly, and delivered robust online monitoring. DDR can improve the current best practice of building performance determination by eliminating assumptions through measurements and parameter estimation, without the effort of elaborate building simulations. More entities can be measured for an elaborate data driven retrofit framework, which in combination yield a precise representation of the current thermal performance of a building. DDR is a powerful tool for a cost effective and efficient retrofit of the building stock.

REFERENCES

1. B. Metz, et. al, *Climate Change 2007: Mitigation of Climate Change : Contribution of Working Group III to the 4th Assess. Report of the IPCC.* Cambridge University Press, 2007
2. M. Sunikka-Blank and R. Galvin, "Introducing the prebound effect: the gap between performance and actual energy consumption," *Build. Res. Inf.*, 40(3), pp. 260–273, 2012
3. A. Papafragkou, et. al "A simple, scalable and low-cost method to generate thermal diagnostics of a domestic building," *Appl. Energy*, vol. 134, pp. 519 – 530, 2014
4. Z. Nagy, et. al, "Balancing envelope and heating system parameters for zero emissions retrofit using building sensor data," *Appl. Energy*, vol. 131, pp. 56 – 66, 2014
5. F. Flourentzou, J.-L. Genre, and C.-A. Roulet, "EPIQR-TOBUS: a new generation of refurbishment decision aid methods," in *Towards Sustainable Buildings 61*, Springer, 2001
6. T. Loga, N. Diefenbach, and B. Stein, *Typology approach for building stock energy assessment. Main results of the TABULA project*. Institut Wohnen und Umwelt GmbH, 2012
7. M. Santamouris, *Energy performance of residential buildings: a practical guide for energy rating and efficiency*. Taylor & Francis, 2010
8. R. Sonderegger, *Diagnostic tests determining the thermal response of a house*. 1977
9. D. Sturzenegger, D. Gyalistras, M. Morari, and R. S. Smith, "Semi-automated modular modeling of buildings for model predictive control," in *Proc. 4th ACM Workshop on Embedded Sensing Systems for Energy-Efficiency in Buildings*, 2012, pp. 99–106
10. C. Miller, Z. Nagy, and A. Schlueter, "Automated daily pattern filtering of measured building performance data," *Autom. Constr.*, vol. 49, pp. 1–17, 2015

ARCHITECTURE AND FIELD TEST OF A RESTFUL WEB SERVICE FOR THE OPTIMISATION OF SPACE HEATING IN A COMMERCIAL OFFICE

D. Lindelöf[1], H. Afshari[1], M. Alisafaee[1], J. Biswas[1], P. Borsò[1], X. Mocellin[1], J. Viaene[1]

[1]*Neurobat AG, Research and Development, Rue de Veyrot 9, 1217 Meyrin, Switzerland*

ABSTRACT

The optimal operation of many building services (including HVAC) requires computational resources that are not necessarily available in commercial building management systems (BMS). Having this computational power available in a dedicated data center will ease the deployment of these algorithms, but raises several issues having mostly to do with getting the data out of the BMS and back to it.

In this work we report on the architecture and field tests of Neurobat Online (NOL), a RESTful web service that implements the NEUROBAT heating control algorithm developed at EPFL. It has been controlling the space heating of a commercial building in Winterthur (Switzerland) for the second half of the 2014–2015 heating season. The original controller operated during the first half of the same heating season. By comparing the energy performance with and without NOL we derive estimates for the relative energy savings that such a system can achieve.

INTRODUCTION

In spite of the availability of advanced heating control systems, most commercial buildings in the developed world are still managed using the same principles as residential homes, e.g. by weather-compensated controllers. These controllers pump a heating fluid heated to a certain temperature whose setpoint is almost always a simple, monotonous function of the outdoor temperature. This scheme, while simple to setup and configure to ensure that the users are warm enough, tends to ignore the physics of the building and, more critically, makes no provision for the inclusion of any weather forecast.

However, more and more buildings are being equipped with building management systems (BMS) that can, through a graphical interface, be configured by the facility manager to obtain values for this flow temperature setpoint from other sources than the heating curve. In particular, it has become possible to provide this value to the BMS either directly over the internet or indirectly, through the building automation and control system used in that building.

Controlling the building services of a building over the internet appears to be a relatively unexplored topic in the academic literature. For example, [1] describes a set of web services for the "smart home", i.e. a central computer in the house connected to sensors, actuators and HVAC systems, and that exposes a set of web services to the public internet. Through these services, the users can monitor their energy consumption or set their preferred setpoints, while utility companies can facilitate demand response or sell excess energy back to the grid when it is economical to do so. The same system has been extended in [2] to improve the demand response aspect and the energy management algorithms.

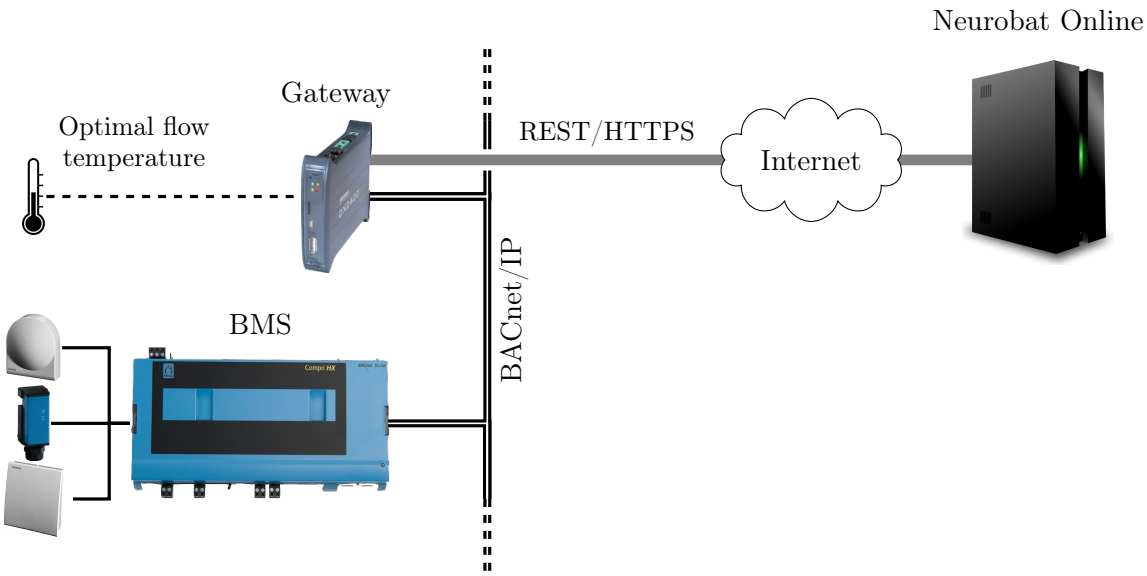

Figure 1: Schematic deployment of the Neurobat Online (NOL) system. The BMS is connected to sensors and actuators and makes them available on the local BACnet network. The NOL gateway is connected to the same network and exposes a so-called `AnalogValue` *BACnet object representing the computed optimal flow temperature. The gateway communicates via the public internet to the NOL server, posting the sensor values and getting the computed flow temperature back.*

Apart from these two examples, we were unable to find other examples of field tests of remotely controlled buildings.

The NEUROBAT technology, described in [3] and references therein, is an adaptive, model-predictive controller for optimising the space heating in buildings. We have extended this technology to handle the optimisation of space heating in commercial buildings, and implemented it as a REST[1] web service. We have installed this system on a commercial building in Winterthur owned (and occupied) by a major facility management firm. In this work we will detail the factors that justify the architectural choices we have made, describe the installation, and report on the results.

SYSTEM ARCHITECTURE

Several assumptions have guided our architectural choices in this project. First, we assume that the buiding is already equipped with the necessary sensors and actuators, and that a central BMS aggregates the data collected from the sensors. We also assume that the data from these sensors is published on a standard bus, BACnet/IP in this case. We assume that we can install a small device on that network, able to read the sensor values published on the bus and able to publish values for the optimal flow temperature back to the bus. This device is also connected to the public internet and serves as a gateway, translating between the local building bus system and a proprietary API that we have developed for this project. The setup is shown schematically in Fig. 1.

We believe that this setup achieves all of the non-functional requirements that can be asked by a customer:

[1] REpresentational State Transfer, a set of guidelines for designing web services.

Security: the communication from the gateway to NOL uses SSL, with HTTP Basic Authentication. This ensures that no eavesdropping is possible, and that two NOL customers cannot intercept each other's data.

Reliability: the gateway transmits sensor data at intervals that are shorter than theoretically necessary, to minimise the probability that any data should be lost due to connectivity issues.

Fault-tolerance: BACnet objects support a status flag that can indicate faults. By checking this flag, the BMS can fall back to its heating curve if a fault is reported.

Simplicity: no connection is initiated from NOL to the local system. All communication is initiated by the gateway over TCP/IP, port 443, which is usually open for arbitrary outgoing traffic in corporate firewalls.

Resiliency: the network connectivity, usually provided by the customer, is a single point of failure. NOL will therefore transmit to the gateway not only the optimal flow temperature for the next timestep, but for the next 6 hours. These values are cached by the gateway to be communicated to the building management system in case the NOL server should not be reachable. An alert is also generated notifying the operator that no message has been received from the installation.

In RESTful web services, every "interesting" piece of information exposed by a server (user accounts, pictures, blog posts, etc) is called a *resource* and is mapped to a URL. All the operations that the server can do are done by sending one of the standard HTTP verbs (`GET`, `POST`, etc) to a resource, possibly with a payload. REST recommends that the HTTP verbs follow several semantic conventions. For example, `GET` operations should return a representation of the resource (typically, a web page) and be safe and idempotent. `POST` is usually sent to a resource representing a collection of other resources, and appends a new element to that collection.

We have tried to follow that convention with NOL. Every NOL site is mapped to the `/sites/######` URL, where `######` is a unique identifier for that site during site creation. A new site can be created by `POST`ing to `/sites`. New sensor data can be `POST`ed to `/sites/######/sensors`. The optimal setpoint for the flow temperature is obtained by performing a `GET` request. We have found that strictly adhering to REST conventions results in a server API that is simpler, easier to document, and easier to test.

DEPLOYMENT

The left side of Fig. 2 shows the three-floor commercial office building in Winterthur where the system has been installed. The building is split in two heating zones. A heating schedule is in effect, applying typical office hours and reduced heating in the evening, nights, and the weekend.

The right side of Fig. 2 shows the rack where the existing BMS, a CompriHX system from Priva, has been installed. The gateway sits at the top of the rack, and is connected to the same LAN as the BMS. All sensors and actuators are available as BACnet objects, and the optimal flow temperature computed by NOL is published by the local gateway as two BACnet `AnalogValue` objects, one per zone. These objects are regularly read by the BMS, whose control algorithms adjust the mixing valves in order to keep the flow temperature as close as possible to these setpoints.

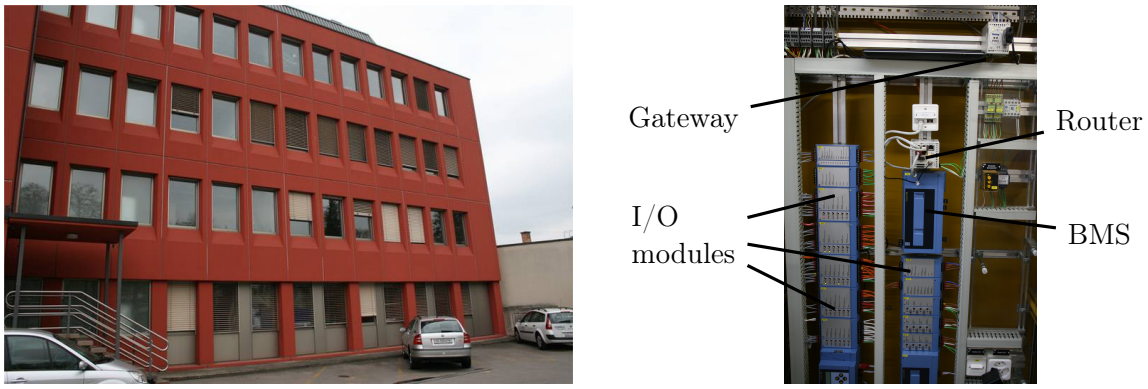

Figure 2: Left: the building in Winterthur. Right: the building management system (BMS), its I/O modules, the industrial router and the local gateway interfacing between the local bus and the NOL server.

The BMS operator can also revert to a standard heating-curve based system, using a setpoint for the flow temperature calculated from the outdoor temperature instead of the value provided by NOL.

The system ran with the standard heating-curve from 29 October 2014 to 8 February 2015, and with NOL since then.

RESULTS

In Fig. 3 we plot the indoor temperature, the outdoor temperature, the solar irradiance and the flow temperature.

For each day of the heating season, we compute the average outdoor temperature and the total space heating energy consumed by each of the two heating circuits. We also know which, of the reference or the NOL controller, was running on each day. Plotting the daily space heating against the average outdoor temperature for that day yields the so-called *energy signature* of the building, i. e. the extra heat required for each extra degree of cold. These signatures are shown in Fig. 4.

These plots show that the linear relationship between outdoor temperature and space heating energy holds very well with the reference controller, with about $16.4\,\mathrm{kWh.d^{-1}.K^{-1}}$ for zone 1 and $18.3\,\mathrm{kWh.d^{-1}.K^{-1}}$ for zone 2. The linear fit is not as good with the NOL controller, which is explained by the presence of days during which *no* heating was applied. These days correspond to weekends, during which the indoor temperature was allowed to naturally fall to the reduced temperature setpoint. The heating was then restarted at the time when doing so was the most energy-efficient.

The NOL controller is thus much better at handling night- and weekend-setback temperatures than the reference controller, which makes a direct comparison of their energy signatures impossible. The reference controller will merely shift its heating curve by a constant offset, while NOL will shut the heating completely off. In spite of this, the difference in slopes between both signatures allows a careful, conservative estimate of about 30–40% energy savings.

Finally we show in Fig. 5 the distribution of the indoor temperature during normal office hours for each zone and each controller. The reference line shows the normal indoor

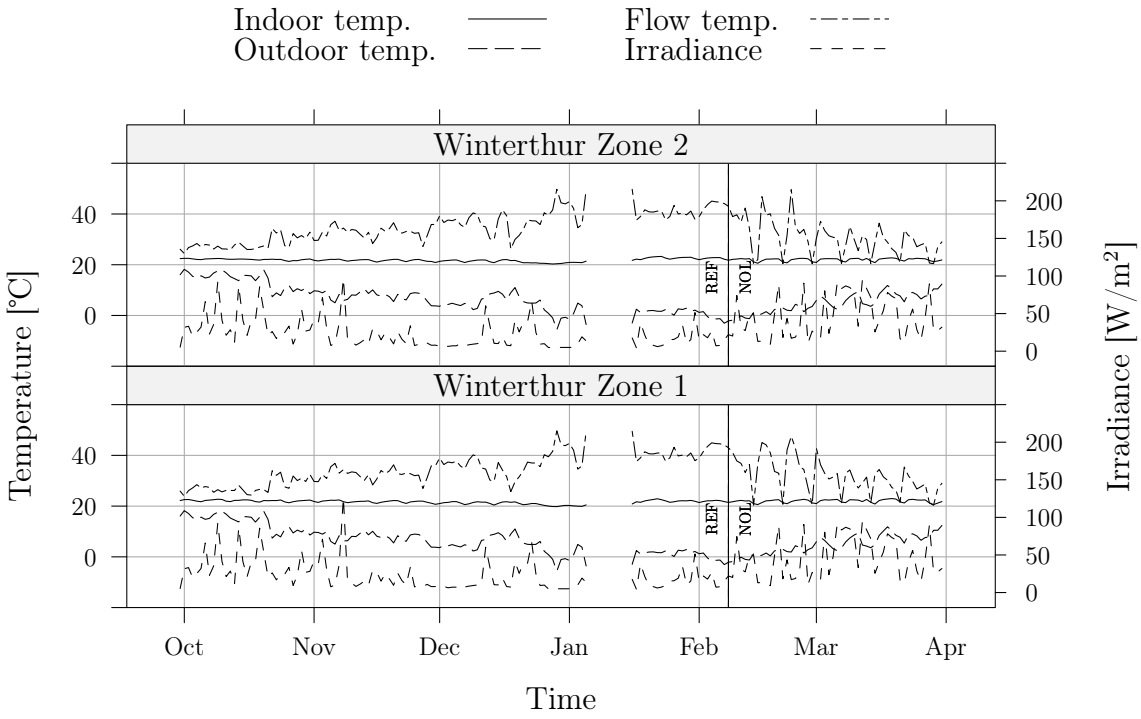

Figure 3: Daily averages of temperatures and solar irradiance measured on the Winterthur site. The vertical line indicates when the controller was switched from the reference controller to NOL. No updates to the BACnet objects were received by the BMS for a few days in January, hence the missing values. Notice the clear tendency by NOL to shut the heating off during weekends.

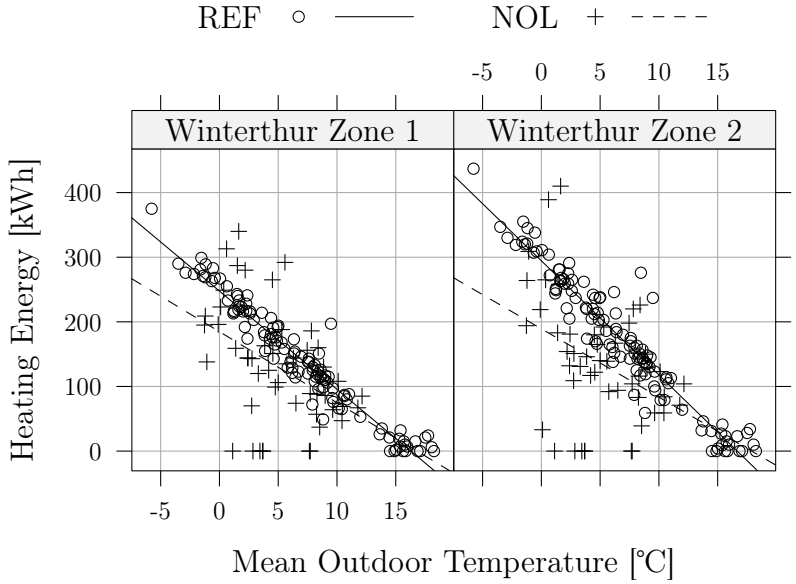

Figure 4: Daily space heating energy against average outdoor temperature. Each point represents one day of measurements. Different symbols are used for the reference controller and for the NOL controller. Each pane shows one of the two heating circuits. A linear regression line is added to each controller.

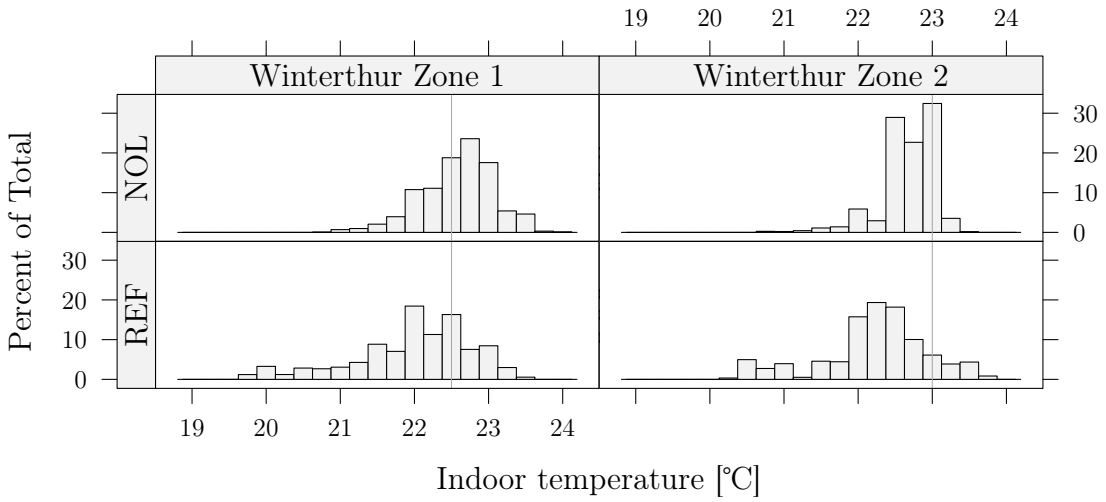

Figure 5: Indoor temperature distribution with both controllers and both heating circuits. These histograms include only samples taken during normal offices hours, and excludes the weekend. A reference line shows the temperature setpoint chosen by the user.

temperature setpoint chosen by the user. This plot shows that the energy savings achieved by the NOL controller have not compromised the indoor comfort, quite the contrary.

CONCLUSION

We have deployed and tested Neurobat Online (NOL), a RESTful web service for the optimisation of space heating in office buildings. We have described the principles that guided its architecture, described its deployment on a commercial building in Winterthur, and found energy savings of the order of 30–40%. These energy savings have not compromised the comfort of the occupants of the building; indeed, the comfort has been improved.

We believe that this demonstration has validated the principle of having a web service responsible for something as critical as the thermal comfort of office workers. We plan to pursue this project during the next heating season, by including other kinds of buildings and also by including building network protocols other than BACnet.

References

1. Khan, A. A. and Mouftah, H. T.: Web services for indoor energy management in a smart grid environment. *2011 IEEE 22nd International Symposium on Personal, Indoor and Mobile Radio Communications*, pages 1036–1040, 2011.

2. Khan, A. A. and Mouftah, H. T.: Energy optimization and energy management of home via web services in smart grid. In *2012 IEEE Electrical Power and Energy Conference*, pages 14–19, 2012.

3. Lindelöf, D., Afshari, H., Alisafaee, M., Biswas, J., Caban, M., Mocellin, X., and Viaene, J.: Field tests of an adaptive, model-predictive heating controller for residential buildings. *Energy and Buildings*, 99:292–302, 2015.

URBAN ENERGY WEB. A TRANSNATIONAL AND COMMON ENERGY CITY PLATFORM FOR SUSTAINABILITY IN THE BUILT ENVIRONMENT

Massimiliano Condotta[1]; Markus Biberacher[2]; Sabine Gadocha[2]; Andrea Mancuso[1]; Stefano Picchio[1]; Giovanni Borga[1].

1: University Iuav of Venice, Department of Design and Planning in Complex Environment. Santa Croce 191, Tolentini, 30135 Venezia, Italia.

2: Research Studios Austria Forschungsgesellschaft mbH – Studio iSPACE, Schillerstraße 25, 5020 Salzburg.

ABSTRACT

Knowledge on the energy related status of urban areas is an important basis for measures to improve sustainability and energy efficiency of the built environment. The "Urban Energy Web" project (UEb) developed an IT solution to share knowledge about energy consumption/energy behaviours of buildings and/or cities. The main output is the "UEb City Platform", a transnational web based platform to be used both as "Information Portal" and "Decision Support System". The platform was implemented and tested in two pilot areas: the city of Feltre, in the Veneto Region (Italy) and the region of Pinzgau Pongau, with a focus on the city of Zell Am See (Austria). The transnational level of the project and cooperation helped to compare policy disparities/differences. The application of the UEb methodology with different premises to the pilots triggered different results. In Feltre the UEb City Platform has been used for developing and integrating the Sustainable Energy Action Plan and to select some critic buildings to be included in a list of retrofitting intervention. In addition, the system triggered a network between experts, public administration and citizens. In Austria is used as an information portal for citizens, politicians and energy consultants. The platform includes indicators on refurbishment rates, average energy savings due to refurbishment, solar insolation on roofs, distances to district heating or gas infrastructure.

Keywords: Energy Saving, City Sensing, City Model, Decision Support System

INTRODUCTION

"Information transfer" and "improved competences" of urban actors are important factors to improve sustainability and energy efficiency of built environment. A wide and detailed "knowledge" of the places and their behaviour is a mandatory – but not sufficient - condition to start policies and initiatives aiming at the protection of the environment. Know-how and awareness of public administrators, building managers and citizens, is the complementary condition to create an enabling environment to make the "knowledge" effective. Moreover, if this information is shared on a common knowledge base it acquires more relevance and transnational cooperation helps to compare policy disparities/differences. This creates a transnational enabling and learning environment for improving the energy efficiency of cities. Against this background the "Urban Energy Web" (UEb) project, co-financed by the Interreg IV cooperation program was set up. The main goal of the UEb project was to create the "UEb City Platform", a transnational web based platform that serves simultaneously as information portal, decision support system and networking platform [1]. The focus is on a shared knowledge of the energetic performance, consumption and behaviour of buildings and cities integrated with information about physical aspects of the built environment.

IMPLEMENTATION METHOD OF THE UEB CITY PLATFORM

Technical implementation

The development of the platform was divided into two tasks. One was dedicated to the creation of the "knowledge", the other one to the implementation of the IT infrastructure to make the "knowledge sharing" possible. Information administrated and provided by the platform is in fact geo-referenced at regional level or at urban level. To support this feature, the platform is map-based: this means that all the information can be visualized and accessed browsing an online map that displays the different kind of data in any possible geographic location.

In Italy the platform has been implemented and tested (at urban level) for the city of Feltre, in Austria for the region of Pinzgau Pongau (at regional level), with a focus on the city of Zell Am See (at urban level). To adapt to the different needs, rules, cultural approaches and available data of the two countries, different information had to be visualized in the platform. For this reason, and also to create an "interoperable" platform, a design approach has been chosen that assures flexibility in the kind of data that need to be managed and displayed. The result is a system that can be adapted to the specific demands of territories/cities.

The platform therefore uses a schema of data implementation that relies on a common map server able to collect and harmonize different kinds of data coming from different sources. The development of the platform is based on *Geonode*, a geospatial CMS for the management and publication of geospatial data. The peculiarity of Geonode is to allow non-specialized users to share data and create interactive maps through a web interface. Geonode uses a Postgres/Postgis database as geospatial data store and *Geoserver* for retrieve and cache spatial information and provide "Open Geospatial Consortium" services.

Special attention was dedicated to the creation of specific styles of data visualization in order to make better interpretable numeric data. Each type of data uses a different visualization style to communicate the appropriate information. This is possible because Geoserver also provides specific functions that allow converting, recoding and interpolating attribute values directly into styling parameters such as color, width and opacity.

To visualize the data an interface that integrates interactive maps inside the CMS *Drupal* was developed. It is the interface that end users interact with and that visualizes the information. The interface uses different layers that can be selected by users via a widget that groups different data sets in three mains categories that can be customized for each specific city. The result is a friendly user interface oriented also to non-technical users.

Data and information structure inside the UEb City Platform

Regarding the "knowledge" organization, in the development of the web platform a general structure of three categories was chosen, whereby each category is customised to the requirements of the specific pilot region.

For the **pilot region of Feltre** (Italy) the three categories were chosen as *City Model*, *City Sensing* [1] and *Energy Model*.

For the category *City Model* two models were developed, based on the fusion of high-resolution aerial images, LIDAR images and terrestrial point clouds laser scanning. One model includes streets, trees and building facades, while the other shows the roofs of the buildings. By the integration of these two models the *City Model* is developed, which is the digital multilevel-knowledge model for the city of Feltre.

In the category *City Sensing* an analysis of existing datasets was carried out to derive information on the real energy consumption and energy losses of buildings, as well as the behaviour of residents and households. The data analysed include gas consumption, heating systems, energy certificates and inhabitants. Furthermore thermographic pictures of buildings were analysed to generate information on the heat losses of building envelopes.

For the category *Energy Model*, information based on the interconnection of the *City Sensing* and the *City Model* was elaborated. This information includes CO_2 emissions of buildings, PV-potential of roofs and the *FEU Index*. It is an index appositively developed to analyse the energy efficiency of a building in relation to the urban surroundings. It is an indicator called "*Firma Energetica Urbana Index*" (Urban Energy Signature Index). It calculates and represents the performance of each building considered as part of the city system. FEU is based on *n* correlated "*performance indicators*" that are related both at energetic characteristics of the building and users behaviours. The parameters that have been considered in this application are:

- **E**nergy consumption (gas, oil, wood, consumption for heating, hot water etc.);
- Energy **D**ispersion of facades (analysed by infrared survey at urban level);
- Users/**P**eoples behaviours (considering moreover energy consumption per person);
- **C**O_2 emissions (calculated on the basis of heating system used).

To each performance indicator a score is assigned that ranges from 1 (good energetic performance, good building) to 5 (bad building). The scale is configured on the basis of the average of all buildings of the city. Considering that these *performance indicators* are reciprocally correlated, the FEU has been conceived as a configurable index where each parameter weight can be increased or decreased to adapt to users needs and demands. The parameters can be adapted by assigning to each parameter variable (αe, αd, αc, αp) a value that range from 1 (to assign low weight to the specific parameter), 4, 6 (medium), 8, to 16 (to assign the maximum relevance to the parameter). The *FEU* formula is:
FEU Index = (E • αe + D • αd + P • αp + C • αc) / (αe + αd + αp + αc).

The platform gives the possibility to the users to customize in real time the Index by giving different weights to each indicator and getting immediate results from the platform (in Fig. 1 a customized configuration of the Index by moving the slider of each specific indicator). This functionality has been realized using a particular characteristic of Geoserver which allows displaying data through the definition of dynamic styles that use formulas processed through WMS requests containing the parameters entered by the user according to the *FEU* index.

For the **pilot region Pinzgau/Pongau** (Austria) the categories were defined as *Energy Coefficients, Energy Indicators* and *3D-City Model*.

For the category *Energy Coefficients* available energy certificates of the pilot region were analysed and coefficients on community level on energy sources for building heating, average heating demand, CO_2 emissions and average savings due to refurbishment were derived.

For the category *Energy Indicators,* indicators maps on building and raster cell level were developed for solar potentials, infrastructure and buildings. Infrastructure distances of buildings to available gas or district heating networks have been computed on a 50m raster cell basis. Regarding the solar potential, indicators on insolation on roofs as well as on whole parcels were elaborated. Roofs are classified in areas of "very good", "good" and "less good" solar insolation and the indicators give the available area of each class for every roof. Furthermore an indicator showing the average solar insolation in kWh/m^2 for different classes was developed. For parcels, the average solar insolation per m^2 was computed. For buildings indicators on the roof pitch and roof orientation have been developed and integrated in online maps. As input for the category *3D-City Model*, a model of selected parts of the pilot region

such as the city centre of Zell am See based on airborne laser scanning data on a 1m raster resolution and cadastre data on buildings was developed.

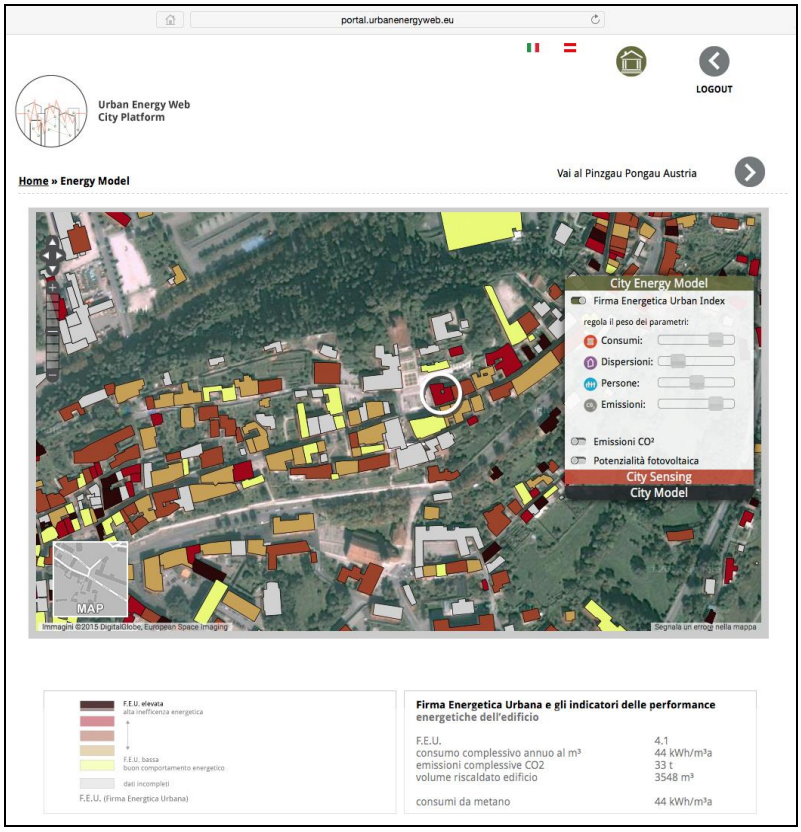

Figure 1: Screenshot of the UEb City Platform about the F.E.U. Index in Feltre.

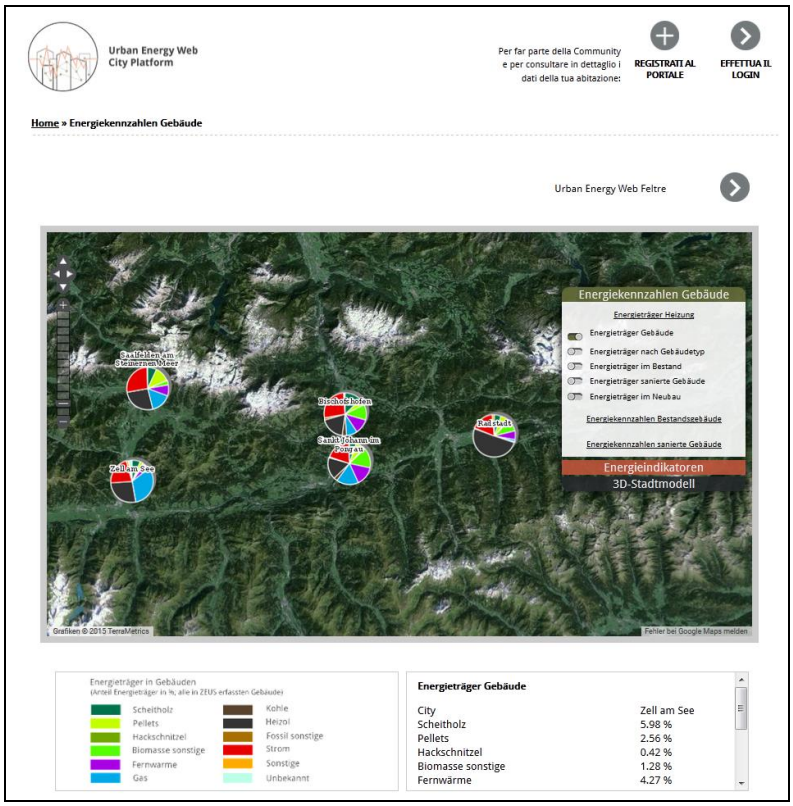

Figure 2: Indicators of share of energy sources for heating purposes in Pinzgau/Pongau.

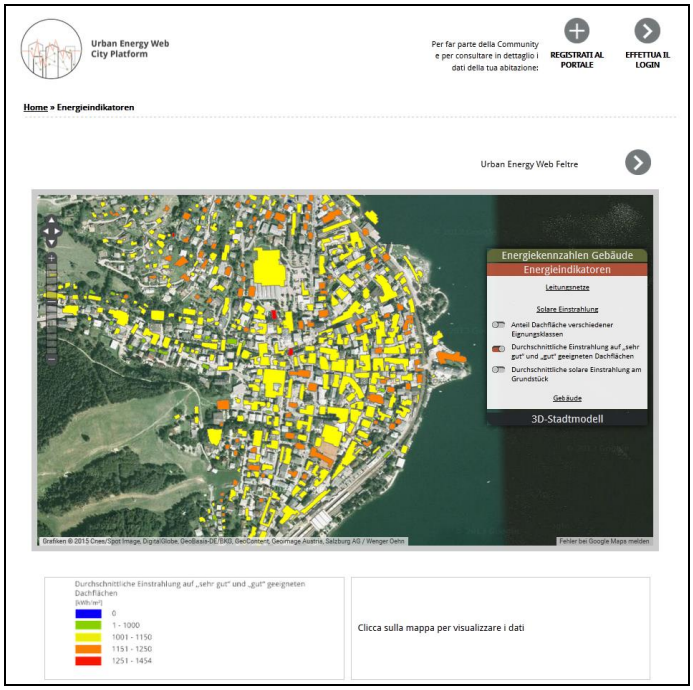

Figure 3: Indicators of solar insolation on roofs in Pinzgau/Pongau.

RESULTS AND OUTCOMES

The Urban Energy Web project reached two main results. The first one is the realization of the transnational UEb City Platform, the second one is the production of a relevant amount of information regarding energy behaviour of the cities and related buildings of the pilot areas. The project platform can be accessed via the project website (www.urbanenergyweb.eu) where the information on the two pilot areas can be obtained. This is the main output of the project that enables the exploitation of all the analysed data and produced information. The platform for Austria includes indicators on energy sources for heating purposes of buildings (Figure 2), refurbishment rates, average energy savings due to refurbishment, solar insolation on roofs (Figure 3), distances to district heating or gas infrastructure and roof pitch. For Feltre, information is given on real consumption of gas, oil or wooden, on CO_2 emissions, on population data, on photovoltaic potential of roofs and the FEU Index (Figure 1). In addition, for both pilot areas, the platform gives access to the 3D City models produced during project lifetime.

The application of the UEb methodology to the pilots, which means the possibility for end users to have access to the shared knowledge of the energetic performance, consumption and behaviour of buildings and cities integrated with information about physical aspects of the built environment, already generated some outcomes. In Feltre the City Platform has been used for developing and integrating the Sustainable Energy Action Plan and to select some critical buildings to be included in a list for retrofitting intervention. In addition, the system triggered a network between experts, public administration and citizens. In Austria the UEb City Platform is used to provide information for citizens, politicians and energy consultants.

DISCUSSION

The experience of the application of the UEb platform to a different context (from a political, geographical and social point view) made evident that is not possible to use exactly the same schema in each occasion. In fact available data and regulations are different and also specific objectives. A simple replication of any IT solution to support energy saving process is therefore not possible. Nevertheless, the overall goal to improve sustainability of the built environment is largely shared. For this reason the approach used in UEb to have a flexible IT structure that can be adapted at specific needs can have more success. The two pilots done in the UEb project demonstrated that it is possible. Moreover the common platform can work as a bridge reducing differences towards a more EU shared approach.

CONCLUSION

The Urban Energy Web City Platform was designed as a transnational web platform for information provision, decision support and networking activities between different actors in the field of energy and energy efficiency. The platform administrates and disseminates information on energy and energy efficiency elaborated during the project and provides it to the different user groups. As the available data, derived indicators and legal regulations are different in the pilot areas, the platform architecture is set up in a flexible way so it can be adapted to the specific needs of the pilot areas. The Urban Energy Web City Platform offers therefore the possibility to share knowledge and experiences on transnational level. Thereby it serves as a basis for the future enhanced use of renewable energy and the increase of energy efficiency in cities and can be considered as a potential tool to tackling non-technological obstacles existing inside EU (such as legislation barriers and know how disparities) towards a more concrete application of already existing energy saving technologies to renovate built environment.

REFERENCES

1. Condotta, M., Onorato, R., Gruber, P., Gadocha, S., Zatta, E., Borga, G., Mancuso, A., Biberacher, M., Picchio, S., Bonan, V. *Urban Energy Web. Conoscenza condivisa per il contenimento dei consumi energetici e sviluppo di energie rinnovabili a scala urbana*. Eds. Condotta, M. Belluno, 2015, Tipografia Tiziano Publisher. ISBN 978-88-900188-8-6
2. Condotta, M., Borga, G. "'Sensing' the city model to improve effectiveness of digital resources." *Territorio Italia. Governo del Territorio, Catasto, Mercato immobiliare. Periodico d'Informazione tecnico-scientifica.* Anno XII no. 2 (2012): 85-93. Published by: Agenzia delle Entrate, Roma, 2013. ISSN 2240-7707

URBAN ACCEPTABILITY OF SOLAR INSTALLATIONS: LESO-QSV GRID, A SOFTWARE TOOL TO SUPPORT MUNICIPALITIES

P. Florio[1]; C. Roecker[1]; M. C. Munari Probst[1].

[1]*LESO-PB, Laboratoire d'Énergie Solaire et Physique du Bâtiment, École Polytechnique Fédérale de Lausanne (EPFL), Station 18, CH-1015 Lausanne, Switzerland*

ABSTRACT

The "LESO-QSV Acceptability" tool is a decision-supporting aid for municipalities in charge of approving new active solar installations. It does not bar any urban zone from being targeted, but requires architectural integration quality, as a function of the "criticity" of the intervention area, i.e. the architectural sensitivity of the local urban zone, combined with the visibility of the proposed solar plant on the building.

This tool includes several elements: the software "LESO-QSV GRID", a detailed description of the approach, documentation on active solar integration in architecture, and finally, an application form for new installations.

The LESO-QSV GRID program fulfils three complementary functions:

- Support municipalities to set their specific levels of required quality for the different "situations" (zones and visibility) of their territory – in practice selecting a grid (GRID).
- Educate architects, installers and building owners through a very large palette of evaluated solar integration examples (positive and negative), that can be filtered according to different criteria (context specificities, solar technology, system size, integration approach …) ,.
- Help municipalities to explain in an interactive and visually convincing way how the method works and justify potential rejections to users

The main purpose of the software tool is to simulate the effect of different severity policies (from lenient to strict) on the existing examples (more than 90 cases). These simulations allow to check in real-time which installations would be approved or rejected and to choose the most suitable severity degree for the municipality.

A difficulty in the application of this approach lays in the "objective" evaluation of the architectural integration quality of a solar plant. LESO-QSV constitutes a simplified method based on objective criteria, which have been synthetized in three questions. All examples in the software database include the answers given by experts to these three questions, allowing the user, in association with the documentation accompanying the method, to understand how to use these criteria.

Additionally, the examples of the database itself provide an important inspiration source to help realize successful architectural integrations in different configurations.

Keywords: architectural integration, BIPV, solar refurbishment, solar planning, criticity

1. INTRODUCTION

The recast of the Energy Performance of Buildings Directive – EPBD [1] pushes towards the implementation of the "nearly zero energy building" concept by stating that by 2020 "the nearly zero or very low amount of energy required should be covered to a very significant

extent by energy from renewable sources, including energy from renewable sources produced on-site or nearby".

Solar energy is a key factor to meet these targets, and new technologies such as BIPV (Building Integrated Photovoltaics) and BIST (Building Integrated Solar Thermal) allow a good exploitation of solar potential in a densely built environment [2]. When cities undertake massive solar refurbishment though, the urgency of the production goals should not exempt them from trying to keep the quality of their urban, landscape and cultural environments as high as possible. The responsibility of preserving this quality within a solar expansion scenario is

- with public authorities, who need to adopt a wise incentive policy to exploit the potential of the territory;
- with solar panels manufacturers, who need to improve the market offer in terms of products for architectural integration;
- with architects and engineers, who need to deal with the energy related constraints and aesthetic impact.

Solar panels should not be considered just as pure technical components for energy production but also as architectural elements.

The LESO-QSV method [3], [4] has been developed to assist authorities on decisional, educational and urban planning aspects of solar integration. This paper focuses on the specific software tool (LESO-QSV GRID), designed to meet the first two goals in a practical way.

2. "LESO-QSV ACCEPTABILITY" TOOL

The "LESO-QSV Acceptability" tool is a decision-supporting aid for municipalities in charge of approving/denying new active solar installations. To help maximizing solar use in cities, it does not bar any urban zone from being treated, but helps users set requirement levels of architectural integration quality. The quality that is requested for a new solar plant depends on the "criticity" of the intervention area, i.e. the socio-cultural value of the local urban zone (its sensitivity), combined with the visibility of the proposed solar plant on the building.

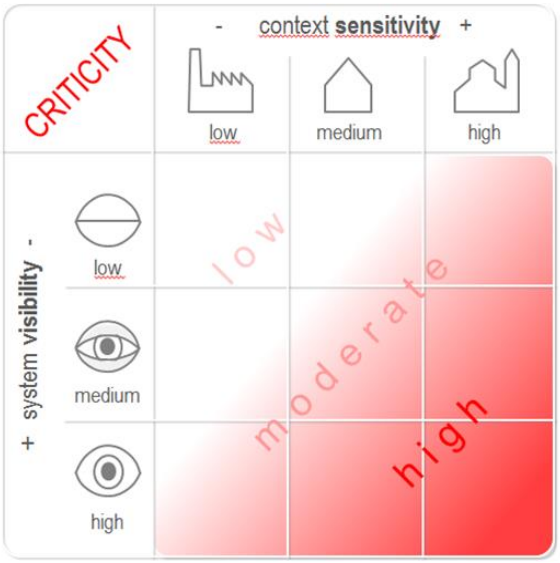

Figure 1: Criticity grid: 9 "situations" defined from 3 sensitivity by 3 visibility levels [4]

In the present method, both the architectural sensitivity of a zone and the visibility of the plant can assume 3 discrete values, high, medium or low. The combination of sensitivity and visibility values results in a 9 cells matrix, representing different "criticity" levels (*Figure 1*).

The authorities can select the minimum level of integration quality expected for each "situational cell" this process implying a way to assess this quality.

In this method, the quality of integration is evaluated through a simplified procedure, based on existing literature [5]. The coherence of the following 3 installation characteristics are judged in relation with the hosting building architecture: the shape and size of the field, the colour and texture of the materials and the modules details (size, jointing, connections). The resulting evaluation is graphically synthesized in a disk, composed of 3 sectors, whose colour depends on the coherence of the associated characteristic: green for high, yellow for medium and red for weak coherence (*Figure 2*).

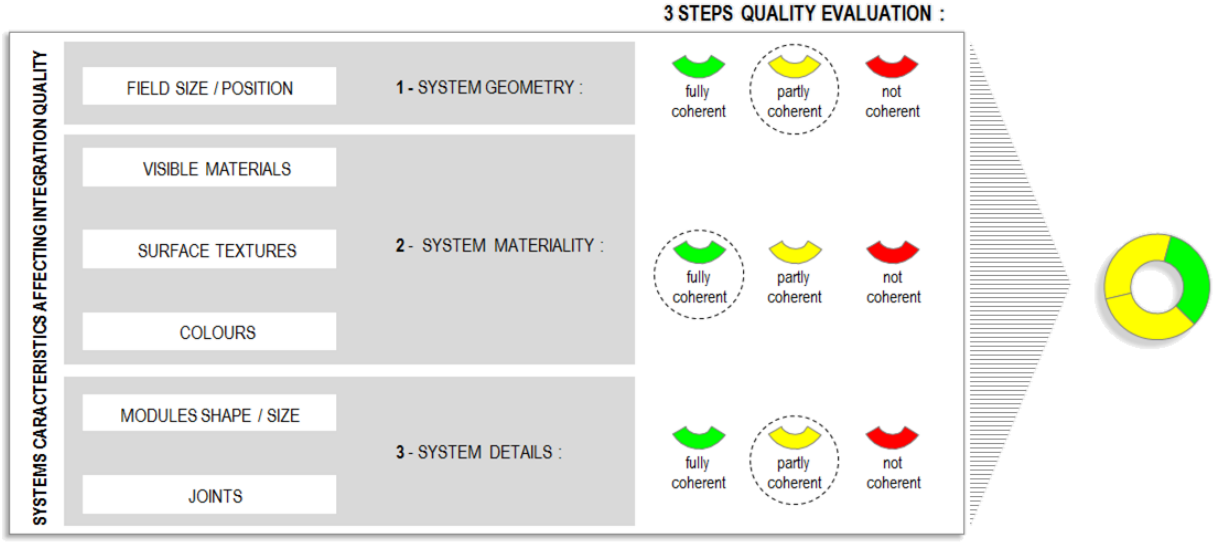

Figure 2 : "Quality disk" resulting from coherence evaluations of 3 global criteria [4]

Using this colour code, the authorities can define the level of quality they require for each "situation". The LESO-QSV GRID tool described hereafter is designed to assist them in this process with immediate feedback as to the effects of their choices over a collection of examples.

3. LESO-QSV GRID TOOL

The LESO-QSV GRID software tool, as stated above, has been conceived to fulfil complementary functions. The first function is to act as a decisional support tool, to help the municipalities set the levels of required quality for the different configurations of "criticity" (visibility + sensitivity) on their territory, selecting acceptability thresholds for every "situation". The second function is to serve as an educational tool by presenting several integration examples, with their positive or negative quality evaluations, in different urban contexts. These examples are provided as references for the process of quality evaluation, through appreciations given by experts, and as inspiration for architects and professionals of the solar industry.

The main window (

Figure 3) shows the acceptability grid (top right), the examples viewport (center), the detail panel (bottom right) and the selection filters (bottom left).

The software tool is in its last stages of development. A first French release is foreseen in 2015 and pilot collaborations with voluntary municipalities and local communities will be initiated in the French-speaking part of Switzerland. The functionalities and components of the tool are described in detail below.

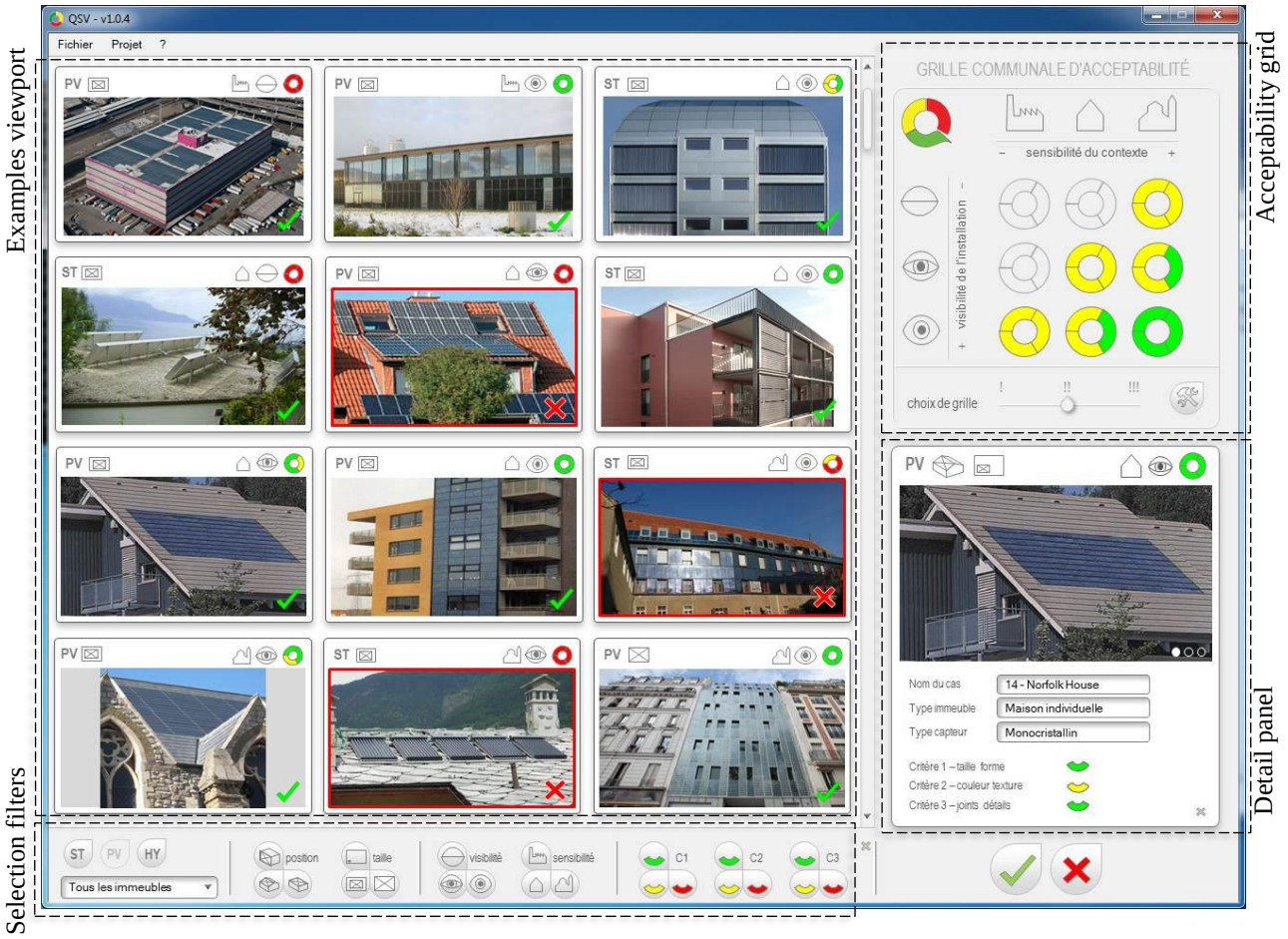

Figure 3: screenshot of the software tool LESO-QSV GRID, main window.

3.1 The acceptability grid: concept, principles and functioning

The core of the tool is the acceptability grid (*Figure 4*), which allows the users to set, for every "situation", the minimum required quality to accept a proposed installation. This grid should be defined at the municipality level by a person or group of persons entitled to manage the assigned territory and its architectural assets (municipal architects, urban planners, architectural commission…).

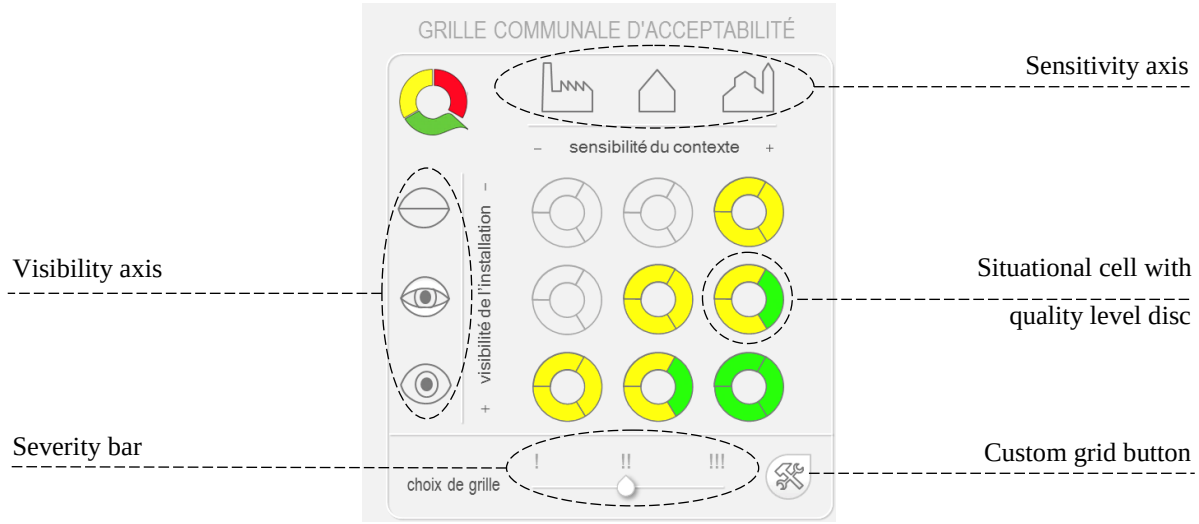

Figure 4: screenshot of the software tool LESO-QSV GRID: the acceptability grid.

The acceptability grid is based on the "criticity" matrix: the 3 sensitivity levels are indicated on the top horizontal axis, whereas the 3 visibility levels are shown on the left vertical axis, and represented by an icon each. Every "situational cell" has its own acceptability threshold, expressed through the colour code assigned to the disk sectors, considering the following conventions:

- The position of each sector does not represent any specific integration criterion, only the number of yellow and green sectors is relevant. A yellow threshold is respected by a yellow / green mark; a green threshold is only respected by a green mark.

- If the situation does not require a specific quality level, the sectors are left blank. In this case, installations with one or more red sectors will be accepted.

The 9 cells of the grid can be either independently set (custom grid), or adopted from one of 3 pre-selected grids, via the selection bar. This bar allows the user to quickly choose out of 3 "severity" degrees and check the effects on the examples catalogue (see below).

3.2 The buildings catalogue: composition and classification

The tool includes a database of both coherent and incoherent architectural integrations of solar plants, in various context and "criticity" situations, to illustrate the LESO-QSV various concepts with practical examples. The database can be fully scrolled through and twelve examples are simultaneously displayed in the examples viewport. Their main characteristics are summarized in the thumbnail showing the system picture (*Figure 5*). The quality appreciations of each example are compared to the thresholds of the selected acceptability grid and the results are instantly displayed, accepted cases marked with a green V mark, rejected ones with a red X and a red framing.

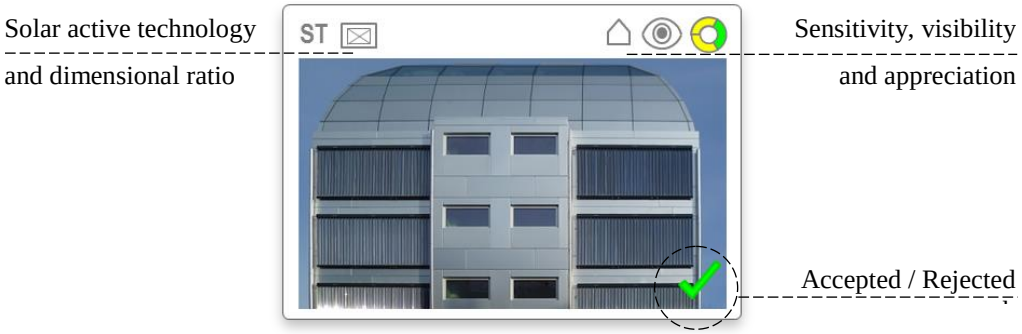

Figure 5 : screenshot of the software tool LESO-QSV GRID, case study thumbnail.

Currently the building database includes 95 sample case studies, from different European countries. Each entry of the database includes different information, the most important marked by different icons in the thumbnail picture, from left to right: the type of solar active technology (glazed, unglazed, evacuated tubes for solar thermal and monocrystalline, polycrystalline, thin film for photovoltaic); the dimensional ratio of the solar field in relation with the building support; the sensitivity of the urban zone; the visibility of the solar plant from the public space; the appreciation of the solar installation under the three criteria. Additionally some more information is available in the detail panel, by clicking on one example: the GPS location of the building site; the category of the building, as used for energy classification [6] with a mention for heritage classed buildings; the material and the type of support where the field is located (pitched roof, flat roof, skylight, glazed façade, sun protection devices, opaque façade) and finally the used products and the producer's contacts when available. By double-clicking on the picture, a pdf sheet appears with all the details, including a map of the building location, detailed pictures of the installation (when available) and a few explanation lines over the case study appreciation made by the expert evaluators.

3.3 The selection filters

The small area at the bottom of the screen allows the user to select various filters and to visualise only the cases matching the chosen features: in this way detailed considerations and studies can be conducted on targeted categories of buildings and solar plants. This feature is especially useful for an educational purpose.

4. THE AUTHORISING PROCESS WITH LESO-QSV GRID

Once the urban planners and the municipality officers have defined the acceptability grid for their territory with the software tool, they can communicate their decision to architects, installers and citizens. The chosen severity will give different acceptability thresholds in each "criticity" situation. When a citizen applies for a solar installation on his building, he will be aware of the expected quality according to the "criticity" of the site and select a suitable solution with the installer. Then, the installer will submit a form to the local authority, describing the chosen solution in detail (by attaching pictures and simple photo-edited simulations). The municipality will analyse the proposition and find whether it is compliant to the relevant acceptability threshold, by assessing its integration quality level (by using the case studies provided in LESO-QSV GRID if needed). The municipality might add its own selected case studies to create a customised database. The proposed installation is then either accepted or rejected, and a notice with evaluation comments and recommendations for improvements is sent to the applicant.

5. CONCLUSION AND EXPECTED DEVELOPMENTS

Given the huge increase of solar installations in urban settings, the presented tool, associated to the QSV-method, offers a valuable way to take into account the formal and aesthetic aspects. It can be used as a protecting tool, blocking inappropriate designs in sensitive areas, and as an educational tool, helping improve the architectural integration quality. This software, with accompanying documents and support, allows municipalities defining the conditions to control the impact of the development of solar in a built context. Further work will be devoted to the elaboration of a proactive tool to tailor solar energy policies to local urban specificities by mapping the architectural "criticity", and crossing this map with the solar irradiation data [4].

REFERENCES

[1] *Directive 2010/31/EU of the European Parliament and of the Council of 19 May 2010 on the energy performance of buildings (recast)*. European Parliament, 2010.

[2] M. C. Munari Probst and C. Roecker ed., *Solar energy systems in architecture*. IEA SHC Task 41 D.A. 2, 2012.

[3] M. C. Munari Probst and C. Roecker, "Urban acceptability of Building Integrated Solar Systems : LESO-QSV approach," in *proceedings Eurosun 2011,* 2011.

[4] M. C. Munari Probst and C. Roecker, "Solar energy promotion & urban context protection: LESO-QSV (Quality - Site - Visibility) Tool," in *proceedings 31th PLEA Conference,* 2015.

[5] M. C. Munari Probst, "Architectural Integration and Design of Solar Thermal Systems," EPFL Thesis 4258, 2009.

[6] *SIA 380/1 L'énergie thermique dans le bâtiment*. Switzerland: SIA, Société Suisse des Ingénieurs et des Architectes, 2009.

DECISION SUPPORT TOOL FOR SUSTAINABLE RENOVATION PROJECTS IN THE DUTCH HOUSING CORPORATIONS

Davide Garufi[1]; Bauke de Vries[1].

1: Department of Built Environment, Eindhoven University of Technology, Eindhoven, The Netherlands

ABSTRACT

In Europe, the Energy Performance of Buildings Directive is a driving force for member states to develop and strengthen energy performance regulations for new and existing buildings. In the Netherlands, 33% of dwellings (2.4 million) are owned by social housing corporations (SHC), and 86% of them do not yet conform to the European 2009/28/EC which states that all the existing houses have to reach at least energy label B by 2020. If the actual retrofitting trend will not significantly increase, the Dutch SHCs will not comply with the European Commission requirements. Due to a lack of information and ambiguity about the performance of such systems, the decision-makers in companies whose core competence is not strictly energy efficiency related, face challenges in selecting the most appropriate sets of measures for their projects. Hence, there is a need for a quick and reliable tool, able to provide accurate predictions energy savings to the users as well as environmental impact and financial feasibility of energy retrofitting projects. This paper describes the challenges and relative solutions of a decision support tool (DST) at house and district level, developed together with the employees of a SHC, so coherent with the company strategy and parameters. This leads to the development of a methodology in which the performance of insulation scenarios is pre-calculated using an energy performance certificate (EPC) software, while low-resolution models **(**LRM) were built for assessing the potential of renewable energy technologies (RET) and financial consequences. As a result, the DST has been already successfully applied in a project of the SHC in Eindhoven. The lessons learned from the design and the implementation of the system have the potential to be applied in other European countries.

Keywords: decision support tool, social housing, energy retrofit, strategic tool.

INTRODUCTION

In recent years the social housing corporations in Europe have been submitting and realizing many retrofitting projects. In the Netherlands, various initiatives are currently being undertaken to improve the energy efficiency of the existing building stock, for example in the cities of Roosendaal in 2010 or in Kerkrade in 2011. Their goal was to explore the financial and energy bill consequences when insulating terraced houses until passivhaus standards and RETs for gas consumption for domestic hot water (DHW) and room heating (RH).

Nomenclature

ASHP	Air Source Heat Pump	*HL Menu*	House Level Menukaart	*PVs*	Photovoltaic panels
DHW	Domestic Hot Water	*IC s*	Investment costs	*RETs*	Renewable Energy Technologies
EI	Energy Index	*IRR*	Investment Rate of Return	*RH*	Room Heating
EL	Energy Label	*IS s*	Insulation Scenarios	*SHC*	Social Housing corporation
ESMs	Energy Saving Measures	*LRM*	Low Resolution Model	*SL Menu*	Strategy Level Menukaart
GSHP	Ground Source Heat Pump	*NL Menu*	Neighborhood Level Menukaart	*STC*	Solar Thermal Collector

The combination of these solutions resulted to be remarkable since the gas demand reduction of more than the half and a small increase (around 10%) of electricity consumption after monitoring. On the other hand, overheating in summer season was experienced by the users and the high retrofitting costs, around €100.000,00 [1] per house, are undesirable for SHC standards. One of the methods to make the process from design to construction of energy retrofitting projects more effective in terms of involved resources and expected results, is the use of a decision support tool (DST). There have been made different DSTs for studies in the sustainable redevelopment of individual objects as the studies of Rosenfeld and Shohet [2] and Alanne [3]. These models support the choice for retrofitting actions in individual dwellings, based on a techno-economic comparison, but not implementing sustainable energy technologies at neighbourhood level. The lack of information in energy retrofitting within the SHCs can be minimised through the DST described in this paper so that to fill this gap.

SYSTEM REQUIREMENTS

In order to reduce the above mentioned weaknesses of the available DSTs, the tool kit was developed together with the target group called "end-users", composed by real estate advisors and project leaders of the company Woonbedrijf, the biggest SHC in the region of North-Brabant, the Netherlands. Five meetings have been scheduled to define the system requirements, preferred inputs and outputs from the DST called *Menukaart*, the word "menu" in Dutch language. In *Figure 1* the main system requirements are presented.

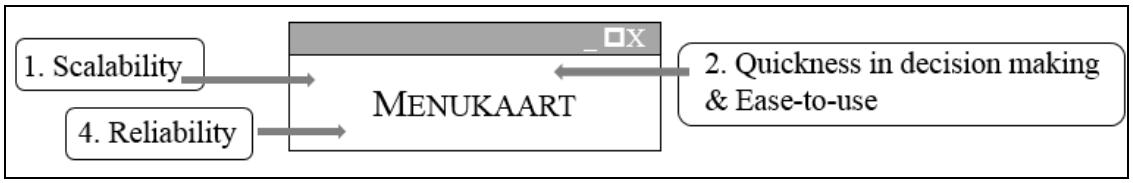

Figure 1: System requirements from the Social Housing Corporation's users.

Below the system requirements definitions are presented:

1. The system must be applicable to all the building complexes with same archetype (terraced houses 1945-1965). It is supposed to combine the data from the background calculations and the variable inputs through a user-friendly interface.
2. The ISs and RETs options provided should be linked to a financial model in line with the company rates. Check boxes and buttons can be part of the system and, to guide the steps to take, some comments and input limitations have to be implemented.
3. Consistence of the embedded LRMs with the national Dutch regulations or broadly recognised institutions is highly desirable. The characteristics of the location, weather data as well as the specific geometry of the archetype are essential prerequisites.

The systems outputs, according to the end-users, have to include the energy index (EI) and the energy label (EL) before and after renovation. The actual energy consumption of the dwellings often differs from the EPC values, which are strictly related to the building performances but, they do not take into account among others, the contribution of the electric appliances [4]. The DST provides the users with a quick way to estimate more accurate scenarios, since the annual energy bills of the tenants, as available data in the company, can be easily implemented in the model. The results of the insulation scenarios (IS), a selection of energy saving measures (ESM) and RET are asked to be converted in terms of environmental,

energy savings and financial impacts. Moreover, a key output for the end-users is the financial contribution to the project from the tenant, i.e. the increment of the monthly rent.

METHOD

A step by step procedure was built so that to define each input-output stage during the decision making process, as usually done in energy planning [5].

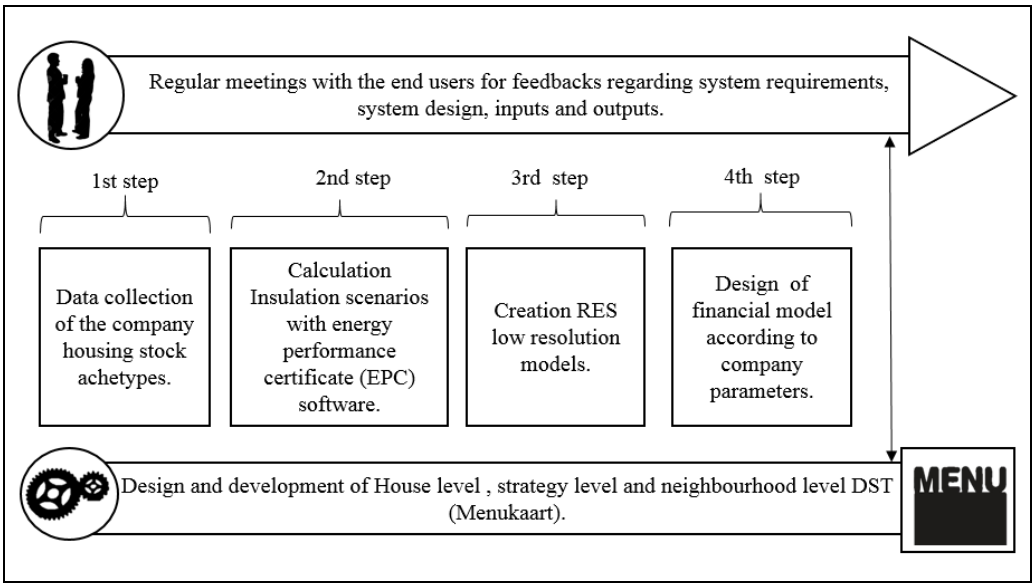

Figure 2: The steps taken in the research methodology are shown.

Since the company's housing stock is very diverse, in the 1st step of the research a data collection about the geometry, components construction and heating systems currently installed has been performed. A sample of 440 terraced houses distributed in two different complexes, sub-units of neighbourhoods, located in the city of Eindhoven was chosen coherently with the strategic plans of renovation projects of Woonbedrijf. To explore the different options of energy reduction based on insulating the houses, as a 2nd step, eight ISs have been calculated with the Dutch EPC software *Vabi Assets Energie 4.3*. In *Table 1* the actual situation of an average terraced house, the scenarios, the increasing thermal properties of the components, the ventilation and heating systems are indicated. The further four IS configurations are called ''No floor'' scenarios, in which the same measures have been applied, and the floor insulation have been excluded. The latter ISs have been selected to deal with situations in which the foundations of the houses are not accessible or their construction layers could contain toxic materials such as asbestos.

Scenarios	Rc Value	Floor	Roof	Façade	Doors	Glazing	Ventilation system	Heating System
Actual	[m².K/W]	0.15	0.22	0.36	Not insulated	Single or double	Natural	High efficiency gas boiler
1 Reasonable	[m².K/W]	2.4	2.6	1.6	Insulated	Double + wooden frame	Mechanical	High efficiency gas boiler
2 Good	[m².K/W]	3.6	4	3.7	Insulated	Double + wooden frame	Mechanical	High efficiency gas boiler
3 Excellent	[m².K/W]	8.7	8	8.3	Insulated	Triple wooden frame	Heat recovery	High efficiency gas boiler
4 Excellent+Triple	[m².K/W]	8.7	8	8.3	Insulated	Triple wooden frame	Heat recovery	High efficiency gas boiler

Table 1: Overview of the selected insulation scenarios.

After getting the outputs in terms of yearly gas consumption depending on the insulation scenarios, the 3rd step has been to define low resolution models (LRM) for a selection of RETs: PVs for electricity conversion, flat plate solar collectors (SC) for DHW , air source and

ground source heat pump (ASHP) and (GSHP) for RH and DHW. The assumptions within the LRMs for RETs are: house orientation 45° southwest, tilt angle of the roof of 20°, a low temperature radiator system 45°C /35°C for room heating distribution, constant occupancy of two inhabitants per house. A selection of ESMs is included in the DST: heat recovery shower plate for reducing DHW consumption, electric stoves for cooking, stand-by killers for minimizing the electricity from appliances, smart meter and app for higher awareness which leads to a lower energy consumption [6]. Then, RET implementation was provided to be integrated in the buildings, to exploit the local available resources so that to achieve a high sustainability level [7]. An extra model was built for the estimation of thermal energy storage at neighbourhood level. With the support of the financial department of the company the 4th step, the financial LRM was built. In order to connect the mentioned steps to the needs of the users group, three different menus have been designed. All the LRMs for RETs have been validated with the results from broadly used softwares showing between 2% and 9% difference in outputs.

DATA SOURCES AND SYSTEM DESIGN

The geometry data of the component surfaces, actual energy bills and financial parameters are provided by the company. The LRM for EI and EL as well as ASHP, GSHP electricity consumption and Aquifer Thermal Energy Storage (ATES) are conforming to the NEderlandse Norm (NEN) 7120, Dutch legislation for calculating the energy performance in buildings. The energy conversion LRM was built in accordance with the guideline provided by the Sustainable Energy Authority of Ireland [8]. One option for the installation of flat plate SC has been calculated on the basis of the ESTIF standards [9]. Moreover, the prices estimation for the chosen insulation materials, the selected technologies and the ESMs is provided by Dutch national price lists for buildings [10]. Below the design per Menukaart is described and in the figures the required inputs per step and outputs are displayed. The menus will be accessed from the system Home page. In the *SL Menu* the user is invited to go through five steps (see *Figure 3*). The system shows the top three on 39 background combinations per selected strategy goal. Minimizing the energy bill for the tenant and the CO_2 production of the housing stock are the priorities two strategic scenarios called *Min CO_2* and *Min Bill* were designed. Two further scenarios called *No Heat pump_Min Bill* and *No heatpump_Min CO_2* were included since the deployement of heat pumps is not included in the commonly in SHCs renovation projects. The fifth and sixth strategic options called *ALL Electric_Min Bill* and *ALL Electric_Min CO_2* provide the user with the option of avoiding the consumption of natural gas. No financial consequences are shown.

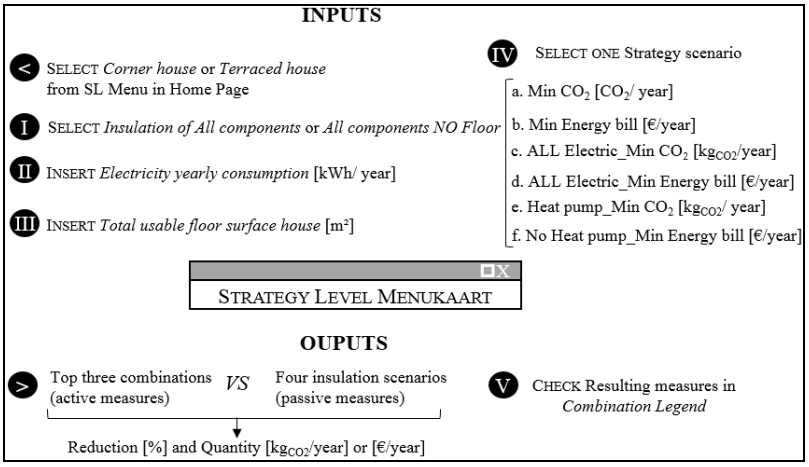

Figure 3: The steps involved in the SL Menu in Roman numerals are indicated.

While in the *SL Menu* average values are in the background data, in nine steps of the *HL Menu* the user can insert the specific geometry inputs per complex. Personalized combinations of ISs, ESMs and RETs can be chosen and the energy, environmental and financial consequences presented as outputs (see *Figure 4*).

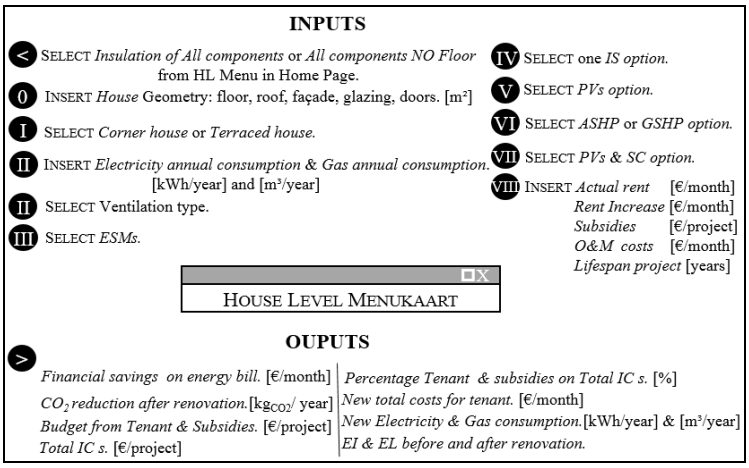

Figure 4: The steps involved in the HL Menu in Roman numerals are indicated.

The *NL Menu* (see *Figure 5*) offers to the user an estimation of the total investment and operational cost for ATES applicable in large scale projects which involve terraced houses and non-residential buildings in two steps: the number of houses, the annual heating and cooling demand of the buildings.

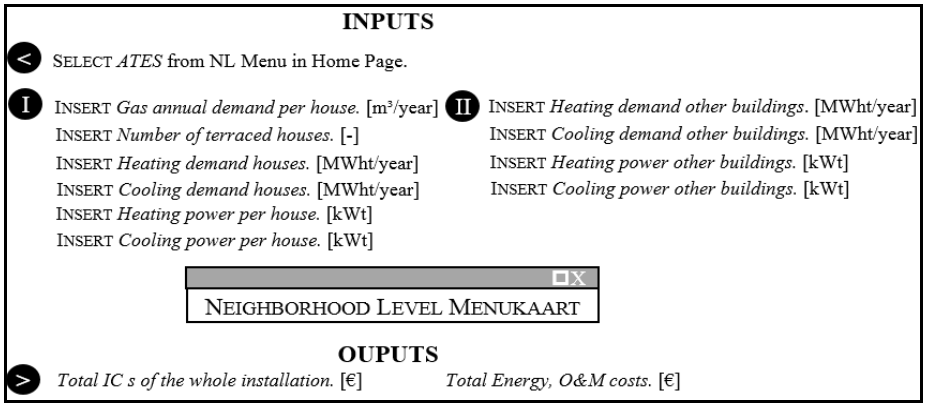

Figure 5: The steps involved in the NL Menu in Roman numerals are indicated.

CONCLUSION

System implementation: case study HL Menu

The DST for retrofitting projects in Dutch SHCs has been implemented in Microsoft Excel to guarantee the accessibility from all the employees of the company and avoid extra licence costs for the company. To have an overview of the possible results of a deep renovation of a corner terraced house in *Table 3* a summary of the choices made (in *italic*) is presented. The DST designed has been easily and successfully applied to all complexes with the same archetype, so the design requirements have been satisfied. The DST is still under development for other archetypes in the housing stock that one kind find in a housing corporation.

Steps	*Insulation ALL components*			
0 &1	Façade [m²]	Roof [m²]	Windows [m²]	Doors [m²]
	90	*43*	*15*	*4*
	Usable floor area [m²]	*Corner House*		
	70			
2	Electricity consumption [kWh/year]	Gas consumption [m³/year]	*Mechanical Ventilation*	
	3000	*1700*		
3	*Stand-by killers*	*Smart meter & Smart app*	*Heat recovery shower plate*	*Electric cooking*
4, 5,6 & 7	*Scenario 2_Good*	*ASHP_RH & DHW*	*18PVs + 1SC*	
8	Lifespan [years]	Actual Rent [€/month]	Rental increase [€/month]	
	25	*€ 450,00*	*€ 70,00*	
	Subsidies [€/project]	Maintenace costs [€/month]	Operating costs [€/month]	
	€ 2.000,00	*€ 100,00*	*€ 100,00*	
Results				
Financial savings on bill [€/month]	New Electricity consumption [kWh/year]	New Gas consumption [m³/year]	New total costs for tenant [€/month]	Total *IC s* [€/project]
€ 120,00	*1247*	*152*	*€ 520,00*	*€ 23.500,00*
Tenant & subsidies	Tenant & subsidies [%] on *IC s*	CO2 reduction [%]	EL before	New EL
€ 15.326,00	*65%*	*78%*	*D*	*A++*

Table 2: HL Menu case study for a corner terraced house deep retrofitting.

ACKNOWLEDGEMENTS

This research was part of the second year project within the Professional Doctorate in Engineering ‘’Smart Energy Buildings and Cities’’ at Eindhoven University of Technology. Woonbedrijf housing corporation has been the industry partner.

REFERENCES

1. Rovers, R.: New energy retrofit concept: ‘renovation trains’ for mass housing. Building Research & Information, 42:6, 757-767, 2014.
2. Alanne, K.: Selection of renovation actions using multi-criteria “knapsack” model. Automation in Construction, 13:3, 377-391, 2003.
3. Rosenfeld, Y. and Shohet, I.M.: Decision support model for semi-automated selection of renovation alternatives. Automation in Construction, 8, 503-510, 1999.
4. Visscher, H.: Effectiveness of energy performance certification for the existing housing stock. Proceedings RICS COBRA 2012 10-13 September 2012, Las Vegas, Nevada USA
5. Nastasi, B., de Santoli, L., Albo, A., Bruschi, D., Lo Basso, G.: RES (Renewable Energy Sources) availability assessments for Eco-fuels production at local scale: carbon avoidance costs associated to a hybrid biomass/H2NG-based energy scenario. Energy Procedia, 2015.
6. Ybema R.: Energietrends 2014, ECN 2014.
7. De Santoli, L., Mancini, F., Nastasi, B., Piergrossi, V.: Building Integrated Bioenergy Production (BIBP): economic sustainability analysis of Bari airport CHP (combined heat and power) upgrade fuelled with bioenergy from short chain, Renewable Energy, 81, 499-508, 2015.
8. SEAI: Best Practice Guide – Photovoltaics. Sustainable Energy Authority of Ireland, 2010.
9. ESTIF: Objective methodology for simple calculation of the energy delivery of (small) Solar Thermal systems, European Solar Thermal Industry Federation, Belgium, 2007.
10. RVO.nl: Maatregelen EPA-Maatwerkadvies Bestaande Woningbouw, The Netherlands, 2013.

BIM BASED CLASSIFICATION OF BUILDING PERFORMANCE DATA FOR ADVANCED ANALYSIS

Stephan Hoerster[1]; Karsten Menzel[1]

1: IRUSE Department, Western Gateway Building, University College Cork, Ireland

ABSTRACT

Data density has increased dramatically through utilization of wireless sensors and smart metering devices. While smart meters are commonly monitored in 15 minute intervals, wireless devices are usually polled at much higher rates. Due to these frequent reading intervals, the high data granularity creates a need for improved analysis and categorisation of data.

This research aims to extract descriptive information from BIM (Building Information Modelling) models in order to classify and structure monitored data. This is achieved through application of the open BIM standard IFC (Industry Foundation Classes). The extracted information gets combined with current DWH (Data Warehouse) methodologies to support superior and efficient analysis. The DWH model is in sync with the IFC standard to enable a straight forward mapping of IFC objects into the DWH.

Several KPIs (Key Performance Indicators) are be applied that support the combination of monitored fact data with the extracted descriptive information. The analysis of monitored data is realised through DWH cubes. These cubes are modelled with selected IFC objects in order to maximise their significance. The envisaged DWH allows the categorisation of data per (i) building system, (ii) building tenant, (iii) building space and (iv) time. Moreover, the DWH allows any combination of afore mentioned categories based on various time intervals. This enables various analysis scenarios, e.g. the calculation of the average electricity consumption per tenant or the peak temperature in a building level.

The benefit of reusing selected objects from BIM models over existing solutions is the elimination of repetitive work. In the past, descriptive data was acquired multiple times. This work demonstrates that data extracted from BIM models can be successfully used to enrich data analysis in a DWH system. The major achievement of this work is the elimination of the need to populate static information in the DWH through other means.

This concept is evaluated with data sets obtained from real buildings. A proof-of-concept DWH is presented in this work. The main obstacles during the ETL (Extract, Transform and Load) process of individual IFC objects and their conversion into DWH compatible elements are highlighted. Lastly it is also demonstrated that the combination of both technologies does not negatively reflect on the speed of database queries.

Keywords: BIM, IFC, Data Warehouse, Smart Metering, Key Performance Indicators

INTRODUCTION

Nowadays, buildings equipped with smart meters and sensors generate a huge amount of performance data. For evaluation purposes, this data needs to be processed and classified. The availability of standardized product and process models allows clustering of vast data by building elements and systems [1]. Sensor and meter readings enriched with spatial information increase their interpretability and meaningfulness [2].

In this research, we use information extracted from BIM models to classify performance data. Conventional BIM models require the analysis of complex 3D models. Our approach extracts only relevant information from an open, standardized BIM (IFC). For processing and complex analysis of IFC models, modern DWH functionality is implemented. The compatibility between an IFC model and DWH architecture allows an easy reuse of relevant BIM information. Classification of the data will then be possible through utilizing KPI's implemented in the DWH.

For this approach, only a subset of elements described in the IFC metadata model is required. The selected objects will be discussed and their successful transformation into a Data Warehouse is the main aspect of this work. Specifically, we select from the building model (i) spatial information, (ii) systems topology, (iii) relationship of different units within a company, and (iv) time reporting intervals. These four domains will be the foundation for the KPI's used for building classification.

BACKGROUND

IFC allows the export of metadata models into files. File types and layouts have been standardized. There is (i) IFC-STEP which has been standardized in ISO-10303-21. Every instance of an IFC object is stored in a single line. Each IFC object has a defined number of attributes. The STEP format enumerates these attributes chronologically, where unset attributes are represented with a dollar sign ($). Additionally, there is (ii) IFC-XML, a definition based on the widely used XML file type. The application of XML is the IFC domain is also standardized in ISO 10303-28. Due to the nature of the XML standard, the XML file comes with an overhead that significantly increases the total file size compared to STEP.

Currently, researchers are working on creating Data Warehouse servers which are compatible to IFC. Their vision is that IFC specifications can be considered as a blueprint for database schemas. Any useful information from an IFC file could then be easily imported into the schema. The expected outcome would be that information already modelled and stored in IFC could be reused for other applications. In the long term, this could eliminate repeated data acquisition for different purposes. The status and implementation of IFC compatible database schemas have been discussed in [3, 4].

Historical meter and sensor readings from buildings act as fact data in the proposed model. Preservation of this kind of data enables a wide field of disciplines. For example, energy analysts have data of much higher granularity for examination. Ways for data acquisition and data storage are outlined in previous research [5, 6].

METHODOLOGY

In this work, we aim to select a manageable subset of IFC objects extracted from the open BIM model to enrich the analysis of building performance data. These subsets can be clustered into four domains. For this, the IFC objects enumerated in table 1 will be of interest to us.

In IFC, a Model View Definition (MVD) is a specified subset of the IFC metadata model. MVD's allow the exchange of AEC information from selected individual domains. The principles of MVD's follow standards defined in ISO 29481. Unfortunately, for the model required by us, no MVD exists.

Domain	IFC Objects	IFC Relationship Objects
Spatial	IfcSpace, IfcBuildingStorey, IfcBuilding, IfcSite,	IfcRelAggregates
Organization	IfcOrganization,	IfcOrganizationRelationship
System	IfcDistributionFlowElement entities, IfcDistributionCircuit,	IfcRelAggregates
Time	IfcDateTimeResource entities, IfcTimeSeries	IfcResourceLevelRelationship

Table 1. Selected IFC objects

To compensate for this, we decided to focus solely on exported raw IFC data model files. This enables us to work with the bare data and select only individual IFC objects as needed. Both file type formats (STEP and XML) can be parsed using either on-board or 3rd party tools. In this work, we decided to use STEP files along with standard UNIX shell commands for parsing and filtering. Through these shell commands, all objects of the four domains as in table 1 can be filtered.

As an example, the objects consolidating the spatial domain are given in figure 1. There is illustrated how objects are linked to each other in IFC. Through resolving their hierarchical relationship, matching of a room to a storey and to a building becomes possible.

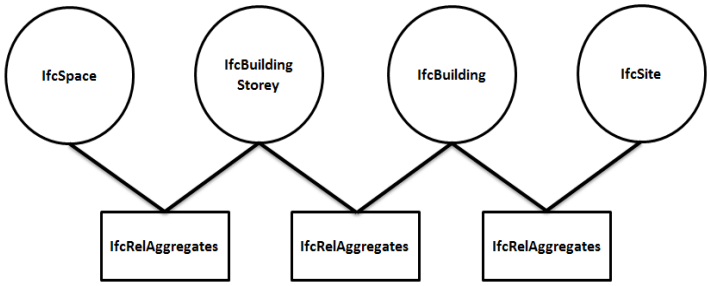

Figure 1. File based relation

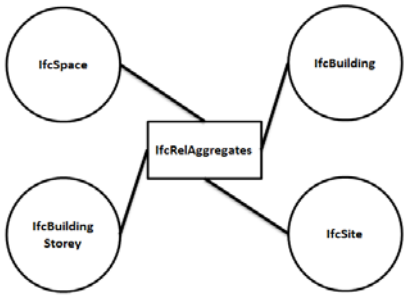

Figure 2. Database relation

To maintain compatibility between the IFC standard and the database, its schema is based upon the IFC object definition. IFC objects like IfcSpace and IfcBuilding hold their entities in dedicated tables. Relationship objects are consolidated in a single relationship table. These tables ensure that single objects, sitting in its own encapsulated tables, can be correctly related to their corresponding objects. Figure 2 highlights that in a database approach only one table IfcRelAggregates exists which maintains the relation of all related IFC entities.

Historical fact data is collected from meters and sensors throughout buildings and stored inside the DWH. IFC is supporting fact data through its IfcTimeSeriesValue entity. Each record consists of a value, a timestamp and meter/sensor identification (ID). Through these attributes, it is possible to identify which source reported what value at a specific time. The ID can be used to lookup further information from the geometrical model, e.g. where the sensor/meter is physically located.

The outlined remodelling process is executed for all four domains. At this stage, an IFC database schema compatible for our methodology has been achieved. However, this schema lacks speed due to its encapsulated design (as seen in the results section). In order to compensate this, we have implemented modern DWH technology on top.

The objects scattered across multiple tables from each domain have been consolidated in MV's (Materialized Views). This is accomplished by resolving the relationship table, effectively pulling all information into a single view. MVs get populated and updated in adjustable intervals and they allow the definition of constraints [7].

The fact table needs to be enriched with a) references to the MVs and b) with KPI's. This enrichment is also realised through the application of a MV. This work focuses on KPI's which were previously compiled and determined as beneficial for the analysis of building performance data [8, 9]. Figure 3 gives a graphical overview about earlier identified KPI categories.

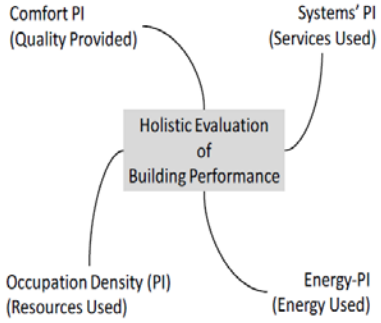

Figure 3. Categories of Key Performance Indicators as identified in [9]

Through the implementation of afore mentioned MV and the generation of a suitable fact table, all requirements are fulfilled. As a result of applying the constraints, a database star schema is created. For analysis purposes, OLAP cubes for each KPI can be generated based on this star schema. Example outputs (rendered in MATLAB) can be seen in the next section.

RESULTS

The selected results focus on the UPR (underperformance) KPI, which belongs to the class of comfort PI (as seen in figure 3). This KPI rates a building between 0% and 100%. In this context, 100% is equal with performance always within set thresholds. The two buildings evaluated are two university buildings, namely Civil and Environmental Engineering Building (CEE) and the Environmental Research Institute (ERI). Performance data for these buildings is collected since 2011. The following figures illustrate the exemplary analysis possibilities given by the outlined methodology.

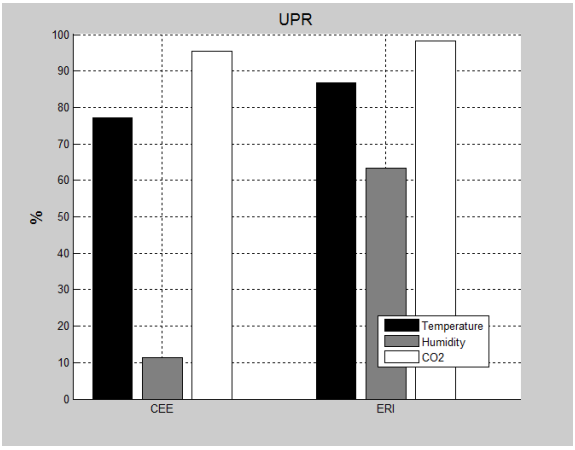

Figure 4a. Overall building comparison

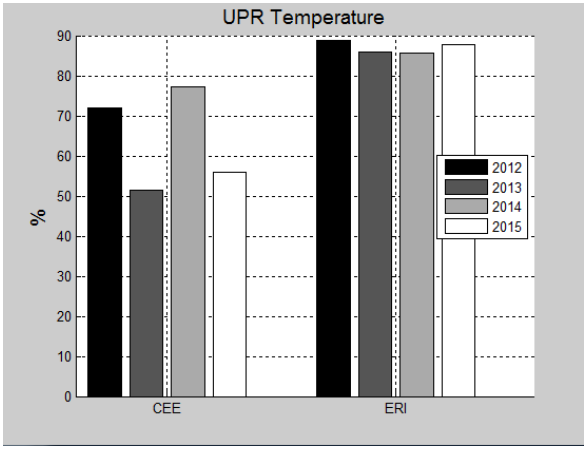

Figure 4b. Temperature comfort

The direct comparison between the two buildings reveals that the ERI buildings performance is superior in all three disciplines with the highest advance in humidity.

Graph 4b identifies clearly how the ERI building is consistently performing close to the desired levels of 100% comfort level, with only marginal changes of 2.5% over 4 years, while in contrast the level of user comfort in the CEE building is unpredictable with large variances in the data recorded

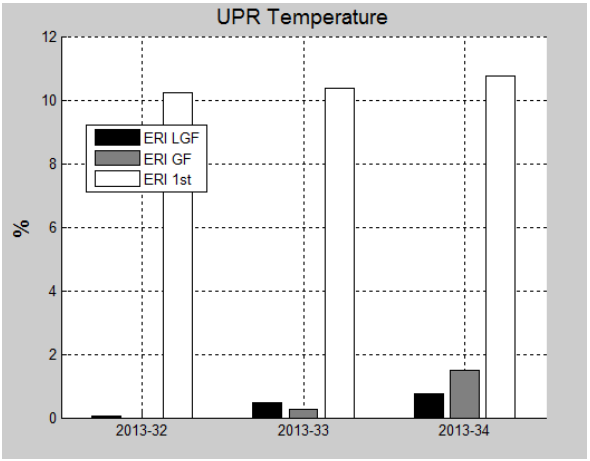

Figure 4c. Storey-based temperature

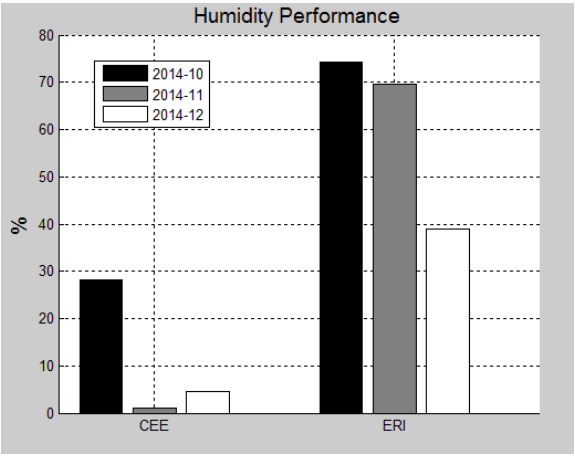

Figure 4d. Humidity comfort

Graph 4c is broken down into a 'story' spatial hierarchy. In this example, the amount of underperformance is displayed. This bad performance of the first floor may be due to its roof exposure.

When focusing on the performance of the two buildings in terms of humidity the CEE building is performing poorest with comfort far below the ERI in same time intervals.

Regular SQL queries to acquire KPI were executed against (i) a regular database schema without any DWH optimizations, and (ii) against a DWH optimized schema as introduced in this work. Both schemas held the same amount of fact data. Average response times can be seen in table 2.

Type of KPI	**Time span**	**Type of fact table**	
		Regular database (in s)	**DWH optimized (in s)**
Average consumption	1 month	75	0
Maximum consumption	1 day	6	0
Underperformance Ratio	1 day	8.7	0
Minimum value	6 month	83	0

Table 2. SQL execution comparison

The application of Data Warehouse technology is known to reduce response times to a minimum. These results prove that our methodology also benefits from this technology.

CONCLUSION

This work has introduced a methodology to process and classify building performance data using descriptive information from BIM models. This has been achieved by combining

selected information from the open BIM standard IFC with DWH technology. This process eliminates the need to reacquire previously gathered information.

The introduced DWH dimensions allow the analysis of individual or grouped sensors/meters. This analysis is supported by the application of KPI. Analysis may be performed against arbitrary combinations of organization units, building systems, spatial zones over time periods. Even huge numbers of installed sensors can be analysed following the same principles.

A downside of this approach is, that even experienced database designers might face difficulties to fully understand the schema if they are not familiar with the IFC standard. Nonetheless, we believe that common schemas could improve rapid comparative analysis of collections of buildings.

For further application scenarios with different subsets of BIM data it is more than likely that other domains, as introduced in this paper, will be required. We are optimistic that the compatibility introduced in this work can be maintained. We envisage that a fully IFC compatible schema could improve efficiencies across the field. Database tools customized to work against IFC schemas could become a future niche product as they would work out-of-the-box with any stored data following the IFC meta-data model.

ACKNOWLEDGMENTS

This work is funded by the Irish HEA PRTLI-5 program and Bilfinger HSG FM.

REFERENCES

1. Ammar Ahmed, Joern Ploennigs, Karsten Menzel, Brian Cahill, Multi-dimensional building performance data management for continuous commissioning, Advanced Engineering Informatics, Volume 24, Issue 4, November 2010, Pages 466-475, ISSN 1474-0346, http://dx.doi.org/10.1016/j.aei.2010.06.007
2. Goekce, H.U., Goekce, K.U., 2013. Multi dimensional energy monitoring, analysis and optimization system for energy efficient building operations. Sustainable Cities and Society, Volume 10, February 2014, Pages 161-173, ISSN 2210-6707, http://dx.doi.org/10.1016/j.scs.2013.08.004
3. Mo, K., Menzel, K., and Hoerster, S. Development of an IFC-compatible data warehouse for a building information model. In: CiB W78. Beijing, 2013.
4. BaaS Deliverable 2.2 , Data Warehouse, EU FP7 project, 2013
5. Stack, P., Cahill, B., Manzoor, F. and Menzel, K., 2011. Data Warehouse Model to support Optimized Operation and Energy Savings in Buildings. ICEBO, New York, 2011.
6. Hoerster, S., Katzemich, F., Menzel, K., 2014. A Methodology for Data Logging and Retrieval from Remote Sites. ECPPM Vienna, 2014
7. Shukla, A., Deshpande, P., Naughton, J.F., Materialized view selection for multidimensional datasets, in: Proceedings of the 24th International Conference on Very Large Data Bases, NY, USA, 1998, pp. 488–499.
8. Menzel, K., Katzemich and F., Mahdavi, A. Impacts of building performance monitoring on integrated energy management. 2nd CESBP Vienna, 2013
9. Menzel, K., Browne, D. and Deng, S. Performance indicators to evaluate buildings' systems' performance. ECPPM Vienna, 2014

ENERGY FLOWS MONITORING AT THE CANTONAL LEVEL

M. Guittet[1]; M.Capezzali[1]

1: Ecole Polytechnique Fédérale de Lausanne (EPFL), Energy Center, Station 5, 1015 Lausanne

ABSTRACT

As an increased number of measures (Swiss or European level) aim at developing more sustainable policies for energy management and reduction of CO_2 emissions in particular (for example, the 3x20 policy), very few tools currently exist at the regional/cantonal level to monitor the multiple existing energy flows. Energy issues at local and territorial level have become considerably more complex in the last twenty years for a number of reasons. First, new technologies penetrated the market and now compete with fossil-based conversion systems. In addition, energy systems are evolving to systematically become multi-fluid and multi-services. Finally, local and state authorities have taken up a stronger and broader role in terms of energy policy and have committed to ambitious goals in terms of both increased energy efficiency and implementation of renewables.

Within this project, a decision-support and monitoring tool for policy makers has been developed, which includes thorough information on the most prominent energy aspects of the Canton of Vaud, and paves the way for establishing more indicators covering environmental and economic aspects. The development of a web-based tool aimed at visualizing the entire energy chain, from energy sources to end-use sectors at the level of a whole Swiss Canton is thus presented here. This tool provides a unifying structure for all the useful information on energy sources, vectors and final consumptions, this approach thereby giving access to a global overview, understanding and monitoring of the energy supply and demand characteristics of any given Canton (or any equivalent subnational territorial entity).

The final goal of this approach is to give access to the direct visualization of all energy flows on the platform, thus translating and broadening the national statistics on the energy chain up to the cantonal (territorial) level. Therefore, this innovative tool will allow quantifying energy profiles, modelling conversion nodes along the energy chain, as well as assessing the overall energy balance per end-use sector.

This very innovative platform constitutes a centralized energy data repository as well as a quantitative evaluation tool, encompassing most useful energy sources.

Keywords: monitoring, Canton, energy flows, web-based tool, decision support

INTRODUCTION

Switzerland has recently committed to phase-out nuclear power contribution to the electricity production mix, while reducing greenhouse gas emissions. While many regulations have already been put in place at the cantonal level to this end, the need to follow the evolution of energy-related data appears of crucial importance. With this goal in mind, a tool has been developed allowing various institutional as well as private entities to visualize the most pertinent energy data necessary. In particular, at the Canton governmental level, the web-based tool shall represent an extremely useful support to thoroughly monitor the effects of policy decisions.

The project has been entirely financed by the Canton of Vaud (Switzerland).

WEB-BASED ARCHITECTURE

The web-service oriented architecture aims at visualizing on a single platform all the relevant energy data that could later be used for both the purposes of communication and decision-making. The main goals are to achieve a maximum flexibility, robustness and security: in fact, the whole development of the platform has been oriented towards adopting widely spread technologies and architecture, thus ensuring overall robustness and replicability, while guaranteeing at the same time an enforced security of all the data.

The platform comprises of two main parts: first, the server handles the requests made by a user and thereafter consults all the relevant data in the database. The second part is the "data management tool" that is used to manage the integration of new data. Both parts are integrated within the same web-service, but are fundamentally different in their usefulness and can be accessed independently. In other words, a user can have access to the server (to consult or make a query), the data management tool (to insert new data on the platform), or even both - depending on the user rights and accreditations.

Server architecture

The basic architecture of the platform is depicted in Figure 1, and comprises:

- the *interface*, developed in Groovy/Grails;
- the *service layer*, which processes all the requests from the user, and invoke the data access layer so that it can get all the useful data needed for further calculations. This layer is also responsible for all the communication between interface and data processing;
- the *data access layer*, which defines the means of accessing data from the database. This module allows to develop a large number of queries of any type (production, consumption and gross final consumption and import/export);
- the *database*, for all the relevant energy data and user accounts.

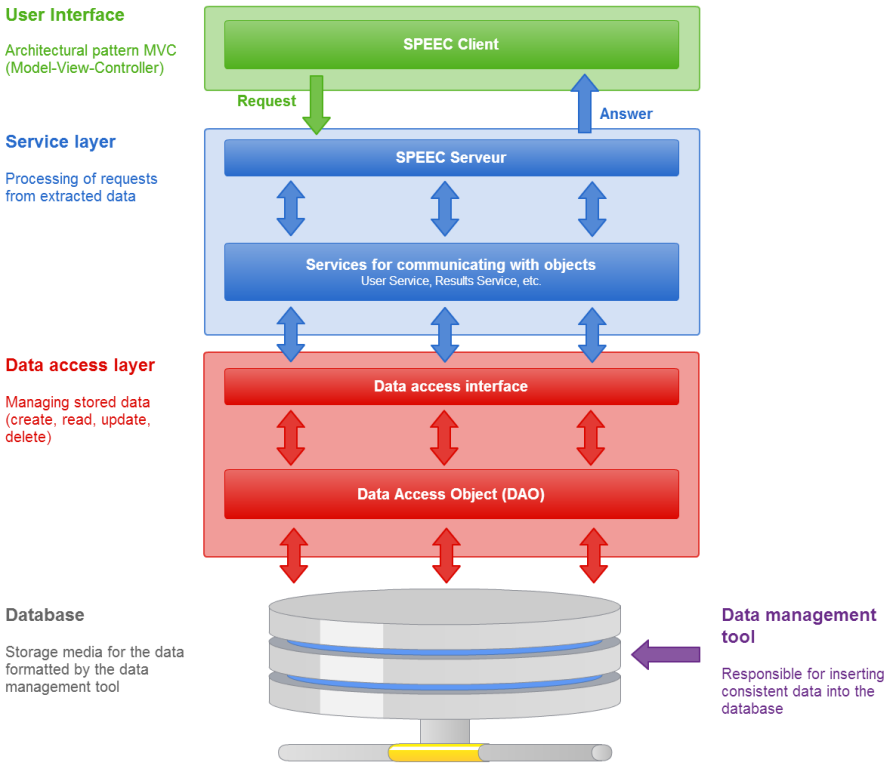

Figure 1 – Three-tier architecture of the tool: the front-end webserver, data processing and data management are fully separated

User management: rights and roles

Different user profiles can be precisely defined with specific data access rights. Three roles have been implemented, namely Administrator, User and Data provider. While the user can only consult the database and make queries, the Data provider can only submit new data. The administrator can do both, and in addition can review the pending data from the data provider, and manually validate them. This double-step process for the data validation is detailed later (see § Data tool management). All the roles are additives.

Granularity of the data

Sub-entities of the considered territory (i.e. either a municipality or a district) cannot be easily considered since most data become sensitive either because of issues related to the commercial nature of energy consumption data or because of privacy protection rights (especially when the granularity decreases down to the urban zone/neighborhood level). Therefore, and despite a construction and implementation of the tool initially designed to accept different granularity levels (municipality, district, canton), only the Canton level has been ultimately considered.

MAIN FUNCTIONALITIES AND DISPLAY OF THE PLATFORM

Two basic visualization modes are currently implemented within the platform: the pie chart and line chart (see Figure 2).

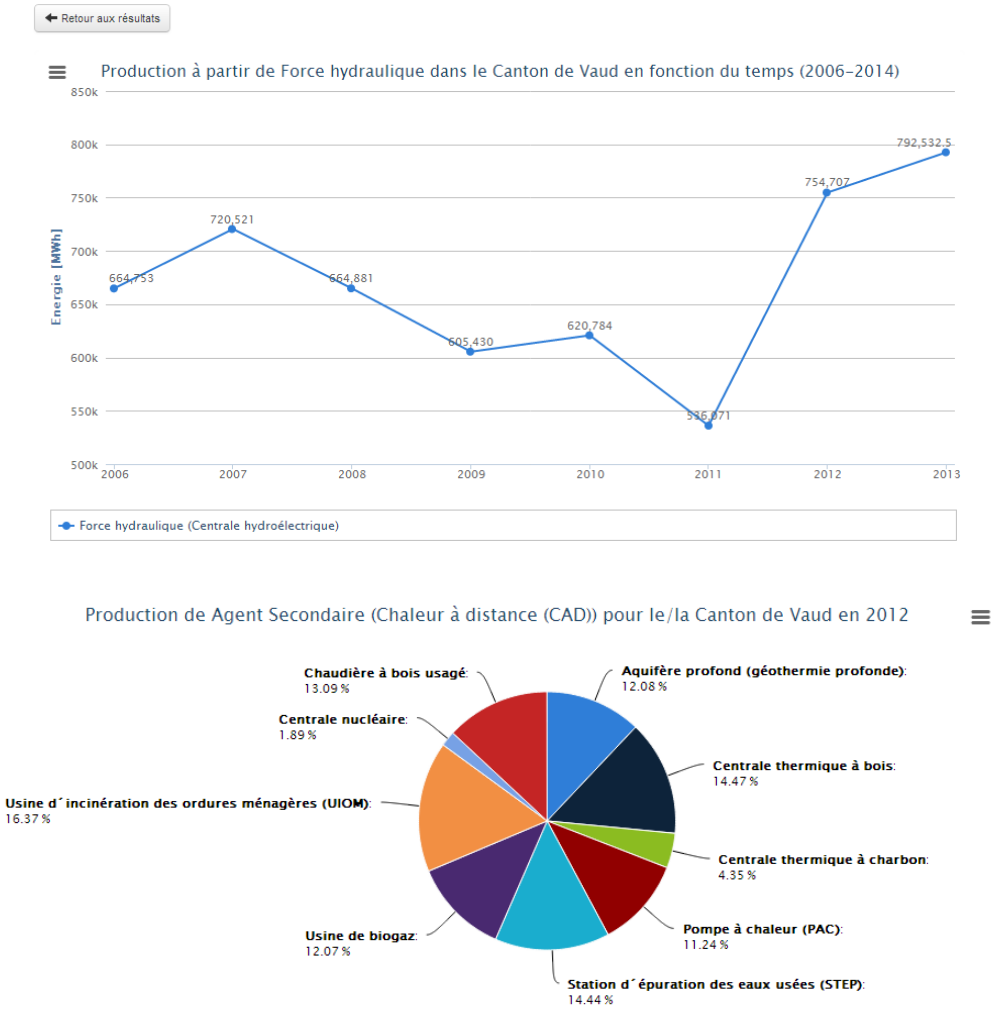

Figure 2 – Possible visualisations: 1) Line chart, 2) Pie chart, legend in French. For confidentiality reasons, the data presented here has been altered.

The viewable data comprises production, raw and final consumption of all energy carriers mentioned in the Swiss Energy Statistics from SFOE (electricity, natural gas, coal, wood, renewables, waste, crude oil, petroleum products…).

DATA MANAGEMENT TOOL

Process

A two-step process has been specifically designed to ensure a complete accuracy of the data inserted in the database. While many automatic tests are being performed as soon as a data provider inserts new data, manual intervention has been deemed necessary to validate the last part of the process. Therefore, a first step of the process concerns the insertion of new data from the data provider: when all the possible errors, typos and numerous checks have been identified and corrected, all the data is then inserted in a temporary database. The data cannot be consulted at this stage by a user with basic rights, but only by an administrator.

During the second step of this process, an administrator will review all the data, aided again by a battery of different tests to help with the validation. Those two steps are detailed in the two following paragraphs, as well as in Figure 3.

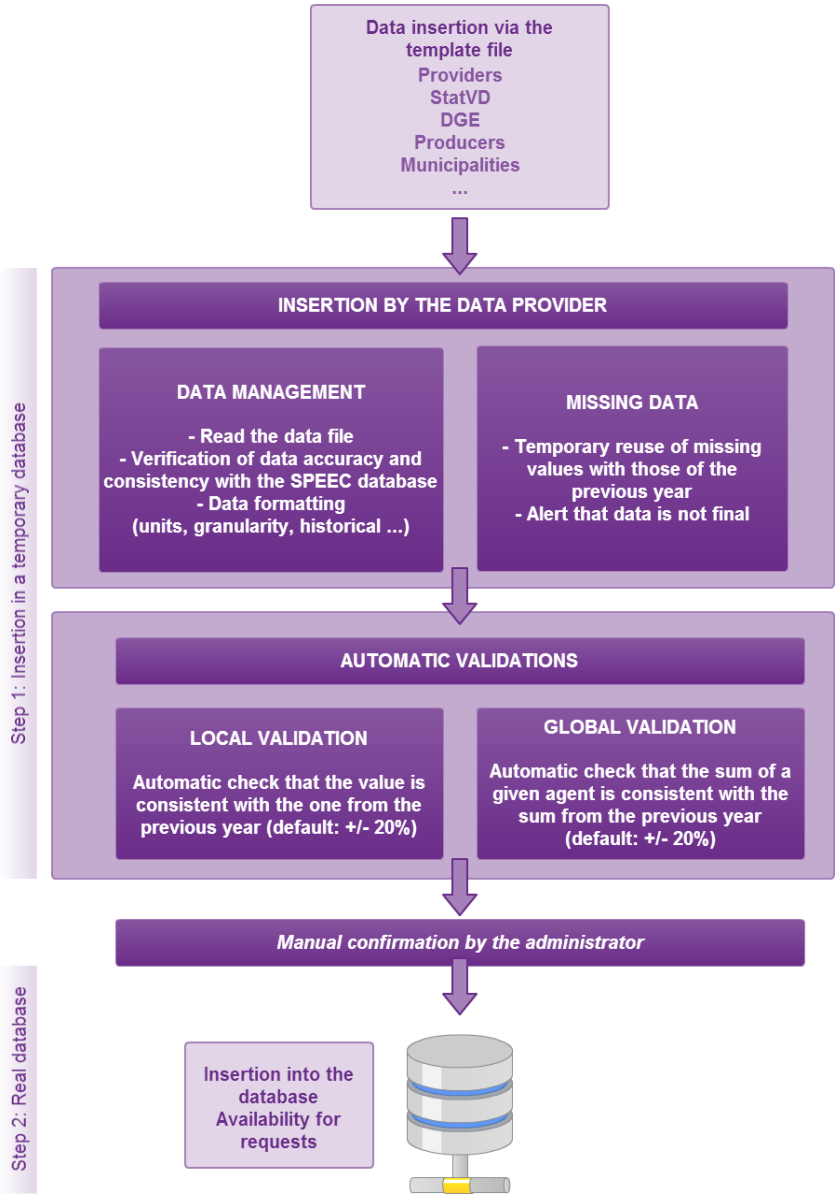

Figure 3 – Two-step process for the data management tool

Insertion

When a user has the specific rights to feed the database (i.e. administrator or data provider), a special menu is unlocked: the *Import Data* menu. The insertion is achieved thanks to specific templates, readily prepared for the type of data to be inserted (production, sales, consumption…). This facilitates the insertion for data providers and ensures readability.

Once the file is imported, the tool checks the consistency of data entries with the database model and sends warnings if something is improper. The occurrences are often typos or a designation not recognized by the database such as acronyms (e.g. "CAD" instead of "district heating", or 6.3k instead of 6'300 [MWh]). Everything can be easily corrected thanks to dropdown menus should it be necessary. Another issue can be that these exact values (for example the electricity production for Vaud in 2012) have already been inserted, with possibly a different value: in this case, the model needs to recognize it and ask whether the user want to replace the existing values or keep the old ones.

When everything has been corrected directly by the data provider, the data is inserted in a temporary database, ready to be validated by an administrator.

Validation

To facilitate the administrator's work, several warnings are implemented so that potentially problematic errors can be readily seen at a glance. These are either focused on the value by itself (local warning, e.g. electricity production of a single company), or on the total value of the energetic agent (global warning, e.g. total electricity production over the whole Canton).

For the local warning, a test checks if the value entered by a data provider is not too different from the years before. While not always a good indication since some energies are bound to explode (e.g. PV or wind, which are very small currently but expected to expand drastically in the years to come), most other energy agents such as electricity, gas, district heating will stay within a fixed boundaries (depending on the weather, the energy policies, the incentives etc.). Therefore, a threshold is assumed at 20% by default, but can be changed thanks to a button to trigger stricter or looser warnings.

The global warning adds all the same agents over the whole Canton, independently of the provider, in other words, it sums the whole production/consumption without singling out the producers. Like in the previous case, a comparison is drawn with the previous years, and a warning is issued if the difference is too important.

Finally, it has been estimated that about 80% of the data can be (relatively) easily found and inserted in the database, while the remaining 20% will be obtained at the price of more effort (much more time will need to be invested to gather it). In the case where some data is missing, a catching routine has been set-up to insert a temporary value in the database, while waiting for the real one. This allows freeing the temporary database much earlier than waiting, and giving access to a number that will not be too far from the reality. For example, in the fictitious case of five electricity producers with one of them not having inserted its data yet, the values of the latter stemming from the previous year are temporarily inserted in the database instead, and added to the total with the five others, along with a clear mention that the value given is not definitive. This is done thanks to the auto-insertion button.

DISCUSSION

Many projects are currently developed in the field of energy management and planning of urban zones. This is the case of widely diverse projects such as the MEU platform (meu.epfl.ch) [1][2], which is a web-based platform serving as a decision support system for decision makers at municipal level, or the PlanETer tool which allows for an energy audit at a

territorial level [3]. Additionally, for example the Swiss-Energyscope web platform allows (thanks to its energy calculator) viewing the current energy situation and create a scenario for 2035/2050, and thus visualize the implications of energy choices for Switzerland [4]. However, to our knowledge, no other Swiss tool allows a specific representation of the energy flows at a cantonal level.

As far as the authors are aware, this is the largest and most comprehensive database for a given year, at a cantonal level. However, the critical mass of data needed to keep the tool updated implies a huge effort. The most recent reports made to comprehensively evaluate the full range of energies flows on a cantonal level date back to 2009 [5], while the perspectives for 2035 date from the beginning of 2010 [6]. This underlines the difficulty to gather useful data, and to keep it up to date. This is especially striking for energy agents such as oil products, which are extremely easy to find at a national level thanks to custom agencies [7], but extremely difficult to estimate at a cantonal level without real borders. Wood would also be such an extremely difficult energy vector to evaluate precisely: it is currently either extensively studied and analysed once every 5-10 years via comprehensive studies such as the Rapport Bois-Eau [8], or either estimated, with a wide range of possible errors.

Nevertheless, populating such a database is greatly dependent on data availability. An appropriate regulatory framework should therefore be consolidated in order to convince the data providers to share the data needed for such a tool.

CONCLUSION

By way of a relatively complex web-based tool, different energy flows at a regional/cantonal level can be readily displayed at various detail levels, while guaranteeing a very robust and secure service for the different types of users. This innovative platform is thus an important database for energy-related data all the while being a useful tool for decision-making and follow-up of policy regulations initiated at regional/cantonal level.

REFERENCES

[1] J. Rager, D. Rebeix, G. Cherix, F. Maréchal, and M. Capezzali, “MEU: An urban energy management tool for communities and multi-energy utilities,” presented at the CISBAT 2013, 2013.

[2] M.-L. Boand Colombini and M. Capezzali, “Un nouvel instrument de planification énergétique bientôt sur le marché,” *Domotech*, no. 1, pp. 16–18, 2015.

[3] L. Darmayan, G. Cherix, M. Cudilleiro, and F. Kuchler, “PlanETer, Planification Energétique Territoriale : Approche territoriale pour définir une stratégie énergétique à l’échelle d’une collectivité locale,” in *Session Collectivités Locales / Energie*, Versailles, 2011.

[4] S. Moret, V. C. Girones, F. Marechal, and D. Favrat, “Swiss-energyscope.ch: a platform to widely spread energy literacy and aid decision-making,” in *Chemical Engineering Transactions*, 2014, vol. 39, pp. 877–882.

[5] Weinmann, “Programme cantonal vaudois visant à améliorer l’efficacité énergétique et à développer la production d’énergie renouvelable - Etat des lieux,” Weinmann-Energies, Lausanne (Suisse), 2009.

[6] Weinmann, “Programme cantonal vaudois visant à améliorer l’efficacité énergétique et à développer la production d’énergie renouvelable - Perspectives énergétiques pour le canton de Vaud à l’horizon 2035,” Weinmann-Energies, Lausanne (Suisse), 2010.

[7] Office fédéral de l’énergie (OFEN), “Statistique globale de l’énergie 2013,” Berne, 2014.

[8] “Analyse du potentiel de bois énergie disponible dans les forêts vaudoises,” Service des forêts, faune, nature, 2008.

THE MEU WEB PLATFORM: A TOOL DEDICATED TO URBAN ENERGY MANAGEMENT

P. Puerto [1], M. Pernet [2], M. Capezzali [2], L. Darmayan [1], G. Cherix [1]

1: CREM, Av. Du Grand-Saint-Bernard 4-CP 256, CH-1920 Martigny

2: EPFL Energy Center, Station 5, CH - 1015 Lausanne

ABSTRACT

The MEU GIS-enabled web-platform [1] has been developed in close collaboration with four Swiss cities. The tool enables detailed monitoring and planning for both energy demand and supply at individual building, neighborhood and whole city scale (http://meu.epfl.ch). This web-platform acts like an interface between different tools and allows to establish detailed energy balances for entire cities comprising several thousand buildings.

In its present configuration, the MEU tool does not allow yet to simulate energy networks behaviors, based on the real or projected energy demand in an urban zone. In order to meet this need from energy utilities partners, a specific data model, as well as an user-interface giving access to networks attributes and edition/simulation tools were developed, which will be then functionally integrated in the MEU platform. The idea is to create a "Natural Gas Networks" module built for energy utilities.

The objectives of this project within the larger MEU endeavor were the following:

- Create a platform gathering topological and geo-referenced data
- Develop a gas network pre-design/planning methodology including demand characteristics and gas supply for buildings in a selected area.
- Interface with gas distribution system operators existing tools and add new functionalities within a single platform.
- Include gas distribution system operator constraints and operational realities in the pre-design/planning process.

In order to achieve those objectives, two tools and several visualization concepts have been created, along with an ad hoc data model: (i) a data model able to allow data import, storage and centralization from energy utilities databases: networks, buildings demands and specifications, as well as interface between edition, simulation and visualization tools; (ii) a network edition tool prototype (LEAFLET JavaScript based web page), which allows to display a network on a map, to add/delete or drag&drop pipes, nodes, consumption and biogas production/injection points and pressure let down stations; (iii) a network flows, and pressures simulation device (MATLAB® compressible fluids model) which computes the network behavior for each hour (pressures, flows, power equivalent and temperatures in each point); (iv) a detailed mock-up for visualization and display concept with interactive and GIS data: buildings area, networks paths, pipes characteristics, results from simulation, studied area energy balance, etc.

This paper focuses more specifically on the visualization and network edition tool, as well as simulation results interactive representation on the MEU platform.

Keywords: urban energy planning, energy flows, GIS, gas networks

INTRODUCTION

Due to high level policy decision, energy systems, especially at local scale, have considerably evolved during the last ten years. European Union for example decided in 2008 the 3x20 strategy: decrease CO_2 emission of 20%, increase energy efficiency of 20% and share at least 20% of renewable energy considering the global energy consumptions, at EU scale and since 2020. Such decision had a direct impact on local energy systems, in terms of demand as well as in terms of supply: buildings refurbishment or more efficient devices implementation, saving energy ; decentralized energy production, based on renewable or distributed energy (e.g. : Combined heat and power); substitution of fossil & fissile fuel by renewable or CO_2 free energy [2].

This pressure, coming from different level regulation [3], combined to the availability of high efficiency and renewable new technologies increase the number of possible solutions to achieve a defined territorial objective, like EU 3x20 applied at local scale through the Covenant of Mayors [4]. The solutions, which local decision makers have to compare are more and more complex, tackling spatial and temporal distribution of energy resources and demand, considering multi-energy centralized and decentralized technologies. Computing becomes necessary as a decision support system, taking into account as many solutions as possible, and benchmarking them based on different relevant indicators (primary energy consumption, CO2 emission, share of renewable energy). Such a computation scheme needs a large energy technology model library, as well as huge quantity of "up to date" territorial energy data [5].

In parallel, Information and Communication Technology science highlighted the potential of Smart Cities, to better collect, process and store territorial data including energy data. This approach can strongly support the way that local administration, as well as utility industry, manage and share territorial energy data. The use of such smart cities energy data enhance the knowledge of the local energy system "state of the art", allow the monitoring of local energy system performances, and support the computation of future energy systems scenarios as help decision tool.

METHOD

Dedicated data model

The MEU platform is built around a database that stores and makes data available for display, indicator computation and simulations [6]. In order to integrate gas networks to the platform, the existing data model covering buildings and conversion technologies had to be extended. This was done considering the three following constrains. Integrate data needed by network energy providers; Integrate topological data needed for network simulations; Comply with existing norms and good practices in terms of network representation.

Based on a bottom up approach, interviews were conducted with industrial partners (SOGAVAL SA, Sinergy, Viteos, ESR, SIL) in order to identify their needs in terms of data accessibility and display. These needs were added to the inputs needed by the simulation tool developed in parallel and translated into objects and attributes, based on the technical guidebook n° 2015 [7] given by the Swiss Society of Engineers and Architects (SIA).

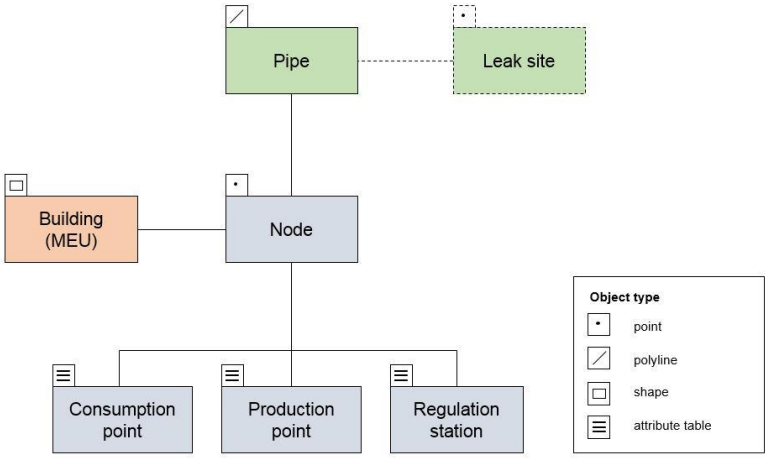

Figure 1: Network data model objects diagram

The resulting data model contains two "geographical" objects: node (point) and pipe (polyline), as well as three "attributes table" objects that can be assigned to a node to form a consumption point, a production point or a regulation point. This basic model can be extended depending on the user's needs (for example with leak site table)

Display and visualization concepts

Georeferenced representations of networks and related data are the key features of MEU+. It is built up on the existing GIS based visualization interface MEU that allows users to activate layers displayed on top of an ortho-picture map and access data by clicking directly on the objects.

The basic representation of the network consists in a layer showing the network's geographical objects on top of the ortho-picture map or any other pre-existing MEU map. Nodes are represented by points or pictograms depending on their type (elbow, junction, production / consumption points, etc.). Pipes are represented by segments joining two nodes and of variable width and color depending on the type of network (mid/low pressure, carrying, delivery, etc.).

In order to avoid over-charging large scale maps, three levels of detail display have been defined depending on the scale. At city scale only the mid pressure network components are shown on the map. At the neighborhood scale the low pressure network components are added. At the street scale the connecting pipes and low pressure consumption points appear.

Figure 2: Concept for the three level network representations (from left to right: city, neighbourhood and street scale)

In addition to the basic representation, the network's geo-referenced data can be used to display thematic maps according to user's needs. Segment width and color scales can be used to highlight aspects of the network state such as flowrate, speed, pressure or location of leaks. Other representation, taking advantage of the building database MEU, highlight new market opportunities like oil heated building within a certain range of the network, or building with higher needs (Figure 3).

Figure 3: Concept of thematic maps (light grey: oil heated buildings, dark grey: big consumers)

Access to network component attributes is done by clicking the object on the map. A pop-up window (Figure 4) displays all information linked to the object. Data are organized in tabs for convenience of use. A first tab displays general information like identification code, coordinates, construction year, etc. A "modify" button allows user to modify the content. The "results" tab displays the simulation results. The "documents" tab shows a list of documents (reports, schematics) related to the object. The "history" tab shows the history of modification. Depending on the object type, additional tabs are used to display specific information (consumption, production, regulation). The same four level metadata (0, 1, 2 or 3 stars) contained in the MEU platform is also used to qualify data quality of networks components (0: default, 1: estimated, 2: simulated, 3: measured)

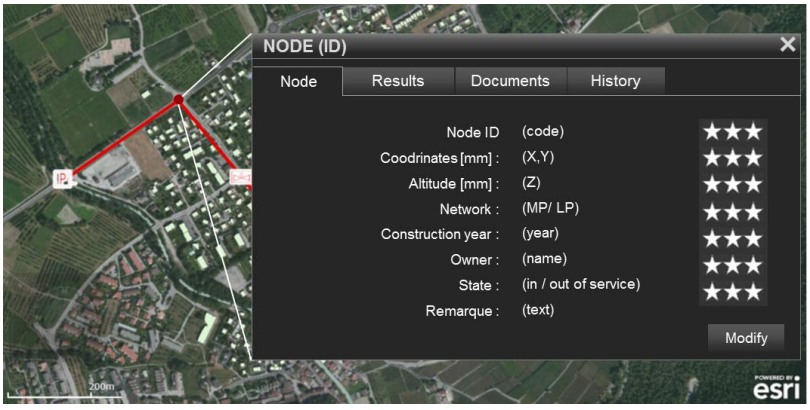

Figure 4: Concept of pop up window for a node

A global network window allows to display synthetic network values like annual volume distributed, global pipe length, average network age, energy vector penetration rate, biogas share, delivered power, etc. as well as graphical representation of the whole network or a selected area.

Network edition tool development

Natural gas network data, are usually owned and directly managed by distribution companies, and are not standardized, at least in Switzerland. Each gas company can rely

upon its own information system and data structure. Thus, natural gas network data, as received from utilities, need pre-processing, in order to ensure matching with the data model described previously.

The main underlying idea of the MEU+ project is to create, test and validate new scenarios for natural gas infrastructure. It allows handling both the modification of existing networks, as well as the creation of a completely new network.

Utilities project partners actually work on two completely separate tools to handle natural gas network modification test and validation. The first one, based on a very precise "drawing" of the existing network, manages and displays spatialized data, necessary for network maintenance and intervention; however, this first tool is not able to deal with topological data or flow simulations. The second one (ex: NEPLAN®) is a flow simulation tool which is not designed to manage GIS data.

The need for a tool integrating both GIS data and topological data thus arose from natural gas utilities project partners, in order to simplify the management and exploitation of network data.

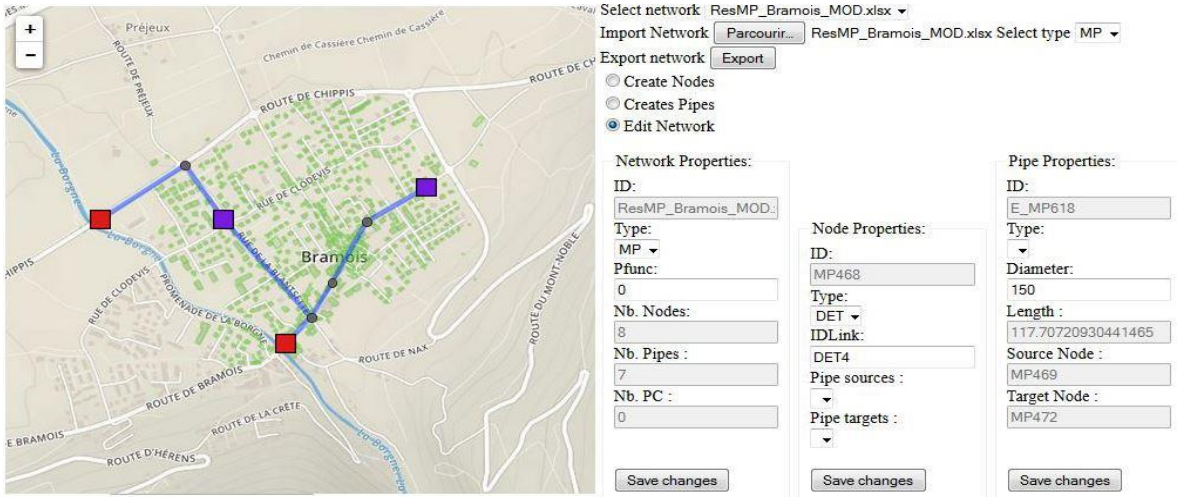

Figure 5: Network edition tool

A more detailed description of the network edition tool features, functionalities and characteristics can be found in [8].

Network flows, and pressure simulation device development

Tool specifications, underlying assumptions and physical modelling, as well as the integrated solving simulation have also been already presented in [8].

RESULTS

Prototype of a gas network simulation module

In order to test and validate natural gas network model with associated technical assumptions, a "basic blocks-like" method has been developed. Basic and simplified network structures have been created and implemented based on real network topology analysis. Those "basic blocks" are designed to simply cover every possible micro-structure occurring in real natural gas network. Overall model computation and simulation have then been performed for each "basic block" structure, while the model core code has been adapted to suit every one of those "miniature network".

The model is currently tested for big-scale network simulation using a comparison between the network simulated behaviour computations and NEPLAN® simulation results on an existing neighbourhood. The results of this validation will be published in a successive dedicated paper..

CONCLUSION

The MEU platform presently allows displaying a precise picture of an urban area, regarding its energy consumption and balances. The platform code is currently undergoing broad refactoring [9], in order to increase robustness, reliability and replicability. New functionalities regarding energy networks and, in particular, natural gas networks are simultaneously developed and tested. MEU tool users from cities and energy utilities will thus be able to perform detailed network pre-dimensioning computations, based on geo-referenced cities energy data. Thus, the impact of selected natural gas network scenarios can be displayed in the MEU platform: the user is enabled to compare current state for a given year to these scenarios, in order to evaluate the impact of foreseen actions. In the future, it shall open the opportunity to directly exchange high added-value data between different local energy stakeholders.

The described platform aims at bringing more transversality in territorial energy planning and management. It will foster urban energy networks analysis and design by precise description and study of fluids flows and energy exchange through energy infrastructures. Such technological and methodological advances will help with: (i) further developments and integration of power and district heating/cooling networks; (ii) modelling, simulating and , improving design methods; (iii) the comprehension of global urban energy metabolism and territorial energy systems.

REFERENCES

1. Capezzali M., Cherix G. : MEU – A cartographic-based web-platform for urban energy management and planning, ESRI World Summit, Palm Spring, 2012
2. Cherix G. : Impact of decentral energy generation on greenhouse gas emissions, Network Industries Quarterly vol. 12 no1, June 2010
3. Cherix G., Finger M., Capezzali M., Püttgen H.B., Chapuis A., Nour A. : Action and influence of the multiple decision levels over the whole energy chain, 5th Dubrovnik Conference on Sustainable Development of Energy, Water and Environment Systems, Dubrovnik, 2009
4. Covenant of Mayors - http://www.conventiondesmaires.eu
5. Blanc G., Cherix G., Darmayan L. : How to plan the desirable development of the energy use and supply of a local territory with the use of GIS tool, 8th Dubrovnik Conference on Sustainable Development of Energy, Water and Environment Systems, Dubrovnik, 2013
6. Rager J., Rebeix D., Maréchal F., Cherix G., Capezzali M. : MEU- an urban energy management tool for communities and multi-energy utilities, CISBAT, Lausanne, 2013
7. GEO 405 – Catalogue de données et de représentations de conduites souterraines, SIA, Cahier technique 2015, Zurich, 2005
8. Puerto P. and al. :Towards pre-dimensioning of natural gas networks on a web-platform, WGC 2015, Paris, 2015
9. Capezzali M. and al. : Evolution of and additional functionalities to the city energy planning platform MEU, IGRC 2014, Copenhagen, 2014

AUTHOR INDEX

Author Index

E

F

G

H

I

J

P

Q

R

S

T

U

V

W

X

Y

Z

ACKNOWLEDGEMENTS

CISBAT can only exist thanks to the patronage of the Swiss Federal Office of Energy and other donors. We are very grateful for their continuing support.

We also thank the Swiss Competence Center for Energy Research “Future Buildings and District”, supported by the Swiss Federal Commission for Technology and Innovation, for their partnership and funding of the Outreach Event.

Our scientific partners from Cambridge University, the Massachusetts Institute of Technology and the Swiss Chapter of the International Building Simulation Association as well as the members of the CISBAT scientific committee and the session chairs have enthusiastically supported the conference and ensured its quality. We would like to express our sincere thanks for the time and effort they have spent to make it a success.

Behind the scenes, we have received much competent support from the EPFL administration as well as from our caterers and diverse suppliers. We herewith express our sincere thanks for their efficient and friendly collaboration.

The active and uncomplicated help of all staff members of the Solar Energy and Building Physics Laboratory was much appreciated. Special thanks go to our technical and IT staff whose professionalism and excellent organisation was essential at every stage of preparation and during the conference.

Finally, we cordially thank all speakers, authors and participants who have brought CISBAT 2015 to life.

Prof. Dr J.-L. Scartezzini
Chairman of CISBAT 2015
Head of Solar Energy and Building Physics Laboratory (LESO-PB), Swiss Federal Institute of Technology Lausanne (EPFL)

Barbara Smith
CISBAT Conference Manager